UNIVERSITY OF SOUTHAMPTON

A Mixed Mode Function – Boundary Element Method for Very Large Floating Structure – Water Interaction Systems Excited by Airplane Landing Impacts

Jingzhe, JIN

Thesis submitted for the degree of Ph.D.

School of Engineering Sciences, Ship Science

October, 2007

UNIVERSITY OF SOUTHAMPTON

ABSTRACT

Doctor of Philosophy

SCHOOL OF ENGINEERING SCIENCES
SHIP SCIENCE

A MIXED MODE FUNCTION – BOUNDARY ELEMENT METHOD FOR VERY LARGE FLOATING STRUCTURE – WATER INTERACTION SYSTEMS EXCITED BY AIRPLANE LANDING IMPACTS

By Jingzhe, JIN

This thesis develops a mixed mode function – boundary element method (BEM) to analyze the dynamics of an integrated airplane – floating structure – water interaction system subject to airplane landing impacts.

The airplane and the floating structure are treated as two solid substructures of which the motions are represented by their respective modal functions. The landing gear system of the airplane is modelled with a few linear spring – damper units connecting the airplane and the floating structure. The water is assumed to be inviscid and incompressible and the fluid motion is irrotational. Under a linear potential theory, the motion of the fluid is governed by the Laplace equation and the related boundary conditions. A linearised composite free surface boundary condition and an undisturbed far field (infinity) radiation condition are considered. The Green function, or kernel, of BEM formulation is a fundamental solution of the Laplace equation assuming an infinite fluid domain. The motion of the floating structure and the surrounding fluid are coupled through the wetted surface interface conditions. The coupled equations of the airplane, the floating structure and the surrounding fluid are solved using a step by step time integration procedure based on the Newmark assumptions.

A FORTRAN program MMFBEP is written to implement the proposed numerical method. A few examples are completed to validate the mathematical model and the developed computer code. In comparing the available numerical and experimental results reported in the literature, sound agreements are reached.

It is hoped that the developed method and computer code may be further improved and modified to provide an engineering tool for the dynamic design of Very Large Floating Structures (VLFS).

Key words: integrated airplane – VLFS – water system, mixed mode function – boundary element method, VLFS dynamics, airplane landing impacts, transient dynamics, time integration scheme.

Acknowledgements

This is my opportunity to say a few words of thanks.

First, I would like to acknowledge the School of Engineering Sciences for the studentship support enabling me to study in the University of Southampton and engage in this research.

I would like to thank my supervisor, Professor Jingtang Xing for his strict supervision, constant support and kind encouragement from the beginning to the end.

I would also like to thank all the colleagues and friends in Ship Science, who have at times provided individual help and support for me over the past few years. In particular, I thank Dr. Yeping Xiong, Dr. Shihua Miao, Dr. Weibo Wang and Haitao Wang for discussing some theoretical, technical and software problems. Dr. Mingyi Tan is thanked for help in solving computer problems and Simon Lewis is acknowledged for reading and suggesting modifications to the manuscript.

I also want to thank Hisayoshi Endo from Japan for kindly providing the experimental data.

I owe a big thankyou to all my friends in Southampton, too many to mention. Without you, I would have had nowhere to escape from office. Among the others, Lin Ji and Wenjuan Sun have to get a mention for the times we spent together.

Last but not least, I wish to thank my parents, all my family back in China and my husband in Norway for their never ending love and support, without which finishing the Ph.D. would have been impossible for me.

List of Contents

List of Figures

List of Tables

Nomenclature

a	added mass coefficient representing hydrodynamic force
a	static stroke parameter of the landing gears
$a_1,...,a_{11}$	coefficients used in the time integration scheme
a_x	horizontal acceleration of the airplane in landing
A	amplitude of a harmonic motion
A_{CG}	acceleration at centre of gravity
$\mathbf{A}_1,...,\mathbf{A}_6$	coefficient matrices and vectors used in expressing first order derivative of velocity potential with respect to time
$\overline{\mathbf{A}}_1,...,\overline{\mathbf{A}}_6$	matrices and vectors truncated from $\mathbf{A}_1,...,\mathbf{A}_6$
b	damping coefficient representing hydrodynamic force
$b_1,\ ...,\ b_4$	constants to determine the spatial function $\Phi(x)$
$b_5,\ b_6$	constants to determine the function $f(t)$
B	width of the floating structure
$B_1,\ B_2$	constants to determine the displacement $\hat{x}$ of the mass–spring–damper system relative to equilibrium position
$c_0,\ c_1$	constants to be determined for the Green function $G(\ )$
C	damping coefficient of spring – damper unit
C_J $(J=1,...,4)$	damping coefficients of the four landing gears
C_l	constant value of the Bernoulli function along a streamline
$\mathbf{C}$	damping matrix of a structure
$\mathbf{C}_{11},\mathbf{C}_{12},\mathbf{C}_{21},\mathbf{C}_{22}$	component damping matrices in the coupled equation of the two substructures
$\overline{\mathbf{C}}$	generalized damping matrix of a structure
d	mean draft of the floating structure
E'	kinetic energy caused by the sink velocity of landing gear carriage
$E^{(I)}(I=1,2)$	Young's modulus of the floating structure and airplane

$\mathbf{E}^{(I)}(I=1,2)$	material matrix of the floating structure and airplane
EI	bending stiffness of a structure
$f(t)$	a function of time
f_e	frequency of external excitation force
f_J $(J=1,...,4)$	force provided by the four landing gears
$F(x,y,z,t)$	free surface function
F'	force provided by spring – damper unit
F_d	damping force applied to a harmonic system
F_w	resultant force from water pressure applied on the floating structure
F_x	constant landing resistance
$\mathbf{F}$	external force applied on a structure
$\mathbf{F}_d^{(1)}$	generalized force from water pressure applied on the floating structure
$\mathbf{F}_d^{(2)}$	generalized force from the inertia of the airplane
$\mathbf{F}_g^{(I)}(I=1,2)$	generalized force from the gravity of the floating structure and airplane
$\mathbf{F}_i^{(I)}(I=1,2)$	generalized force from the landing gear system
$\hat{\mathbf{F}}$	a vector
$\overline{\mathbf{F}}$	body force per unit mass
g	acceleration of gravity
$\mathbf{g}^{(I)}(I=1,2)$	external force applied on the floating structure and airplane
$G(\ )$	Green function of fluid domain
$\mathbf{G}_1, \mathbf{G}_2, \mathbf{G}_3$	coefficient matrices to determine the generalized force from water pressure $\mathbf{F}_d^{(1)}$
$\mathbf{G}_4$	coefficient matrix in the coupled fluid – structure interaction equation
$\mathbf{G}, \mathbf{H}, \overline{\mathbf{G}}$	coefficient matrices in the boundary element equation
H	Bernoulli function
i	$=\sqrt{-1}$
$\mathbf{i}, \mathbf{j}, \mathbf{k}$	unit vector along three coordinate axes
$\mathbf{I}^{(I)}(I=1,2)$	unit diagonal matrix of order $M^{(I)}(I=1,2)$
k	spring coefficient representing hydrostatic force

k	wave number
k_1	equivalent spring coefficient at static stroke of the landing gear
k_2	equivalent spring coefficient at working stroke of the landing gear
K	spring coefficient of spring – damper unit
K_J $(J=1,...,4)$	spring coefficients of the four landing gears
$\mathbf{K}$	stiffness matrix of a structure
$\mathbf{K}_{11},\mathbf{K}_{12},\mathbf{K}_{21},\mathbf{K}_{22}$	component stiffness matrices in the coupled equation of the two substructures
$\mathbf{K}^{(I)}(I=1,2)$	generalized stiffness matrices of the floating structure and airplane
$\overline{\mathbf{K}}$	generalized stiffness matrix of a structure
$\tilde{\mathbf{K}},\tilde{\mathbf{C}},\tilde{\mathbf{M}}$	coefficient matrices in the effective stiffness matrix
L	length of the floating structure
$m^{(1)}$	total mass of the floating structure
$m^{(2)}$	total mass of the airplane
$\overline{m}$	mass per unit length of a beam
M	number of retained modes
M'	mass sustained on one landing gear
$M^{(I)}(I=1,2)$	number of retained modes of the floating structure and airplane
$\mathbf{M}$	mass matrix of a structure
$\mathbf{M}^{(I)}(I=1,2)$	generalized mass matrices of the floating structure and airplane
$\overline{\mathbf{M}}$	generalized mass matrix of a structure
n	outward normal of fluid domain
n'	load factor of landing gear
$\mathbf{n}$	unit outward normal vector of a closed surface
N	number of degrees of freedom
N_f	number of element on the free surface
N_Σ	number of element on the wetted interaction interface
$\overline{N}_f$	element identifying number on the free surface
$\overline{N}_\Sigma$	element identifying number on the wetted interaction interface

$p(x_p^{(1)}, y_p^{(1)}, z_p^{(1)})$	field point in fluid domain
P	water pressure
P_a	atmospheric pressure at the free surface
P_s	static load on landing gear
P_w	load on landing gear at working stroke
$q(x_q^{(1)}, y_q^{(1)}, z_q^{(1)})$	source point in fluid domain
$\mathbf{q}$	natural mode vector of a structure
$\mathbf{Q}$	generalized coordinate vector of a structure
$\mathbf{Q}^{(I)}(I=1,2)$	generalized coordinates of the floating structure and airplane
r	distance between field and source points
$\mathbf{R}_a, \mathbf{R}_v, \mathbf{R}$	coefficient vectors in the effective load vector
S	$=\Gamma_f + \Gamma_\infty + \Gamma_b + \sum$
S_s	static stroke of the shock absorber of landing gears
S_w	working stroke of the shock absorber of landing gears
t	time
Δt	time step used in the time integration scheme
Δt_{cr}	critical time step
T	thickness of the floating structure
T_e	period of the external excitation force
T_n	smallest period of a system
$u(x,t)$	vertical displacement of a beam
$\mathbf{u}$	displacement vector of a structure
U	a potential function
$\mathbf{U}_0^{(2)}$	initial deformation of the airplane
$\mathbf{U}^{(I)}(I=1,2)$	displacement vector of the floating structure and airplane
V	amplitude of fluid velocity
V	volume enclosed by a closed surface
V_n	velocity of floating structure along the outward normal of wetted surface
V_s	sink velocity of the landing gear carriage in the drop test

V_x	horizontal velocity of the mass centre of the airplane
$\mathbf{V}(u,v,w)$	velocity vector of fluid
$\mathbf{V}_0(V_{x0}, 0, V_{z0})$	initial landing velocity of the airplane
W	work done by the damping force of a harmonic system in one cycle
W_d	dissipated energy within one stroke of shock absorber
$\hat{x}$	displacement of mass–spring–damper system relative to equilibrium position
$\tilde{x}$	displacement of a harmonic motion
$\mathbf{x}$	a field point on the boundary of the fluid domain
$\mathbf{x}'$	a source point on the boundary of the fluid domain
$\hat{X}$	displacement of mass–spring– damper system relative to initial position
$\mathbf{X}$	a field point inside the fluid domain
$\mathbf{X}'$	a source point inside the fluid domain

α, δ	parameters from Newmark assumptions
$\overline{\alpha}, \overline{\beta}$	coefficients of Rayleigh damping
β'	phase angle of a harmonic motion
Γ_b	sea bed boundary
Γ_f	free surface boundary
Γ_∞	far field boundary
δ_{ij}	Kronecker delta function
$\Delta(\ )$	Dirac's delta function
ε	radius of a spherical control surface
ε'	damping ratio
$\boldsymbol{\varepsilon}^{(I)}(I=1,2)$	strain vector of the floating structure and airplane
$\varsigma(x,y,t)$	vertical elevation of free surface
η	energy absorption efficiency of the shock absorber of landing gears
$\eta^{(I)}(I=1,2)$	material damping factor of the floating structure and airplane
$\boldsymbol{\eta}$	unit outward normal vector of fluid domain

$\mathbf{\Lambda}^{(I)}(I=1,2)$	diagonal matrix of the square of the natural frequencies of the floating structure and airplane
$\mu^{(I)}(I=1,2)$	Poisson's ratio of the floating structure and airplane
$\mathbf{v}^{(I)}(I=1,2)$	unit outward normal vector of the floating structure and airplane
ξ	modal damping parameter
π	ratio of circumference to diameter
ρ	mass density of water
$\rho^{(I)}(I=1,2)$	mass density of the floating structure and airplane
$\boldsymbol{\sigma}^{(I)}(I=1,2)$	stress vector of the floating structure and airplane
τ	a small increase of time
$\phi(x^{(1)},y^{(1)},z^{(1)},t)$	velocity potential of fluid
ϕ'	transfer coefficient of landing gears
$\Phi(x)$	a spatial function
$\mathbf{\Phi}$	modal matrix of a structure
$\mathbf{\Phi}^{(I)}\ (I=1,2)$	normal natural mode matrices of the floating structure and airplane
χ	energy dissipation coefficient of landing gears
ψ	a potential function
$\mathbf{\Psi}$	velocity potential vector
$\mathbf{\Psi}_n$	vector of normal derivative of velocity potential
$\overline{\mathbf{\Psi}}$	truncated velocity potential vector along the wetted interface
ω	frequency of a harmonic motion
$\omega^{(I)}(I=1,2)$	natural frequency of the floating structure and airplane
ω_d	frequency of a damped motion
ω_t	truncation frequency
$\Omega^{(1)}$	floating structure
$\Omega^{(2)}$	airplane structure
Ω_f	fluid domain
$\mathbf{\Omega}$	curl of velocity vector of fluid

$\sum$	wetted interaction interface
Π	a scalar function
∇	Hamilton operator
∇^2	Laplace operator

Notations for Coordinate Reference Axes and Key Points

$o^{(1)}-x^{(1)}y^{(1)}z^{(1)}$	a Cartesian coordinate system fixed in space
$o^{(2)}-x^{(2)}y^{(2)}z^{(2)}$	a moving Cartesian coordinate system
$O^{(1)}-X^{(1)}Y^{(1)}Z^{(1)}$	Lagrangian coordinate system of the floating structure
$O^{(2)}-X^{(2)}Y^{(2)}Z^{(2)}$	Lagrangian coordinate system of the airplane
$\mathbf{x}_c^{(1)}\left(x_c^{(1)},y_c^{(1)},z_c^{(1)}\right)$	position of the mass centre of the airplane
$\mathbf{x}_{c0}^{(1)}\left(x_{c0}^{(1)},y_{c0}^{(1)},z_{c0}^{(1)}\right)$	initial position of the mass centre of the airplane
$\mathbf{X}^{(I)}\left(X^{(I)},Y^{(I)},Z^{(I)}\right)(I=1,2)$	a material point of the floating structure and airplane
$\mathbf{X}_J^{(1)}\left(X_J^{(1)},Y_J^{(1)},Z_J^{(1)}\right)\ (J=1,...,4)$	landing gear position on the floating structure
$\mathbf{X}_{J0}^{(1)}\ \left(X_{J0}^{(1)},Y_{J0}^{(1)},Z_{J0}^{(1)}\right)(J=1,...,4)$	initial position of the landing gears on the floating structure
$\mathbf{X}_J^{(2)}\left(X_J^{(2)},Y_J^{(2)},Z_J^{(2)}\right)\ (J=1,...,4)$	fixed landing gear position on the airplane

Chapter 1

Introduction

1.1 Very Large Floating Structures (VLFS)

1.1.1 Overview of VLFS

It is well known that seventy percent of the earth surface is covered by water, which contains abundant resources, such as: chemicals, minerals, natural gas, oil, etc. Marine resource exploitation has always been an important task for future developments. Together with the growing population and the corresponding expansion of urban areas in land-scarce countries and countries with long coastlines, interest in utilising ocean space has increased constantly in recent years. As a consequence, the concept of Very Large Floating Structures (VLFS) was proposed. Such structures can serve as a sea base where various operations and activities are carried out.

The original concept of VLFS seemed to be “the huge metal vessel” described by the 19th century French novelist, Jules Verne, in his science fiction “Twenty Thousand Leagues Under the Sea” (ISSC 2006). The first VLFS promoted in earnest was the Armstrong Seadrome proposed initially to enable airline routes across the world’s oceans (Armstrong 1924).

The VLFS concept has not been taken into serious consideration until the potential of modern shipbuilding technology became apparent in the 1950s (ISSC 2006). Before then the only manner in which ocean space could be exploited on a large scale was through land reclamation. Such exploitations are limited to shallow regions of the continental shelf.

In the 1950s, architects were drawn to the idea of large floating structures. This new research interest was reflected through the proposal of a floating airport for the new Kansai International Airport in 1973 (ISSC 2006) and the semi-submersible unit of a floating city at the Okinawa International Ocean Exhibition in 1975 (ISSC 2006). Since the early 1970s the technology for VLFS has been continually developed.

VLFS is a unique concept of ocean structures primarily because of its unprecedented length (10^3-10^4 m), displacement (10^6-10^7 tons), cost (5-15 billion $US) and the associated analysis methods and design procedures (ISSC 2006). There are two basic VLFS hull types.

1) Pontoon type: a complex of pontoon hulls designed for operation in protected waters, also known as Mega-Float. A pontoon type floating airport is shown in Figure 1.1.

2) Semi-submersible type: a complex of semi-submersible hulls designed for operation in deeper water and/or open sea. The semi-submersible hull may be an array of columns, or it may be a system of columns resting on submerged pontoons. A semi-submersible type Mobile Offshore Base (MOB) is depicted in Figure 1.2.

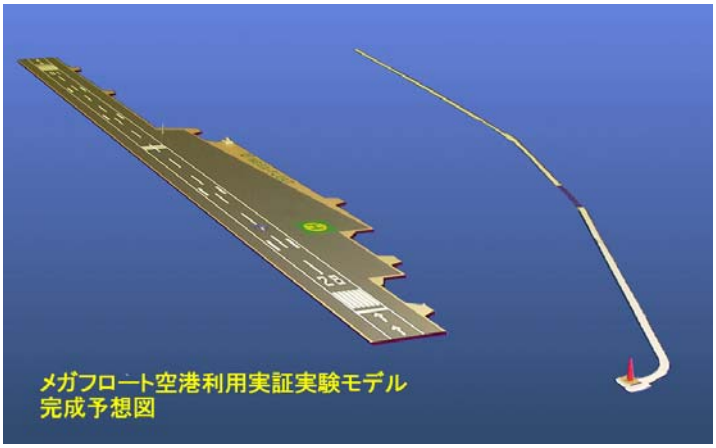

Figure 1.1 A pontoon type floating airport (Isobe 1999)

Figure 1.2 A semi-submersible type MOB (Remmers et al 1999)

1.1.2 Application of VLFS

VLFS may be applied to serve many different purposes in reality. A few examples of these applications are listed below, among the others (ISSC 2006).

1) Airport

Due to the limited land space near to the coastlines of densely populated areas, there will be a need in the future for floating airports. A floating airport can reduce pollution and noise level in the surrounding residential areas compared to a land based airport.

2) MOB

MOB is mainly for military application. It can be assembled/disassembled on the site of military operations. A similar concept may be envisaged for a mobile emergency rescue base to support humanitarian relief operations worldwide.

3) Offshore port facilities

Offshore container terminals are being considered to service large ocean-going vessels. It will be beneficial to site offshore terminals for potentially hazardous vessels, such as LNG ships.

4) Offshore storage and waste disposal facilities

In the densely populated coastal regions, setting up offshore storage facilities, waste processing and treatment plants is very attractive. Examples of offshore storage facilities exist in Japan, where two of the nation’s ten national oil stockpiles are floating stockpiles sited off the islands of Kamigoto (1988) and Shirashima (1996) respectively.

5) Energy islands

Depending on the prevailing climate, an offshore energy facility may include wind turbines, wave power generators, tidal current turbines and ocean thermal energy conversion units.

6) Habitats

Considering the pressure on coastal zones from the growing population and the threat of environmental changes, offshore habitats may provide a solution for the future. There are current proposals for offshore sports facilities and theme parks in Japan and South Korea (ISSC 2006).

Among all these applications of VLFS, a floating airport is one of the important research areas. Proposals to use floating structures for airplane landing/take-off were first considered in the 1920s (Armstrong 1924). These concepts were investigated more seriously for military applications by the US in the 1940s and a demonstration project was built and tested successfully in 1943 (ISSC 2006). In recent years, due in large part to the efforts of the Technological Research Association of Mega-Float (TRAM) in Japan, the fundamental design and construction needs of a floating airport have been extensively studied. Numerical analysis methods were developed alongside an experimental programme carried out by TRAM, which resulted in the construction of a 1000m by 60m technology demonstrator. Although a floating airport has yet to be approved for construction in reality, research interest regarding it remains strong.

1.1.3 Characteristics of VLFS

The engineers will face profound challenges regarding the design and construction of VLFS, as they are different from conventional ship and offshore structures. VLFS have the following characteristics (ISSC 2006):

1) Large size

VLFS are unprecedented large structures. Due to the large length/depth ratio, they are very flexible thus the elastic response is dominant for VLFS. Consequently, hydroelastic analysis becomes necessary for estimating the response of VLFS under waves and other external loadings.

2) Environment condition

Physical environmental conditions in which VLFS must operate may not be simply considered spatially uniform in the sense that coherence of environmental conditions such as wind, wave and current must be considered.

3) Connection at sea

VLFS are modularized structures. In the assembly of VLFS, base modules/units need to be joined together at sea. Control of thermal deformation and alignment of units are key issues in the construction.

4) Positioning

Reliability of the station keeping system is crucial to the operational availability of VLFS. In general, station keeping of MOB is accomplished by Dynamic Positioning System (DPS) and that of Mega-Float is accomplished with dolphin moorings.

5) Design life

Design life is typically 50 years for MOB and 100 years for Mega-Float. These criteria are substantially greater than those for conventional ship and offshore structures.

6) Model test

As there is no experience in designing such huge floating structures, model test plays an important role in clarifying key issues of the hydroelastic responses of VLFS. How to set up and carry out model tests in the current towing tank and ocean basin facilities is itself a new experimental technology.

When considering the characteristics of a floating airport, the following aspects are recognized. The problem of an airplane landing/take-off from a floating structure necessitates interdisciplinary studies relating the airplane, the floating airport and the surrounding fluid. Solving this problem requires a knowledge of structural dynamics, hydrodynamics and hydroelasticity theory. It is also a transient problem due to the time dependent landing/take-off impacts of the airplane, thus solutions need to be obtained in the time domain. The airplane and the floating airport are connected through the landing gear system, whose mechanics is entirely nonlinear. This nonlinearity will increase the computation efforts significantly, unless a proper linearization scheme is applied.

1.2 Hydroelasticity Theory

Hydroelasticity is concerned with the phenomena involving mutual interactions among inertial, hydrodynamic and elastic forces (Heller & Abramson 1959). The interaction between fluid pressure and structural deformation is the key point in classifying a problem as hydroelastic.

In theory, any problem of fluid (liquid) – structure interaction is a problem of

hydroelasticity as the fluid pressure acting on the wetted surface of the structure will induce both rigid-body motion and structural distortion and in return the rigid-body motion and distortion of the structure will disturb the pressure field, flow and wave pattern of the surrounding fluid. However, for most traditional marine structures such as ships and platforms, the distortion of these structures is so small in comparison with their rigid body motions that the effect of the elastic distortion of the structure on the fluid field can be neglected. The hydrodynamics book of Newman (1977) contributed a fundamental theoretical approach to the problems of ship – water interactions. Within this theory, the structure is assumed to be a rigid body for the determination of the water pressure acting on the wetted surface. The distortion of the structure can be calculated by applying either the distributed pressure or the resultant integrated global forces acting on the structure in a subsequent structural analysis.

Although the concept that floating structures behave like elastic bodies has been accepted, hydroelastic analysis hasn't been brought into the scope of marine technology until the 1970s when Bishop (1971) suggested that ship response could be evaluated based on hydroelasticity theory. This was then followed by the development of "wet modes" method employed by Bishop et al (1973) and Bishop & Eatock Taylor (1973) to determine symmetric stress and structural dynamics of ship hulls in waves. The idea of the "wet modes" method was that dynamic characteristics of the ship hull were to be determined after both structural properties and fluid actions had been taken into account. On the other hand, Bishop & Price (1974) introduced the use of "dry modes" method in which the modal analysis of a ship hull is carried out in vacuo and the influence of the surrounding fluid is treated as external loadings of the ship hull. Bishop & Price (1976) later discussed comparisons between these two approaches.

The hydroelasticity theory was originally described for two dimensional (2D) cases based on the "dry modes" method. The ship hull was assumed to be a "beamlike" structure whose dynamic characteristics in vacuo were determined in a "dry hull analysis" in the absence of any damping or external forces. The fluid field was represented by strip theory. The strip theory was adopted by Betts et al (1977) to represent the generalized

hydrodynamic forces, which formed a preliminary step for the dynamic response analysis of a symmetric ship subject to waves (Bishop et al 1977). Later Bishop et al (1980) studied the asymmetric responses of a container ship in regular waves. The study on asymmetric offshore structures or ships with an angle of heel was brought into scope by Conceicao et al (1984). The detailed theory of 2D hydroelasticity was established in a well known book "Hydroelasticity Theory of Ships" (Bishop & Price 1979).

The application of the 2D hydroelasticity theory is limited to slender or beam-like structures. In order to examine the fluid-structure interaction behaviour of non-beamlike structures, Wu (1984), Price & Wu (1982,1983,1986) and Bishop et al (1986a) presented a general linear three dimensional (3D) hydroelasticity theory of floating structures moving in a seaway. In this theory, a linear finite element approach is used to describe the dynamic behaviour of the 3D dry structure in vacuo. The singularity distribution method was used to determine the fluid actions associated with the distorting 3D wetted structure.

Most of the early studies were undertaken in the frequency domain assuming time harmonic motion of the structure. However, transient phenomena observed in fluid-structure interactions of ships and other floating structures, such as whipping induced by slamming, transient responses due to aircraft landing/take-off, underwater explosion, dynamic capsizing, collision and grounding can only be studied in the time domain. Gu et al (1989) and Xia & Wang (1997) described a time domain strip theory and used it to study the vertical motion and longitudinal bending of a ship. The associated linear hydrodynamic forces were formulated in terms of time convolutions and the structure was treated as a Timoshenko beam. Janardhanan et al (1992) developed a 3D time domain approach, incorporating time history effects and nonlinear fluid loading from wave effects. In his method the fluid field was represented in terms of the frequency domain Green function. Wu & Moan (1996) and Wu et al (1996) reported a time domain hydroelastic analysis for ships at high forward speed. Wang (1996) and Wang & Wu (1998) presented a time domain 3D hydroelasticity method for ships advancing in waves. In their method the time domain Green function (Liapis & Beck 1985) and the impulsive response function were employed.

Although linear hydroelasticity theory can be applied in many cases, nonlinear issues

involving the hydrodynamic loading and the structure response have to be addressed. Bishop et al (1978) and later Belik et al (1980) were among the first to use modal analysis to predict the transient responses due to slamming in regular head waves, using impact and momentum slamming theories. This was then extended by Belik & Price (1982) and Belik et al (1983) to study slamming responses in irregular head waves. Faltinsen (1996) studied the bottom slamming of a floating airport and later provided an overview on hydroelastic slamming Faltinsen (2000). Faltinsen states that “when the angle between the impacting free surface and the body surface is small, hydroelasticity has to be considered and the importance of hydroelasticity depends on the impact velocity and the highest natural period of the local structure”. Maeda et al (1997) and Ikoma et al (1998) calculated the second-order wave loads acting on large floating structures. Chen et al (2003a) studied the motion of a moored floating body with the consideration of second order fluid forces induced by the large rigid body rotations in high waves, the variation of the instantaneous wetted surface and the coupling of the first order wave potentials. The hydroelastic responses of a structure manoeuvring in viscous fluid were prescribed by Du (1999). With regards to the structural nonlinearity, Chen et al (2003b) proposed a method for analyzing the hydroelastic characteristics of VLFS in multidirectional monochromatic incident waves taking into account the effect of the membrane forces.

The 2D and 3D hydroelasticity theory has been widely used by many researchers to investigate the hydrodynamic/hydroelastic behaviour of floating structures since they were proposed. Bishop et al (1986b) and Price et al (1987) predicted hydroelastic behaviour of a SWATH (Small Water Area Twin Hull). Fu et al (1985,1986,1987) studied the towage of a jack-up. Price et al (1988) applied the theory to a submerged flexible cylindrical shell.

The 1990s has seen more and more application of hydroelasticity theory into the dynamics of VLFS. The huge length/draught ratio makes VLFS very flexible. This causes significant wave – structure interactions and therefore a hydroelastic analysis is necessary. One of the essential steps in the design stage is to estimate the hydroelastic wave induced responses of VLFS and the influence of other external loadings to guarantee structural integrity and serviceability. Extensive research, regarding this aspect, has been carried out

over many years. The main research publications on this subject may be divided into two categories: frequency domain analysis methods and time domain analysis methods. Each approach is considered in turn next.

1.3 Frequency Domain Analysis Methods

When the motions of VLFS and the surrounding water are time harmonic, they can be analyzed in the frequency domain. The relevant analysis methods are known as frequency domain methods. In this case it is the amplitudes of the motions that is to be determined.

This section provides a brief review on the frequency domain analysis methods for pontoon type VLFS. Practical calculations of the responses of VLFS in regular waves have been attained and fundamental characteristics of the responses are also clarified (Ohmatsu 1998a, Iwahashi et al 1998). As a result, the wave induced hydroelastic responses of VLFS can now be predicted with good accuracy in the frequency domain within a linear regime.

There exist a large number of publications involving frequency domain analysis. The interested readers may start from the following review papers to obtain a general idea of the existing analysis methods, which include a Report of the Special Task Committee on VLFS (ISSC 2006), Ohmatsu (2005), Chen et al (2006), Watanabe et al (2004), Cui (2002), Cui et al (2001) and Kashiwagi (2000a).

1.3.1 Analysis methods regarding fluid motion

In general, the surrounding water is assumed to be inviscid, incompressible and the fluid motion is irrotational. Therefore, the potential flow theory is valid. The governing equation of fluid motion is the Laplace equation together with suitable boundary conditions. This problem is often solved by using a boundary element method (panel method) or eigenfunction expansion-matching method (domain decomposition method).

BEM may be further classified as either direct or indirect. In the direct BEM (Yasuzawa et al 1997), both the velocity potential and its spatial derivatives are used in the boundary integral equation formulation, whilst in the indirect BEM (Okada et al 1999), the velocity

potential is expressed in terms of a fictitious source distribution function. Yago & Endo (1996), Yasuzawa et al (1996) and Hamamoto et al (1997) independently developed a method to determine the water pressure distribution using a BEM. Ohkusu & Namba (1996) and Namba & Ohkusu (1999) introduced the modified Green function approach, which corresponds to a modified free surface condition to reflect the presence of a floating plate. Initially they considered an infinitely long plate, and later the method was extended to a finite 3D problem.

In conventional BEM (low order BEM), the submerged surface of the floating structure is represented by a number of small quadrilateral plane elements, and the velocity potential is assumed to be constant over each element. As the wave length of the incident wave is much smaller than the length of the floating structure, the number of elements required for sufficient accuracy is very large, which makes the conventional BEM very time consuming. Newman & Lee (2002) described two methods to overcome the problems experienced in the conventional BEM. One is a higher-order method of which the geometry shapes of the submerged surface are represented exactly or approximated to a high degree of accuracy using B-spline functions, and the velocity potential is also approximated by B-splines. For the same accuracy, the number of unknowns in higher-order methods is less than that used in the low-order methods. As a result of this, the required memory space and computational time are reduced whilst the accuracy and continuity of the solution are improved. Higher-order boundary element methods are also used by Yasuzawa et al (1996), Hamamoto et al (1998) and Utsunomiya et al (1998). The other development is to use the pre-corrected Fast Fourier Transform method (pFFT) to improve the efficiency of conventional BEM. pFFT was developed by Phillips & White (1997) for electro-static and electro-dynamic applications and subsequently extended to the analysis of wave-body interactions by Korsmeyer et al (1999).

In the eigenfunction expansion-matching method, the entire fluid domain is divided into an inner domain covered by VLFS and an outer domain. Velocity potential within each sub-domain is approximated by using the vertical orthogonal eigenfunction expansion and is forced to match each other on the interfaces of the sub-domains. Ohmatsu (1997, 2001) employed the eigenfunction expansion-matching method to analyze fluid motion. The

surface integral for the hydrodynamic force calculation was simplified to a line integral with a significant reduction of computation time. Seto & Ochi (1998) and Seto et al (2003) used a hybrid finite/infinite element formulation for the fluid flow based on the eigenfunction expansion-matching method. The inner and outer fluid sub-domains were discretised with planar finite elements and hybrid infinite elements, respectively. Kim & Ertekin (1998) introduced the eigenfunction expansion-matching method into the fluid region beneath VLFS. They also efficiently utilized the representation of solutions of the Helmholtz equation for rectangular regions.

In Kim & Ertekin (2002) and Ertekin & Kim (1999), the governing fluid motion equations are based on the linear level I Green-Naghdi equations (Green & Naghdi 1976). The velocity fields in regions with and without the plate were matched using the continuity of mean mass flux and pressure. The resulting Helmholtz equations were solved by the boundary-integral-equation method and the finite difference method was used for discretizing the boundary conditions at the edges of the floating structure. Xia et al (2004) further studied the nonlinear hydroelasticity of VLFS with the nonlinear, Level I Green-Naghdi theory.

The fluid motion can also be dealt with Finite Element Method (FEM) based on the variational principle. Watanabe & Utsunomiya (1996) and Kyoung et al (2006) employed FEM for solving fluid motion. Although the methods proposed in these two papers are for time domain analysis, the treatment for fluid domain can obviously be adopted in a frequency domain analysis.

1.3.2 Analysis methods regarding structure motion

VLFS are generally steel or concrete structures and they are often modeled as elastic plates, shells or sandwich-grillages in the primary design stage. FEM is often used for the structural analysis of VLFS. Alternatively, the differential motion equation of VLFS can be solved using a finite difference scheme.

The motion of VLFS can be solved by either direct or modal superposition method. The direct method is straightforward, but must solve a large scale matrix equation and this

means that a large amount of memory space and CPU time is required. Mamidipudi & Webster (1994) used the direct method for VLFS. In their solution procedure, the deflection of VLFS was determined by solving the combined hydroelastic equation via the finite difference scheme and the hydrodynamic aspects were considered by the panel method. Their method was modified by Yago & Endo (1996) who applied the pressure distribution method (Yamashita 1979) for fluid and the equation of motion of VLFS was solved using FEM.

In the modal superposition method, the motion of VLFS is represented in terms of the dry or wet natural modes. Compared to the direct solution method, the modal superposition method is more efficient. However, it is important to judge the effectiveness and rationality of the mode truncation technique. Takaki & Gu (1996) and Lin & Takaki (1998a) calculated numerically the dry modes of the structure using FEM. Maeda et al (1995), Wu et al (1995), Nagata et al (1998), Utsunomiya et al (1998) and Ohmatsu (1998a) employed the simple products of free-free beam modes as the modal function of rectangular plates with free edges, which are analytically given and thus able to avoid numerical differentiations and integrations. Lin & Takaki (1998b) showed that the B-spline functions can also be used to approximate the modal functions of a plate. Wang et al (2001) adopted 2D polynomial functions as modal functions for the structure. It should be remarked that all the modes aforementioned are of a dry type. While most analysts use the dry-mode approach, because of its simplicity and easy accessibility, Hamamoto et al (1996) and Hamamoto & Fujita (2002) conducted studies using the wet-mode approach.

Based on the modal superposition method for solving the motion of a structure, Kashiwagi (1997) proposed an effective calculation scheme for computing wave forces on an elastic plate in the regime of very short wave-lengths. The scheme employed bi-cubic B-spline functions for representing the unknown pressure and a Galerkin method for converting the integral equation into a linear system of simultaneous equations. Kashiwagi (1998) further proposed a method using B-spline functions to represent both the pressure and elastic deflections of structure.

Murai et al (1998, 1999) used an assembly of substructures to model VLFS whose deformation was represented with a succession of discrete vertical displacement of each

substructure. The substructures are treated as if they were independent, freely floating rigid bodies, while the structural constraint is taken into account as an additional restoring force on the motion of the substructures. The structural constraint is evaluated based on the displacements of the associated substructures.

Eatock Taylor & Ohkusu (2000) used a Green function method to describe the deformation of VLFS with the Green function giving the response at any point in the structure due to a harmonic point excitation at any position along the structure. The Green function of a free–free beam was first developed. The analysis was then extended to the case of free–free rectangular plates of arbitrary aspect ratio.

1.3.3 Comparative study of responses of VLFS in waves

It is very promising to see that a comparative study of the hydroelastic responses of a pontoon type VLFS under regular waves from five different computer codes was reported in the recent International Ship and Offshore Structures Congress (ISSC 2006). The five computer programs are: HYDRAN (OCI 2005), KU-VLFS (Yasuzawa et al 1997), MEGA (Seto et al 2003), VODAC (Iijima et al 1997) and LGN (Ertekin & Kim 1999). HYDRAN uses a traditional constant panel Green function formulation for the fluid and a 3D shell finite element model for the structure. KU-VLFS uses bi-linear direct BEM formulation and an equivalent plate finite element model. MEGA uses a hybrid finite/infinite element fluid model with vertical modal expansion of the wave field and an equivalent plate finite element structural model. VODAC uses a traditional constant panel Green function formulation for the fluid and a 3D grillage model for the structure. LGN uses the Green-Naghdi equations for the fluid and a linear Kirchhoff plate model for structure. Despite some small discrepancies, the five computer codes give similar results.

The above basically summarizes the main method used to analysis the hydroelastic responses of VLFS in regular waves. The responses of VLFS in irregular wave can be estimated with a stochastic approach based on the spectrum of linear responses in regular waves as shown in Hirayama et al (1994).

1.4 Time Domain Analysis Methods

When the motions of VLFS and the surrounding fluid are time dependent or transient, they must be analyzed in the time domain. The corresponding methods are known as time domain methods and it is the time histories of the structural motions that are determined.

One of the promising applications of VLFS is a floating airport. General design principles of a floating airport can be referenced in Hirayama et al (1996), Suzuki (2001) and Fukuoka et al (2002). When designing such a floating airport, the naval architect needs to address not only the response of the structure to ocean waves, but also its transient dynamic response due to the impulsive and moving loads excited by airplane landing/take-off.

The next subsection summarizes the major methods developed to solve the transient responses of a floating airport subject to airplane landing/take-off impacts.

1.4.1 Various methods

Watanabe & Utsunomiya (1996) showed a numerical method for analyzing the transient response of a VLFS at airplane landing. Their method employed FEM for both structure and fluid. The structure was modeled as an elastic floating plate having circular shape and the impulsive load modeling the airplane landing was applied at the centre of the plate. In the FEM solution of fluid, a set of variables equaling the water pressure at specific points (nodes) were chosen. The fluid domain was divided into sub-regions called fluid elements and shape functions were employed to express the variation of water pressure within each element in terms of their values at the nodes. Compressibility of fluid and the effect of gravity on the free surface were both included. The advantage of this method is its simplicity in terms of the theoretical background and the computational schemes. The disadvantages are: 1) the radiation condition at infinity is not satisfied, thus the outgoing waves will be reflected on the boundary walls; 2) the meshing of the entire fluid domain is necessary and this significantly increases computational requirements.

Kim & Webster (1996) studied the drag on an airplane when taking off from a floating

runway. Since the floating runway is no longer flat, the airplane needs to climb out of the low points of the runway undulation and this will translate into an additional drag applied on the plane. In their paper, it was assumed that the floating runway behaves like a simple, infinitely long beam and the Bernoulli-Euler beam equation was adopted. The motion of fluid was governed by the Laplace equation. Fourier and inverse Fourier transformations were utilized to relate the responses in time and frequency domain. This simple configuration was analyzed in closed-form with the following observations obtained: 1) the deformation of the runway resulting from the take off is wave like and moves in the same direction as the airplane; 2) the maximum additional drag occurs when the plane catches up with the wave; 3) the additional drag imposed on the plane increases approximately proportional to the square root of the flexibility of the floating runway; 4) maximum additional drag ranges from 1% to 10% of the drag on a flat runway for different bending rigidities of the floating runway.

Yeung & Kim (1998) further studied the drag and deformation caused by a translating load on a flexible runway floating on the surface of deep water. The runway was modeled as an infinite isotropic elastic plate and thin plate theory was used to describe its motion. The boundary value problem of fluid domain was solved analytically using a free surface condition incorporating the flexural rigidity of the plate. The 3D load was modeled as axisymmetric, translating pressure distribution. Yeung and Kim found that the drag attains a discontinuous but finite value as the translation speed of the moving load approaches the critical speed, which is the minimum velocity of the generated structural waves. This is also known as the resonant phenomenon due to the energy accumulation near the load (Davys et al 1985). On the other hand, the deflection around the loading at the critical speed tends to grow infinitely. The additional drag is about 0.2% of the weight of airplane in the most severe case and this could constitute as much as 1% of the take off thrust. Based on the calculation results of this paper, it is suggested that the resonant phenomenon at critical speed does not appear to critically affect the take off operation except for a very flexible floating runway.

Ohmatsu (1998b) proposed a numerical scheme for the hydroelastic behavior of VLFS in the time domain. By using frequency dependent responses in regular waves, a time

domain analysis of VLFS in irregular waves was performed by appealing to the linear superposition principle. This calculation scheme was validated by the comparison with experimental results (Ohta et al 1998). Furthermore, the superposition principle was applied to consider the airplane landing/take-off impact onto VLFS. In order to do so, the frequency response function to a periodic load acting at a certain point of VLFS in still water was calculated first. This was then used to evaluate the impulse response function. With the obtained impulse response function, the response of VLFS to any arbitrary changing load can be computed by the convolution integral of the changing load. Validation of this calculation was confirmed by comparing with the experiment carried out by Endo & Yago (1999).

Endo (2000) suggested a time domain analysis method for the transient behaviour of VLFS subject to both airplane landing/take-off impacts and incident waves. The method uses: 1) a FEM model of the structure, 2) Wilson's method to perform the time integrations and 3) a memory effect function to include the hydrodynamic influences. The memory effect function was computed from the frequency dependent fluid damping coefficient evaluated using a frequency domain analysis. Endo observes that: 1) when the incident wave is included, the magnitude of the vertical displacement of VLFS is much greater than that induced only by airplane landing/take-off; 2) the time history of the drag is keenly related to the propagation of structural wave and the magnitude of the additional drag is less than 0.2% of the airplane weight; 3) the characteristics of the structural wave are governed by the dispersion relation and the velocity of this structural wave increases with increasing frequency in the range of normal incident wave frequency.

Kashiwagi (2004) presented a numerical simulation of the transient response of a floating airport during airplane landing/take-off. A rectangular floating airport of length 5km and width 1km was considered. The time histories of the imparted force, the position and velocity of the airplane during landing/take-off were modeled with the data of a Boeing 747-400 jumbo jet. The time domain mode expansion method (Kashiwagi 2000b) was adopted, so that the elastic deflection of the floating airport was expressed as the superposition of mathematical modal functions with unknown time dependent amplitudes. The hydrodynamic force was evaluated through the memory effect function and the added

mass at infinite frequency. Special care was paid to obtain good numerical accuracy. From the simulation, it is observed that the displacement of the floating airport is of the order of 1.0cm at maximum. The load from airplane landing/take-off develops smoothly, thus there is no high-frequency variation in the time history of the deflection of the floating airport. It is also found that in landing, the airplane moves faster than the generated waves in the early stage and the waves overtake as the speed of the airplane decreases to stop; in take off, it takes a relatively long time for the airplane to move in the early stage and thus the disturbance on the VLFS develops slowly.

1.4.2 Summary

The main methods proposed for analyzing the transient responses of a floating airport during airplane landing/take-off have been summarized. In all these studies it is assumed that a prescribed external load applied to the floating airport represents the dynamic loading caused by airplane landing/take-off. Thus the problem of an airplane landing/take-off from a floating airport reduces to a problem of a floating airport subject to a point load whose magnitude and position are time dependent. This approach simplifies the solution procedure. However, it is impossible to consider and investigate the interactions between the airplane and the floating airport.

Except for the FEM scheme proposed by Watanabe & Utsunomiya (1996), all the other time domain methods aforementioned involve frequency domain solutions in one way or another. For example in Ohmatsu (1998b), the frequency response function of a VLFS in regular waves needs to be addressed before the transient response in irregular wave can be considered; in Endo (2000), the memory effect function is evaluated from the frequency dependent damping coefficients. Although the solutions in the time and frequency domains can be conveniently linked through the Fourier and inverse Fourier transforms, it is time consuming and difficult to perform these transforms in some cases. One of the difficulties in undertaking an inverse Fourier transform from the frequency domain to time domain is the evaluation of the integrals over an infinite frequency range. Thus it is necessary to truncate the integral at a finite frequency and to assess the accuracy of the truncated

integral.

Having reviewed the different aspects of VLFS and airplane landing/take-off analysis, it is possible to identify tasks undertaken in the reported research that require careful consideration.

1.5 Research Aims and Dissertation Contents

1.5.1 Aims

A mixed mode function – boundary element method is proposed to analyze the dynamics of an airplane – floating structure – water interaction system subject to airplane landing impacts.

The airplane and the floating structure are treated as two solid substructures with the motions represented by their respective modal functions. The landing gear system of the airplane is linearised and modelled as a few linear spring – damper units that connect the airplane and the floating structure. In this way, the coupling effect between the airplane and the floating structure can be considered.

The water domain is a horizontally unbounded domain with infinite depth. The water is assumed to be inviscid, incompressible and subject to irrotational flow. Under linear potential theory, the motion of the fluid is governed by the Laplace equation. The surface disturbance satisfies a linearised free surface wave condition and an undisturbed condition at infinity. The Laplace equation in association with particular boundary conditions is solved with BEM in which the fundamental solution of the Laplace equation in an infinite fluid domain is used as the Green function. The motion of the floating structure and the surrounding fluid domain are coupled through the wetted interaction interface condition. Finally, the coupled equations of the airplane, the floating structure and the surrounding fluid are directly solved in time domain based on Newmark assumptions through a step by step procedure.

1.5.2 Contents

In Chapter 2, the theoretical background for solving the dynamics of airplane – floating structure – water interaction systems is introduced. This includes the mode theory and modal superposition method for structural dynamics; time integration schemes for solving time differential equations; linear potential flow theory for hydrodynamics and BEM for solving the boundary value problem of the fluid domain.

In Chapter 3, a linearization scheme is proposed to model the landing gears of an airplane with a few suspension units, each of which consists of a linear spring and damper.

In Chapter 4, the mixed mode function – boundary element method is formulated. The coupled governing equations are derived to describe the dynamics of the airplane – floating structure – water interaction system.

In Chapter 5, the time integration scheme for solving the coupled equations derived in Chapter 4 is discussed.

In Chapter 6, the developed Mixed Mode Function – Boundary Element Program – MMFBEP is introduced in association with the User Manual.

In Chapter 7, the dynamics of a mass – spring – damper system dropping onto a floating mass is examined with the computer program MMFBEP.

In Chapter 8, the dynamics of an elastic beam landing and travelling on another floating elastic beam is investigated. The examples in Chapter 7 and 8 provide the validations of the developed method and program.

In Chapter 9, the proposed mixed mode function – boundary element method is applied to approximately simulate the landing of a Boeing 747-400 jumbo plane onto a floating structure. With the developed program MMFBEP, the responses of both the airplane and the floating structure are solved during a landing process.

In Chapter 10, the work presented in this thesis is concluded. It also points the way forward for a continued investigation into the dynamics of airplane – floating structure – water interaction systems.

The structure of this thesis is illustrated in Figure 1.3.

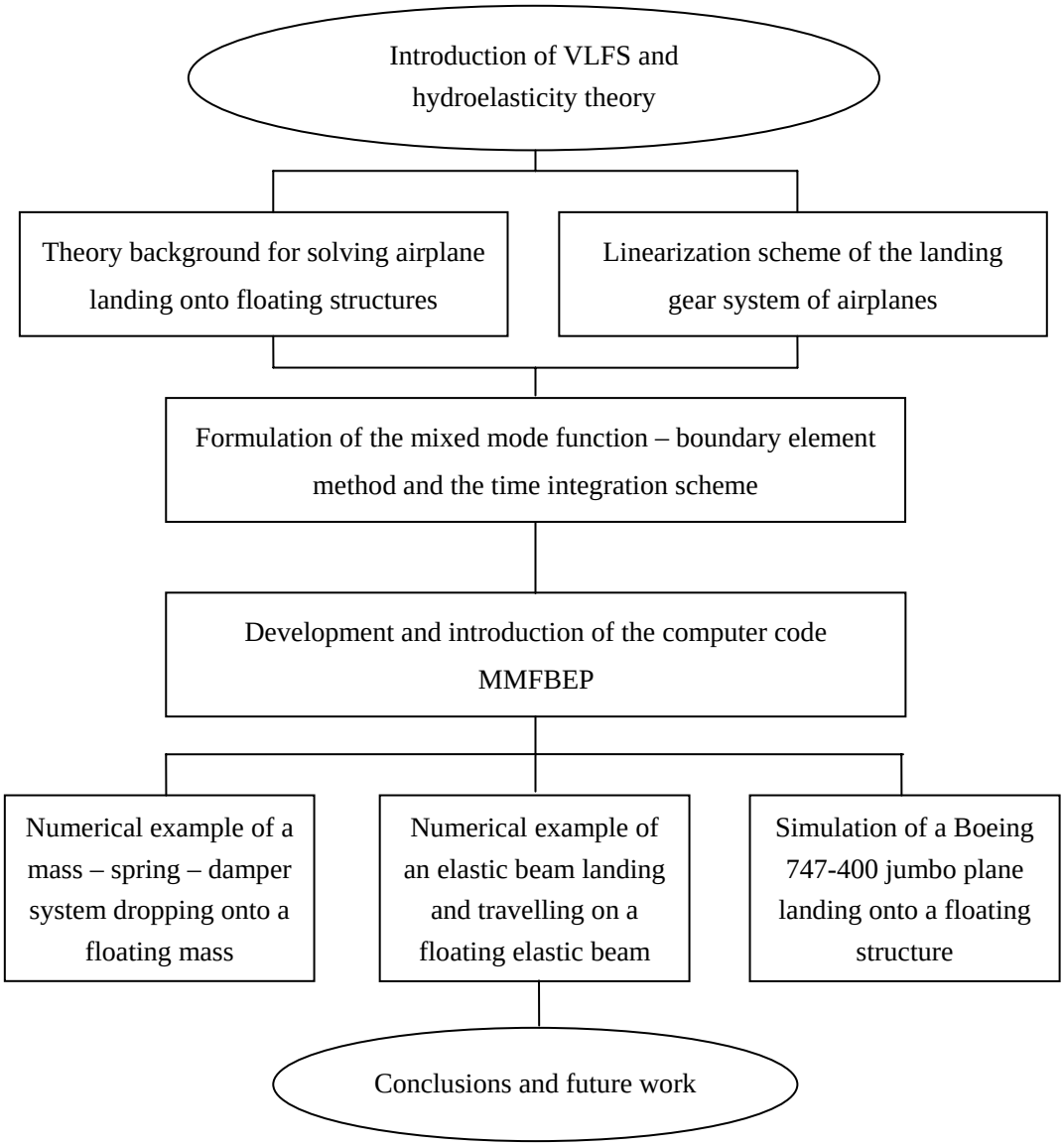

Figure 1.3 Structure of thesis

Chapter 2

Theory Background

In this chapter, the theoretical background for solving the dynamics of airplane – floating structure – water interaction systems is presented.

Firstly, the mode theory of structural dynamics and the modal superposition method are introduced. These are used to model the motion of the airplane and the floating structure. Secondly, the commonly-used time integration schemes are described with particular attention to the Newmark method that is applied to solve the coupled equations of motion of the airplane – floating structure – water interaction system.

Thirdly, the potential flow theory of hydrodynamics regarding fluid – structure interaction problem is illuminated. Lastly, the boundary element method is presented, with which the motion of the surrounding fluid is solved.

2.1 Mode Theory of Structural Dynamics

A knowledge of the natural characteristics of a structure, including natural frequencies and modes is the foundation to its dynamic analysis. This knowledge coupled with the modal superposition method can be used to investigate the motion of the structure in a mode space, which greatly reduces the degrees of freedom that need to be included. The modal superposition method is the most efficient approach to obtaining the dynamic responses of structures, thus it is adopted to analyse the motion of the airplane and the floating structure. In this section, we briefly summarize the required theory on natural vibrations and the modal superposition method of structural dynamics.

2.1.1 Equation of natural vibrations

Let us consider the dynamic problem of a structural system. Using a finite element idealisation, the dynamic equilibrium equation of the system is written in a matrix form as

(Paz & Leigh 2004)

$$\mathbf{M}\ddot{\mathbf{u}} + \mathbf{C}\dot{\mathbf{u}} + \mathbf{K}\mathbf{u} = \mathbf{F}, \tag{2.1}$$

where $\mathbf{M}$, $\mathbf{C}$ and $\mathbf{K}$ denote respectively the mass, damping and stiffness matrices of the structural system. In general, $\mathbf{M}$ and $\mathbf{K}$ are symmetric matrices whilst $\mathbf{C}$ is non-symmetric. $\mathbf{u}$ is the displacement vector and $\mathbf{F}$ is the external force vector. To determine the natural vibrations of this structural system, damping and external loads are ignored and hence Equation (2.1) reduces to

$$\mathbf{M}\ddot{\mathbf{u}} + \mathbf{K}\mathbf{u} = \mathbf{0}. \tag{2.2}$$

It is assumed that the solution of Equation (2.2) has the harmonic form

$$\mathbf{u} = \mathbf{q}\, e^{\mathrm{i}\omega t}, \tag{2.3}$$

which upon substitution into Equation (2.2) leads to

$$(\mathbf{K} - \omega^2\mathbf{M})\,\mathbf{q} = \mathbf{0}. \tag{2.4}$$

Equation (2.4) is a linear homogenous algebraic system of equations with unknown vector $\mathbf{q}$ and ω^2. This is known as the eigenvalue problem of the structural system, with ω and $\mathbf{q}$ representing the natural frequency and the corresponding mode vector respectively.

2.1.2 Solutions of natural vibration

A nontrivial solution of Equation (2.4) requires the determinant of the coefficient matrix to be zero, that is

$$\left|\mathbf{K} - \omega^2\mathbf{M}\right| = 0. \tag{2.5}$$

The expansion of the determinant in Equation (2.5) results in a polynomial equation of ω^2 designated the characteristic equation of the structural system. If the system has N degrees of freedom, N solutions of ω^2 can be obtained from Equation (2.5).

Substituting each of these values of ω^2 into Equation (2.4), we can obtain the corresponding natural mode vector, or eigenvector $\mathbf{q}$.

2.1.3 Orthogonality of natural modes

An important property of the natural modes is the orthogonal property which constitutes the basis of modal superposition method.

On writing Equation (2.4) for the r^{th} mode of the structural system (Hurty & Rubinstein 1964), it is found that

$$\mathbf{K}\mathbf{q}_r - \omega_r^2 \mathbf{M}\,\mathbf{q}_r = \mathbf{0}. \tag{2.6}$$

Pre-multiplying both sides of Equation (2.6) by the transpose of the s^{th} mode vector of the system, $\mathbf{q}_s$ say, leads to

$$\mathbf{q}_s^{\mathrm{T}}\mathbf{K}\mathbf{q}_r - \omega_r^2 \mathbf{q}_s^{\mathrm{T}}\mathbf{M}\,\mathbf{q}_r = 0. \tag{2.7}$$

Since the matrices $\mathbf{M}$ and $\mathbf{K}$ are symmetric and each term of Equation (2.7) is a real number, the transpose of Equation (2.7) does not change the equation, therefore we obtain

$$\mathbf{q}_r^{\mathrm{T}}\mathbf{K}\mathbf{q}_s - \omega_r^2 \mathbf{q}_r^{\mathrm{T}}\mathbf{M}\,\mathbf{q}_s = 0. \tag{2.8}$$

In performing the above operation the symmetric property of matrices $\mathbf{M}$ and $\mathbf{K}$ is utilized.

Next, Equation (2.6) is used to represent the s^{th} mode of the system in the form

$$\mathbf{K}\mathbf{q}_s - \omega_s^2 \mathbf{M}\,\mathbf{q}_s = \mathbf{0}. \tag{2.9}$$

Pre-multiplying both sides of Equation (2.9) by the transpose of the r^{th} mode vector gives

$$\mathbf{q}_r^{\mathrm{T}}\mathbf{K}\mathbf{q}_s - \omega_s^2 \mathbf{q}_r^{\mathrm{T}}\mathbf{M}\,\mathbf{q}_s = 0. \tag{2.10}$$

Subtracting Equation (2.10) from Equation (2.8) provides the relationship:

$$\left(\omega_r^2 - \omega_s^2\right)\mathbf{q}_r^{\mathrm{T}}\mathbf{M}\,\mathbf{q}_s = 0. \tag{2.11}$$

Clearly, provided $\omega_r \neq \omega_s$, then

$$\mathbf{q}_r^{\mathrm{T}}\mathbf{M}\,\mathbf{q}_s = 0. \tag{2.12}$$

The substitution of this equation into Equation (2.8) gives

$$\mathbf{q}_r^{\mathrm{T}}\mathbf{K}\,\mathbf{q}_s = 0. \tag{2.13}$$

Equations (2.12) and (2.13) express the orthogonal relationship between the natural modes of the structural system. On setting $s = r$, the triple product in Equation (2.11) is equal to a non-zero constant, say M_r, i.e.

$$\mathbf{q}_r^{\mathrm{T}}\mathbf{M}\,\mathbf{q}_r = M_r. \tag{2.14}$$

Substituting Equation (2.14) into Equation (2.8) or (2.10) implies that

$$\mathbf{q}_r^{\mathrm{T}}\mathbf{K}\,\mathbf{q}_r = \omega_r^2 M_r. \tag{2.15}$$

It is clear from Equation (2.4) that the mode vector $\mathbf{q}$ can only be determined with an arbitrary multiplicative constant. This constant is often selected so that one of the $\mathbf{q}$ elements is unity. Hence, the absolute magnitudes of the mode vector are not determined. It is convenient to normalize the mode vectors for the constant M_r equalling 1. As a result of this, Equations (2.14) and (2.15) are expressible in the form

$$\mathbf{q}_r^{\mathrm{T}}\mathbf{M}\,\mathbf{q}_r = 1 \tag{2.16}$$

and

$$\mathbf{q}_r^{\mathrm{T}}\mathbf{K}\,\mathbf{q}_r = \omega_r^2. \tag{2.17}$$

The mode vectors satisfying Equations (2.16) and (2.17) are called the normalized mode vectors of the system.

It is worth noting that when repeated roots are found in the characteristic equation of

Equation (2.5), the corresponding natural mode vectors are not unique, and consequently a linear combination of such mode vectors will also satisfy Equation (2.6). For example, the natural frequency of all the rigid body modes is zero thus any linear combination of the rigid body modes is a natural mode of the system. In this case, the Gram – Schmidt Process (Trefethen & Bau 1997) may be used to obtain a set of orthogonal rigid body modes that can be further modified to satisfy Equations (2.16) and (2.17).

2.1.4 Different approaches to obtain natural modes

A brief summary of the approaches commonly used to obtain the natural modes of a structural system now follows.

Modal testing

Modal testing is widely practised in all those engineering disciplines where vibration and other dynamic phenomena affect the behaviour and performance of structures and machines (Ewins 2000). Through modal testing, the natural frequencies, natural modes and modal damping coefficients of a structure are measured. This can provide insight and a basic understanding of how a structure will respond to dynamic forces in a real operating environment.

Modal testing based on Frequency Response Functions (FRFs) obtained from measured input forces and output responses of a structure is a well established application, often referred to as classical modal analysis. The excitation applied to the structure under test can be transient, random or sinusoidal. Typically, transient excitation is applied using an impact hammer, whereas random and sinusoidal excitation is applied using one or more shakers. The most common and inexpensive way of measuring the structural responses is by using accelerometers. They are available in a number of different types to fulfill requirements concerning mass, sensitivity, frequency range, temperature range, mounting method, etc.

On the other hand, Operational Modal Analysis (OMA) is based on only measuring the responses and using the ambient and operating forces as unmeasured input. OMA is,

therefore, also known as output-only or ambient modal analysis. Major advantages of OMA over the classical modal analysis are as follows: 1) As the measurements are obtained under real operating conditions, true boundary conditions, actual force and vibration levels are guaranteed ensuring an optimal modal model. 2) The structure does not have to be moved into a laboratory to test under controlled conditions. Thus, the test does not affect or interrupt the daily use of the structure and can even be applied in parallel with other applications. 3) No shakers or hammers are used, making the physical setup very straightforward and fast.

Modal testing is often used to check the accuracy of theoretical and numerical predictions of the modal characteristics of engineering structures.

Theoretical analysis

Generally speaking, it is not possible to obtain the natural modes in analytical form for most engineering structures. However, analytical natural modes exist for some relatively simple structures such as uniform beams subjected to different boundary conditions. In this thesis, the airplane and the floating structure are both approximately modelled by free – free beams in the first approximation. Thus the derivation of the analytical natural modes of a free – free beam is illustrated next.

The free vibration of a uniform beam, as shown in Figure 2.1 is governed by the following equation of motion (Paz & Leigh 2004)

$$EI\frac{\partial^4 u}{\partial x^4}+\overline{m}\frac{\partial^2 u}{\partial t^2}=0\,, \tag{2.18}$$

where EI, $\overline{m}$ and $u(x,t)$ represent the bending stiffness, mass per unit length and vertical displacement of the beam, respectively.

The solution of Equation (2.18) can be found by the method of separation of variables. It is assumed that the solution may be expressed as the product of a spatial function $\Phi(x)$ and a function $f(t)$ of time, that is

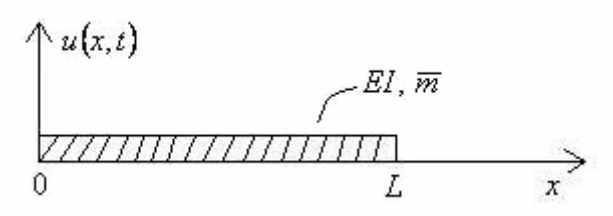

Figure 2.1 A uniform beam with free – free ends

$$u(x,t) = \Phi(x) f(t). \tag{2.19}$$

The substitution of Equation (2.19) into Equation (2.18) leads to

$$\frac{EI}{\overline{m}} \frac{\Phi^{IV}(x)}{\Phi(x)} = -\frac{\ddot{f}(t)}{f(t)}, \tag{2.20}$$

where the Roman superscript indicates fourth derivative with respect to the coordinate x and the over dot indicates derivatives with respect to time. Since the left hand side of Equation (2.20) is a function of position coordinate only, whilst the right hand side is a function of time only, each side of the equation must be equal to the same constant value. We designate this constant by ω^2. Hence Equation (2.20) gives the following two equations

$$\Phi^{IV}(x) - \beta^4 \Phi(x) = 0 \tag{2.21}$$

and

$$\ddot{f}(t) + \omega^2 f(t) = 0, \tag{2.22}$$

subject to

$$\beta^4 = \frac{\overline{m}\omega^2}{EI} \tag{2.23}$$

and one may also write

$$\omega = (\beta L)^2 \sqrt{\frac{EI}{\overline{m} L^4}}, \tag{2.24}$$

upon introducing L, the length of beam.

By using the standard solution schemes for differential equations (Stroud & Booth 2003),

Equations (2.21) and (2.22) can be solved. Their general solutions are expressed as

$$\Phi(x) = b_1 \sin \beta x + b_2 \cos \beta x + b_3 \sinh \beta x + b_4 \cosh \beta x \tag{2.25}$$

and

$$f(t) = b_5 \cos \omega t + b_6 \sin \omega t \,. \tag{2.26}$$

The arbitrary constants b_1, b_2, b_3 and b_4 can be evaluated by considering the boundary conditions at the two ends of the beam and the constants b_5 and b_6 can be determined from initial conditions.

Performing the above operations, the spatial function $\Phi(x)$ for the bending of a uniform beam with free-free ends is obtained as (Paz & Leigh 2004)

$$\Phi_m(x) = \cosh \beta_m x + \cos \beta_m x - \sigma_m (\sinh \beta_m x + \sin \beta_m x), \tag{2.27}$$

where

$$\sigma_m = \frac{\sin \beta_m L + \sinh \beta_m L}{\cosh \beta_m L - \cos \beta_m L}, \tag{2.28}$$

and the subscript m represents the m^{th} mode of the beam. β_m denotes the positive real roots of the equation

$$\cos \beta_m L \cdot \cosh \beta_m L - 1 = 0 \,. \tag{2.29}$$

For uniform beams with different boundary conditions, such as both ends fixed or simply supported, the spatial function $\Phi(x)$ can be derived in a similar way.

Numerical solution from FEA software

The Finite Element Method (FEM) is a numerical procedure for obtaining approximate solutions to many of the problems encountered in engineering analysis. It is achieved by discretizing a continuum into an assemblage of elements of finite dimension. The concepts of FEM have evolved over a long period. The term “finite element” was first coined by

Clough (1960) and since then the FEM has rapidly become a very popular technique for the computer solution of complex problems in engineering.

Many text books have been published regarding FEM, for example Zienkiewicz & Cheung (1967) and Bathe (1996). Together with the theoretical development of FEM, its application has been realized with various Finite Element Analysis (FEA) software packages including ANSYS, ABAQUS, ADINA, NASTRAN, SESAM, COSMOSWORKS, etc.

Modal analysis is an important function of FEA software, through which natural frequencies and modes of a structure are readily obtained. For the modelling of the airplane and floating structure in this thesis, ANSYS (2004) is adopted to undertake the modal analysis.

Approximate numerical methods

The exact analysis for the vibration of systems with many degrees of freedom is generally difficult, and its associated calculations are laborious. In many cases, only a few of the lower modes, rather than all of the natural modes, of a structural system are sufficient to estimate its dynamic responses (Thomson 1988). There are some approximate methods for determining the natural frequencies and mode shapes of the first few vibration modes, for example, the Rayleigh-Ritz method.

In the Rayleigh-Ritz method, the deflection of the structural system is expressed by a series of shape functions multiplied by constant coefficients. The shape functions are known functions, which should satisfy the geometric boundary conditions of the problem and are differentiable at least to the order of the derivatives appearing in the energy equations. The coefficients are adjusted by minimizing the frequency ω with respect to each of the coefficients, which results in a system of algebraic equations in ω^2 and the constant coefficients. The determinant of this system of equations should be zero and it forms another system of algebraic equations in ω^2 only, whose solution results in the natural frequencies. With the obtained natural frequencies, the constant coefficients and the deflection of the structural system can be evaluated, respectively.

Using approximate numerical methods to obtain the natural frequencies and modes of a structural system often requires judgement and experience, in particular, the choice of shape functions. Therefore, this kind of method is not entirely amenable to treatment by routine computing procedures.

2.1.5 Modal superposition method

Modal superposition method is based on the idea that the motion of a structural system can be described in terms of its natural modes of vibration and that the total response may be obtained as the superposition of the solutions of the independent modal equations. By using natural modes, the coupled differential equations of a system are transformed to a set of uncoupled equations known as mode equations, each of which contains only one variable.

Reverting to the forced motion described in Equation (2.1) and expressing the displacement of the structural system in terms of its natural modes $\mathbf{q}_i \left(i = 1, 2, ..., M\right)$ and generalized coordinates $Q_i \left(i = 1, 2, ..., M\right)$, then

$$\mathbf{u} = \mathbf{\Phi Q}, \tag{2.30}$$

with $\mathbf{\Phi}$ denoting the modal matrix and $\mathbf{Q}$ the generalized coordinate vector defined respectively by

$$\mathbf{\Phi} = \left[\mathbf{q}_1,\ \mathbf{q}_2,\ \cdots,\ \mathbf{q}_M\right] \tag{2.31}$$

and

$$\mathbf{Q} = \left[Q_1,\ Q_2,\ \cdots,\ Q_M\ \right]^{\mathrm{T}}. \tag{2.32}$$

Hence M represents the number of natural modes and in theory it should equal the number of degrees of freedom N of the structural system.

Introducing Equation (2.30) into Equation (2.1) yields

$$\mathbf{M\Phi\ddot{Q}} + \mathbf{C\Phi\dot{Q}} + \mathbf{K\Phi Q} = \mathbf{F}. \tag{2.33}$$

On pre-multiplying Equation (2.33) by the transpose of the modal matrix $\mathbf{\Phi}$ and utilizing the orthogonal property of the natural modes, as given in Equations (2.14) and (2.15), it is found

$$\overline{\mathbf{M}}\ddot{\mathbf{Q}} + \overline{\mathbf{C}}\dot{\mathbf{Q}} + \overline{\mathbf{K}}\mathbf{Q} = \mathbf{\Phi}^{\mathrm{T}}\mathbf{F}, \tag{2.34}$$

where

$$\mathbf{\Phi}^{\mathrm{T}}\mathbf{M}\mathbf{\Phi} = \overline{\mathbf{M}} = \begin{bmatrix} 1 & \cdots & \cdots & 0 \\ 0 & 1 & \cdots & 0 \\ \vdots & \vdots & \vdots & \vdots \\ 0 & \cdots & \cdots & 1 \end{bmatrix} \tag{2.35}$$

is a unit matrix,

$$\mathbf{\Phi}^{\mathrm{T}}\mathbf{C}\mathbf{\Phi} = \overline{\mathbf{C}} = \begin{bmatrix} \overline{\alpha} + \overline{\beta}\omega_1^2 & \cdots & \cdots & 0 \\ 0 & \overline{\alpha} + \overline{\beta}\omega_2^2 & \cdots & 0 \\ \vdots & \vdots & \vdots & \vdots \\ 0 & \cdots & \cdots & \overline{\alpha} + \overline{\beta}\omega_M^2 \end{bmatrix} \tag{2.36}$$

and

$$\mathbf{\Phi}^{\mathrm{T}}\mathbf{K}\mathbf{\Phi} = \overline{\mathbf{K}} = \begin{bmatrix} \omega_1^2 & \cdots & \cdots & 0 \\ 0 & \omega_2^2 & \cdots & \cdots \\ \vdots & \vdots & \vdots & \vdots \\ 0 & \cdots & \cdots & \omega_M^2 \end{bmatrix} \tag{2.37}$$

are diagonal matrices.

In deriving Equation (2.34), it is assumed that the natural modes are normalized with respect to the mass matrix $\mathbf{M}$ and that Rayleigh damping is applicable (Bathe 1996) and so

$$\mathbf{C} = \overline{\alpha}\mathbf{M} + \overline{\beta}\mathbf{K}. \tag{2.38}$$

The two constants $\overline{\alpha}$ and $\overline{\beta}$ are to be determined.

Assuming that the structural system exhibits proportional damping, we have

$$\mathbf{q}_i^{\mathrm{T}}\mathbf{C}\mathbf{q}_j = 2\omega_i\xi_i\delta_{ij}, \tag{2.39}$$

where ξ_i is a modal damping parameter and δ_{ij} is the Kronecker delta ($\delta_{ij} = 1$ for

$i = j$, $\delta_{ij} = 0$ for $i \neq j$). Based on the two modal damping parameters ξ_1 and ξ_2 corresponding respectively to two unequal frequencies ω_1 and ω_2 in the interested range of frequency, constants $\overline{\alpha}$ and $\overline{\beta}$ can be determined from Equations (2.36) and (2.39). That is to solve the following equations

$$2\omega_1\xi_1 = \overline{\alpha} + \overline{\beta}\omega_1^2 \tag{2.40}$$

and

$$2\omega_2\xi_2 = \overline{\alpha} + \overline{\beta}\omega_2^2 . \tag{2.41}$$

As already stated the damping characteristics of the structure have been assumed to display proportional damping. This assumption holds true in many analyses. However, non proportional damping is necessary in some cases, which means the mode Equation (2.34) can not be decoupled and therefore it needs to be solved simultaneously.

In practice, it's not always necessary to include all the natural modes of a structural system in Equation (2.34). According to the frequency range of the external force $\mathbf{F}$, a truncation frequency ω_t can be set up for the structural system assuming that the contribution from those natural modes with a frequency higher than ω_t to the total response are negligibly small. Therefore, only those natural modes with a frequency lower than ω_t need to be considered. This mode truncation technique reduces the number of equations in Equation (2.34).

2.2 Time Integration Schemes

The dynamic response of a structural system is governed by Equation (2.1). This equation is derived from the principle of virtual work (Bathe 1996). The effect of acceleration – dependent inertia forces and velocity – dependent damping forces are included in the derivation. Mathematically, Equation (2.1) represents a system of linear differential equations of second order and the solution of this equation can be obtained by standard solution procedures for differential equations (Collatz 1966 and Crandall 1956).

However, the procedures proposed for the solution of general systems of differential equations are very expensive when the order of the matrices is very high.

In practice, a few effective methods known as time integration schemes are used to obtain numerical solutions of Equation (2.1). Four commonly used time integration schemes are considered next.

2.2.1 The central difference method

When Equation (2.1) is regarded as a system of ordinary differential equations, it allows any convenient finite difference expressions to approximate the acceleration and velocity in terms of the displacements, provided that the solution scheme is effective. One procedure that can be very effective in the solution of some problems is the central difference method (Collatz 1966). In this method it is assumed that

$$ {}^{t}\ddot{\mathbf{u}} = \frac{1}{\Delta t^2}\left({}^{t-\Delta t}\mathbf{u} - 2\,{}^{t}\mathbf{u} + {}^{t+\Delta t}\mathbf{u}\right) \tag{2.42} $$

and

$$ {}^{t}\dot{\mathbf{u}} = \frac{1}{2\Delta t}\left(-{}^{t-\Delta t}\mathbf{u} + {}^{t+\Delta t}\mathbf{u}\right). \tag{2.43} $$

The error in the above two expansions is of order $(\Delta t)^2$. The substitution of Equations (2.42) and (2.43) into Equation (2.1) produces

$$ \left(\frac{1}{\Delta t^2}\mathbf{M} + \frac{1}{2\Delta t}\mathbf{C}\right){}^{t+\Delta t}\mathbf{u} = {}^{t}\mathbf{F} - \left(\mathbf{K} - \frac{2}{\Delta t^2}\mathbf{M}\right){}^{t}\mathbf{u} - \left(\frac{1}{\Delta t^2}\mathbf{M} - \frac{1}{2\Delta t}\mathbf{C}\right){}^{t-\Delta t}\mathbf{u}\,, \tag{2.44} $$

from which ${}^{t+\Delta t}\mathbf{u}$ can be calculated.

It should be noted that the solution for ${}^{t+\Delta t}\mathbf{u}$ is based on using the dynamic equation at time t. For this reason the integration procedure is called an explicit integration method. On the other hand, the Houbolt, Wilson and Newmark methods discussed in the following subsections all use the equilibrium equation at time $t+\Delta t$ and are thus called implicit integration methods.

The calculation of ${}^{t+\Delta t}\mathbf{u}$ involves ${}^{t}\mathbf{u}$ and ${}^{t-\Delta t}\mathbf{u}$ in the central difference method. Therefore, in order to calculate ${}^{t+\Delta t}\mathbf{u}$, a special starting procedure must be used to evaluate ${}^{t-\Delta t}\mathbf{u}$. With Equations (2.42) and (2.43), ${}^{t-\Delta t}\mathbf{u}$ can be obtained as follows

$$ {}^{t-\Delta t}\mathbf{u} = {}^{t}\mathbf{u} - \Delta t\, {}^{t}\dot{\mathbf{u}} + \frac{\Delta t^2}{2}\, {}^{t}\ddot{\mathbf{u}} . \tag{2.45} $$

Assume the system has no physical damping ($\mathbf{C} = \mathbf{0}$) and the mass matrix $\mathbf{M}$ is diagonal, then Equation (2.44) can be solved with matrix multiplications and without factorizing a matrix. If neither the stiffness nor the mass matrix has to be triangularised, it is also not necessary to assemble the global stiffness and mass matrices in FEM analysis. This means that the right hand side of Equation (2.44) can be calculated on the element level, by summing the contributions from each element, which will ease the solution process significantly.

Considering the shortcomings of central difference method, it is recognized that the effectiveness of this method depends heavily on the choice of time step Δt. It must be smaller than a critical value Δt_{cr}, which can be determined from the smallest natural period of the structural system, i.e.

$$ \Delta t \le \Delta t_{cr} = T_n / \pi . \tag{2.46} $$

As the central difference method requires the use of a time step Δt smaller than a critical value Δt_{cr}, it is a conditionally stable time integration scheme. If a time step used is larger than Δt_{cr}, the integration will be unstable. This means that any errors resulting from the numerical integration or round-off in the computer might grow uncontrollably and make the results worthless.

2.2.2 The Houbolt method

The Houbolt time integration scheme is somewhat related to the central difference method in that standard finite difference expressions are used to approximate the acceleration and velocity components in terms of the displacement component. The following finite difference expansions are employed in the Houbolt method (Houbolt 1950)

$$ {}^{t+\Delta t}\ddot{\mathbf{u}} = \frac{1}{\Delta t^2}\left(2\,{}^{t+\Delta t}\mathbf{u} - 5\,{}^{t}\mathbf{u} + 4\,{}^{t-\Delta t}\mathbf{u} - {}^{t-2\Delta t}\mathbf{u}\right), \tag{2.47} $$

$$ {}^{t+\Delta t}\dot{\mathbf{u}} = \frac{1}{6\Delta t}\left(11\,{}^{t+\Delta t}\mathbf{u} - 18\,{}^{t}\mathbf{u} + 9\,{}^{t-\Delta t}\mathbf{u} - 2\,{}^{t-2\Delta t}\mathbf{u}\right), \tag{2.48} $$

the error of each of which is of order $(\Delta t)^2$.

Substituting Equations (2.47) and (2.48) into Equation (2.1) and arranging all known vectors on the right-hand side of the resultant equation gives

$$ \begin{aligned} \left(\frac{2}{\Delta t^2}\mathbf{M} + \frac{11}{6\Delta t}\mathbf{C} + \mathbf{K}\right){}^{t+\Delta t}\mathbf{u} = {}^{t+\Delta t}\mathbf{F} + \left(\frac{5}{\Delta t^2}\mathbf{M} + \frac{3}{\Delta t}\mathbf{C}\right){}^{t}\mathbf{u} - \left(\frac{4}{\Delta t^2}\mathbf{M} + \frac{3}{2\Delta t}\mathbf{C}\right){}^{t-\Delta t}\mathbf{u} \\ + \left(\frac{1}{\Delta t^2}\mathbf{M} + \frac{1}{3\Delta t}\mathbf{C}\right){}^{t-2\Delta t}\mathbf{u} \end{aligned} . \tag{2.49} $$

The solution of ${}^{t+\Delta t}\mathbf{u}$ in Equation (2.49) requires knowledge of ${}^{t}\mathbf{u}$, ${}^{t-\Delta t}\mathbf{u}$ and ${}^{t-2\Delta t}\mathbf{u}$. With the initial ${}^{0}\mathbf{u}$, ${}^{0}\dot{\mathbf{u}}$ and ${}^{0}\ddot{\mathbf{u}}$ known, special starting procedures should be employed to calculate ${}^{-\Delta t}\mathbf{u}$ and ${}^{-2\Delta t}\mathbf{u}$. One way of proceeding is to integrate Equation (2.1) and use a different time integration scheme for the solution of ${}^{-\Delta t}\mathbf{u}$ and ${}^{-2\Delta t}\mathbf{u}$, possibly the central difference scheme.

A basic difference between the Houbolt scheme and the central difference method is the appearance of the stiffness matrix $\mathbf{K}$ as a factor to the required displacements vector ${}^{t+\Delta t}\mathbf{u}$. As the equilibrium is considered at time $t+\Delta t$, the Houbolt method is an implicit integration scheme. The integration time step Δt has no critical limit, and therefore Δt can in general be selected much larger than that used in the central difference method.

A noteworthy point is that the step – by – step solution scheme based on the Houbolt

method reduces directly to a static analysis, if mass and damping effects are neglected.

2.2.3 The Wilson θ method

The Wilson θ method is essentially an extension of the linear acceleration method, in which a linear variation of acceleration from time t to $t+\Delta t$ is assumed. In the Wilson θ method, the acceleration is assumed to be linear from time t to $t+\theta\Delta t$, with $\theta \geq 1.0$ (Wilson et al 1973). When $\theta = 1.0$, the method reduces to the linear acceleration scheme. For unconditional stability it is necessary to use $\theta \geq 1.37$ and $\theta = 1.40$ is usually used.

Let τ $(0 \leq \tau \leq \theta\Delta t)$ denote the increase of time. For the time interval from t to $t+\theta\Delta t$, it is assumed that

$$ {}^{t+\tau}\ddot{\mathbf{u}} = {}^{t}\ddot{\mathbf{u}} + \frac{\tau}{\theta\Delta t}\left({}^{t+\theta\Delta t}\ddot{\mathbf{u}} - {}^{t}\ddot{\mathbf{u}}\right). \tag{2.50} $$

Integrating Equation (2.50) once, we obtain

$$ {}^{t+\tau}\dot{\mathbf{u}} = {}^{t}\dot{\mathbf{u}} + \tau\,{}^{t}\ddot{\mathbf{u}} + \frac{\tau^2}{2\theta\Delta t}\left({}^{t+\theta\Delta t}\ddot{\mathbf{u}} - {}^{t}\ddot{\mathbf{u}}\right). \tag{2.51} $$

Integrating Equation (2.50) twice yields

$$ {}^{t+\tau}\mathbf{u} = {}^{t}\mathbf{u} + \tau\,{}^{t}\dot{\mathbf{u}} + \frac{\tau^2}{2}{}^{t}\ddot{\mathbf{u}} + \frac{\tau^3}{6\theta\Delta t}\left({}^{t+\theta\Delta t}\ddot{\mathbf{u}} - {}^{t}\ddot{\mathbf{u}}\right). \tag{2.52} $$

On setting $\tau = \theta\Delta t$, Equations (2.51) and (2.52) are re-written as

$$ {}^{t+\theta\Delta t}\dot{\mathbf{u}} = {}^{t}\dot{\mathbf{u}} + \frac{\theta\Delta t}{2}\left({}^{t+\theta\Delta t}\ddot{\mathbf{u}} + {}^{t}\ddot{\mathbf{u}}\right) \tag{2.53} $$

and

$$ {}^{t+\theta\Delta t}\mathbf{u} = {}^{t}\mathbf{u} + \theta\Delta t\,{}^{t}\dot{\mathbf{u}} + \frac{\theta^2\Delta t^2}{6}\left({}^{t+\theta\Delta t}\ddot{\mathbf{u}} + 2\,{}^{t}\ddot{\mathbf{u}}\right). \tag{2.54} $$

Next ${}^{t+\theta\Delta t}\ddot{\mathbf{u}}$ and ${}^{t+\theta\Delta t}\dot{\mathbf{u}}$ can be expressed in terms of ${}^{t+\theta\Delta t}\mathbf{u}$ and that is

$$ {}^{t+\theta\Delta t}\ddot{\mathbf{u}} = \frac{6}{\theta^2\Delta t^2}\left({}^{t+\theta\Delta t}\mathbf{u} - {}^{t}\mathbf{u}\right) - \frac{6}{\theta\Delta t}\,{}^{t}\dot{\mathbf{u}} - 2\,{}^{t}\ddot{\mathbf{u}}\,. \tag{2.55} $$

and

$$ {}^{t+\theta\Delta t}\dot{\mathbf{u}} = \frac{3}{\theta\Delta t}\left({}^{t+\theta\Delta t}\mathbf{u} - {}^{t}\mathbf{u}\right) - 2\,{}^{t}\dot{\mathbf{u}} - \frac{\theta\Delta t}{2}\,{}^{t}\ddot{\mathbf{u}} . \tag{2.56} $$

As the accelerations are assumed to vary linearly, a linear projected load vector is used to give the load vector at time $t+\theta\Delta t$ using

$$ {}^{t+\theta\Delta t}\mathbf{F} = {}^{t}\mathbf{F} + \theta\left({}^{t+\Delta t}\mathbf{F} - {}^{t}\mathbf{F}\right). \tag{2.57} $$

On considering the equilibrium equation of Equation (2.1) at time $t+\theta\Delta t$ and substituting Equations (2.55) - (2.57) into Equation (2.1), it is found that

$$ \begin{aligned} \left(\frac{6}{\theta^2\Delta t^2}\mathbf{M} + \frac{3}{\theta\Delta t}\mathbf{C} + \mathbf{K}\right){}^{t+\theta\Delta t}\mathbf{u} = {}^{t}\mathbf{F} + \theta\left({}^{t+\Delta t}\mathbf{F} - {}^{t}\mathbf{F}\right) + \mathbf{C}\left(\frac{3}{\theta\Delta t}\,{}^{t}\mathbf{u} + 2\,{}^{t}\dot{\mathbf{u}} + \frac{\theta\Delta t}{2}\,{}^{t}\ddot{\mathbf{u}}\right) \\ + \mathbf{M}\left(\frac{6}{\theta^2\Delta t^2}\,{}^{t}\mathbf{u} + \frac{6}{\theta\Delta t}\,{}^{t}\dot{\mathbf{u}} + 2\,{}^{t}\ddot{\mathbf{u}}\right) \end{aligned} , \tag{2.58} $$

from which ${}^{t+\theta\Delta t}\mathbf{u}$ can be solved. With Equations (2.55) and (2.56), ${}^{t+\theta\Delta t}\dot{\mathbf{u}}$ and ${}^{t+\theta\Delta t}\ddot{\mathbf{u}}$ are calculated. ${}^{t+\Delta t}\ddot{\mathbf{u}}$, ${}^{t+\Delta t}\dot{\mathbf{u}}$ and ${}^{t+\Delta t}\mathbf{u}$ can be evaluated from Equations (2.50) - (2.52) at $\tau = \Delta t$.

The Wilson θ method is also an implicit integration method. No special starting procedures are needed as the velocity and acceleration at time $t+\theta\Delta t$ are respectively expressed in terms of the displacement at time $t+\theta\Delta t$ and other known quantities at the previous time step. The Wilson θ method has second – order accuracy and it is an unconditionally stable time integration scheme.

2.2.4 The Newmark method

The Newmark integration scheme (Newmark 1959) can also be understood as an extension of the linear acceleration method, under which the following assumptions are used

$$ {}^{t+\Delta t}\dot{\mathbf{u}} = {}^{t}\dot{\mathbf{u}} + \left[(1-\delta)\,{}^{t}\ddot{\mathbf{u}} + \delta\,{}^{t+\Delta t}\ddot{\mathbf{u}}\right]\Delta t \tag{2.59} $$

and

$$ {}^{t+\Delta t}\mathbf{u} = {}^{t}\mathbf{u} + {}^{t}\dot{\mathbf{u}}\Delta t + \left[(0.5-\alpha)\,{}^{t}\ddot{\mathbf{u}} + \alpha\,{}^{t+\Delta t}\ddot{\mathbf{u}}\right]\Delta t^{2}. \tag{2.60} $$

The parameters α and δ can be determined according to the requirement of accuracy and stability. The Newmark scheme is unconditionally stable provided that $\delta \geq 0.5$ and $\alpha \geq 0.25(\delta + 0.5)^2$ and with $\delta = 0.5$ it has second order accuracy. The Newmark method is an implicit time integration scheme and no special starting procedures are needed for it. Newmark originally proposed an unconditionally stable scheme: the constant – average – acceleration method (also known as trapezoidal rule), in which $\alpha = 1/4$ and $\delta = 1/2$ are used. When $\alpha = 1/6$ and $\delta = 1/2$, relations in Equations (2.59) and (2.60) correspond to the linear acceleration method.

From Equations (2.59) and (2.60), ${}^{t+\Delta t}\ddot{\mathbf{u}}$ and ${}^{t+\Delta t}\dot{\mathbf{u}}$ can be expressed in terms of ${}^{t+\Delta t}\mathbf{u}$ as follows

$$ {}^{t+\Delta t}\ddot{\mathbf{u}} = \frac{1}{\alpha\Delta t^{2}}\,{}^{t+\Delta t}\mathbf{u} - \frac{1}{\alpha\Delta t^{2}}\,{}^{t}\mathbf{u} - \frac{1}{\alpha\Delta t}\,{}^{t}\dot{\mathbf{u}} - \frac{0.5-\alpha}{\alpha}\,{}^{t}\ddot{\mathbf{u}} \tag{2.61} $$

and

$$ {}^{t+\Delta t}\dot{\mathbf{u}} = \frac{\delta}{\alpha\Delta t}\,{}^{t+\Delta t}\mathbf{u} - \frac{\delta}{\alpha\Delta t}\,{}^{t}\mathbf{u} - \left(1-\frac{\delta}{\alpha}\right){}^{t}\dot{\mathbf{u}} - \left(1-\frac{\delta}{2\alpha}\right)\Delta t\,{}^{t}\ddot{\mathbf{u}}. \tag{2.62} $$

The substitution of Equations (2.61) and (2.62) into Equation (2.1) at time $t + \Delta t$ yields

$$ \begin{aligned} \left(\frac{1}{\alpha\Delta t^{2}}\mathbf{M} + \frac{\delta}{\alpha\Delta t}\mathbf{C} + \mathbf{K}\right){}^{t+\Delta t}\mathbf{u} = {}^{t+\Delta t}\mathbf{F} &+ \mathbf{M}\left(\frac{1}{\alpha\Delta t^{2}}\,{}^{t}\mathbf{u} + \frac{1}{\alpha\Delta t}\,{}^{t}\dot{\mathbf{u}} + \left(\frac{1}{2\alpha}-1\right){}^{t}\ddot{\mathbf{u}}\right) \\ &+ \mathbf{C}\left(\frac{\delta}{\alpha\Delta t}\,{}^{t}\mathbf{u} + \left(\frac{\delta}{\alpha}-1\right)\dot{\mathbf{u}} + \frac{\Delta t}{2}\left(\frac{\delta}{\alpha}-2\right){}^{t}\ddot{\mathbf{u}}\right) \end{aligned}. \tag{2.63} $$

From Equation (2.63) the displacement ${}^{t+\Delta t}\mathbf{u}$ is solved and with Equations (2.61) and (2.62) the acceleration ${}^{t+\Delta t}\ddot{\mathbf{u}}$ and velocity ${}^{t+\Delta t}\dot{\mathbf{u}}$ can be calculated, respectively.

The trapezoidal rule is adopted as the time integration scheme in this thesis, due to its accuracy and good performance in solving relevant engineering problems.

2.3 Basic Theory of Hydrodynamics

Hydrodynamics is the science of investigating the dynamics of liquids. In this section, the basic theory of hydrodynamics involved in solving the dynamic equation of airplane – floating structure – water interaction systems subject to airplane landing impacts is introduced.

2.3.1 Governing equation

In hydrodynamic theory, the flow is assumed to be continuous throughout the region under consideration. The continuity of flow states that the mass of fluid is conserved, hence no addition or depletion of fluid mass is possible. Assume that a closed surface S encloses the volume V that is fixed in the fluid domain. The mass of fluid that flows out of the closed surface S per unit time can be expressed as

$$\iint_S (\rho \mathbf{V}) \cdot \mathbf{n} \mathrm{dS}, \tag{2.64}$$

where ρ represents the density of fluid, $\mathbf{V}(u, v, w)$ is the velocity of fluid and $\mathbf{n}$ is the outward unit normal vector to the surface S. According to the law of mass conservation, the mass of fluid that flows into the volume V (negative of Equation (2.64)) should equal the rate of change of the fluid mass inside volume V. That is

$$\frac{\partial}{\partial t} \iiint_V \rho \, \mathrm{d}V = -\iint_S (\rho \mathbf{V}) \cdot \mathbf{n} \, \mathrm{dS}. \tag{2.65}$$

On using Gauss's theorem (Stroud & Booth 2003), the surface integral on the right hand side of Equation (2.65) can be transformed into a volume integral as follows

$$\iint_S (\rho \mathbf{V}) \cdot \mathbf{n} \, \mathrm{dS} = \iiint_V \left(\frac{\partial(\rho u)}{\partial x} + \frac{\partial(\rho v)}{\partial y} + \frac{\partial(\rho w)}{\partial z} \right) \mathrm{d}V. \tag{2.66}$$

Substituting Equation (2.66) into Equation (2.65) and rearranging the resultant equation follows

$$\iiint_V \left(\frac{\partial \rho}{\partial t} + \frac{\partial (\rho u)}{\partial x} + \frac{\partial (\rho v)}{\partial y} + \frac{\partial (\rho w)}{\partial z} \right) \mathrm{d}V = 0 . \tag{2.67}$$

Since Equation (2.67) applies to any volume V in the fluid domain, it is necessary that

$$\frac{\partial \rho}{\partial t} + \frac{\partial (\rho u)}{\partial x} + \frac{\partial (\rho v)}{\partial y} + \frac{\partial (\rho w)}{\partial z} = 0 . \tag{2.68}$$

This equation is known as the continuity equation. On expanding the partial derivatives of ρu, ρv and ρw in Equation (2.68) and using the Hamilton operator $\nabla = \frac{\partial}{\partial x}\mathbf{i} + \frac{\partial}{\partial y}\mathbf{j} + \frac{\partial}{\partial z}\mathbf{k}$, the continuity Equation (2.68) is rewritten as

$$\frac{\partial \rho}{\partial t} + \mathbf{V} \cdot \nabla \rho + \rho \nabla \cdot \mathbf{V} = 0 . \tag{2.69}$$

For an incompressible fluid $D\rho / Dt = 0$, that is

$$\frac{\partial \rho}{\partial t} + \mathbf{V} \cdot \nabla \rho = 0 . \tag{2.70}$$

Thus Equation (2.69) can be reduced to

$$\nabla \cdot \mathbf{V} = 0 \tag{2.71}$$

or

$$\frac{\partial u}{\partial x} + \frac{\partial v}{\partial y} + \frac{\partial w}{\partial z} = 0 . \tag{2.72}$$

For an irrotational flow *curl* $\mathbf{V} = \mathbf{0}$, and since *curl grad* of any scalar function is identically zero, the fluid velocity field can be defined in terms of the velocity potential ϕ subject to

$$u = \frac{\partial \phi}{\partial x}, \qquad v = \frac{\partial \phi}{\partial y}, \qquad w = \frac{\partial \phi}{\partial z} . \tag{2.73}$$

The substitution of Equation (2.73) into Equation (2.72) yields

$$\frac{\partial^2 \phi}{\partial x^2} + \frac{\partial^2 \phi}{\partial y^2} + \frac{\partial^2 \phi}{\partial z^2} = 0 , \tag{2.74}$$

which is known as Laplace's equation. It is one of the most powerful relationships applied in many hydrodynamic problems.

The derivation of Laplace equation is based on two assumptions. One is incompressible fluid and the other is irrotational flow. It has been found that for large submerged structures and especially those having streamline boundaries, the assumption of irrotational flow provides realistic results in solving the fluid – structure interaction problem. Therefore the potential flow theory is adopted in this thesis to investigate the dynamics of airplane – floating structure – water interaction systems.

2.3.2 Bernoulli's theorem

To deduce Bernoulli's theorem, it is necessary to introduce the equation of fluid motion in Eulerian form. It is generally expressed in the form (Liu et al 1990)

$$\frac{\partial \mathbf{V}}{\partial t} + \nabla\left(\frac{\mathrm{V}^2}{2}\right) - \mathbf{V} \times \boldsymbol{\Omega} = \overline{\mathbf{F}} - \frac{1}{\rho}\nabla P , \tag{2.75}$$

where $\boldsymbol{\Omega}$ represents the vorticity, that is

$$\boldsymbol{\Omega} = \nabla \times \mathbf{V} , \tag{2.76}$$

$\overline{\mathbf{F}}$ is body force per unit mass and P is fluid pressure.

From a mathematical point of view, Equation (2.75) is a nonlinear partial differential equation, which can only be integrated under special circumstances. To integrate this equation, two assumptions are used.

Firstly, the body force $\overline{\mathbf{F}}$ is a conservative force. In mathematical terms, a conservative force is a potential force expressible in the form

$$\overline{\mathbf{F}} = -\nabla U , \tag{2.77}$$

where U is a potential energy function.

Secondly, the density of fluid ρ is a function of fluid pressure P only, from which we have

$$\Pi(P) = \int_0^P \frac{dP}{\rho}, \tag{2.78}$$

where Π is a scalar function. The gradient of this scalar function is calculated as

$$\nabla \Pi = \Pi'(P)\nabla P = \frac{1}{\rho}\nabla P. \tag{2.79}$$

On substituting Equations (2.77) and (2.79) into Equation (2.75), it is found

$$\frac{\partial \mathbf{V}}{\partial t} = -\nabla\left(U + \Pi + \frac{\mathrm{V}^2}{2}\right) + \mathbf{V} \times \boldsymbol{\Omega}. \tag{2.80}$$

If the fluid flow is steady, Equation (2.80) reduces to

$$\nabla\left(U + \Pi + \frac{\mathrm{V}^2}{2}\right) = \mathbf{V} \times \boldsymbol{\Omega}, \tag{2.81}$$

and the Bernoulli function (Liu et al 1990) is defined as

$$H = U + \Pi + \frac{\mathrm{V}^2}{2}. \tag{2.82}$$

The dot product of both sides of Equation (2.81) with respect to a small piece of arc, $\mathrm{d}\mathbf{l}$, along the streamline produces

$$\nabla H \cdot \mathrm{d}\mathbf{l} = (\mathbf{V} \times \boldsymbol{\Omega}) \cdot \mathrm{d}\mathbf{l}. \tag{2.83}$$

The right hand side of Equation (2.83) is zero, as the vector $\mathbf{V} \times \boldsymbol{\Omega}$ is perpendicular to the plane containing vector $\mathrm{d}\mathbf{l}$. This means the value of Bernoulli function is a constant along the same streamline. Thus the Bernoulli's theorem is interpreted as

$$H = U + \Pi + \frac{\mathrm{V}^2}{2} = C_l, \tag{2.84}$$

where C_l is the different constant value for different streamlines.

If the flow is irrotational, Equation (2.80) can be rewritten as

$$\nabla\left(\frac{\partial\phi}{\partial t}+U+\Pi+\frac{\mathrm{V}^2}{2}\right)=0, \tag{2.85}$$

which gives another form of Bernoulli's theorem, namely

$$\frac{\partial\phi}{\partial t}+U+\Pi+\frac{\mathrm{V}^2}{2}=f(t). \tag{2.86}$$

As the velocity of fluid only involves the spatial derivatives of velocity potential, the absolute value of the function $f(t)$ in Equation (2.86) will not affect the evaluation of the fluid velocity. For convenience, $f(t)=0$ may be used.

For an incompressible fluid with uniform mass density ρ and a body force $\overline{\mathbf{F}}$ based on gravitational acceleration it follows that

$$\Pi(P)=\int_0^P\frac{dP}{\rho}=\frac{P}{\rho} \tag{2.87}$$

and

$$U=\int_z^0(-g)\mathrm{d}z=g\,z, \tag{2.88}$$

where g is the gravitational acceleration and z is the vertical coordinate. Here, the plane at $z=0$ is chosen as the reference position where $U=0$. The potential energy U at the position z is calculated by the work, as expressed by Equation (2.88), done by the gravitational force moving from the position z to the reference position $z=0$.

Bernoulli's theorem in Equation (2.86) can be rewritten as

$$\frac{\partial\phi}{\partial t}+gz+\frac{P}{\rho}+\frac{\mathrm{V}^2}{2}=f(t), \tag{2.89}$$

which can be linearised by neglecting the velocity related term $\mathrm{V}^2/2$. This gives

$$\frac{\partial \phi}{\partial t} + gz + \frac{P}{\rho} = f(t). \tag{2.90}$$

Equation (2.90) will be used hereafter to derive the relation between fluid pressure P and velocity potential ϕ.

2.3.3 Boundary conditions

Irrotational flow of an incompressible fluid is governed by the Laplace equation and this is subject to certain boundary conditions that are discussed in this subsection.

Kinematical condition at the floor

Kinematical condition at the bottom of fluid domain states that the normal component of fluid velocity at any point on the bottom surface should be zero. This is required in order that there is no flow into the bottom or no voids created at the bottom resulting from fluid flow. Mathematically, it is simply written as

$$\frac{\partial \phi}{\partial n} = 0, \tag{2.91}$$

where n represents the outward normal of the fluid domain.

Kinematical condition at the fluid – structure interaction interface

For the same, the normal fluid velocity must equal the normal velocity of the floating structures at the fluid – structure interface. This condition is expressed as

$$\frac{\partial \phi}{\partial n} = V_n, \tag{2.92}$$

where V_n is the normal velocity of the floating structure along the outward normal of the fluid domain at the wetted surface.

Combined linear condition at the free surface

Kinematical condition

The free surface is the boundary between water and air. The water particles at the free surface can only move along this surface; they can not leave this surface. The free surface is mathematically described as satisfying

$$F(x, y, z, t) = z - \varsigma(x, y, t) = 0, \tag{2.93}$$

where $\varsigma(x, y, t)$ is the vertical elevation of free surface measured from the undisturbed free surface.

Since the free surface is a material surface, its material derivative vanishes and so

$$\frac{DF}{Dt} = \frac{\partial F}{\partial t} + u\frac{\partial F}{\partial x} + v\frac{\partial F}{\partial y} + w\frac{\partial F}{\partial z} = 0. \tag{2.94}$$

With (u, v, w) defined by Equation (2.73) and F defined by Equation (2.93), Equation (2.94) is rearranged in the form

$$\frac{\partial \phi}{\partial z} = \frac{\partial \varsigma}{\partial t} + \frac{\partial \phi}{\partial x}\frac{\partial \varsigma}{\partial x} + \frac{\partial \phi}{\partial y}\frac{\partial \varsigma}{\partial y}. \tag{2.95}$$

The kinematical condition in Equation (2.95) is nonlinear. For simplicity, many fluid – structure interaction problems are solved by linearising this equation. If the wave amplitude is assumed to be small in describing the wave profile, the second order quantities in Equation (2.95) can be neglected. The corresponding linearised kinematical free surface condition becomes

$$\frac{\partial \phi}{\partial z} = \frac{\partial \varsigma}{\partial t}. \tag{2.96}$$

Dynamic condition

Dynamic condition describes the pressure at free surface. It is obtained by applying Bernoulli's theorem. Assuming $f(t) = 0$, Equation (2.90) has the following form

$$\frac{\partial \phi}{\partial t} + g\varsigma + \frac{P_a}{\rho} = 0. \tag{2.97}$$

Here P_a is the constant atmospheric pressure acting on the free surface. It can be set to zero without loss of generality since it is pressure gradient that causes fluid flow.

Combined linear condition

The kinematical condition in Equation (2.96) and dynamic condition in Equation (2.97) can be merged to form the combined linear condition at free surface assuming there is no variation of the pressure on the free surface

$$\frac{\partial^2 \phi}{\partial t^2} + g\frac{\partial \phi}{\partial z} = 0 . \tag{2.98}$$

Boundary conditions at infinity

At the far field boundary of the infinite water domain, two forms of the boundary condition are adopted in numerical simulations.

Undisturbed condition

This condition assumes that the disturbance in water does not transmit to the far field of the water domain during the interested time period. This condition requires the velocity of the fluid to vanish at infinity, that is

$$\frac{\partial \phi}{\partial n} = 0 . \tag{2.99}$$

Radiation condition

This condition ensures that the energy radiated as a result of fluid structure interaction must scatter toward infinity, but no such energy may be radiated back from infinity into the field. Assuming the water domain under consideration is a time harmonic field, the 3D radiation condition for wave propagating problem is expressed as (Sommerfeld 1949)

$$\lim_{R\to\infty} \sqrt{R}\left(\frac{\partial \phi}{\partial R} + \mathrm{i}k\phi\right) = 0 , \tag{2.100}$$

where $R = \sqrt{x^2 + y^2}$, k is the deep water wave number.

For the problem investigated in this thesis, due to the short impact time period of interest,

the undisturbed condition of Equation (2.99) is adopted at infinity.

2.4 Boundary Element Method

The boundary element method (BEM) can be viewed as a general numerical technique to solve boundary integral equations. The method possesses a few advantages. Firstly, the discretization is restricted only to the boundaries of a domain, which greatly reduces the degrees of freedom of the problem and makes data generation much easier. Secondly, BEM is more suitable to solve problems involving an infinite external domain since discretizations are only required on the internal boundaries for some cases. Thirdly, BEM provides a convenient approach to deal with problems involving some types of discontinuity or singularity, due to the use of singular fundamental solutions.

BEM will be used to model the external water domain in this research. Its basic formulation and numerical solution procedure are introduced herein for the convenient use in the following chapters.

2.4.1 Basic concepts

Gauss's theorem

The main properties of potential functions can be derived from Gauss's theorem, also known as the divergence theorem, and its corollaries known as Green's identities (Wrobel 2002). The Gauss's theorem establishes that the total flux of vector $\hat{\mathbf{F}}$ across a single connected closed surface S must be equal to the volume integral of the divergence of vector $\hat{\mathbf{F}}$ over the volume V enclosed within the surface S, that is

$$\iint_S \hat{\mathbf{F}} \cdot \mathbf{n}\, dS = \iiint_V \nabla \cdot \hat{\mathbf{F}}\, dV \,. \tag{2.101}$$

Flux conservation for potential flows

Applying Gauss's theorem to the velocity of fluid $\nabla\phi$, we obtain

$$\iint_S \nabla\phi \cdot \mathbf{n}\, dS = \iiint_V \nabla^2\phi\, dV = 0. \tag{2.102}$$

Physically, this result represents potential flow problems with no internal sources as the net flux across the closed surface S must vanish.

Green's first identity

Substituting $\hat{\mathbf{F}} = \phi \nabla \psi$ into Gauss theorem, in Equation (2.101), we obtain

$$\iint_S \phi \frac{\partial \psi}{\partial n} dS = \iiint_V \nabla \cdot (\phi \nabla \psi) dV, \tag{2.103}$$

where ψ is another potential function.

On using the chain rule, it follows that

$$\nabla \cdot (\phi \nabla \psi) = \nabla\phi \cdot \nabla \psi + \phi \nabla^2 \psi. \tag{2.104}$$

The substitution of Equation (2.104) into the right-hand side of Equation (2.103) yields Green's first identity

$$\iint_S \phi \frac{\partial \psi}{\partial n} dS = \iiint_V \left(\nabla\phi \cdot \nabla \psi + \phi \nabla^2 \psi\right) dV. \tag{2.105}$$

Green's second identity

The identity Equation (2.105) is also valid when interchanging ϕ and ψ, namely

$$\iint_S \psi \frac{\partial \phi}{\partial n} dS = \iiint_V \left(\nabla \psi \cdot \nabla\phi + \psi \nabla^2 \phi\right) dV. \tag{2.106}$$

Subtracting Equation (2.106) from Equation (2.105) gives Green's second identity

$$\iint_S \left(\phi \frac{\partial \psi}{\partial n} - \psi \frac{\partial \phi}{\partial n}\right) dS = \iiint_V \left(\phi \nabla^2 \psi - \psi \nabla^2 \phi\right) dV. \tag{2.107}$$

In the expressions of Green's identities, the scalar functions ϕ and ψ must be differentiable at least to the orders that appear in the integrands.

Fundamental solution of Laplace equation

The solution of Laplace Equation (2.74) defined in an unbounded region, for a point source of unit strength, is called the fundamental solution or free-space Green's function of the problem. For a homogeneous and isotropic water domain, the 3D fundamental solution must have spherical symmetry. Mathematically, it can be defined as a scalar function G that is at least twice differentiable with respect to the coordinates of any field point $\mathbf{X}$, and satisfies Laplace's equation at all points except at $\mathbf{X}'$, the point of application of the source. That is

$$\nabla^2 G(\mathbf{X}', \mathbf{X}) = \Delta(\mathbf{X} - \mathbf{X}') = \begin{cases} 0 & \mathbf{X} \neq \mathbf{X}' \\ \infty & \mathbf{X} = \mathbf{X}' \end{cases}. \tag{2.108}$$

The solution of Equation (2.108) can be found by writing it in spherical coordinates and taking into account its central symmetrical character, that is

$$\nabla^2 G = \frac{1}{r^2}\frac{d}{dr}\left(r^2 \frac{dG}{dr}\right) = 0, \tag{2.109}$$

where r is the distance between the source and field points. This is an ordinary differential equation whose solution is

$$G = c_0 + \frac{c_1}{r}, \tag{2.110}$$

where c_0 is an arbitrary additive constant corresponding to the reference level adopted for measuring velocity potential. c_0 has no influence on the calculation of fluid velocities. The constant c_1 can be determined from mass conservation by considering a spherical control surface of radius ε centred at the source point $\mathbf{X}'$. For the convenience of derivation, it is assumed that a sink source is located at point $\mathbf{X}'$. From the principle of mass conservation, the total flux across the spherical surface must be equal to the mass flux into the unit sink source at point $\mathbf{X}'$, thus

$$\iint_{S_\varepsilon} \frac{\partial G}{\partial n} dS = 1. \tag{2.111}$$

Substituting Equation (2.110) into Equation (2.111) and noting $\frac{\partial}{\partial n} = -\frac{\partial}{\partial r}$ on the spherical control surface gives the following equation

$$c_1 \frac{1}{\varepsilon^2} \iint_{S_\varepsilon} dS = 1. \tag{2.112}$$

Since the area of the spherical surface is $4\pi\varepsilon^2$, we obtain the constant $c_1 = 1/4\pi$. Assuming $c_0 = 0$, the expression for the fundamental solution of the Laplace equation in a 3D water domain of infinite extent is expressible as

$$G = \frac{1}{4\pi r}. \tag{2.113}$$

2.4.2 Formulation of boundary integral equation

Green's second identity in Equation (2.107) is valid for any two regular functions, thus it can be applied to relate the sought velocity potential ϕ and the fundamental solution G of Laplace equation. As G is singular at the source point $\mathbf{X}'$, it's necessary to exclude this point from the solution domain V by introducing a sphere of radius ε centred at $\mathbf{X}'$, that is

$$\iiint_{V-V_\varepsilon} \left(\phi \nabla^2 G - G \nabla^2 \phi\right) dV = \iint_S \left(\phi \frac{\partial G}{\partial n} - G \frac{\partial \phi}{\partial n}\right) dS + \iint_{S_\varepsilon} \left(\phi \frac{\partial G}{\partial n} - G \frac{\partial \phi}{\partial n}\right) dS. \tag{2.114}$$

Both ϕ and G satisfy Laplace's equation in the new region $V - V_\varepsilon$ so the volume integral on the left hand side of Equation (2.114) vanishes. Next the surface integral over S_ε in Equation (2.114) is analysed. Initially, the value of velocity potential at source point $\mathbf{X}'$, is subtracted from and then added to $\phi(\mathbf{x})$. This gives

$$\iint_{S_\varepsilon} \phi(\mathbf{x}) \frac{\partial G(\mathbf{X}', \mathbf{x})}{\partial n} dS = \iint_{S_\varepsilon} [\phi(\mathbf{x}) - \phi(\mathbf{X}')] \frac{\partial G(\mathbf{X}', \mathbf{x})}{\partial n} dS + \phi(\mathbf{X}') \iint_{S_\varepsilon} \frac{\partial G(\mathbf{X}', \mathbf{x})}{\partial n} dS. \tag{2.115}$$

We now concentrate on the second integral on the right-hand side of Equation (2.115). The normal derivative of the fundamental solution G over S_ε is given as

$$\frac{\partial G(\mathbf{X}', \mathbf{x})}{\partial n} = \frac{1}{4\pi r^2}, \tag{2.116}$$

and the limit of its integral produces the result

$$\lim_{\varepsilon \to 0} \iint_{S_\varepsilon} \frac{\partial G(\mathbf{X}', \mathbf{x})}{\partial n} dS = \lim_{\varepsilon \to 0} \int_0^{2\pi} \int_{-\pi/2}^{\pi/2} \frac{1}{4\pi\varepsilon^2} \varepsilon^2 \cos\alpha' \, d\alpha' \, d\theta' = 1. \tag{2.117}$$

For the first integral on the right-hand side of Equation (2.115), assuming that the velocity potential ϕ is continuous at source point $\mathbf{X}'$, it's obvious that

$$\lim_{\varepsilon \to 0} \iint_{S_\varepsilon} [\phi(\mathbf{x}) - \phi(\mathbf{X}')] \frac{\partial G(\mathbf{X}', \mathbf{x})}{\partial n} dS = 0, \tag{2.118}$$

thus

$$\lim_{\varepsilon \to 0} \iint_{S_\varepsilon} \phi(\mathbf{x}) \frac{\partial G(\mathbf{X}', \mathbf{x})}{\partial n} dS = \phi(\mathbf{X}'). \tag{2.119}$$

The second term of the surface integral over S_ε in Equation (2.114) is evaluated as

$$\lim_{\varepsilon \to 0} \iint_{S_\varepsilon} G(\mathbf{X}', \mathbf{x}) \frac{\partial \phi(\mathbf{x})}{\partial n} dS = \lim_{\varepsilon \to 0} \int_0^{2\pi} \int_{-\pi/2}^{\pi/2} \frac{1}{4\pi\varepsilon} \frac{\partial \phi(\mathbf{x})}{\partial n} \varepsilon^2 \cos\alpha' \, d\alpha' \, d\theta' = 0. \tag{2.120}$$

The substitution of Equations (2.119) and (2.120) into Equation (2.114) yields

$$\phi(\mathbf{X}') = \iint_S \left[G(\mathbf{X}', \mathbf{x}) \frac{\partial \phi(\mathbf{x})}{\partial n} - \phi(\mathbf{x}) \frac{\partial G(\mathbf{X}', \mathbf{x})}{\partial n} \right] dS, \tag{2.121}$$

which is known as Green's third identity.

To obtain the boundary integral equation relating only boundary values, the limit is taken when the source point $\mathbf{X}'$ tends to a point $\mathbf{x}'$ on the boundary S. Again, it is necessary to exclude point $\mathbf{x}'$ before taking the limit. In this case, Equation (2.121) has the following form

$$c(\mathbf{x}')\phi(\mathbf{x}') = \iint_S \left[G(\mathbf{x}', \mathbf{x}) \frac{\partial \phi(\mathbf{x})}{\partial n} - \phi(\mathbf{x}) \frac{\partial G(\mathbf{x}', \mathbf{x})}{\partial n} \right] dS \,, \tag{2.122}$$

where the coefficient $c(\mathbf{x}')$ can be evaluated from Equation (2.117) according to the local geometry of the boundary surface at the location of source point $\mathbf{x}'$. For example, if $\mathbf{x}'$ belongs to a smooth part of the boundary S, a hemi-sphere will suffice to exclude $\mathbf{x}'$ from the entire domain V and in this case $c(\mathbf{x}') = 1/2$.

2.4.3 Numerical solution

Analytical solutions of the boundary integral equation of Equation (2.122) only exist for some very simple problems. For more general problems, a numerical solution procedure is needed. The BEM, based on a discretization procedure, is such a method to solve boundary integral equations. Application of BEM requires two approximations. The first is geometrical, involving a subdivision of the boundary S into N_e small elements $S_j (j = 1, 2, ..., N_e)$, such that

$$\sum_{j=1}^{N_e} S_j \approx S \,, \tag{2.123}$$

and taking this into consideration, Equation (2.122) is rewritten in the form

$$c(\mathbf{x}')\phi(\mathbf{x}') = \sum_{j=1}^{N_e} \iint_{S_j} \left[G(\mathbf{x}', \mathbf{x}) \frac{\partial \phi(\mathbf{x})}{\partial n} - \phi(\mathbf{x}) \frac{\partial G(\mathbf{x}', \mathbf{x})}{\partial n} \right] dS \,. \tag{2.124}$$

Within a certain level of approximation, Equation (2.123) permits any complex geometry S to be modelled using simple geometrical forms S_j. One important aspect is that the approximate geometrical representation can always be improved by increasing the number of elements, or increasing the order of approximation.

The second approximation required by BEM is functional, which is necessary because although the entire boundary has been reduced to a summation of elements, we don't know how the velocity potential and its normal derivative vary within each element. Thus their

variations within each element need to be approximated by expressing their local behaviour in terms of their values at the nodes of each element with a suitable set of interpolation functions. The simplest approximation assumes that ϕ and $\partial\phi/\partial n$ are constant within each element and equal to their values at the midpoint of each element, respectively. By introducing this approximation into Equation (2.124), we obtain

$$c(\mathbf{x}')\phi(\mathbf{x}') = \sum_{j=1}^{N_e} \frac{\partial \phi_j}{\partial n} \iint_{S_j} G(\mathbf{x}', \mathbf{x}) dS - \sum_{j=1}^{N_e} \phi_j \iint_{S_j} \frac{\partial G(\mathbf{x}', \mathbf{x})}{\partial n} dS \,, \tag{2.125}$$

where ϕ_j and $\partial\phi_j/\partial n$ are the corresponding values at the midpoint of element j.

With a finite number N_e of unknowns, it is necessary to generate the same number of equations. These equations are generated by applying Equation (2.125) to the midpoint of each element along the boundary. For example, for the midpoint of element i, we have

$$c_i\phi_i = \sum_{j=1}^{N_e} \frac{\partial \phi_j}{\partial n} \iint_{S_j} G(\mathbf{x}_i', \mathbf{x}) dS - \sum_{j=1}^{N_e} \phi_j \iint_{S_j} \frac{\partial G(\mathbf{x}_i', \mathbf{x})}{\partial n} dS \,. \tag{2.126}$$

Calling

$$G_{ij} = \iint_{S_j} G(\mathbf{x}_i', \mathbf{x}) dS \,, \tag{2.127}$$

and

$$\hat{H}_{ij} = \iint_{S_j} \frac{\partial G(\mathbf{x}_i', \mathbf{x})}{\partial n} dS, \qquad H_{ij} = \hat{H}_{ij} + c_i\delta_{ij} \,, \tag{2.128}$$

where integrations in Equations (2.127) and (2.128) must be determined so as not to include the source point.

With Equations (2.127) and (2.128), Equation (2.126) is rewritten as

$$\sum_{j=1}^{N_e} H_{ij}\phi_j = \sum_{j=1}^{N_e} G_{ij} \frac{\partial \phi_j}{\partial n} \,. \tag{2.129}$$

On applying Equation (2.129) to the midpoint of all elements along boundary S, a system of equations is generated as

$$\hat{\mathbf{H}}\boldsymbol{\psi} = \hat{\mathbf{G}}\boldsymbol{\psi}_n, \tag{2.130}$$

where $\hat{\mathbf{H}}$ and $\hat{\mathbf{G}}$ are square matrices of influence coefficients, $\boldsymbol{\psi}$ and $\boldsymbol{\psi}_n$ are vectors containing the values of velocity potential and its normal derivative at the midpoints of all boundary elements. Once the boundary conditions of the problem are applied to the system, Equation (2.130) can be solved by standard schemes such as Gaussian elimination or iterative schemes.

Chapter 3

Modelling of Landing Gear System of Airplane

The modelling of the landing gear system of the airplane investigated in this research is very important for the following two main reasons: 1) The landing gear system is a main energy dissipation unit in the total system and it is a high order nonlinear system involving oil and gas dynamic behaviour. 2) The landing gear system connects the airplane and the floating structure thus affecting the interactions between these two solid structures. Therefore, the modelling of the landing gear system will directly affect the simulation results of the integrated model of airplane – floating structure – water interaction systems.

Due to the complexity of modern landing gears, it is very difficult to consider the detailed dynamic behaviour of real landing gears. As a first approximation to establish the integrated linear model for airplane – floating structure – water interaction systems, each landing gear of the airplane is modelled by a suspension unit consisting of a linear spring and damper. This chapter indicates how the required linear spring and damper coefficients are assigned.

To validate the developed approach, a drop test of a landing gear carriage is simulated. Under the prescribed initial conditions, the responses of the mass – spring – damper unit used to model the landing gear carriage and the forces provided by the linear spring – damper system are calculated. On comparing these results with those measured from the drop test, it is demonstrated that the linear spring – damper system is capable of describing the basic mechanics of a landing gear. Thereafter, the proposed linearization approach is used in the following chapters to model the landing gears of an airplane.

3.1 Introduction

3.1.1 History of development

The landing gear system of an airplane, also known as an undercarriage, serves a triple

purpose in providing a stable support for an airplane at rest on the ground, forming a suitable shock absorbing device for landing and acting as a rolling chassis for taxiing. It accounts for around 3 – 5 percent of the gross airplane weight and also represents a considerable cost item in the total manufacturing and maintenance bills.

The first wheeled landing gear appeared shortly after the Wright Brothers' maiden flight in December 1903 (Currey 1988). By the time of World War I, most of the landing gear arrangements were tail wheel types. The shock absorber fitted to each wheel consisted of springs or bungee cords allowing a few inches of vertical motion of the wheel with respect to the bracing.

Towards the end of World War I, oil damping was introduced to supplement the rubber spring shock absorbers to control recoil (Conway 1958). It was about 1928 – 1929 that the oleo – pneumatic shock absorber became popular, although it was proposed much early. Most of today's airplanes use oleo – pneumatic shock absorbers because they have the highest efficiency among all shock absorber types and also exhibit the best energy dissipation capacity.

The earliest retractable landing gear was produced in the late 1920's. However, the problems of retraction by mechanical means were considerable and the general adoption of retraction awaited the development of hydraulic means (Conway 1958). By the time of World War II, most of the operational fighters and bombers had retractable landing gears (Currey 1988).

Airplane design has now become a very sophisticated form of engineering and so has the landing gear design. In order to satisfy the sometimes conflicting demands of structural engineers, aerodynamicists, runway designers and operational personnel, the landing gear design has been made more and more efficient and reliable.

3.1.2 Landing gear's structure and operation principle

A landing gear normally consists of shock absorber, wheels, tyres, brakes, steering system, retraction/extension system, etc. Among these components, the shock absorber is usually the most complex part of a landing gear. The basic function of a shock absorber is

to absorb and dissipate the kinetic energy during airplane landing and taxiing to the extent that accelerations imposed upon the airframe are reduced to a tolerable level. There are two basic types of shock absorbers: those using a solid spring made of steel or rubber and those using a fluid spring with gas, oil, or a mixture of gas and oil which is generally referred to as an oleo – pneumatic shock absorber, as shown in Figure 3.1.

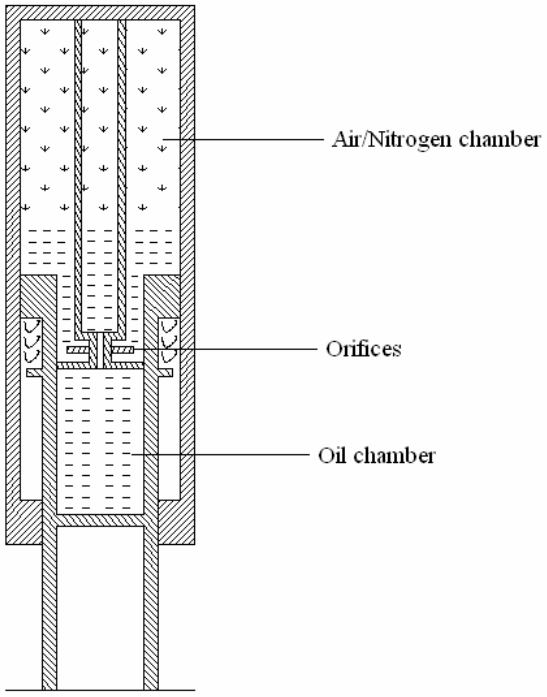

Figure 3.1 Oleo – pneumatic shock absorber

Oleo – pneumatic shock absorbers absorb energy by pushing a chamber of oil against a chamber of dry air or nitrogen and then compressing the gas and the oil. Energy is dissipated by the oil being forced through one or more orifices between the two chambers. For example as in Figure 3.1, when the airplane lands the oil is forced from the lower chamber to the upper chamber of air through the orifices. After the initial impact, the rebound is controlled by the air pressure forcing the oil to flow back into its chamber through the orifices. After a few cycles of this process, the kinetic energy of the airplane induced by the “sink velocity” is dissipated and the airplane tends to its static equilibrium position.

During a landing process, the ideal force provided by a shock absorber should rise as fast as possible to the maximum allowed value, remain constant till the centre of gravity

(CG) of the airplane reaches its lowest position, and decay afterwards. This corresponds to one stroke of the shock absorber and it consists of a compression half and an extension half. Neglecting the inertia of the wheels, tyres, etc., the grounding force between the tyres and the ground can be approximated by the force provided by the shock absorber.

Figure 3.2 (Currey 1988) shows an ideal curve of grounding force versus CG position of an airplane, which is also known as the efficiency diagram of landing gears. This diagram is usually obtained by experiments in the design stage of an airplane. It is worthy to note that the same CG position corresponds to two different values of grounding force, one for the compression state and the other for the extension state of the shock absorber. The area S_2 contained by the grounding force – CG position curve indicates the energy dissipated in one stroke. S_1 represents the area contained by the upper half of the grounding force – CG position curve and the vertical axis whilst S_3 indicates the area contained by the lower half of the same curve and the horizontal axis.

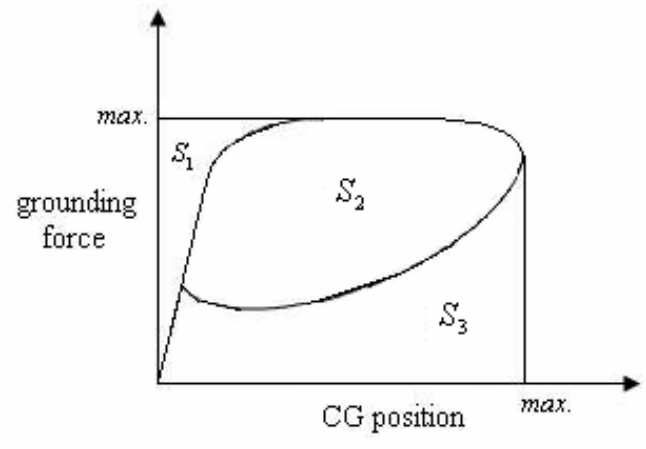

Figure 3.2 Efficiency diagram of landing gears.

With the efficiency diagram of the landing gears of an airplane, it is very straightforward to simulate the landing impact. However, this relationship between the grounding force and CG position is very nonlinear. Modelling this nonlinearity costs a lot of computer time. For our linear integrated model of airplane – floating structure – water interaction systems, it is necessary to use a linear relationship to approximate this diagram. The adopted approach is presented next.

3.2 Modelling of Landing Gear System of Airplane

3.2.1 General description

The force provided by the shock absorber inside a landing gear consists of an elastic component representing the compression of the gas and a viscous component representing the energy dissipation through the oil orifice. Strictly speaking, the effect of the landing gear tyres is also considered, since the tyres are included in the test to measure the landing gear efficiency diagram shown in Figure 3.2. Thus the mechanics of the landing gear may be understood as a non linear spring – damper system, as illustrated in Figure 3.3. It is assumed that the effect of the tyres is included in the spring – damper system.

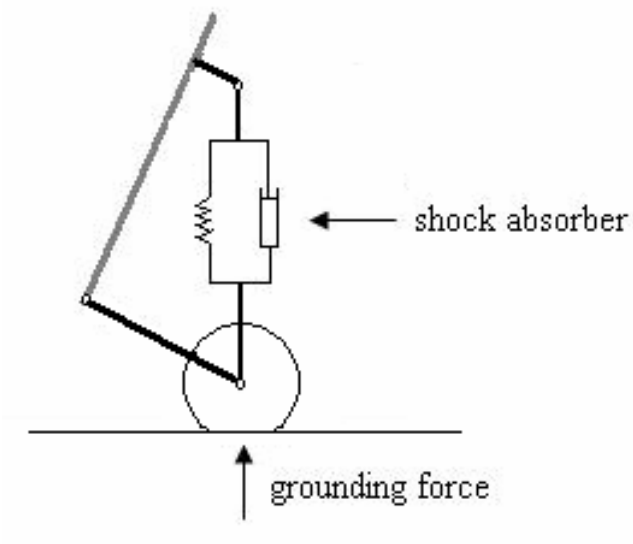

Figure 3.3 Simplified landing gear model

The spring and damper parameters are required to model the landing gear system. Therefore, the grounding force is calculated by the force provided by the spring – damper unit. To further reduce modelling complexity, a linear spring – damper system is used to model the entire landing gear.

3.2.2 Coefficients of linear spring – damper system

In order to determine the spring and damping coefficients of the linear spring – damper system shown in Figure 3.3, an approximate scheme is proposed that assumes some

parameters of the landing gear are already known.

Spring coefficient

Assume the sink velocity of an airplane in landing is V_s and the weight sustained on one of the landing gears is $M'g$. The corresponding kinetic energy may be expressed as

$$E' = \frac{1}{2} M' V_s^2 . \tag{3.1}$$

This energy is first absorbed and then dissipated by the shock absorber of the landing gear.

The working stroke of the shock absorber, S_w, may be approximated as (Feng 1991)

$$S_w = \frac{E'}{P_s n' \phi' \eta}, \tag{3.2}$$

where P_s is the static load equal to the weight $M'g$. n' is the landing gear load factor with values ranging from 0.75 to 5.0 for different types of airplanes (Currey 1988). ϕ' is a transfer coefficient that is determined by the structural layout of the landing gear. As a rough approximation, the transfer coefficient ϕ' may be equalled to 1.0. η is the energy absorption efficiency of the landing gear given by the ratio $(S_2 + S_3)/(S_1 + S_2 + S_3)$. The areas S_1, S_2 and S_3 are shown in Figure 3.2. The value of η is normally between 0.6 and 0.8 (Feng 1991).

The stroke of the shock absorber at the static load P_s is estimated as (Currey 1988)

$$S_s = S_w(1 - a), \tag{3.3}$$

where a is the static stroke parameter varying between 0.1 and 0.4 for various types of airplane.

At stroke S_s, the shock absorber provides a force P_s, and at a working stroke S_w, it provides a force $P_w = n' P_s$. If we draw a force – stroke curve, its gradients at stroke S_s

and S_w are respectively

$$k_1 = \frac{P_s}{S_s} \tag{3.4}$$

and

$$k_2 = \frac{P_w}{S_w}. \tag{3.5}$$

As an approximation of the spring coefficient of the linear spring – damper system, the average of the two gradients in Equations (3.4) and (3.5) is used. The linear spring stiffness is

$$K = \frac{k_1 + k_2}{2}. \tag{3.6}$$

Damping coefficient

To approximate the damping coefficient of the idealised spring – damper system shown in Figure 3.3, the energy dissipated in one stroke is equal to the work done by the damping force. This energy dissipation can be obtained by experiments or is estimated as (Feng 1991)

$$W_d = P_w S_w \eta \chi, \tag{3.7}$$

where χ is the landing gear energy dissipation coefficient. χ equals the ratio of dissipated energy over absorbed energy given by the ratio of $S_2/(S_2 + S_3)$. The value of χ is usually between 0.6 and 0.7 (Feng 1991).

Next consider a harmonic motion whose displacement is expressed as

$$\tilde{x} = A\cos(\omega t - \beta'), \tag{3.8}$$

where A is the motion amplitude, ω is the frequency and β' is the phase angle. If the damping force of this harmonic system is expressed as

$$F_d = -C\dot{\tilde{x}}, \tag{3.9}$$

where C is the damping coefficient, then the work done by this damping force over one period is

$$\begin{aligned} W &= \int -F_d \, d\tilde{x} \\ &= \int_0^{\frac{2\pi}{\omega}} C\left(\dot{\tilde{x}}\right)^2 dt \\ &= C\omega^2 A^2 \int_0^{\frac{2\pi}{\omega}} \sin^2\left(\omega t - \beta'\right) dt \\ &= \pi \, C \, \omega \, A^2 . \end{aligned} \tag{3.10}$$

If it is assumed that Equation (3.10) is also applicable to approximate the work done in one cycle by the damping force of the spring – damper system illustrated in Figure 3.3, then it follows that

$$W_d = \pi \, C \, \omega \, A^2 , \tag{3.11}$$

where

$$A = \frac{S_w}{2} \tag{3.12}$$

and

$$\omega = \sqrt{\frac{K}{M'}} . \tag{3.13}$$

The damping coefficient of the linear spring – damper system may be obtained by equating Equations (3.7) and (3.11), that is

$$C = \frac{4 P_w \eta \chi}{\pi \sqrt{\frac{K}{M'}} S_w} . \tag{3.14}$$

Thus provided certain parameters ($V_s, M', a, n', \phi', \eta$ and χ) are known for a landing gear, following the scheme proposed in this subsection, the spring and damping coefficients of the linear spring – damper system representing the shock absorber can be approximated.

3.3 Simulation of a Drop Test

In order to validate the proposed approach using the linear spring – damper systems to model the landing gears of an airplane, the drop test of a landing gear is simulated.

The main landing gear of a light jet trainer was used in a drop test (Ghiringhelli 2000). It was equipped with a standard oleo – pneumatic shock absorber. The drop test facility was a vertical test fixture, constructed from two vertical steel rails that guide a sliding carriage. The maximum drop height was 5m. The drop ballast mass was 275kg. Different sink velocities V_s, 1.5m/s, 2.0m/s and 2.5m/s, were used in the drop test. Lift has not been considered. The measures of CG position, CG acceleration, grounding force, etc. were collected during the test.

To simulate this drop test, we use the mass – spring – damper system depicted in Figure 3.4 with the mass M' representing the ballast mass 275kg and the spring – damper system representing the landing gear.

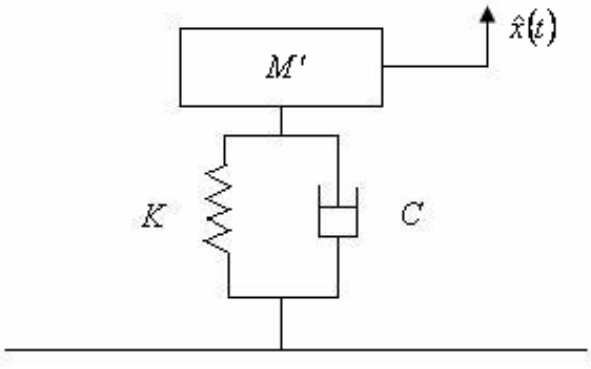

Figure 3.4 Mass – spring – damper system used to simulate the drop test

Following the scheme proposed in Section 3.2, the spring and damping coefficients K and C can be determined with the parameters of the landing gear estimated in Table 3.1.

The motion of a mass – spring – damper system is a classical dynamical problem and its solution for small damping is given as

$$\hat{x}(t) = e^{-\varepsilon'\omega t}\left(B_1 \cos \omega_d t + B_2 \sin \omega_d t\right), \tag{3.15}$$

where

Table 3.1 Parameters of landing gear

Landing gear load factor n'	1.3 (V_s=1.5m/s) 1.8 (V_s=2.0m/s) 2.3 (V_s=2.5m/s)
Transfer coefficient ϕ'	1
Energy absorption efficiency of landing gear η	0.6
Energy dissipation efficiency of landing gear χ	0.6
Static stroke parameter a	0.2

$$\varepsilon' = \frac{C}{2M'\omega}, \tag{3.16}$$

$$\omega_d = \sqrt{1-\varepsilon'^2}\,\omega. \tag{3.17}$$

Constants B_1 and B_2 are determined from the initial conditions

$$\hat{x}(0) = \frac{M'g}{K} \tag{3.18}$$

and

$$\dot{\hat{x}}(0) = -V_s. \tag{3.19}$$

From Equations (3.15), (3.18) and (3.19), the coefficients B_1 and B_2 may be obtained and hence Equation (3.15) is rearranged in the form

$$\hat{x}(t) = e^{-\varepsilon'\omega t}\left(\hat{x}(0)\cos\omega_d t + \frac{\dot{\hat{x}}(0)+\varepsilon'\omega\hat{x}(0)}{\omega_d}\sin\omega_d t\right). \tag{3.20}$$

It should be noted that $\hat{x}(t)$ is the position of the mass measured relative to its equilibrium position. In the following context, we use $\hat{X}(t)$ to represent the position of the mass relative to its initial position, so we have

$$\hat{X}(t) = \hat{x}(t) - \hat{x}(0) . \tag{3.21}$$

The forces provided by the spring – damper system can be expressed as

$$F'(t) = -K\hat{X}(t) - C\dot{\hat{X}}(t) . \tag{3.22}$$

The time histories of the acceleration at the CG of the landing gear carriage measured in the drop test are presented in Figure 3.5 for three different sink velocities (Ghiringhelli 2000). The acceleration is in non dimensional form and the reference acceleration is the gravitational acceleration. From Equation (3.20), the acceleration A_{CG} of the mass of the mass – spring – damper system can be calculated. Figure 3.6 shows the time histories of the calculated non-dimensional acceleration of the mass – spring – damper system for the three different sink velocities.

Figure 3.7 indicates the grounding force – CG position curve measured in the drop test (Ghiringhelli 2000). Figure 3.8 presents the calculated relation between the force provided by the spring – damper system $F'(t)$ and the CG position of the mass of the mass – spring – damper system relative to its initial position.

Comparing Figures 3.5 and 3.6 and Figures 3.7 and 3.8, the trends indicate that the proposed linear spring – damper system can model a landing gear and provide reasonable predictions for the motion of the landing gear and the grounding force – CG position relation. Therefore, this scheme is adopted in the following chapters to model the landing gears of an airplane.

With the basic theory of Chapter 2 and the linear landing gear model of this chapter, one may now proceed with the modelling of an airplane landing on a floating structure.

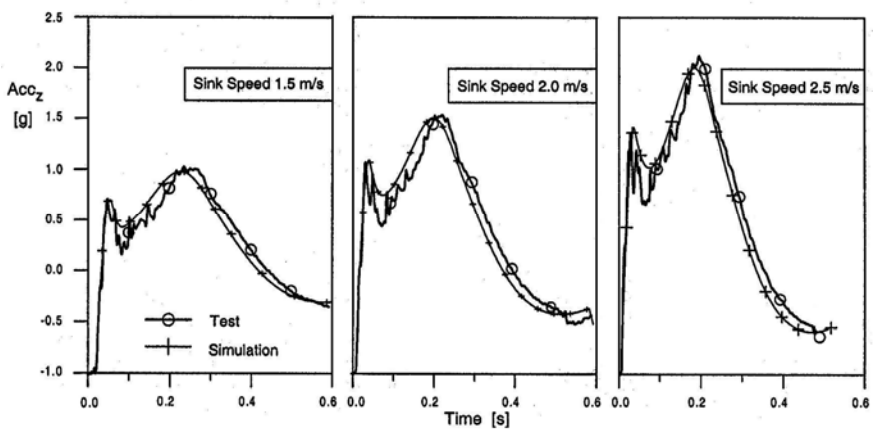

Figure 3.5 Measured acceleration at the CG position of landing gear carriage

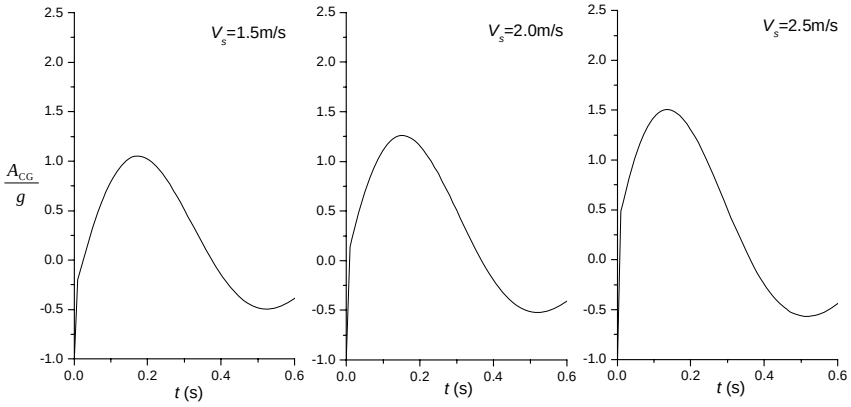

Figure 3.6 Calculated acceleration of mass – spring – damper system

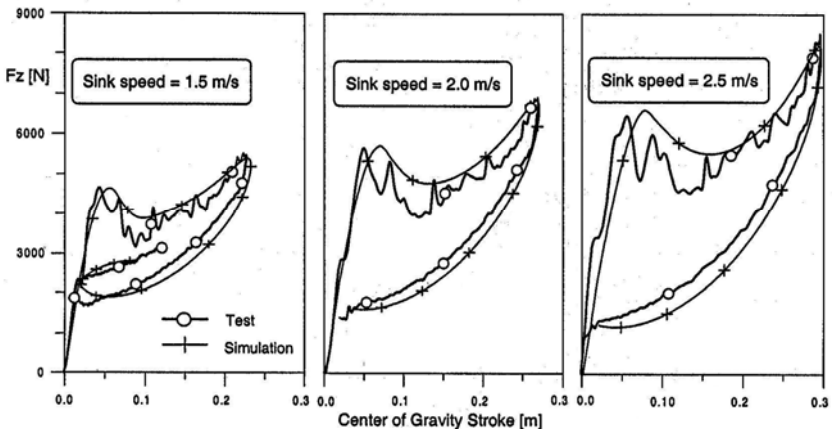

Figure 3.7 Measured grounding force – CG position of landing gear carriage

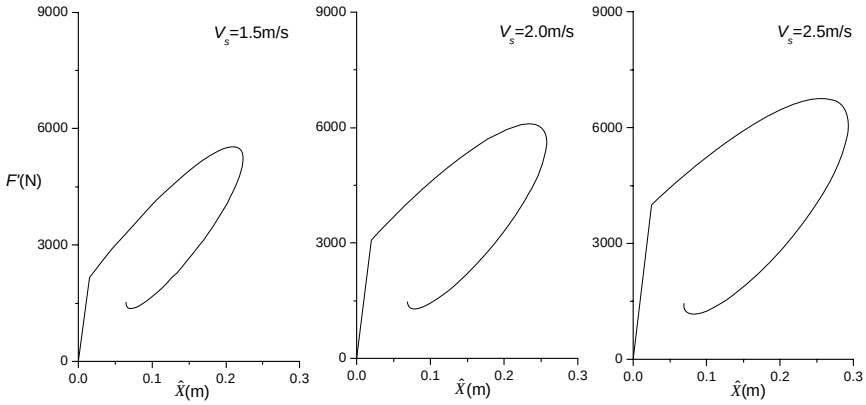

Figure 3.8 Calculated spring – damper force – CG position of mass – spring – damper system

Chapter 4

Mixed Mode Function – Boundary Element Method

Based on the fundamental theories summarized in Chapters 2 and 3, this chapter presents the mixed mode function – boundary element method for the dynamic analysis of an airplane landing onto a floating structure developed in this thesis.

The airplane and the floating structure are considered as two elastic substructures that are governed by their dynamic equations of equilibrium, respectively. The modal superposition method is utilized to transform these dynamic equations, established in the physical space, into the mode space to reduce the degrees of freedom of the substructures. The fluid, occupying a horizontally unbounded 3D domain Ω_f, is assumed to be incompressible, inviscid with irrotational motion. These assumptions allow the potential flow theory to be applicable. Therefore, the fluid flows are governed by the Laplace equation in association with suitable boundary conditions, which are modelled and solved by BEM.

The motion of the airplane and the floating structure are interacted through the landing gear system of the airplane. The landing gear system is approximately modelled using the spring – damper unit discussed in Chapter 3. The motion of the floating structure and the fluid flow are coupled through the fluid – structure interaction conditions defined on the wetted interface. The mixed mode function – boundary element equation is derived to describe the coupled dynamics of the integrated airplane – floating structure – water interaction system.

4.1 General Description

As illustrated in Figure 4.1, a large – scale flexible structure $\Omega^{(1)}$ with unit outward normal vector $\mathbf{v}^{(1)} = \left[v_x^{(1)}, v_y^{(1)}, v_z^{(1)}\right]^{\mathrm{T}}$ floats on the calm surface of a fluid domain Ω_f with

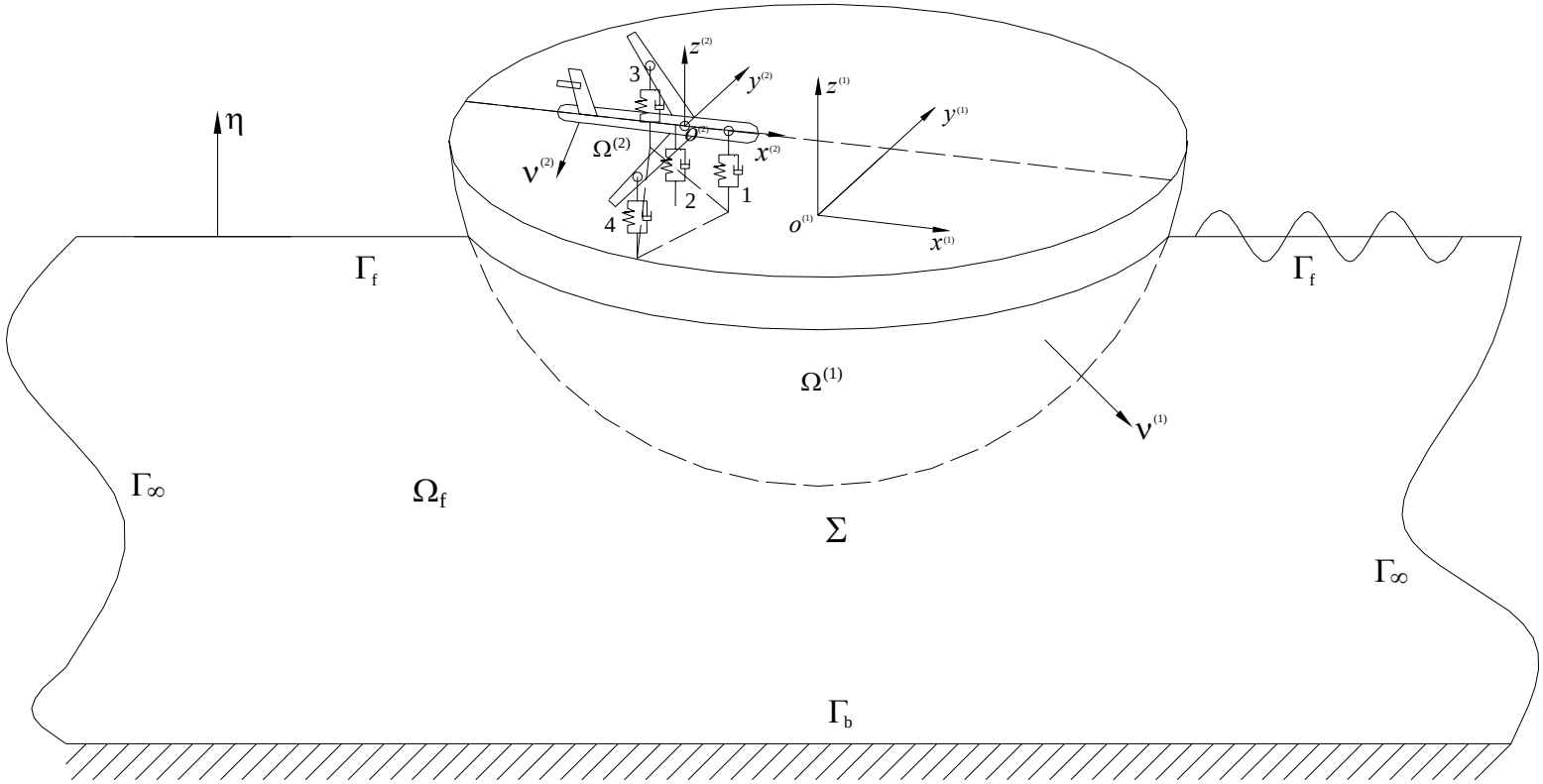

Figure 4.1 An integrated airplane - floating structure - water interaction system subject to airplane landing impact.

unit outward normal vector $\boldsymbol{\eta} = \left[\eta_x, \eta_y, \eta_z\right]^{\mathrm{T}}$. The depth of the fluid domain is assumed to be infinite. An airplane $\Omega^{(2)}$ with unit outward normal vector $\mathbf{v}^{(2)} = \left[v_x^{(2)}, v_y^{(2)}, v_z^{(2)}\right]^{\mathrm{T}}$ lands and travels on the floating structure $\Omega^{(1)}$.

To formulate the governing equations describing this complex airplane – floating structure – water interaction system, a 3D Cartesian coordinate system $o^{(1)} - x^{(1)}y^{(1)}z^{(1)}$ fixed at point $o^{(1)}$ in the physical space is chosen as an absolute reference frame. The origin $o^{(1)}$ of this absolute system is chosen such that the mass centre of the floating structure coincides with it at time $t = 0$ when the dynamic interaction starts. In this system, the coordinate plane $o^{(1)} - x^{(1)}y^{(1)}$ is horizontal and the axis $o^{(1)} - z^{(1)}$ is vertical and positive upward. To investigate the large horizontal motion of the airplane travelling on the floating structure, another moving coordinate system $o^{(2)} - x^{(2)}y^{(2)}z^{(2)}$ is also chosen. The origin $o^{(2)}$ of this moving system coincides with the mass centre of the airplane at time $t = 0$ and moves with the instant horizontal velocity V_x of the mass centre of the airplane. The coordinate plane $o^{(2)} - x^{(2)}y^{(2)}$ of this moving system is also horizontal with the coordinate axis $o^{(2)} - x^{(2)}$ pointing in the positive direction of the horizontal translation of the airplane. For convenience but not losing any generality, we choose that axis $o^{(1)} - x^{(1)}$ has the same direction as axis $o^{(2)} - x^{(2)}$.

To investigate the deformation of the airplane and the floating structure, two material or Lagrangian coordinate systems $O^{(1)} - X^{(1)}Y^{(1)}Z^{(1)}$ and $O^{(2)} - X^{(2)}Y^{(2)}Z^{(2)}$ respectively fixed in the floating structure and the airplane are chosen so that they coincide with the two systems $o^{(1)} - x^{(1)}y^{(1)}z^{(1)}$ and $o^{(2)} - x^{(2)}y^{(2)}z^{(2)}$ at time $t = 0$, respectively.

The airplane lands onto the floating structure with an initial vertical velocity V_{z0} and horizontal velocity V_{x0} and travels along the $o^{(1)} - x^{(1)}$ axis. It is assumed that the airplane is subject to a constant landing resistance F_x and therefore it travels with a

negative acceleration along the $o^{(1)}-x^{(1)}$ axis until its final stop. Obviously, the horizontal velocity V_x of the mass centre of the airplane is not a constant and the moving coordinate system $o^{(2)}-x^{(2)}y^{(2)}z^{(2)}$ is a non-inertial system, in which the inertial forces of the airplane need to be considered when the relative motion of the airplane in this moving coordinate system is investigated.

It is assumed that there are four sets of landing gears supporting the airplane. The $J-th$ landing gear fixed at point $\mathbf{X}_J^{(2)}\left(X_J^{(2)},Y_J^{(2)},Z_J^{(2)}\right)\left(J=1,2,3,4\right)$ on the airplane is modelled by a suspension unit lying in the vertical direction. Each suspension unit consists of a linear spring of stiffness K_J and a damper of damping coefficient C_J as described in Chapter 3, which produces a supporting force f_J. To simplify the problem, the following assumptions are used.

1) The motion of the suspension units is constrained along the vertical direction and all wheels smoothly roll along the floating structure during a landing process;

2) The four suspension units are always in their compression state because of airplane weight and landing gear's damping. Thus, there is no separation between the lower end of the suspension units and the floating structure since the landing started;

3) The dynamic displacements of both the airplane and the floating structure are negligibly small compared to the horizontal translation of the mass centre of the airplane. Therefore, the contact point between the suspension units and the floating structure can be calculated using only the horizontal motion equation of the mass centre of the airplane.

4.2 Governing Equations

4.2.1 Fluid domain

As shown in Figure 4.1, a 3D domain Ω_f is occupied by water of mass density ρ, which is assumed to be incompressible, inviscid and subject to irrotational motion.

$\Gamma_b, \Gamma_\infty, \Gamma_f$ and $\sum$ denote the horizontal flat sea bed, a suitable far-field boundary, the free surface and the fluid – structure interaction interface of the water domain, respectively. The velocity potential $\phi\left(x^{(1)}, y^{(1)}, z^{(1)}, t\right)$ of the fluid satisfies the following equations defined under the fixed coordinate system $o^{(1)} - x^{(1)} y^{(1)} z^{(1)}$.

Laplace's equation [See Equation (2.74)]

$$\nabla^2 \phi = 0, \qquad \text{in } \Omega_f, \tag{4.1}$$

where ∇^2 is the 3D Laplace operator.

Pressure – velocity potential relationship [See Equation (2.90)]

$$P = -\rho \frac{\partial \phi}{\partial t} - \rho g z^{(1)}. \tag{4.2}$$

Boundary conditions

Linearised free surface condition [See Equation (2.98)]

$$\frac{\partial^2 \phi}{\partial t^2} + g \frac{\partial \phi}{\partial z^{(1)}} = 0, \qquad \text{on } \Gamma_f. \tag{4.3}$$

Non-impermeable condition at the sea bed [See Equation (2.91)]

$$\frac{\partial \phi}{\partial x^{(1)}} \eta_x + \frac{\partial \phi}{\partial y^{(1)}} \eta_y + \frac{\partial \phi}{\partial z^{(1)}} \eta_z = 0, \qquad \text{on } \Gamma_b, \tag{4.4}$$

with outward unit normal $\boldsymbol{\eta}$ defined previously.

Boundary condition at the far-field [See Equation (2.99)]

For airplane landing impact analysis, the interested load happens in a very short time period since the impact start. During this short time period, the waves generated by the landing impacts can not reach the far field boundary. Thus the undisturbed condition derived in Chapter 2 is adopted, which gives

$$\frac{\partial \phi}{\partial x^{(1)}}\eta_x + \frac{\partial \phi}{\partial y^{(1)}}\eta_y + \frac{\partial \phi}{\partial z^{(1)}}\eta_z = 0, \qquad \text{on} \quad \Gamma_\infty . \tag{4.5}$$

4.2.2 Floating structure and airplane

The dynamic behaviour of the floating structure and the airplane are governed by the dynamic equations of equilibrium defined in the two Lagrangian coordinate systems identified by superscript $I = 1 \text{ and } 2$ respectively. Here $I = 1$ represents the floating structure, with all variables defined in the coordinate system $O^{(1)} - X^{(1)}Y^{(1)}Z^{(1)}$. Similarly, $I = 2$ represents the airplane, with all variables defined in the coordinate system $O^{(2)} - X^{(2)}Y^{(2)}Z^{(2)}$.

Dynamic equation of equilibrium (Fung 1977)

$$\mathbf{d}^{(I)}\boldsymbol{\sigma}^{(I)} - \mathbf{g}^{(I)} = \rho^{(I)}\ddot{\mathbf{U}}^{(I)}, \qquad I = 1,2 , \tag{4.6}$$

where

$$\boldsymbol{\sigma}^{(I)} = \left[\sigma_{xx}^{(I)}, \sigma_{yy}^{(I)}, \sigma_{zz}^{(I)}, \sigma_{xy}^{(I)}, \sigma_{yz}^{(I)}, \sigma_{zx}^{(I)}\right]^{\mathrm{T}}, \tag{4.7}$$

$$\mathbf{U}^{(I)} = \left[U_x^{(I)}, U_y^{(I)}, U_z^{(I)}\right]^{\mathrm{T}}, \tag{4.8}$$

$$\mathbf{d}^{(I)} = \begin{bmatrix} \dfrac{\partial}{\partial X^{(I)}} & 0 & 0 & \dfrac{\partial}{\partial Y^{(I)}} & 0 & \dfrac{\partial}{\partial Z^{(I)}} \\ 0 & \dfrac{\partial}{\partial Y^{(I)}} & 0 & \dfrac{\partial}{\partial X^{(I)}} & \dfrac{\partial}{\partial Z^{(I)}} & 0 \\ 0 & 0 & \dfrac{\partial}{\partial Z^{(I)}} & 0 & \dfrac{\partial}{\partial Y^{(I)}} & \dfrac{\partial}{\partial X^{(I)}} \end{bmatrix}, \tag{4.9}$$

$$\mathbf{g}^{(1)} = \left[0,\ 0,\ \rho^{(1)}g - \sum_{J=1}^{4} f_J \Delta\left(\mathbf{X}^{(1)} - \mathbf{X}_J^{(1)}\right)\right]^{\mathrm{T}}, \tag{4.10}$$

$$\mathbf{g}^{(2)} = \left[\rho^{(2)}a_x,\ 0,\ \rho^{(2)}g + \sum_{J=1}^{4} f_J \Delta\left(\mathbf{X}^{(2)} - \mathbf{X}_J^{(2)}\right)\right]^{\mathrm{T}}. \tag{4.11}$$

In these equations $\boldsymbol{\sigma}^{(I)}$ and $\mathbf{U}^{(I)}$ respectively represents the stress and displacement

vectors; $\rho^{(I)}$ is the mass density; a_x is the horizontal acceleration of the mass centre of the airplane; $\mathbf{X}^{(I)}\left(X^{(I)},Y^{(I)},Z^{(I)}\right)$ indicates a material point of substructure $I(=1,2)$ and $\mathbf{X}_J^{(1)}\left(X_J^{(1)},Y_J^{(1)},Z_J^{(1)}\right)$ indicates the position of the $J-th$ landing gear on the floating structure.

The stress and strain relation

$$\boldsymbol{\sigma}^{(I)}=\left(1+\mathrm{i}\eta^{(I)}\right)\mathbf{E}^{(I)}\boldsymbol{\varepsilon}^{(I)},\qquad I=1,2\,, \tag{4.12}$$

where the material matrix $\mathbf{E}^{(I)}$ and the strain vector $\boldsymbol{\varepsilon}^{(I)}$ are given as

$$\mathbf{E}^{(I)}=\frac{E^{(I)}\left(1-\mu^{(I)}\right)}{\left(1+\mu^{(I)}\right)\left(1-2\mu^{(I)}\right)}\begin{bmatrix} 1 & \frac{\mu^{(I)}}{1-\mu^{(I)}} & \frac{\mu^{(I)}}{1-\mu^{(I)}} & 0 & 0 & 0 \\ \frac{\mu^{(I)}}{1-\mu^{(I)}} & 1 & \frac{\mu^{(I)}}{1-\mu^{(I)}} & 0 & 0 & 0 \\ \frac{\mu^{(I)}}{1-\mu^{(I)}} & \frac{\mu^{(I)}}{1-\mu^{(I)}} & 1 & 0 & 0 & 0 \\ 0 & 0 & 0 & \frac{1-2\mu^{(I)}}{2\left(1-\mu^{(I)}\right)} & 0 & 0 \\ 0 & 0 & 0 & 0 & \frac{1-2\mu^{(I)}}{2\left(1-\mu^{(I)}\right)} & 0 \\ 0 & 0 & 0 & 0 & 0 & \frac{1-2\mu^{(I)}}{2\left(1-\mu^{(I)}\right)} \end{bmatrix}, \tag{4.13}$$

and

$$\boldsymbol{\varepsilon}^{(I)}=\left[\varepsilon_{xx}^{(I)},\varepsilon_{yy}^{(I)},\varepsilon_{zz}^{(I)},\varepsilon_{xy}^{(I)},\varepsilon_{yz}^{(I)},\varepsilon_{zx}^{(I)}\right]^{\mathrm{T}}. \tag{4.14}$$

Here, $E^{(I)}$ denotes the Young's modulus, $\mu^{(I)}$ is the Poisson ratio and $\eta^{(I)}$ represents the non – dimensional material damping factor (Fung 1977).

Strain and displacement relation

$$\boldsymbol{\varepsilon}^{(I)}=\left(\mathbf{d}^{(I)}\right)^{\mathrm{T}}\mathbf{U}^{(I)},\qquad I=1,2\,. \tag{4.15}$$

Force conditions on free boundaries of substructures

$$\sigma_{xx}^{(I)}\nu_x^{(I)}+\sigma_{xy}^{(I)}\nu_y^{(I)}+\sigma_{zx}^{(I)}\nu_z^{(I)}=0, \qquad I=1,2, \tag{4.16.1}$$

$$\sigma_{xy}^{(I)}\nu_x^{(I)}+\sigma_{yy}^{(I)}\nu_y^{(I)}+\sigma_{yz}^{(I)}\nu_z^{(I)}=0, \tag{4.16.2}$$

$$\sigma_{zx}^{(I)}\nu_x^{(I)}+\sigma_{yz}^{(I)}\nu_y^{(I)}+\sigma_{zz}^{(I)}\nu_z^{(I)}=0. \tag{4.16.3}$$

Dynamic equation of airplane's horizontal translation

The horizontal motion of the airplane satisfies the third Law of Newton and is governed by the following equations

$$F_x=m^{(2)}a_x, \tag{4.17.1}$$

$$X_J^{(1)}(t)=X_{J0}^{(1)}+\left(V_{x0}t+\frac{a_x t^2}{2}\right), \tag{4.17.2}$$

$$V_x=V_{x0}+a_x t, \tag{4.17.3}$$

where $m^{(2)}$ represents the total mass of the airplane. $\mathbf{X}_{J0}^{(1)}\left(X_{J0}^{(1)},Y_{J0}^{(1)},Z_{J0}^{(1)}\right)$ denotes the initial position of the $J-th$ landing gear on the floating structure. Equation (4.17.2) is derived based on the third assumption given at the end of Section 4.1.

Dynamic force of $J-th$ landing gear

$$f_J=K_J\left[U_z^{(2)}\left(\mathbf{X}_J^{(2)}\right)-U_z^{(1)}\left(\mathbf{X}_J^{(1)}\right)\right]+C_J\left[\dot{U}_z^{(2)}\left(\mathbf{X}_J^{(2)}\right)-\dot{U}_z^{(1)}\left(\mathbf{X}_J^{(1)}\right)\right], \quad J=1,2,3,4. \tag{4.18}$$

4.2.3 Coupling conditions on fluid – structure interaction interface

On the fluid –structure interaction interface $\sum$, the velocity of both the floating structure and the fluid are consistent along the normal direction of the interface. The internal stress of the floating structure balances the external water pressure applied on it. Therefore on the interaction interface $\sum$, the velocity of the floating structure and the velocity potential of

fluid, the stress of the floating structure and the water pressure satisfy the following conditions, respectively.

Velocity consistent condition [See Equation (2.92)]

$$\frac{\partial \phi}{\partial x^{(1)}}\eta_x + \frac{\partial \phi}{\partial y^{(1)}}\eta_y + \frac{\partial \phi}{\partial z^{(1)}}\eta_z = -\left(\dot{U}_x^{(1)}\nu_x^{(1)} + \dot{U}_y^{(1)}\nu_y^{(1)} + \dot{U}_z^{(1)}\nu_z^{(1)}\right). \tag{4.19}$$

Force equilibrium condition

$$\sigma_{xx}^{(1)}\nu_x^{(1)} + \sigma_{xy}^{(1)}\nu_y^{(1)} + \sigma_{zx}^{(1)}\nu_z^{(1)} = P\eta_x, \tag{4.20.1}$$

$$\sigma_{xy}^{(1)}\nu_x^{(1)} + \sigma_{yy}^{(1)}\nu_y^{(1)} + \sigma_{yz}^{(1)}\nu_z^{(1)} = P\eta_y, \tag{4.20.2}$$

$$\sigma_{zx}^{(1)}\nu_x^{(1)} + \sigma_{yz}^{(1)}\nu_y^{(1)} + \sigma_{zz}^{(1)}\nu_z^{(1)} = P\eta_z. \tag{4.20.3}$$

4.2.4 Initial conditions

At time $t = 0$, the fluid and the floating structure are assumed to be in their stationary equilibrium position of the system. The airplane lands with an initial velocity $\mathbf{V}_0(V_{x0}, 0, V_{z0})$ onto the floating structure. The aerodynamic lift force applied to the airplane is assumed to be released immediately when the landing commences. These initial conditions are represented as follows.

Fluid

$$\phi = 0, \qquad \dot{\phi} = 0, \qquad \ddot{\phi} = 0. \tag{4.21}$$

Floating structure

$$\mathbf{U}^{(1)} = \mathbf{0}, \qquad \dot{\mathbf{U}}^{(1)} = \mathbf{0}, \qquad \ddot{\mathbf{U}}^{(1)} = \mathbf{0}. \tag{4.22}$$

Airplane

$$\mathbf{U}^{(2)} = \mathbf{U}_0^{(2)}, \qquad \dot{\mathbf{U}}^{(2)} = \left[0, 0, V_{z0}\right]^{\mathrm{T}}, \qquad \ddot{\mathbf{U}}^{(2)} = \mathbf{0}, \tag{4.23}$$

where $\mathbf{U}_0^{(2)}$ represents the initial deformation of the airplane.

Mass centre of airplane

$$\mathbf{x}_c^{(1)} = \mathbf{x}_{c0}^{(1)}, \qquad \dot{\mathbf{x}}_c^{(1)} = \mathbf{V}_0, \qquad \ddot{\mathbf{x}}_c^{(1)} = \left[a_x,\ 0, 0\right]^{\mathrm{T}}, \tag{4.24}$$

where $\mathbf{x}_c^{(1)}\left(x_c^{(1)}, y_c^{(1)}, z_c^{(1)}\right)$ represents the position of the mass centre of the airplane in the fixed coordinate system $o^{(1)} - x^{(1)}y^{(1)}z^{(1)}$ and $\mathbf{x}_{c0}^{(1)}\left(x_{c0}^{(1)}, y_{c0}^{(1)}, z_{c0}^{(1)}\right)$ denotes its initial position.

4.3 Mode Equations of Solid Substructures

In this section, the equilibrium equation, Equation (4.6) of the two solid substructures, is transformed to the corresponding mode equation using the modal superposition method (Paz & Leigh 2004). The coupled equations of the two solid substructures are obtained through the interaction force provided by the landing gear system.

4.3.1 Mode equations of floating structure and airplane

It is assumed that the normalized natural mode matrix $\mathbf{\Phi}^{(I)}$ $\left(I = 1,2\right)$ and the corresponding natural frequencies $\omega_j^{(I)}\left(j = 1, 2,..., M^{(I)}\right)$ are obtained using the methods described in Chapter 2. Here $M^{(I)}$ represents the number of retained modes. The application of the modal superposition method allows the displacement of substructure I to be expressed as

$$\mathbf{U}^{(I)} = \begin{bmatrix} U_x^{(I)} \\ U_y^{(I)} \\ U_z^{(I)} \end{bmatrix} = \mathbf{\Phi}^{(I)}\mathbf{Q}^{(I)}, \tag{4.25}$$

where

$$\mathbf{\Phi}^{(I)} = \begin{bmatrix} \mathbf{\Phi}_x^{(I)} \\ \mathbf{\Phi}_y^{(I)} \\ \mathbf{\Phi}_z^{(I)} \end{bmatrix} = \begin{bmatrix} \Phi_{x1}^{(I)}, & \Phi_{x2}^{(I)}, & \cdots & \Phi_{xM^{(I)}}^{(I)} \\ \Phi_{y1}^{(I)}, & \Phi_{y2}^{(I)} & \cdots & \Phi_{yM^{(I)}}^{(I)} \\ \Phi_{z1}^{(I)}, & \Phi_{z2}^{(I)} & \cdots & \Phi_{zM^{(I)}}^{(I)} \end{bmatrix}, \tag{4.26}$$

$$\mathbf{Q}^{(I)} = \left[Q_1^{(I)}, Q_2^{(I)}, ..., Q_{M^{(I)}}^{(I)} \right]^{\mathrm{T}}, \tag{4.27}$$

and $\Phi_{xj}^{(I)}, \Phi_{yj}^{(I)}, \Phi_{zj}^{(I)} \left(j = 1, 2, ..., M^{(I)} \right)$ represent the displacement components of the $j-th$ mode in the three directions of the coordinate axes, respectively. $Q_j^{(I)}$ represents the corresponding generalized coordinate, which is a function of time t.

On substituting Equation (4.12) into Equation (4.6) and using the relationships of Equations (4.15) and (4.25), equilibrium equation of Equation (4.6) assumes the form

$$\left(1 + i\eta^{(I)}\right)\mathbf{d}^{(I)}\{\mathbf{E}^{(I)}\left(\mathbf{d}^{(I)}\right)^{\mathrm{T}}\mathbf{\Phi}^{(I)}\}\mathbf{Q}^{(I)} - \mathbf{g}^{(I)} = \rho^{(I)}\mathbf{\Phi}^{(I)}\ddot{\mathbf{Q}}^{(I)}, \qquad I = 1,2\,. \tag{4.28}$$

By pre-multiplying both sides of Equation (4.28) with $\left(\mathbf{\Phi}^{(I)}\right)^{\mathrm{T}}$ and integrating the resultant equation over the domain $\Omega^{(I)}$ and using Gauss theorem as well as the boundary conditions of Equations (4.16) and (4.20), Equation (4.28) is transformed into the following mode equation (see Appendix A)

$$\mathbf{M}^{(I)}\ddot{\mathbf{Q}}^{(I)} + \left(1 + i\eta^{(I)}\right)\mathbf{K}^{(I)}\mathbf{Q}^{(I)} = \mathbf{F}_i^{(I)} + \mathbf{F}_g^{(I)} + \mathbf{F}_d^{(I)}, \tag{4.29}$$

where

$$\mathbf{M}^{(I)} = \int_{\Omega^{(I)}} \left(\mathbf{\Phi}^{(I)}\right)^{\mathrm{T}} \rho^{(I)}\, \mathbf{\Phi}^{(I)} dV\,, \tag{4.30}$$

$$\mathbf{K}^{(I)} = \int_{\Omega^{(I)}} \left(\left(\mathbf{d}^{(I)}\right)^{T}\mathbf{\Phi}^{(I)}\right)^{\mathrm{T}} \mathbf{E}^{(I)}\left(\mathbf{d}^{(I)}\right)^{\mathrm{T}}\mathbf{\Phi}^{(I)} dV\,. \tag{4.31}$$

Upon appealing to Equations (4.10) and (4.11), it follows that the $\mathbf{g}^{(I)}$ term of Equation (4.6) leads to

$$\mathbf{F}_i^{(I)} = (-1)^{I+1}\sum_{J=1}^{4} \int_{\Omega^{(I)}} \left(\mathbf{\Phi}_z^{(I)}\right)^{\mathrm{T}} f_J \Delta\left(\mathbf{X}^{(I)} - \mathbf{X}_J^{(I)}\right) dV \tag{4.32}$$

and

$$\mathbf{F}_g^{(I)} = -\int_{\Omega^{(I)}} \left(\mathbf{\Phi}_z^{(I)}\right)^{\mathrm{T}} \rho^{(I)} g \, dV \tag{4.33}$$

As demonstrated in Appendix A, on applying Gauss theorem to the equilibrium equation of the floating structure, the first term of Equation (4.28) yields two terms. One term is $\mathbf{K}^{(1)}$ in Equation (4.31). The other term is related to the water pressure, given in Equation (4.20), exerted on the bottom surface of the floating structure and it is expressible in the form

$$\mathbf{F}_d^{(1)} = -\int_{\Sigma} \left(\mathbf{\Phi}^{(1)}\right)^{\mathrm{T}} \boldsymbol{\eta} \, P dS \, . \tag{4.34}$$

And Equation (4.11) leads to

$$\mathbf{F}_d^{(2)} = -\int_{\Omega^{(2)}} \left(\mathbf{\Phi}_x^{(2)}\right)^{\mathrm{T}} \rho^{(2)} a_x \, dV \, . \tag{4.35}$$

Here, $\mathbf{M}^{(I)}$ is the generalized mass matrix and $\mathbf{K}^{(I)}$ is the generalized stiffness matrix. $\mathbf{F}_i^{(I)}$ and $\mathbf{F}_g^{(I)}$ represent respectively the generalized force from the landing gear system and gravity. $\mathbf{F}_d^{(1)}$ is the generalized force from the water pressure applied on the floating structure. $\mathbf{F}_d^{(2)}$ is the generalized force from the inertia of the airplane.

On substituting Equation (4.25) into Equation (4.18), the interaction force f_J in Equation (4.32), provided by each suspension unit, can be expressed as

$$f_J = K_J \left[\mathbf{\Phi}_z^{(2)}\left(\mathbf{X}_J^{(2)}\right)\mathbf{Q}^{(2)} - \mathbf{\Phi}_z^{(1)}\left(\mathbf{X}_J^{(1)}\right)\mathbf{Q}^{(1)}\right] + C_J\left[\mathbf{\Phi}_z^{(2)}\left(\mathbf{X}_J^{(2)}\right)\dot{\mathbf{Q}}^{(2)} - \mathbf{\Phi}_z^{(1)}\left(\mathbf{X}_J^{(1)}\right)\dot{\mathbf{Q}}^{(1)}\right],$$

$$J = 1,2,3,4 \, . \tag{4.36}$$

Upon comparing Equations (2.34) and (4.29) and then appealing to Equations (2.35) and (2.37) respectively, the normalized characteristics of the mode matrix $\mathbf{\Phi}^{(I)}$ allow $\mathbf{M}^{(I)}$ and $\mathbf{K}^{(I)}$ of Equation (4.29) to be expressed as

$$\mathbf{M}^{(I)} = \mathbf{I}^{(I)} \tag{4.37}$$

and

$$\mathbf{K}^{(I)} = \mathbf{\Lambda}^{(I)}, \tag{4.38}$$

where

$$\mathbf{\Lambda}^{(I)} = \begin{bmatrix} \left(\omega_1^{(I)}\right)^2 & & & \\ & \left(\omega_2^{(I)}\right)^2 & & \\ & & \ddots & \\ & & & \left(\omega_{M^{(I)}}^{(I)}\right)^2 \end{bmatrix}. \tag{4.39}$$

Clearly $\mathbf{I}^{(I)}$ represents a unit diagonal matrix of order $M^{(I)}$.

4.3.2 Coupled equation of two substructures

On substituting Equation (4.36) into Equation (4.32) and utilizing the characteristics of the Dirac delta function $\Delta(\ )$, the mode equations for the two distinct solid substructures in Equation (4.29), subject to Equations (4.37) and (4.38), are merged into the coupled form

$$\begin{bmatrix} \ddot{\mathbf{Q}}^{(1)} \\ \ddot{\mathbf{Q}}^{(2)} \end{bmatrix} + \begin{bmatrix} \mathbf{C}_{11}(t) & \mathbf{C}_{12}(t) \\ \mathbf{C}_{21}(t) & \mathbf{C}_{22} \end{bmatrix} \begin{bmatrix} \dot{\mathbf{Q}}^{(1)} \\ \dot{\mathbf{Q}}^{(2)} \end{bmatrix} + \begin{bmatrix} \left(1+i\eta^{(1)}\right)\mathbf{\Lambda}^{(1)} + \mathbf{K}_{11}(t) & \mathbf{K}_{12}(t) \\ \mathbf{K}_{21}(t) & \left(1+i\eta^{(2)}\right)\mathbf{\Lambda}^{(2)} + \mathbf{K}_{22} \end{bmatrix} \begin{bmatrix} \mathbf{Q}^{(1)} \\ \mathbf{Q}^{(2)} \end{bmatrix} = \begin{bmatrix} \mathbf{F}_g^{(1)} \\ \mathbf{F}_g^{(2)} \end{bmatrix} + \begin{bmatrix} \mathbf{F}_d^{(1)} \\ \mathbf{F}_d^{(2)} \end{bmatrix}, \tag{4.40}$$

where the landing system damping dependent terms $\mathbf{C}_{ij}(t)$ are expressed in the form

$$\mathbf{C}_{11}(t) = \sum_{J=1}^{4} \left(\mathbf{\Phi}_z^{(1)}\left(\mathbf{X}_J^{(1)}\right)\right)^{\mathrm{T}} C_J \mathbf{\Phi}_z^{(1)}\left(\mathbf{X}_J^{(1)}\right), \tag{4.41}$$

$$\mathbf{C}_{12}(t) = -\sum_{J=1}^{4} \left(\mathbf{\Phi}_z^{(1)}\left(\mathbf{X}_J^{(1)}\right)\right)^{\mathrm{T}} C_J \mathbf{\Phi}_z^{(2)}\left(\mathbf{X}_J^{(2)}\right), \tag{4.42}$$

$$\mathbf{C}_{21}(t) = -\sum_{J=1}^{4} \left(\mathbf{\Phi}_z^{(2)}\left(\mathbf{X}_J^{(2)}\right)\right)^{\mathrm{T}} C_J \mathbf{\Phi}_z^{(1)}\left(\mathbf{X}_J^{(1)}\right), \tag{4.43}$$

$$\mathbf{C}_{22} = \sum_{J=1}^{4} \left(\mathbf{\Phi}_z^{(2)}\left(\mathbf{X}_J^{(2)}\right)\right)^{\mathrm{T}} C_J \mathbf{\Phi}_z^{(2)}\left(\mathbf{X}_J^{(2)}\right) \tag{4.44}$$

and the landing gear system stiffness dependent terms $\mathbf{K}_{ij}(t)$ assume the form

$$\mathbf{K}_{11}(t)=\sum_{J=1}^{4}\left(\boldsymbol{\Phi}_{z}^{(1)}\left(\mathbf{X}_{J}^{(1)}\right)\right)^{\mathrm{T}}K_{J}\boldsymbol{\Phi}_{z}^{(1)}\left(\mathbf{X}_{J}^{(1)}\right), \tag{4.45}$$

$$\mathbf{K}_{12}(t)=-\sum_{J=1}^{4}\left(\boldsymbol{\Phi}_{z}^{(1)}\left(\mathbf{X}_{J}^{(1)}\right)\right)^{\mathrm{T}}K_{J}\boldsymbol{\Phi}_{z}^{(2)}\left(\mathbf{X}_{J}^{(2)}\right), \tag{4.46}$$

$$\mathbf{K}_{21}(t)=-\sum_{J=1}^{4}\left(\boldsymbol{\Phi}_{z}^{(2)}\left(\mathbf{X}_{J}^{(2)}\right)\right)^{\mathrm{T}}K_{J}\boldsymbol{\Phi}_{z}^{(1)}\left(\mathbf{X}_{J}^{(1)}\right), \tag{4.47}$$

$$\mathbf{K}_{22}=\sum_{J=1}^{4}\left(\boldsymbol{\Phi}_{z}^{(2)}\left(\mathbf{X}_{J}^{(2)}\right)\right)^{\mathrm{T}}K_{J}\boldsymbol{\Phi}_{z}^{(2)}\left(\mathbf{X}_{J}^{(2)}\right). \tag{4.48}$$

Having formulated the structural problem, the fluid problem will be addressed next.

4.4 Boundary Element Equation of Fluid Domain

The fundamental solution or Green function $G(p,q)$ of a 3D infinite fluid domain is required to satisfy the following equations [See Equation (2.108)]

$$\nabla^{2}G=\Delta(p-q), \quad \text{in} \quad \Omega_{f} \tag{4.49}$$

and

$$\frac{\partial G}{\partial x^{(1)}}\eta_{x}+\frac{\partial G}{\partial y^{(1)}}\eta_{y}+\frac{\partial G}{\partial z^{(1)}}\eta_{z}=0, \quad \text{on} \quad \text{both } \Gamma_{\infty} \text{ and } \Gamma_{b} \tag{4.50}$$

subject to p denoting a generic fluid field point located at $(x_{p}^{(1)},y_{p}^{(1)},z_{p}^{(1)})$ and q indicating the location of a source point $(x_{q}^{(1)},y_{q}^{(1)},z_{q}^{(1)})$ within the fluid domain described with respect to the fixed coordinate system $o^{(1)}-x^{(1)}y^{(1)}z^{(1)}$.

The Green function $G(p,q)$ is simply a Rankine source satisfying [See Equation (2.113)]

$$G(p,q)=\frac{1}{4\pi r}, \tag{4.51}$$

where $r = \sqrt{(x_p^{(1)} - x_q^{(1)})^2 + (y_p^{(1)} - y_q^{(1)})^2 + (z_p^{(1)} - z_q^{(1)})^2}$. From Equation (2.121), the sought velocity potential ϕ satisfies

$$\phi_q = \int_S \left\{ G(p,q)\left(\frac{\partial \phi_p}{\partial x^{(1)}}\eta_x + \frac{\partial \phi_p}{\partial y^{(1)}}\eta_y + \frac{\partial \phi_p}{\partial z^{(1)}}\eta_z \right) - \phi_p\left(\frac{\partial G(p,q)}{\partial x^{(1)}}\eta_x + \frac{\partial G(p,q)}{\partial y^{(1)}}\eta_y + \frac{\partial G(p,q)}{\partial z^{(1)}}\eta_z \right) \right\} dS, \tag{4.52}$$

where $S = \Gamma_f \cup \Gamma_\infty \cup \Gamma_b \cup \Sigma$ is the boundary of fluid domain. ϕ_p represents the velocity potential at field point p and ϕ_q represents the velocity potential at source point q. On substituting Equations (4.3) to (4.5), (4.19) and (4.50) into Equation (4.52) and letting the field point p approach the boundary of the fluid domain, it is found (Subsection 2.4.2) that

$$\frac{\phi_q}{2} = \int_{\Gamma_f + \Sigma} \left(-\phi_p \left(\frac{\partial G(p,q)}{\partial x^{(1)}}\eta_x + \frac{\partial G(p,q)}{\partial y^{(1)}}\eta_y + \frac{\partial G(p,q)}{\partial z^{(1)}}\eta_z \right) \right) dS - \int_{\Gamma_f} \frac{G(p,q)}{g}\ddot{\phi}_p dS + \int_{\Sigma} G(p,q)\left(\dot{\mathbf{U}}^{(1)}\right)^{\mathrm{T}} \cdot \boldsymbol{\eta}\, dS, \tag{4.53}$$

where the integrations and the derivatives are defined for the field point p on the boundaries. In the last term of Equation (4.53), the V_n of Equation (2.92) has been expressed in terms of the structural displacement $\mathbf{U}^{(1)}$ of Equation (4.25).

For simplicity, constant boundary elements are used herein to discretize the boundary of the fluid domain. It is assumed that the boundaries Γ_f and Σ of the fluid domain are divided into N_f and N_Σ constant elements, respectively. The two sets of boundary elements associated with the free surface Γ_f and fluid-structure interaction interface Σ are designated $\overline{N}_f$ and $\overline{N}_\Sigma$. The constant value of the velocity potential on the j^{th}

boundary element is represented by $\phi_j(t)$. Implementing the numerical solution explained in Subsection 2.4.3, the integrations in Equation (4.53) are expressible in the form

$$\begin{aligned}\frac{\phi_i}{2} = &\sum_{j=1}^{N_f+N_\Sigma} \phi_j \int_{S_j} -\left(\frac{\partial G(j,i)}{\partial x^{(1)}}\eta_x + \frac{\partial G(j,i)}{\partial y^{(1)}}\eta_y + \frac{\partial G(j,i)}{\partial z^{(1)}}\eta_z \right) dS \\ &-\frac{1}{g}\sum_{j\in\overline{N}_f} \ddot{\phi}_j \int_{S_j} G(j,i)dS + \sum_{j\in\overline{N}_\Sigma} \int_{S_j} G(j,i)\left(\dot{\mathbf{U}}^{(1)}\right)^{\mathrm{T}} \cdot \boldsymbol{\eta} dS,\end{aligned} \tag{4.54}$$

where $i = 1,2,..., N_f + N_\Sigma$. Equation (4.54) can be rewritten in the matrix form

$$\mathbf{G}\ddot{\boldsymbol{\Psi}} + \mathbf{H}\boldsymbol{\Psi} = \overline{\mathbf{G}}\dot{\mathbf{Q}}^{(1)}, \tag{4.55}$$

with ij^{th} element of the matrices $\mathbf{G}$, $\mathbf{H}$ and $\overline{\mathbf{G}}$ defined by

$$G_{ij} = \begin{cases} \dfrac{1}{g}\displaystyle\int_{S_j} G(j,i)dS, & j \in \overline{N}_f, \\ 0, & j \notin \overline{N}_f, \end{cases} \qquad i, j = 1,2,..., N_f + N_\Sigma, \tag{4.56}$$

$$\begin{gathered}H_{ij} = \int_{S_j} \left(\frac{\partial G(j,i)}{\partial x^{(1)}}\eta_x + \frac{\partial G(j,i)}{\partial y^{(1)}}\eta_y + \frac{\partial G(j,i)}{\partial z^{(1)}}\eta_z \right) dS + \frac{\delta_{ij}}{2}, \\ i, j = 1,2,..., N_f + N_\Sigma,\end{gathered} \tag{4.57}$$

$$\begin{gathered}\overline{G}_{ij} = \int_\Sigma G(p,i)\left(\Phi_{xj}^{(1)}\eta_x + \Phi_{yj}^{(1)}\eta_y + \Phi_{zj}^{(1)}\eta_z\right) dS, \\ i = 1,2,..., N_f + N_\Sigma,\ j = 1,2,..., M^{(1)},\end{gathered} \tag{4.58}$$

and

$$\boldsymbol{\Psi} = [\phi_1(t), \phi_2(t), ..., \phi_{N_f+N_\Sigma}(t)]^{\mathrm{T}} \ . \tag{4.59}$$

Here the first N_Σ components of the velocity potential vector $\boldsymbol{\Psi}$ lay on the fluid – structure interaction interface Σ and is denoted by $\overline{\boldsymbol{\Psi}}$. The other components of $\boldsymbol{\Psi}$ are on the free surface Γ_f.

According to the definition in Equation (4.56), $\mathbf{G}$ is a matrix whose first N_Σ

columns are zero. Matrix $\mathbf{H}$ defined in Equation (4.57) is an anti-symmetric matrix provided that the normal of the boundaries $\Gamma_f + \sum$ is a constant. Therefore, the matrices $\mathbf{G}$ and $\mathbf{H}$ are not symmetric.

4.5 Mixed Mode Function - Boundary Element Equation

Equations (4.40) and (4.55) provide a set of matrix equations formulating the mixed mode function – boundary element method to simulate the dynamics of the airplane – floating structure – water interaction system subject to airplane landing impacts.

The vertical position $z^{(1)}$ of the wetted interaction interface $\sum$ is expressed in terms of the displacement of the floating structure and the initial draught as

$$z^{(1)} = U_z^{(1)} - d = \mathbf{\Phi}_z^{(1)}\mathbf{Q}^{(1)} - d\,, \tag{4.60}$$

upon appealing to Equation (4.25) and the definition of $\mathbf{\Phi}^{(1)}$ in Equation (4.26).

Substitution of Equation (4.60) into Equation (4.2) yields the following expression for water pressure

$$P = -\rho\frac{\partial\phi}{\partial t} - \rho g\left(\mathbf{\Phi}_z^{(1)}\mathbf{Q}^{(1)} - d\right). \tag{4.61}$$

The generalized force $\mathbf{F}_d^{(1)}$ of Equation (4.34) can be rewritten as follows

$$\mathbf{F}_d^{(1)} = -\rho\int_{\sum}\left(\mathbf{\Phi}^{(1)}\right)^{\mathrm{T}}\boldsymbol{\eta}\frac{\partial\phi}{\partial t}dS - \rho g\int_{\sum}\left(\mathbf{\Phi}^{(1)}\right)^{\mathrm{T}}\boldsymbol{\eta}\mathbf{\Phi}_z^{(1)}\mathbf{Q}^{(1)}dS + \rho g d\int_{\sum}\left(\mathbf{\Phi}^{(1)}\right)^{\mathrm{T}}\boldsymbol{\eta}\,dS\,, \tag{4.62}$$

upon substitution of the expression for P in Equation (4.61).

The integrals on the right hand side of Equation (4.62) need to be transformed to a summation of integrals over all the boundary elements defining on the wetted surface $\sum$. Performing this transformation, it is found that

$$\mathbf{F}_d^{(1)} = -\rho\sum_{j=1}^{N_\Sigma}\dot{\phi}_j\int_{S_j}\left(\mathbf{\Phi}^{(1)}\right)^{\mathrm{T}}\boldsymbol{\eta}dS - \rho g\sum_{j=1}^{N_\Sigma}\int_{S_j}\left(\mathbf{\Phi}^{(1)}\right)^{\mathrm{T}}\boldsymbol{\eta}\mathbf{\Phi}_z^{(1)}\mathbf{Q}^{(1)}dS + \rho g d\sum_{j=1}^{N_\Sigma}\int_{S_j}\left(\mathbf{\Phi}^{(1)}\right)^{\mathrm{T}}\boldsymbol{\eta}\,dS\,. \tag{4.63}$$

Upon defining

$$\mathbf{G}_1 = \left[\int_{S_1} \left(\mathbf{\Phi}^{(1)}\right)^{\mathrm{T}} \boldsymbol{\eta}\, dS,\ \int_{S_2} \left(\mathbf{\Phi}^{(1)}\right)^{\mathrm{T}} \boldsymbol{\eta}\, dS,\ \cdots,\ \int_{S_{N_\Sigma}} \left(\mathbf{\Phi}^{(1)}\right)^{\mathrm{T}} \boldsymbol{\eta}\, dS \right], \tag{4.64}$$

$$\mathbf{G}_2 = \sum_{j=1}^{N_\Sigma} \int_{S_j} \left(\mathbf{\Phi}^{(1)}\right)^{\mathrm{T}} \boldsymbol{\eta}\, \mathbf{\Phi}_z^{(1)} dS \tag{4.65}$$

and

$$\mathbf{G}_3 = \sum_{j=1}^{N_\Sigma} \int_{S_j} \left(\mathbf{\Phi}^{(1)}\right)^{\mathrm{T}} \boldsymbol{\eta}\ dS\ , \tag{4.66}$$

Equation (4.63) can be written in the matrix form

$$\mathbf{F}_d^{(1)}(t) = -\rho\, \mathbf{G}_1 \overline{\dot{\mathbf{\Psi}}}(t) - \rho g \mathbf{G}_2 \mathbf{Q}^{(1)}(t) + \rho g d \mathbf{G}_3 . \tag{4.67}$$

$\overline{\dot{\mathbf{\Psi}}}(t)$ represents the first order time derivative of the unknown velocity potential on the wetted surface $\sum$.

The substitution of Equation (4.67) into Equation (4.40) produces the following equation

$$\begin{bmatrix} \ddot{\mathbf{Q}}^{(1)}(t) \\ \ddot{\mathbf{Q}}^{(2)}(t) \end{bmatrix} + \begin{bmatrix} \mathbf{C}_{11}(t) & \mathbf{C}_{12}(t) \\ \mathbf{C}_{21}(t) & \mathbf{C}_{22} \end{bmatrix} \begin{bmatrix} \dot{\mathbf{Q}}^{(1)}(t) \\ \dot{\mathbf{Q}}^{(2)}(t) \end{bmatrix} + \begin{bmatrix} \mathbf{\Lambda}^{(1)} + \mathbf{K}_{11}(t) + \rho g \mathbf{G}_2 & \mathbf{K}_{12}(t) \\ \mathbf{K}_{21}(t) & \mathbf{\Lambda}^{(2)} + \mathbf{K}_{22} \end{bmatrix} \begin{bmatrix} \mathbf{Q}^{(1)}(t) \\ \mathbf{Q}^{(2)}(t) \end{bmatrix} = \begin{bmatrix} -\rho \mathbf{G}_1 \overline{\dot{\mathbf{\Psi}}}(t) \\ \mathbf{F}_g^{(2)} + \mathbf{F}_d^{(2)} \end{bmatrix}. \tag{4.68}$$

Here, it is assumed that the gravity of the floating structure is balanced by the hydrostatic force induced by the initial draught d and the dynamic displacement and hydro-pressure measured from the static equilibrium state is considered, so that the term involving the draught d has been cancelled in Equation (4.68).

The Equations (4.55) and (4.68) are coupled through the first order derivative $\overline{\dot{\mathbf{\Psi}}}(t)$ of velocity potential defined on the wetted surface $\sum$ and the generalized velocity vector $\dot{\mathbf{Q}}^{(1)}$. These two equations are next rewritten in the global form

$$\begin{bmatrix} \mathbf{I}^{(1)} & \mathbf{0} & \mathbf{0} \\ \mathbf{0} & \mathbf{I}^{(2)} & \mathbf{0} \\ \mathbf{0} & \mathbf{0} & \mathbf{G} \end{bmatrix} \begin{bmatrix} \ddot{\mathbf{Q}}^{(1)}(t) \\ \ddot{\mathbf{Q}}^{(2)}(t) \\ \ddot{\mathbf{\Psi}} \end{bmatrix} + \begin{bmatrix} \mathbf{C}_{11}(t) & \mathbf{C}_{12}(t) & \mathbf{G}_4 \\ \mathbf{C}_{21}(t) & \mathbf{C}_{22} & \mathbf{0} \\ -\overline{\mathbf{G}} & \mathbf{0} & \mathbf{0} \end{bmatrix} \begin{bmatrix} \dot{\mathbf{Q}}^{(1)}(t) \\ \dot{\mathbf{Q}}^{(2)}(t) \\ \dot{\mathbf{\Psi}} \end{bmatrix}$$
$$+ \begin{bmatrix} \mathbf{\Lambda}^{(1)} + \mathbf{K}_{11}(t) + \rho g \mathbf{G}_2 & \mathbf{K}_{12}(t) & \mathbf{0} \\ \mathbf{K}_{21}(t) & \mathbf{\Lambda}^{(2)} + \mathbf{K}_{22} & \mathbf{0} \\ \mathbf{0} & \mathbf{0} & \mathbf{H} \end{bmatrix} \begin{bmatrix} \mathbf{Q}^{(1)}(t) \\ \mathbf{Q}^{(2)}(t) \\ \mathbf{\Psi} \end{bmatrix} = \begin{bmatrix} \mathbf{0} \\ \mathbf{F}_g^{(2)} + \mathbf{F}_d^{(2)} \\ \mathbf{0} \end{bmatrix}, \tag{4.69}$$

where

$$\mathbf{G}_4 = \begin{bmatrix} \rho \mathbf{G}_1 & \mathbf{0} \end{bmatrix}. \tag{4.70}$$

The coupled Equation (4.69) has two main characteristics. First, the aircraft's travelling on the floating structure produces transient time – dependent interaction loads between the airplane and the floating structure, hence the stiffness and damping matrices in Equation (4.69) are time – dependent.

Secondly, the fluid –structure interaction brings in some non symmetrical matrices in Equation (4.69), which involves the velocity potential $\mathbf{\Psi}$, its first $\dot{\mathbf{\Psi}}$ and second order derivatives $\ddot{\mathbf{\Psi}}$ with respect to time t, and the generalized velocity $\dot{\mathbf{Q}}^{(1)}$. As explained above $\mathbf{G}$ and $\mathbf{H}$ are not symmetric matrices. On comparing Equation (4.58) with Equation (4.64), it is readily observed that matrix $\mathbf{G}_4$ is not the transpose of the matrix $-\overline{\mathbf{G}}$. As a result of this, none of the three coefficient matrices on the left hand side of Equation (4.69) is symmetric. This characteristic makes the classical time integration schemes based on symmetrical matrices unable to be used to solve Equation (4.69). The developed approach to solve this non-symmetrical matrix equation is discussed next in Chapter 5.

Chapter 5

Time Integration Scheme

In this chapter, the time integration scheme of the mixed mode function – boundary element equation as formulated in Equation (4.69) is discussed.

Generally speaking, Equation (4.69) is a set of second order differential equations whose coefficient matrices are not symmetric. Due to the large size and the non-symmetrical characteristics, the current available time integration methods discussed in Section 2.2 and the related software can not be directly used to solve Equation (4.69). To address this difficulty, instead of solving the final coupled formulation of Equation (4.69), a time integration scheme is proposed to solve Equation (4.68) describing the motions of the two solid substructures and Equation (4.55) describing the fluid flows. The ideas are based on the Newmark procedure and it is referred to as a substitution scheme. Details of the solution procedure are explained next.

5.1 Solution Procedure

As observed in Equations (4.55) and (4.68), the fluid – structure interaction equations are coupled through the first order derivatives $\overline{\dot{\boldsymbol{\Psi}}}$ and $\dot{\mathbf{Q}}^{(1)}$. To solve these coupled equations, we intend to express $\overline{\dot{\boldsymbol{\Psi}}}$ as a function of $\dot{\mathbf{Q}}^{(1)}$ and other obtained values at the previous time step. The Newmark formulation (Newmark 1959) provides a bridge to realise our aim. Appealing to Equations (2.60) and (2.59) respectively, the velocity potential $\boldsymbol{\Psi}(t)$ and its first order time derivative $\dot{\boldsymbol{\Psi}}(t)$ are expressed as

$$\boldsymbol{\Psi}(t) = \boldsymbol{\Psi}(t-\Delta t) + \dot{\boldsymbol{\Psi}}(t-\Delta t)\Delta t + [(\frac{1}{2}-\alpha)\ddot{\boldsymbol{\Psi}}(t-\Delta t) + \alpha\ddot{\boldsymbol{\Psi}}(t)]\Delta t^2 \tag{5.1}$$

and

$$\dot{\boldsymbol{\Psi}}(t) = \dot{\boldsymbol{\Psi}}(t-\Delta t) + [(1-\delta)\ddot{\boldsymbol{\Psi}}(t-\Delta t) + \delta\ddot{\boldsymbol{\Psi}}(t)]\Delta t\,, \tag{5.2}$$

where α and δ are two parameters from Newmark formulation and Δt is the time step.

The values of the three parameters α, δ and Δt and their influence on the numerical results will be discussed in Subsection 5.2.1 and 5.2.2.

In order to transform Equation (4.55) into one equation which only involves $\dot{\boldsymbol{\Psi}}(t)$ and $\dot{\mathbf{Q}}^{(1)}(t)$, the velocity potential $\boldsymbol{\Psi}(t)$ and its second order time derivative $\ddot{\boldsymbol{\Psi}}(t)$ are expressed in terms of $\dot{\boldsymbol{\Psi}}(t)$ as

$$\boldsymbol{\Psi}(t) = a_1\dot{\boldsymbol{\Psi}}(t) + \boldsymbol{\Psi}(t-\Delta t) + a_2\dot{\boldsymbol{\Psi}}(t-\Delta t) + a_3\ddot{\boldsymbol{\Psi}}(t-\Delta t), \tag{5.3}$$

$$\ddot{\boldsymbol{\Psi}}(t) = a_4[\dot{\boldsymbol{\Psi}}(t) - \dot{\boldsymbol{\Psi}}(t-\Delta t)] + a_5\ddot{\boldsymbol{\Psi}}(t-\Delta t), \tag{5.4}$$

where $a_1 = \dfrac{\alpha\,\Delta t}{\delta}$, $a_2 = (1-\dfrac{\alpha}{\delta})\Delta t$, $a_3 = (\dfrac{1}{2}-\dfrac{\alpha}{\delta})\Delta t^2$, $a_4 = \dfrac{1}{\delta\,\Delta t}$, $a_5 = 1-\dfrac{1}{\delta}$.

The substitution of Equations (5.3) and (5.4) into Equation (4.55) yields

$$\begin{aligned}\dot{\boldsymbol{\Psi}}(t)[a_4\mathbf{G} + a_1\mathbf{H}] = \overline{\mathbf{G}}\dot{\mathbf{Q}}^{(1)} - \mathbf{H}\boldsymbol{\Psi}(t-\Delta t) + [a_4\mathbf{G} - a_2\mathbf{H}]\dot{\boldsymbol{\Psi}}(t-\Delta t)\\ -[a_5\mathbf{G} + a_3\mathbf{H}]\ddot{\boldsymbol{\Psi}}(t-\Delta t),\end{aligned} \tag{5.5a}$$

also written as

$$\dot{\boldsymbol{\Psi}}(t) = \mathbf{A}_4\dot{\mathbf{Q}}^{(1)}(t) + \mathbf{A}_6(t-\Delta t). \tag{5.5b}$$

Subject to

$$\mathbf{A}_4 = \mathbf{A}_5\overline{\mathbf{G}}, \tag{5.6}$$

$$\mathbf{A}_5 = [a_4\mathbf{G} + a_1\mathbf{H}]^{-1}, \tag{5.7}$$

$$\mathbf{A}_6(t-\Delta t) = \mathbf{A}_1\boldsymbol{\Psi}(t-\Delta t) + \mathbf{A}_2\dot{\boldsymbol{\Psi}}(t-\Delta t) + \mathbf{A}_3\ddot{\boldsymbol{\Psi}}(t-\Delta t) \tag{5.8}$$

and the additional parameters

$$\mathbf{A}_1 = -\mathbf{A}_5\mathbf{H}, \tag{5.9}$$

$$\mathbf{A}_2 = \mathbf{A}_5[a_4\mathbf{G} - a_2\mathbf{H}], \tag{5.10}$$

and

$$\mathbf{A}_3 = -\mathbf{A}_5[a_5\mathbf{G} + a_3\mathbf{H}]. \tag{5.11}$$

As observed in Equation (5.5b), the first order time derivative of the velocity potential $\dot{\boldsymbol{\Psi}}(t)$ is expressed in terms of the generalized velocity $\dot{\mathbf{Q}}^{(1)}(t)$ in association with other known quantities $\mathbf{A}_6(t-\Delta t)$ at the previous time step $t-\Delta t$. Thus Equation (5.5b) are of a form consistent with the assumptions of the Newmark method. Extracting those $\dot{\boldsymbol{\Psi}}(t)$ which is now denoted by $\overline{\dot{\boldsymbol{\Psi}}}(t)$ on the fluid – structure interaction interface $\sum$ from Equation (5.5b) we can formulate a truncated equation. That is

$$\overline{\dot{\boldsymbol{\Psi}}}(t)=\overline{\mathbf{A}}_4\dot{\mathbf{Q}}^{(1)}(t)+\overline{\mathbf{A}}_6(t-\Delta t), \tag{5.12}$$

where

$$\overline{\mathbf{A}}_4=\overline{\mathbf{A}}_5\overline{\mathbf{G}}, \tag{5.13}$$

$$\overline{\mathbf{A}}_6(t-\Delta t)=\overline{\mathbf{A}}_1\boldsymbol{\Psi}(t-\Delta t)+\overline{\mathbf{A}}_2\dot{\boldsymbol{\Psi}}(t-\Delta t)+\overline{\mathbf{A}}_3\ddot{\boldsymbol{\Psi}}(t-\Delta t), \tag{5.14}$$

and matrices $\overline{\mathbf{A}}_1,...,\overline{\mathbf{A}}_6$ are truncated from $\mathbf{A}_1,...,\mathbf{A}_6$ in a similar way as that of $\overline{\dot{\boldsymbol{\Psi}}}(t)$ from $\dot{\boldsymbol{\Psi}}(t)$.

The substitution of Equation (5.12) into Equation (4.68) yields the alternative equation

$$\begin{bmatrix}\ddot{\mathbf{Q}}^{(1)}(t)\\ \ddot{\mathbf{Q}}^{(2)}(t)\end{bmatrix}+\begin{bmatrix}\mathbf{C}_{11}(t)+\rho\,\mathbf{G}_1\overline{\mathbf{A}}_4 & \mathbf{C}_{12}(t)\\ \mathbf{C}_{21}(t) & \mathbf{C}_{22}\end{bmatrix}\begin{bmatrix}\dot{\mathbf{Q}}^{(1)}(t)\\ \dot{\mathbf{Q}}^{(2)}(t)\end{bmatrix}+\begin{bmatrix}\boldsymbol{\Lambda}^{(1)}+\mathbf{K}_{11}(t)+\rho g\mathbf{G}_2 & \mathbf{K}_{12}(t)\\ \mathbf{K}_{21}(t) & \boldsymbol{\Lambda}^{(2)}+\mathbf{K}_{22}\end{bmatrix}\begin{bmatrix}\mathbf{Q}^{(1)}(t)\\ \mathbf{Q}^{(2)}(t)\end{bmatrix}=\begin{bmatrix}-\rho\mathbf{G}_1\overline{\mathbf{A}}_6(t-\Delta t)\\ \mathbf{F}_g^{(2)}+\mathbf{F}_d^{(2)}\end{bmatrix}. \tag{5.15}$$

It is necessary to clarify that the term $\rho\,\mathbf{G}_1\overline{\mathbf{A}}_4$ causes the non-symmetry of the generalized damping matrix in Equation (5.15), whilst the generalized stiffness matrix is symmetric. In this case, the traditional Newark solution procedure based on symmetrical matrices is still not applicable. Therefore the direct solution of Equation (5.15) will be more time – consuming than those with symmetric coefficient matrices. However, considering the capacity of current PCs, the computation time for solving Equation (5.15) is bound to be practical. For this reason, we stick to solving Equation (5.15) directly with

the non – symmetrical matrix.

It is also worthy noting that there is yet an alternative method to solve Equation (5.15) by moving the non – symmetrical term $\rho \mathbf{G}_1 \overline{\mathbf{A}}_4 \dot{\mathbf{Q}}^{(1)}(t)$ from the left hand side to the right hand side with its value at time *t* replaced by the approximate value at the previous time step $t - \Delta t$. This approximation avoids solving a large non – symmetrical matrix equation (Bathe 1996).

Using Newmark's formulation again, we express the generalized acceleration $\ddot{\mathbf{Q}}^{(1)}(t), \ddot{\mathbf{Q}}^{(2)}(t)$ and velocity $\dot{\mathbf{Q}}^{(1)}(t), \dot{\mathbf{Q}}^{(2)}(t)$ in the following forms

$$\begin{bmatrix} \ddot{\mathbf{Q}}^{(1)}(t) \\ \ddot{\mathbf{Q}}^{(2)}(t) \end{bmatrix} = a_6 \left(\begin{bmatrix} \mathbf{Q}^{(1)}(t) \\ \mathbf{Q}^{(2)}(t) \end{bmatrix} - \begin{bmatrix} \mathbf{Q}^{(1)}(t-\Delta t) \\ \mathbf{Q}^{(2)}(t-\Delta t) \end{bmatrix} \right) - a_7 \begin{bmatrix} \dot{\mathbf{Q}}^{(1)}(t-\Delta t) \\ \dot{\mathbf{Q}}^{(2)}(t-\Delta t) \end{bmatrix} - a_8 \begin{bmatrix} \ddot{\mathbf{Q}}^{(1)}(t-\Delta t) \\ \ddot{\mathbf{Q}}^{(2)}(t-\Delta t) \end{bmatrix}, \quad (5.16)$$

$$\begin{bmatrix} \dot{\mathbf{Q}}^{(1)}(t) \\ \dot{\mathbf{Q}}^{(2)}(t) \end{bmatrix} = a_9 \left(\begin{bmatrix} \mathbf{Q}^{(1)}(t) \\ \mathbf{Q}^{(2)}(t) \end{bmatrix} - \begin{bmatrix} \mathbf{Q}^{(1)}(t-\Delta t) \\ \mathbf{Q}^{(2)}(t-\Delta t) \end{bmatrix} \right) - a_{10} \begin{bmatrix} \dot{\mathbf{Q}}^{(1)}(t-\Delta t) \\ \dot{\mathbf{Q}}^{(2)}(t-\Delta t) \end{bmatrix} - a_{11} \begin{bmatrix} \ddot{\mathbf{Q}}^{(1)}(t-\Delta t) \\ \ddot{\mathbf{Q}}^{(2)}(t-\Delta t) \end{bmatrix}, \quad (5.17)$$

where $a_6 = \frac{1}{\alpha \Delta t^2}, a_7 = \frac{1}{\alpha \Delta t}, a_8 = \frac{1}{2\alpha} - 1, a_9 = \frac{\delta}{\alpha \Delta t}, a_{10} = \frac{\delta}{\alpha} - 1$ and $a_{11} = \frac{\Delta t}{2}(\frac{\delta}{\alpha} - 2)$.

Substituting Equations (5.16) and (5.17) into Equation (5.15) yields a time integration equation

$$\left[\tilde{\mathbf{K}} + a_6 \tilde{\mathbf{M}} + a_9 \tilde{\mathbf{C}}\right] \begin{bmatrix} \mathbf{Q}^{(1)}(t) \\ \mathbf{Q}^{(2)}(t) \end{bmatrix} = \mathbf{R}(t-\Delta t) + \mathbf{R}_{\mathbf{a}}(t-\Delta t) + \mathbf{R}_{\mathbf{v}}(t-\Delta t), \quad (5.18)$$

where on the left hand side

$$\tilde{\mathbf{K}} = \begin{bmatrix} \mathbf{\Lambda}^{(1)} + \mathbf{K}_{11}(t) + \rho g \mathbf{G}_2 & \mathbf{K}_{12}(t) \\ \mathbf{K}_{21}(t) & \mathbf{\Lambda}^{(2)} + \mathbf{K}_{22} \end{bmatrix}, \quad (5.19)$$

$$\tilde{\mathbf{M}} = \begin{bmatrix} \mathbf{I}^{(1)} & \mathbf{0} \\ \mathbf{0} & \mathbf{I}^{(2)} \end{bmatrix}, \quad (5.20)$$

$$\tilde{\mathbf{C}} = \begin{bmatrix} \mathbf{C}_{11}(t) + \rho \mathbf{G}_1 \overline{\mathbf{A}}_4 & \mathbf{C}_{12}(t) \\ \mathbf{C}_{21}(t) & \mathbf{C}_{22} \end{bmatrix} \quad (5.21)$$

and on the right hand side

$$\mathbf{R}(t-\Delta t)=\begin{bmatrix} -\rho\mathbf{G}_1\overline{\mathbf{A}}_6(t-\Delta t) \\ \mathbf{F}_g^{(2)}+\mathbf{F}_d^{(2)} \end{bmatrix}, \tag{5.22}$$

$$\mathbf{R}_{\mathbf{a}}(t-\Delta t)=\tilde{\mathbf{M}}\left[a_6\begin{bmatrix}\mathbf{Q}^{(1)}(t-\Delta t)\\ \mathbf{Q}^{(2)}(t-\Delta t)\end{bmatrix}+a_7\begin{bmatrix}\dot{\mathbf{Q}}^{(1)}(t-\Delta t)\\ \dot{\mathbf{Q}}^{(2)}(t-\Delta t)\end{bmatrix}+a_8\begin{bmatrix}\ddot{\mathbf{Q}}^{(1)}(t-\Delta t)\\ \ddot{\mathbf{Q}}^{(2)}(t-\Delta t)\end{bmatrix}\right] \tag{5.23}$$

and

$$\mathbf{R}_{\mathbf{v}}(t-\Delta t)=\tilde{\mathbf{C}}\left[a_9\begin{bmatrix}\mathbf{Q}^{(1)}(t-\Delta t)\\ \mathbf{Q}^{(2)}(t-\Delta t)\end{bmatrix}+a_{10}\begin{bmatrix}\dot{\mathbf{Q}}^{(1)}(t-\Delta t)\\ \dot{\mathbf{Q}}^{(2)}(t-\Delta t)\end{bmatrix}+a_{11}\begin{bmatrix}\ddot{\mathbf{Q}}^{(1)}(t-\Delta t)\\ \ddot{\mathbf{Q}}^{(2)}(t-\Delta t)\end{bmatrix}\right]. \tag{5.24}$$

Equations (5.5b), (5.12) and (5.18) provide a set of time integration equations to solve the mixed mode function – boundary element equations describing the complex transient dynamics of the airplane – floating structure – water interaction system. To apply these equations, it is assumed that the values of the required variables at time $t-\Delta t$ are available, for example $t-\Delta t=0$ representing time at which the initial conditions are prescribed. Figure 5.1 shows a flow chart to integrate the numerical equations derived previously to obtain the values of all required variables at time t. Following completion of all calculations for time step t, the calculation can advance to the next time step for time $t+\Delta t$. The calculation process illustrated in Figure 5.1 continues until such time as there is no interest in further analysis of the problem.

5.2 Stability and Accuracy Analyses

The proposed time integration process is a variation of the traditional Newmark scheme and so the requirement for stability and accuracy of the analysis is considered to be similar to that for the Newmark method of time integration. The stability and accuracy of the proposed time integration scheme is discussed and summarized in this section, which is primarily concerned with the selection of the two parameters α and δ (used in the Newmark formulation) and the time step Δt.

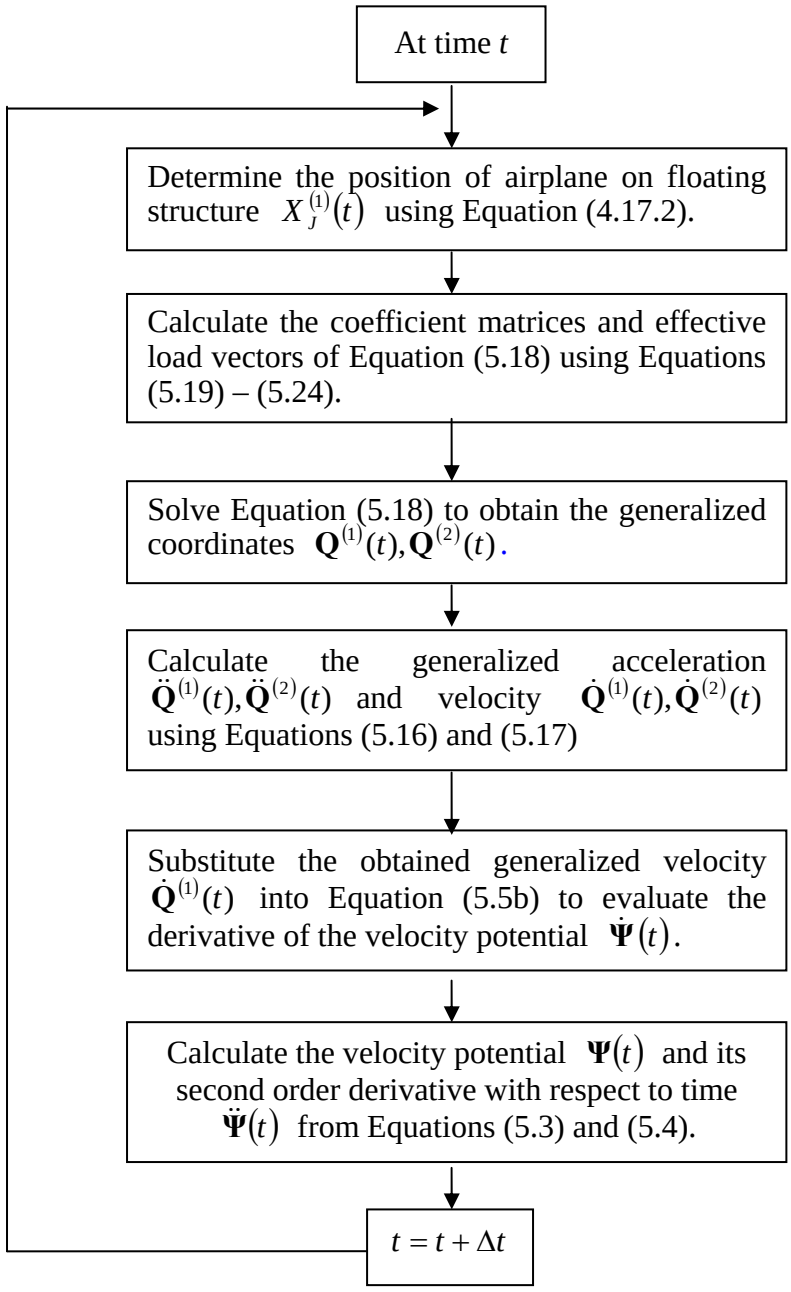

Figure 5.1 Flow chart of the time integration scheme

5.2.1 Selection of parameters α and δ

The two parameters α and δ of a Newmark time integration scheme can be varied to obtain optimum stability and accuracy. The Newmark integration scheme is unconditionally stable provided that $\delta \geq 0.5$ and $\alpha \geq 0.25(\delta + 0.5)^2$. And the two

expressions of the Newmark assumption have second – order accuracy when $\delta = 0.5$. Newmark originally proposed an unconditionally stable scheme, the constant – average – acceleration method also known as trapezoidal rule, where $\delta = 0.5$ and $\alpha = 0.25$ are adopted**.** The trapezoidal rule is an unconditionally stable time integration scheme with second – order accuracy and it is commonly used in many engineering situations due to its good performance. Thus, it is adopted in this thesis for the time integration scheme.

5.2.2 Selection of time step Δt

The choice of an appropriate time step Δt is very important, especially for those conditionally stable time integration schemes.

For general time integration equation, for example Equation (5.18), the time step Δt would have to be selected according to the "smallest period" of the retained natural vibration modes of the system. If the smallest period of the system is T_n, then Δt would have to be about $T_n / 10$.

To determine the smallest period T_n of a structure system, it is necessary to consider the period of the external excitation force T_e. It is generally accepted that the primary response of the system lies in those modes with a natural period greater than $T_e / 3$. Therefore in most cases retaining only these modes should be sufficient to describe the dynamic response of the system under the prescribed external force. This principle is adopted in this thesis to determine the truncation frequency of the modal analysis of the airplane and the floating structure according to the frequency of the landing impacts.

Chapter 6

Program Implementation

Following the derivations presented in Chapters 4 and 5, a Mixed Mode Function – Boundary Element Program, designated MMFBEP, is developed to solve the dynamic responses of the airplane – floating structure – water interaction system excited by airplane landing impacts. In this chapter the developed program MMFBEP is introduced.

6.1 Introduction of Program MMFBEP

Program MMFBEP (presented in Appendix B) is written using FORTRAN-90 language and it consists of 1688 original FORTRAN sentences. To execute this program, two input files need to be prepared.

The first input file is INPUTP.DAT in which main control parameters are provided. These include the number of nodes, degrees of freedom and retained modes of both airplane and floating structure; dimension of floating structure and surrounding fluid domain; initial landing velocity and landing position of airplane; coefficients of landing gear system, etc.

The second input file is INPUTM.DAT in which the modal information including the retained natural frequencies and the corresponding modes of both the airplane and the floating structure are provided. These natural frequencies and modes should be obtained using one of the available approaches including theoretical analysis methods, finite element calculations and experimental measurements as discussed in Chapter 2. For example, if the airplane or the floating structure is approximately modelled by a beam then the analytical frequencies and modes can be readily found. However, for a real airplane and floating structure, the most efficient approach to obtain the modal information is using FEA method. In this thesis, ANSYS (2004) is adopted to carry out the modal analysis for both the airplane and the floating structure.

The output file of program MMFBEP can provide the following simulation results: 1)

the dynamic displacement, velocity and acceleration responses of the airplane and the floating structure; 2) the hydrodynamic pressure at the wetted surface of the floating structure, as well as the resultant forces and moments; 3) the impact forces of the landing gear system. These output data can be used as input information to further calculate the dynamic stresses in the airplane and the floating structure using the same commercial FEA software as used to obtain the modal information to prepare input file INPUTM.DAT

The detailed format, contents and data structures of these two input files and the output file are described and illustrated in Section 6.5.

Program MMFBEP is currently executed based on any PC machines with a 2.4 GHz processor, memory of 512MB, a hard disk of 80GB and supported by the Microsoft Windows XP Home Edition (Version 2002) operating system. The running times of the program are indicated following each of the numerical simulations presented in the following chapters.

6.2 Function of Program MMFBEP

Program MMFBEP allows the airplane to have rather arbitrary structural types, such as a mass, an elastic beam, a beam frame or a more complex structure.

A real floating airport must have a flat surface of length in kilometres and width in hundreds of metres. Therefore, this type of structure can be simplified as a thin plate. When the length/width ratio is large enough, we can even use a beam to model the floating airport. For this reason, three structural types, namely a mass, an elastic beam and a flexible thin plate, are considered to model the floating structure in program MMFBEP. A MMFBEP program control parameter NDFS is used to specify the structural type of the floating structure with the settings:

$$\mathrm{NDFS} = \begin{cases} 1, & \text{mass type floating structure,} \\ 2, & \text{beam type floating structure,} \\ 3, & \text{plate type floating structure.} \end{cases}$$

Program MMFBEP is capable of dealing with 2D and 3D fluid domain. Parameter

NDFD is used to indicate the dimension of fluid domain:

$$\text{NDFD} = \begin{cases} 2, & \text{2D fluid domain,} \\ 3, & \text{3D fluid domain.} \end{cases}$$

Based on these two control parameters, program MMFBEP provides a tool for analyzing the dynamic responses of a structure landing and travelling on another floating structure in a general sense. To illustrate the proposed mixed mode function – boundary element method, as developed in program MMFBEP, three distinct numerical examples are provided in Chapters 7, 8, and 9. The situations investigated are

1) A mass – spring – damper system drops onto a mass floating on the surface of a 2D and 3D fluid domain, respectively. In this example, both the airplane and the floating structure are modelled with mass, which may be useful in the preliminary design stage of a floating airport in order to evaluate the initial landing impact.

2) An elastic beam supported by a spring – damper unit at its centre lands and travels on another floating beam in 2D and 3D fluid domain, in which the airplane and the floating structure are simplified as two elastic beams, respectively. This example may provide some insights into the airplane's landing and travelling effect onto a flexible floating structure.

3) An approximate model of a Boeing 747-400 jumbo jet lands and travels on a thin – plate type floating structure in a 3D fluid domain. The airplane is modelled as a beam frame. This example can give us a more realistic understanding of the dynamics of the airplane – floating structure – water interaction system.

6.3 Structure of Program MMFBEP

The structure of program MMFBEP is summarized in the flow chart of Figure 6.1. The program consists of the following four principal stages.

Stage 1

Read in the control parameters from input file INPUTP.DAT together with the nodal and modal information of both the airplane and the floating structure from input file

INPUTM.DAT.

Stage 2

Evaluate all the time – independent coefficients involved in Equation (5.15). This requires the evaluation of matrices $\mathbf{\Lambda}^{(I)}(I=1,2)$, $\mathbf{C}_{22}$, $\mathbf{K}_{22}$, $\mathbf{G}_1$, $\mathbf{G}_2$ and $\overline{\mathbf{A}}_4$, and vectors $\mathbf{F}_g^{(2)}$ and $\mathbf{F}_d^{(2)}$.

Stage 3

Carry out time integration scheme for the coupled Equations (5.15) and (4.55) within a time stepping DO-LOOP statement. Within each loop, the time – dependent coefficients in Equation (5.15) need to be determined first. These coefficients include matrices $\mathbf{C}_{11}(t)$, $\mathbf{K}_{11}(t)$, $\mathbf{C}_{12}(t)$, $\mathbf{K}_{12}(t)$, $\mathbf{C}_{21}(t)$, $\mathbf{K}_{21}(t)$ and vector $\overline{\mathbf{A}}_6(t-\Delta t)$. After all the coefficient matrices and vectors are determined, Equation (5.15) is solved using the time integration approach described in Chapter 5. Starting from the prescribed initial condition, the floating structure and airplane generalized coordinates $\mathbf{Q}^{(1)}(t)$ and $\mathbf{Q}^{(2)}(t)$, their velocities $\dot{\mathbf{Q}}^{(1)}(t)$ and $\dot{\mathbf{Q}}^{(2)}(t)$ and the accelerations $\ddot{\mathbf{Q}}^{(1)}(t)$ and $\ddot{\mathbf{Q}}^{(2)}(t)$ are determined. Knowledge of the generalized velocity of the floating structure $\dot{\mathbf{Q}}^{(1)}(t)$ permits the velocity potential $\mathbf{\Psi}(t)$ and its first and second order time derivatives $\dot{\mathbf{\Psi}}(t)$ and $\ddot{\mathbf{\Psi}}(t)$ to be calculated from Equations (5.3), (5.4) and (5.5b). When all the quantities at the current time step t have been evaluated, the loop will go to the next time instant $t+\Delta t$ until reaching the end of simulation. After the execution of the DO-LOOP statement, the solution of the coupled Equations (5.15) and (4.55) is available as a time series covering the whole simulation process.

Stage 4

Produce the output file with the dynamic responses of the airplane – floating structure – water interaction system stored in a predefined order and format.

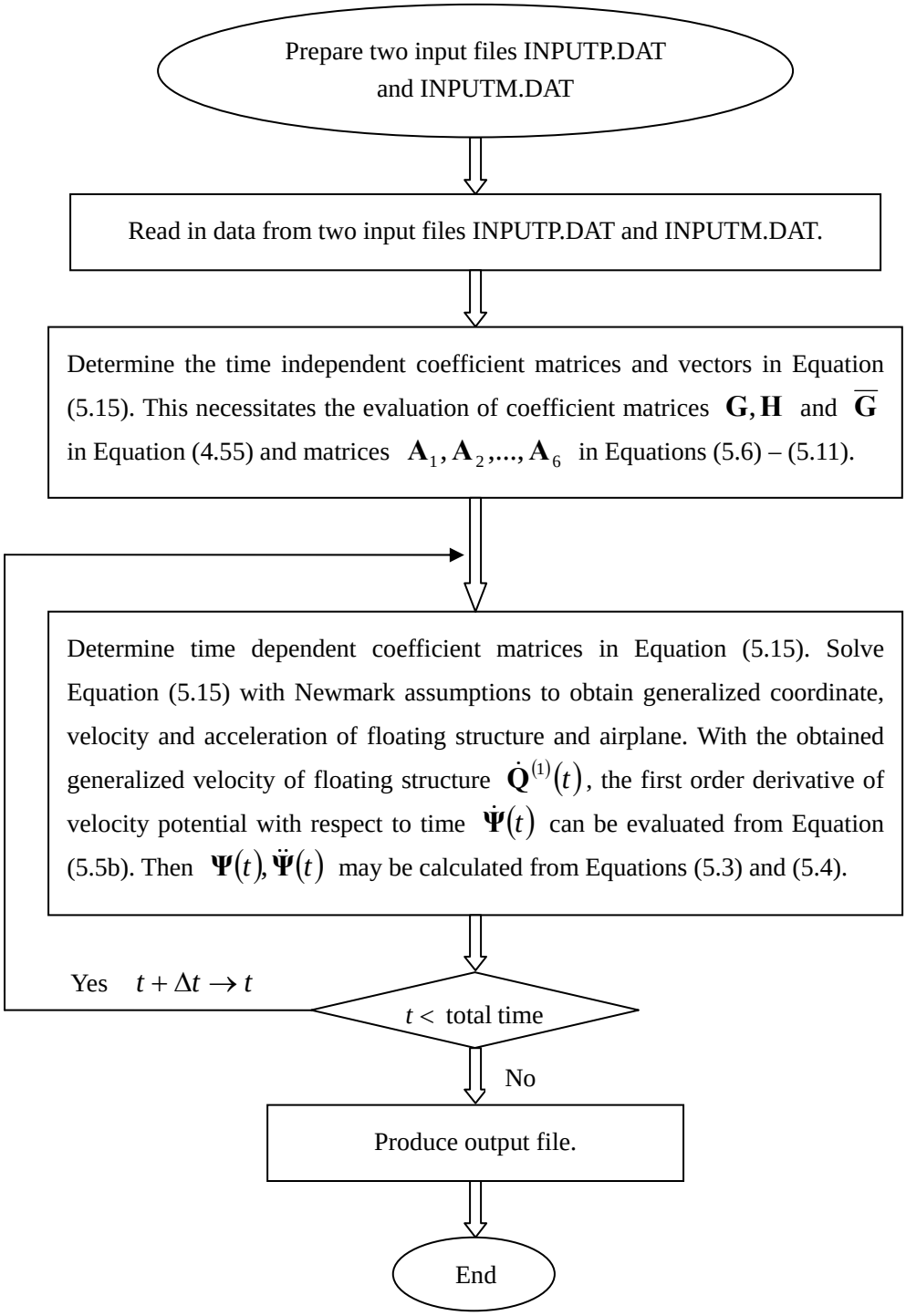

Figure 6.1 Flow chart of program MMFBEP

6.4 Characteristics of Program MMFBEP

MMFBEP has been developed as a user – friendly program and is straightforward to use. Some of its characteristics are summarized next.

User control of input file INPUTP.DAT

Every parameter required to set up the model of the airplane – floating structure – water interaction system is defined in the input file INPUTP.DAT. The user controls all aspects of the problem by specifying the control parameters. For example, the user can define the structural type of the floating structure by parameter NDFS.

User control over output file

The user can define when and where the simulation results should be written into the output file. For example, the user can define at which time step and on which node the responses of the airplane and the floating structure are required. The control parameters for the output file are also defined in the input file INPUTP.DAT.

Modularized structure

The structure of program MMFBEP is modularized with four key subroutines whose names and functions are listed in Table 6.1. As explained in Section 6.3, stages 2 and 3 of program MMFBEP form the main body of the numerical calculation, which only consist of 300 original FORTRAN sentences. Thus the main structure of program MMFBEP is simple to be understood by the user.

Table 6.1 Subroutines of program MMFBEP

Name	Function
GF3	Calculate coefficient matrices **G** and **H** in Equation (4.55) for 3D fluid domain
GF2	Calculate coefficient matrices **G** and **H** in Equation (4.55) for 2D fluid domain
GG2AND3	Calculate two transform matrices. One is used to transform the nodal displacement vector of the floating structure to the vertical displacement vector at the centre of each element. Another is used to transform the water pressure vector at the centre of each element of the floating structure to its equivalent nodal force vector.
B11TO44	Calculate four transform matrices. They are used to transform the nodal displacement vector of the floating structure to the vertical displacement at the position of the $J-th$ landing gear $(J=1,2,3,4)$, respectively.

Readability

Program MMFBEP has plenty of comment lines to help to increase its readability. Furthermore all the variables, constants, functions and subroutines appearing in the program are named in a way according to their physical meaning or their corresponding symbol used in the general derivation in Chapters 4 and 5.

Memory saving

A large number of quantities are used in program MMFBEP and thus the usage of PC memory is considerable when executing the program. To reduce the use of memory and speed up the execution process, an ALLOCATABLE ARRAY is used to define all the vector and matrix variables in the program. The benefit of doing this is that when a variable is no longer in use in the program, the memory used to store it can be released by a DEALLOCATE statement. To further reduce memory demands without losing numerical accuracy, single precision data type is adopted throughout the entire program.

Direct solution scheme of equation

The interactions between the floating structure and the surrounding water introduce non – symmetric terms into the mode equation of the floating structure. Consequently a conventional triangularization scheme is not applicable in terms of solving the coupled mode equation of the airplane and the floating structure herein. Instead, the coupled Equation (5.15) has to be solved directly in program MMFBEP, which can make the solution process more time-consuming.

6.5 User Manual for Program MMFBEP

6.5.1 Write input file INPUTP.DAT

INPUTP.DAT comes together with program MMFBEP and it is given by the program developer. What the user needs to do is to fill in all the required control parameters following a designed sequence and format. A sample of input file INPUTP.DAT is given in Appendix C.

Two points should be stressed before filling in the input file INPUTP.DAT:

1) INPUTP.DAT provides explanations for all the input parameters. Each input parameter should occupy one single line of the file and it should be input in the line just after its explanation line. There is a blank line between one input parameter and the explanation line for the next input parameter. The line structure of INPUTP.DAT mustn't be changed.

2) When the data type for an input parameter is real, it must be input in decimal format, for example, unity should be input as "1.0" rather than integer "1".

To further provide a clear understanding, all the parameters appearing in INPUTP.DAT are listed below together with their definitions and input units. The data type of each parameter is defined by FORTRAN default rules, for example, variables beginning with I, J, K, L, M, and N are of integer type while all others are of real type.

N1	number of nodes of floating structure
ND1	number of degrees of freedom of floating structure
NM1	number of retained modes of floating structure
NE1	number of elements of floating structure
NEX1	number of elements along longitudinal axis of floating structure
NEY1	number of elements along transverse axis of floating structure
N2	number of nodes of airplane
ND2	number of degrees of freedom of airplane
NM2	number of retained modes of airplane
NT	number of time steps used in time integration scheme
NZ	ratio of length/width of water surface over length/width of floating structure
NDFD	dimension of fluid domain which equals two for 2D fluid domain and three for 3D fluid domain
NDFS	type of floating structure which equals one for mass type, two for beam type and three for thin plate type

	floating structure
NOUTPUT1, **…**, **NOUTPUT5**	number of five time steps at which responses are output
AMASS	total mass of airplane, unit kilogram
TIME	total time of simulation, unit second
ANGLEX	angle between runway and longitudinal axis of floating structure, unit radian
VH	initial horizontal velocity of airplane, unit m/s
AH	horizontal deceleration of airplane, unit m/s^2
VZ	initial vertical velocity of airplane, unit m/s
FLX	length of floating structure, unit m
FLY	width of floating structure, unit m
DF	initial draught of floating structure, unit m
SK1, C1,…, SK4, C4	spring and damping coefficients of landing gear 1, …, 4, unit of spring coefficient N/s, unit of damping coefficient Ns/m. (When the number of landing gears or the connecting points between the two solid structures is less than four, make the spring and damping coefficients of the non-existent landing gears equal to those of landing gear 1. For example, when the number of landing gears is three, SK4= SK1 and C4= C1. This also applies to the definition of the following parameters X01, Y01, …, X04, Y04 and NS1, …, NS4.)
X01, **Y01**, **…**, **X04**, **Y04**	initial coordinates of the connecting point between landing gear 1, …, 4 and the floating structure, unit m
NS1, …, **NS4**	number of the four nodes on airplane which are connected to landing gear 1, …, 4
NF1, **…**, **NF10**	number of ten nodes on floating structure at which the responses are outputted. (When the number of interested nodes for output is less than ten for the floating structure, make the number of the non – interested node

	equal to NF1. For example when the number of interested nodes is eight, NF10= NF9= NF1. The same applies to the definition of parameters NEF1, …, NEF10 and NL1,…, NL5.)
NEF1, **…**, **NEF10**	number of ten elements on floating structure at which time history of water pressure is output
NL1, **…**, **NL5**	number of five nodes on airplane at which the responses are output

6.5.2 Generation of input file INPUTM.DAT

The input file INPUTM.DAT is produced by the user according to the specified sequence and format defined by the program developer. As explained in previous sections, INPUTM.DAT should contain the nodal coordinates, natural frequencies and modes of both the airplane and the floating structure. A sample of input file INPUTM.DAT is given in Appendix D.

The numbering of node and element should follow the rules indicated in Figure 6.2 for a beam or a plate – type floating structure, respectively. The numbering of node and element of the airplane is rather arbitrary. It is assumed in the program that each node of the airplane and the floating structure has three degrees of freedom: One vertical displacement and two rotations about the longitudinal and transverse axes of the two solid substructures, respectively.

The required input data of INPUTM.DAT is listed next according to the order they appear in the file.

X22(N2)	longitudinal nodal coordinate of airplane in its Lagrangian coordinate system from node 1 to node N2, unit in metre
Y22(N2)	transverse nodal coordinate of airplane in its Lagrangian coordinate system from node 1 to node N2, unit in metre

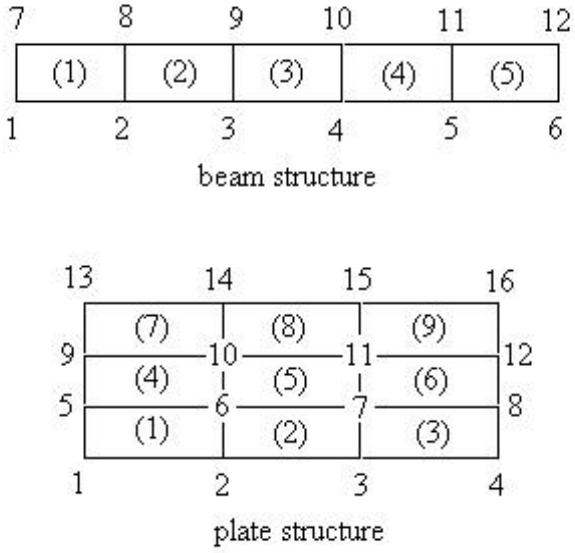

Figure 6.2 Numbering of nodes and elements for floating structure

OMEG2(NM2) natural frequencies of airplane from mode 1 to mode NM2, unit in Hz

FAI2(ND2, NM2) natural modes of airplane from mode 1 to mode NM2. Within each mode, the first N2 input data are the nodal vertical displacement with unit in metre; the next N2 input data are the nodal rotation about longitudinal axis and the last N2 input data are the nodal rotation about the transverse axis with unit in radian

X11(N1) longitudinal nodal coordinate of floating structure in its Lagrangian coordinate system from node 1 to node N1, unit in metre

Y11(N1) transverse nodal coordinate of floating structure in its Lagrangian coordinate system from node 1 to node N1, unit in metre

OMEG1(NM1) natural frequencies of floating structure from mode 1 to mode NM1, unit in Hz

FAI1(ND1, NM1) natural modes of floating structure from mode 1 to mode NM1. Within each mode, the first N1 input data are the nodal vertical

displacement with unit in metre; the next N1 input data are the nodal rotation about longitudinal axis and the last N1 input data are the nodal rotation about transverse axis with unit in radian

6.5.3 Contents of output file

The responses of the airplane – floating structure – water interaction system are written into an output file automatically once program MMFBEP is executed. A sample of the output file is given in Appendix E. As explained in Section 6.4, the user can control when and where the responses are outputted by setting relevant control parameters in the input file INPUTP.DAT. In this section, all the output data are listed according to their sequence in the output file.

WZ2(N2)	distribution of the vertical displacement of the airplane, unit in metre; **W1**(N1) distribution of the vertical displacement of the floating structure, unit in metre; **PD**(NE1) distribution of the water pressure at the bottom of the floating structure, unit in N/m^2 at the five time instants defined by parameter NOUTPUT1, …, NOUTPUT5
WL1(NT), **…**, **WL5**(NT)	time history of the vertical displacement at the five nodes of the airplane defined by NL1,…, NL5
WLV1(NT), …, **WLV5**(NT)	time history of the vertical velocity at the five nodes of the airplane defined by NL1,…, NL5
WLA1(NT), …, **WLA5**(NT)	time history of the vertical acceleration at the five nodes of the airplane defined by NL1, …, NL5
WF1(NT), …, **WF10**(NT)	time history of the vertical displacement at the ten nodes of the floating structure defined by NF1,…, NF10
WFV1(NT), …, **WFV10**(NT)	time history of the vertical velocity at the ten nodes of the floating structure defined by NF1, …, NF10
WFA1(NT), …, **WFA10**(NT)	time history of the vertical acceleration at the ten nodes

	of the floating structure defined by NF1, …, NF10
PD1(NT), …, **PD10**(NT)	time history of the water pressure applied at the ten elements on the bottom of the floating structure defined by parameter NEF1, …, NEF10
RW1(NT), **…**, **RW4**(NT)	time history of the relative displacement between the airplane and the floating structure at the four landing gears
FKC1(NT), **…**, **FKC4**(NT)	time history of the force provided by the four landing gears
FKC(NT)	time history of the total force provided by the landing gear system
FD(NT)	time history of the total force from water pressure applied on the floating structure

Having explained how the computer program reflects the problem formulation of Chapters 4 and 5, the application of the generated code is now presented in the next three chapters for three distinct scenarios defined at the end of Section 6.2.

Chapter 7

A Mass–Spring–Damper System Dropping onto a Floating Mass

The first application of the developed analysis procedure addresses the dynamics of a mass – spring – damper system dropping onto a floating mass. In this case both the airplane and the floating structure are modelled as two masses and the landing gear system is modelled as a linear spring – damper unit. This scenario is solved using three models.

Initially the problem is solved in a 2D fluid domain using the author's program MMFBEP. Under prescribed initial conditions, the dynamic responses of the dropping mass and the floating mass, as well as the forces acting on the floating mass due to the spring – damper unit and the surrounding water are calculated. Next, the same problem is solved for a 3D fluid domain. The simulation results for the case of 2D and 3D fluid domains are compared at the end of this chapter.

Finally, to validate the computer simulated results for a 2D fluid domain a different approach is used to solve the problem. The hydrodynamic force applied on the floating mass is now approximated by an additional inertial force and a damping force that are represented by a frequency dependent added mass and damping coefficient, respectively. In order to do so, we assume that the floating mass undergoes a sinusoidal heave motion. The amplitude of the heave motion is constant and relatively small. Several examples of the added mass and damping coefficients for the heave motion of 2D cylinders are given by Wehausen (1971). With these results, the added mass and damping coefficients of the floating mass considered herein can be obtained. The hydrostatic buoyancy force due to the heave motion of the floating mass is modelled with a spring. Thus the original problem of a mass – spring – damper system dropping onto a floating mass in a 2D fluid domain is replaced by the approximate problem of a mass – spring – damper system dropping onto another mass – spring – damper system, which has theoretical solutions. Results obtained from this approximate scheme compare very favourably with those obtained from program MMFBEP.

7.1 General Description

The airplane and the floating structure used in the general derivation described in Chapter 4 are now reduced to two rigid bodies in this chapter, namely the dropping mass and the floating mass. The motions of these masses are constrained to the vertical direction and consequently we have $\mathbf{U}^{(I)} = \left[0, 0, U_z^{(I)},\right]^{\mathrm{T}}$ $(I = 1,2)$. The mass – spring – damper system drops onto the mass centre of the floating mass with an initial velocity $\mathbf{V}_0\left(0, 0, V_{z0}\right)$. Since there is no horizontal translation of the dropping mass along the floating mass, the horizontal velocity $V_{x0} = V_x = 0$ and the horizontal acceleration $a_x = 0$. The number of suspension units is reduced to one and this is fixed to the mass centre of the dropping mass (we use $J = 1$ to denote it). Figure 7.1 describes the mass – spring – damper system dropping onto a floating mass. The floating mass is denoted by $m^{(1)}$ and it has width B, length L, thickness T and initial draught d.

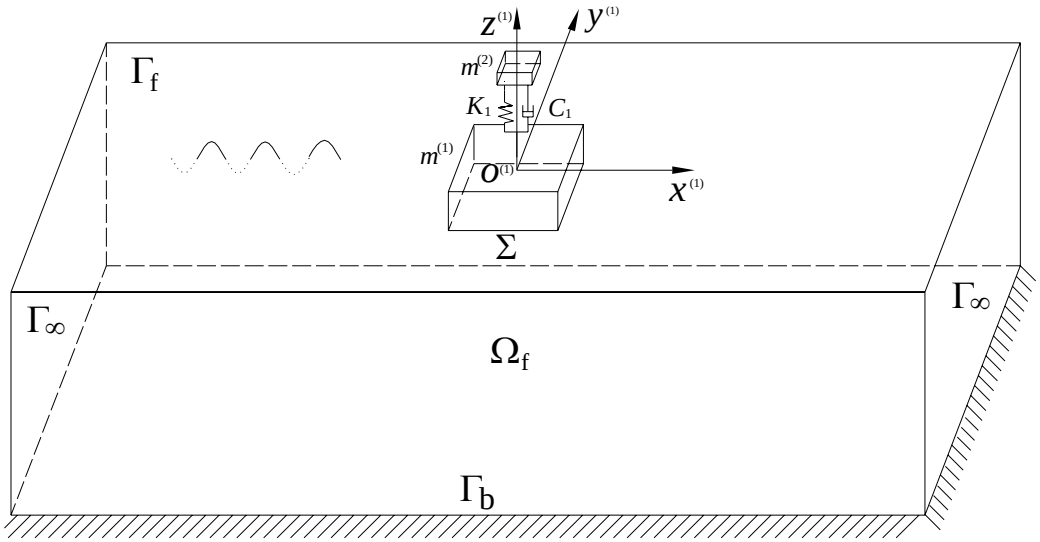

Figure 7.1 A mass – spring – damper system dropping onto a floating mass

The derivation of the problem investigated in this chapter may be understood as a simplification of the general derivation presented in Chapter 4. On considering a 2D fluid domain, the Green function given in Equation (4.51) should be replaced by its 2D

equivalent

$$G(p,q) = -\frac{1}{2\pi}\ln r\,, \tag{7.1}$$

where $r = \sqrt{(x_p^{(1)} - x_q^{(1)})^2 + (z_p^{(1)} - z_q^{(1)})^2}$.

With the basic problem defined, its numerical solution can be investigated next.

7.2 Numerical Simulation

7.2.1 Simulation in 2D fluid domain

The mass – spring – damper system of mass $m^{(2)} = 10.0\text{kg}$ has a spring coefficient of $K_1 = 1\times10^3\text{N/m}$ and a damping value $C_1 = 1\times10^2\text{Ns/m}$ drops onto the floating structure of mass $m^{(1)} = 125.0\text{kg}$, length $L = 1.0\text{m}$, width $B = 0.5\text{m}$, depth $T = 0.5\text{m}$ and initial draught $d = 0.25\text{m}$, with an initial velocity of $V_{z0} = -0.2\text{m/s}$. The motion of the dropping mass and the floating mass are measured in the coordinate system $o^{(2)} - x^{(2)}y^{(2)}z^{(2)}$ and $o^{(1)} - x^{(1)}y^{(1)}z^{(1)}$, respectively. The gravitational acceleration $g = 9.80\text{m/s}^2$ and the mass density of water $\rho = 1000\text{kg/m}^3$ are used in the calculation.

The natural frequency of the floating mass in salt water is given by $\sqrt{\rho gBL/m^{(1)}}/2\pi$ (ignoring added mass influences). For the parameter values provided this equals 1.0Hz. The corresponding natural frequency of the dropping mass is equal to $\sqrt{K_1/m^{(2)}}/2\pi = 1.6\text{Hz}$ and by considering the damper's damping effect, the frequency of the dropping mass – spring – damper system is equal to 1.38Hz.

The water depth of the 2D fluid domain is assumed to be infinite. The range of free surface retained on each side of the floating mass is about 300 times the floating mass's width and it is assumed that the velocity of fluid at the far field boundary is negligibly small, thus satisfying the undisturbed condition. The wetted interaction interface and the retained free surface are idealized by 1 and 600 constant boundary elements, respectively.

The total simulation time is 10s and the time step $\Delta t = 1.0 \times 10^{-2}\text{s}$ is used in the time integration scheme.

The two input files INPUTP.DAT and INPUTM.DAT can be easily formulated following the guidance provided in Chapter 6. The running time of program MMFBEP is about 15 seconds for solving the problem in the 2D fluid domain.

The responses of the mass – spring – damper system dropping onto the floating mass in 2D fluid domain are shown in Figures 7.4 – 7.11 and indicated by "2D".

7.2.2 Simulation in 3D fluid domain

The dynamic responses of the mass – spring – damper system dropping onto the floating mass are now solved in a 3D fluid domain with program MMFBEP. The surface of the retained fluid domain is rectangular with its centre point at $o^{(1)}$, length $41L$ and width $41B$. At the corresponding far field boundary of the retained fluid domain, it is assumed that the velocity of fluid is negligibly small thus the undisturbed condition is satisfied. The fluid – structure interaction interface and the free surface are idealized by 1 and $41 \times 41 - 1 = 1680$ constant boundary elements, respectively. The total simulation time and the time step are the same as those used in the simulation with a 2D fluid domain.

By re-setting NDFD=3 and NZ=41 in the input file INPUTP.DAT for 2D fluid domain, the corresponding input file for 3D fluid domain is obtained. The input file INPUTM.DAT for 3D fluid domain remains the same as that for 2D fluid domain. The running time of program MMFBEP is about 3 minutes for solving the problem in the 3D fluid domain.

The responses of the mass – spring – damper system dropping onto the floating mass in 3D fluid domain are presented in Figures 7.4 – 7.11 and indicated by "3D".

7.3 Validation

Assuming the heave motion of the floating mass in a 2D fluid domain is small and sinusoidal in time, we can approximate the hydrodynamic force applied on it with two

component reactive force, with one component proportional to acceleration and the other proportional to velocity (Newman 1977). Together with the hydrostatic restoration force, the total force from water pressure is approximated as

$$F_w = \mathrm{a}\ddot{U}_z^{(1)} + \mathrm{b}\dot{U}_z^{(1)} + \mathrm{k}U_z^{(1)}, \tag{7.2}$$

where a and b are the added mass and damping coefficients used to represent the hydrodynamic force. $\mathrm{k} = \rho g L B$ is the spring coefficient representing the hydrostatic restoring force.

The added mass and damping coefficients used to approximate the hydrodynamic force applied on a floating structure are dependent on the frequency of the motion of the structure. Many investigations have been carried out to compute these two coefficients as function of frequency for various body forms. The majority of this work pertains to 2D cylinders in deep water. For example, Vugts (1968) studied the added mass and damping coefficients for a family of 2D rectangular cylinders heaving in deep water. Sample results of Vugts are presented in Figure 7.2 for the added mass and damping coefficients for rectangular cylinders with width/draught =2, 4 and 8. It is important to note that the symbol T appearing in Figure 7.2 represents the draught of the cylinder and it corresponds to the symbol d in the text.

To determine the added mass and damping coefficients for the floating mass considered in this exercise, the frequency of the heave motion is initially estimated from

$$\omega = \sqrt{\frac{\mathrm{k}}{m^{(1)}}}\,. \tag{7.3}$$

The frequency estimated in Equation (7.3) does not reflect the influence of the corresponding added mass and damping coefficients, which can be interpolated from the curves with width/draught =2 in Figure 7.2. On taking the estimated added mass and damping coefficients into consideration, the frequency of the heave motion of the floating mass changes to ω'', namely

$$\omega'' = \omega'\sqrt{1-\varepsilon'^2}\,, \tag{7.4}$$

where

$$\varepsilon' = \frac{\mathrm{b}}{2\left(m^{(1)}+\mathrm{a}\right)\omega'} \quad \text{and} \quad \omega' = \sqrt{\frac{\mathrm{k}}{m^{(1)}+\mathrm{a}}}\,. \tag{7.5}$$

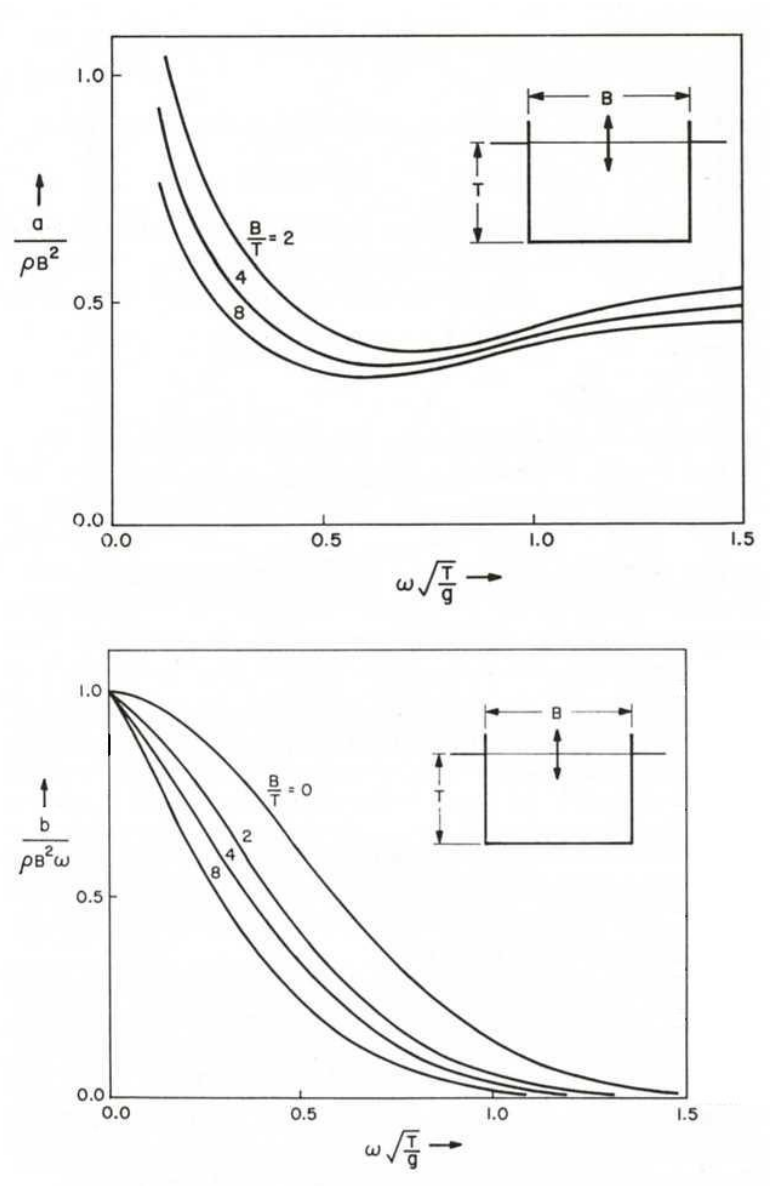

Figure 7.2 Added mass and damping coefficients for a family of 2D rectangular cylinders Vugts (1968)

To assign the approximate value of added mass and damping coefficients it is necessary that ω and ω'' are close to each other and this may necessitate an iteration procedure. The added mass $\mathrm{a} = 99.25\,\mathrm{kg}$ and damping coefficient $\mathrm{b} = 203.15\,\mathrm{Ns/m}$ are obtained for the heave motion of the floating mass at the frequency of 0.74Hz after a few iterations.

With the obtained added mass and damping coefficients, the heave motion of the floating mass on water is represented by a mass – spring – damper system of mass $m^{(1)} + \mathrm{a}$, spring coefficient k and damping coefficient b. As a result of this, the problem described in Figure 7.1 is replaced by a mass – spring – damper system dropping onto another mass – spring – damper system, as depicted in Figure 7.3.

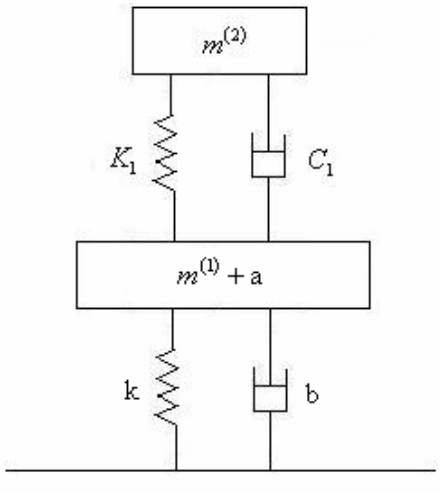

Figure 7.3 A mass – spring – damper system dropping onto another mass – spring – damper system

The free vibration of the system described in Figure 7.3 is a well known dynamic problem (Paz & Leigh 2004). Its oscillatory responses have the following analytical form

$$U_z^{(1)} + \overline{U}_z^{(1)} = D_1 e^{-\eta' t} \cos\left(\omega_d' t - \varphi_1\right) + D_2 e^{-\eta'' t} \cos\left(\omega_d'' t - \varphi_2\right), \tag{7.6}$$

$$U_z^{(2)} + \overline{U}_z^{(2)} = \mu_1 D_1 e^{-\eta' t} \cos\left(\omega_d' t - \varphi_1 - \theta_1\right) + \mu_2 D_2 e^{-\eta'' t} \cos\left(\omega_d'' t - \varphi_2 - \theta_2\right), \tag{7.7}$$

where $\overline{U}_z^{(2)}$ and $\overline{U}_z^{(1)}$ represent the final equilibrium position of the dropping and floating mass in coordinate system $o^{(2)} - x^{(2)} y^{(2)} z^{(2)}$ and $o^{(1)} - x^{(1)} y^{(1)} z^{(1)}$, respectively. The solution parameters $D_1, D_2; \varphi_1, \varphi_2$ are determined from the initial conditions of the system. η', η''; ω_d', ω_d'' are determined from the eigenvalues of the system. μ_1, μ_2; θ_1, θ_2 are determined from the amplitude ratio of the motion of the two masses.

The responses of the system in Figure 7.3 under prescribed initial conditions are calculated and presented in Figures 7.4 – 7.11 and indicated by “Approx. 2D”.

7.4 Results and Discussions

Figure 7.4 shows the time history of the displacement of the dropping mass, which falls from its initial position to the lowest position and then oscillates with decreasing amplitude until it comes to rest at its static equilibrium position $U_z^{(2)} = -0.118\,\text{m}$. Figure 7.5 indicates the time history of the displacement of the floating mass. Similarly the motion of the floating mass behaves as a damped oscillation and tends to its static equilibrium state at position $U_z^{(1)} = -0.02\,\text{m}$.

Figures 7.6 and 7.7 present the time histories of the velocity of the dropping and floating masses respectively. The velocities of both masses reach their minimum value first and then oscillate about their final static value zero.

Figures 7.8 and 7.9 respectively reveal the time histories of the acceleration of the dropping and floating mass. The discrepancies of the initial value of acceleration in these two figures are due to the different initial conditions. When the problem is solved with program MMFBEP in 2D or 3D fluid domain, the initial acceleration of the dropping and floating mass are assumed to be zero according to the general derivations presented in Chapter 4. When the approximate approach using 2D added mass and damping coefficients is used, the initial acceleration of both the dropping and floating mass are automatically determined (not zero) as we constrain their initial displacement and velocity in Equations (7.6) and (7.7).

The dropping mass and the floating mass form a coupled system, thus their motions consist of two frequency component one of which comes from the dropping mass – spring – damper system and the other of which comes from the heave motion of the floating mass. Due to the relatively large damping coefficient, the frequency component induced by the dropping mass – spring – damper system is damped very quickly so it doesn't make significant contributions to the motion of the coupled system. As a result, the motion of both the dropping and floating mass is dominated by the frequency related to the heave motion of the floating mass, which is about 0.67Hz.

Figure 7.10 gives the time history of the interaction force provided by the spring –

damper unit. The interaction force increases continuously until it reaches the maximum value and then tends to its static value equalling the weight of the dropping mass. The trend of this interaction force shown in Figure 7.10 is rather smooth, thus representing a relatively light landing impact onto the floating structure. However, when increasing the spring coefficient or decreasing the damping coefficient of the dropping mass – spring – damper system, we find that the oscillatory character of this interaction force becomes obvious, which may worsen the landing condition.

Figure 7.11 shows the time history of the induced water pressure force applied on the bottom of the floating mass, which presents a typical damped oscillation with a frequency 0.67Hz. When increasing the spring coefficient or decreasing the damping coefficient of the dropping mass – spring – damper system, we can observe a high frequency component added onto the damped oscillation of the water pressure force.

The numerical results obtained with program MMFBEP in a 2D fluid domain and those obtained with the 2D added mass and damping coefficients generally agree with each other as shown in Figures 7.4 – 7.11. This agreement validates the reliability of the proposed mixed mode function – boundary element method and the accuracy of the developed program MMFBEP. However, these two sets of results are not identical as the hydrodynamic force applied on the floating mass can only be approximated with the constant added mass and damping coefficients. The numerical results with 2D added mass and damping coefficients tend to have a higher oscillatory frequency and a lower damping value compared with the results from program MMFBEP.

On comparing the numerical results for a 2D and a 3D fluid domain in Figures 7.4 – 7.11, the two sets of predictions have the same oscillatory frequency for each corresponding responses but the amplitude of these responses in the 3D case is relatively larger than that in the 2D case.

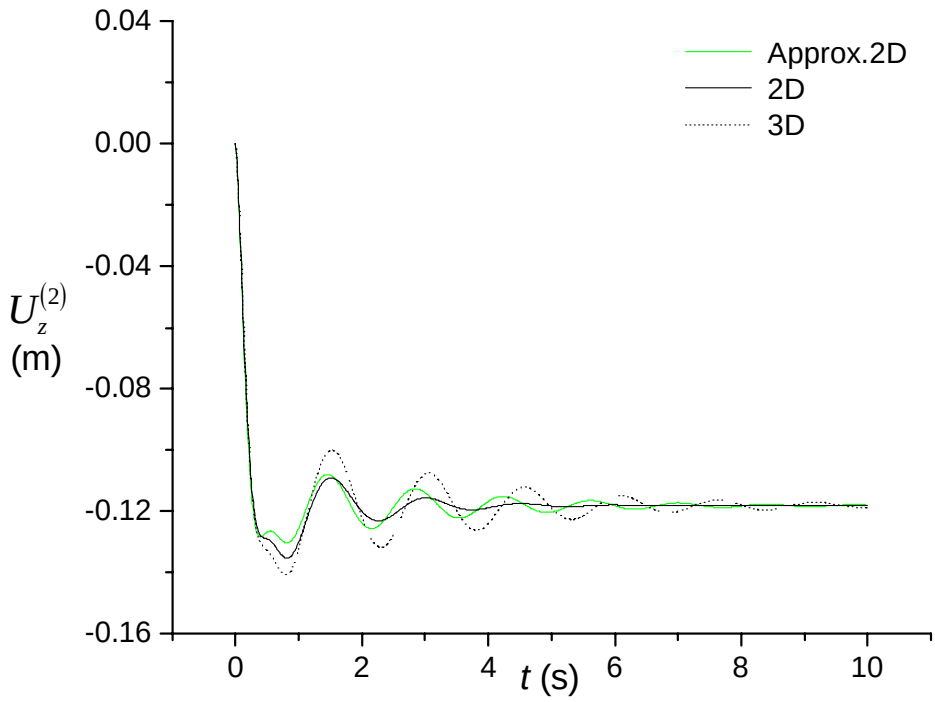

Figure 7.4 Time history of the displacement of the dropping mass

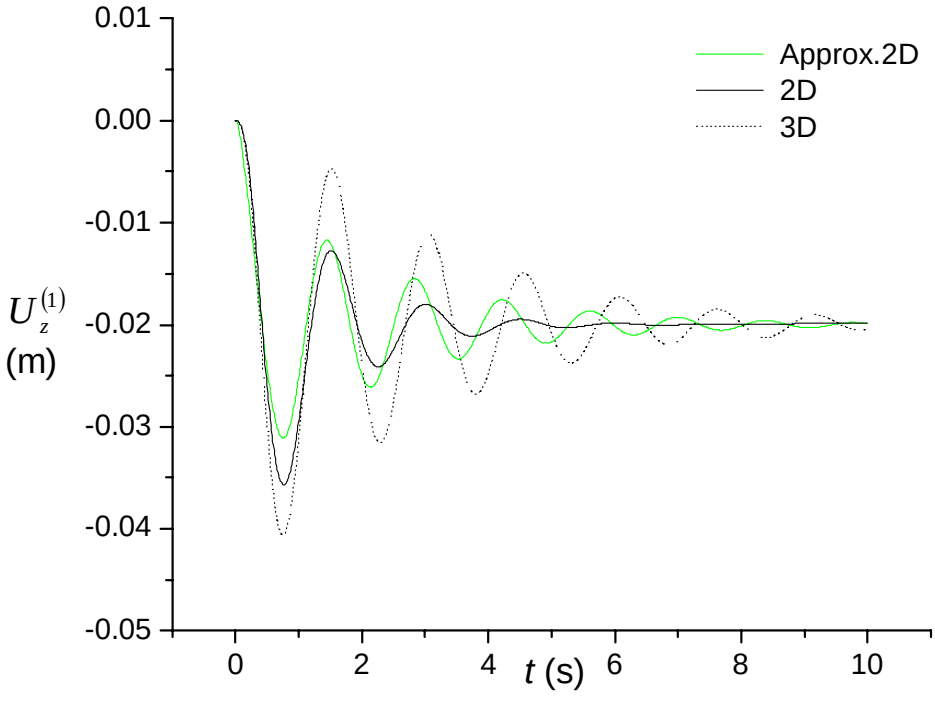

Figure 7.5 Time history of the displacement of the floating mass

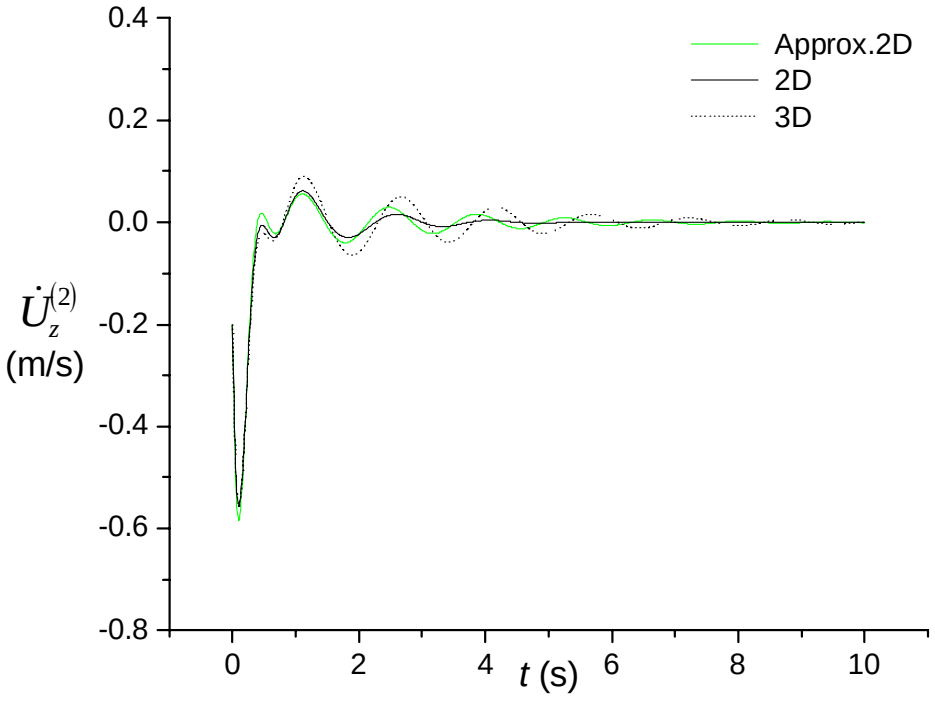

Figure 7.6 Time history of the velocity of the dropping mass

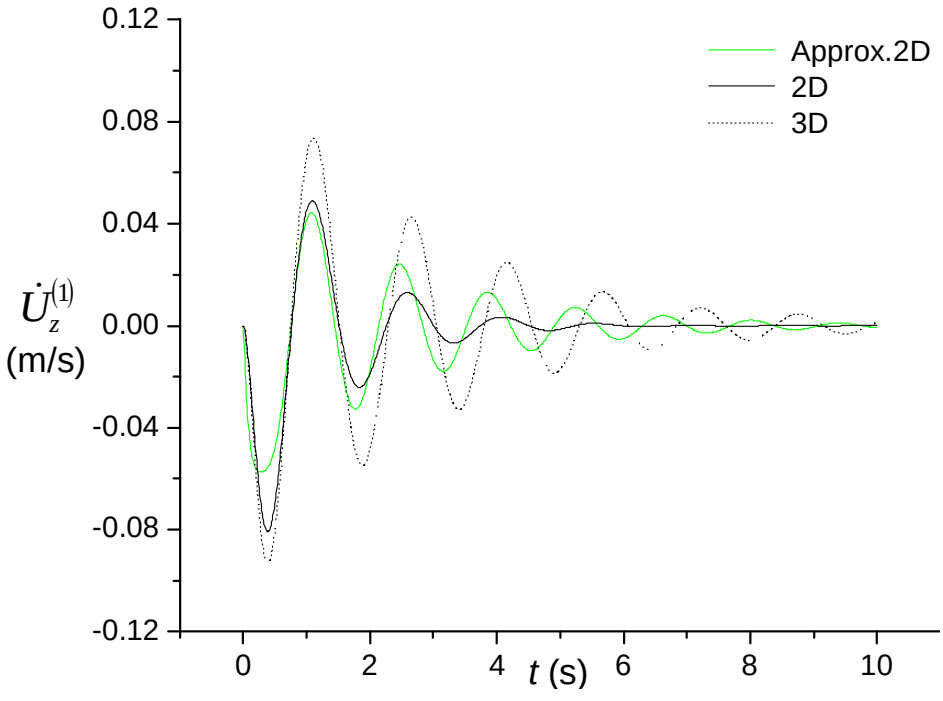

Figure 7.7 Time history of the velocity of the floating mass

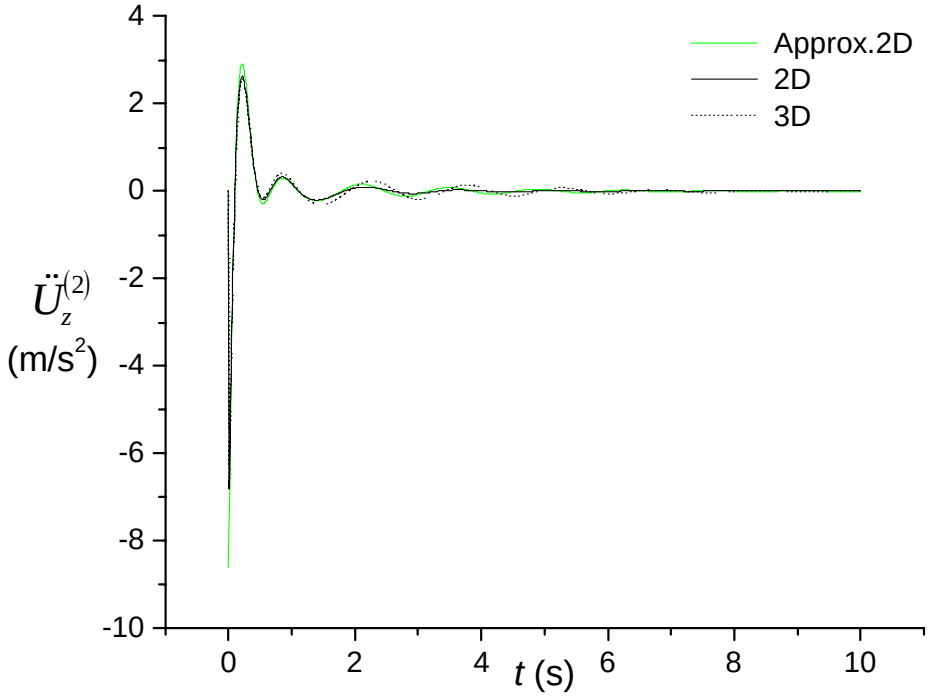

Figure 7.8 Time history of the acceleration of the dropping mass

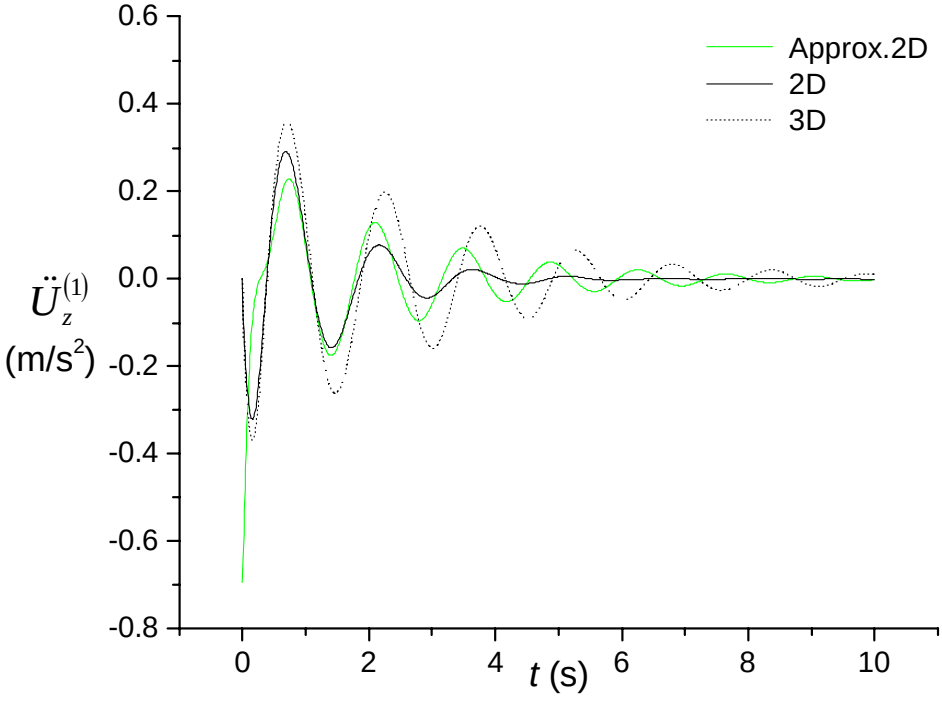

Figure 7.9 Time history of the acceleration of the floating mass

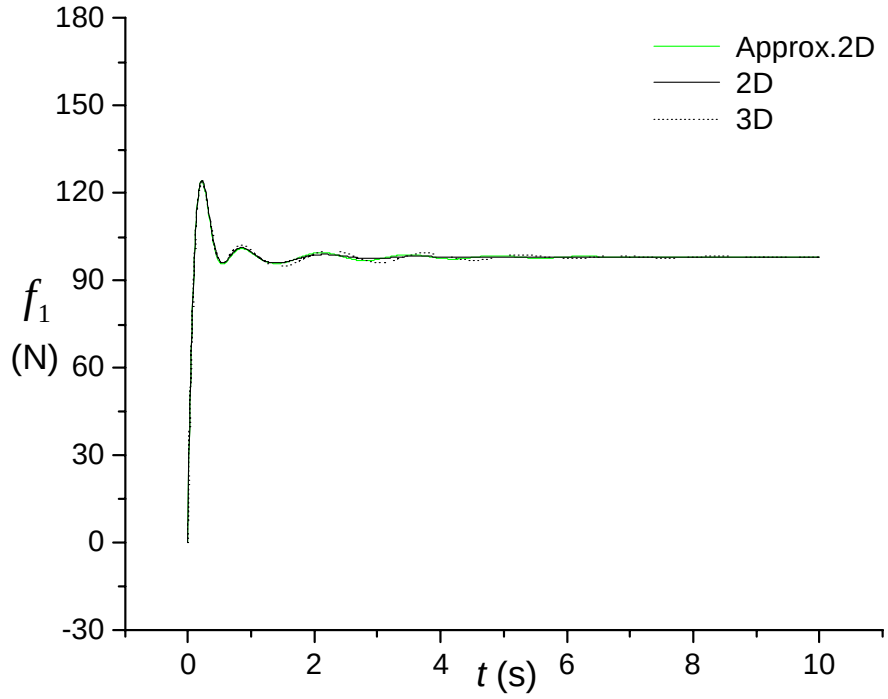

Figure 7.10 Time history of the interaction force from the spring – damper unit

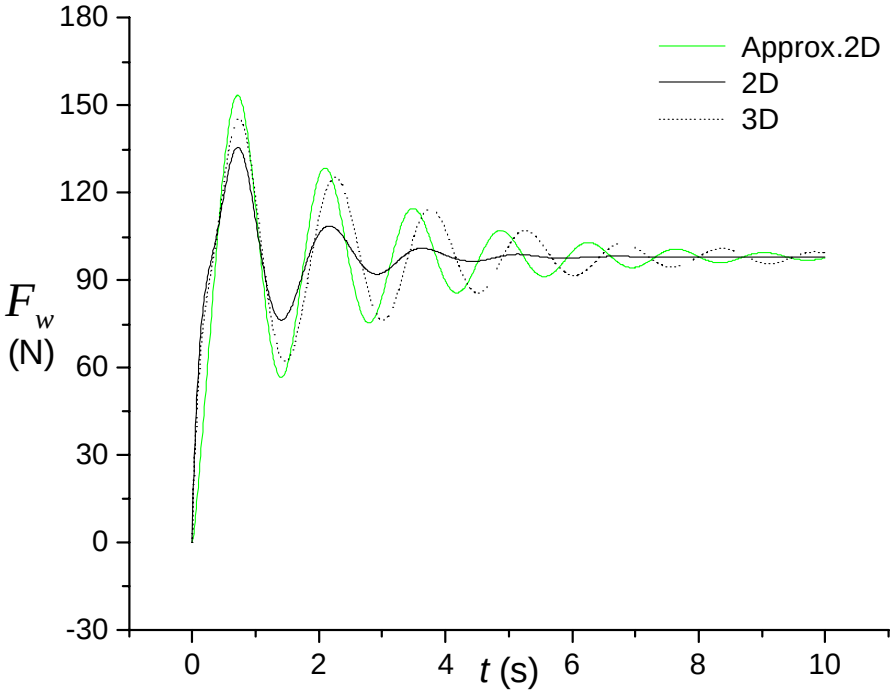

Figure 7.11 Time history of the force from water pressure applied on the floating mass

Chapter 8

An Elastic Beam Landing onto another Floating Elastic Beam

To further validate the proposed analysis method implemented in the computer program MMFBEP a numerical simulation of the car running test conducted by Endo & Yago (1999) is investigated. This numerical application is presented to reveal the dynamic behaviour of a coupled problem through an application of the program MMFBEP. The good agreement between the numerical predictions and the experimental measures provided in Subsection 8.2.3 demonstrates the validity of the proposed method and the developed program.

To investigate the interaction of the landing beam, the floating beam and the surrounding water, the dynamics of an elastic beam landing and travelling along another floating elastic beam is examined. The predicted dynamic responses of the coupled system in both a 2D and a 3D fluid domain are discussed.

8.1 General Description

The general derivations given in Chapters 4 and 5 can be applied directly to the problem discussed in this chapter. The “airplane” and the “flexible floating structure” generally described in Chapter 4 are simplified as two elastic beams, the landing beam and the floating beam. The number of suspension units is reduced to one, which is fixed at the middle point of the landing beam (denoted by $J = 1$). A horizontally unbounded 2D or 3D fluid domain is assumed.

Figure 8.1 describes an elastic beam (the car) with a supporting system consisting of a linear spring of stiffness K_1 and a damper of damping coefficient C_1 landing and travelling on another elastic beam floating on the surface of a water domain.

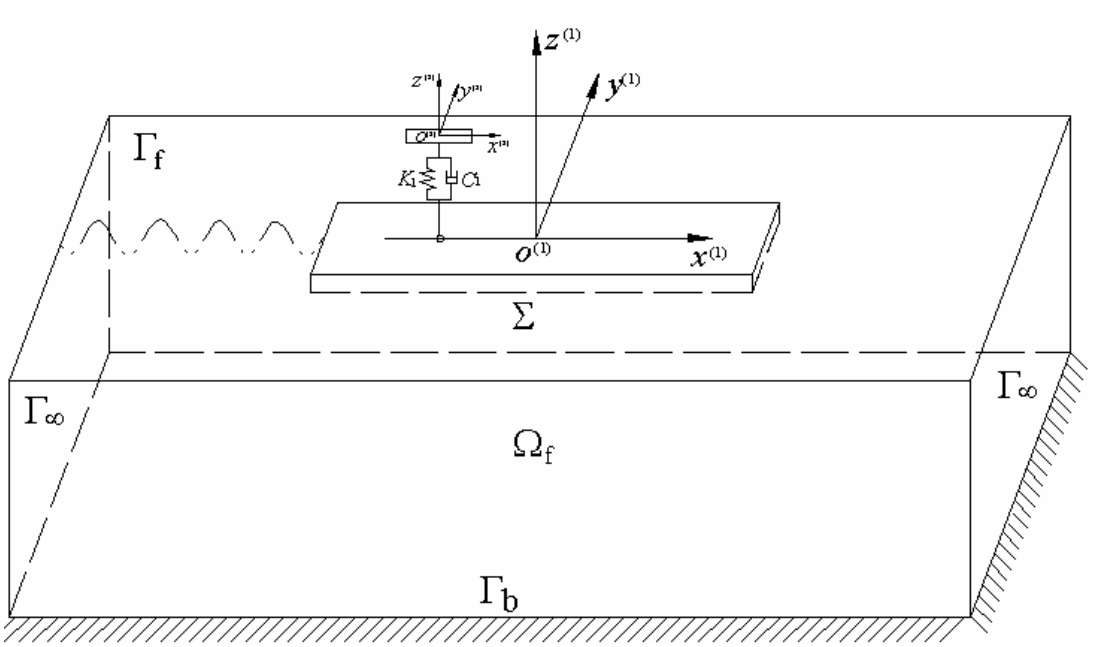

Figure 8.1 A landing beam - floating beam - water interaction system subject to landing impacts

8.2 A Car Running Test

8.2.1 Description

In Endo and Yago's test (Endo & Yago 1999), a small carriage (car) of mass 6.91kg was towed along the rail on a floating plate model as shown in Figure 8.2. The plate, whose geometrical and physical data are listed in Table 8.1, floats on the free surface of a basin of length 40m, width 27.5m and water depth 1.9m. The rail was shifted 0.18m from the centreline of the plate model. The carriage moved with a constant towing velocity of 0.61m/s along the positive direction of the $O-X$ axis. The vertical displacements at the five points Z1, Z3, Z5, Z7, Z9 along the centreline of the plate model were measured during the test.

To simulate this test using the developed landing beam – floating beam – water interaction system, the landing beam is assumed to have a very large bending stiffness of $2\times10^{10}\,\mathrm{Nm}^2$, a mass density of $6.91\,\mathrm{kg/m}$ and length $1\mathrm{m}$, which approximately provides a rigid body of total mass 6.91kg like the carriage used in the test. The supporting system is

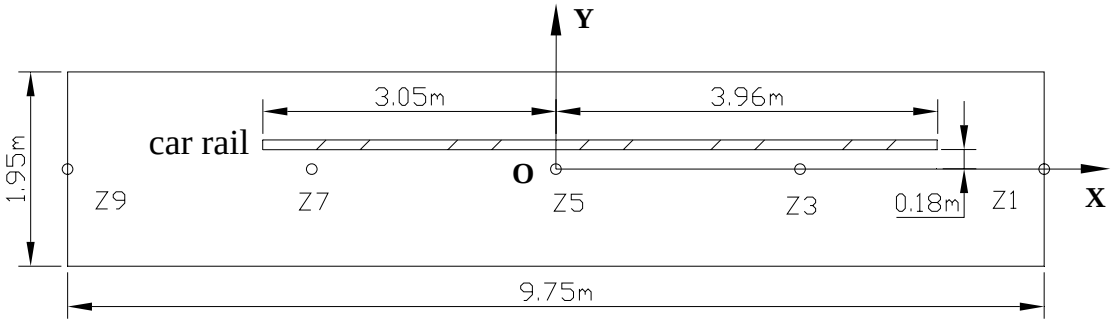

Figure 8.2 Arrangements of displacement measure points and car moving rail on the plate model

Table 8.1 Particulars of the floating plate model

Length × Breadth × Depth	9.75m × 1.95m × 0.0545 m
Draught	0.0163m
Bending Rigidity	17.53kNm^2

reduced to an extremely strong spring of $K_1 = 2.0 \times 10^9$ N/m and no damping mechanism, so $C_1 = 0$ Ns/m. The landing beam has a zero vertical landing velocity ($V_{z0} = 0$ m/s) and a constant horizontal velocity $V_{x0} = V_x = 0.61$m/s to reflect the towing velocity of the "car" of the experimental test.

The water depth / plate draught ratio used in the test is $1.9/0.0163 \approx 116$. This is sufficiently large to assume that the water depth is infinite in the numerical simulation. For the case of a 2D fluid domain, the length of the retained fluid domain in the numerical simulation is $31\text{m} \times 9.75\,\text{m}$ with its centre at point $o^{(1)}$. The fluid surface is divided into 31×50 constant elements of which $1 \times 50 = 50$ elements are on the wetted interaction interface and $30 \times 50 = 1500$ elements are on the free surface. For the case of a 3D fluid domain, the retained fluid surface is a rectangle of length $9\text{m} \times 9.75\,\text{m}$, width $9\text{m} \times 1.95\,\text{m}$ and with its centre at point $o^{(1)}$. The fluid surface is divided into 81×50 constant elements of which $1 \times 50 = 50$ elements are on the wetted interaction interface and $80 \times 50 = 4000$ elements are located on the free surface.

The number of modes retained for the two elastic beams are $M^{(1)} = M^{(2)} = 16$. The first

two retained modes are rigid body modes. The total simulation time for the car running test is 11.5s and the time step $\Delta t = 0.0115$ s is used in the numerical time integration scheme.

8.2.2 Execution of program MMFBEP

The input file INPUTP.DAT for simulating the car running test in 2D and 3D fluid domain can be generated following the explanations in Subsection 6.5.1.

The input file INPUTM.DAT for the two beams is readily formulated due to the existence of the analytical modal functions for free – free beams. The landing beam is modelled with 20 elements and 42 nodes whilst the floating beam is modelled with 50 elements and 102 nodes. The numbering rules of the elements and nodes for beam structures are described in Subsection 6.5.2. It should be noted that each node of the two beam structures used herein only have two degrees of freedom and the rotation about the longitudinal axis shall be zero.

The running time of program MMFBEP is about 5 minutes for the 2D fluid domain and 45 minutes for the 3D fluid domain.

8.2.3 Results and discussions

The time histories of the vertical displacement measured at the five points Z1, Z3, Z5, Z7, Z9 are depicted in Figure 8.3. The mean value of the numerical time histories shows a good agreement with the experimental data (Endo & Yago 1999), which validates the proposed mixed mode function – boundary element method and the developed program.

It has been observed that there is a high frequency oscillation component on the numerical curves and a large initial displacement discrepancy at point Z7. This is due to the different initial conditions in the test and the numerical simulation. In the test, the carriage was placed on the floating plate model before the test started so the floating plate model and the carriage were in their initial static equilibrium state. However, in the numerical simulation, the landing beam with a zero vertical velocity lands on the floating beam at the initial time. The landing beam behaves as a suddenly applied added mass on

the floating beam and this causes an initial dynamic deflection of the floating beam. This dynamic deflection is twice as large as that produced by the static carriage in the test, which produces the oscillation.

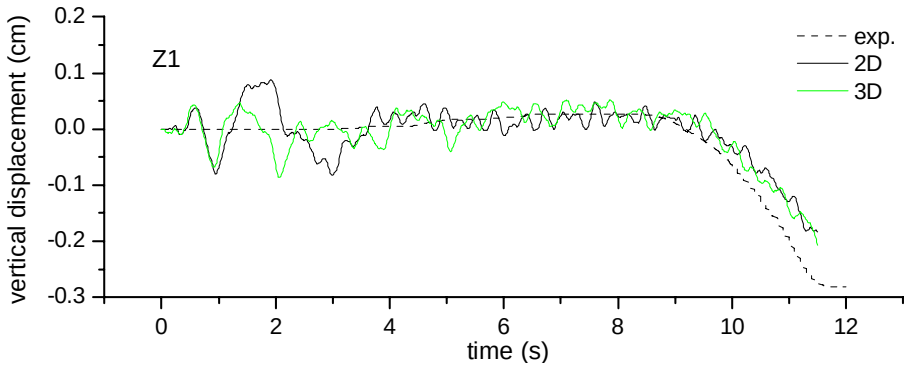

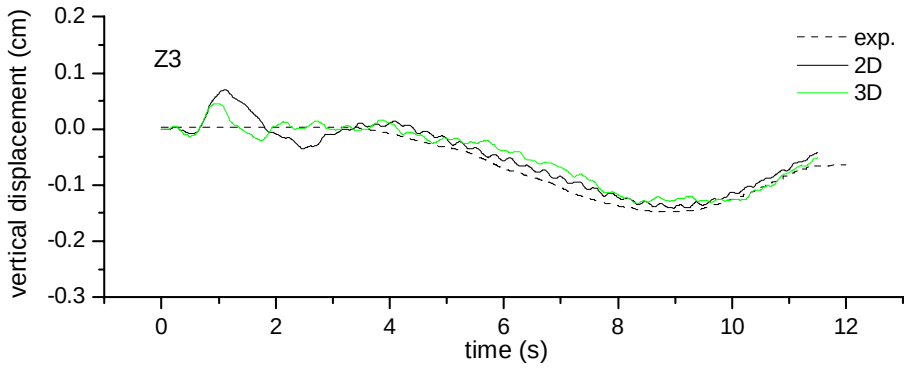

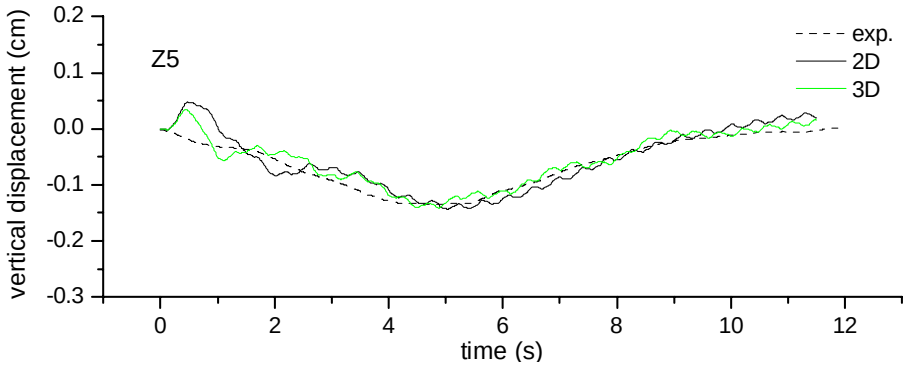

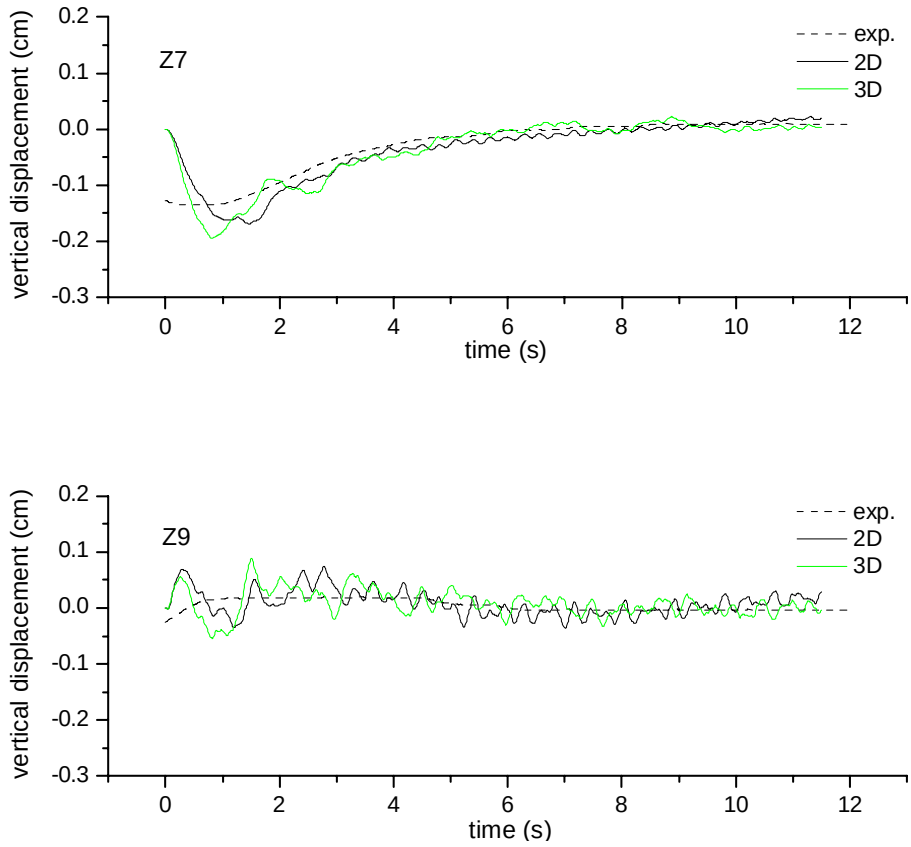

Figure 8.3 Time histories of the vertical displacement measured at the five points on the plate model

Having indicated that car test situation can be modelled correctly, we next replace the car by an elastic beam “airplane”.

8.3 Landing Beam–Floating Beam–Water Interaction System

8.3.1 Description and program execution

To investigate numerically the interactions of the landing beam (“car”), the floating beam and the surrounding water, the following system is simulated to reveal the dynamic behaviour of this coupled system. The landing beam has bending stiffness $2\times10^2\,\mathrm{Nm}^2$, mass density 20kg/m and length 1m. The floating beam has bending stiffness $2\times10^3\,\mathrm{Nm}^2$, mass density 50kg/m, length 15m, width 1m, thickness 0.1m and initial draught 0.05m. The spring and damping coefficient of the supporting system are $K_1 = 2.0\times10^4\,\mathrm{N/m}$ and

$C_1 = 1.0 \times 10^4$ Ns/m, respectively. The landing beam lands onto the floating beam at position $\mathbf{x}_{c0}^{(1)}(-2.5, 0, 0)$ with an initial vertical velocity of $V_{z0} = -0.1$m/s and a horizontal velocity of $V_{x0} = 2$ m/s. The landing resistance applied on the landing beam produces a constant deceleration $a_{x0} = -0.4\text{m/s}^2$.

For 2D fluid domain, the length of the retained fluid domain in the numerical simulation is 31×15 m with its centre at point $o^{(1)}$. For 3D fluid domain, the retained fluid surface is a rectangle of length 9×15 m, width 9×1 m and with its centre at point $o^{(1)}$. The meshes adopted for the two elastic beams and the water domain are exactly the same as those used in the numerical simulation of the car running test discussed in Section 8.2.

The number of modes retained for the two elastic beams are both 16. The total time of simulation is 5s and the time step $\Delta t = 0.005$ s is used in the time integration scheme.

The input file INPUTP.DAT for the simulation in 2D fluid domain is presented in Appendix C. For 3D fluid domain, the input file in Appendix C is modified by setting NDFD=3 and NZ=9. The input file INPUTM.DAT can be generated according to Subsection 8.2.2 and is given in Appendix D. The output file produced by program MMFBEP for 2D fluid domain is presented in Appendix E.

The running time of program MMFBEP is about the same as that for the simulation of car running test as the same meshes of the two elastic beams and the fluid domain are used in both cases.

8.3.2 Results and discussions

To present the dynamic responses of the landing beam – floating beam – water interaction system non – dimensional forms are presented. The reference length is water depth d, the reference velocity is V_{z0}, reference acceleration is g, reference pressure is $P_0 = \rho g d$ and the resultant reference force is $F_0 = \rho g d L$ with L representing the length of the floating beam. The graphical results of the simulation and their physical

explanations are described next.

Figure 8.4 presents the distribution of the non – dimensional vertical displacement $U_z^{(2)}/d$ of the 1m long landing beam at time $t = 1,2,3,4,5$ s. The landing beam shows a relatively stable configuration that is dominated by gravity.

Figure 8.5 shows the distribution of the non – dimensional vertical displacement, $U_z^{(1)}/d$, of the 15m long floating beam at time $t = 1,2,3,4,5$ s. Figure 8.6 provides the corresponding distribution of the non – dimensional water pressure P/P_0 along the floating beam at time $t = 1,2,3,4,5$ s. The floating beam displacement $U_z^{(1)}/d$, for each different time shown always exhibits a minimum displacement value when the water pressure value of Figure 8.6 is a maximum. The floating beam displacement exhibits a very flat distribution over the left hand half quite unlike the water pressure, which is significantly influenced by the floating beam bending stiffness but not other parameters.

From Figures 8.4 to 8.6, it is observed that the numerical predictions in 2D and 3D fluid domain generally agree with each other. However, in Figure 8.5, the minimum value of the non – dimensional displacement of the floating beam at time $t = 2$ s shows a relatively large discrepancy, which originates from the different water pressure prediction at time $t = 2$ s in Figure 8.6. This discrepancy also causes the different displacement of the landing beam at time $t = 2$ s in Figure 8.4.

Figures 8.7 to 8.9 present the responses at the “left end” and “middle point” of the landing beam. As the spring – damper unit is fixed at the middle point of the landing beam, the response of the landing beam is symmetric about its middle point. Figure 8.7 describes the time histories of the non – dimensional vertical displacement $U_z^{(2)}/d$ at the left end and middle point of the landing beam. The displacement at both points decreases to the minimum value prior to increasing to the equilibrium value. The displacement at the left end of the landing beam shows initial fluctuations that disappear after the first two seconds. The corresponding displacement at the middle point of the landing beam presents a relatively flat trend over the five - second time period.

Figure 8.8 gives the landing beam time histories of the non – dimensional vertical

velocity $\dot{U}_z^{(2)}/V_{z0}$ at the left end and middle points. The vertical velocity at the left end of the landing beam shows a typical damped oscillation, whilst the vertical velocity at the middle point of the landing beam goes to the minimum value first and then tends to oscillate about the zero value of equilibrium points. The magnitude of the initial vertical velocity at the left end point is about five times larger than that at the middle point.

Figure 8.9 shows the landing beam time histories of the non – dimensional vertical acceleration $\ddot{U}_z^{(2)}/g$ at the left end and middle points. The vertical acceleration at both points indicates a damped oscillation. The amplitude of this oscillation at the left end point is much larger than that at the middle point. The simulation results for 2D and 3D fluid domains seem very similar. Figures 8.7 to 8.9 indicate that the landing beam responses at the left end point show oscillations with a relatively stable frequency of 7Hz.

Figures 8.10 to 8.12 present the responses at the left end, middle and right end point of the floating beam. Figure 8.10 gives the floating beam time histories of the non – dimensional vertical displacement $U_z^{(1)}/d$ at the three points. The floating beam vertical displacement at the left end point oscillates about the equilibrium value with relatively small amplitudes. The floating beam displacement at the middle point increases to the maximum value first and then reduces to the minimum value while the landing beam passes by. After this, the floating beam displacement gradually tends to its static equilibrium position. The initial increase of the floating beam displacement at the middle point is caused by the elastic deformation of the beam. The displacement at the right end point of the floating beam indicates the formulation and travelling effect of the generated waves.

Figure 8.11 describes the floating beam time histories of the non – dimensional vertical velocity $\dot{U}_z^{(1)}/V_{z0}$ at the left end, middle and right end points. Figure 8.12 shows the corresponding floating beam time histories of the non – dimensional vertical acceleration $\ddot{U}_z^{(1)}/g$ at these three points. From Figures 8.11 and 8.12, it is observed that the velocity and acceleration responses at the middle point of the floating beam are much smaller than those at the two end points.

Figure 8.13 shows the floating beam time histories of the non – dimensional water pressure P/P_0 at the left end, middle and right end points. The large fluctuation of the water pressure applied on the floating beam is a result of the initial impact of the landing beam.

Figure 8.14 gives the time history of the non – dimensional relative displacement $\left(U_z^{(2)} - U_z^{(1)}\right)/d$ between the two elastic beams at the supporting system. The relative displacement, representing the compression of the spring – damper unit, gradually tends to the equilibrium value. Figure 8.14 confirms that the spring – damper unit is in a compressive state during the entire landing process, thus satisfying the assumption made in the general derivation presented in Chapter 4.

Figure 8.15 presents the time history of the non – dimensional force provided by the supporting system f_1/F_0. It is found that this force f_1/F_0 shows a damp oscillation with a relatively stable frequency 7 Hz, which is the same as the frequency of the responses at the left end of the landing beam. This frequency is larger than the first order natural frequency of 4.31 Hz for the landing system that is fixed at the end of the supporting system. If the parameters of the landing system are changed, the stable frequency of the resultant force f_1/F_0 experiences a corresponding change. This demonstrates that the stable frequency of the force f_1/F_0 is strongly related to the landing system.

Figure 8.16 depicts the time history of the non – dimensional resultant vertical force, F_w/F_0, induced by the water pressure. This force has a damped oscillation of the same frequency as that of the force from the supporting system.

The results presented in this chapter indicated that the developed analysis method and program can be used to simulate the dynamics of a landing beam – floating beam – water interaction system with the extent of the fluid domain having small influences.

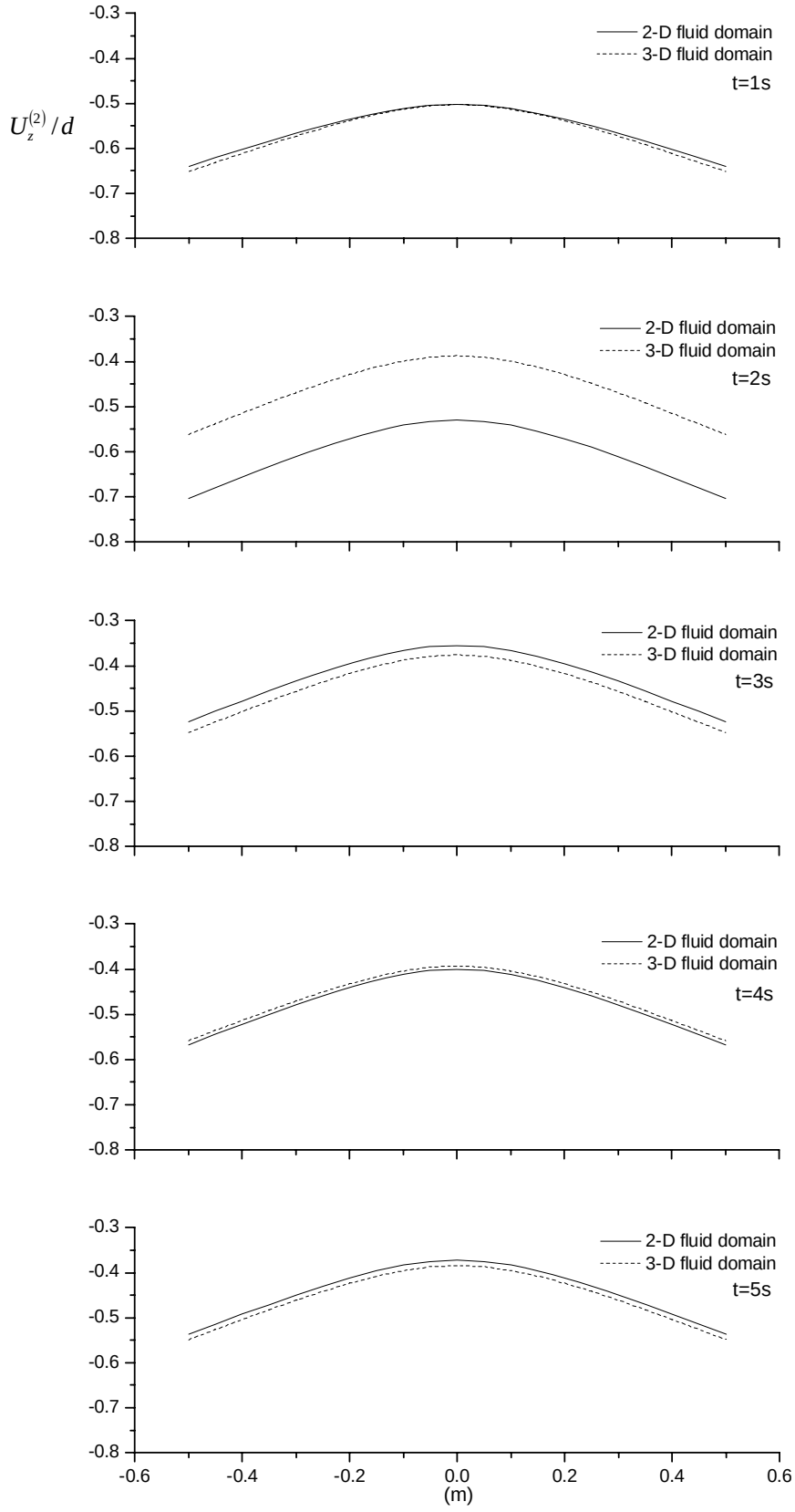

Figure 8.4 Distribution of the non – dimensional vertical displacement of the 1m long landing beam at time $t = 1,2,3,4,5$ s.

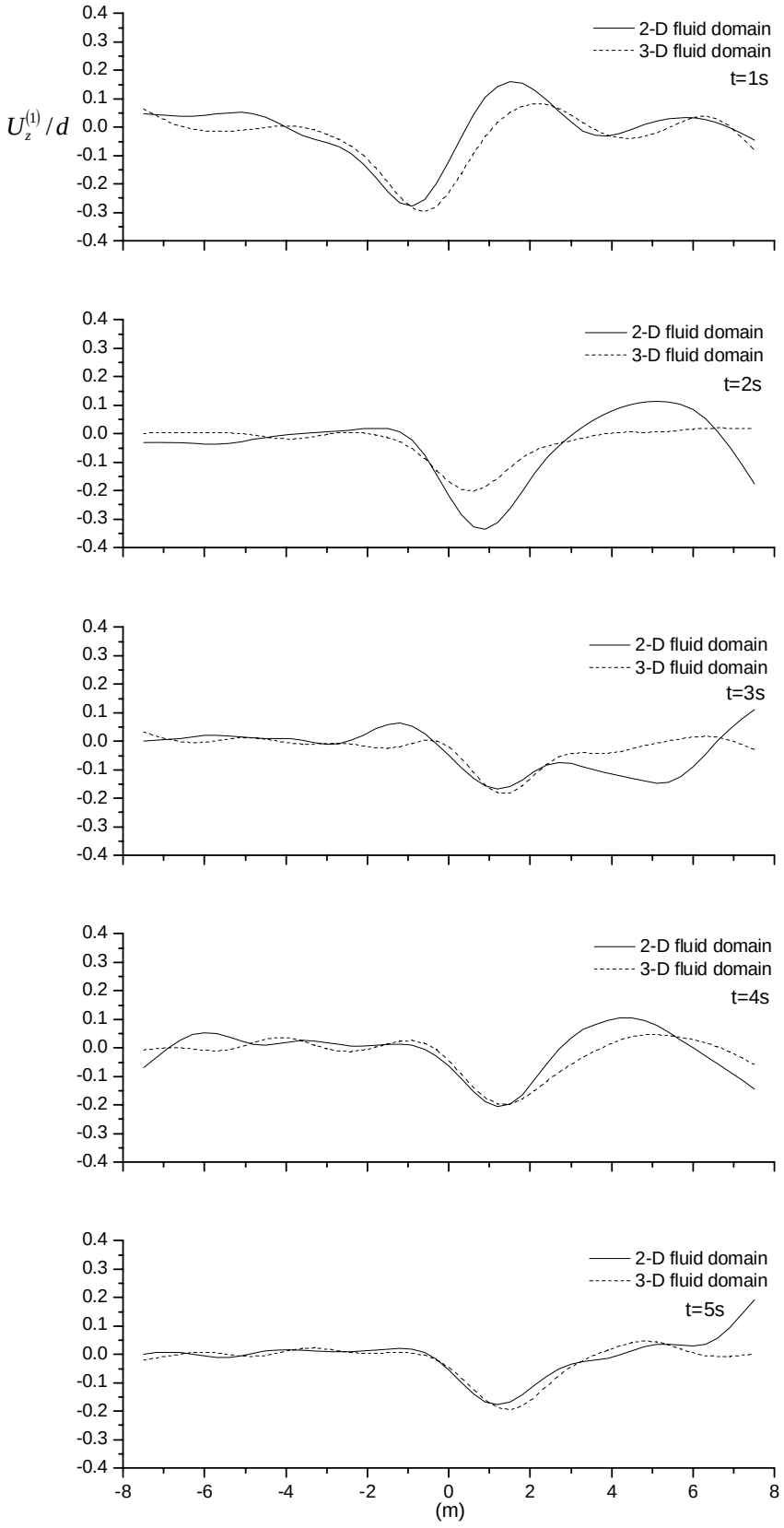

Figure 8.5 Distribution of the non – dimensional vertical displacement of the 15m long floating beam at time $t = 1,2,3,4,5$ s.

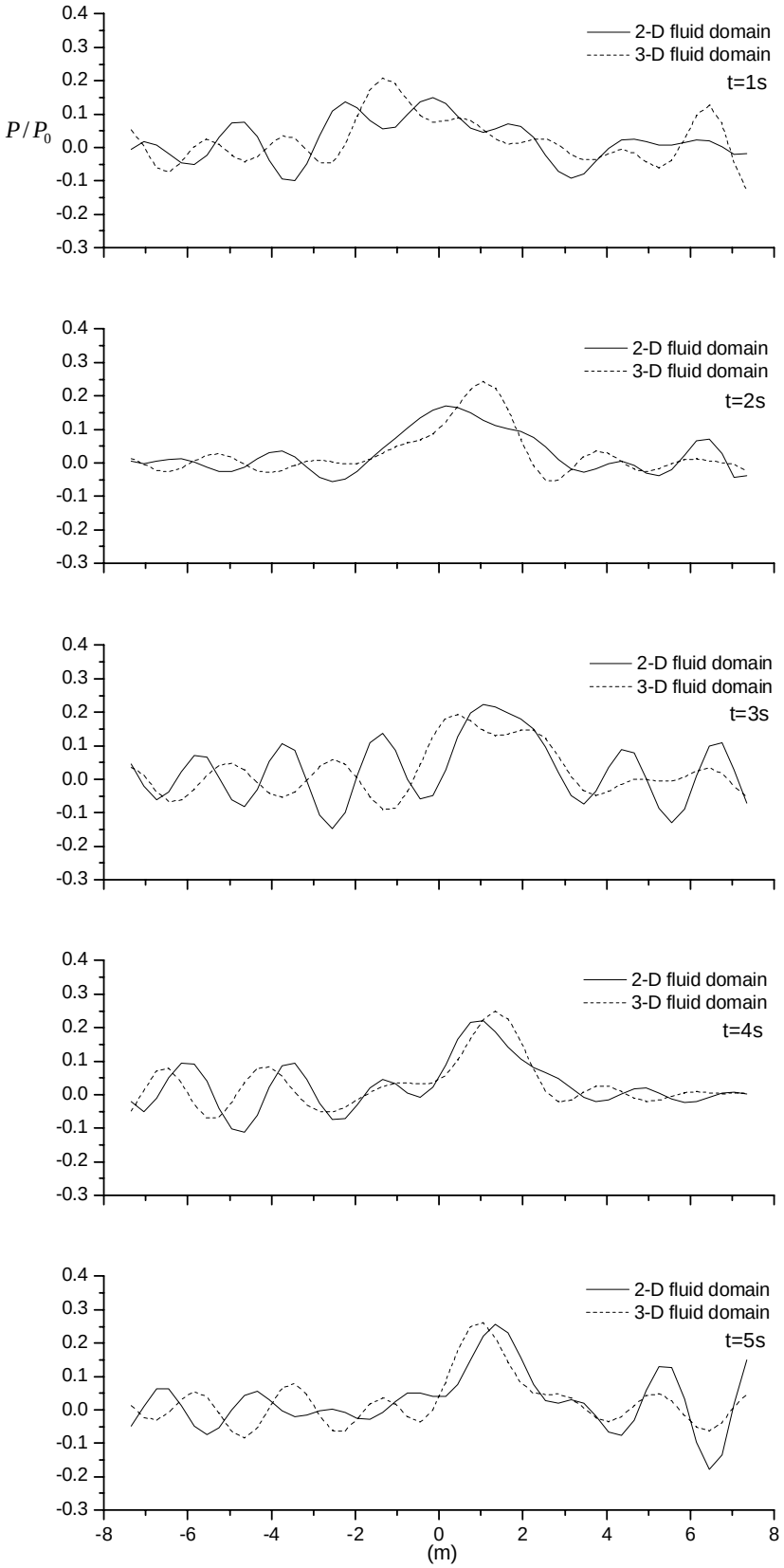

Figure 8.6 Distribution of the non – dimensional water pressure along the 15m long floating beam at time $t = 1,2,3,4,5$ s.

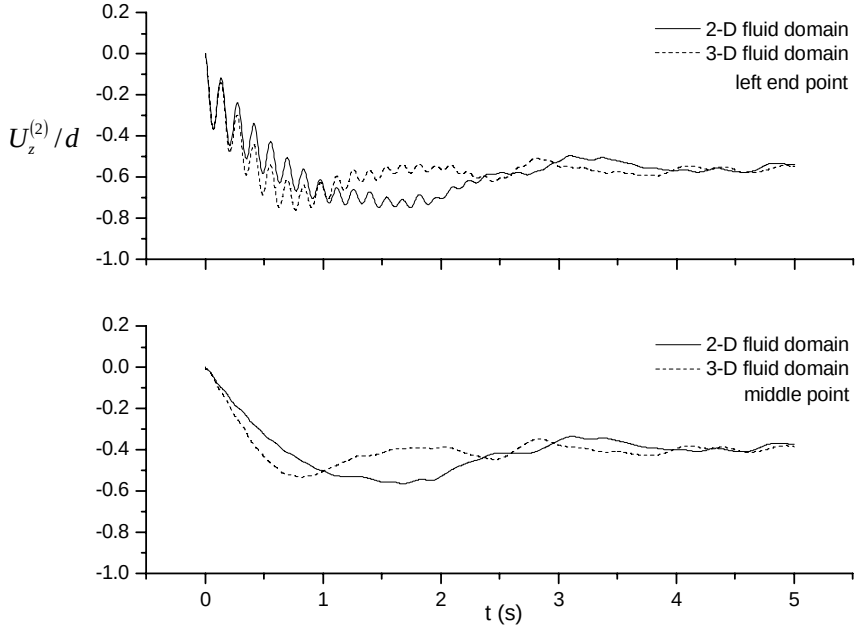

Figure 8.7 Time histories of the non – dimensional vertical displacement at the left end and middle point of the landing beam.

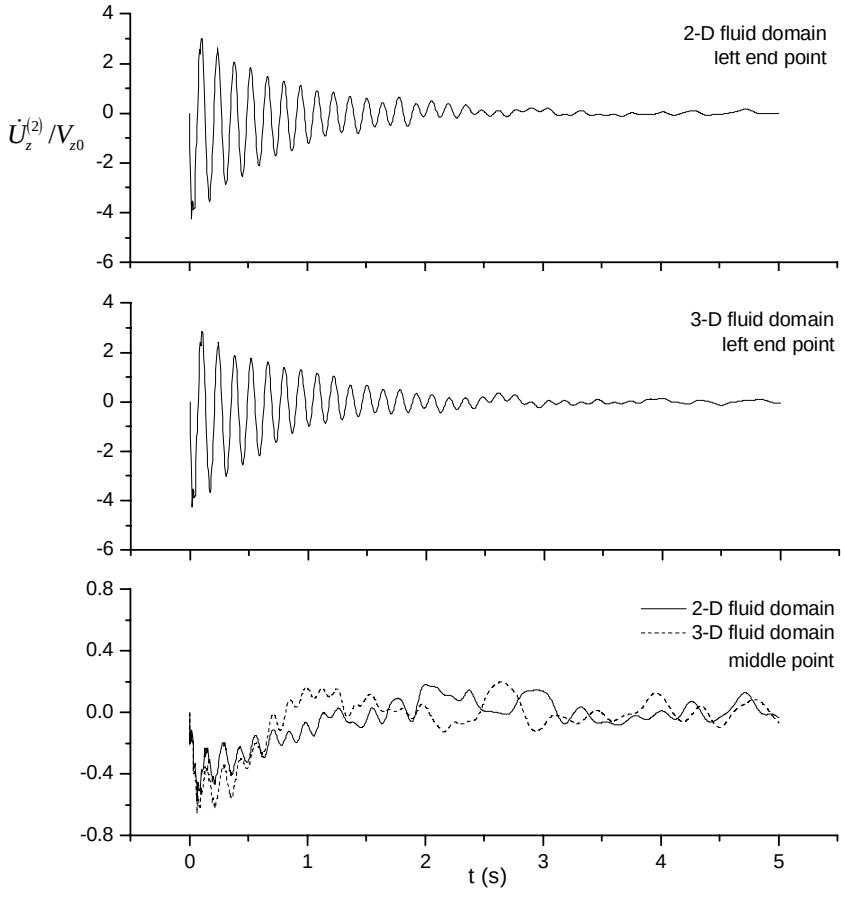

Figure 8.8 Time histories of the non – dimensional vertical velocity at the left end and middle point of the landing beam.

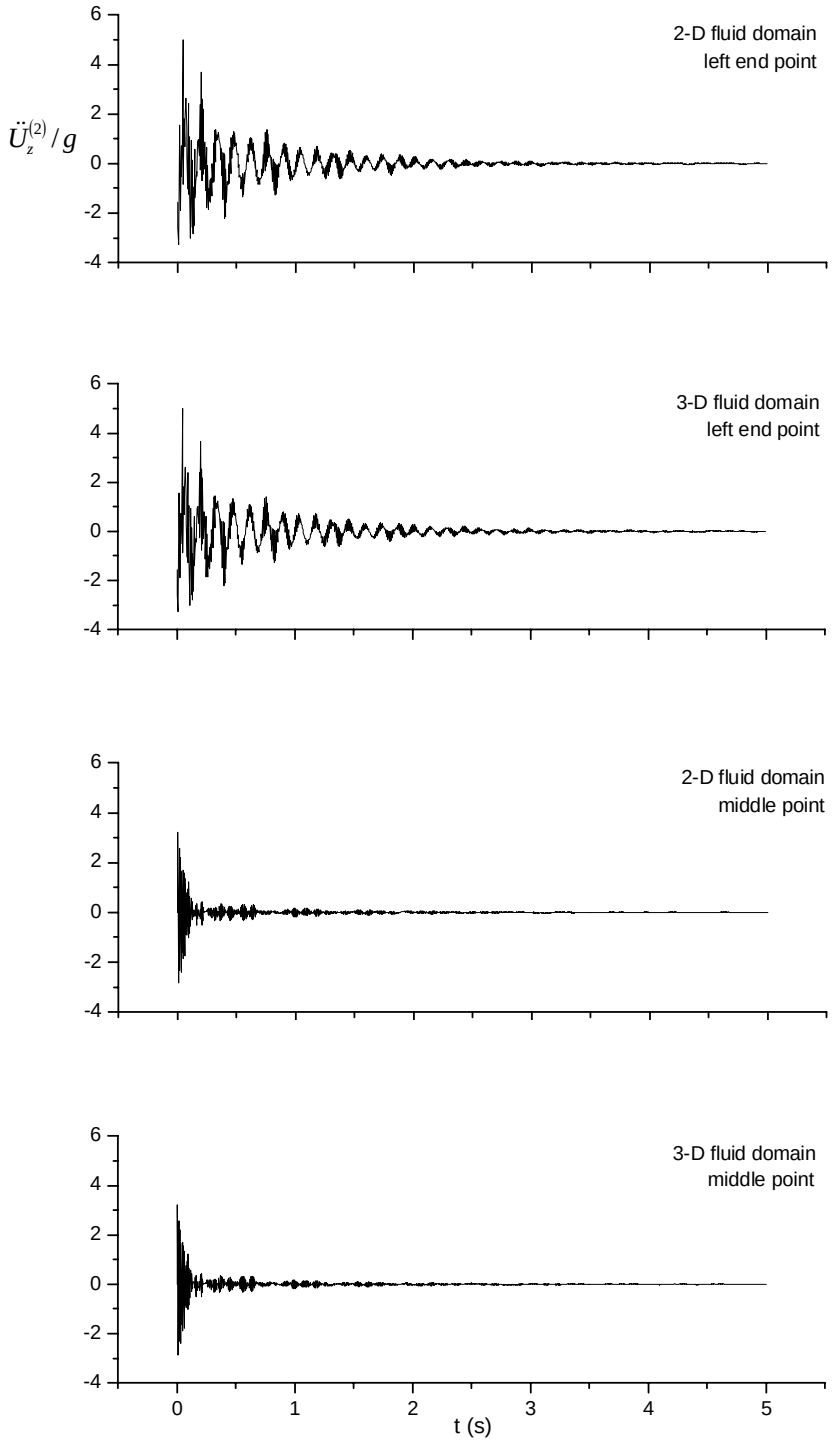

Figure 8.9 Time histories of the non – dimensional vertical acceleration at the left end and middle point of the landing beam.

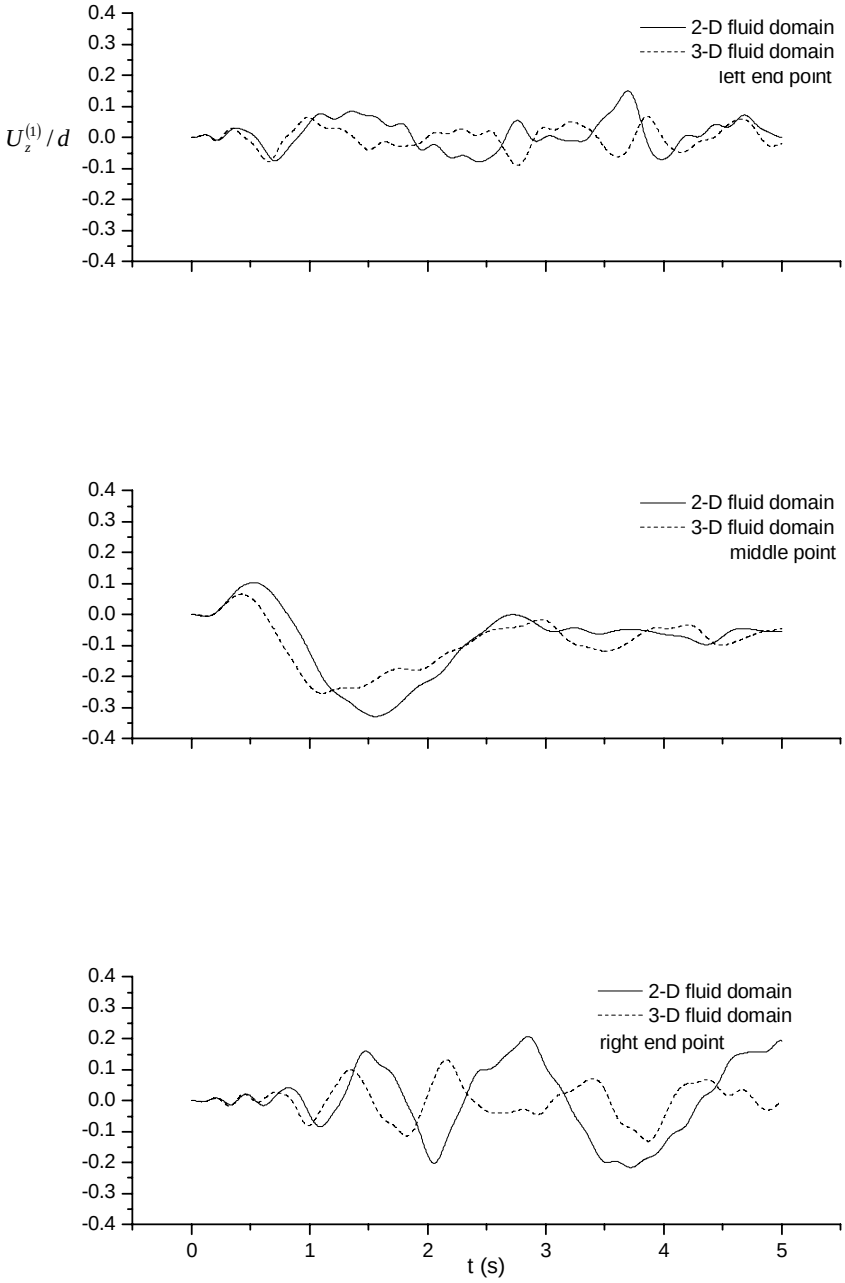

Figure 8.10 Time histories of the non – dimensional vertical displacement at the left end, middle and right end point of the floating beam

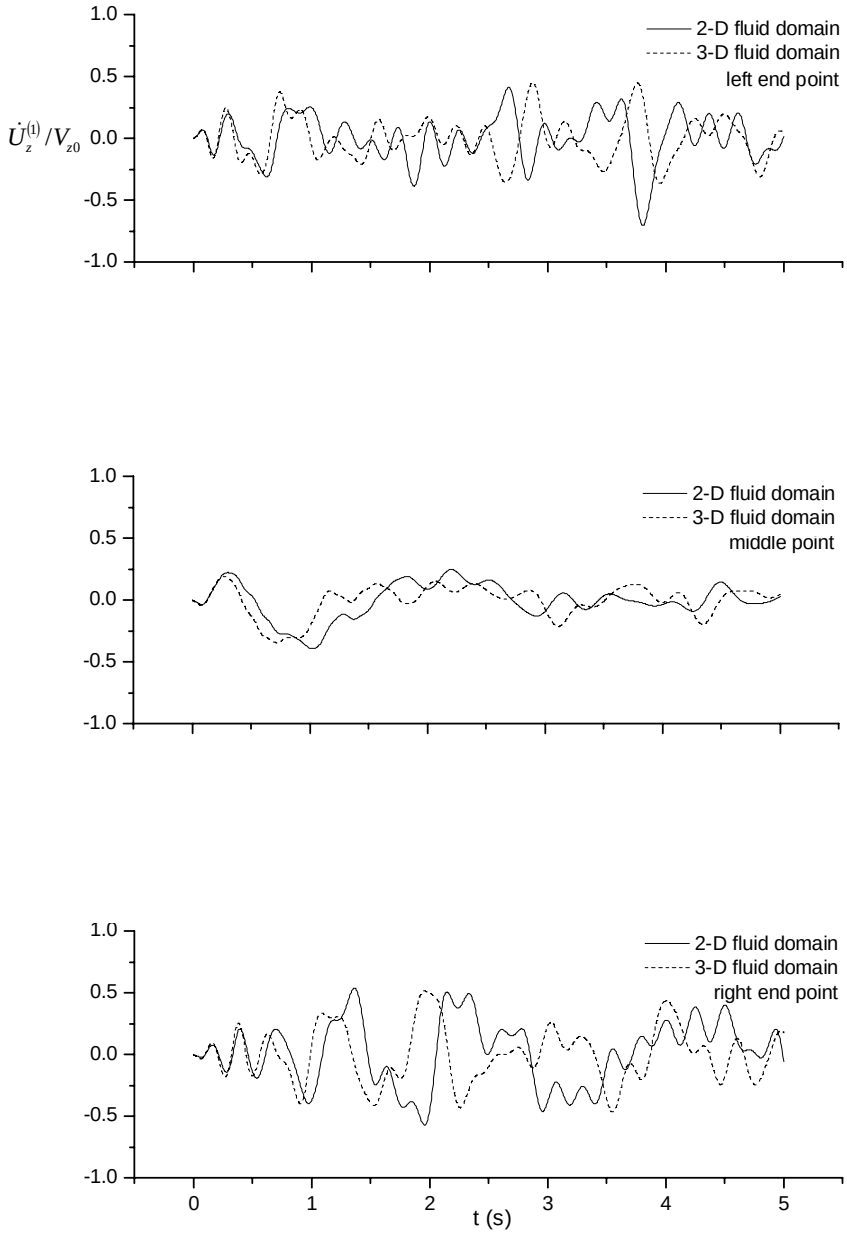

Figure 8.11 Time histories of the non – dimensional vertical velocity at the left end, middle and right end point of the floating beam

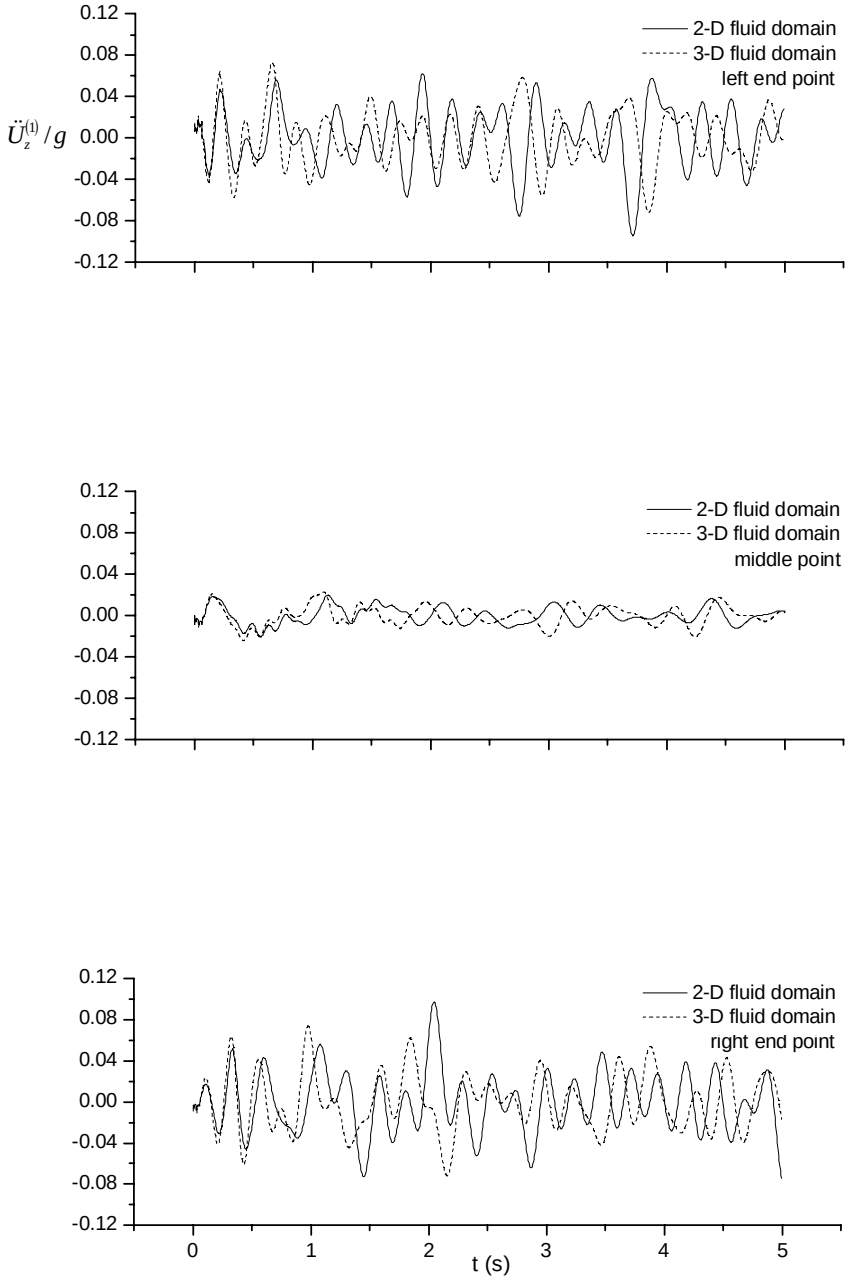

Figure 8.12 Time histories of the non – dimensional vertical acceleration at the left end, middle and right end point of the floating beam

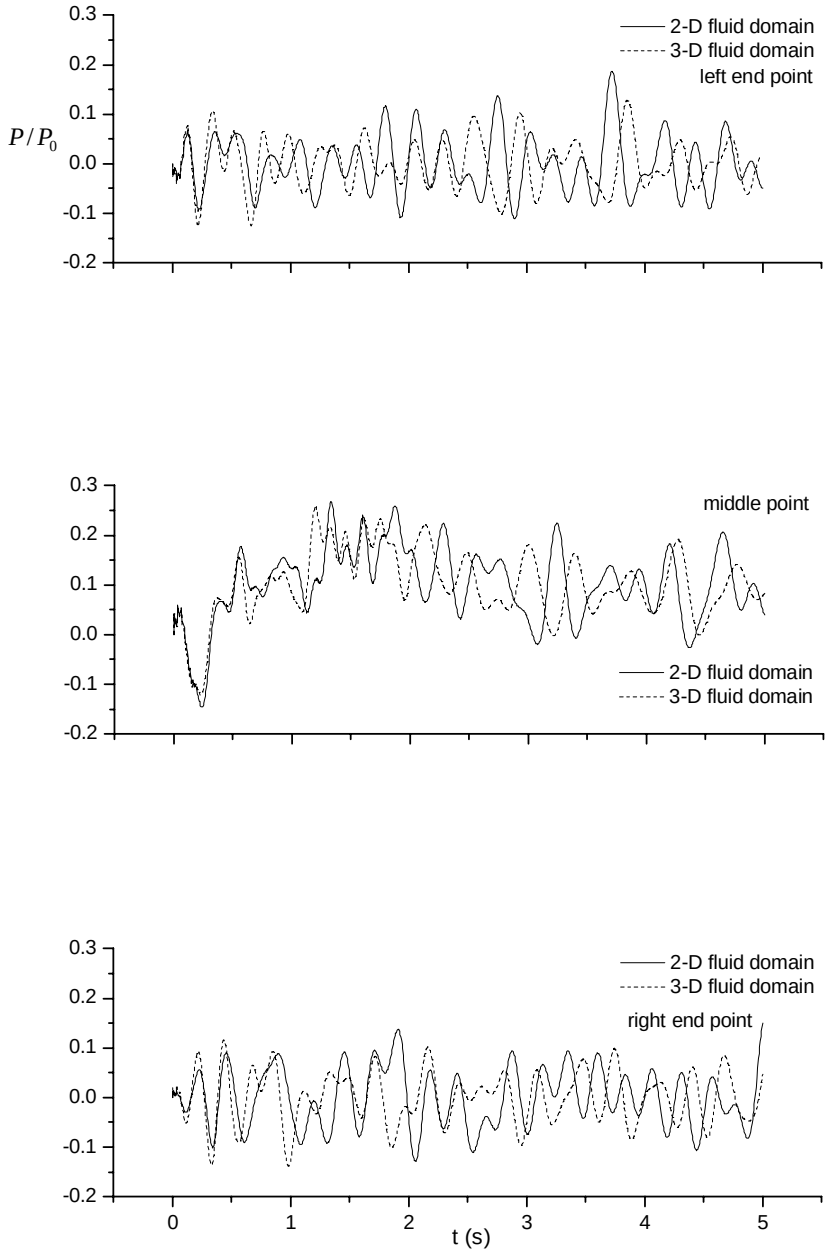

Figure 8.13 Time histories of the non – dimensional water pressure at the left end, middle and right end point of the floating beam

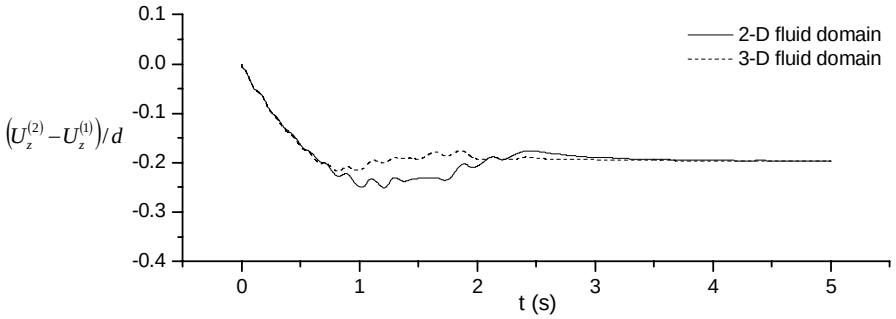

Figure 8.14 Time history of the non – dimensional relative displacement between the two elastic beams at the supporting system

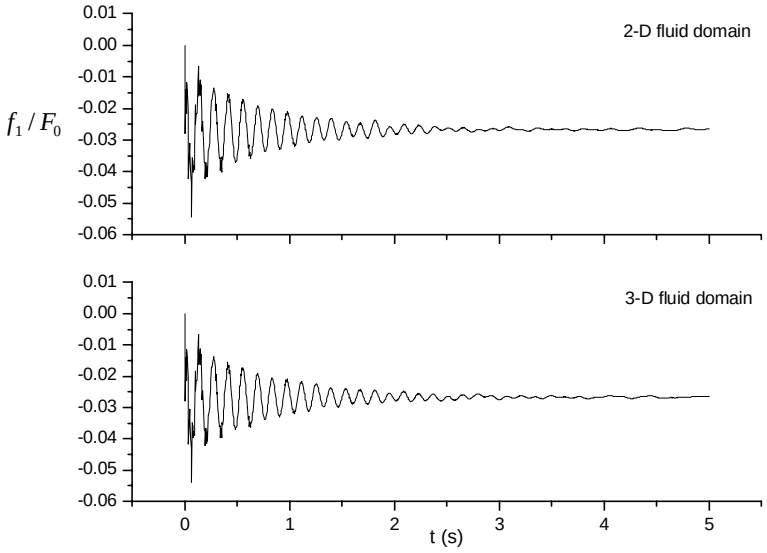

Figure 8.15 Time history of the non – dimensional interaction force provided by the supporting system

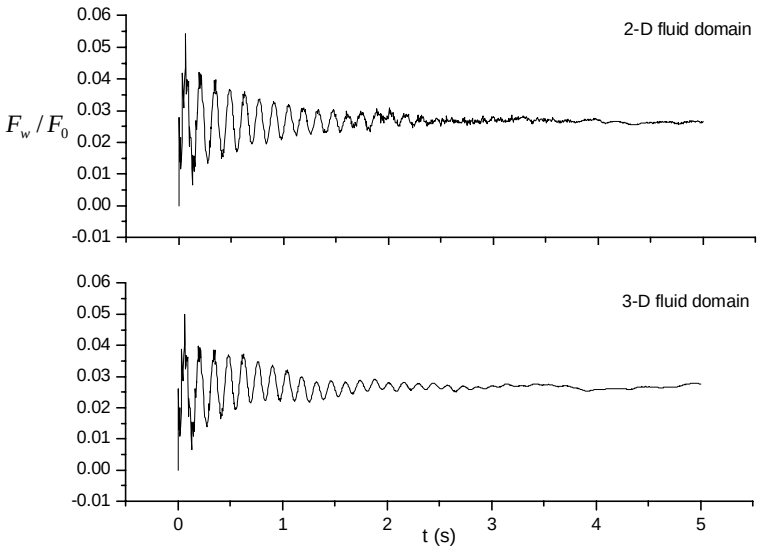

Figure 8.16 Time history of the non – dimensional resultant vertical force from induced water pressure

Chapter 9

An Airplane Landing onto a Floating Structure

The final investigation uses the proposed analysis method to simulate the landing of a simplified Boeing 747-400 jumbo plane onto a floating structure.

Modal analysis is carried out with ANSYS (2004) for both the airplane and the floating structure. The natural frequencies and the numerical modes of the two solid substructures are obtained. The landing gear system of Boeing 747-400 jumbo plane is simplified with 4 linear spring-damper units using the linearization scheme discussed in Chapter 3.

With the developed program MMFBEP, the responses of both the airplane and the floating structure during the landing process are solved. The numerical results are presented and discussed. Some physical explanations may be useful for the future design of a floating airport.

9.1 General Description

Figure 9.1 schematically illustrates a Boeing 747-400 jumbo plane landing and travelling on a floating structure on the calm surface of a 3D water domain. The landing gear system of the airplane is modelled by four sets of linear spring-damper units $K_1 - C_1, \ldots, K_4 - C_4$. The airplane lands onto the floating structure with an initial vertical velocity V_{z0} and horizontal velocity V_{x0}. Due to the constant landing resistance F_x in the horizontal direction, the airplane travels with a negative acceleration a_x along the $o^{(1)} - x^{(1)}$ axis until it finally stops. The general derivations presented in Chapters 4 and 5, as well as the program MMFBEP discussed in Chapter 6, are directly applied to solve the proposed airplane landing problem.

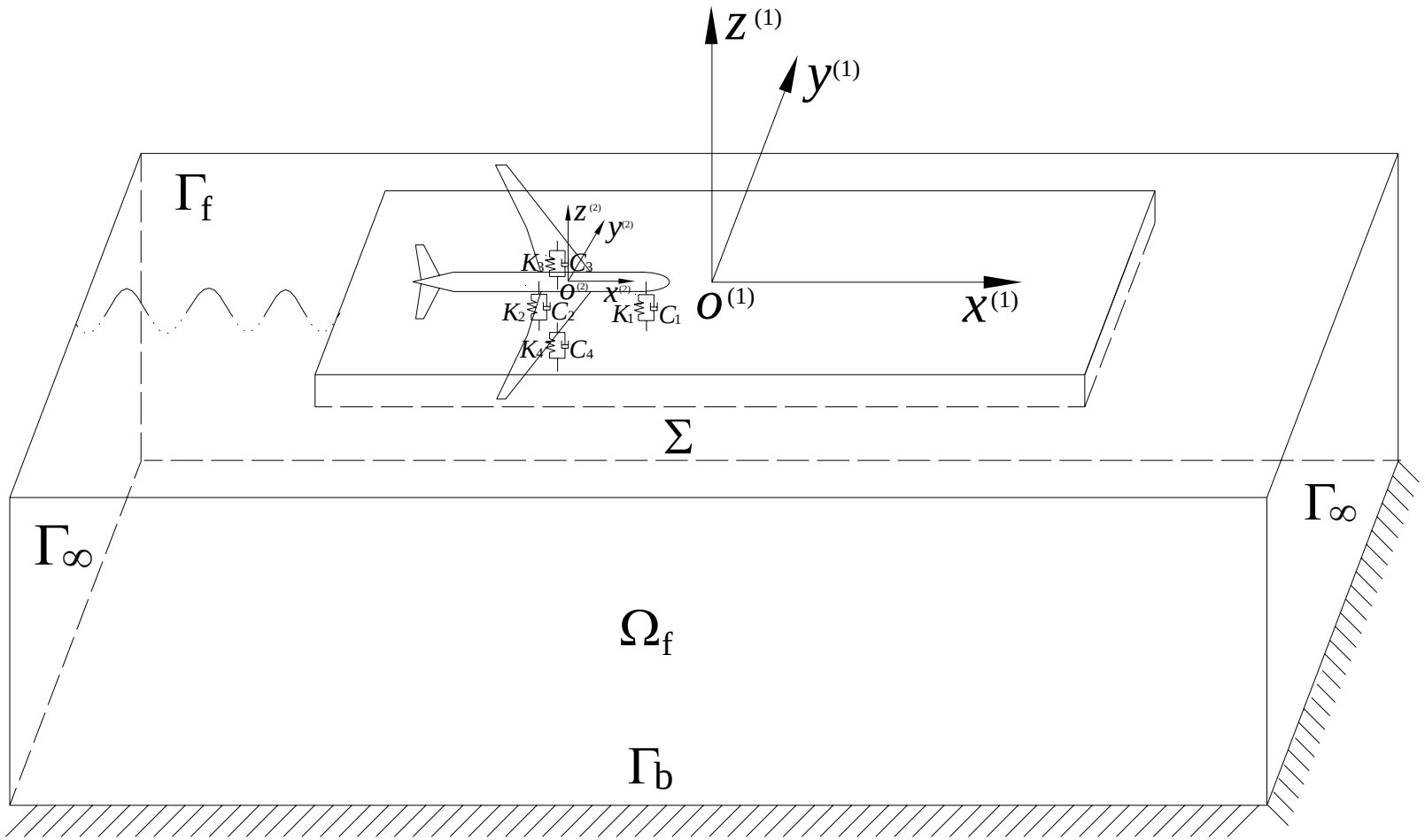

Figure 9.1 A Boeing 747-400 jumbo plane landing on a floating structure

9.2 Modelling of the System

In this study the airplane is modelled as an elastic structure landing and travelling on the runway of a floating airport. The vertical landing velocity of the airplane is considered whilst lift force is neglected. In Kashiwagi's paper (2004), he used a moving and time-varying external load model to represent the airplane landing/take-off and the value of the external load is taken as the difference between the airplane weight and the lift force. Though Kashiwagi (2004) and the author of this thesis addressed the same engineering problem, the analysis details and the relevant parameters used are different due to the different solution methods adopted. The approach presented here provides a complete and realistic model of the airplane- landing problem with a significant increase in modelling complexity.

9.2.1 Model of Boeing 747-400 airplane

A Boeing 747-400 airplane is presented in Figure 9.2. The basic parameters of the airplane are indicated in Table 9.1.

Figure 9.2 Boeing 747-400 jumbo plane (BOEING webpage)

Table 9.1 Basic parameters of Boeing 747-400 airplane (BOEING webpage)

Overall weight	3883.54kN
Wing weight (two wings in total)	422.282kN
Fuselage weight	1568.0kN
Engine weight (four engines in total)	171.99kN
Fuel weight	1721.272kN
Wing span	64.44m
Overall length	70.66m
Tail height	19.41m
Initial horizontal speed in landing	69.35m/s
Initial vertical speed in landing	-3.0m/s
Horizontal acceleration in landing	$-1.26m/s^2$

To illustrate the applications of the developed method in this thesis, the detailed modelling of the complex structure of Boeing 747-400 airplane is not practical or necessary. Instead, a simplified model of the airplane is set up, in which the fuselage and the two wings are modelled by three uniform beams, respectively. The two beams representing the two wings are identical. The simplified model of Boeing 747-400 airplane is depicted in Figure 9.3. *A1*, *A3*, and *A2* represent the two end points and the middle point of the fuselage whilst *A4* and *A5* indicate the middle and end point of the left wing of the airplane. The responses at these five points are to be generated.

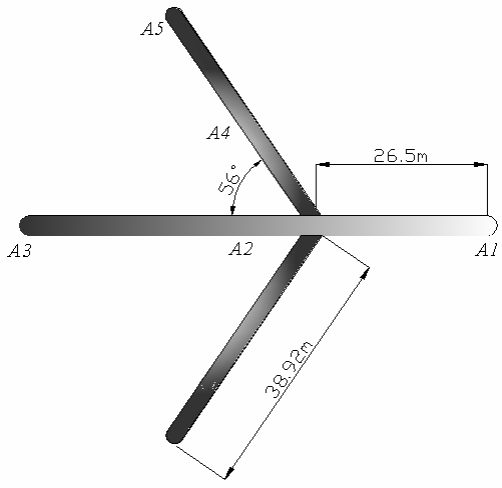

Figure 9.3 Simplified model of Boeing 747-400 jumbo plane

It is assumed that the mass distribution is uniform along the fuselage and the wings of the airplane. The four engines fixed under the two wings are modelled by four concentrated masses and each of these engines is attached to a corresponding node on the wing. To determine the bending rigidity of the beams used to represent the airplane, the following three principles should be followed:

1) The bending rigidity of the wings is relatively smaller than that of the fuselage;

2) The frequency of the first flexible mode of the airplane is around 1-2 Hz and it is the first bending mode of the wings;

3) The first bending mode of the fuselage occurs at a frequency of about 7-8Hz.

According to these principles, the beams' parameters were evaluated and are listed in Table 9.2.

Table 9.2 Parameters of beams used to model Boeing 747-400 airplane

	length	mass density	bending rigidity
beam for fuselage	70.66 m	2761.51 kg/m	2.616×10^{11} Nm^2
beam for wings	38.92 m	2358.71 kg/m	1.08×10^{10} Nm^2

When setting up the airplane model, using ANSYS, the 3D elastic beam element BEAM4 is used to model the fuselage and the wings. Structural mass element MASS21 is adopted to model the engines. In fact 40 BEAM4 elements are used to represent the fuselage, 20 BEAM4 elements are used to model each of the two wings and 4 MASS21 elements are used to represent the four engines. In total, there are 84 elements used to model the Boeing 747-400 airplane. The number of total nodes is 81. Each node is allowed to have three degrees of freedom to model the vertical bending deformation of the airplane. Since the bending stiffness of the airplane in the horizontal direction is very large, the horizontal bending deformation is neglected. Once the finite element model of the airplane is set up, the modal analysis can be conducted.

In general, the period of the landing impacts of an airplane onto a land – based runway is less than 1s (Raymer 1999). The landing period for a sea – based runway is enlarged due to the flexibility of the floating runway. As a rough approximation, we assume that the period of the landing impacts onto a floating runway is between 1s – 2s, which corresponds to a frequency of 0.5 Hz – 1Hz. According to the principles discussed in Chapter 5, those modes of the airplane and the floating structure with a natural frequency smaller than three times the frequency of the landing impacts should be retained. Therefore, the truncation

frequency for the two substructures is taken as 1.5Hz – 3Hz herein.

The first ten modes including three rigid body modes are retained for the airplane. The highest frequency of these ten modes is 13.408 Hz which is much higher than the required truncation frequency. Thus the first ten modes should be sufficient to describe the airplane dynamics response in a landing process. The frequencies of the first ten modes are listed in Table 9.3 and the corresponding modal shapes are presented in Figure 9.4.

Table 9.3 Frequencies of the first ten modes of the airplane model

1^{st} mode	2^{nd} mode	3^{rd} mode	4^{th} mode	5^{th} mode
0Hz	0Hz	0Hz	0.9510 Hz	2.8440 Hz
6^{th} mode	7^{th} mode	8^{th} mode	9^{th} mode	10^{th} mode
4.5978 Hz	6.5231 Hz	6.8658 Hz	13.191 Hz	13.408 Hz

9.2.2 Linearization of landing gear system

A Boeing 747-400 airplane has a landing gear system consisting of five landing gears. The nose gear is approximately located 8m aft of the front end of the airplane. The nose gear has two wheels. The other four are main gears. Two of the main gears are attached to the fuselage at a position approximately half of the overall length of the airplane. The other two main gears are fixed at the two wings, respectively, which are approximately 6m apart from the centerline of the fuselage, and 3m ahead of the main gears on the fuselage. Each of the four main gears has four wheels.

The discussion presented in Chapter 3 shows that the simulation of the landing gear system with a few linear spring-damper units is acceptable. Based on this, the 5 landing gears of the Boeing 747-400 airplane are simulated with four linear spring-damper units of which the two main gears on the fuselage are modelled as one spring-damper unit.

To utilize the linearization scheme proposed in Chapter 3, it is necessary to know the sustained weight on each of the landing gears. On performing a static analysis using ANSYS, it is found that the nose gear sustains 15%, the two main gears on the fuselage sustain 40% and each of the main gears under the wing sustains 22.5% of the overall weight of the airplane. It is also necessary to determine a few parameters of the landing gears of an airplane before the approximate scheme developed in Chapter 3 can be used. As finding these parameters for a commercial airplane such as Boeing 747-400 jumbo jet is very difficult, we have to approximate them herein. The definition and approximation of

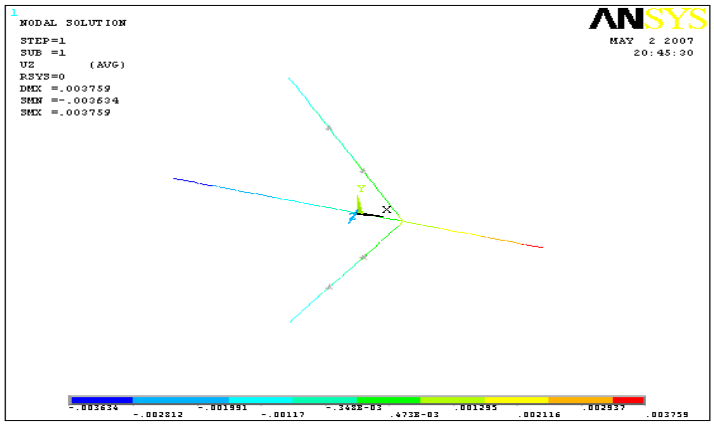
NODAL SOLUTION
STEP=1
SUB =1
UZ (AVG)
RSYS=0
DMX =.003759
SMN =-.003694
SMX =.003759
ANSYS
MAY 2 2007
20:45:30

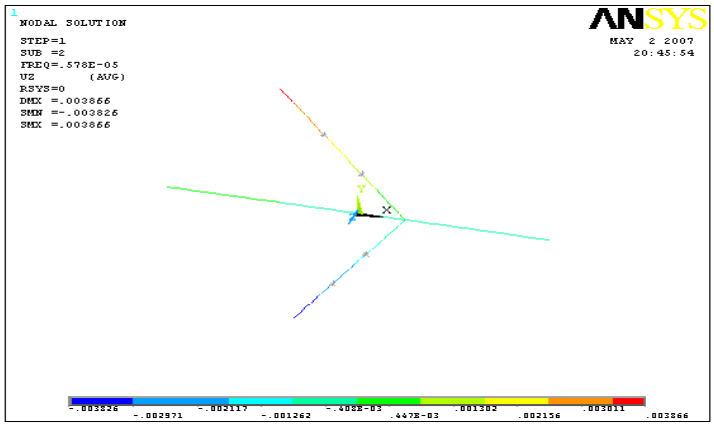
NODAL SOLUTION
STEP=1
SUB =2
FREQ=.578E-05
UZ (AVG)
RSYS=0
DMX =.003866
SMN =-.003826
SMX =.003866
ANSYS
MAY 2 2007
20:45:54

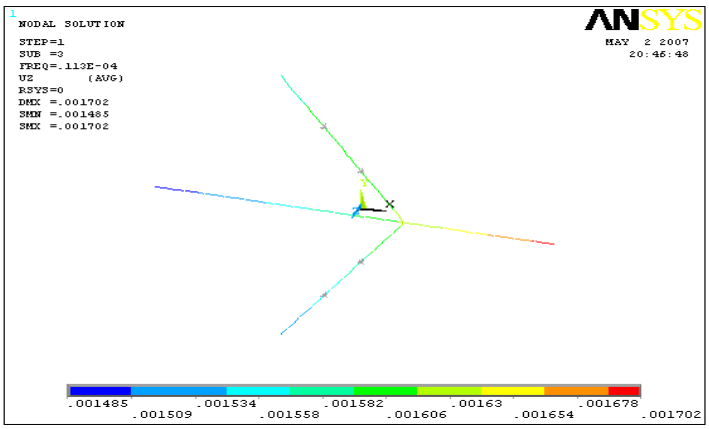
NODAL SOLUTION
STEP=1
SUB =3
FREQ=.113E-04
UZ (AVG)
RSYS=0
DMX =.001702
SMN =.001485
SMX =.001702
ANSYS
MAY 2 2007
20:46:48
.001485
.001509
.001534
.001558
.001582
.001606
.00163
.001654
.001678
.001702

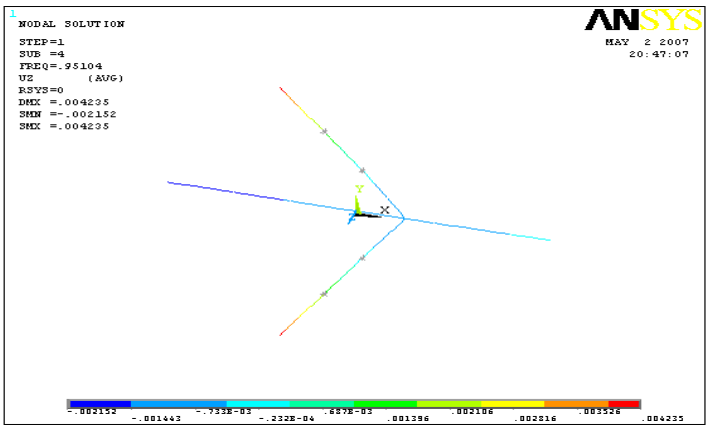
NODAL SOLUTION
STEP=1
SUB =4
FREQ=.95104
UZ (AVG)
RSYS=0
DMX =.004235
SMN =-.002152
SMX =.004235
ANSYS
MAY 2 2007
20:47:07

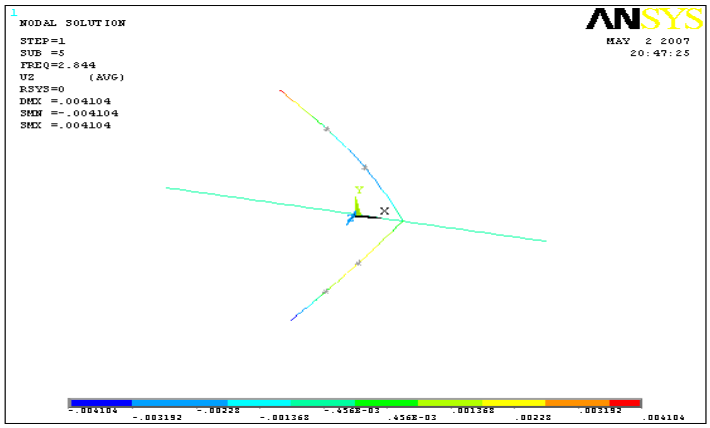
NODAL SOLUTION
STEP=1
SUB =5
FREQ=2.844
UZ (AVG)
RSYS=0
DMX =.004104
SMN =-.004104
SMX =.004104
ANSYS
MAY 2 2007
20:47:25

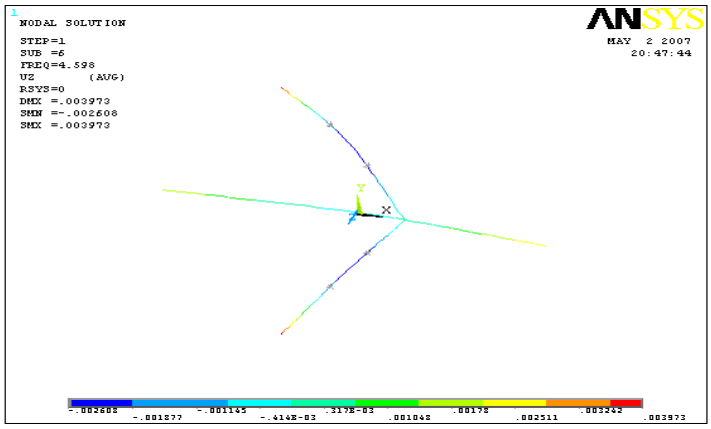
NODAL SOLUTION
STEP=1
SUB =6
FREQ=4.598
UZ (AVG)
RSYS=0
DMX =.003973
SMN =-.002608
SMX =.003973
ANSYS
MAY 2 2007
20:47:44

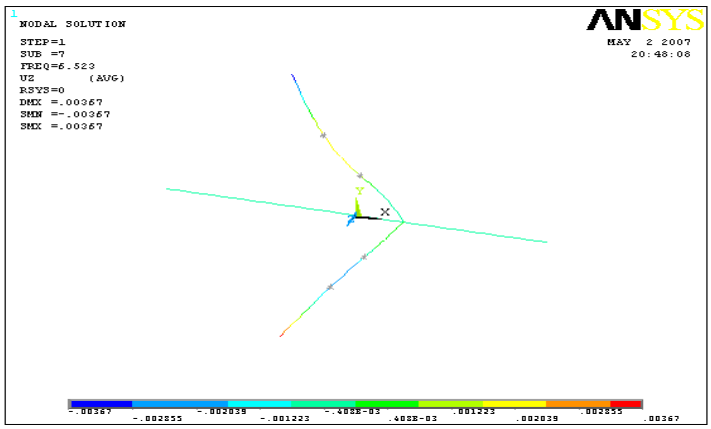
NODAL SOLUTION
STEP=1
SUB =7
FREQ=6.523
UZ (AVG)
RSYS=0
DMX =.00367
SMN =-.00367
SMX =.00367
ANSYS
MAY 2 2007
20:48:08

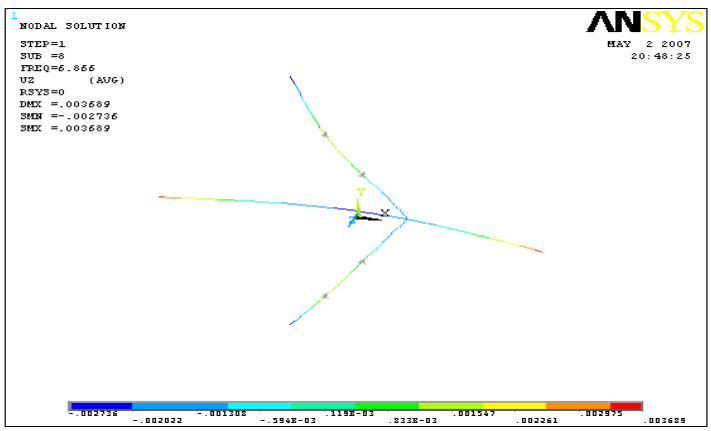
NODAL SOLUTION
STEP=1
SUB =8
FREQ=6.866
UZ (AVG)
RSYS=0
DMX =.003689
SMN =-.002736
SMX =.003689
ANSYS
MAY 2 2007
20:48:25

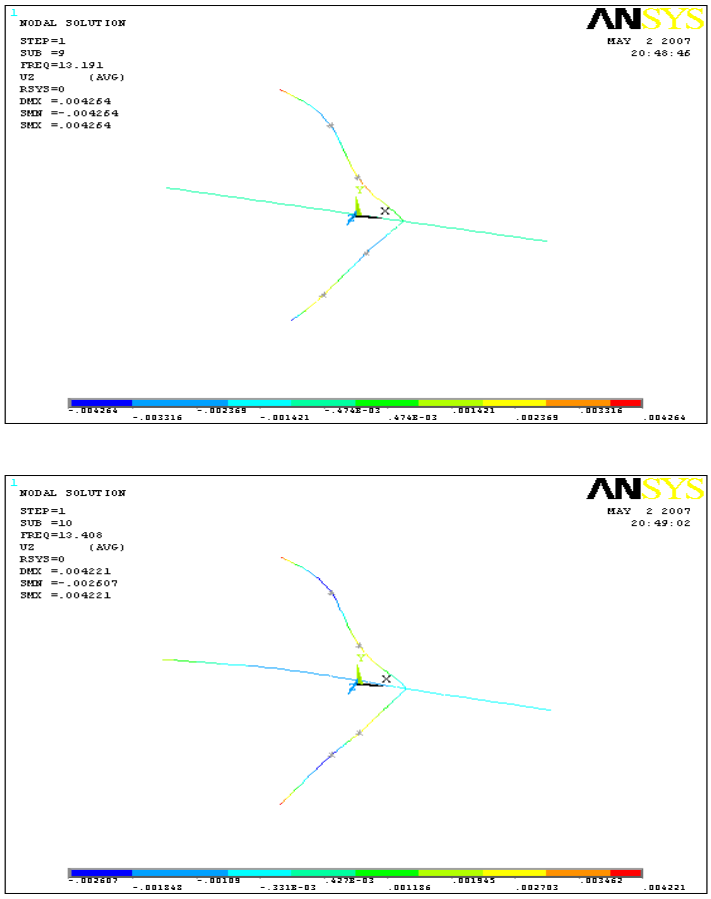

Figure 9.4 First ten modes of airplane model

these parameters are explained in Chapter 3. On assuming that these parameters are all the same for the landing gears of 747-400 airplane, their values are listed in Table 9.4.

Table 9.4 Parameters of the landing gears of Boeing 747-400 airplane

Parameter	Value
load factor n'	1.5
transfer coefficient ϕ'	1
energy absorption efficiency η	0.7
static stroke parameter a	0.25
energy dissipation coefficient χ	0.65

Following the schemes presented in Chapter 3, the spring and damper coefficients of the four linear spring-damper units used to simulate the five landing gears of Boeing 747-400 airplane are determined and given in Table 9.5.

Table 9.5 Coefficients of the four linear spring-damper units

Spring – damper unit	Spring coefficient	Damping coefficient
nose gear	1.875×10^{6} N/m	2.052×10^{5} Ns/m
two main gears on fuselage	5.0×10^{6} N/m	5.473×10^{5} Ns/m
main gear on each wing	2.8125×10^{6} N/m	3.079×10^{5} Ns/m

9.2.3 Model of floating structure

The floating structure considered herein is a rectangular thin plate as depicted in Figure 9.5.

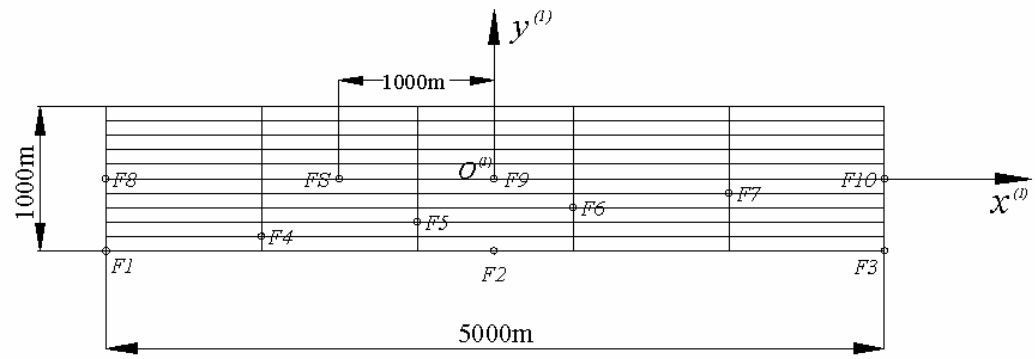

Figure 9.5 Model of floating structure

Within Figure 9.5 the labels *F1*, *F2*, …, *F10* indicate the position of the ten nodes at which responses are to be generated. The runway is located along the longitudinal axis of the floating structure. The initial landing position of the airplane is at point *FS*. The parameters of the floating structure are presented in Table 9.6.

Table 9.6 Parameters of floating structure (Kashiwagi 2004)

Length L	5000m
Breadth B	1000m
Depth T	10m
Draught d	5m
Flexural Rigidity EI/B	1.764×10^{11}Nm
Poisson's Ratio $\mu^{(1)}$	0.3

Elastic shell element SHELL63 is used to mesh the floating structure in ANSYS. There are 50 elements along the longitudinal axis and 10 elements across the transverse axis of the floating structure. In total, the number of elements is 500 and the number of nodes is 561. Each node is assumed to have three degrees of freedom, one of which is vertical displacement and the other two are rotations about the longitudinal and transverse axes, respectively.

The natural frequency of the large floating structure is relatively low. So in order to meet the required truncation frequency 1.5Hz – 3Hz as discussed in Subsection 9.2.1, it is necessary to keep the first 1000 or even more modes. This means a large amount of memory space and CPU time. To save computational effort and to improve efficiency, the convergence check regarding the proper number of the retained modes is carried out. From the convergence check it is found that the primary response of the floating structure lies in the first 300 modes, thus retaining these modes should be sufficient to describe the dynamic response of the floating structure subject to airplane landing impacts. Ten modes of the floating structure are presented in Figure 9.6, with the associated natural frequencies listed in Table 9.7.

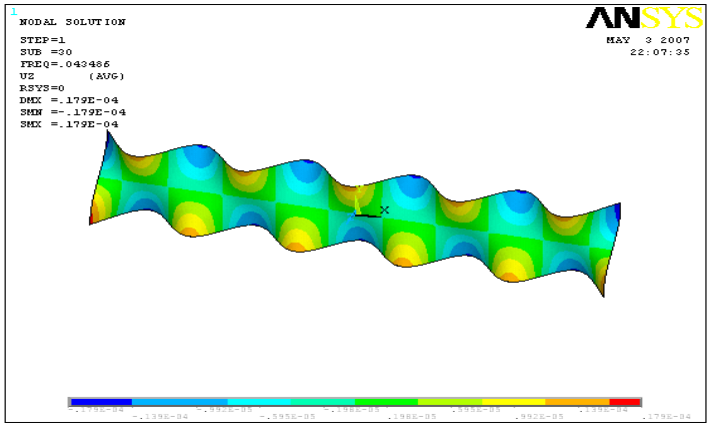

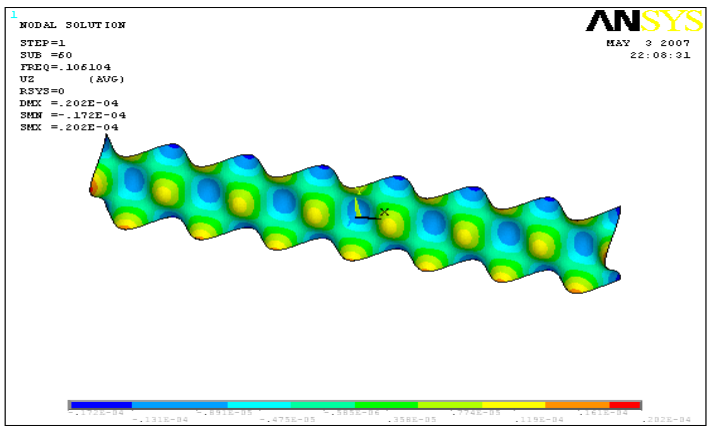

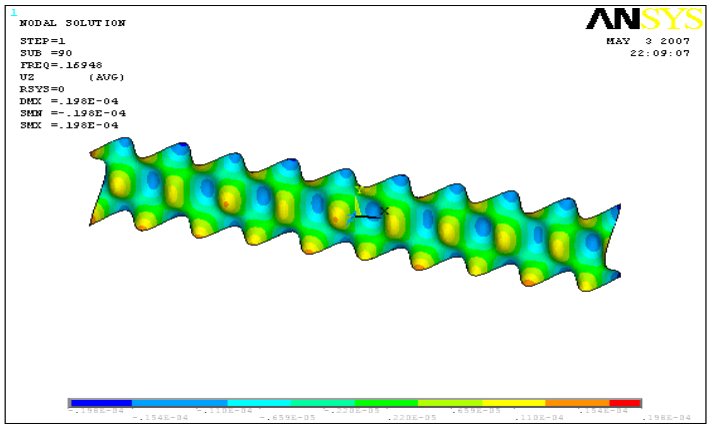
NODAL SOLUTION
STEP=1
SUB =90
FREQ=.16948
UZ (AVG)
RSYS=0
DMX =.198E-04
SMN =-.198E-04
SMX =.198E-04
ANSYS
MAY 3 2007
22:09:07

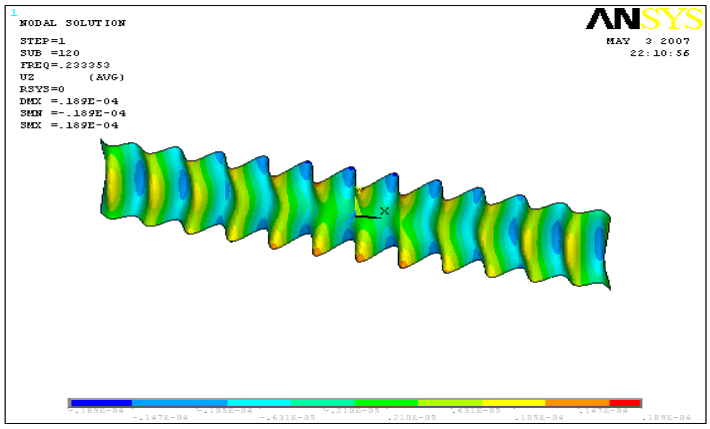
NODAL SOLUTION
STEP=1
SUB =120
FREQ=.233353
UZ (AVG)
RSYS=0
DMX =.189E-04
SMN =-.189E-04
SMX =.189E-04
ANSYS
MAY 3 2007
22:10:56

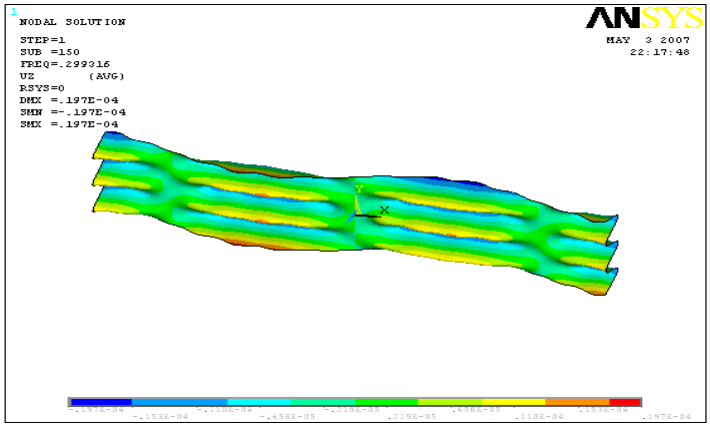
NODAL SOLUTION
STEP=1
SUB =150
FREQ=.299316
UZ (AVG)
RSYS=0
DMX =.197E-04
SMN =-.197E-04
SMX =.197E-04
ANSYS
MAY 3 2007
22:17:48

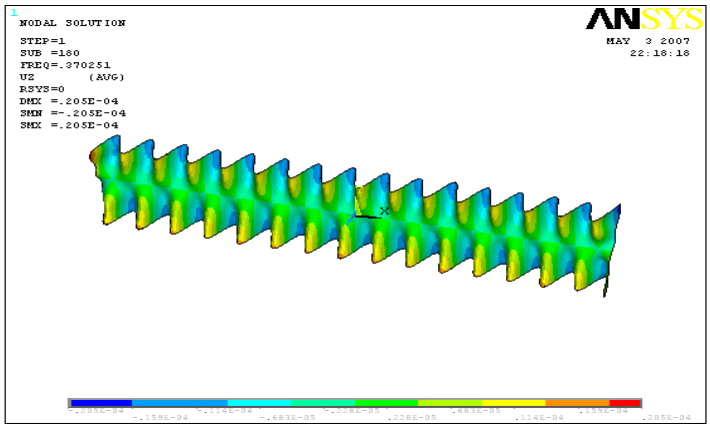
NODAL SOLUTION
STEP=1
SUB =180
FREQ=.370251
UZ (AVG)
RSYS=0
DMX =.205E-04
SMN =-.205E-04
SMX =.205E-04
ANSYS
MAY 3 2007
22:18:18

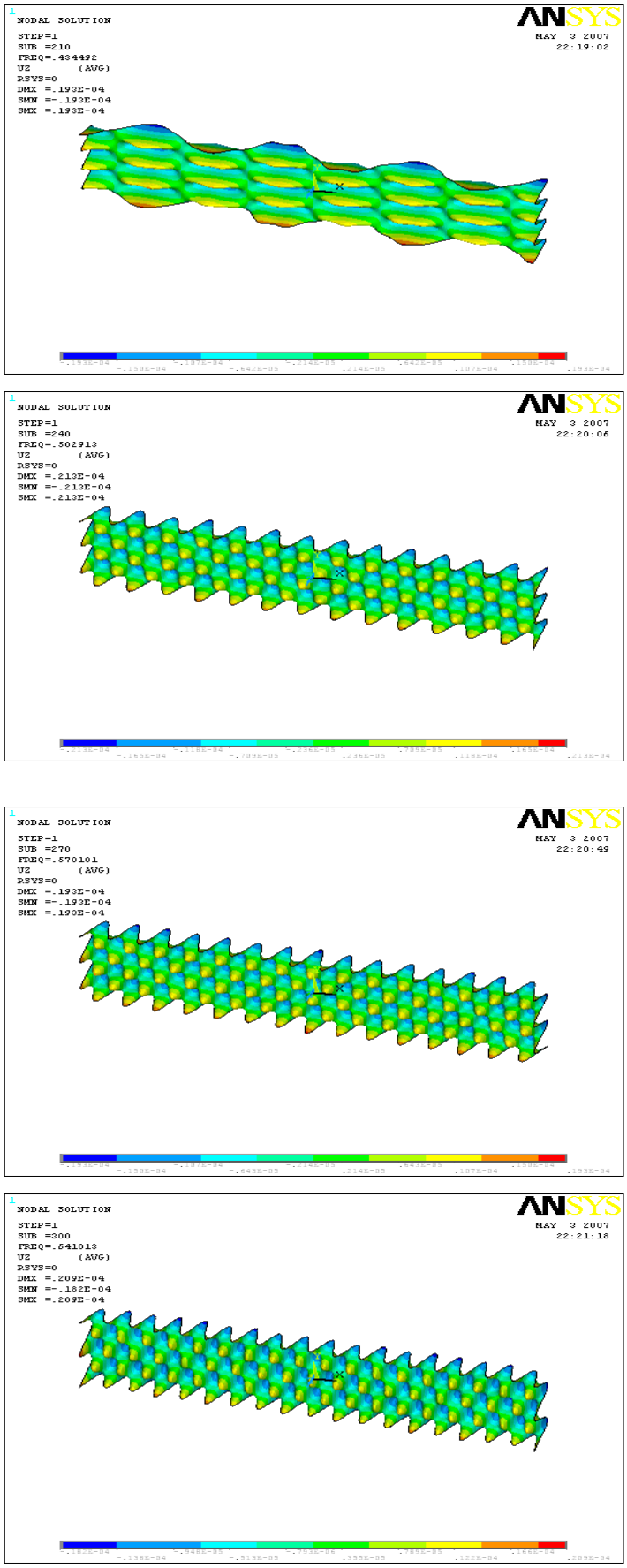

Figure 9.6 Ten picked modes of floating structure

Table 9.7 Frequencies of the ten picked modes of the floating structure

30^{th} mode	60^{th} mode	90^{th} mode	120^{th} mode	150^{th} mode
0.0435 Hz	0.1061 Hz	0.1695 Hz	0.2334 Hz	0.2993 Hz
180^{th} mode	210^{th} mode	240^{th} mode	270^{th} mode	300^{th} mode
0.3703 Hz	0.4345 Hz	0.5029 Hz	0.5701 Hz	0.6410 Hz

9.2.4 Truncation of fluid domain

The free surface of the retained fluid domain in the numerical simulation is a rectangle of length 3×5000 m, width 3×1000 m and with its centre at point $o^{(1)}$. At the corresponding far field boundary, it is assumed that the undisturbed condition is satisfied as within the interested time period, the generated waves can not reach the assumed far field boundary. The whole fluid surface is divided into 9×500 constant boundary elements, of which $N_{\Sigma}=1\times 500$ elements are on the wetted interaction interface and $N_f=8\times 500$ elements are on the free surface. It is assumed that the 500 boundary elements on the wetted interaction interface coincide with the 500 structural elements of the floating structure.

Due to the capacity of current computers, a convergence check concerning influence of fluid domain truncation has not been extensively investigated. In theory, the larger the retained fluid domain, the better the results of the simulation.

The total time of the landing process is 55s. And the time step $\Delta t=0.055$ s is used in the time integration scheme. The running time of program MMFBEP for the current problem is about 16 hours and 30 minutes.

9.3 Results and Discussions

Figure 9.7 presents the vertical deformation $U_z^{(2)}$ of the airplane at time $t=11$s. The vertical oscillation of the airplane is damped significantly within the first ten seconds, after which the airplane tends to its static equilibrium position dominated by gravity.

Figure 9.8 describes the vertical deformation $U_z^{(1)}$ of the floating structure at times $t=11, 22, 33, 44$ and 55s, which illustrate the traveling effect of the airplane. Although the

airplane stops at $t = 55$ s, the generated structural waves keep propagating towards the forward end of the floating structure. On taking the initial landing position as a reference point, it is observed that the deformation at the forward part of the floating structure is much larger than that at the aft part. And the extreme value of the deformation seems to occur at the two forward corners, with a magnitude maintained within 0.02m.

Figure 9.9 gives the distribution of water pressure P at the bottom of the floating structure at time $t = 11, 22, 33, 44$ and 55s. At the beginning of the landing process, the peak value of the water pressure is rather obvious and corresponds to the instantaneous position of the airplane. As time goes on, the water pressure distribution at the forward part of the floating structure seems to exhibit larger amplitudes than that of the aft part. Toward the end of the landing process, the fluctuation of the water pressure along the floating structure tends to be comparable over the forward and aft parts of the floating structure.

Figures 9.10 to 9.12 respectively present the time histories of the deformation $U_z^{(2)}$, the vertical velocity $\dot{U}_z^{(2)}$ and the acceleration $\ddot{U}_z^{(2)}$ at the five nodes *A1* to *A5* of the airplane defined in Figure 9.3. All these time histories indicate damped oscillations with a relatively stable frequency of 0.67Hz, which is found to be related to the natural frequency of the airplane at the fixed end of the landing gears. Generally speaking, the response of the wings is relatively larger than that of the fuselage. The responses at the three fuselage nodes *A1* to *A3* are quite alike, which implies that during the landing process, the fuselage of the airplane behaves rather like a rigid body. A high frequency oscillation component is observed on the velocity and acceleration responses at the two fuselage end points *A1* and *A3*, especially at point *A3*. The maximum value of the response of the airplane occurs at point *A5* on the tip of the wing.

Figures 9.13 – 9.15 show the time histories of the displacement $U_z^{(1)}$, the vertical velocity $\dot{U}_z^{(1)}$ and acceleration $\ddot{U}_z^{(1)}$ at the ten nodes *F1* to *F10* of the floating structure defined in Figure 9.5. The responses at those nodes behind the initial landing position are relatively small, for example node *F1*, *F4* and *F8*. The responses at those nodes along or close to the runway, for example *F6* and F9, indicate the travelling effect of the airplane. The displacement responses reach their minimum value once the airplane has passed by. The responses at the front end of the floating structure, for example *F3* and F10, clearly show the formulation and the travelling of the generated waves. Extreme responses seem to occur at the two forward corners with the maximum displacement of the order of 0.02m.

Figure 9.16 indicates the time histories of water pressure P at the ten selected nodes of

the floating structure. The maximum value of water pressure occurs at node *F9* when the airplane passes by. The water pressure at those nodes behind the initial landing position is relatively small, for example at nodes *F1, F4* and *F8*. The water pressure shows relatively large fluctuation at those nodes close to the runway, for example at nodes *F2, F5, F6* and *F7*.

Figure 9.17 gives the time histories of the relative deformation between the airplane and the floating structure $\left(U_z^{(2)} - U_z^{(1)}\right)$ at the four linear spring-damper units, each of which presents a damped oscillation with a frequency 0.67Hz. Figure 9.17 confirms that the four linear spring – damper units are in a compressive state throughout the whole landing process.

Figures 9.18 and 9.19 present the time histories of the force f_i $(\mathrm{i} = 1,2,3,4)$ provided by each of the four linear spring-damper units and the resultant total force $\sum_{i=1}^{4} f_i$, respectively. The forces provided by the linear spring-damper units oscillate with the same frequency as that of the responses of the airplane and tend to the static value after the first 10s.

Figure 9.20 gives the time history of the resultant vertical force F_w induced by water pressure. The resultant force exhibits a damped oscillation with the same frequency as that of force from the spring – damper units in the first few seconds, thereafter it tends to oscillate with a relatively lower frequency before achieving its final static value. For such a huge floating structure, it may take a long time for it to rest at its static equilibrium position after the airplane comes to a stop.

The third quite realistic simulation indicates how insight on the impact of a landing airplane may be gained and hence how beneficial changes to the airplane and the floating structure might be achieved.

Comparing the results of this study and those of Kashiwagi (2004), the displacement of the runway at selected points on the centre line are found to be different in terms of the oscillatory pattern, graphical smoothing of the overall movement of the runway displacement in Kashiwagi's study and the raw results presented in this study, and the overall magnitude of the displacement, bounded by ± 1cm in Kashiwagi's study and generally bounded by ± 2cm in this study. The reasons causing these discrepancies are probably:

1) As stated earlier in section 9.2, lift force is included in Kashiwagi's study but

excluded in this study;

2) In subsection 9.2.1, a rather severe landing condition is considered in this study with the vertical landing velocity equal to 3m/s, which normally ranges from 1-3 m/s . The influence of the vertical landing velocity was not considered in Kashiwagi's study.

The above suggests that the two sets of results are not very comparable due to the difference of the two approaches. In order to compare them in a realistic way, the external load used in Kashiwagi's study shall be measured from a real landing test onto a floating airport under a particular landing condition.

Here only the landing situation has been investigated whereas Kashiwagi presents corresponding results for landing and take-off. In future work, addressed more fully in the next chapter it would be useful to integrate the loads acting on the airplane to see if drag is increased and hence more fuel or a longer floating structure is required for safe take-off of the Boeing 747-400.

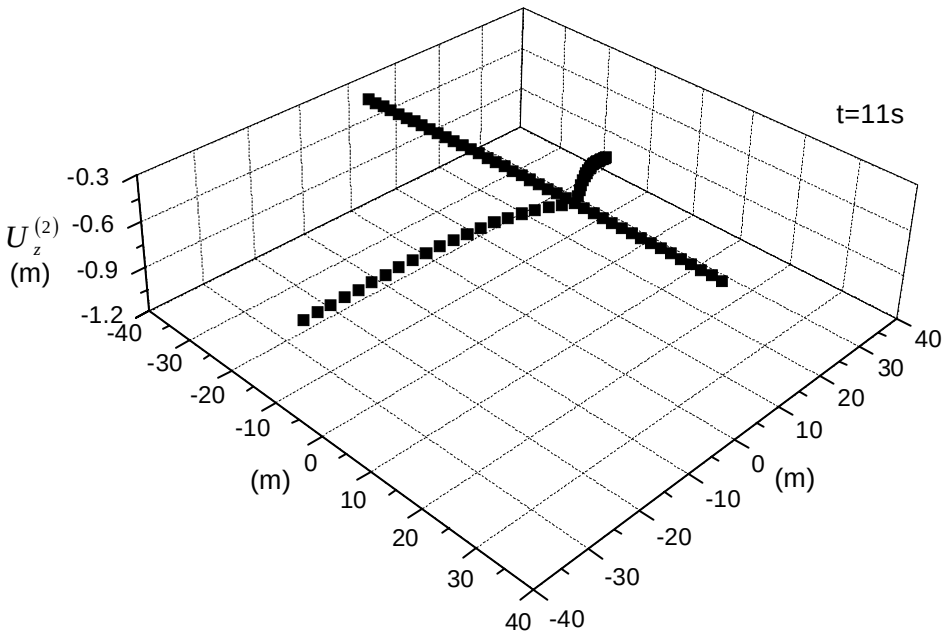

Figure 9.7 Distribution of the displacement of airplane at time t=11s.

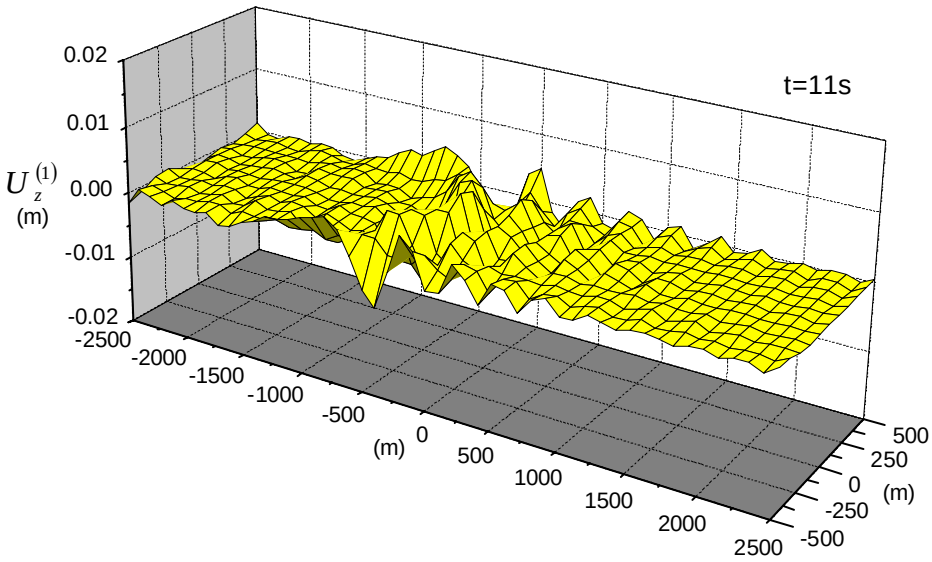
t=11s
$U_z^{(1)}$
(m)
0.02
0.01
0.00
-0.01
-0.02
-2500
-2000
-1500
-1000
-500
0
500
1000
1500
2000
2500
(m)
500
250
0
-250
-500
(m)

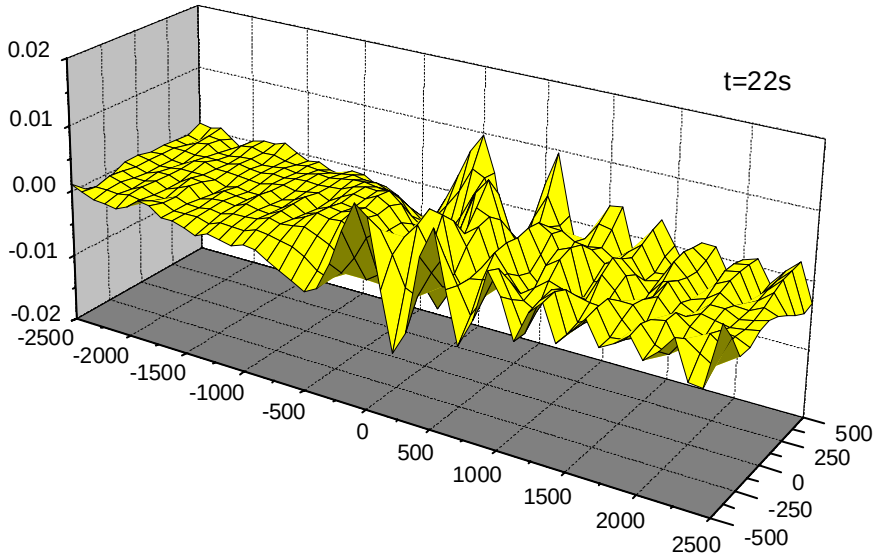
t=22s
0.02
0.01
0.00
-0.01
-0.02
-2500
-2000
-1500
-1000
-500
0
500
1000
1500
2000
2500
500
250
0
-250
-500

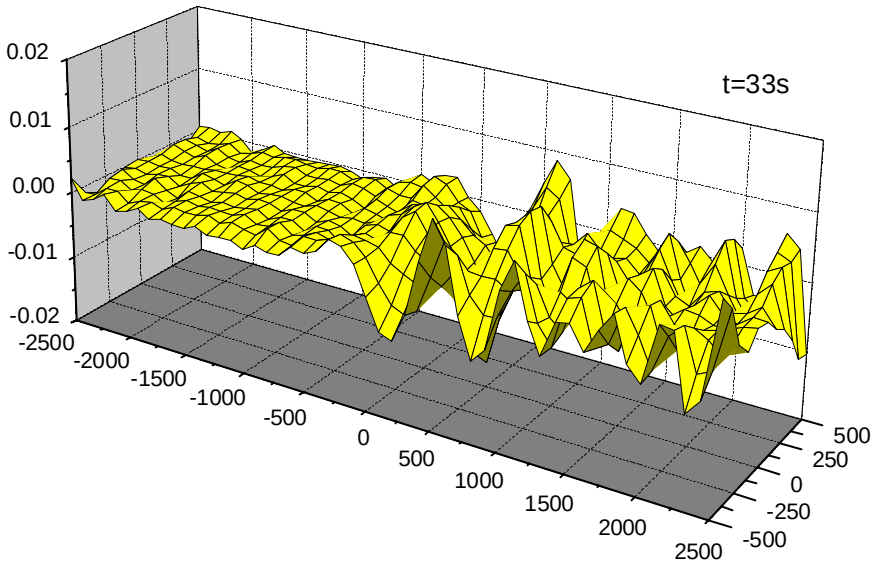
t=33s
0.02
0.01
0.00
-0.01
-0.02
-2500
-2000
-1500
-1000
-500
0
500
1000
1500
2000
2500
500
250
0
-250
-500

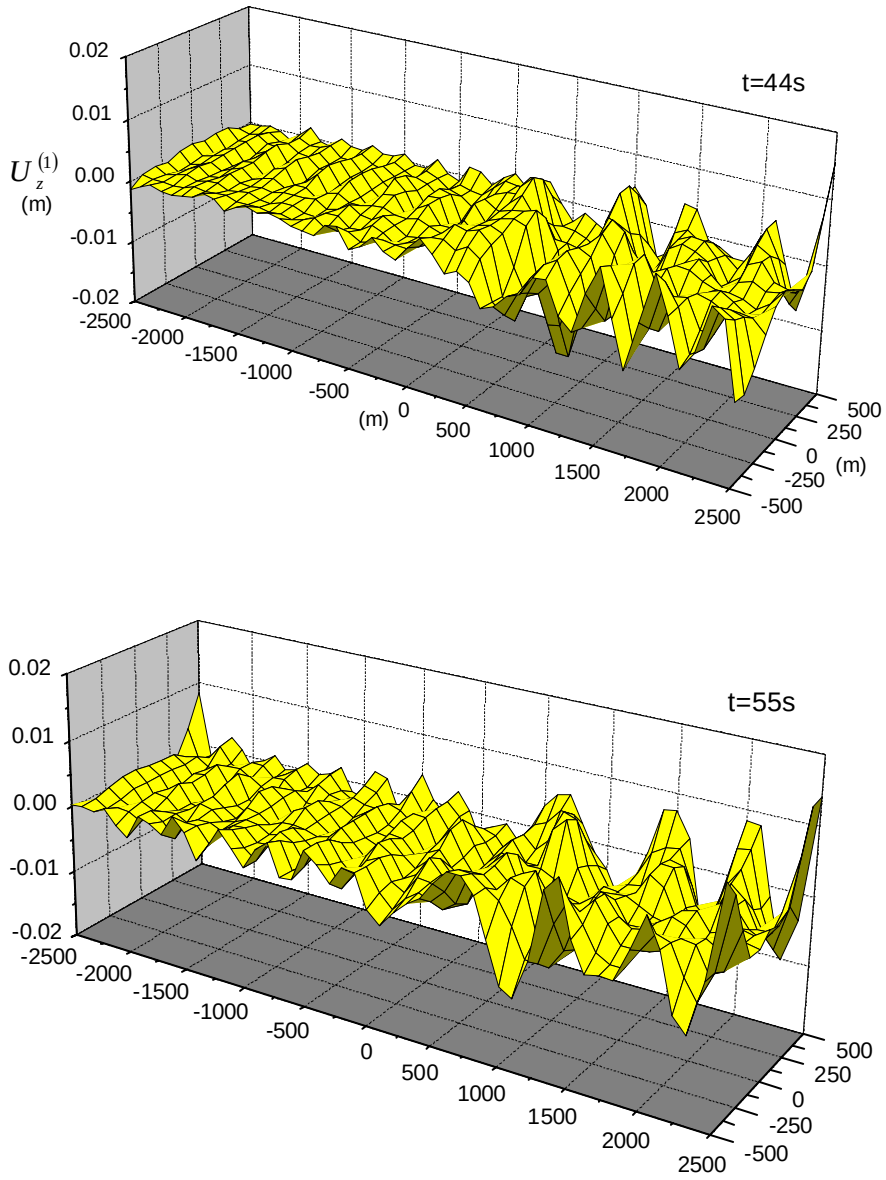

Figure 9.8 Distribution of the deformation of floating structure at five distinct times

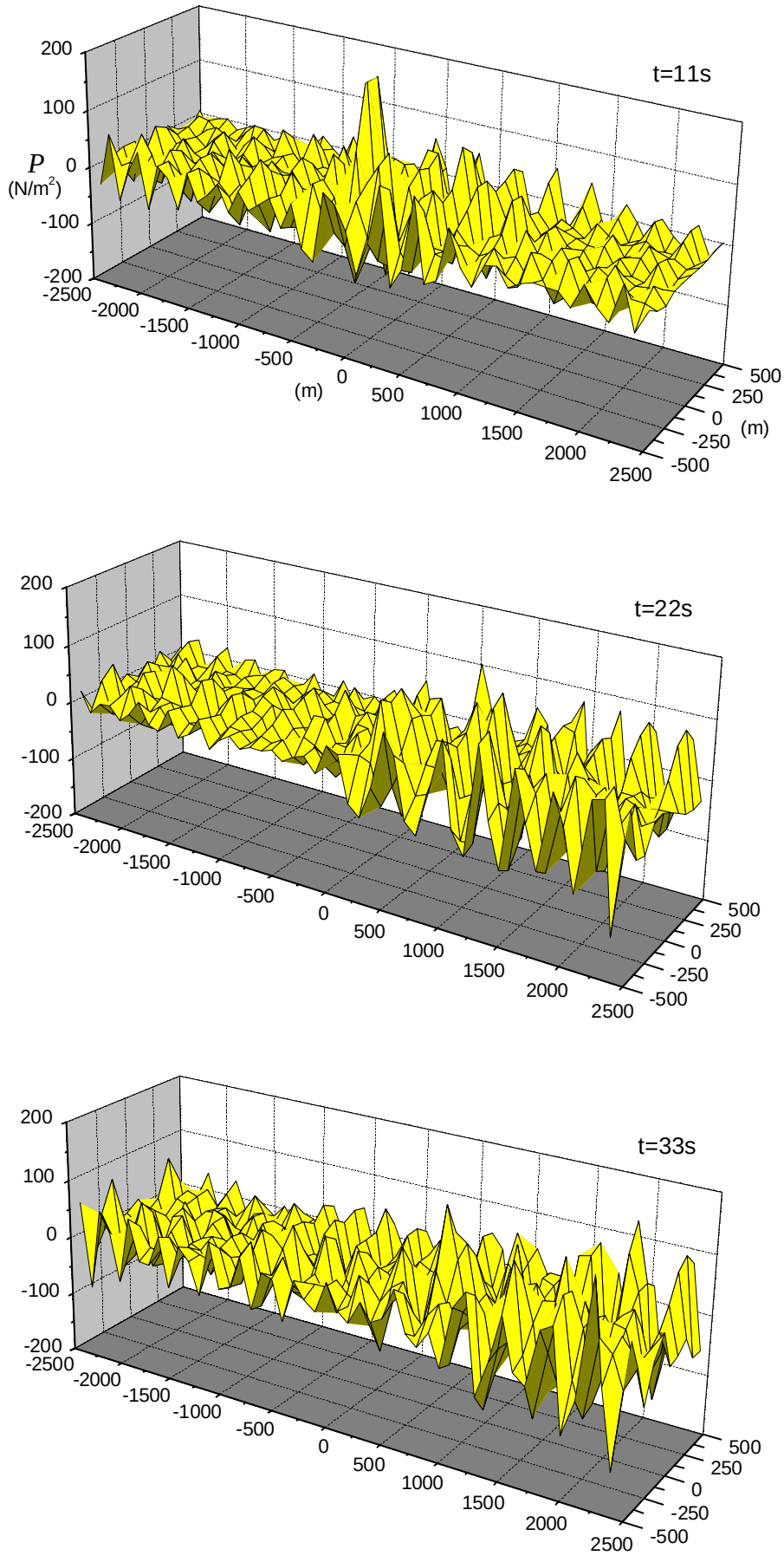
t=11s
t=22s
t=33s
P
(N/m2)
200
100
0
-100
-200
-2500
-2000
-1500
-1000
-500
0
500
1000
1500
2000
2500
(m)
500
250
0
-250
-500
(m)

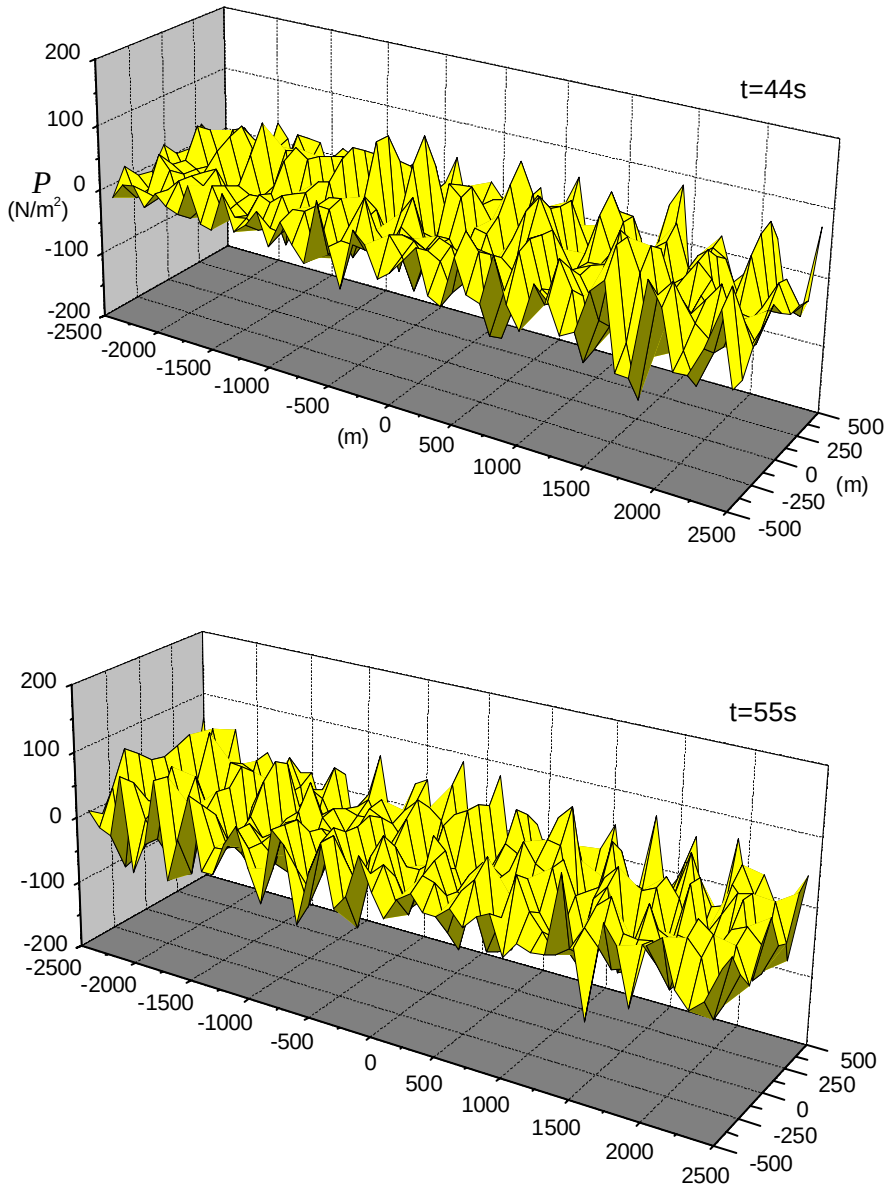

Figure 9.9 Distribution of water pressure along the floating structure at five distinct times

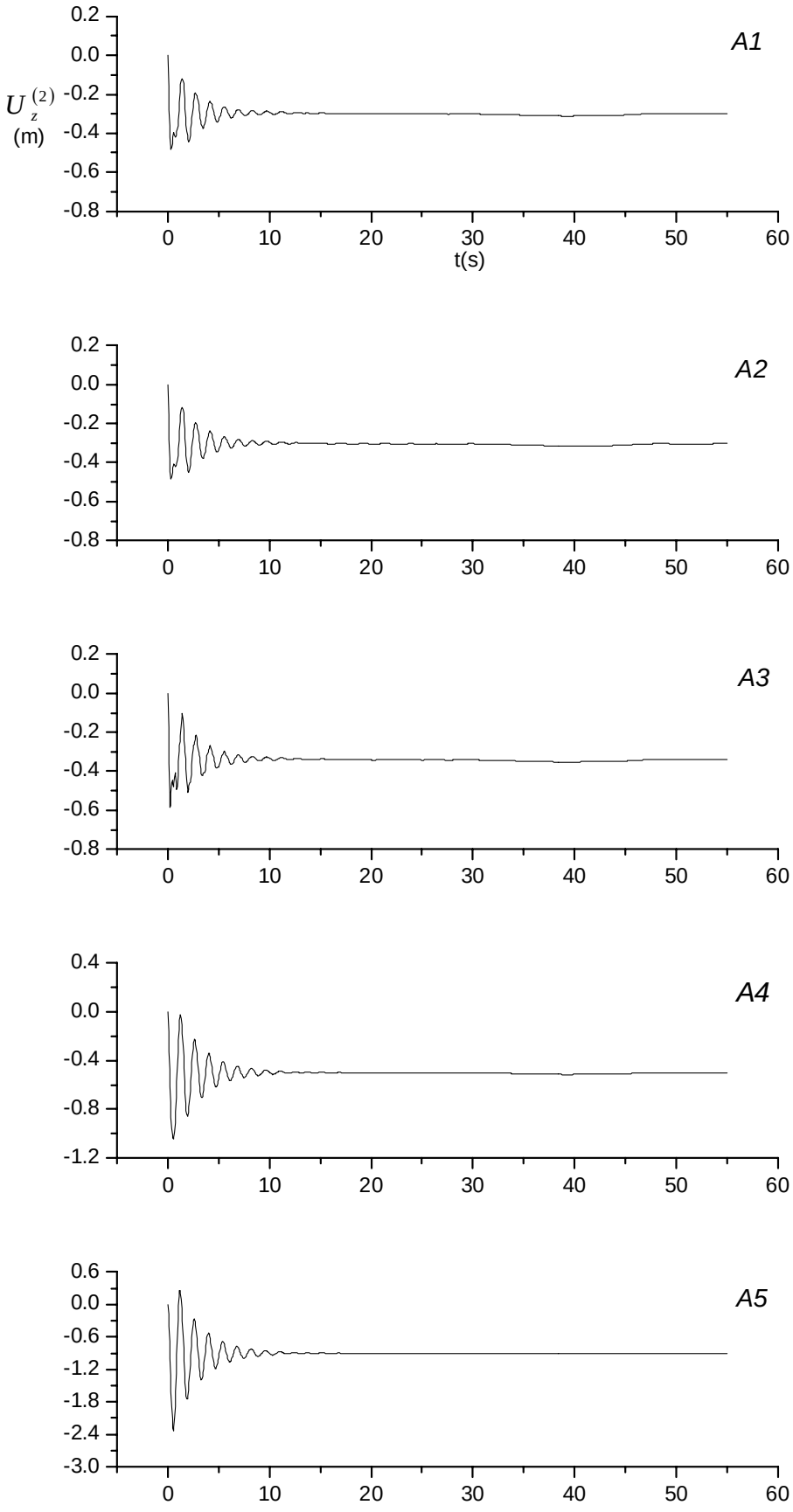

Figure 9.10 Time histories of the deformation at the five nodes of the airplane

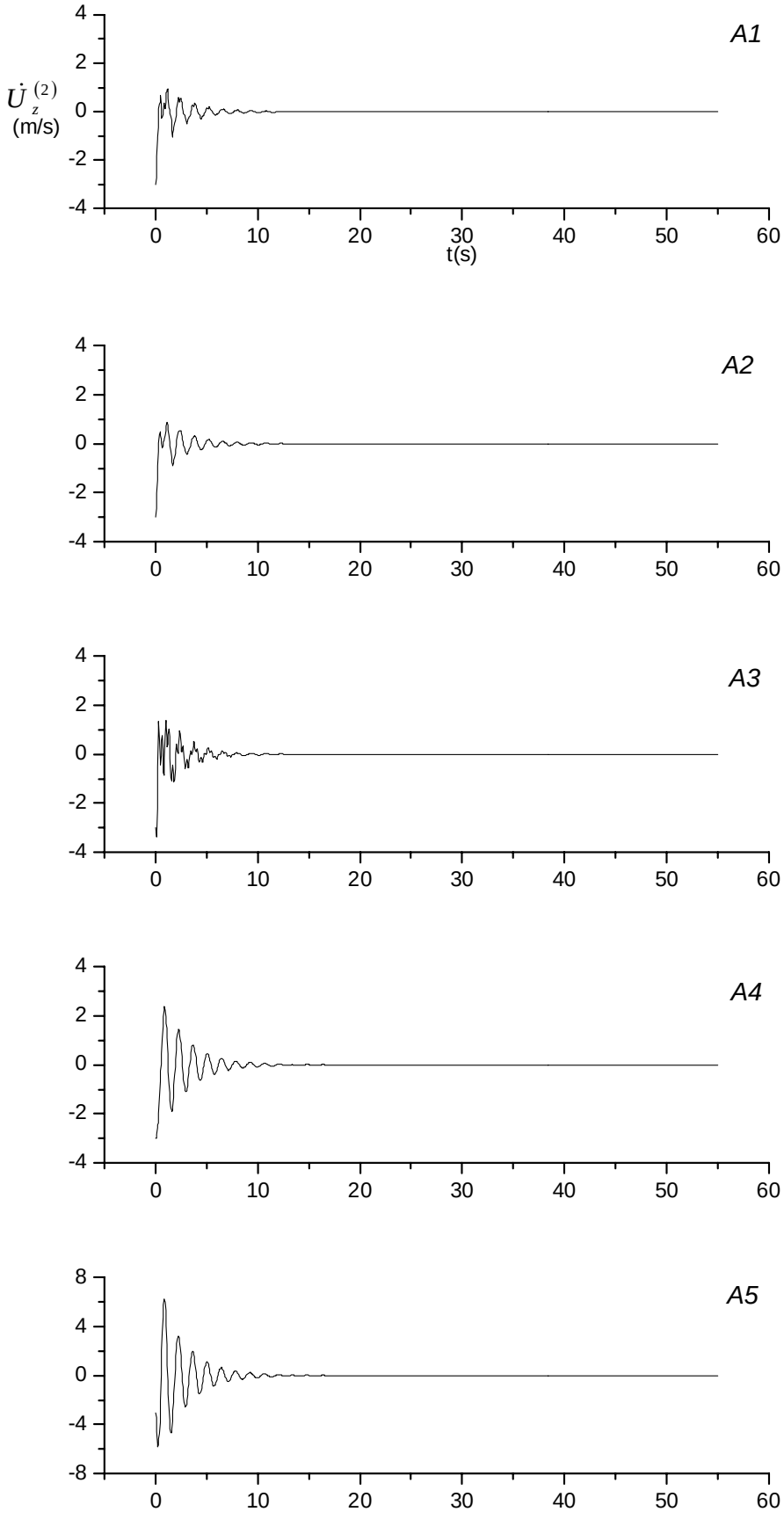

Figure 9.11 Time histories of the vertical velocity at the five nodes of the airplane

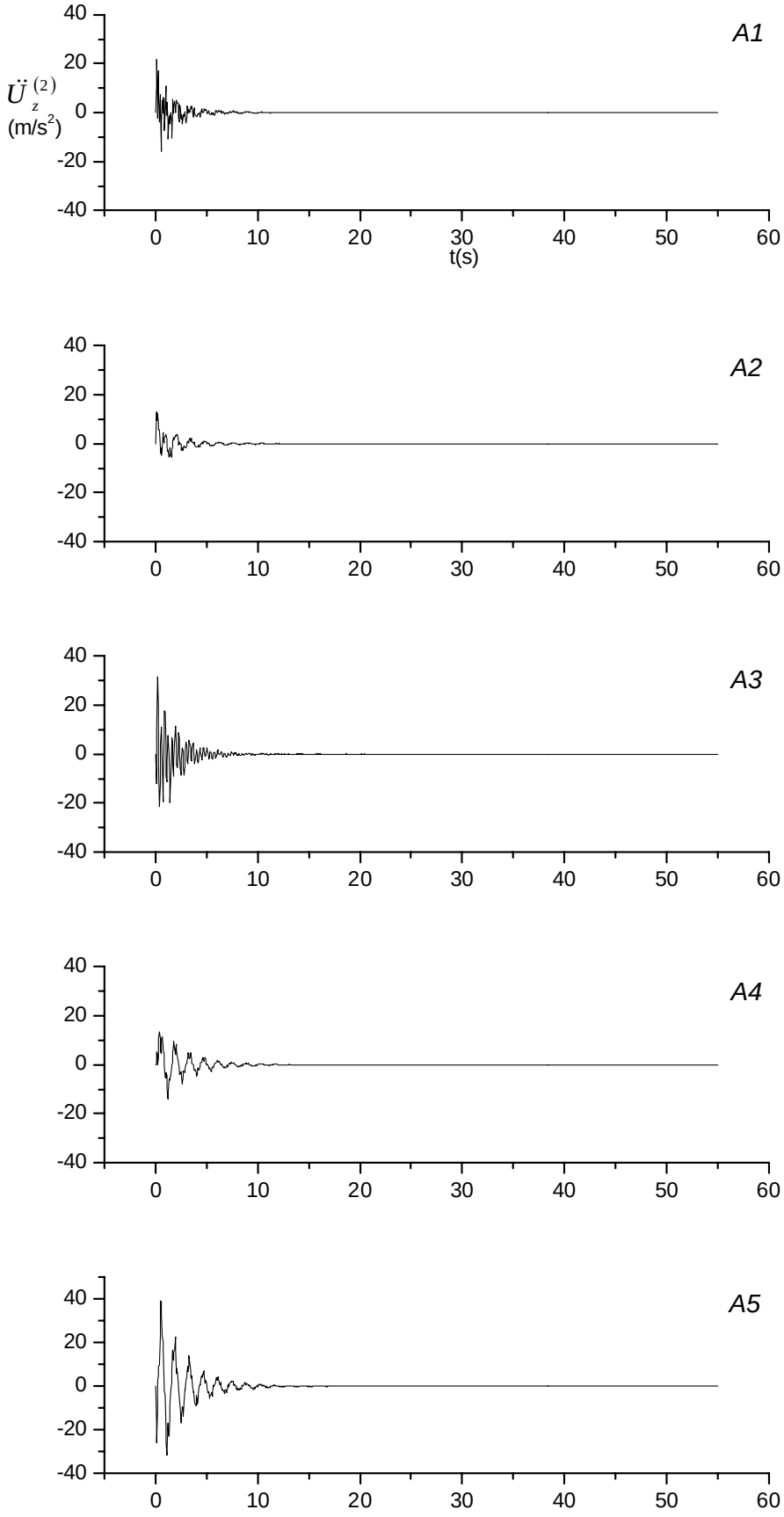

Figure 9.12 Time histories of the vertical acceleration at the five nodes of the airplane

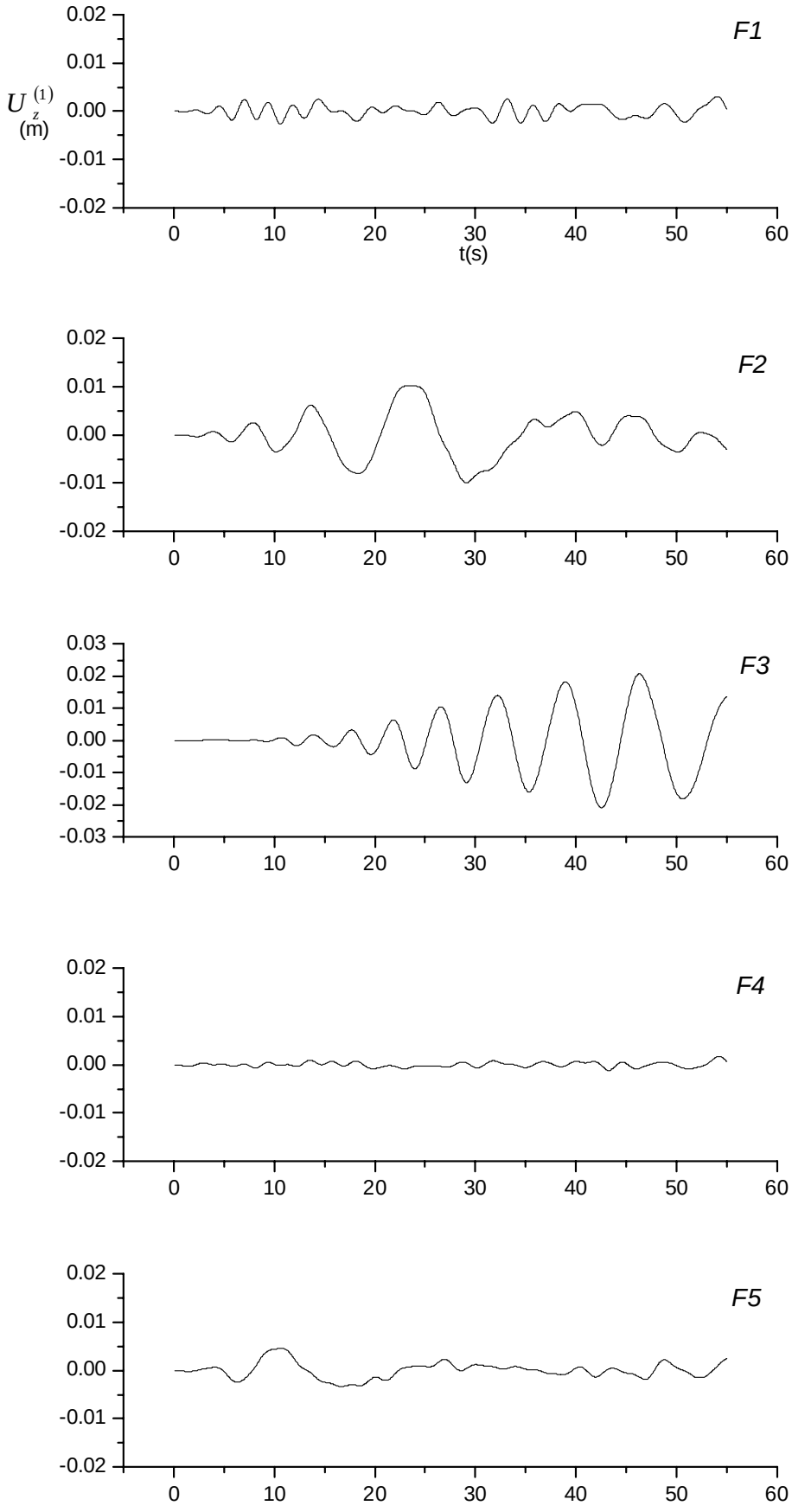
F1
F2
F3
F4
F5
$U_z^{(1)}$ (m)
t(s)
0.02
0.01
0.00
-0.01
-0.02
0.03
-0.03
0
10
20
30
40
50
60

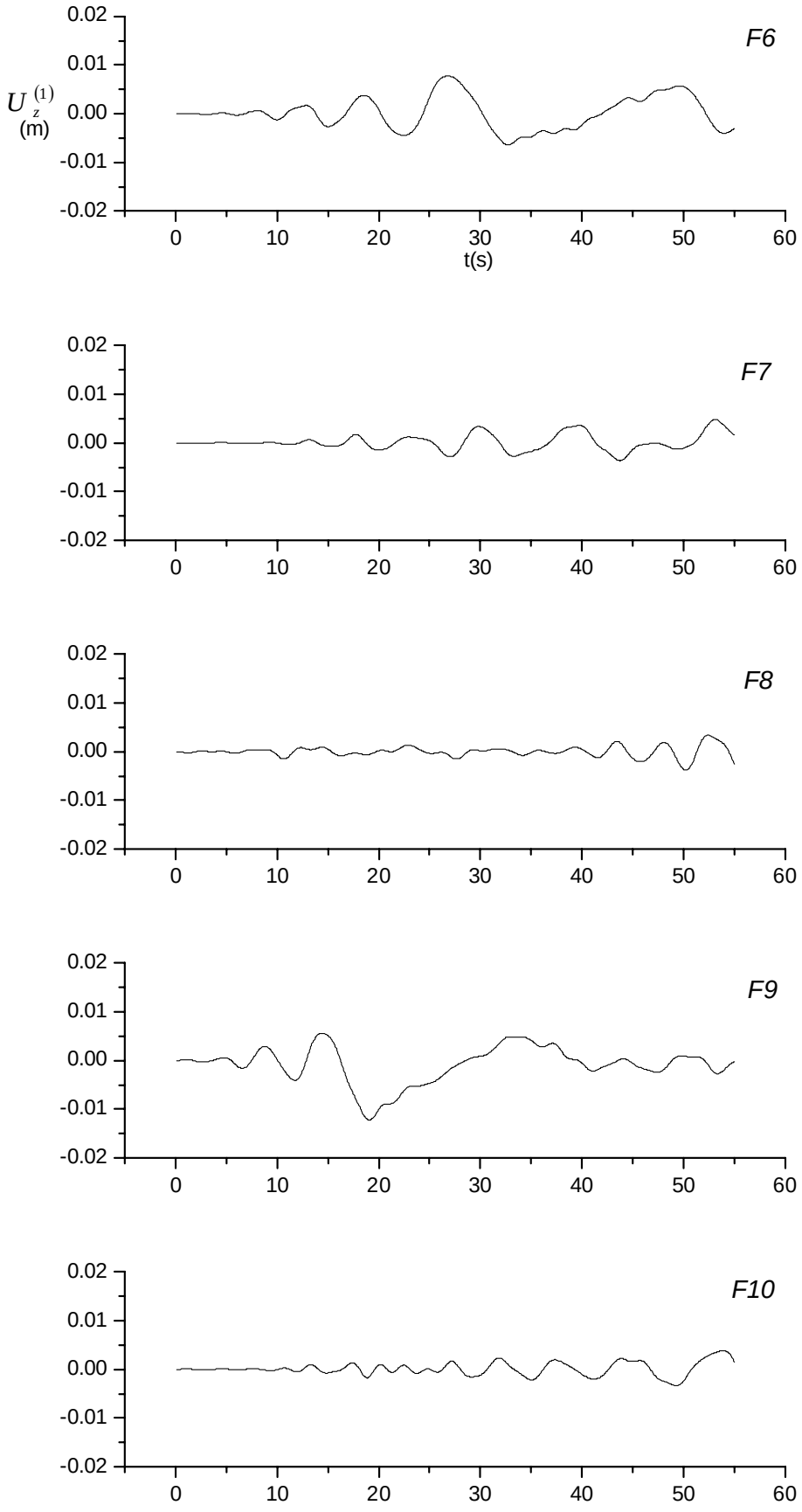

Figure 9.13 Time histories of the deformation of floating structure at the ten selected nodes *F1 – F10*

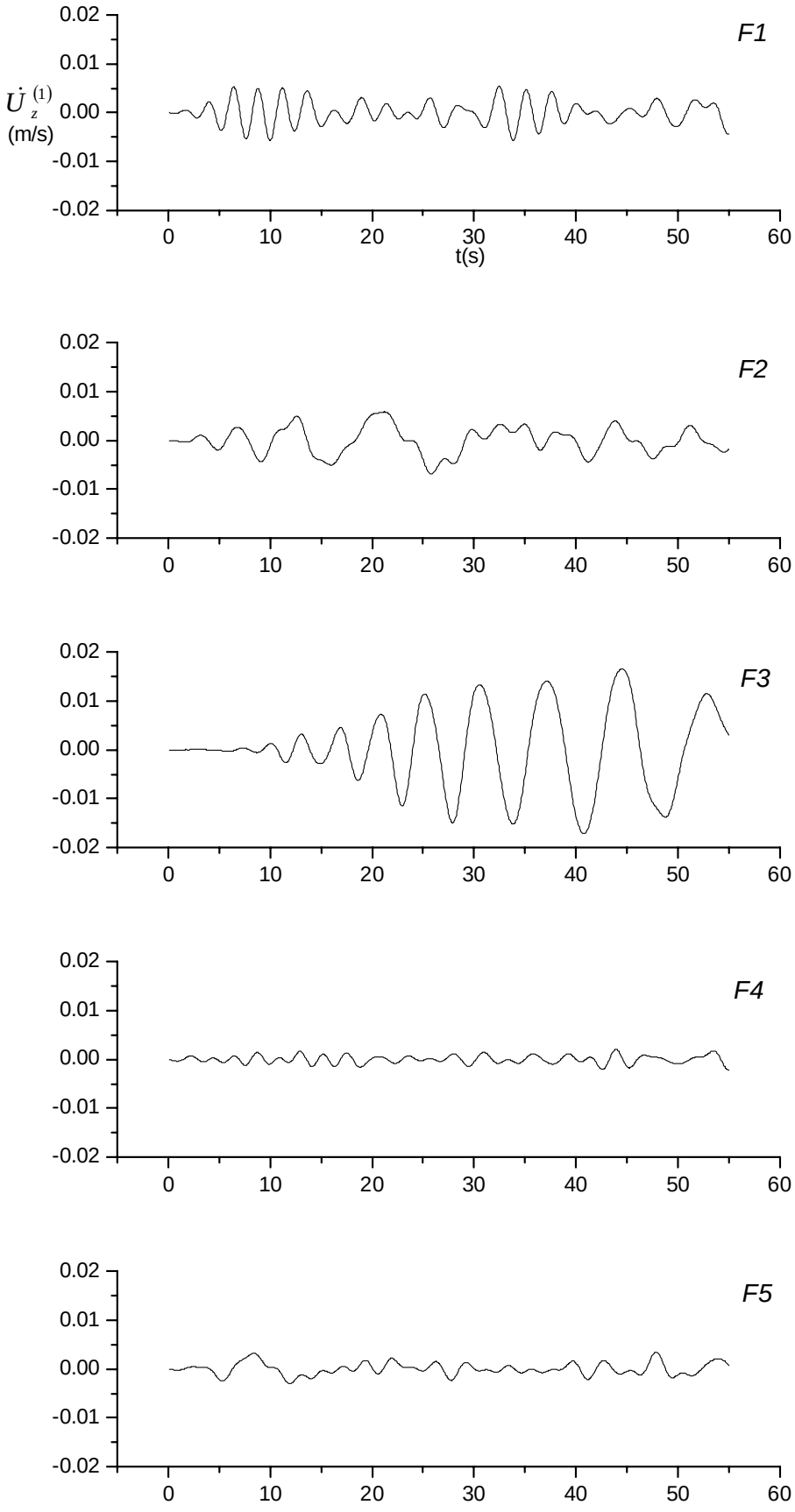
F1
F2
F3
F4
F5
$\dot{U}_z^{(1)}$
(m/s)
t(s)
0.02
0.01
0.00
-0.01
-0.02
0
10
20
30
40
50
60

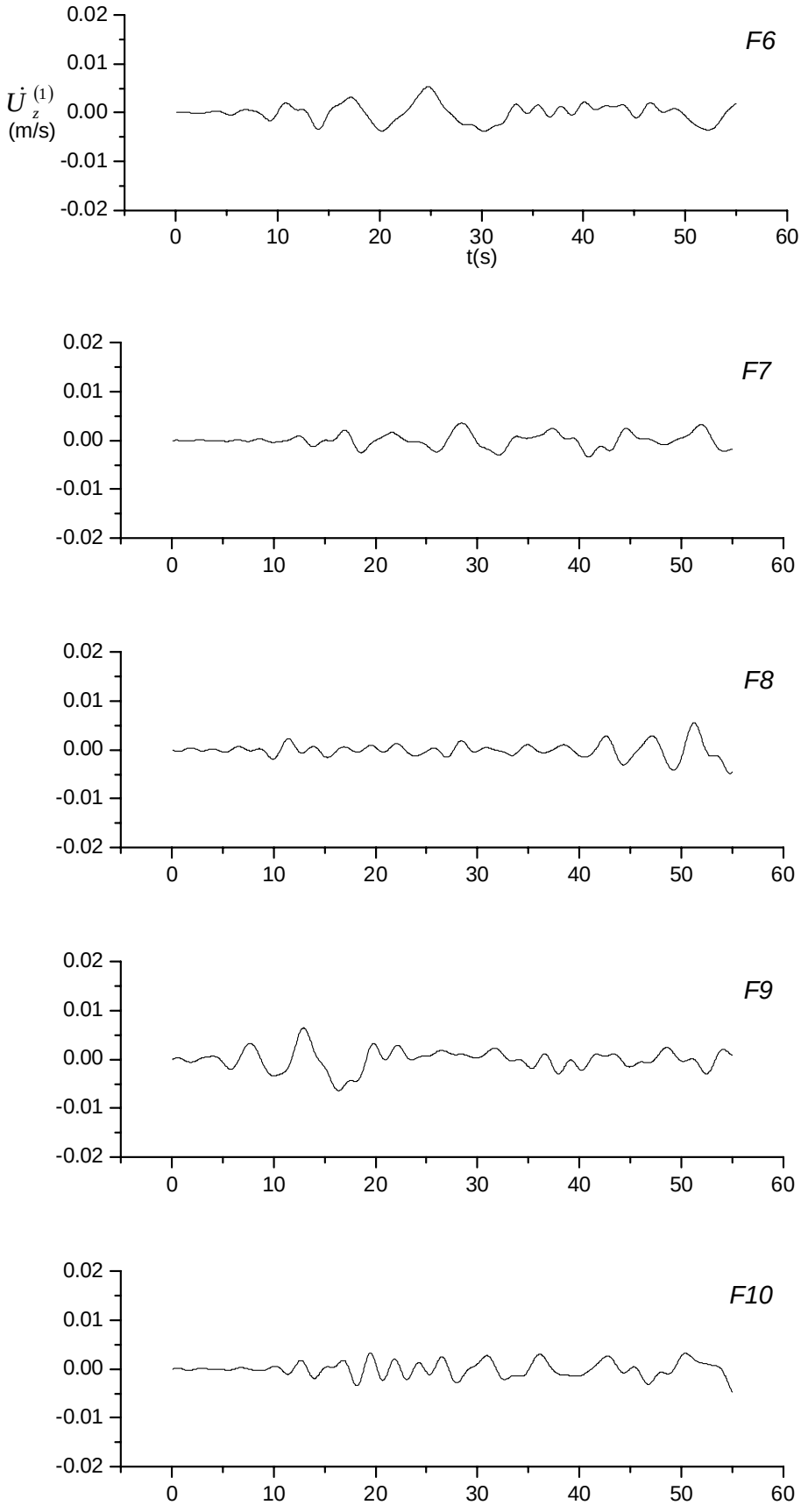

Figure 9.14 Time histories of the vertical velocity of floating structure at the ten selected nodes *F1 – F10*

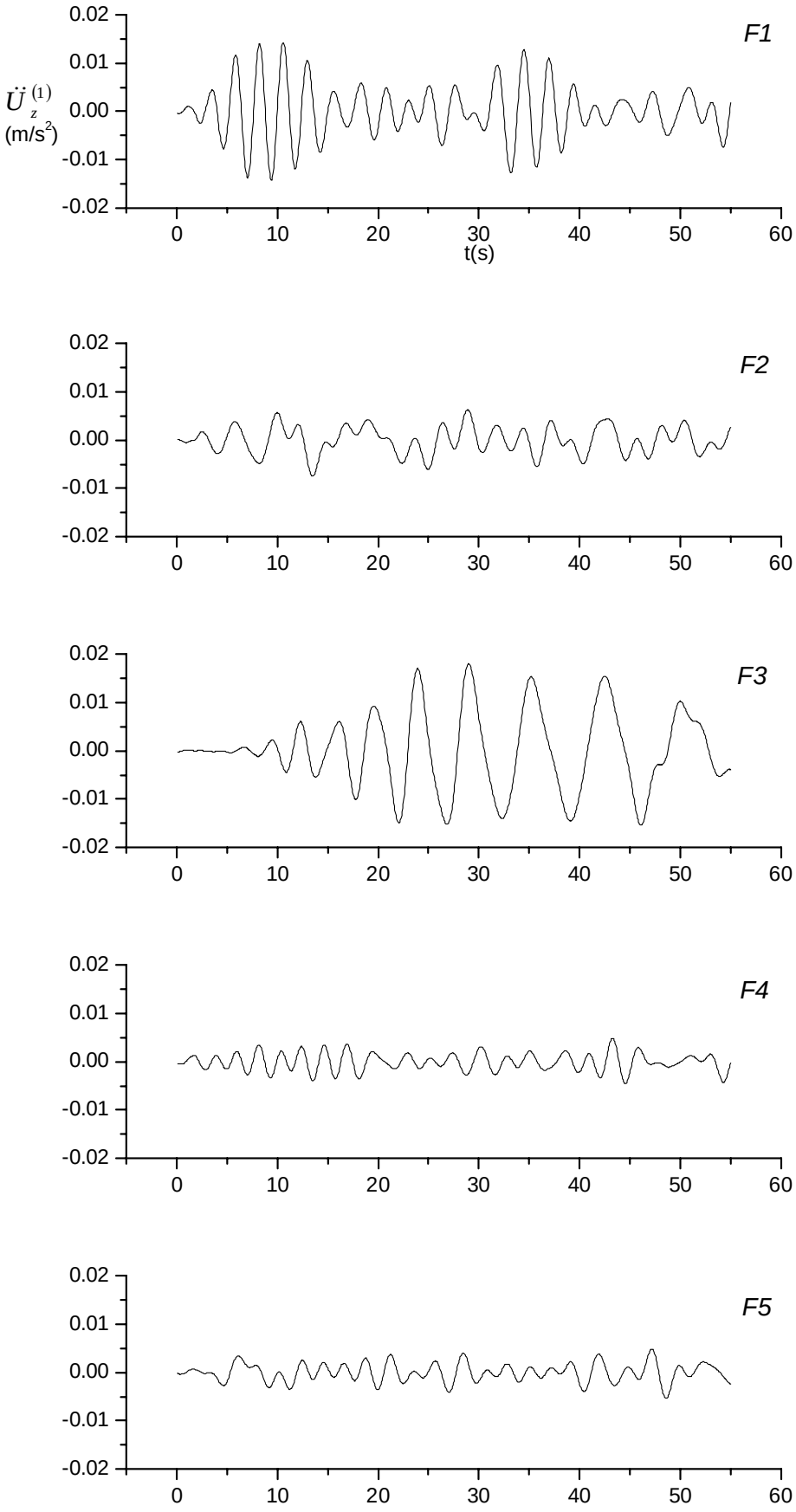
F1
F2
F3
F4
F5
$\ddot{U}_z^{(1)}$
(m/s^2)
t(s)
0.02
0.01
0.00
-0.01
-0.02
0
10
20
30
40
50
60

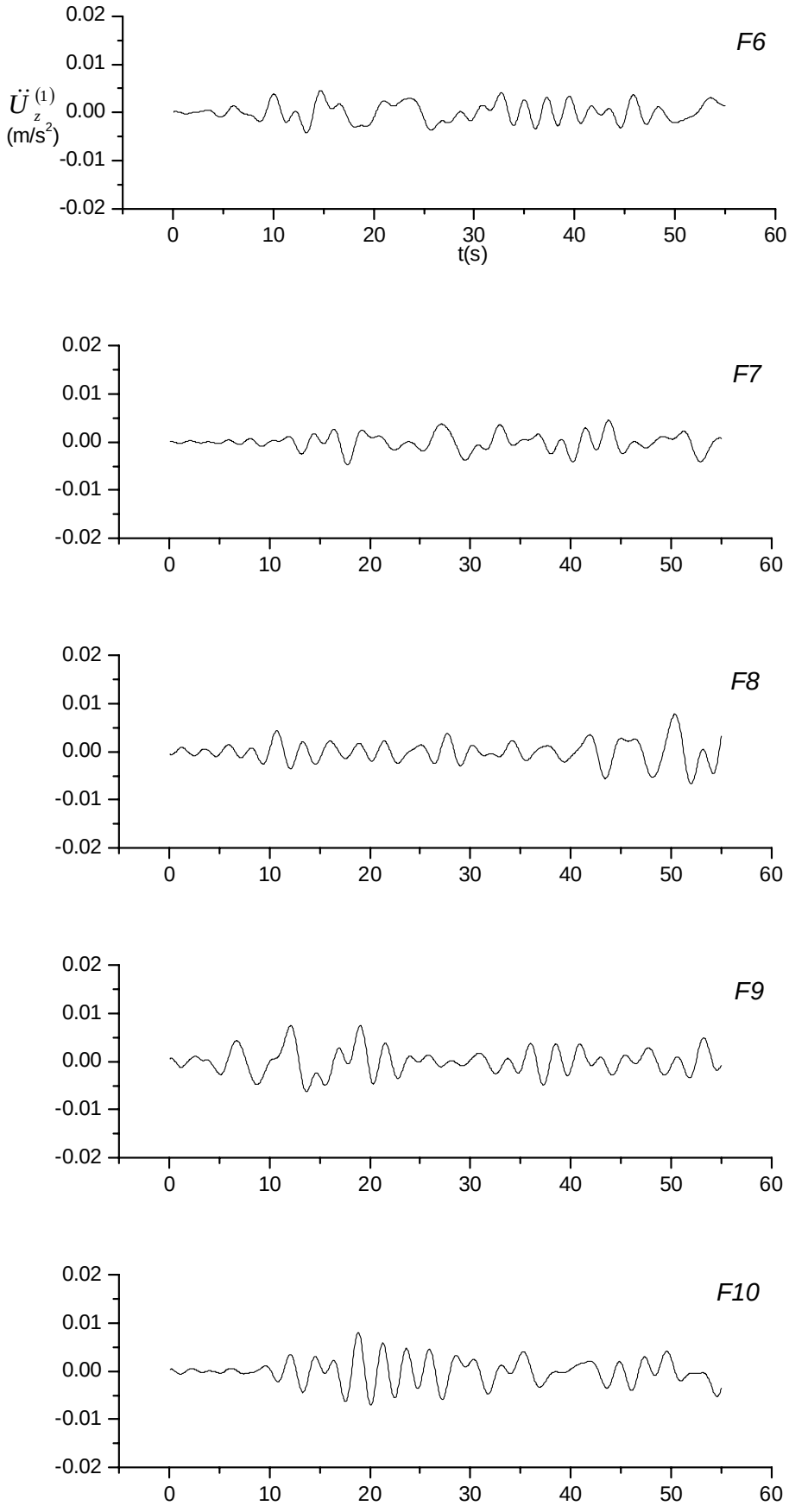

Figure 9.15 Time histories of the vertical acceleration of floating structure at the ten selected nodes *F1 – F10*

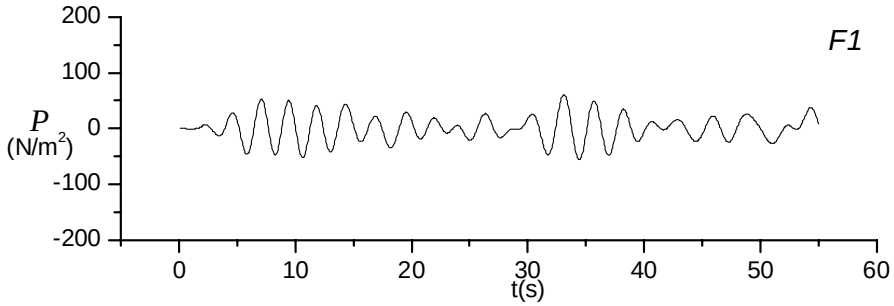
F1
P
(N/m2)
200
100
0
-100
-200
0
10
20
30
40
50
60
t(s)

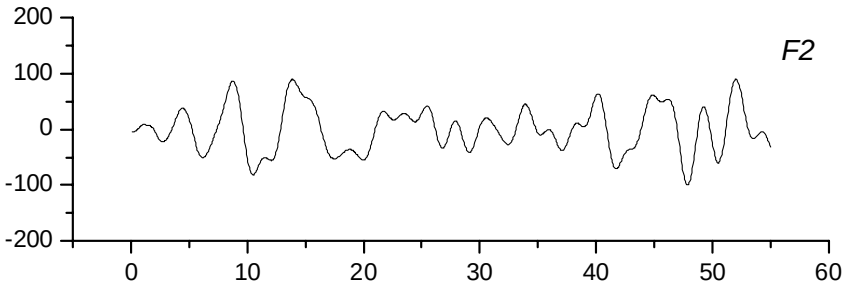
F2
200
100
0
-100
-200
0
10
20
30
40
50
60

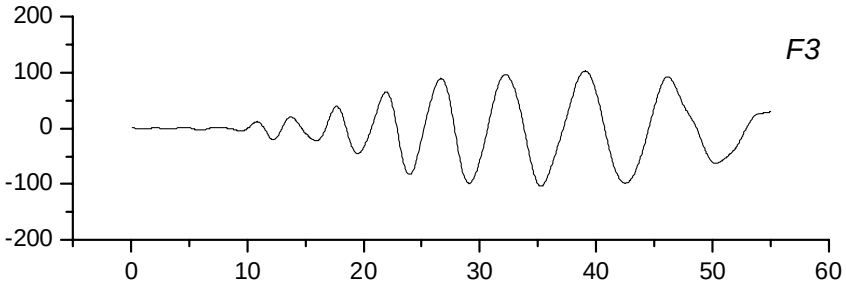
F3
200
100
0
-100
-200
0
10
20
30
40
50
60

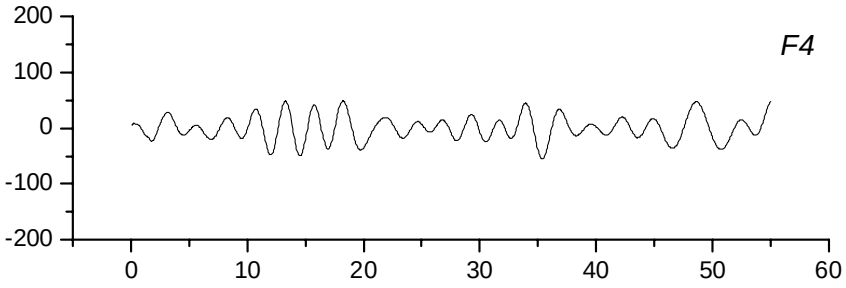
F4
200
100
0
-100
-200
0
10
20
30
40
50
60

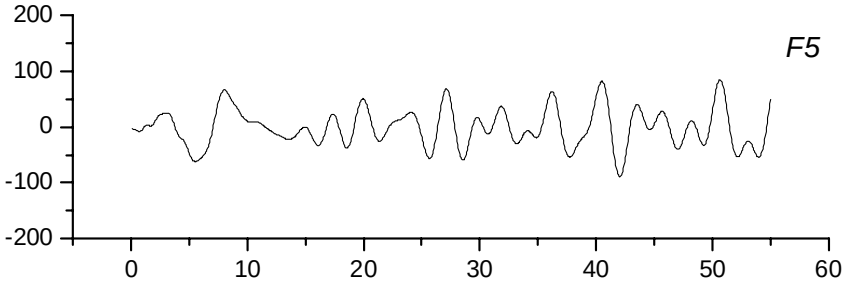
F5
200
100
0
-100
-200
0
10
20
30
40
50
60

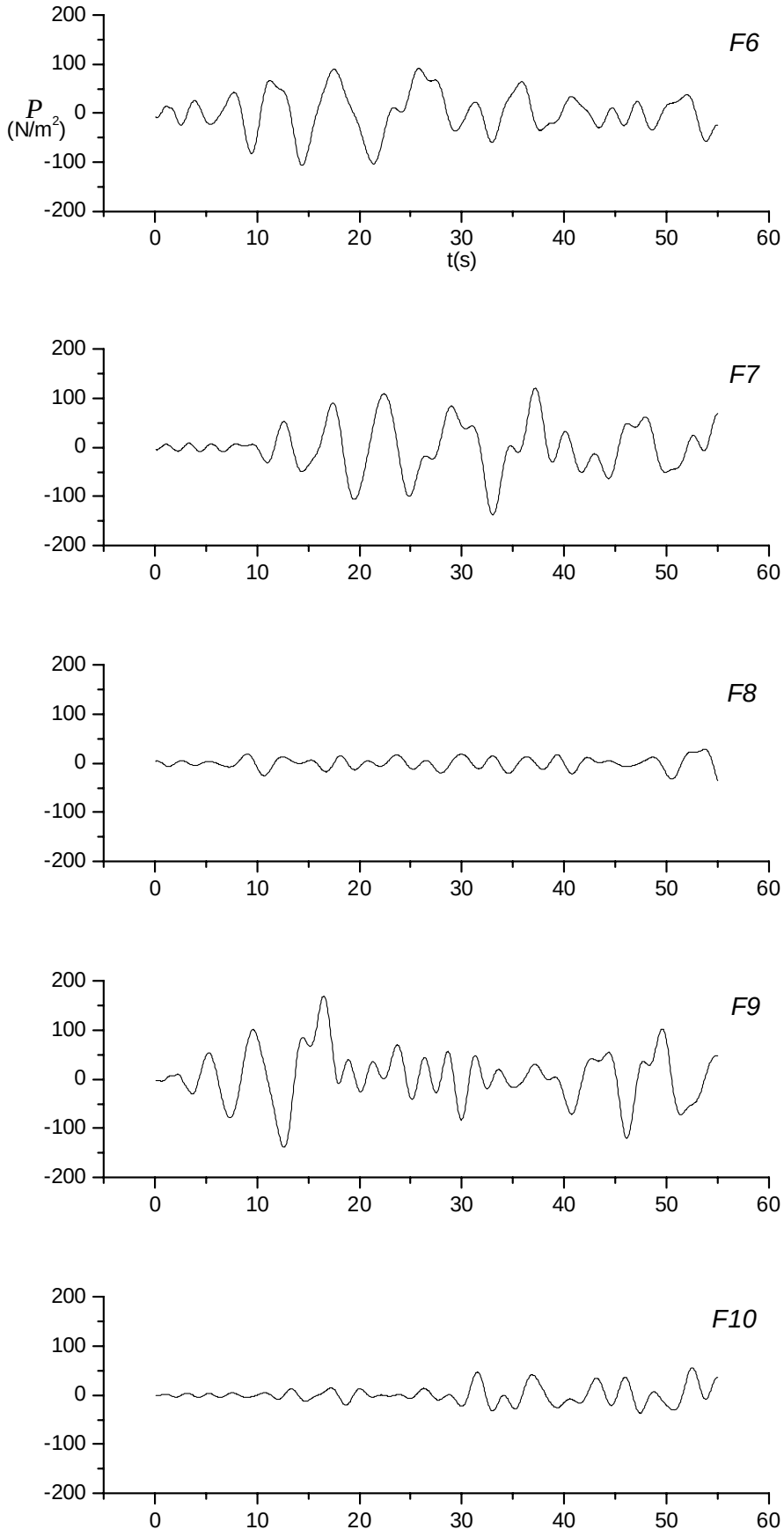

Figure 9.16 Time histories of water pressure of floating structure at the ten selected nodes *F1 – F10*

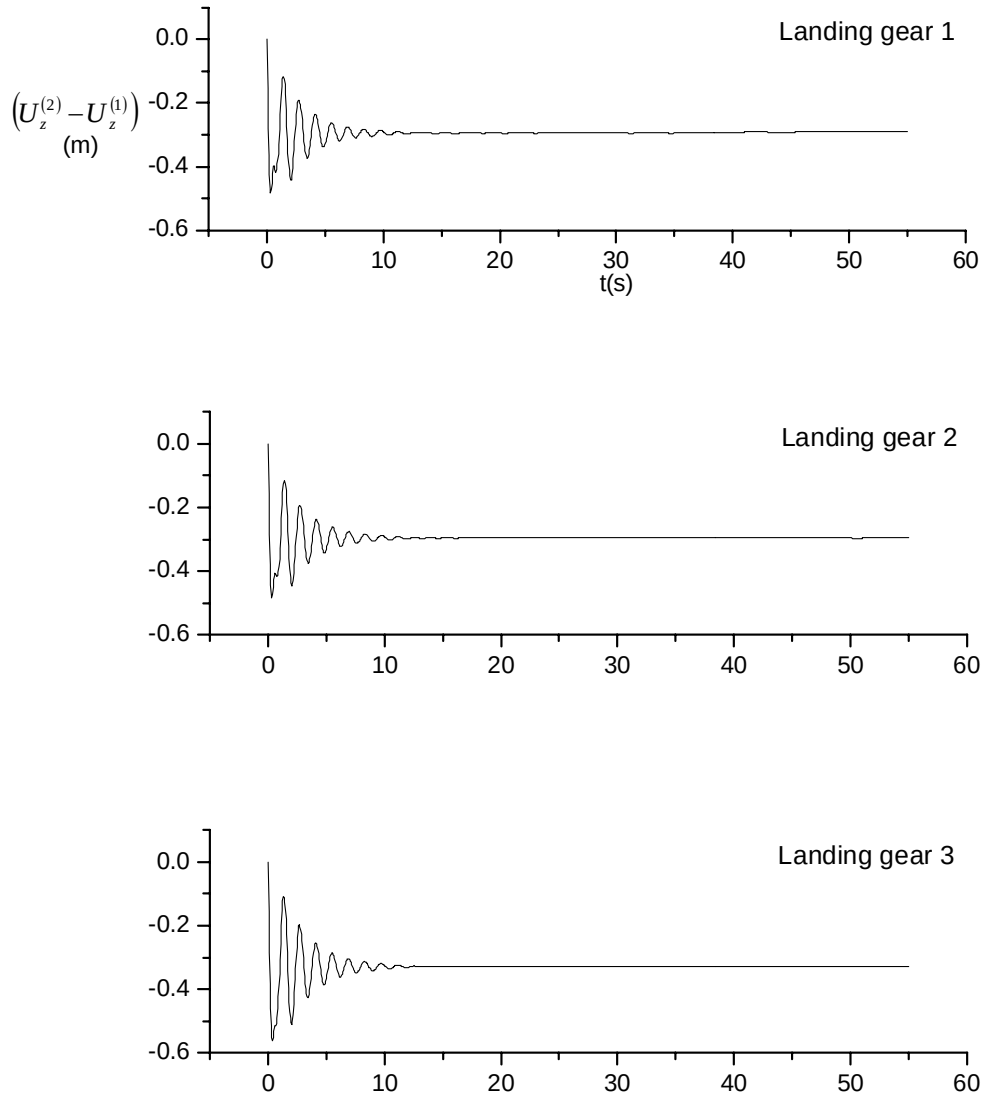

Figure 9.17 Time histories of the relative deformation between the airplane and the floating structure at the four linear spring-damper units

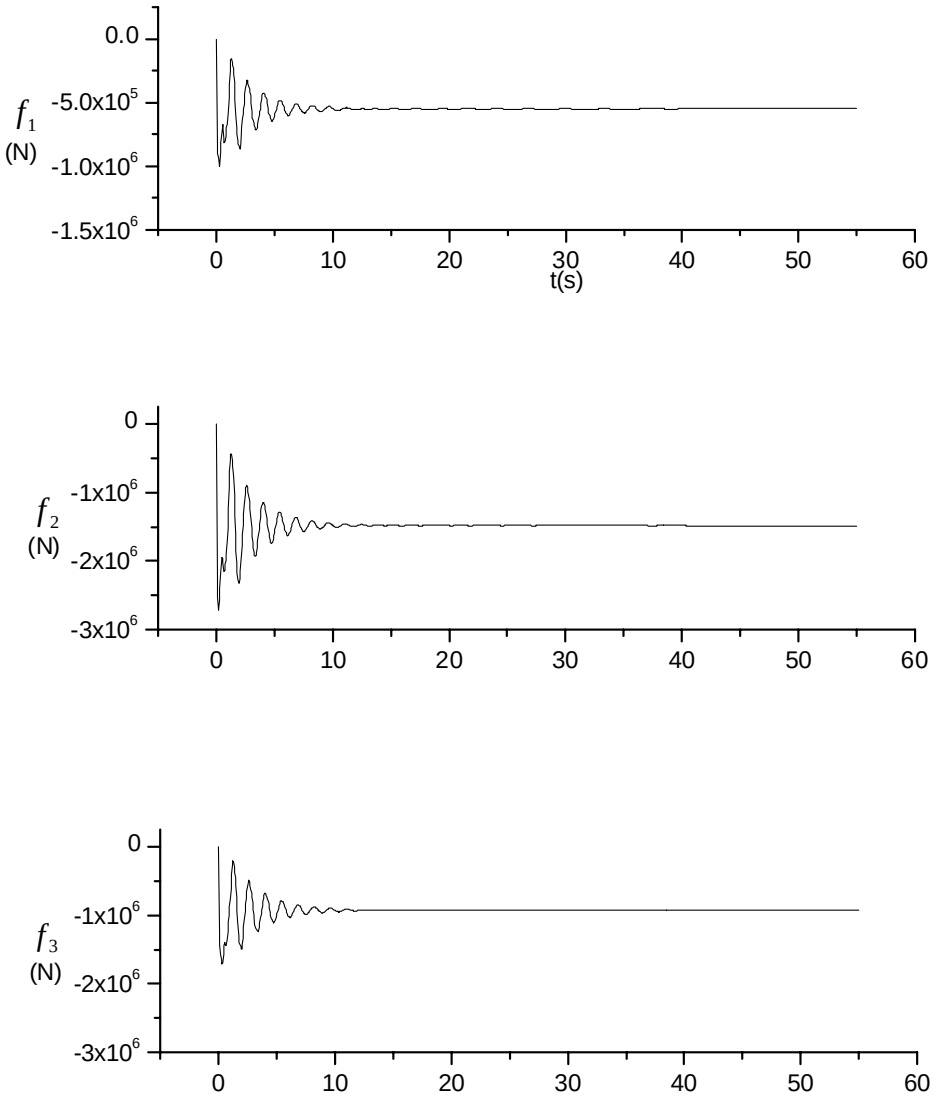

Figure 9.18 Time histories of the force provided by each linear spring-damper unit

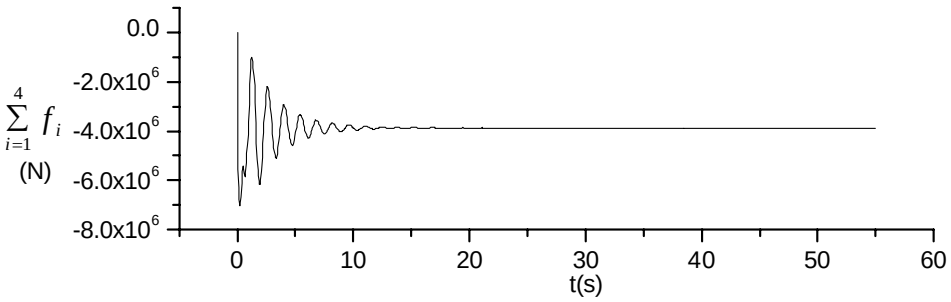

Figure 9.19 Time history of the total force provided by the four linear spring-damper units

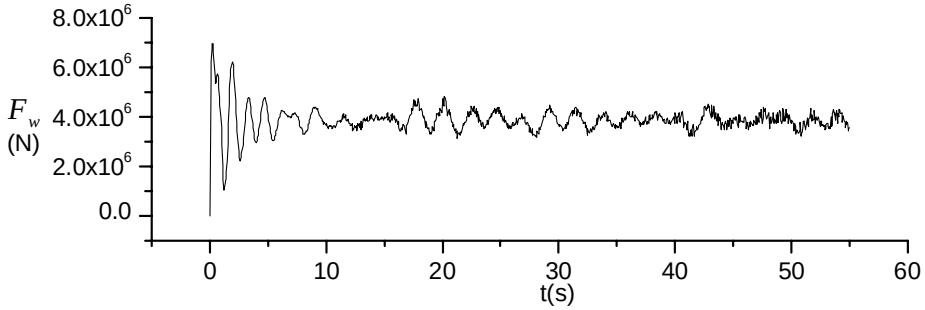

Figure 9.20 Time history of the resultant force from water pressure

Chapter 10

Conclusions and Future Work

10.1 Conclusions

To address the dynamic problems of an airplane – floating structure – water interaction system excited by airplane landing impacts, a mixed mode function – boundary element method and its corresponding computer code MMFBEP have been developed and tested.

The motion of the airplane and the floating structure are solved by using the modal superposition method through which the dynamic equations established in the physical space are transformed into the mode space in order to reduce the degrees of freedom. The fluid, occupying a horizontally unbounded domain, is assumed to be incompressible, inviscid and subject to irrotational motion. The potential flow theory is used to solve the fluid motion. BEM is adopted to solve the Laplace equation in association with the boundary conditions of the fluid domain. The motion of the airplane and the floating structure are interacted through the landing gear system which is linearised by a few linear spring – damper units. The motion of the floating structure and the surrounding fluid are coupled through the wetted interface conditions. The mixed mode function – boundary element equations governing the airplane – floating structure – water interaction system are directly solved in the time domain.

By considering the airplane and the floating structure as two substructures, respectively, a complete and realistic model describing the dynamics of an airplane landing on a floating structure is set up, through which the interactions between each component of this coupled system can be investigated. This capability in association with the obtained numerical results is helpful for the practical design of a floating airport.

As the impacts induced by airplane landing are transient, the responses of the airplane – floating structure – water interaction system need to be studied in the time domain. Based on the assumptions and approach of the Newmark integration method, a direct solution scheme has been developed to solve the coupled equation of the two solid substructures

and the fluid by expressing the first order derivative of the velocity potential in terms of the velocity of the floating structure and using a substitution approach. This solution scheme is suitable for both symmetric and non-symmetric systems of equations.

The adoption of the fundamental solution of Laplace equation in an infinite fluid domain as the Green function of the integral equation simplifies the fluid structure interaction formulation and the boundary element solution. The resultant algebraic equations involve the velocity potential of fluid, the Green function and their normal derivatives over the wetted surface and undisturbed free surface rather than the surface of the complete fluid domain and thus save computation effort and improve efficiency.

To implement the proposed mixed mode function – boundary element method, a Fortran program MMFBEP is developed, in which the structure type of the airplane is rather arbitrary, the floating structure can be a mass, a beam or a thin plate and the fluid domain can be either 2D or 3D. Two input files need to be prepared for the execution of program MMFBEP, one of which defines all the control parameters and the other contains the nodal and modal information of the two solid substructures.

To illustrate the proposed method and the developed computer code, numerical applications of increasing complexity were examined in Chapters 7, 8 and 9.

Initially, a mass – spring – damper system dropping onto a mass floating on the surface of a 2D and 3D fluid domain was investigated and compared with an appropriate semi-analytic solution of the 2D formulation. Next, an elastic beam supported by a spring – damper unit at its centre lands and travels along another floating elastic beam in 2D and 3D fluid domain. Experimental investigation of a car travelling along a floating structure was used to demonstrate that the vertical displacement of the floating structure was reasonably modelled. Finally, an approximate model of a Boeing 747-400 jumbo plane landing and travelling along a thin – plate type floating structure in a 3D fluid domain is simulated.

By comparing the obtained numerical results with the available numerical and experimental results, the efficiency of the method was demonstrated and the program was validated.

10.2 Future Work

In the proposed method, the infinite fluid domain needs to be truncated at a suitable far field boundary and the boundary integral is evaluated for the retained fluid domain instead of the infinite fluid domain. As the undisturbed condition is assumed at the far field boundary, the larger the retained fluid domain is, the better the simulation results are. However, as the complexity of the simulation increases, there is a certain limit size for the retained fluid domain imposed by the capability of current computers. Therefore, to maintain a fluid domain as large as possible, an efficient numerical scheme is necessary to keep the balance between efficiency and accuracy.

The process of an airplane landing onto a floating structure has been investigated in this thesis. In a similar way, the take-off process can be analyzed. In that case, the airplane causes an initial deformation of the floating structure, which can be solved by a static analysis using ANSYS.

The stress distribution inside the floating structure will be needed in a practical design procedure. Based on the obtained deformation of the floating structure, the stress distribution can be achieved either by substituting the deformation back to ANSYS and performing a static analysis or by calculating the stress directly based on the relationship between deformation and stress.

It is more realistic to look at the hydrodynamic/elastic responses of floating runways subject to both airplane landing/take-off impacts and incident waves. The former is a transient problem and has to be analysed in the time domain, whilst the latter can normally be regarded as a problem in the frequency domain. Special attention may be paid to investigate the effect of the phase and approach angle of incident waves on the landing/take-off operation.

The amplitude of the structural motion and the generated waves are both assumed to be small in this thesis, allowing the problem to be solved in a linear regime. However, nonlinearities regarding large deformations of structure, nonlinear waves and instant wetted interface and nonlinear free surface conditions will have to be considered in some cases.

References

ANSYS 2004 *A Finite Element Package*, Version 8.1.

Armstrong, E.R. 1924 *Sea Station*. Patent No. 1,511,153.

Bathe, K.J. 1996 *Finite Element Procedures*. Prentice-Hall, Englewood Cliffs, New Jersey.

Belik, Ö., Bishop, R.E.D. and Price, W.G. 1980 On the slamming response of ships to regular head waves. *Transactions of the Royal Institution of Naval Architects* **122** 325-337.

Belik, Ö. and Price, W.G. 1982 Comparison of slamming theories in the time simulation of ship response in irregular waves. *International Shipbuilding Progress* **29** 173-187.

Belik, Ö., Bishop, R.E.D. and Price, W.G. 1983 A simulation of ship responses due to slamming in irregular head waves. *Transactions of the Royal Institution of Naval Architects* **125** 237-253.

Betts, C.V., Bishop, R.E.D. and Price, W.G. 1977 The symmetric generalized fluid forces applied to a ship in a seaway. *Transactions of the Royal Institution of Naval Architects* **119** 265-278.

Bishop, R.E.D. 1971 On the strength of large ships in heavy seas. *South African Mechanical Engineer* **December** 338-353.

Bishop, R.E.D. and Eatock Taylor, R. 1973 On wave induced stress in a ship executing symmetric motions. *Philosophical of Transactions of the Royal Society of London* **A275** 1-32.

Bishop, R.E.D., Eatock Taylor, R. and Jackson, K.L. 1973 On the structural dynamics of ships hulls in waves. *Transactions of the Royal Institution of Naval Architects* **115** 257-274.

Bishop, R.E.D. and Price, W.G. 1974 On modal analysis of ship strength. *Proceedings of the Royal Society of London* **A341** 121-134.

Bishop, R.E.D. and Price, W.G. 1976 On the relationship between “dry modes” and “wet modes” in the theory of ship response. *Journal of Sound and Vibration* **45** 157-164.

Bishop, R.E.D., Price, W.G. and Tam, P.K.Y. 1977 A unified dynamic analysis of ship

response to waves. *Transactions of the Royal Institution of Naval Architects* **119** 363-390.

Bishop, R.E.D., Price, W.G. and Tam, P.K.Y. 1978 On the dynamics of slamming. *Transactions of the Royal Institution of Naval Architects* **120** 259-280.

Bishop, R.E.D. and Price, W.G. 1979 *Hydroelasticity of Ships*. Cambridge University Press.

Bishop, R.E.D., Price, W.G. and Temarel, P. 1980 A unified dynamic analysis of antisymmetric ship response to waves. *Transactions of the Royal Institution of Naval Architects* **122** 349-365.

Bishop, R.E.D., Price, W.G. and Wu, Y.S. 1986a A general linear hydroelasticity theory of floating structures moving in a seaway. *Philosophical of Transactions of the Royal Society of London* **A316** 375-426.

Bishop, R.E.D., Price, W.G. and Temarel, P. 1986b On the hydroelastic response of a SWATH to regular oblique waves, in Smith, C.S. and Clarke, J.D. (Editors) *Advances in Marine Structures*. Elsevier Applied Science, London, 89-110.

BOEING webpage *www.boeing.com*.

Chen, X.J., Wu, Y.S., Cui, W.C. and Tang, X.F. 2003a Nonlinear hydroelastic analysis of a moored floating body. *Ocean Engineering* **30(8)** 965-1003.

Chen, X.J., Jensen, J.J., Cui, W.C. and Fu, S.X. 2003b Hydroelasticity of a floating plate in multi-directional waves. *Ocean Engineering* **30(15)** 1997-2017.

Chen, X.J., Wu, Y.S., Cui, W.C. and Jensen, J.J. 2006 Review of hydroelasticity theories for global response of marine structures. *Ocean Engineering* **33(3-4)** 439-457.

Clough, R.W. 1960 The finite element in plane stress analysis. *Proceedings of the 2nd ASCE Conference on Electronic Computation*. Pittsburgh.

Collatz, L. 1966 *The Numerical Treatment of Differential Equations (3rd Edition).* Springer, Berlin.

Conceicao, C.A.L., Price, W.G. and Temarel, P. 1984 The influence of heel on the hydrodynamic coefficients of ship like sections and a trawler form. *International Shipbuilding Progress* **31(355)** 56-66.

Conway, H.G. 1958 *Landing Gear Design*. Chapman & Hall, London.

Crandall, S.H. 1956 *Engineering Analysis: a Survey of Numerical Procedures*.

McGraw-Hill, New York.

Cui, W.C., Wu, Y.S. and Li, R.P. 2001 Recent researches on dynamic performances of very large floating structures. *Journal of Ship Mechanics* **5(1)** 73-81 (in Chinese).

Cui, W.C. 2002 Current status and future directions in predicting the hydroelastic response of very large floating structures. *Journal of Ship Mechanics* **6(1)** 73-90 (in Chinese).

Currey, N.S. 1988 *Aircraft Landing Gear Design: Principles and Practices*. American Institute of Aeronautics and Astronautics, Education Series, Washington.

Davys, J.W., Hosking, R.J. and Sneyd, A.D. 1985 Waves due to a steadily moving source on a floating ice plate. *Journal of Fluid Mechanics* **158** 269-287.

Du, S.X. 1996 *A Complete Frequency Domain Analysis Method of Linear Three-dimensional Hydroelastic Responses of Floating Structure Traveling in Waves*. Ph.D. Thesis, China Ship Scientific Research Center, Wuxi, China (in Chinese).

Du, S.X. 1999 A general theory for the hydroelastic response of a structure maneuvering in viscous fluid. *Journal of Ship Mechanics* **3(3)** 21-34 (in Chinese).

Eatock Taylor, R. and Ohkusu, M. 2000 Green functions for hydroelastic analysis of vibrating free-free beams and plates. *Applied Ocean Research* **22(5)** 295-314.

Endo, H. and Yago, K. 1999 Time history response of a large floating structure subjected to dynamic load. *Journal of the Society of Naval Architects of Japan* **186** 369-376.

Endo, H. 2000 The behaviour of a VLFS and an airplane during takeoff/landing run in wave condition. *Marine Structures* **13(4-5)** 477-491.

Ertekin, R.C. and Kim, J.W. 1999 Hydroelastic response of a floating, mat-type structure in oblique, shallow-water waves. *Journal of Ship Research* **43(4)** 241-254.

Ewins, D. J. 2000 *Modal Testing: Theory, Practice and Application*. Research Studies Press, Baldock, Hertsfordshire, England.
Faltinsen, O.M. 1996 Bottom slamming on a floating airport. *Proceedings of the 1st International Workshop on Very Large Floating Structures*. Hayama, Japan, 97-106.

Faltinsen, O.M. 2000 Hydroelastic slamming. *Journal of Marine Science and Technology* **5(2)** 49-65.

Feng, Y.Z. 1991 *Analysis of Airplane Structure and Advanced Design Principles*. Northwestern Polytechnical University Press, Xi’an, China (in Chinese).

Fu, Y., Price, W.G. and Temarel, P. 1985 The behaviour of a jack-up rig in transit in waves. *Proceedings of the International Conference on Offshore Transportation and Installation*. Royal Institution of Naval Architects, London, UK, paper 15.

Fu, Y., Price, W.G. and Temarel, P. 1986 Directional waves spectra and the response spectra of a flexible jack-up rig in transit. *Proceedings of the 5th International Conference on Offshore Mechanics and Arctic Engineering*. Tokyo, Japan, paper OMAE-904 102-112.

Fu, Y., Price, W.G. and Temarel, P. 1987 The 'dry' and 'wet' towage of a jack-up rig in regular and irregular waves. *Transactions of the Royal Institution of Naval Architects* **129** 147-159.

Fukuoka, T., Miyajima, S., Sato, C. and Ohta, M. 2002 Assessment of structural safety and functionality of a floating airport model. *Proceedings of the 12th International Offshore and Polar Engineering Conference*. Kitakyushu, Japan, 379-384.

Fung, Y.C. 1977 *A First Course in Continuum Mechanics (2nd Edition)*. Prentice-Hall, Englewood Cliffs, New Jersey.

Ghiringhelli, G.L. 2000 Testing of semiactive landing gear control for a general aviation aircraft. *Journal of Aircraft* **37(4)** 606-616.

Green, A.E. and Naghdi, P.M. 1976 A derivation of equations for wave propagation in water of variable depth. *Journal of Fluid Mechanics* **78(2)** 237-246.

Gu, M.X., Wu, Y.S. and Xia, J.Z. 1989 Time domain analysis of non-linear hydroelastic response of ships. *Proceedings of the International Symposium on Practical Design of Ships and Mobile Units*. Varna, Bulgaria.

Hamamoto, T., Hayashi, T. and Fujita, K. 1996 3D BEM-FEM coupled hydroelastic analysis of irregular shaped, module-linked large floating structures. *Proceedings of the 6th International Offshore and Polar Engineering Conference*. Los Angels, CA, **1** 362-369.

Hamamoto, T., Suzuki, A. and Fujita, K. 1997 Hybrid dynamic analysis of large tension leg floating structures using plate elements. *Proceedings of the 7th International Offshore and Polar Engineering Conference*. Honolulu, HI, **1** 285-292.

Hamamoto, T., Suzuki, A., Tsujioka, N. and Fujita, K. 1998 3D BEM-FEM hybrid hydroelastic analysis of module linked large floating structures subjected to regular waves. *Proceedings of the 8th International Offshore and Polar Engineering Conference*. Montreal, Canada, **1** 192-199.

Hamamoto, T. and Fujita, K. 2002 Wet-mode superposition for evaluating the hydroelastic response of floating structures with arbitrary shape. *Proceedings of the 12th International*

Offshore and Polar Engineering Conference. Kitakyushu, Japan, 290-297.

Heller, S.R. and Abramson, H.N. 1959 Hydroelasticity: a new naval science. *Journal of the America Society of Naval Engineers* **71(2)** 205-209.

Hirayama, T., Ma, N. and Ueno, S. 1994 Influence of flexibility on the motions and deflections of an airport-oriented floating long offshore structure. *Proceedings of the 1st International Conference on Hydroelasticity in Marine Technology*. Trondheim, Norway, 377-388.

Hirayama, T., Ma, N., Miyakawa, K. and Takayama, T. 1996 Long life floating airport conceptual proposal and basic study on response and attitude control. *Proceedings of the 2nd International Workshop on Very Large Floating Structures*. Hayama, Japan, 193-200.

Houbolt, J.C. 1950 A recurrence matrix solution for the dynamic response of elastic aircraft. *Journal of Aeronautical Science* **17** 540-550.

Hurty, W.C. and Rubinstein, M.F. 1964 *Dynamics of Structures*. Prentice-Hall, Englewood Cliffs, New Jersey.

Iijima, K., Yoshida, K. and Suzuki, H. 1997 Hydrodynamic and hydroelastic analyses of very large floating structures in waves. *Proceedings of the 16th International Conference on Offshore Mechanics and Arctic Engineering*. Yokohama, Japan, **6** 139-145.

Ikoma, T., Maeda, H., Masuda, K. and Rheem, C.K. 1998 Hydroelastic responses of pontoon type very large floating offshore structure (The 4th report. Estimation method of slowly varying wave drift force and fender reaction force). *Journal of the Society of Naval Architects of Japan* **184** 291–296.

Isobe, E. 1999 Research and development of Mega-Float. *Proceedings of the Third International Workshop on Very Large Floating Structures*. Honolulu, Hawaii, USA, **1** 7-13.

ISSC 2006 Report of Specialist Task Committee VI.2. Very Large Floating Structures, in Frieze, P.A. and Shenoi, R.A. (Editors) *Proceedings of the 16th International Ship and Offshore Structures Congress*. Elsevier, Southampton, UK, 391-442.

Iwahashi, Y., Ohmatsu, S. and Tsubogo, T. 1998 Hydroelastic response characteristics of a pontoon type VLFS in waves. *Journal of the Society of Naval Architects of Japan* **183** 211-218.

Janardhanan, K., Price, W.G. and Wu, Y.S. 1992 Generalized fluid impulse functions for oscillating marine structures. *Journal of Fluids and Structures* **6(2)** 207-222.

Kashiwagi, M. 1997 A B-spline Galerkin scheme for computing wave forces on a floating very large elastic plate. *Proceedings of the 7th International Offshore and Polar Engineering Conference*. Honolulu, HI, **1** 229-236.

Kashiwagi, M. 1998 A direct method versus a mode-expansion method for calculating hydroelastic response of a VLFS in waves. *Proceedings of the 8th International Offshore and Polar Engineering Conference*. Montreal, Canada, **1** 215-222.

Kashiwagi, M. 2000a Research on hydroelastic responses of VLFS: recent progress and future work. *International Journal of Offshore and Polar Engineering* **10(2)** 81-90.

Kashiwagi, M. 2000b A time-domain mode-expansion method for calculating transient elastic responses of a pontoon-type VLFS. *Journal of Marine Science and Technology* **5(2)** 89-100.

Kashiwagi, M. 2004 Transient responses of a VLFS during landing and take-off of an airplane. *Journal of Marine Science and Technology* **9(1)** 14-23.

Kim, J.W. and Webster, W.C. 1996 The drag of an airplane taking off from a floating runway. *Proceedings of the 2nd International Workshop on Very Large Floating Structures.* Hayama, Japan, 235-241.

Kim, J.W. and Ertekin, R.C. 1998 An eigenfunction-expansion method for predicting hydroelastic behaviour of a shallow-draft VLFS. *Proceedings of the 2nd International Conference on Hydroelasticity in Marine Technology*. Fukuoka, Japan, 47-59.

Kim, J.W. and Ertekin, R.C. 2002 Hydroelasticity of an infinitely-long plate floating in oblique waves: linear Green-Naghdi theory. *Journal of Engineering for the Maritime Environment (Proceedings of the Institution of Mechanical Engineers, Part M)* **216(M2)** 179-197.

Korsmeyer, F.T., Klemas, T.J., White, J.K. and Phillips, J.R. 1999 Fast hydrodynamic analysis of large offshore structures. *Proceedings of the International Symposium on Offshore and Polar Engineering*. Brest, France.

Kyoung, J.H., Hong, S.Y. and Kim, B.W. 2006 Time domain analysis on hydroelastic responses of VLFS using finite element method. *Proceedings of the International Conference on Hydroelasticity in Marine Technology*. Wuxi, China, 273-282.

Liapis, S. and Beck, R.F. 1985 Seakeeping computation using time-domain analysis. *Proceedings of the 4th International Conference on Numerical Ship Hydrodynamics.* Washington.

Lin, X. and Takaki, M. 1998a A B-spline element method for predicting the hydroelastic

responses of a very large floating structure in waves. *Journal of the Society of Naval Architects of Japan* **183** 219-225.

Lin, X. and Takaki, M. 1998b On B-spline element methods for predicting hydroelastic responses of very large floating structure in waves. *Proceedings of the 2nd International Conference on Hydroelasticity in Marine Technology.* Fukuoka, Japan, 219-228.

Liu, Y.Y., Feng, T.C. and Liu, Y.Z. 1990 *Fundamental Theory in Hydrodynamics*. Shanghai Jiao Tong University Press, Shanghai, China (in Chinese).

Maeda, H., Miyajima, S., Masuda, K. and Ikoma, T. 1995 Hydroelastic responses of pontoon type very large floating offshore structure. *Journal of the Society of Naval Architects of Japan* **178** 203-212.

Maeda, H., Masuda, K. and Ikoma, T. 1997 Hydroelastic responses of pontoon type very large floating offshore structure (The 3rd report: The effects of 2nd-order wave loads). *Journal of the Society of Naval Architects of Japan* **182** 319–328.

Mamidipudi, P. and Webster, W.C. 1994 The motions performance of a mat-like floating airport. *Proceedings of the 1st International Conference on Hydroelasticity in Marine Technology.* Trondheim, Norway, 363-375.

Murai, M., Kagemoto, H. and Fujino, M. 1998 On the predictions of hydroelastic behaviours of a huge floating structure in waves: 3rd report. *Journal of the Society of Naval Architects of Japan* **183** 199-210.

Murai, M., Kagemoto, H. and Fujino, M. 1999 On the hydroelastic responses of a very large floating structure in waves. *Journal of Marine Science and Technology* **4(3)** 123-153.

Nagata, S., Yoshida, H., Fujita, T. and Isshiki, H. 1998 Reduction of the motion of an elastic floating plate in waves by breakwaters. *Proceedings of the 2nd International Conference on Hydroelasticity in Marine Technology*. Fukuoka, Japan, 229-238.

Namba, Y. and Ohkusu, M. 1999 Hydroelastic behavior of floating artificial islands in waves. *Journal of Offshore and Polar Engineering* **9(1)** 67-94.

Newman, J.N. 1977 *Marine Hydrodynamics*. The MIT Press, Cambridge, MA, USA.

Newman, J.N. and Lee, C.H. 2002 Boundary-element methods in offshore structure analysis. *Journal of Offshore Mechanics and Arctic Engineering* **124** 81-89.

Newmark, N.M. 1959 A method of computation for structural dynamics. *Journal of the Engineering Mechanics Division, ASME* **85** 67-94.

OCI. 2005 *HYDRAN: A Computer Program for the HYDroelastic Response ANalysis of Ocean Structures*. v. 1.52, OffCoast, Inc., Kailua, HI, USA.

Ohkusu, M. and Namba, Y. 1996 Analysis of hydroelastic behaviour of a large floating platform of thin plate configuration in waves. *Proceedings of the 2nd International Workshop on Very Large Floating Structures*. Hayama, Japan, 143-148.

Ohmatsu, S. 1997 Numerical calculation of hydroelastic responses of pontoon-type VLFS. *Journal of the Society of Naval Architects of Japan* **182** 329-340.

Ohmatsu, S. 1998a Numerical calculation of hydroelastic behaviour of pontoon type VLFS in waves. *Proceedings of 17th International Conference on Offshore Mechanics and Arctic Engineering.* Lisbon, Portugal, paper OMAE-984333.

Ohmatsu, S. 1998b Numerical calculation of hydroelastic behaviour of VLFS in time domain. *Proceedings of the 2nd International Conference on Hydroelasticity in Marine Technology.* Fukuoka, Japan, 89-98.

Ohmatsu, S. 2001 Numerical calculation method for the hydroelastic response of a pontoon-type very large floating structure close to a breakwater. *Journal of Marine Science and Technology* **5(4)** 147-160.

Ohmatsu, S. 2005 Overview: research on wave loading and responses of VLFS. *Marine Structure* **18(2)** 149-168.

Ohta, M., Ikegami, K. and Yamaguchi, Y. 1998 Experimental study on elastic behaviour of a huge floating structure in waves. *Transactions of the West-Japan Society of Naval Architects of Japan* **95** 99-108 (in Japanese).

Okada, S., Shibuta, S., Negayama, H. and Okamura, H. 1999 Hydroelastic response and structural analysis of a 1000m Mega-Float model. *Proceedings of the 18th International Conference on Offshore Mechanics and Arctic Engineering.* Newfoundland, Canada, paper OMAE99/OSU-3060.

Paz, M. and Leigh, W. 2004 *Structural Dynamics: Theory and Computation (5th Edition).* Kluwer Academic Publishers, Norwell, MA, USA.

Phillips, J.R. and White, J.K. 1997 A precorrected-FFT method for electrostatic analysis of complicated 3-D structures. *IEEE Transactions on Computer-Aided Design of Integrated Circuits and Systems* **16(10)** 1059-1072.

Price, W.G. and Wu, Y.S. 1982 Hydrodynamic coefficients and responses of semi-submersibles in waves. *Proceedings of the 2nd International Symposium on Ocean Engineering and Ship Handling.* Gothenburg, Sweden, 393-415.

Price, W.G. and Wu, Y.S. 1983 Fluid interaction in multi-hull structures travelling in waves. *Proceedings of the 2nd International Symposium in the Practical Design of Ships*. Tokyo and Seoul, 251-263.

Price, W.G. and Wu, Y.S. 1986 *Hydroelasticity of Marine Structures*. China Ship Scientific Research Center, Report 86001, Wuxi, China.

Price, W.G., Temarel, P. and Wu, Y.S. 1987 Responses of a SWATH travelling in unidirectional irregular seas. *Journal of Underwater Technology* **13** 2-10.

Price, W.G., Randall, R. and Temarel, P. 1988 Fluid-structure interaction of submerged shells. *Proceedings of the Conference on Stress Determination and Strain Measurements in Aeronautics, Naval Architecture and Offshore Engineering, Joint Aero Marine Group of RAeS, RINA and SUT*. Guildford, UK.

Raymer, Daniel P. 1999 *Aircraft Design: A Conceptual Approach***.** AIAA (American Institute of Aeronautics & Astronautics), 3rd edition.

Remmers, G., Taylor, R., Palo, P. and Brackett R. 1999 Mobile Offshore Base: A seabasing option. *Proceedings of the Third International Workshop on Very Large Floating Structures*. Honolulu, Hawaii, USA, **1** 1-6.

Seto, H. and Ochi, M. 1998 A hybrid element approach to hydroelastic behavior of a very large floating structure in regular waves. *Proceedings of the 2nd International Conference on Hydroelasticity in Marine Technology*. Fukuoka, Japan, 185-194.

Seto, H., Ochi, M., Ohta, M. and Kawakado, S. 2003 Hydroelastic response analysis of real very large floating structures in regular waves in open/sheltered sea. *Proceedings of the 4th International Workshop on Very Large Floating Structures*. Tokyo, Japan, 65-73.

Sommerfeld, A. 1949 *Partial Differential Equations in Physics*. Academic Press, New York.

Stroud, K.A. and Booth, D.J. 2003 *Advanced Engineering Mathematics (4th Edition).* Palgrave Macmillan, New York.

Suzuki, H. 2001 Safety target of very large floating structure used as a floating airport. *Marine Structures* **14(1-2)** 103-113.

Takaki, M. and Gu, X. 1996 Motions of a floating elastic plate in waves. *Journal of the Society of Naval Architects of Japan* **180** 331-339.

Thomson, W.T. 1988 *Theory of Vibration with Applications (3rd Edition)*. Prentice-Hall, London.

Trefethen, L.N. and David Bau, III. 1997 *Numerical Linear Algebra*. Society for Industrial and Applied Mathematics.

Utsunomiya, T., Watanabe, E. and Eatock Taylor, R. 1998 Wave response analysis of a box-like VLFS close to a breakwater. *Proceedings of the 17th International Conference Offshore Mechanics and Arctic Engineering.* Lisbon, Portugal, paper OMAE-984331.

Vugts, J.H. 1968 The hydrodynamic coefficient for swaying, heaving and rolling cylinder in a free surface. *International Shipbuilding Progress* **15** 251–276.

Wang, D.Y. 1996 *Three Dimensional Hydroelastic Analysis of Ships in Time Domain*. Ph.D. Thesis, China Ship Scientific Research Center, Wuxi, China (in Chinese).

Wang, D.Y. and Wu, Y.S. 1998 Three dimensional hydroelastic analysis in time domain with application to an elastic ship model. *Journal of Hydrodynamics* **10** 57-64.

Wang, C.M., Xiang, Y., Utsunomiya, T. and Watanabe, E. 2001 Evaluation of modal stress resultants in freely vibrating plates. *International Journal of Solids and Structures* **38(36-37)** 6525-6558.

Watanabe, E. and Utsunomiya, T. 1996 Transient response analysis of a VLFS at airplane landing. *Proceedings of the 2nd International Workshop On Very Large Floating Structures.* Hayama, Japan, 243-247.

Watanabe, E., Utsunomiya, T. and Wang, C.M. 2004 Hydroelastic analysis of pontoon-type VLFS: a literature survey. *Engineering Structures* **26(2)** 245-256.

Wehausen, J.V. 1971 The motion of floating bodies. *Annual Review of Fluid Mechanics* **3** 237-268.

Wilson, E.L., Farhoomand, I. and Bathe, K.J. 1973 Nonlinear dynamic analysis of complex structures. *International Journal of Earthquake Engineering and Structural Dynamics* **1(3)** 241-252.

Wrobel, L.C. 2002 *The Boundary Element Method, Volume 1: Applications in Thermo-Fluids and Acoustics*. John Wiley, West Sussex, England.

Wu, C., Watanabe, E. and Utsunomiya, T. 1995 An eigenfuction expansion-matching method for analysing the wave-induced responses of an elastic floating plate. *Applied Ocean Research* **17(5)** 301-310.

Wu, Y.S. 1984 *Hydroelasticity of Floating Bodies*. Ph.D. Thesis, Brunel University, UK.

Wu, M.K. and Moan, T. 1996 Linear and nonlinear hydroelectric analysis of high-speed

vessels. *Journal of Ship Research* **40(2)** 149-163.

Wu, M.K., Aarsnes, J.V., Hermundstad, O. and Moan, T. 1996 A practical prediction of wave-induced structural responses in ships with large amplitude motion. *Proceedings of the 21st Symposium on Naval Hydrodynamics*. Trondheim, Norway.

Xia, D.W., Ertekin, R.C. and Kim, J.W. 2004 Nonlinear hydroelastic response of a two-dimensional mat-type VLFS by the Green-Naghdi Theory. *Proceedings of the 23rd International Conference on Offshore Mechanics and Arctic Engineering.* Vancouver, Canada, paper OMAE2004-51484.

Xia, J.Z. and Wang, Z.H. 1997 Time-domain hydroelasticity theory of ships responding to waves. *Journal of Ship Research* **41(4)** 286-300.

Yago, K. and Endo, H. 1996 On the hydroelastic response of box-shaped floating structure with shallow draft. *Journal of the Society of Naval Architects of Japan* **180** 341-352.

Yamashita, S. 1979 Motions and hydrodynamic pressures of a box-shaped floating structure of shallow draft in regular waves: comparisons between calculations by the use of pulsating pressure distributions and experiments. *Journal of the Society of Naval Architects of Japan* **146** 165-172.

Yasuzawa, Y., Kagawa, K., Kawano, D. and Kitabayashi, K. 1996 Wave response analysis of a flexible large floating structure. *Proceedings of the 2nd International Workshop on Very Large Floating Structures.* Hayama, Japan, 221-228.

Yasuzawa, Y., Kagawa, K., Kawano, D. and Kitabayashi, K. 1997 Dynamic response of a large flexible floating structure in regular waves. *Proceedings of the 16th Conference on Offshore Mechanics and Arctic Engineering.* Yokohama, Japan, **4** 187-194.

Yeung, R.W. and Kim, J.W. 1998 Structural drag and deformation of a moving load on a floating plate. *Proceedings of the 2nd International Conference on Hydroelasticity in Marine Technology.* Fukuoka, Japan, 77-88.

Zienkiewicz, O.C. and Cheung, Y.K. 1967 *The Finite Element Method in Structural and Continuum Mechanics*. McGraw-Hill, London, UK.

Publications

1. Jin, J. and Xing, J.T. 2007 Transient dynamic analysis of a floating beam – water interaction system excited by the impact of a landing beam. *Journal of Sound and Vibration* **303** 371 – 390.

2. Jin, J. and Xing, J.T. 2006 The dynamic analysis of a three dimensional landing beam – floating beam – water interaction system subject to landing impacts. *9th International Conference on Recent Advances in Structural Dynamics*. 17–19 July, Southampton, UK.

3. Xing, J.T. and Jin, J. 2005 A dynamic analysis of an integrated aircraft – floating structure – water interaction system excited by the impact of an aircraft landing. *International Journal of Offshore and Polar Engineering* **15(4)** 257 – 263.

4. Xing, J.T. and Jin, J. 2004 A mixed mode function – boundary element method for the transient impact analysis of an aircraft landing on a floating structure. *9th Symposium on Practical Design of Ships and Other Floating Structures*. 12–17 September, Lubeck - Travemunde, Germany, **2** 816 – 826.

5. Xing, J.T., Jin, J. and Price, W.G. 2004 A mathematical model describing a floating structure – water interaction system impacted by an aircraft landing. 14th *International Symposium on Trends in Application of Mathematics to Mechanics*. 22– 8 August, Seeheim, Germany, 603 – 613.

Appendix A

By pre-multiplying both sides of Equation (4.28) with $\left(\mathbf{\Phi}^{(I)}\right)^{\mathrm{T}}$ and integrating the resultant equation over the domain $\Omega^{(I)}$, Equations (4.28) is transformed into the following equation

$$\begin{aligned}&\int_{\Omega}\left(\mathbf{\Phi}^{(I)}\right)^{\mathrm{T}}\mathbf{d}^{(I)}\left\{\left(1+i\eta^{(I)}\right)\mathbf{E}^{(I)}\left(\mathbf{d}^{(I)}\right)^{\mathrm{T}}\mathbf{\Phi}^{(I)}\mathbf{Q}^{(I)}\right\}dV-\int_{\Omega}\left(\mathbf{\Phi}^{(I)}\right)^{\mathrm{T}}\mathbf{g}^{(I)}\,dV\\&=\int_{\Omega}\left(\mathbf{\Phi}^{(I)}\right)^{\mathrm{T}}\rho^{(I)}\mathbf{\Phi}^{(I)}\ddot{\mathbf{Q}}^{(I)}\,dV,\qquad I=1,2.\end{aligned}\tag{A.1}$$

Clearly, the term on the right hand side of Equation (A.1) corresponds to the generalized mass matrix given in Equation (4.30).

The substitution of Equation (4.10) into the second term on the left hand side of Equation (A.1) yields

$$\begin{aligned}-\int_{\Omega}\left(\mathbf{\Phi}^{(1)}\right)^{\mathrm{T}}\mathbf{g}^{(1)}\,dV&=-\int_{\Omega}\left(\mathbf{\Phi}^{(1)}\right)^{\mathrm{T}}\left(0,\,0,\,\rho^{(1)}g-\sum_{J=1}^{4}f_J\Delta\left(\mathbf{X}^{(1)}-\mathbf{X}_J^{(1)}\right)\right)^{\mathrm{T}}dV\\&=-\int_{\Omega}\left(\mathbf{\Phi}_z^{(1)}\right)^{\mathrm{T}}\rho^{(1)}g\,dV+\int_{\Omega}\left(\mathbf{\Phi}_z^{(1)}\right)^{\mathrm{T}}\sum_{J=1}^{4}f_J\Delta\left(\mathbf{X}^{(1)}-\mathbf{X}_J^{(1)}\right)dV\\&=-\int_{\Omega}\left(\mathbf{\Phi}_z^{(1)}\right)^{\mathrm{T}}\rho^{(1)}g\,dV+\sum_{J=1}^{4}\int_{\Omega}\left(\mathbf{\Phi}_z^{(1)}\right)^{\mathrm{T}}f_J\Delta\left(\mathbf{X}^{(1)}-\mathbf{X}_J^{(1)}\right)dV.\end{aligned}\tag{A.2}$$

The two terms on the right hand side of Equation (A.2) represent the generalized forces applied on the floating structure, as given in Equations (4.33) and (4.32), respectively.

In a similar manner, upon substituting Equation (4.11) into the second term on the left hand side of Equation (A.1), the generalized forces represented in Equations (4.32), (4.33) and (4.35) can be obtained for the airplane.

Next, write the first term on the left hand side of Equation (A.1) in form

$$\begin{aligned}&\int_{\Omega}\left(\mathbf{\Phi}^{(I)}\right)^{\mathrm{T}}\mathbf{d}^{(I)}\left\{\left(1+i\eta^{(I)}\right)\mathbf{E}^{(I)}\left(\mathbf{d}^{(I)}\right)^{\mathrm{T}}\mathbf{\Phi}^{(I)}\mathbf{Q}^{(I)}\right\}dV\\&=\int_{\Omega}\mathbf{d}^{(I)}\left\{\left(\mathbf{\Phi}^{(I)}\right)^{\mathrm{T}}\left(1+i\eta^{(I)}\right)\mathbf{E}^{(I)}\left(\mathbf{d}^{(I)}\right)^{\mathrm{T}}\mathbf{\Phi}^{(I)}\mathbf{Q}^{(I)}\right\}dV\\&-\int_{\Omega}\left(\left(\mathbf{d}^{(I)}\right)^{\mathrm{T}}\mathbf{\Phi}^{(I)}\right)^{\mathrm{T}}\left\{\left(1+i\eta^{(I)}\right)\mathbf{E}^{(I)}\left(\mathbf{d}^{(I)}\right)^{\mathrm{T}}\mathbf{\Phi}^{(I)}\mathbf{Q}^{(I)}\right\}dV.\end{aligned}\tag{A.3}$$

The second term on the right hand side of Equation (A.3) corresponds to the generalized stiffness matrices given in Equation (4.31). On applying the Gauss's theorem (Stroud &

Booth 2003), the first term on the right hand side of Equation (A.3) is transformed to

$$\begin{aligned}&\int_{\Omega} \mathbf{d}^{(I)}\left\{\left(\mathbf{\Phi}^{(I)}\right)^{\mathrm{T}}\left(1+i\eta^{(I)}\right)\mathbf{E}^{(I)}\left(\mathbf{d}^{(I)}\right)^{\mathrm{T}}\mathbf{\Phi}^{(I)}\mathbf{Q}^{(I)}\right\}dV\\&=\oint_{S}\left(\mathbf{\Phi}^{(I)}\right)^{\mathrm{T}}\overline{\mathbf{n}}^{(I)}\left\{\left(1+i\eta^{(I)}\right)\mathbf{E}^{(I)}\left(\mathbf{d}^{(I)}\right)^{\mathrm{T}}\mathbf{\Phi}^{(I)}\mathbf{Q}^{(I)}\right\}dS,\end{aligned} \tag{A.4}$$

where

$$\overline{\mathbf{n}}^{(I)}=\begin{bmatrix} v_x^{(I)} & 0 & 0 & v_y^{(I)} & 0 & v_z^{(I)} \\ 0 & v_y^{(I)} & 0 & v_x^{(I)} & v_z^{(I)} & 0 \\ 0 & 0 & v_z^{(I)} & 0 & v_y^{(I)} & v_x^{(I)} \end{bmatrix}. \tag{A.5}$$

Upon using the boundary conditions given in Equations (4.16) and (4.20), it is found that for the airplane

$$\oint_{S}\left(\mathbf{\Phi}^{(2)}\right)^{\mathrm{T}}\overline{\mathbf{n}}^{(2)}\left\{\left(1+i\eta^{(2)}\right)\mathbf{E}^{(2)}\left(\mathbf{d}^{(2)}\right)^{\mathrm{T}}\mathbf{\Phi}^{(2)}\mathbf{Q}^{(2)}\right\}dS=0 \tag{A.6}$$

and for the floating structure

$$\oint_{S}\left(\mathbf{\Phi}^{(1)}\right)^{\mathrm{T}}\overline{\mathbf{n}}^{(1)}\left\{\left(1+i\eta^{(1)}\right)\mathbf{E}^{(1)}\left(\mathbf{d}^{(1)}\right)^{\mathrm{T}}\mathbf{\Phi}^{(1)}\mathbf{Q}^{(1)}\right\}dS=-\int_{\Sigma}\left(\mathbf{\Phi}^{(1)}\right)^{\mathrm{T}}\boldsymbol{\eta}\,P\,dS\,, \tag{A.7}$$

which gives the generalized force from water pressure P, as given in Equation (4.34) for the floating structure.

Appendix B: Program MMFBEP

```
program       MMFBEP
use           msimsl
implicit      none
C-------------------------------------------------------------------------------------------------------------------------------
C   Program MMFBEP has been developed to solve the dynamics of an airplane landing onto a floating structure. The
C   airplane can be an arbitrary structure while the floating structure can be a rigid body, an elastic beam or a thin plate.
C   The surrounding fluid domain can be either two or three dimensional. The maximum number of landing gears is four.
CCC-------------------------------------------------------------------------------------------------------------------------------

integer   m,n,i,j,k,l,NDFS,NDFD
integer   n1,nm1,nd1,n2,nm2,nd2,nm12,ne1,nex1,ney1,nz,nzh,news
integer   irule,ipath,nt,ntt,ns1,ns2,ns3,ns4,n11,i1,ifn,ix,iy
integer   nf1,nf2,nf3,nf4,nf5,nf6,nf7,nf8,nf9,nf10
integer   nef1,nef2,nef3,nef4,nef5,nef6,nef7,nef8,nef9,nef10
integer   noutput1,noutput2,noutput3,noutput4,noutput5
integer   nl1,nl2,nl3,nl4,nl5
C-------------------------------------------------------------------------------------------------------------------------------
C   NDFS        dimension of floating structure, 1 for rigid body, 2 for beam and 3 for thin plate
C   NDFD        dimension of fluid domain either 2 or 3
C   n1          number of nodes of the floating structure
C   nm1         number of retained modes of the floating structure
C   nd1         number of DOFs of the floating structure
C   n2          number of nodes of the landing structure
C   nm2         number of retained modes of the landing structure
C   nd2         number of DOFs of the landing structure
C   nm12        nm1+nm2
C   ne1         number of elements of the floating structure
C   nex1,ney1   number of elements along x, y direction of floating structure
C   nz          the ratio of length/width of water surface over length/width of the floating structure
C   nzh         (nz-1)/2
C   news        number of boundary elements along the whole water surface
C   irule       parameter for function TWODQ
C   ipath       parameter for function LSARG
C   nt          number of time steps
C   ntt         when counting the boundary element along the whole water surface from left to right, bottom to top,
C               ntt represents the number of elements on the free surface before the counting reaches the first element
C               on the wetted body surface
C   n11         constant 1
C   i1          element number where the connecting points between floating structure and landing gears are located
C   ifn         the first node number in element i1
C   ix,iy       integer variable for the calculation of i1
```

```
C    ns1-ns4        node number of the landing structure on which the landing system are connected to
C    nf1-nf10       node number of the floating structure on which time history of responses are outputted
C    nef1-nef10     element number of the floating structure where water pressure history are outputted
C    nl1-nl5        node number of the landing structure on which time history of responses are outputted
C    noutput1-noutput5          number of time steps at which data are outputted
CCC-------------------------------------------------------------------------------------------------------------------------------------------

real   g,pi,densityw,flx,fly,lex1,ley1,sk1,sk2,sk3,sk4,c1,c2,c3,c4,xp,yp,zp,zq,df,vh,ah,vz,time,amass
real   errabs,errrel,errest,result0,lowy,highy,lowx,highx,alfa,dita,ts,a1,a2,a3,a4,a5,a6,a7,a8,a9,a10,a12
real   xem1,yem1,x1,y1,x2,y2,x3,y3,x4,y4,s1,anglex,x01,y01,x02,y02,x03,y03,x04,y04
real   xa1,ya1,xa2,ya2,xa3,ya3,xa4,ya4,tw1(1,1),twv1(1,1)

real,ALLOCATABLE:: fai1(:,:),fai2(:,:),omeg1(:,:),omeg2(:,:),fg2n(:,:),fg2(:,:),x11(:),y11(:),x22(:),y22(:)
real,ALLOCATABLE:: a11(:,:),a22(:,:),a33(:,:),a44(:,:),akc22(:,:),b11(:,:),b22(:,:),b33(:,:),b44(:,:),tkc22(:,:)
real,ALLOCATABLE:: gg2(:,:),gg5(:,:),gg6(:,:),gg7(:,:),aa(:,:),bb(:,:),cc(:,:),dd(:,:),mz(:,:),fz(:),cz(:,:),kz(:,:),f(:,:),az(:,:)
real,ALLOCATABLE:: temp6(:,:),temp7(:,:),temp8(:,:),temp9(:,:),temp10(:,:),temp11(:,:),temp12(:,:),
*                  temp13(:,:),temp14(:,:),temp15(:,:),temp16(:,:),temp17(:,:),temp18(:,:)
real,ALLOCATABLE:: k12(:,:),k21(:,:),c12(:,:),c21(:,:),k11(:,:),c11(:,:),k22(:,:),c22(:,:)
real,ALLOCATABLE:: fai(:,:),faiv(:,:),faia(:,:),fain(:,:),faivn(:,:),faian(:,:),
real,ALLOCATABLE:: u(:,:),uv(:,:),ua(:,:),un(:),u1(:,:),uvn(:,:),uan(:,:)
real,ALLOCATABLE:: wf1(:),wf3(:),wf5(:),wf7(:),wf9(:),wf2(:),wf4(:),wf6(:),wf8(:),wf10(:)
real,ALLOCATABLE:: wfv1(:),wfv3(:),wfv5(:),wfv7(:),wfv9(:),wfv2(:),wfv4(:),wfv6(:),wfv8(:),wfv10(:)
real,ALLOCATABLE:: wfa1(:),wfa3(:),wfa5(:),wfa7(:),wfa9(:),wfa2(:),wfa4(:),wfa6(:),wfa8(:),wfa10(:)
real,ALLOCATABLE:: wl1(:),wl2(:),wl3(:),wl4(:),wl5(:),wlv1(:),wlv2(:),wlv3(:),wlv4(:),wlv5(:)
real,ALLOCATABLE:: wla1(:),wla2(:),wla3(:),wla4(:),wla5(:)
real,ALLOCATABLE:: pd1(:),pd3(:),pd5(:),pd7(:),pd9(:),pd2(:),pd4(:),pd6(:),pd8(:),pd10(:)
real,ALLOCATABLE:: wa1(:),wp1(:),wav1(:),wpv1(:),wa2(:),wp2(:),wav2(:),wpv2(:)
real,ALLOCATABLE:: wa3(:),wp3(:),wav3(:),wpv3(:),wa4(:),wp4(:),wav4(:),wpv4(:)
real,ALLOCATABLE:: fkc1(:),fkc2(:),fkc3(:),fkc4(:),faivbs(:),wze1(:,:),pd(:),fd(:),
real,ALLOCATABLE:: w1(:,:),wv1(:,:),waa1(:,:),wz2(:),wvz2(:),waz2(:)
real,ALLOCATABLE:: gg(:,:),gg1(:,:),hh(:,:),hhn(:,:),temp1(:,:),ee(:,:),ddt(:,:),gg3(:,:)
real,ALLOCATABLE:: gg00(:,:),gg01(:,:),gg10(:,:),gg11(:,:),hh00(:,:),hh01(:,:),hh10(:,:),hh11(:,:)

real,external::    gr3,grn3,gl,hl,gr2,grn2
C-------------------------------------------------------------------------------------------------------------------------------------------
C    g              gravitional acceleration
C    pi             ratio of the circumference to the diameter of a circle
C    densityw       mass density of water
C    flx,fly        length, width of the floating structure
C    lex1,ley1      length, width of the element of floating structure
C    sk1-sk4        spring coefficients of landing system
C    c1-c4          damping coefficients of landing system
C    xp,yp,zp       coordinates of field point p
C    zq             z coordinate of source point q
```

```
C   df          initial draft of floating structure
C   vh,ah       horizontal landing velocity, deceleration
C   vz          vertical landing velocity
C   time        total time of landing process
C   amass       mass of the landing structure
C   alfa,dita   two parameters from Newmark time integration scheme
C   ts          time step
C   a1-a10,a12  relevant coefficients for Newmark time integration scheme
C   xem1,yem1   coordinates of the centre of each element of the floating structure
C   x1,y1-x4,y4 relative coordinates in element of the four connecting points along the floating structure
C   s1          horizontal travel distance of the landing structure
C   anglex      orientation of the runway to the positive direction of x axis
C   tw1,twv1    temporary matrices
C   fai1,fai2   mode matrix for floating, landing structure
C   fg2n,fg2    equivalent nodal force from gravity for landing struture, generalized format of fg2n
C   a11-a44     transform matrix to get the vertical displacement at each connecting point 1-4 on the landing structure
C               from its nodal displacement vector
C   b11-b44     similar as a11-a44 for the floating structure
C   akc22,tkc22 temporary matrices for calculation
C   gg2         transform matrix to get the vertical displacement at the centre of each element of the floating structure
C               from its nodal displacement vector
C   gg3         transform matrix to get the equivalent nodal force vector from water pressure for the floating structure
C   gg5         gg3*(Tranpose fai1)
C   gg6         in the expression of nodal force vector from water pressure, it's the matrix in front of the velocity
C               coorcinate vector of the floating structure/(-densityw)
C   gg7         in the expression of nodal force vector from water pressure, it's the matrix in front of the displacement
C               coorcinate vector of the floating structure/(-densityw*g)
C   aa          in the expression of the first order derivative of velocity potential, it's the matrix in front of the velocity
C               potential at previous time step
C   bb          in the expression of the first order derivative of velocity potential, it's the matrix in front of the first
C               order derivative of velocity potential at previous time step
C   cc          in the expression of the first order derivative of velocity potential, it's the matrix in front of the second
C               order derivative of velocity potential at previous time step
C   dd          in the expression of the first order derivative of velocity potential, it's the matrix in front of the velocity
C               coordinate of the floating structure
C   kz,cz,mz    in the equation about the displacement, velocity, acceleration coordinates of the two structure, they are
C               the coefficient matrices
C   az,fz       in the equation only about displacement coordinates of the two structures, az coefficient matrix, fz load
C               vector on the right hand side
C   f           part of fz which is only related to velocity potential/(-densityw*gg5)
C   temp6-18    temporary matrices for calculation
C   fai,faiv,faia velocity potential, it's first order derivative, second order derivative (previous time step)
C   u,uv,ua     displacement, velocity, acceleration coordinates vector (previous time step)
C   un,uvn,uan  displacement, velocity, acceleration coordinates vector (current time step)
```

```
C   u1              displacement coordinate vector for floating structure only
C   wf1-wf10        displacement of the floating structure at ten points
C   wfv1-wfv10      velocity of the floating structure at ten points
C   wfa1-wfa10      acceleration of the floating structure at ten points
C   wl1-wl5         displacement of the landing structure at five points
C   wlv1-wlv5       velocity of the landing structure at five points
C   wla1-wla5       acceleration of the landing structure at five points
C   pd1-pd10        water pressure at ten points of the bottom of the floating structure
C   wa1-wa4         displacement at four connecting points on the landing structure
C   wav1-wav4       velocity at four connecting points on the landing structure
C   wp1-wp4         displacement at four connecting points on the floating structure
C   wpv1-wpv4       velocity at four connecting points on the floating structure
C   fkc1-4          force of the landing system at four connecting points
C   faivbs          first order of velocity potential at the centre of each element along the wet body surface
C   wze1            displacement at the centre of each element of the floating structure
C   pd              water pressure at centre of each element of the floating structure
C   fd              total force from water pressure
C   w1              nodal displacement for floating structure
C   wv1             nodal velocity for floating structure
C   waa1            nodal acceleration for floating structure
C   wz2             nodal displacement for landing structure
C   wvz2            nodal velocity for landing structure
C   waz2            nodal acceleration for landing structure
C   gr3             basic 3-D Green function
C   grn3            derivative of 3-D Green function
C   gr2             basic 2-D Green function
C   grn2            derivative of 2-D Green function
C   gl              lower limit function of integral (TWODQ)
C   hl              higher limit funciton of integral (TWODQ)
C   errabs,errrel,errest,result0    parameters of 2-D [qdags] and 3-D integral function [TWODQ]
C   lowy,highy,lowx,highx           lower and upper limit of the integral
C   x01,y01-x04,y04                 initial position of the four connecting points on the floating structure
C   xa1,ya1-xa4,ya4                 instant position of the four connecting points on the floating structure
C   omeg1,omeg2                     frequency matrix for floating, landing structure
C   x11,y11,x22,y22                 nodal coordinates for floating, landing structure
C   fain,faivn,faian                velocity potential, it's first and second order derivative at current time step
C   k11,k12,k21,k22                 component matrices of kz
C   c11,c12,c21,c22                 component matrices of cz
C   gg00,gg01,gg10,gg11             the integral of Green function at each boundary element along the whole water surface
C                                    for a fixed source point
C   hh00,hh01,hh10,hh11             the integral of Green function's derivative at each boundary element along the whole
C                                    water surface for a fixed source point
CCC-------------------------------------------------------------------------------------------------------------------------------------------
```

```
character*12    files

common /lowhighy/ lowy,highy
common /xzt/    xp,yp,zp,zq
common /cgf3/ nz,nzh,flx,fly,lex1,ley1,nex1,ney1,df,news,pi, errabs,errrel,nd1,ne1,NDFS,s1
common /cb11to44/ vh,ah,ts,k,anglex,x01,y01,x02,y02,x03,y03, x04,y04,xa1,nt

WRITE(6,80)
80          FORMAT(3X,'Please enter the input-file name for parameters',':')
READ(5,'(A)') FILES
OPEN(10,FILE=FILES,STATUS='OLD')
C-------------------------------------------------------------------------------------------------------------------------------
C    Read in all the parameters which shall be defined by the user.
CCC-----------------------------------------------------------------------------------------------------------------------------
read(10,90)       n1,nd1,nm1,ne1,nex1,ney1,n2,nd2,nm2,nt,nz, NDFD,NDFS,noutput1,noutput2,noutput3,noutput4,
*                 noutput5, amass,time,anglex,vh,ah,vz,flx,fly,df,sk1,c1,sk2,c2,sk3, c3,sk4,c4,x01,y01,x02,y02,x03,y03,
*                 x04,y04,ns1,ns2,ns3,ns4,nf1,nf2,nf3,nf4,nf5,nf6,nf7,nf8,nf9,nf10,nef1,nef2, nef3,nef4,nef5,nef6,
*                 nef7,nef8,nef9,nef10,nl1,nl2,nl3,nl4,nl5
90          FORMAT (8/,i5,17(3/,i5),9(3/,f15.4),3/,16(3/,f15.4),4(3/,i5),3/,20(3/,i5),5(3/,i5))

n11=1
ipath=1
nm12=nm1+nm2
nzh=(nz-1)/2

if (NDFD.eq.2) then
ntt=nzh*nex1
news=nex1*ney1*nz
else if (NDFD.eq.3) then
ntt=nz*nex1*ney1*nzh+nzh*nex1
news=nex1*ney1*nz**2
else
end if
g=DCONST("StandardGravity")
PI=DCONST("PI")
densityw=1000.0d0
lex1=flx/nex1
ley1=fly/ney1
alfa=0.25
dita=0.5
ts=time/nt
a1=alfa*ts/dita
a2=(1-alfa/dita)*ts
a3=(0.5-alfa/dita)*ts**2
```

```
a4=1/(dita*ts)
a5=1-1/dita
a6=1/(alfa*ts**2)
a7=1/(alfa*ts)
a8=1/(2*alfa)-1
a9=dita/(alfa*ts)
a10=dita/alfa-1
a12=ts*(dita/(2*alfa)-1)
errabs=1.0d-3
errrel=1.0d-3

allocate (fai1(nd1,nm1),fai2(nd2,nm2),omeg1(nm1,nm1), omeg2(nm2,nm2))
allocate (fg2n(nd2,1),fg2(nm2,1),x11(n1),y11(n1),x22(n2),y22(n2))
allocate (a11(nd2,1),a22(nd2,1),a33(nd2,1),a44(nd2,1), akc22(nd2,nd2),b11(1,nd1),b22(1,nd1),b33(1,nd1),
*       b44(1,nd1),tkc22(nm2,nd2))
allocate (gg2(ne1,nd1),gg5(nm1,ne1),gg6(nm1,nm1),gg7(nm1,nm1))
allocate (aa(news,news),bb(news,news),cc(news,news),dd(news,nm1))
allocate (mz(nm12,nm12),fz(nm12),cz(nm12,nm12),kz(nm12,nm12), f(ne1,1),az(nm12,nm12))
allocate (temp6(nm2,nm1),temp7(nm2,nm1),temp8(nm2,nm1), temp9(nm2,nm1),temp10(nm1,nm1),temp11(nm1,nm1),
*       temp12(nm1,nm1),temp13(nm12,nm12),temp14(nm12,1), temp15(nm1,1),temp16(nm12,1),temp17(nm12,1),
*       temp18(nm1,nm1))
allocate (k12(nm1,nm2),k21(nm2,nm1),c12(nm1,nm2),c21(nm2,nm1), k11(nm1,nm1),c11(nm1,nm1),k22(nm2,nm2),
*       c22(nm2,nm2))
allocate (fai(news,1),faiv(news,1),faia(news,1),fain(news,1), faivn(news,1),faian(news,1))
allocate (u(nm12,1),uv(nm12,1),ua(nm12,1),un(nm12),u1(nm1,1),uvn(nm12,1),uan(nm12,1))
allocate (wf1(nt),wf3(nt),wf5(nt),wf7(nt),wf9(nt),wf2(nt),wf4(nt),wf6(nt),wf8(nt),wf10(nt))
allocate (wfv1(nt),wfv3(nt),wfv5(nt),wfv7(nt),wfv9(nt),wfv2(nt),wfv4(nt),wfv6(nt),wfv8(nt),wfv10(nt))
allocate (wfa1(nt),wfa3(nt),wfa5(nt),wfa7(nt),wfa9(nt),wfa2(nt),wfa4(nt),wfa6(nt),wfa8(nt),wfa10(nt))
allocate (wl1(nt),wl2(nt),wl3(nt),wl4(nt),wl5(nt),wlv1(nt),wlv2(nt),wlv3(nt),wlv4(nt),wlv5(nt))
allocate (wla1(nt),wla2(nt),wla3(nt),wla4(nt),wla5(nt),fkc1(nt),fkc2(nt),fkc3(nt),fkc4(nt))
allocate (pd1(nt),pd3(nt),pd5(nt),pd7(nt),pd9(nt),pd2(nt),pd4(nt),pd6(nt),pd8(nt),pd10(nt))
allocate (wa1(nt),wp1(nt),wav1(nt),wpv1(nt),wa2(nt),wp2(nt),wav2(nt),wpv2(nt))
allocate (wa3(nt),wp3(nt),wav3(nt),wpv3(nt),wa4(nt),wp4(nt),wav4(nt),wpv4(nt))
allocate (faivbs(ne1),wze1(ne1,1),pd(ne1),fd(nt), w1(nd1,1),wv1(nd1,1),waa1(nd1,1),wz2(n2),wvz2(n2), waz2(n2))

WRITE(6,100)
100     FORMAT(3X,'Please enter input-file name for nodal and modal information for two solid substructure',':')
READ(5,'(A)') FILES
OPEN(3,FILE=FILES,STATUS='OLD')
WRITE(6,110)
110     FORMAT(3X,'PLEASE ENTER OUTPUT_FILE NAME',T50,':')
READ(5,'(A)') FILES
OPEN(4,FILE=FILES,STATUS='UNKNOWN')
write(4,*) "*****************************************************"
```

```
write(4,*)        "Output file for Program MMFBEP"
write(4,*)        "Unit system: m for displacement and coordinate,"
write(4,*)        "m/s for velocity, m/s**2 for acceleration,"
write(4,*)        "s for time, N for force and N/m**2 for pressure."
write(4,*) "*****************************************************"
write(4,260)

C-------------------------------------------------------------------------------------------------------------------------------
C    Read in the coordinates and modal information for airplane and floating structure.
CCC------------------------------------------------------------------------------------------------------------------------------
do i=1,n2
read(3,*) x22(i)
end do
do i=1,n2
read(3,*) y22(i)
end do

do m=1,nm2
read(3,*) omeg2(m,m)
omeg2(m,m)=(omeg2(m,m)*2*pi)**2
end do

do m=1,nm2
do n=1,n2
read(3,*) fai2(3*n-2,m)
end do
end do
do m=1,nm2
do n=1,n2
read(3,*) fai2(3*n-1,m)
end do
end do
do m=1,nm2
do n=1,n2
read(3,*) fai2(3*n,m)
end do
end do

do i=1,n1
read(3,*) x11(i)
end do
do i=1,n1
read(3,*) y11(i)
end do
```

```
do m=1,nm1
read(3,*) omeg1(m,m)
omeg1(m,m)=(omeg1(m,m)*2*pi)**2
end do

do m=1,nm1
do n=1,n1
read(3,*) fai1(3*n-2,m)
end do
end do
do m=1,nm1
do n=1,n1
read(3,*) fai1(3*n-1,m)
end do
end do
do m=1,nm1
do n=1,n1
read(3,*) fai1(3*n,m)
end do
end do

do i=1,nm12
mz(i,i)=1.0
end do

do i=1,n2
fg2n(3*i-2,1)=-amass*g/n2
end do
CALL MXTYF (nd2,nm2,fai2,nd2,nd2,n11,fg2n,nd2,nm2,n11,fg2,nm2)

C-------------------------------------------------------------------------------------------------------------------------------
C    Formulate a11-a44 and k22,c22.
C    This program can consider four connecting points between the landing and floating structure. If the number of
C    connecting points is less than 4, just put the revelant spring and damping coefficients to those of landing gear 1.
C    For example, if only one connecting point is considered, simply put sk2=sk3=sk4= sk1, c2=c3=c4=c1and
C    ns2=ns3=ns4=ns1
CCC------------------------------------------------------------------------------------------------------------------------------
a11(3*ns1-2,1)=1.0d0
a22(3*ns2-2,1)=1.0d0
a33(3*ns3-2,1)=1.0d0
a44(3*ns4-2,1)=1.0d0
akc22(3*ns4-2,3*ns4-2)=sk4
akc22(3*ns3-2,3*ns3-2)=sk3
akc22(3*ns2-2,3*ns2-2)=sk2
```

```
akc22(3*ns1-2,3*ns1-2)=sk1
CALL MXTYF (nd2,nm2,fai2,nd2,nd2,nd2,akc22,nd2,nm2,nd2,tkc22,nm2)
CALL MRRRR (nm2,nd2,tkc22,nm2,nd2,nm2,fai2,nd2,nm2,nm2,k22,nm2)
akc22(3*ns4-2,3*ns4-2)=c4
akc22(3*ns3-2,3*ns3-2)=c3
akc22(3*ns2-2,3*ns2-2)=c2
akc22(3*ns1-2,3*ns1-2)=c1
CALL MXTYF (nd2,nm2,fai2,nd2,nd2,nd2,akc22,nd2, nm2,nd2,tkc22,nm2)
CALL MRRRR (nm2,nd2,tkc22,nm2,nd2,nm2,fai2,nd2,nm2,nm2,c22,nm2)

C-------------------------------------------------------------------------------------------------------------------------------
C    Formulate the two coefficient matrices G and H in the boundary integral equation according to the dimension of
C    the fluid domain.
CCC-------------------------------------------------------------------------------------------------------------------------------
allocate (gg(news,news),hh(news,news))
if (NDFD.eq.3) then
call gf3(gg,hh)
else if (NDFD.eq.2)    then
call gf2(gg,hh)
else
end if

allocate     (gg1(news,ne1))
do m=1,news
do l=1,ney1
do n=1,nex1
gg1(m,n+(l-1)*nex1)=gg(m,ntt+n+(l-1)*nz*nex1)
gg(m,ntt+n+(l-1)*nz*nex1)=0.0d0
end do
end do
end do
gg=gg/g

C-------------------------------------------------------------------------------------------------------------------------------
C    Formulate the two transform matrices gg2 and gg3 based on the element shape function of the floating structure.
CCC-------------------------------------------------------------------------------------------------------------------------------
allocate (gg3(nd1,ne1))
call gg2and3(gg2,gg3)

allocate     (temp1(news,nd1))
CALL MRRRR (news,ne1,gg1,news,ne1,nd1,gg2,ne1,news,nd1,temp1,news)
deallocate (gg1)
allocate     (gg1(news,nm1))
CALL MRRRR (news,nd1,temp1,news,nd1,nm1,fai1,nd1,news,nm1,gg1,news)
```

```
deallocate (temp1)

C-----------------------------------------------------------------------------------------------------------------------------------------
C    Formulate matrices aa,bb,cc,dd.
CCC---------------------------------------------------------------------------------------------------------------------------------------
allocate       (temp1(news,news),ee(news,news))
temp1=-(a1*hh+a4*gg)
call LINRG (news,temp1,news,ee,news)
CALL MRRRR (news,news,ee,news,news,news,hh,news,news,news,aa,news)
temp1=a2*hh-a4*gg
CALL MRRRR (news,news,ee,news,news,news,temp1,news,news,news,bb,news)
temp1=a3*hh+a5*gg
CALL MRRRR (news,news,ee,news,news,news,temp1,news,news,news,cc,news)
deallocate (gg,hh,temp1)
CALL MRRRR (news,news,ee,news,news,nm1,gg1,news,news,nm1,dd,news)
deallocate (gg1,ee)
dd=-dd

allocate     (ddt(ne1,nm1))
do l=1,ney1
do m=1,nex1
do n=1,nm1
ddt(m+(l-1)*nex1,n)=dd(m+ntt+(l-1)*nex1*nz,n)
end do
end do
end do

C-----------------------------------------------------------------------------------------------------------------------------------------
C    Calculate matrices gg5,gg6 and gg7.
CCC---------------------------------------------------------------------------------------------------------------------------------------
allocate     (temp1(nm1,nd1))
CALL MXTYF (nd1,nm1,fai1,nd1,nd1,ne1,gg3,nd1,nm1,ne1,gg5,nm1)
deallocate (gg3)
CALL MRRRR (nm1,ne1,gg5,nm1,ne1,nm1,ddt,ne1,nm1,nm1,gg6,nm1)
CALL MRRRR (nm1,ne1,gg5,nm1,ne1,nd1,gg2,ne1,nm1,nd1,temp1,nm1)
CALL MRRRR (nm1,nd1,temp1,nm1,nd1,nm1,fai1,nd1,nm1,nm1,gg7,nm1)
deallocate (temp1,ddt)

uv(nm1+1,1)=-vz/fai2(1,1)

do i=1+nm1,nm12
do j=1+nm1,nm12
cz(i,j)=c22(i-nm1,j-nm1)
kz(i,j)=k22(i-nm1,j-nm1)+omeg2(i-nm1,j-nm1)
```

```
end do
end do
C-----------------------------------------------------------------------------------------------------------------------------------------
C    From this point, the program enters a loop which carries out the time integration scheme.
CCC---------------------------------------------------------------------------------------------------------------------------------------
do k=1,nt
write (6,*)    k

do i=nm1+1,nm12
fz(i)=fg2(i-nm1,1)
end do

C-----------------------------------------------------------------------------------------------------------------------------------------
C    Formulate the transform matrices b11,b22,b33 and b44 for the floaitng structure.
CCC---------------------------------------------------------------------------------------------------------------------------------------
do i=1,nd1
b11(1,i)=0.0d0
b22(1,i)=0.0d0
b33(1,i)=0.0d0
b44(1,i)=0.0d0
end do
call b11to44 (b11,b22,b33,b44)
C-----------------------------------------------------------------------------------------------------------------------------------------
C    Formulate matrices k12,k21,c12,c21,k11 and c11.
CCC---------------------------------------------------------------------------------------------------------------------------------------
allocate       (temp1(nd2,nd1),gg1(nm2,nd1))
CALL MRRRR (nd2,n11,a11,nd2,n11,nd1,b11,n11,nd2,nd1,temp1,nd2)
CALL MXTYF (nd2,nm2,fai2,nd2,nd2,nd1,temp1,nd2,nm2,nd1,gg1,nm2)
CALL MRRRR (nm2,nd1,gg1,nm2,nd1,nm1,fai1,nd1,nm2,nm1,temp6,nm2)

CALL MRRRR (nd2,n11,a22,nd2,n11,nd1,b22,n11,nd2,nd1,temp1,nd2)
CALL MXTYF (nd2,nm2,fai2,nd2,nd2,nd1,temp1,nd2,nm2,nd1,gg1,nm2)
CALL MRRRR (nm2,nd1,gg1,nm2,nd1,nm1,fai1,nd1,nm2,nm1,temp7,nm2)

CALL MRRRR (nd2,n11,a33,nd2,n11,nd1,b33,n11,nd2,nd1,temp1,nd2)
CALL MXTYF (nd2,nm2,fai2,nd2,nd2,nd1,temp1,nd2,nm2,nd1,gg1,nm2)
CALL MRRRR (nm2,nd1,gg1,nm2,nd1,nm1,fai1,nd1,nm2,nm1,temp8,nm2)

CALL MRRRR (nd2,n11,a44,nd2,n11,nd1,b44,n11,nd2,nd1,temp1,nd2)
CALL MXTYF (nd2,nm2,fai2,nd2,nd2,nd1,temp1,nd2,nm2,nd1,gg1,nm2)
CALL MRRRR (nm2,nd1,gg1,nm2,nd1,nm1,fai1,nd1,nm2,nm1,temp9,nm2)
deallocate    (temp1,gg1)

do i=1,nm2
```

```
do j=1,nm1
k21(i,j)=sk1*temp6(i,j)+sk2*temp7(i,j)+sk3*temp8(i,j) +sk4*temp9(i,j)
k12(j,i)=k21(i,j)
c21(i,j)=c1*temp6(i,j)+c2*temp7(i,j)+c3*temp8(i,j)+c4*temp9(i,j)
c12(j,i)=c21(i,j)
end do
end do

allocate       (temp1(nd1,nd1),gg1(nm1,nd1))
CALL MXTYF (n11,nd1,b11,n11,n11,nd1,b11,n11, nd1,nd1,temp1,nd1)
CALL MXTYF (nd1,nm1,fai1,nd1,nd1,nd1,temp1,nd1, nm1,nd1,gg1,nm1)
CALL MRRRR (nm1,nd1,gg1,nm1,nd1,nm1,fai1,nd1, nm1,nm1,temp10,nm1)

CALL MXTYF (n11,nd1,b22,n11,n11,nd1,b22,n11, nd1,nd1,temp1,nd1)
CALL MXTYF (nd1,nm1,fai1,nd1,nd1,nd1,temp1,nd1, nm1,nd1,gg1,nm1)
CALL MRRRR (nm1,nd1,gg1,nm1,nd1,nm1,fai1,nd1, nm1,nm1,temp11,nm1)

CALL MXTYF (n11,nd1,b33,n11,n11,nd1,b33,n11, nd1,nd1,temp1,nd1)
CALL MXTYF (nd1,nm1,fai1,nd1,nd1,nd1,temp1,nd1, nm1,nd1,gg1,nm1)
CALL MRRRR (nm1,nd1,gg1,nm1,nd1,nm1,fai1,nd1, nm1,nm1,temp12,nm1)

CALL MXTYF (n11,nd1,b44,n11,n11,nd1,b44,n11, nd1,nd1,temp1,nd1)
CALL MXTYF (nd1,nm1,fai1,nd1,nd1,nd1,temp1,nd1, nm1,nd1,gg1,nm1)
CALL MRRRR (nm1,nd1,gg1,nm1,nd1,nm1,fai1,nd1, nm1,nm1,temp18,nm1)
deallocate    (temp1,gg1)

k11=sk1*temp10+sk2*temp11+sk3*temp12+sk4*temp18
c11=c1*temp10+c2*temp11+c3*temp12+c4*temp18

C-------------------------------------------------------------------------------------------------------------------------------
C    Formulate matrices kz and cz.
CCC-----------------------------------------------------------------------------------------------------------------------------
do i=1,nm1
do j=1,nm1
cz(i,j)=c11(i,j)+densityw*gg6(i,j)
kz(i,j)=k11(i,j)+omeg1(i,j)+densityw*g*gg7(i,j)
end do
end do
do i=1,nm1
do j=1+nm1,nm12
cz(i,j)=-c12(i,j-nm1)
kz(i,j)=-k12(i,j-nm1)
cz(j,i)=cz(i,j)
kz(j,i)=kz(i,j)
```

```
end do
end do
C-----------------------------------------------------------------------------------------------------------------------------------------
C    Formulate coefficient matrix az and load vector fz.
CCC---------------------------------------------------------------------------------------------------------------------------------------
allocate (gg(news,n11),hh(news,n11),gg1(news,n11),temp1(news,n11))
CALL MRRRR (news,news,aa,news,news,n11,fai,news, news,n11,hh,news)
CALL MRRRR (news,news,bb,news,news,n11,faiv,news, news,n11,gg1,news)
CALL MRRRR (news,news,cc,news,news,n11,faia,news, news,n11,temp1,news)

do l=1,ney1
do i=1,nex1
f(i+(l-1)*nex1,1)=hh(i+ntt+(l-1)*nex1*nz,1)+ gg1(i+ntt+(l-1)*nex1*nz,1)+temp1(i+ntt+(l-1)*nex1*nz,1)
end do
end do
CALL MRRRR (nm1,ne1,gg5,nm1,ne1,n11,f,ne1, nm1,n11,temp15,nm1)
do i=1,nm1
fz(i)=-densityw*temp15(i,1)
end do

temp13=a6*mz+a9*cz
CALL MRRRR (nm12,nm12,temp13,nm12,nm12,n11,u,nm12, nm12,n11,temp14,nm12)
temp13=a7*mz+a10*cz
CALL MRRRR (nm12,nm12,temp13,nm12,nm12,n11,uv,nm12, nm12,n11,temp16,nm12)
temp13=a8*mz+a12*cz
CALL MRRRR (nm12,nm12,temp13,nm12,nm12,n11,ua,nm12, nm12,n11,temp17,nm12)
do i=1,nm12
fz(i)=fz(i)+temp14(i,1)+temp16(i,1)+temp17(i,1)
end do

az=a6*mz+a9*cz+kz

C-----------------------------------------------------------------------------------------------------------------------------------------
C    Calculate un,uvn,uan; fain,faivn,faian.
CCC---------------------------------------------------------------------------------------------------------------------------------------
CALL LSARG (nm12,az,nm12,fz,IPATH,un)
do i=1,nm12
uvn(i,1)=a9*un(i)-a9*u(i,1)-a10*uv(i,1)-a12*ua(i,1)
uan(i,1)=a6*un(i)-a6*u(i,1)-a7*uv(i,1)-a8*ua(i,1)
end do

u1=uvn
CALL MRRRR (news,nm1,dd,news,nm1,n11,u1,nm1, news,n11,gg,news)
faivn=temp1+gg1+hh+gg
```

```
deallocate (gg,hh,gg1,temp1)
fain=a1*faivn+fai+a2*faiv+a3*faia
faian=a4*(faivn-faiv)+a5*faia

fai=fain
faiv=faivn
faia=faian
do i=1,nm12
u(i,1)=un(i)
end do
uv=uvn
ua=uan

C-------------------------------------------------------------------------------------------------------------------------------------------
C    From this point on, the program will deal with the generation of the output data and output file.
CCC-----------------------------------------------------------------------------------------------------------------------------------------
do l=1,ney1
do m=1,nex1
faivbs(m+(l-1)*nex1)=faiv(m+ntt+(l-1)*nex1*nz,1)
end do
end do

do i=1,nd1
w1(i,1)=0.0d0
wv1(i,1)=0.0d0
waa1(i,1)=0.0d0
end do
do i=1,nd1
do j=1,nm1
w1(i,1)=w1(i,1)+fai1(i,j)*u(j,1)
wv1(i,1)=wv1(i,1)+fai1(i,j)*uv(j,1)
waa1(i,1)=waa1(i,1)+fai1(i,j)*ua(j,1)
end do
end do

CALL MRRRR (ne1,nd1,gg2,ne1,nd1,n11,w1,nd1,ne1,n11,wze1,ne1)

do i=1,ne1
pd(i)=-densityw*faivbs(i)-densityw*g*wze1(i,1)
end do

pd1(k)=pd(nef1)
pd2(k)=pd(nef2)
pd3(k)=pd(nef3)
```

```
pd4(k)=pd(nef4)
pd5(k)=pd(nef5)
pd6(k)=pd(nef6)
pd7(k)=pd(nef7)
pd8(k)=pd(nef8)
pd9(k)=pd(nef9)
pd10(k)=pd(nef10)

do i=1,ne1
fd(k)=pd(i)*lex1*ley1+fd(k)
end do

do i=1,n2
wz2(i)=0.0d0
wvz2(i)=0.0d0
waz2(i)=0.0d0
end do
do i=1,n2
do j=1,nm2
wz2(i)=wz2(i)+fai2(3*i-2,j)*u(nm1+j,1)
wvz2(i)=wvz2(i)+fai2(3*i-2,j)*uv(nm1+j,1)
waz2(i)=waz2(i)+fai2(3*i-2,j)*ua(nm1+j,1)
end do
end do

wa1(k)=wz2(ns1)
wav1(k)=wvz2(ns1)
wa2(k)=wz2(ns2)
wav2(k)=wvz2(ns2)
wa3(k)=wz2(ns3)
wav3(k)=wvz2(ns3)
wa4(k)=wz2(ns4)
wav4(k)=wvz2(ns4)

wl1(k)=wz2(nl1)
wl2(k)=wz2(nl2)
wl3(k)=wz2(nl3)
wl4(k)=wz2(nl4)
wl5(k)=wz2(nl5)

wlv1(k)=wvz2(nl1)
wlv2(k)=wvz2(nl2)
wlv3(k)=wvz2(nl3)
wlv4(k)=wvz2(nl4)
```

```
wlv5(k)=wvz2(nl5)

wla1(k)=waz2(nl1)
wla2(k)=waz2(nl2)
wla3(k)=waz2(nl3)
wla4(k)=waz2(nl4)
wla5(k)=waz2(nl5)

CALL MRRRR (n11,nd1,b11,n11,nd1,n11,w1,nd1,n11,n11,tw1,n11)
CALL MRRRR (n11,nd1,b11,n11,nd1,n11,wv1,nd1,n11,n11,twv1,n11)
wp1(k)=tw1(1,1)
wpv1(k)=twv1(1,1)

CALL MRRRR (n11,nd1,b22,n11,nd1,n11,w1,nd1,n11,n11,tw1,n11)
CALL MRRRR (n11,nd1,b22,n11,nd1,n11,wv1,nd1,n11,n11,twv1,n11)
wp2(k)=tw1(1,1)
wpv2(k)=twv1(1,1)

CALL MRRRR (n11,nd1,b33,n11,nd1,n11,w1,nd1,n11,n11,tw1,n11)
CALL MRRRR (n11,nd1,b33,n11,nd1,n11,wv1,nd1,n11,n11,twv1,n11)
wp3(k)=tw1(1,1)
wpv3(k)=twv1(1,1)

CALL MRRRR (n11,nd1,b44,n11,nd1,n11,w1,nd1,n11,n11,tw1,n11)
CALL MRRRR (n11,nd1,b44,n11,nd1,n11,wv1,nd1,n11,n11,twv1,n11)
wp4(k)=tw1(1,1)
wpv4(k)=twv1(1,1)

fkc1(k)=sk1*(wa1(k)-wp1(k))+c1*(wav1(k)-wpv1(k))
fkc2(k)=sk2*(wa2(k)-wp2(k))+c2*(wav2(k)-wpv2(k))
fkc3(k)=sk3*(wa3(k)-wp3(k))+c3*(wav3(k)-wpv3(k))
fkc4(k)=sk4*(wa4(k)-wp4(k))+c4*(wav4(k)-wpv4(k))

wf1(k)=w1(3*nf1-2,1)
wf2(k)=w1(3*nf2-2,1)
wf3(k)=w1(3*nf3-2,1)
wf4(k)=w1(3*nf4-2,1)
wf5(k)=w1(3*nf5-2,1)
wf6(k)=w1(3*nf6-2,1)
wf7(k)=w1(3*nf7-2,1)
wf8(k)=w1(3*nf8-2,1)
wf9(k)=w1(3*nf9-2,1)
wf10(k)=w1(3*nf10-2,1)
```

```
wfv1(k)=wv1(3*nf1-2,1)
wfv2(k)=wv1(3*nf2-2,1)
wfv3(k)=wv1(3*nf3-2,1)
wfv4(k)=wv1(3*nf4-2,1)
wfv5(k)=wv1(3*nf5-2,1)
wfv6(k)=wv1(3*nf6-2,1)
wfv7(k)=wv1(3*nf7-2,1)
wfv8(k)=wv1(3*nf8-2,1)
wfv9(k)=wv1(3*nf9-2,1)
wfv10(k)=wv1(3*nf10-2,1)

wfa1(k)=waa1(3*nf1-2,1)
wfa2(k)=waa1(3*nf2-2,1)
wfa3(k)=waa1(3*nf3-2,1)
wfa4(k)=waa1(3*nf4-2,1)
wfa5(k)=waa1(3*nf5-2,1)
wfa6(k)=waa1(3*nf6-2,1)
wfa7(k)=waa1(3*nf7-2,1)
wfa8(k)=waa1(3*nf8-2,1)
wfa9(k)=waa1(3*nf9-2,1)
wfa10(k)=waa1(3*nf10-2,1)

160         FORMAT(f10.4,3x,f10.4,3x,f10.4)
180         FORMAT (x,"Time step",i5,",",3X,"Time=",f5.2,"s")
if (k.eq.noutput1.or.k.eq.noutput2.or.k.eq.noutput3.or. k.eq.noutput4.or.k.eq.noutput5) then
write(4,180) k,k*ts
write(4,*)"Displacement distribution of landing structure:"
write(4,*)"        X                Y                WZ2"
do i=1,n2
write(4,160)    x22(i),y22(i),wz2(i)
end do

write(4,*)"Displacement distribution of floating structure:"
write(4,*)"        X                Y                W1"
do i=1,n1
write(4,160)    x11(i),y11(i),w1(3*i-2,1)
end do

write(4,*) "Water pressure distribution along floating structure:"
write(4,*)"        X                Y                PD"
i=1
do n=1,ney1
do m=1,nex1
xem1=-flx/2+(m-1)*lex1+lex1/2
```

```
yem1=-fly/2+(n-1)*ley1+ley1/2
write(4,160)    xem1, yem1, pd(i)
i=i+1
end do
end do
write(4,260)
else
end if
end do

270         FORMAT(e12.4,e12.4,e12.4,e12.4)
260         FORMAT (/)
write(4,*)"Time history of displacement at node NL1:"
write(4,270)        wl1
write(4,260)

write(4,*)"Time history of displacement at node NL2:"
write(4,270)        wl2
write(4,260)

write(4,*)"Time history of displacement at node NL3:"
write(4,270)        wl3
write(4,260)

write(4,*)"Time history of displacement at node NL4:"
write(4,270)        wl4
write(4,260)

write(4,*)"Time history of displacement at node NL5:"
write(4,270)        wl5
write(4,260)

write(4,*)"Time history of vertical velocity at node NL1:"
write(4,270)        wlv1
write(4,260)

write(4,*)"Time history of vertical velocity at node NL2:"
write(4,270)        wlv2
write(4,260)

write(4,*)"Time history of vertical velocity at node NL3:"
write(4,270)        wlv3
write(4,260)
```

```
write(4,*)"Time history of vertical velocity at node NL4:"
write(4,270)        wlv4
write(4,260)

write(4,*)"Time history of vertical velocity at node NL5:"
write(4,270)        wlv5
write(4,260)

write(4,*)"Time history of vertical acceleration at node NL1:"
write(4,270)        wla1
write(4,260)

write(4,*)"Time history of vertical acceleration at node NL2:"
write(4,270)        wla2
write(4,260)

write(4,*)"Time history of vertical acceleration at node NL3:"
write(4,270)        wla3
write(4,260)

write(4,*)"Time history of vertical acceleration at node NL4:"
write(4,270)        wla4
write(4,260)

write(4,*)"Time history of vertical acceleration at node NL5:"
write(4,270)        wla5
write(4,260)

write(4,*)"Time history of displacement at node NF1:"
write(4,270)        wf1
write(4,260)

write(4,*)"Time history of displacement at node NF2:"
write(4,270)        wf2
write(4,260)

write(4,*)"Time history of displacement at node NF3:"
write(4,270)        wf3
write(4,260)

write(4,*)"Time history of displacement at node NF4:"
write(4,270)        wf4
write(4,260)
```

```
write(4,*)"Time history of displacement at node NF5:"
write(4,270)        wf5
write(4,260)

write(4,*)"Time history of displacement at node NF6:"
write(4,270)        wf6
write(4,260)

write(4,*)"Time history of displacement at node NF7:"
write(4,270)        wf7
write(4,260)

write(4,*)"Time history of displacement at node NF8:"
write(4,270)        wf8
write(4,260)

write(4,*)"Time history of displacement at node NF9:"
write(4,270)        wf9
write(4,260)

write(4,*)"Time history of displacement at node NF10:"
write(4,270)        wf10
write(4,260)

write(4,*)"Time history of vertical velocity at node NF1:"
write(4,270)        wfv1
write(4,260)

write(4,*)"Time history of vertical velocity at node NF2:"
write(4,270)        wfv2
write(4,260)

write(4,*)"Time history of vertical velocity at node NF3:"
write(4,270)        wfv3
write(4,260)

write(4,*)"Time history of vertical velocity at node NF4:"
write(4,270)        wfv4
write(4,260)

write(4,*)"Time history of vertical velocity at node NF5:"
write(4,270)        wfv5
write(4,260)
```

```
write(4,*)"Time history of vertical velocity at node NF6:"
write(4,270)        wfv6
write(4,260)

write(4,*)"Time history of vertical velocity at node NF7:"
write(4,270)        wfv7
write(4,260)

write(4,*)"Time history of vertical velocity at node NF8:"
write(4,270)        wfv8
write(4,260)

write(4,*)"Time history of vertical velocity at node NF9:"
write(4,270)        wfv9
write(4,260)

write(4,*)"Time history of vertical velocity at node NF10:"
write(4,270)        wfv10
write(4,260)

write(4,*)"Time history of vertical acceleration at node NF1:"
write(4,270)        wfa1
write(4,260)

write(4,*)"Time history of vertical acceleration at node NF2:"
write(4,270)        wfa2
write(4,260)

write(4,*)"Time history of vertical acceleration at node NF3:"
write(4,270)        wfa3
write(4,260)

write(4,*)"Time history of vertical acceleration at node NF4:"
write(4,270)        wfa4
write(4,260)

write(4,*)"Time history of vertical acceleration at node NF5:"
write(4,270)        wfa5
write(4,260)

write(4,*)"Time history of vertical acceleration at node NF6:"
write(4,270)        wfa6
write(4,260)
```

```
write(4,*)"Time history of vertical acceleration at node NF7:"
write(4,270)        wfa7
write(4,260)

write(4,*)"Time history of vertical acceleration at node NF8:"
write(4,270)        wfa8
write(4,260)

write(4,*)"Time history of vertical acceleration at node NF9:"
write(4,270)        wfa9
write(4,260)

write(4,*)"Time history of vertical acceleration at node NF10:"
write(4,270)        wfa10
write(4,260)

write(4,*)"Time history of water pressure at element NEF1:"
write(4,270)        pd1
write(4,260)

write(4,*)"Time history of water pressure at element NEF2:"
write(4,270)        pd2
write(4,260)

write(4,*)"Time history of water pressure at element NEF3:"
write(4,270)        pd3
write(4,260)

write(4,*)"Time history of water pressure at element NEF4:"
write(4,270)        pd4
write(4,260)

write(4,*)"Time history of water pressure at element NEF5:"
write(4,270)        pd5
write(4,260)

write(4,*)"Time history of water pressure at element NEF6:"
write(4,270)        pd6
write(4,260)

write(4,*)"Time history of water pressure at element NEF7:"
write(4,270)        pd7
write(4,260)
```

```
write(4,*)"Time history of water pressure at element NEF8:"
write(4,270)        pd8
write(4,260)

write(4,*)"Time history of water pressure at element NEF9:"
write(4,270)        pd9
write(4,260)

write(4,*)"Time history of water pressure at element NEF10:"
write(4,270)        pd10
write(4,260)

write(4,*)"Relative displacement at landing gear 1"
write(4,270)        wa1-wp1
write(4,260)

write(4,*)"Relative displacement at landing gear 2"
write(4,270)        wa2-wp2
write(4,260)

write(4,*)"Relative displacement at landing gear 3"
write(4,270)        wa3-wp3
write(4,260)

write(4,*)"Relative displacement at landing gear 4"
write(4,270)        wa4-wp4
write(4,260)

write(4,*)"Force provided by landing gear 1"
write(4,270)        fkc1
write(4,260)

write(4,*)"Force provided by landing gear 2"
write(4,270)        fkc2
write(4,260)

write(4,*)"Force provided by landing gear 3"
write(4,270)        fkc3
write(4,260)

write(4,*)"Force provided by landing gear 4"
write(4,270)        fkc4
write(4,260)
```

```
write(4,*)"Total force provided by landing gear system"
write(4,270)        fkc1+fkc2+fkc3+fkc4
write(4,260)

write(4,*)"Total force from water pressure"
write(4,270)        fd
write(4,260)

end

C-------------------------------------------------------------------------------------------------------------------------------
C    Defined function for the lower and upper limit for integral function TWODQ.
CCC-------------------------------------------------------------------------------------------------------------------------------
REAL FUNCTION GL()
implicit none
real                lowy,highy
common              /lowhighy/    lowy,highy
GL=lowy
RETURN
END
REAL FUNCTION HL()
Implicit     none
Real         lowy,highy
common     /lowhighy/    lowy,highy
HL=highy
RETURN
END

C-------------------------------------------------------------------------------------------------------------------------------
C    Three dimensional green function and its normal derivative function.
CCC-------------------------------------------------------------------------------------------------------------------------------
real function gr3(xq,yq)
use msimsl
implicit none
real xp,xq,zp,zq,yp,yq,r
common /xzt/ xp,yp,zp,zq
r=sqrt((xp-xq)**2+(yp-yq)**2+(zp-zq)**2)
gr3=1/r
return
end
real function grn3(xq,yq)
use msimsl
implicit none
real xp,xq,zp,zq,yp,yq,r
```

```
common /xzt/ xp,yp,zp,zq
r=sqrt((xp-xq)**2+(yp-yq)**2+(zp-zq)**2)
grn3=(zp-zq)/r**3
return
end

C-----------------------------------------------------------------------------------------------------------------------------
C    Two dimensional green function and its normal derivative function.
CCC----------------------------------------------------------------------------------------------------------------------------
real function Gr2(xq)
use msimsl
implicit none
real xp,xq,zp,zq,r,yp
common /xzt/ xp,yp,zp,zq
r=sqrt((xp-xq)**2+(zp-zq)**2)
Gr2=log(r)
return
end
real function Grn2(xq)
use msimsl
implicit none
real xp,xq,zp,zq,r,yp
common /xzt/ xp,yp,zp,zq
r=sqrt((xp-xq)**2+(zp-zq)**2)
Grn2=-(zp-zq)/r**2
return
end

C-----------------------------------------------------------------------------------------------------------------------------
C    Subroutine to calculate coefficient matrices G and H in the boundary integral equation for three dimensional
C    fluid domain.
CCC----------------------------------------------------------------------------------------------------------------------------
subroutine gf3(gg,hh)
implicit none
common /cgf3/ nz,nzh,flx,fly,lex1,ley1,nex1,ney1,df,news,pi, errabs,errrel,nd1,ne1,NDFS,s1
common /xzt/ xp,yp,zp,zq
common /lowhighy/    lowy,highy

integer irule,m,n,i,j,k,l
integer nz,nzh,nex1,ney1,news,nd1,ne1,NDFS
real xp,yp,zp,zq,lowy,highy,lowx,highx,errest,result0
real flx,fly,lex1,ley1,df,pi,errabs,errrel,s1
real gg(news,news),hh(news,news)
real,ALLOCATABLE:: gg00(:,:),gg01(:,:),gg10(:,:),gg11(:,:)
```

```
real,ALLOCATABLE:: hh00(:,:),hh01(:,:),hh10(:,:),hh11(:,:)
real,external:: gr3,grn3,gl,hl
allocate    (gg00(nz*nex1,nz*ney1),gg01(nz*nex1,nz*ney1), gg10(nz*nex1,nz*ney1),gg11(nz*nex1,nz*ney1))
allocate    (hh00(nz*nex1,nz*ney1),hh01(nz*nex1,nz*ney1), hh10(nz*nex1,nz*ney1),hh11(nz*nex1,nz*ney1))

xp=-nz*flx/2+lex1/2
yp=-nz*fly/2+ley1/2
zp=0.0
zq=0.0
do n=1,nz*ney1
do m=1,nz*nex1
lowy=-nz*fly/2+(n-1)*ley1
highy=lowy+ley1
lowx=-nz*flx/2+(m-1)*lex1
highx=lowx+lex1
if (n.eq.1.and.m.eq.1) then
highy=highy-ley1/2
highx=highx-lex1/2
irule=1
CALL TWODQ (gr3,LOWx,HIGHx,GL,HL,ERRABS,ERRREL, IRULE,RESULT0,ERREST)
gg00(m,n)=4*result0
CALL TWODQ (grn3,LOWx,HIGHx,GL,HL,ERRABS,ERRREL, IRULE,RESULT0,ERREST)
hh00(m,n)=4*result0
else
irule=6
CALL TWODQ (gr3,LOWx,HIGHx,GL,HL,ERRABS,ERRREL, IRULE,RESULT0,ERREST)
gg00(m,n)=result0
CALL TWODQ (grn3,LOWx,HIGHx,GL,HL,ERRABS,ERRREL, IRULE,RESULT0,ERREST)
hh00(m,n)=result0
end if
end do
end do

zp=0
zq=-df
do n=1,nz*ney1
lowy=-nz*fly/2+(n-1)*ley1
highy=lowy+ley1
do m=1,nz*nex1
lowx=-nz*flx/2+(m-1)*lex1
highx=lowx+lex1
irule=6
CALL TWODQ (gr3,LOWx,HIGHx,GL,HL,ERRABS,ERRREL, IRULE,RESULT0,ERREST)
gg01(m,n)=result0
```

```
CALL TWODQ (grn3,LOWx,HIGHx,GL,HL,ERRABS,ERRREL, IRULE,RESULT0,ERREST)
hh01(m,n)=result0
end do
end do

zp=-df
zq=0
do n=1,nz*ney1
lowy=-nz*fly/2+(n-1)*ley1
highy=lowy+ley1
do m=1,nz*nex1
lowx=-nz*flx/2+(m-1)*lex1
highx=lowx+lex1
irule=6
CALL TWODQ (gr3,LOWx,HIGHx,GL,HL,ERRABS,ERRREL, IRULE,RESULT0,ERREST)
gg10(m,n)=result0
CALL TWODQ (grn3,LOWx,HIGHx,GL,HL,ERRABS,ERRREL, IRULE,RESULT0,ERREST)
hh10(m,n)=result0
end do
end do

zp=-df
zq=-df
do n=1,nz*ney1
do m=1,nz*nex1
lowy=-nz*fly/2+(n-1)*ley1
highy=lowy+ley1
lowx=-nz*flx/2+(m-1)*lex1
highx=lowx+lex1
if (n.eq.1.and.m.eq.1) then
highy=highy-ley1/2
highx=highx-lex1/2
irule=1
CALL TWODQ (gr3,LOWx,HIGHx,GL,HL,ERRABS,ERRREL, IRULE,RESULT0,ERREST)
gg11(m,n)=4*result0
CALL TWODQ (grn3,LOWx,HIGHx,GL,HL,ERRABS,ERRREL, IRULE,RESULT0,ERREST)
hh11(m,n)=4*result0
else
irule=6
CALL TWODQ (gr3,LOWx,HIGHx,GL,HL,ERRABS,ERRREL, IRULE,RESULT0,ERREST)
gg11(m,n)=result0
CALL TWODQ (grn3,LOWx,HIGHx,GL,HL,ERRABS,ERRREL, IRULE,RESULT0,ERREST)
hh11(m,n)=result0
end if
```

```
end do
end do
k=1
do j=1,nz*ney1
do i=1,nz*nex1
l=1
do n=1,nz*ney1
do m=1,nz*nex1
if (i.le.nzh*nex1.or.i.gt.(nzh*nex1+nex1).or.j.le.nzh*ney1.or. j.gt.(nzh*ney1+ney1))  then
if (m.le.nzh*nex1.or.m.gt.(nzh*nex1+nex1).or.n.le.nzh*ney1.or. n.gt.(nzh*ney1+ney1))  then
gg(k,l)=gg00(abs(m-i)+1,abs(n-j)+1)
hh(k,l)=hh00(abs(m-i)+1,abs(n-j)+1)
else
gg(k,l)=gg01(abs(m-i)+1,abs(n-j)+1)
hh(k,l)=hh01(abs(m-i)+1,abs(n-j)+1)
end if
else
if (m.le.nzh*nex1.or.m.gt.(nzh*nex1+nex1).or.n.le.nzh*ney1.or. n.gt.(nzh*ney1+ney1))  then
gg(k,l)=gg10(abs(m-i)+1,abs(n-j)+1)
hh(k,l)=hh10(abs(m-i)+1,abs(n-j)+1)
else
gg(k,l)=gg11(abs(m-i)+1,abs(n-j)+1)
hh(k,l)=hh11(abs(m-i)+1,abs(n-j)+1)
end if
end if
l=l+1
end do
end do
k=k+1
end do
end do
deallocate  (gg00,gg01,gg10,gg11)
deallocate  (hh00,hh01,hh10,hh11)

do n=1,news
hh(n,n)=hh(n,n)+2*pi
end do
return
end

C-----------------------------------------------------------------------------------------------------------------------------
C  Subroutine to calculate coefficient matrices G and H in the boundary integral equation for two dimensional fluid
C  domain.
CCC----------------------------------------------------------------------------------------------------------------------------
```

```
subroutine gf2(gg,hh)
implicit none
common /cgf3/ nz,nzh,flx,fly,lex1,ley1,nex1,ney1,df,news,pi, errabs,errrel,nd1,ne1,NDFS,s1
common /xzt/ xp,yp,zp,zq

integer m,n,i,j,k,l
integer nz,nzh,nex1,ney1,news,nd1,ne1,NDFS
real xp,yp,zp,zq,lowy,highy,lowx,highx,errest,result0
real flx,fly,lex1,ley1,df,pi,errabs,errrel,s1
real gg(news,news),hh(news,news)
real,ALLOCATABLE:: gg00(:,:),gg01(:,:),gg10(:,:),gg11(:,:)
real,ALLOCATABLE:: hh00(:,:),hh01(:,:),hh10(:,:),hh11(:,:)
real,external:: gr2,grn2

allocate    (gg00(nz*nex1,1),gg01(nz*nex1,1), gg10(nz*nex1,1),gg11(nz*nex1,1))
allocate    (hh00(nz*nex1,1),hh01(nz*nex1,1), hh10(nz*nex1,1),hh11(nz*nex1,1))

xp=-nz*flx/2+lex1/2
zp=0.0
zq=0.0
do m=1,nz*nex1
lowx=-nz*flx/2+(m-1)*lex1
highx=lowx+lex1
if (m.eq.1) then
highx=highx-lex1/2
CALL qdags (Gr2,LOWx,HIGHx,ERRABS,ERRREL,RESULT0,ERREST)
gg00(m,1)=2*result0
CALL qdags (Grn2,LOWx,HIGHx,ERRABS,ERRREL,RESULT0,ERREST)
hh00(m,1)=2*result0
else
CALL qdags (Gr2,LOWx,HIGHx,ERRABS,ERRREL,RESULT0,ERREST)
gg00(m,1)=result0
CALL qdags (Grn2,LOWx,HIGHx,ERRABS,ERRREL,RESULT0,ERREST)
hh00(m,1)=result0
end if
end do

zp=0.0
zq=-df
do m=1,nz*nex1
lowx=-nz*flx/2+(m-1)*lex1
highx=lowx+lex1
CALL qdags (Gr2,LOWx,HIGHx,ERRABS,ERRREL,RESULT0,ERREST)
gg01(m,1)=result0
```

```
CALL qdags (Grn2,LOWx,HIGHx,ERRABS,ERRREL,RESULT0,ERREST)
hh01(m,1)=result0
end do

zp=-df
zq=0.0
do m=1,nz*nex1
lowx=-nz*flx/2+(m-1)*lex1
highx=lowx+lex1
CALL qdags (Gr2,LOWx,HIGHx,ERRABS,ERRREL,RESULT0,ERREST)
gg10(m,1)=result0
CALL qdags (Grn2,LOWx,HIGHx,ERRABS,ERRREL,RESULT0,ERREST)
hh10(m,1)=result0
end do

zp=-df
zq=-df
do m=1,nz*nex1
lowx=-nz*flx/2+(m-1)*lex1
highx=lowx+lex1
if (m.eq.1) then
highx=highx-lex1/2
CALL qdags (Gr2,LOWx,HIGHx,ERRABS,ERRREL,RESULT0,ERREST)
gg11(m,1)=2*result0
CALL qdags (Grn2,LOWx,HIGHx,ERRABS,ERRREL,RESULT0,ERREST)
hh11(m,1)=2*result0
else
CALL qdags (Gr2,LOWx,HIGHx,ERRABS,ERRREL,RESULT0,ERREST)
gg11(m,1)=result0
CALL qdags (Grn2,LOWx,HIGHx,ERRABS,ERRREL,RESULT0,ERREST)
hh11(m,1)=result0
end if
end do

k=1
do i=1,nz*nex1
l=1
do m=1,nz*nex1
if (i.le.nzh*nex1.or.i.gt.(nzh*nex1+nex1))    then
if (m.le.nzh*nex1.or.m.gt.(nzh*nex1+nex1))    then
gg(k,l)=gg00(abs(m-i)+1,1)
hh(k,l)=hh00(abs(m-i)+1,1)
else
gg(k,l)=gg01(abs(m-i)+1,1)
```

```
hh(k,l)=hh01(abs(m-i)+1,1)
end if
else
if (m.le.nzh*nex1.or.m.gt.(nzh*nex1+nex1))    then
gg(k,l)=gg10(abs(m-i)+1,1)
hh(k,l)=hh10(abs(m-i)+1,1)
else
gg(k,l)=gg11(abs(m-i)+1,1)
hh(k,l)=hh11(abs(m-i)+1,1)
end if
end if
l=l+1
end do
k=k+1
end do
deallocate    (gg00,gg01,gg10,gg11)
deallocate    (hh00,hh01,hh10,hh11)

do n=1,news
hh(n,n)=hh(n,n)-pi
end do
return
end

C-----------------------------------------------------------------------------------------------------------------------------------------
C    Subroutine to calculate transform matrices gg2 and gg3 based on the element shape function of the floating structure.
CCC----------------------------------------------------------------------------------------------------------------------------------------
subroutine gg2and3(gg2,gg3)
implicit none
common /cgf3/ nz,nzh,flx,fly,lex1,ley1,nex1,ney1,df,news,pi, errabs,errrel,nd1,ne1,NDFS,s1
integer m,n,i,j,k,l
integer nz,nzh,nex1,ney1,news,nd1,ne1,NDFS
real flx,fly,lex1,ley1,df,pi,errabs,errrel,s1
real gg3(nd1,ne1),gg2(ne1,nd1)

if (NDFS.eq.1) then
gg3(1,1)=ley1*lex1
gg3(2,1)=0.0
gg3(3,1)=0.0
else
do i=1,ne1
gg3(3*(i+int((i-1)/nex1))-2,i)=ley1*lex1/4.0
gg3(3*(i+int((i-1)/nex1))-1,i)=ley1*lex1*(ley1/24)
gg3(3*(i+int((i-1)/nex1)),i)=-ley1*lex1*(lex1/24)
```

```
gg3(3*(1+i+int((i-1)/nex1))-2,i)=ley1*lex1/4.0
gg3(3*(1+i+int((i-1)/nex1))-1,i)=ley1*lex1*(ley1/24)
gg3(3*(1+i+int((i-1)/nex1)),i)=ley1*lex1*(lex1/24)

gg3(3*(nex1+2+i+int((i-1)/nex1))-2,i)=ley1*lex1/4.0
gg3(3*(nex1+2+i+int((i-1)/nex1))-1,i)=-ley1*lex1*(ley1/24)
gg3(3*(nex1+2+i+int((i-1)/nex1)),i)=ley1*lex1*(lex1/24)

gg3(3*(nex1+1+i+int((i-1)/nex1))-2,i)=ley1*lex1/4.0
gg3(3*(nex1+1+i+int((i-1)/nex1))-1,i)=-ley1*lex1*(ley1/24)
gg3(3*(nex1+1+i+int((i-1)/nex1)),i)=-ley1*lex1*(lex1/24)
end do
end if

if (NDFS.eq.1) then
gg2(1,1)=1.0
gg2(1,2)=0.0
gg2(1,3)=0.0
else
do i=1,ne1
gg2(i,3*(i+int((i-1)/nex1))-2)=1.0/4.0
gg2(i,3*(i+int((i-1)/nex1))-1)=ley1/16.0
gg2(i,3*(i+int((i-1)/nex1)))=-lex1/16.0

gg2(i,3*(1+i+int((i-1)/nex1))-2)=1.0/4.0
gg2(i,3*(1+i+int((i-1)/nex1))-1)=ley1/16.0
gg2(i,3*(1+i+int((i-1)/nex1)))=lex1/16.0

gg2(i,3*(nex1+2+i+int((i-1)/nex1))-2)=1.0/4.0
gg2(i,3*(nex1+2+i+int((i-1)/nex1))-1)=-ley1/16.0
gg2(i,3*(nex1+2+i+int((i-1)/nex1)))=lex1/16.0

gg2(i,3*(nex1+1+i+int((i-1)/nex1))-2)=1.0/4.0
gg2(i,3*(nex1+1+i+int((i-1)/nex1))-1)=-ley1/16.0
gg2(i,3*(nex1+1+i+int((i-1)/nex1)))=-lex1/16.0
end do
end if
return
end

C-----------------------------------------------------------------------------------------------------------------------------
C    Subroutine to calculate transform matrices b11 to b44 based on the element shape function of the floating structure.
CCC----------------------------------------------------------------------------------------------------------------------------
subroutine b11to44 (b11,b22,b33,b44)
```

```
implicit none
common /cgf3/ nz,nzh,flx,fly,lex1,ley1,nex1,ney1,df,news,pi, errabs,errrel,nd1,ne1,NDFS,s1
common /cb11to44/ vh,ah,ts,k,anglex,x01,y01,x02,y02,x03,y03, x04,y04,xa1,nt
integer m,n,i,j,l,k,nt
integer nz,nzh,nex1,ney1,news,nd1,ne1,NDFS
integer ix,iy,i1,ifn
real flx,fly,lex1,ley1,df,pi,errabs,errrel
real vh,ah,ts,anglex,x01,y01,x02,y02,x03,y03,x04,y04
real x1,y1,x2,y2,x3,y3,x4,y4,xa1,ya1,xa2,ya2,xa3,ya3,xa4,ya4,s1
real b11(1,nd1),b22(1,nd1),b33(1,nd1),b44(1,nd1)

if (NDFS.eq.1) then
b11(1,1)=1.0d0
else
s1=(vh*ts*k-0.5*ah*(ts*k)**2)
xa1=x01+s1*cos(anglex)
ya1=y01+s1*sin(anglex)
ix=int((xa1+0.5*flx)/(lex1))
iy=int((ya1+0.5*fly)/(ley1))
i1=iy*nex1+ix+1
ifn=(i1+int((i1-1)/nex1))
x1=2.0*(xa1+0.5*flx-ix*lex1-lex1/2.0)/lex1
y1=2.0*(ya1+0.5*fly-iy*ley1-ley1/2.0)/ley1

b11(1,3*ifn-2)=(1-x1)*(1-y1)*(2-x1-y1-x1**2-y1**2)/8.0
b11(1,3*ifn-1)=-ley1*(1-x1)*(1-y1)**2*(-1-y1)/16.0
b11(1,3*ifn)=lex1*(1-x1)**2*(-1-x1)*(1-y1)/16.0

b11(1,3*(ifn+1)-2)=(1+x1)*(1-y1)*(2+x1-y1-x1**2-y1**2)/8.0
b11(1,3*(ifn+1)-1)=-ley1*(1+x1)*(1-y1)**2*(-1-y1)/16.0
b11(1,3*(ifn+1))=-lex1*(1+x1)**2*(-1+x1)*(1-y1)/16.0

b11(1,3*(ifn+nex1+2)-2)=(1+x1)*(1+y1)*(2+x1+y1-x1**2-y1**2) /8.0
b11(1,3*(ifn+nex1+2)-1)=ley1*(1+x1)*(1+y1)**2*(-1+y1)/16.0
b11(1,3*(ifn+nex1+2))=-lex1*(1+x1)**2*(-1+x1)*(1+y1)/16.0

b11(1,3*(ifn+nex1+1)-2)=(1-x1)*(1+y1)*(2-x1+y1-x1**2-y1**2) /8.0
b11(1,3*(ifn+nex1+1)-1)=ley1*(1-x1)*(1+y1)**2*(-1+y1)/16.0
b11(1,3*(ifn+nex1+1))=lex1*(1-x1)**2*(-1-x1)*(1+y1)/16.0

xa2=x02+s1*cos(anglex)
ya2=y02+s1*sin(anglex)
ix=int((xa2+0.5*flx)/(lex1))
iy=int((ya2+0.5*fly)/(ley1))
```

```
i1=iy*nex1+ix+1
ifn=(i1+int((i1-1)/nex1))
x2=2.0*(xa2+0.5*flx-ix*lex1-lex1/2.0)/lex1
y2=2.0*(ya2+0.5*fly-iy*ley1-ley1/2.0)/ley1

b22(1,3*ifn-2)=(1-x2)*(1-y2)*(2-x2-y2-x2**2-y2**2)/8.0
b22(1,3*ifn-1)=-ley1*(1-x2)*(1-y2)**2*(-1-y2)/16.0
b22(1,3*ifn)=lex1*(1-x2)**2*(-1-x2)*(1-y2)/16.0

b22(1,3*(ifn+1)-2)=(1+x2)*(1-y2)*(2+x2-y2-x2**2-y2**2)/8.0
b22(1,3*(ifn+1)-1)=-ley1*(1+x2)*(1-y2)**2*(-1-y2)/16.0
b22(1,3*(ifn+1))=-lex1*(1+x2)**2*(-1+x2)*(1-y2)/16.0

b22(1,3*(ifn+nex1+2)-2)=(1+x2)*(1+y2)*(2+x2+y2-x2**2-y2**2) /8.0
b22(1,3*(ifn+nex1+2)-1)=ley1*(1+x2)*(1+y2)**2*(-1+y2)/16.0
b22(1,3*(ifn+nex1+2))=-lex1*(1+x2)**2*(-1+x2)*(1+y2)/16.0

b22(1,3*(ifn+nex1+1)-2)=(1-x2)*(1+y2)*(2-x2+y2-x2**2-y2**2) /8.0
b22(1,3*(ifn+nex1+1)-1)=ley1*(1-x2)*(1+y2)**2*(-1+y2)/16.0
b22(1,3*(ifn+nex1+1))=lex1*(1-x2)**2*(-1-x2)*(1+y2)/16.0

xa3=x03+s1*cos(anglex)
ya3=y03+s1*sin(anglex)
ix=int((xa3+0.5*flx)/(lex1))
iy=int((ya3+0.5*fly)/(ley1))
i1=iy*nex1+ix+1
ifn=(i1+int((i1-1)/nex1))
x3=2.0*(xa3+0.5*flx-ix*lex1-lex1/2.0)/lex1
y3=2.0*(ya3+0.5*fly-iy*ley1-ley1/2.0)/ley1

b33(1,3*ifn-2)=(1-x3)*(1-y3)*(2-x3-y3-x3**2-y3**2)/8.0
b33(1,3*ifn-1)=-ley1*(1-x3)*(1-y3)**2*(-1-y3)/16.0
b33(1,3*ifn)=lex1*(1-x3)**2*(-1-x3)*(1-y3)/16.0

b33(1,3*(ifn+1)-2)=(1+x3)*(1-y3)*(2+x3-y3-x3**2-y3**2)/8.0
b33(1,3*(ifn+1)-1)=-ley1*(1+x3)*(1-y3)**2*(-1-y3)/16.0
b33(1,3*(ifn+1))=-lex1*(1+x3)**2*(-1+x3)*(1-y3)/16.0

b33(1,3*(ifn+nex1+2)-2)=(1+x3)*(1+y3)*(2+x3+y3-x3**2-y3**2) /8.0
b33(1,3*(ifn+nex1+2)-1)=ley1*(1+x3)*(1+y3)**2*(-1+y3)/16.0
b33(1,3*(ifn+nex1+2))=-lex1*(1+x3)**2*(-1+x3)*(1+y3)/16.0

b33(1,3*(ifn+nex1+1)-2)=(1-x3)*(1+y3)*(2-x3+y3-x3**2-y3**2) /8.0
b33(1,3*(ifn+nex1+1)-1)=ley1*(1-x3)*(1+y3)**2*(-1+y3)/16.0
```

```
b33(1,3*(ifn+nex1+1))=lex1*(1-x3)**2*(-1-x3)*(1+y3)/16.0
xa4=x04+s1*cos(anglex)
ya4=y04+s1*sin(anglex)
ix=int((xa4+0.5*flx)/(lex1))
iy=int((ya4+0.5*fly)/(ley1))
i1=iy*nex1+ix+1
ifn=(i1+int((i1-1)/nex1))
x4=2.0*(xa4+0.5*flx-ix*lex1-lex1/2.0)/lex1
y4=2.0*(ya4+0.5*fly-iy*ley1-ley1/2.0)/ley1

b44(1,3*ifn-2)=(1-x4)*(1-y4)*(2-x4-y4-x4**2-y4**2) /8.0
b44(1,3*ifn-1)=-ley1*(1-x4)*(1-y4)**2*(-1-y4)/16.0
b44(1,3*ifn)=lex1*(1-x4)**2*(-1-x4)*(1-y4)/16.0

b44(1,3*(ifn+1)-2)=(1+x4)*(1-y4)*(2+x4-y4-x4**2-y4**2)/8.0
b44(1,3*(ifn+1)-1)=-ley1*(1+x4)*(1-y4)**2*(-1-y4)/16.0
b44(1,3*(ifn+1))=-lex1*(1+x4)**2*(-1+x4)*(1-y4)/16.0

b44(1,3*(ifn+nex1+2)-2)=(1+x4)*(1+y4)*(2+x4+y4-x4**2-y4**2)/8.0
b44(1,3*(ifn+nex1+2)-1)=ley1*(1+x4)*(1+y4)**2*(-1+y4)/16.0
b44(1,3*(ifn+nex1+2))=-lex1*(1+x4)**2*(-1+x4)*(1+y4)/16.0

b44(1,3*(ifn+nex1+1)-2)=(1-x4)*(1+y4)*(2-x4+y4-x4**2-y4**2)/8.0
b44(1,3*(ifn+nex1+1)-1)=ley1*(1-x4)*(1+y4)**2*(-1+y4)/16.0
b44(1,3*(ifn+nex1+1))=lex1*(1-x4)**2*(-1-x4)*(1+y4)/16.0
end if
return
end
```

Appendix C: Input file INPUTP.DAT for landing beam-floating beam-water interaction system in 2D fluid domain

****
This is the input file for all the input control parameters of program MMFBEP. When the data type is real, it must be input in decimal format, the decimal digits shall be less than 5 and integral digits shall be less than 11. Each parameter should be input at the line just after its explanation line.
****

*****number of nodes of floating structure "N1" (integer)
102

*****number of DOFs of floating structure "ND1" (integer)
306

*****number of retained modes of floating structure "NM1" (integer)
16

*****number of element of floating structure "NE1" (integer)
50

*****number of elements along longitudinal axis of floating structure "NEX1" (integer)
50

*****number of elements along transverse axis of floating structure "NEY1" (integer)
1

*****number of nodes of landing structure "N2" (integer)
42

*****number of DOFs of landing structure "ND2" (integer)
126

*****number of retained modes of landing structure "NM2" (integer)
16

*****number of time steps "NT" (integer)
1000

***** ratio of length/width of water surface over length/width of floating structure "NZ" (integer)
31

*****dimension of fluid domain "NDFD" (integer), 2 for two-dimensional fluid domain and 3 for three-dimensional fluid domain
2

*****type of floating structure "NDFS" (integer), 1 for mass, 2 for beam or 3 for plate type structure.
2

*****number1 of time step when responses are outputted "NOUTPUT1" (integer)
200

*****number2 of time step when responses are outputted " NOUTPUT 2" (integer)
400

*****number3 of time step when responses are outputted " NOUTPUT 3" (integer)
600

*****number4 of time step when responses are outputted " NOUTPUT 4" (integer)
800

*****number5 of time step when responses are outputted " NOUTPUT 5" (integer)
1000

*****total mass of landing structure "AMASS" (real number, unit kilogram)
20

*****total time of simulation "TIME" (real number, unit second)
5

*****angle between runway and positive direction of longitudinal axis of floating structure "ANGLEX" (real number, unit radian)
0.0

*****initial horizontal velocity of landing structure "VH" (real number, unit m/s)
2

*****horizontal deceleration of landing structure "AH" (real number, unit m/s^2)
0.4

*****initial vertical velocity of landing structure "VZ" (real number, unit m/s)
0.1

*****length of floating structure "FLX" (real number, unit m)
15

*****width of floating structure "FLY" (real number, unit m)
1.0

*****draft of floating structure "DF" (real number, unit m)
0.05

!!!!!Attention please, if the number of spring-damper units is less than 4, put the relevant parameters for the non-existent spring-damper unit to that of landing gear 1. For example if it equals 2, then SK3= SK 4= SK1, C3=C4=C1, X03=X04=X01, Y03=Y04=Y01, NS3=NS4=NS1.
*****spring coefficient of landing gear1 "SK1" (real number, unit N/m)
20000.0

*****damping coefficient of landing gear1 "C1" (real number, unit Ns/m)
10000.0

*****spring coefficient of landing gear2 "SK2" (real number, unit N/m)
20000.0

*****damping coefficient of landing gear2 "C2" (real number, unit Ns/m)
10000.0

*****spring coefficient of landing gear3 "SK3" (real number, unit N/m)
20000.0

*****damping coefficient of landing gear3 "C3" (real number, unit Ns/m)
10000.0

*****spring coefficient of landing gear4 "SK4" (real number, unit N/m)
20000.0

*****damping coefficient of landing gear4 "C4" (real number, unit Ns/m)
10000.0

*****x coordinate of position of landing gear1 on floating structure "X01" (real number, unit m)
-2.5

*****y coordinate of position of landing gear1 on floating structure "Y01" (real number, unit m)
0.0

*****x coordinate of position of landing gear2 on floating structure "X02" (real number, unit m)
-2.5

*****y coordinate of position of landing gear2 on floating structure "Y02" (real number, unit m)
0.0

*****x coordinate of position of landing gear3 on floating structure "X03" (real number, unit m)
-2.5

*****y coordinate of position of landing gear3 on floating structure "Y03" (real number, unit m)
0.0

*****x coordinate of position of landing gear4 on floating structure "X04" (real number, unit m)
-2.5

*****y coordinate of position of landing gear4 on floating structure "Y04" (real number, unit m)
0.0

*****node number of landing structure connected to landing gear1 "NS1" (integer)
11

*****node number of landing structure connected to landing gear2 "NS2" (integer)
11

*****node number of landing structure connected to landing gear3 "NS3" (integer)
11

*****node number of landing structure connected to landing gear4 "NS4" (integer)
11

!!!!!Attention please, if the number of interested nodes to output is less than10 for the floating structure, for example if it is 7, then NF8=NF9=NF10=NF1. And the same applies to NEF1-NEF10 and NL1-NL5.
*****node number of floating structure where responses are outputted, "NF1" (integer)
1

*****node number of floating structure where responses are outputted, "NF2" (integer)
26

*****node number of floating structure where responses are outputted, "NF3" (integer)
51

*****node number of floating structure where responses are outputted, "NF4" (integer)
1

*****node number of floating structure where responses are outputted, "NF5" (integer)
1

*****node number of floating structure where responses are outputted, "NF6" (integer)
1

*****node number of floating structure where responses are outputted, "NF7" (integer)
1

*****node number of floating structure where responses are outputted, "NF8" (integer)
1

*****node number of floating structure where responses are outputted, "NF9" (integer)
1

*****node number of floating structure where responses are outputted, "NF10" (integer)
1

*****element number of floating structure where water pressure are outputted, "NEF1" (integer)
1

*****element number of floating structure where water pressure are outputted, "NEF2" (integer)
26

*****element number of floating structure where water pressure are outputted, "NEF3" (integer)
50

*****element number of floating structure where water pressure are outputted, "nef4" (integer)
1

*****element number of floating structure where water pressure are outputted, "NEF5" (integer)
1

*****element number of floating structure where water pressure are outputted, "NEF6" (integer)
1

*****element number of floating structure where water pressure are outputted, "NEF7" (integer)
1

*****element number of floating structure where water pressure are outputted, "NEF8" (integer)
1

*****element number of floating structure where water pressure are outputted, "NEF9" (integer)
1

*****element number of floating structure where water pressure are outputted, "NEF10" (integer)
1

*****node number of landing structure where responses are outputted, "NL1" (integer)
1

*****node number of landing structure where responses are outputted, "NL2" (integer)
11

*****node number of landing structure where responses are outputted, "NL3" (integer)
1

*****node number of landing structure where responses are outputted, "NL4" (integer)
1

*****node number of landing structure where responses are outputted, "NL5" (integer)
1

Appendix D: Input file INPUTM.DAT for landing beam-floating beam-water interaction system

Longitudinal nodal coordinate of landing structure

-0.5000E+00 -0.4500E+00 -0.4000E+00 -0.3500E+00
-0.3000E+00 -0.2500E+00 -0.2000E+00 -0.1500E+00
-0.1000E+00 -0.5000E-01 0.0000E+00 0.5000E-01
0.1000E+00 0.1500E+00 0.2000E+00 0.2500E+00
0.3000E+00 0.3500E+00 0.4000E+00 0.4500E+00
0.5000E+00 -0.5000E+00 -0.4500E+00 -0.4000E+00
-0.3500E+00 -0.3000E+00 -0.2500E+00 -0.2000E+00
-0.1500E+00 -0.1000E+00 -0.5000E-01 0.0000E+00
0.5000E-01 0.1000E+00 0.1500E+00 0.2000E+00
0.2500E+00 0.3000E+00 0.3500E+00 0.4000E+00
0.4500E+00 0.5000E+00

Transverse nodal coordinate of landing structure

-0.5000E-01 -0.5000E-01 -0.5000E-01 -0.5000E-01
-0.5000E-01 -0.5000E-01 -0.5000E-01 -0.5000E-01
-0.5000E-01 -0.5000E-01 -0.5000E-01 -0.5000E-01
-0.5000E-01 -0.5000E-01 -0.5000E-01 -0.5000E-01
-0.5000E-01 -0.5000E-01 -0.5000E-01 -0.5000E-01
-0.5000E-01 0.5000E-01 0.5000E-01 0.5000E-01
0.5000E-01 0.5000E-01 0.5000E-01 0.5000E-01
0.5000E-01 0.5000E-01 0.5000E-01 0.5000E-01
0.5000E-01 0.5000E-01 0.5000E-01 0.5000E-01
0.5000E-01 0.5000E-01 0.5000E-01 0.5000E-01
0.5000E-01 0.5000E-01

Natural frequency of landing structure

0.0000E+00 0.0000E+00 0.1126E+02 0.3104E+02
0.6085E+02 0.1006E+03 0.1503E+03 0.2099E+03
0.2794E+03 0.3589E+03 0.4483E+03 0.5476E+03
0.6569E+03 0.7761E+03 0.9053E+03 0.1044E+04

Nodal vertical displacement for the 1st mode of landing structure

0.2236E+00 0.2236E+00 0.2236E+00 0.2236E+00
0.2236E+00 0.2236E+00 0.2236E+00 0.2236E+00
0.2236E+00 0.2236E+00 0.2236E+00 0.2236E+00
0.2236E+00 0.2236E+00 0.2236E+00 0.2236E+00
0.2236E+00 0.2236E+00 0.2236E+00 0.2236E+00
0.2236E+00 0.2236E+00 0.2236E+00 0.2236E+00
0.2236E+00 0.2236E+00 0.2236E+00 0.2236E+00
0.2236E+00 0.2236E+00 0.2236E+00 0.2236E+00
0.2236E+00 0.2236E+00

Nodal vertical displacement for the 2nd mode of landing structure

-0.3873E+00 -0.3486E+00 -0.3098E+00 -0.2711E+00
-0.2324E+00 -0.1936E+00 -0.1549E+00 -0.1162E+00
-0.7746E-01 -0.3873E-01 0.0000E+00 0.3873E-01
0.7746E-01 0.1162E+00 0.1549E+00 0.1936E+00
0.2324E+00 0.2711E+00 0.3098E+00 0.3486E+00
0.3873E+00 -0.3873E+00 -0.3486E+00 -0.3098E+00
-0.2711E+00 -0.2324E+00 -0.1936E+00 -0.1549E+00
-0.1162E+00 -0.7746E-01 -0.3873E-01 0.0000E+00
0.3873E-01 0.7746E-01 0.1162E+00 0.1549E+00
0.1936E+00 0.2324E+00 0.2711E+00 0.3098E+00
0.3486E+00 0.3873E+00

Nodal vertical displacement for the 3rd mode of landing structure

0.4472E+00 0.3434E+00 0.2402E+00 0.1395E+00
0.4370E-01 -0.4437E-01 -0.1216E+00 -0.1853E+00
-0.2327E+00 -0.2619E+00 -0.2718E+00 -0.2619E+00
-0.2327E+00 -0.1853E+00 -0.1216E+00 -0.4437E-01
0.4370E-01 0.1395E+00 0.2402E+00 0.3434E+00
0.4472E+00 0.4472E+00 0.3434E+00 0.2402E+00
0.1395E+00 0.4370E-01 -0.4437E-01 -0.1216E+00
-0.1853E+00 -0.2327E+00 -0.2619E+00 -0.2718E+00
-0.2619E+00 -0.2327E+00 -0.1853E+00 -0.1216E+00
-0.4437E-01 0.4370E-01 0.1395E+00 0.2402E+00
0.3434E+00 0.4472E+00

Nodal vertical displacement for the 4th mode of landing structure

-0.4472E+00 -0.2719E+00 -0.1017E+00 0.5255E-01
0.1777E+00 0.2615E+00 0.2961E+00 0.2793E+00
0.2160E+00 0.1175E+00 0.0000E+00 -0.1175E+00
-0.2160E+00 -0.2793E+00 -0.2961E+00 -0.2615E+00
-0.1777E+00 -0.5255E-01 0.1017E+00 0.2719E+00
0.4472E+00 -0.4472E+00 -0.2719E+00 -0.1017E+00
0.5255E-01 0.1777E+00 0.2615E+00 0.2961E+00
0.2793E+00 0.2160E+00 0.1175E+00 0.0000E+00
-0.1175E+00 -0.2160E+00 -0.2793E+00 -0.2961E+00
-0.2615E+00 -0.1777E+00 -0.5255E-01 0.1017E+00
0.2719E+00 0.4472E+00

Nodal vertical displacement for the 5th mode of landing structure

0.4472E+00 0.2029E+00 -0.2324E-01 -0.1975E+00
-0.2875E+00 -0.2778E+00 -0.1775E+00 -0.1987E-01
0.1466E+00 0.2717E+00 0.3181E+00 0.2717E+00
0.1466E+00 -0.1987E-01 -0.1775E+00 -0.2778E+00
-0.2875E+00 -0.1975E+00 -0.2324E-01 0.2029E+00
0.4472E+00 0.4472E+00 0.2029E+00 -0.2324E-01
-0.1975E+00 -0.2875E+00 -0.2778E+00 -0.1775E+00
-0.1987E-01 0.1466E+00 0.2717E+00 0.3181E+00
0.2717E+00 0.1466E+00 -0.1987E-01 -0.1775E+00
-0.2778E+00 -0.2875E+00 -0.1975E+00 -0.2324E-01
0.2029E+00 0.4472E+00

Nodal vertical displacement for the 6th mode of landing structure

-0.4472E+00 -0.1351E+00 0.1315E+00 0.2807E+00
0.2685E+00 0.1145E+00 -0.1009E+00 -0.2712E+00
-0.3131E+00 -0.2057E+00 0.0000E+00 0.2057E+00
0.3131E+00 0.2712E+00 0.1009E+00 -0.1145E+00
-0.2685E+00 -0.2807E+00 -0.1315E+00 0.1351E+00
0.4472E+00 -0.4472E+00 -0.1351E+00 0.1315E+00
0.2807E+00 0.2685E+00 0.1145E+00 -0.1009E+00
-0.2712E+00 -0.3131E+00 -0.2057E+00 0.0000E+00
0.2057E+00 0.3131E+00 0.2712E+00 0.1009E+00
-0.1145E+00 -0.2685E+00 -0.2807E+00 -0.1315E+00
0.1351E+00 0.4472E+00

Nodal vertical displacement for the 7th mode of landing structure

0.4472E+00 0.6944E-01 -0.2161E+00 -0.2907E+00
-0.1365E+00 0.1240E+00 0.3020E+00 0.2702E+00
0.4970E-01 -0.2053E+00 -0.3161E+00 -0.2053E+00
0.4970E-01 0.2702E+00 0.3020E+00 0.1240E+00
-0.1365E+00 -0.2907E+00 -0.2161E+00 0.6944E-01
0.4472E+00 0.4472E+00 0.6944E-01 -0.2161E+00
-0.2907E+00 -0.1365E+00 0.1240E+00 0.3020E+00
0.2702E+00 0.4970E-01 -0.2053E+00 -0.3161E+00
-0.2053E+00 0.4970E-01 0.2702E+00 0.3020E+00
0.1240E+00 -0.1365E+00 -0.2907E+00 -0.2161E+00
0.6944E-01 0.4472E+00

Nodal vertical displacement for the 8th mode of landing structure

-0.4472E+00 -0.6736E-02 0.2717E+00 0.2300E+00
-0.5323E-01 -0.2935E+00 -0.2563E+00 0.2463E-01
0.2817E+00 0.2696E+00 0.0000E+00 -0.2696E+00
-0.2817E+00 -0.2463E-01 0.2563E+00 0.2935E+00
0.5323E-01 -0.2300E+00 -0.2717E+00 0.6736E-02
0.4472E+00 -0.4472E+00 -0.6736E-02 0.2717E+00
0.2300E+00 -0.5323E-01 -0.2935E+00 -0.2563E+00
0.2463E-01 0.2817E+00 0.2696E+00 0.0000E+00
-0.2696E+00 -0.2817E+00 -0.2463E-01 0.2563E+00
0.2935E+00 0.5323E-01 -0.2300E+00 -0.2717E+00
0.6736E-02 0.4472E+00

Nodal vertical displacement for the 9th mode of landing structure

0.4472E+00 -0.5216E-01 -0.2950E+00 -0.1145E+00
0.2256E+00 0.2928E+00 0.1939E-03 -0.2921E+00
-0.2236E+00 0.1210E+00 0.3162E+00 0.1210E+00
-0.2236E+00 -0.2921E+00 0.1939E-03 0.2928E+00
0.2256E+00 -0.1145E+00 -0.2950E+00 -0.5216E-01
0.4472E+00 0.4472E+00 -0.5216E-01 -0.2950E+00
-0.1145E+00 0.2256E+00 0.2928E+00 0.1939E-03
-0.2921E+00 -0.2236E+00 0.1210E+00 0.3162E+00
0.1210E+00 -0.2236E+00 -0.2921E+00 0.1939E-03
0.2928E+00 0.2256E+00 -0.1145E+00 -0.2950E+00
-0.5216E-01 0.4472E+00

Nodal vertical displacement for the 10th mode of landing structure

-0.4472E+00 0.1064E+00 0.2853E+00 -0.2888E-01
-0.3134E+00 -0.1213E+00 0.2557E+00 0.2404E+00
-0.1436E+00 -0.3075E+00 0.0000E+00 0.3075E+00
0.1436E+00 -0.2404E+00 -0.2557E+00 0.1213E+00

0.3134E+00 0.2888E-01 -0.2853E+00 -0.1064E+00
0.4472E+00 -0.4472E+00 0.1064E+00 0.2853E+00
-0.2888E-01 -0.3134E+00 -0.1213E+00 0.2557E+00
0.2404E+00 -0.1436E+00 -0.3075E+00 0.0000E+00
0.3075E+00 0.1436E+00 -0.2404E+00 -0.2557E+00
0.1213E+00 0.3134E+00 0.2888E-01 -0.2853E+00
-0.1064E+00 0.4472E+00

Nodal vertical displacement for the 11th mode of landing structure

0.4472E+00 -0.1551E+00 -0.2445E+00 0.1678E+00
0.2823E+00 -0.1209E+00 -0.3007E+00 0.7382E-01
0.3123E+00 -0.2481E-01 -0.3162E+00 -0.2481E-01
0.3123E+00 0.7382E-01 -0.3007E+00 -0.1209E+00
0.2823E+00 0.1678E+00 -0.2445E+00 -0.1551E+00
0.4472E+00 0.4472E+00 -0.1551E+00 -0.2445E+00
0.1678E+00 0.2823E+00 -0.1209E+00 -0.3007E+00
0.7382E-01 0.3123E+00 -0.2481E-01 -0.3162E+00
-0.2481E-01 0.3123E+00 0.7382E-01 -0.3007E+00
-0.1209E+00 0.2823E+00 0.1678E+00 -0.2445E+00
-0.1551E+00 0.4472E+00

Nodal vertical displacement for the 12th mode of landing structure

-0.4472E+00 0.1975E+00 0.1776E+00 -0.2712E+00
-0.1439E+00 0.2921E+00 0.9771E-01 -0.3075E+00
-0.4947E-01 0.3152E+00 0.0000E+00 -0.3152E+00
0.4947E-01 0.3075E+00 -0.9771E-01 -0.2921E+00
0.1439E+00 0.2712E+00 -0.1776E+00 -0.1975E+00
0.4472E+00 -0.4472E+00 0.1975E+00 0.1776E+00
-0.2712E+00 -0.1439E+00 0.2921E+00 0.9771E-01
-0.3075E+00 -0.4947E-01 0.3152E+00 0.0000E+00
-0.3152E+00 0.4947E-01 0.3075E+00 -0.9771E-01
-0.2921E+00 0.1439E+00 0.2712E+00 -0.1776E+00
-0.1975E+00 0.4472E+00

Nodal vertical displacement for the 13th mode of landing structure

0.4472E+00 -0.2329E+00 -0.9169E-01 0.3162E+00
-0.4930E-01 -0.2921E+00 0.1859E+00 0.2054E+00
-0.2817E+00 -0.7382E-01 0.3162E+00 -0.7382E-01
-0.2817E+00 0.2054E+00 0.1859E+00 -0.2921E+00
-0.4930E-01 0.3162E+00 -0.9169E-01 -0.2329E+00
0.4472E+00 0.4472E+00 -0.2329E+00 -0.9169E-01
0.3162E+00 -0.4930E-01 -0.2921E+00 0.1859E+00
0.2054E+00 -0.2817E+00 -0.7382E-01 0.3162E+00
-0.7382E-01 -0.2817E+00 0.2054E+00 0.1859E+00
-0.2921E+00 -0.4930E-01 0.3162E+00 -0.9169E-01
-0.2329E+00 0.4472E+00

Nodal vertical displacement for the 14th mode of landing structure

-0.4472E+00 0.2608E+00 -0.4394E-02 -0.2928E+00
0.2235E+00 0.1210E+00 -0.3162E+00 0.1210E+00
0.2236E+00 -0.2921E+00 0.0000E+00 0.2921E+00
-0.2236E+00 -0.1210E+00 0.3162E+00 -0.1210E+00
-0.2235E+00 0.2928E+00 0.4394E-02 -0.2608E+00
0.4472E+00 -0.4472E+00 0.2608E+00 -0.4394E-02
-0.2928E+00 0.2235E+00 0.1210E+00 -0.3162E+00
0.1210E+00 0.2236E+00 -0.2921E+00 0.0000E+00
0.2921E+00 -0.2236E+00 -0.1210E+00 0.3162E+00
-0.1210E+00 -0.2235E+00 0.2928E+00 0.4394E-02
-0.2608E+00 0.4472E+00

Nodal vertical displacement for the 15th mode of landing structure

0.4472E+00 -0.2806E+00 0.1009E+00 0.2058E+00
-0.3123E+00 0.1210E+00 0.1859E+00 -0.3152E+00
0.1436E+00 0.1652E+00 -0.3162E+00 0.1652E+00
0.1436E+00 -0.3152E+00 0.1859E+00 0.1210E+00
-0.3123E+00 0.2058E+00 0.1009E+00 -0.2806E+00
0.4472E+00 0.4472E+00 -0.2806E+00 0.1009E+00
0.2058E+00 -0.3123E+00 0.1210E+00 0.1859E+00
-0.3152E+00 0.1436E+00 0.1652E+00 -0.3162E+00
0.1652E+00 0.1436E+00 -0.3152E+00 0.1859E+00
0.1210E+00 -0.3123E+00 0.2058E+00 0.1009E+00
-0.2806E+00 0.4472E+00

Nodal vertical displacement for the 16th mode of landing structure

-0.4472E+00 0.2923E+00 -0.1882E+00 -0.7406E-01
0.2817E+00 -0.2922E+00 0.9773E-01 0.1652E+00
-0.3123E+00 0.2405E+00 0.0000E+00 -0.2405E+00
0.3123E+00 -0.1652E+00 -0.9773E-01 0.2922E+00
-0.2817E+00 0.7406E-01 0.1882E+00 -0.2923E+00
0.4472E+00 -0.4472E+00 0.2923E+00 -0.1882E+00
-0.7406E-01 0.2817E+00 -0.2922E+00 0.9773E-01
0.1652E+00 -0.3123E+00 0.2405E+00 0.0000E+00

-0.2405E+00 0.3123E+00 -0.1652E+00 -0.9773E-01
0.2922E+00 -0.2817E+00 0.7406E-01 0.1882E+00
-0.2923E+00 0.4472E+00

Nodal rotation about longitudinal axis for the 1st mode of landing structure

0.0000E+00 0.0000E+00 0.0000E+00 0.0000E+00
0.0000E+00 0.0000E+00 0.0000E+00 0.0000E+00
0.0000E+00 0.0000E+00 0.0000E+00 0.0000E+00
0.0000E+00 0.0000E+00 0.0000E+00 0.0000E+00
0.0000E+00 0.0000E+00 0.0000E+00 0.0000E+00
0.0000E+00 0.0000E+00 0.0000E+00 0.0000E+00
0.0000E+00 0.0000E+00 0.0000E+00 0.0000E+00
0.0000E+00 0.0000E+00 0.0000E+00 0.0000E+00
0.0000E+00 0.0000E+00 0.0000E+00 0.0000E+00
0.0000E+00 0.0000E+00

Nodal rotation about longitudinal axis for the 2nd mode of landing structure

0.0000E+00 0.0000E+00 0.0000E+00 0.0000E+00
0.0000E+00 0.0000E+00 0.0000E+00 0.0000E+00
0.0000E+00 0.0000E+00 0.0000E+00 0.0000E+00
0.0000E+00 0.0000E+00 0.0000E+00 0.0000E+00
0.0000E+00 0.0000E+00 0.0000E+00 0.0000E+00
0.0000E+00 0.0000E+00 0.0000E+00 0.0000E+00
0.0000E+00 0.0000E+00 0.0000E+00 0.0000E+00
0.0000E+00 0.0000E+00 0.0000E+00 0.0000E+00
0.0000E+00 0.0000E+00 0.0000E+00 0.0000E+00
0.0000E+00 0.0000E+00

Nodal rotation about longitudinal axis for the 3rd mode of landing structure

0.0000E+00 0.0000E+00 0.0000E+00 0.0000E+00
0.0000E+00 0.0000E+00 0.0000E+00 0.0000E+00
0.0000E+00 0.0000E+00 0.0000E+00 0.0000E+00
0.0000E+00 0.0000E+00 0.0000E+00 0.0000E+00
0.0000E+00 0.0000E+00 0.0000E+00 0.0000E+00
0.0000E+00 0.0000E+00 0.0000E+00 0.0000E+00
0.0000E+00 0.0000E+00 0.0000E+00 0.0000E+00
0.0000E+00 0.0000E+00 0.0000E+00 0.0000E+00
0.0000E+00 0.0000E+00 0.0000E+00 0.0000E+00
0.0000E+00 0.0000E+00

Nodal rotation about longitudinal axis for the 4th mode of landing structure

0.0000E+00 0.0000E+00 0.0000E+00 0.0000E+00
0.0000E+00 0.0000E+00 0.0000E+00 0.0000E+00
0.0000E+00 0.0000E+00 0.0000E+00 0.0000E+00
0.0000E+00 0.0000E+00 0.0000E+00 0.0000E+00
0.0000E+00 0.0000E+00 0.0000E+00 0.0000E+00
0.0000E+00 0.0000E+00 0.0000E+00 0.0000E+00
0.0000E+00 0.0000E+00 0.0000E+00 0.0000E+00
0.0000E+00 0.0000E+00 0.0000E+00 0.0000E+00
0.0000E+00 0.0000E+00 0.0000E+00 0.0000E+00
0.0000E+00 0.0000E+00

Nodal rotation about longitudinal axis for the 5th mode of landing structure

0.0000E+00 0.0000E+00 0.0000E+00 0.0000E+00
0.0000E+00 0.0000E+00 0.0000E+00 0.0000E+00
0.0000E+00 0.0000E+00 0.0000E+00 0.0000E+00
0.0000E+00 0.0000E+00 0.0000E+00 0.0000E+00
0.0000E+00 0.0000E+00 0.0000E+00 0.0000E+00
0.0000E+00 0.0000E+00 0.0000E+00 0.0000E+00
0.0000E+00 0.0000E+00 0.0000E+00 0.0000E+00
0.0000E+00 0.0000E+00 0.0000E+00 0.0000E+00
0.0000E+00 0.0000E+00 0.0000E+00 0.0000E+00
0.0000E+00 0.0000E+00

Nodal rotation about longitudinal axis for the 6th mode of landing structure

0.0000E+00 0.0000E+00 0.0000E+00 0.0000E+00
0.0000E+00 0.0000E+00 0.0000E+00 0.0000E+00
0.0000E+00 0.0000E+00 0.0000E+00 0.0000E+00
0.0000E+00 0.0000E+00 0.0000E+00 0.0000E+00
0.0000E+00 0.0000E+00 0.0000E+00 0.0000E+00
0.0000E+00 0.0000E+00 0.0000E+00 0.0000E+00
0.0000E+00 0.0000E+00 0.0000E+00 0.0000E+00
0.0000E+00 0.0000E+00 0.0000E+00 0.0000E+00
0.0000E+00 0.0000E+00 0.0000E+00 0.0000E+00
0.0000E+00 0.0000E+00

Nodal rotation about longitudinal axis for the 7th mode of landing structure

0.0000E+00 0.0000E+00 0.0000E+00 0.0000E+00
0.0000E+00 0.0000E+00 0.0000E+00 0.0000E+00
0.0000E+00 0.0000E+00 0.0000E+00 0.0000E+00
0.0000E+00 0.0000E+00 0.0000E+00 0.0000E+00
0.0000E+00 0.0000E+00 0.0000E+00 0.0000E+00
0.0000E+00 0.0000E+00 0.0000E+00 0.0000E+00
0.0000E+00 0.0000E+00 0.0000E+00 0.0000E+00
0.0000E+00 0.0000E+00 0.0000E+00 0.0000E+00
0.0000E+00 0.0000E+00 0.0000E+00 0.0000E+00
0.0000E+00 0.0000E+00

Nodal rotation about longitudinal axis for the 8th mode of landing structure

0.0000E+00 0.0000E+00 0.0000E+00 0.0000E+00
0.0000E+00 0.0000E+00 0.0000E+00 0.0000E+00
0.0000E+00 0.0000E+00 0.0000E+00 0.0000E+00
0.0000E+00 0.0000E+00 0.0000E+00 0.0000E+00
0.0000E+00 0.0000E+00 0.0000E+00 0.0000E+00
0.0000E+00 0.0000E+00 0.0000E+00 0.0000E+00
0.0000E+00 0.0000E+00 0.0000E+00 0.0000E+00
0.0000E+00 0.0000E+00 0.0000E+00 0.0000E+00
0.0000E+00 0.0000E+00 0.0000E+00 0.0000E+00
0.0000E+00 0.0000E+00

Nodal rotation about longitudinal axis for the 9th mode of landing structure

0.0000E+00 0.0000E+00 0.0000E+00 0.0000E+00
0.0000E+00 0.0000E+00 0.0000E+00 0.0000E+00
0.0000E+00 0.0000E+00 0.0000E+00 0.0000E+00
0.0000E+00 0.0000E+00 0.0000E+00 0.0000E+00
0.0000E+00 0.0000E+00 0.0000E+00 0.0000E+00
0.0000E+00 0.0000E+00 0.0000E+00 0.0000E+00
0.0000E+00 0.0000E+00 0.0000E+00 0.0000E+00
0.0000E+00 0.0000E+00 0.0000E+00 0.0000E+00
0.0000E+00 0.0000E+00 0.0000E+00 0.0000E+00
0.0000E+00 0.0000E+00

Nodal rotation about longitudinal axis for the 10th mode of landing structure

0.0000E+00 0.0000E+00 0.0000E+00 0.0000E+00
0.0000E+00 0.0000E+00 0.0000E+00 0.0000E+00
0.0000E+00 0.0000E+00 0.0000E+00 0.0000E+00
0.0000E+00 0.0000E+00 0.0000E+00 0.0000E+00
0.0000E+00 0.0000E+00 0.0000E+00 0.0000E+00
0.0000E+00 0.0000E+00 0.0000E+00 0.0000E+00
0.0000E+00 0.0000E+00 0.0000E+00 0.0000E+00
0.0000E+00 0.0000E+00 0.0000E+00 0.0000E+00
0.0000E+00 0.0000E+00 0.0000E+00 0.0000E+00
0.0000E+00 0.0000E+00

Nodal rotation about longitudinal axis for the 11th mode of landing structure

0.0000E+00 0.0000E+00 0.0000E+00 0.0000E+00
0.0000E+00 0.0000E+00 0.0000E+00 0.0000E+00
0.0000E+00 0.0000E+00 0.0000E+00 0.0000E+00
0.0000E+00 0.0000E+00 0.0000E+00 0.0000E+00
0.0000E+00 0.0000E+00 0.0000E+00 0.0000E+00
0.0000E+00 0.0000E+00 0.0000E+00 0.0000E+00
0.0000E+00 0.0000E+00 0.0000E+00 0.0000E+00
0.0000E+00 0.0000E+00 0.0000E+00 0.0000E+00
0.0000E+00 0.0000E+00 0.0000E+00 0.0000E+00
0.0000E+00 0.0000E+00

Nodal rotation about longitudinal axis for the 12th mode of landing structure

0.0000E+00 0.0000E+00 0.0000E+00 0.0000E+00
0.0000E+00 0.0000E+00 0.0000E+00 0.0000E+00
0.0000E+00 0.0000E+00 0.0000E+00 0.0000E+00
0.0000E+00 0.0000E+00 0.0000E+00 0.0000E+00
0.0000E+00 0.0000E+00 0.0000E+00 0.0000E+00
0.0000E+00 0.0000E+00 0.0000E+00 0.0000E+00
0.0000E+00 0.0000E+00 0.0000E+00 0.0000E+00
0.0000E+00 0.0000E+00 0.0000E+00 0.0000E+00
0.0000E+00 0.0000E+00 0.0000E+00 0.0000E+00
0.0000E+00 0.0000E+00

Nodal rotation about longitudinal axis for the 13th mode of landing structure

0.0000E+00 0.0000E+00 0.0000E+00 0.0000E+00
0.0000E+00 0.0000E+00 0.0000E+00 0.0000E+00

0.0000E+00 0.0000E+00 0.0000E+00 0.0000E+00
0.0000E+00 0.0000E+00 0.0000E+00 0.0000E+00
0.0000E+00 0.0000E+00 0.0000E+00 0.0000E+00
0.0000E+00 0.0000E+00 0.0000E+00 0.0000E+00
0.0000E+00 0.0000E+00 0.0000E+00 0.0000E+00
0.0000E+00 0.0000E+00 0.0000E+00 0.0000E+00
0.0000E+00 0.0000E+00 0.0000E+00 0.0000E+00
0.0000E+00 0.0000E+00 0.0000E+00 0.0000E+00
0.0000E+00 0.0000E+00

Nodal rotation about longitudinal axis for the 14th mode of landing structure

0.0000E+00 0.0000E+00 0.0000E+00 0.0000E+00
0.0000E+00 0.0000E+00 0.0000E+00 0.0000E+00
0.0000E+00 0.0000E+00 0.0000E+00 0.0000E+00
0.0000E+00 0.0000E+00 0.0000E+00 0.0000E+00
0.0000E+00 0.0000E+00 0.0000E+00 0.0000E+00
0.0000E+00 0.0000E+00 0.0000E+00 0.0000E+00
0.0000E+00 0.0000E+00 0.0000E+00 0.0000E+00
0.0000E+00 0.0000E+00 0.0000E+00 0.0000E+00
0.0000E+00 0.0000E+00 0.0000E+00 0.0000E+00
0.0000E+00 0.0000E+00

Nodal rotation about longitudinal axis for the 15th mode of landing structure

0.0000E+00 0.0000E+00 0.0000E+00 0.0000E+00
0.0000E+00 0.0000E+00 0.0000E+00 0.0000E+00
0.0000E+00 0.0000E+00 0.0000E+00 0.0000E+00
0.0000E+00 0.0000E+00 0.0000E+00 0.0000E+00
0.0000E+00 0.0000E+00 0.0000E+00 0.0000E+00
0.0000E+00 0.0000E+00 0.0000E+00 0.0000E+00
0.0000E+00 0.0000E+00 0.0000E+00 0.0000E+00
0.0000E+00 0.0000E+00 0.0000E+00 0.0000E+00
0.0000E+00 0.0000E+00 0.0000E+00 0.0000E+00
0.0000E+00 0.0000E+00

Nodal rotation about longitudinal axis for the 16th mode of landing structure

0.0000E+00 0.0000E+00 0.0000E+00 0.0000E+00
0.0000E+00 0.0000E+00 0.0000E+00 0.0000E+00
0.0000E+00 0.0000E+00 0.0000E+00 0.0000E+00
0.0000E+00 0.0000E+00 0.0000E+00 0.0000E+00
0.0000E+00 0.0000E+00 0.0000E+00 0.0000E+00
0.0000E+00 0.0000E+00 0.0000E+00 0.0000E+00
0.0000E+00 0.0000E+00 0.0000E+00 0.0000E+00
0.0000E+00 0.0000E+00 0.0000E+00 0.0000E+00
0.0000E+00 0.0000E+00

Nodal rotation about transverse axis for the 1st mode of landing structure

0.0000E+00 0.0000E+00 0.0000E+00 0.0000E+00
0.0000E+00 0.0000E+00 0.0000E+00 0.0000E+00
0.0000E+00 0.0000E+00 0.0000E+00 0.0000E+00
0.0000E+00 0.0000E+00 0.0000E+00 0.0000E+00
0.0000E+00 0.0000E+00 0.0000E+00 0.0000E+00
0.0000E+00 0.0000E+00 0.0000E+00 0.0000E+00
0.0000E+00 0.0000E+00 0.0000E+00 0.0000E+00
0.0000E+00 0.0000E+00 0.0000E+00 0.0000E+00
0.0000E+00 0.0000E+00

Nodal rotation about transverse axis for the 2nd mode of landing structure

0.7746E+00 0.7746E+00 0.7746E+00 0.7746E+00
0.7746E+00 0.7746E+00 0.7746E+00 0.7746E+00
0.7746E+00 0.7746E+00 0.7746E+00 0.7746E+00
0.7746E+00 0.7746E+00 0.7746E+00 0.7746E+00
0.7746E+00 0.7746E+00 0.7746E+00 0.7746E+00
0.7746E+00 0.7746E+00 0.7746E+00 0.7746E+00
0.7746E+00 0.7746E+00 0.7746E+00 0.7746E+00
0.7746E+00 0.7746E+00 0.7746E+00 0.7746E+00
0.7746E+00 0.7746E+00

Nodal rotation about transverse axis for the 3rd mode of landing structure

0.4307E-04 0.4422E+00 0.7685E+00 0.9806E+00
0.1082E+01 0.1081E+01 0.9872E+00 0.8142E+00
0.5788E+00 0.3004E+00 0.0000E+00 -0.3004E+00
-0.5788E+00 -0.8142E+00 -0.9872E+00 -0.1081E+01
-0.1082E+01 -0.9806E+00 -0.7685E+00 -0.4422E+00
-0.4307E-04 0.4307E-04 0.4422E+00 0.7685E+00

0.9806E+00 0.1082E+01 0.1081E+01 0.9872E+00
0.8142E+00 0.5788E+00 0.3004E+00 0.0000E+00
-0.3004E+00 -0.5788E+00 -0.8142E+00 -0.9872E+00
-0.1081E+01 -0.1082E+01 -0.9806E+00 -0.7685E+00
-0.4422E+00 -0.4307E-04

Nodal rotation about transverse axis for the 4th mode of landing structure

0.3515E+01 0.3483E+01 0.3287E+01 0.2838E+01
0.2125E+01 0.1202E+01 0.1734E+00 -0.8279E+00
-0.1665E+01 -0.2221E+01 -0.2415E+01 -0.2221E+01
-0.1665E+01 -0.8279E+00 0.1734E+00 0.1202E+01
0.2125E+01 0.2838E+01 0.3287E+01 0.3483E+01
0.3515E+01 0.3515E+01 0.3483E+01 0.3287E+01
0.2838E+01 0.2125E+01 0.1202E+01 0.1734E+00
-0.8279E+00 -0.1665E+01 -0.2221E+01 -0.2415E+01
-0.2221E+01 -0.1665E+01 -0.8279E+00 0.1734E+00
0.1202E+01 0.2125E+01 0.2838E+01 0.3287E+01
0.3483E+01 0.3515E+01

Nodal rotation about transverse axis for the 5th mode of landing structure

0.1989E-04 0.1962E+01 0.2488E+01 0.1786E+01
0.2717E+00 -0.1487E+01 -0.2903E+01 -0.3517E+01
-0.3125E+01 -0.1828E+01 0.0000E+00 0.1828E+01
0.3125E+01 0.3517E+01 0.2903E+01 0.1487E+01
-0.2717E+00 -0.1786E+01 -0.2488E+01 -0.1962E+01
-0.1989E-04 0.1989E-04 0.1962E+01 0.2488E+01
0.1786E+01 0.2717E+00 -0.1487E+01 -0.2903E+01
-0.3517E+01 -0.3125E+01 -0.1828E+01 0.0000E+00
0.1828E+01 0.3125E+01 0.3517E+01 0.2903E+01
0.1487E+01 -0.2717E+00 -0.1786E+01 -0.2488E+01
-0.1962E+01 -0.1989E-04

Nodal rotation about transverse axis for the 6th mode of landing structure

0.6322E+01 0.6016E+01 0.4386E+01 0.1423E+01
-0.1842E+01 -0.4038E+01 -0.4206E+01 -0.2313E+01
0.7110E+00 0.3406E+01 0.4476E+01 0.3406E+01
0.7110E+00 -0.2313E+01 -0.4206E+01 -0.4038E+01
-0.1842E+01 0.1423E+01 0.4386E+01 0.6016E+01
0.6322E+01 0.6322E+01 0.6016E+01 0.4386E+01
0.1423E+01 -0.1842E+01 -0.4038E+01 -0.4206E+01
-0.2313E+01 0.7110E+00 0.3406E+01 0.4476E+01
0.3406E+01 0.7110E+00 -0.2313E+01 -0.4206E+01
-0.4038E+01 -0.1842E+01 0.1423E+01 0.4386E+01
0.6016E+01 0.6322E+01

Nodal rotation about transverse axis for the 7th mode of landing structure

-0.1522E-03 0.3819E+01 0.2525E+01 -0.1565E+01
-0.4990E+01 -0.5099E+01 -0.1710E+01 0.2846E+01
0.5393E+01 0.4153E+01 0.0000E+00 -0.4153E+01
-0.5393E+01 -0.2846E+01 0.1710E+01 0.5099E+01
0.4990E+01 0.1565E+01 -0.2525E+01 -0.3819E+01
0.1522E-03 -0.1522E-03 0.3819E+01 0.2525E+01
-0.1565E+01 -0.4990E+01 -0.5099E+01 -0.1710E+01
0.2846E+01 0.5393E+01 0.4153E+01 0.0000E+00
-0.4153E+01 -0.5393E+01 -0.2846E+01 0.1710E+01
0.5099E+01 0.4990E+01 0.1565E+01 -0.2525E+01
-0.3819E+01 0.1522E-03

Nodal rotation about transverse axis for the 8th mode of landing structure

0.9132E+01 0.7924E+01 0.2588E+01 -0.3980E+01
-0.6301E+01 -0.2443E+01 0.3805E+01 0.6441E+01
0.2933E+01 -0.3373E+01 -0.6457E+01 -0.3373E+01
0.2933E+01 0.6441E+01 0.3805E+01 -0.2443E+01
-0.6301E+01 -0.3980E+01 0.2588E+01 0.7924E+01
0.9132E+01 0.9132E+01 0.7924E+01 0.2588E+01
-0.3980E+01 -0.6301E+01 -0.2443E+01 0.3805E+01
0.6441E+01 0.2933E+01 -0.3373E+01 -0.6457E+01
-0.3373E+01 0.2933E+01 0.6441E+01 0.3805E+01
-0.2443E+01 -0.6301E+01 -0.3980E+01 0.2588E+01
0.7924E+01 0.9132E+01

Nodal rotation about transverse axis for the 9th mode of landing structure

-0.2917E-03 0.5262E+01 -0.4992E+00 -0.7037E+01
-0.5316E+01 0.2837E+01 0.7446E+01 0.2850E+01
-0.5269E+01 -0.6884E+01 0.0000E+00 0.6884E+01
0.5269E+01 -0.2850E+01 -0.7446E+01 -0.2837E+01
0.5316E+01 0.7037E+01 0.4992E+00 -0.5262E+01
0.2917E-03 -0.2917E-03 0.5262E+01 -0.4992E+00
-0.7037E+01 -0.5316E+01 0.2837E+01 0.7446E+01
0.2850E+01 -0.5269E+01 -0.6884E+01 0.0000E+00
0.6884E+01 0.5269E+01 -0.2850E+01 -0.7446E+01
-0.2837E+01 0.5316E+01 0.7037E+01 0.4992E+00

-0.5262E+01 0.2917E-03

Nodal rotation about transverse axis for the 10th mode of landing structure

0.1194E+02 0.8771E+01 -0.2196E+01 -0.8309E+01
-0.1292E+01 0.7809E+01 0.4965E+01 -0.5483E+01
-0.7524E+01 0.1971E+01 0.8444E+01 0.1971E+01
-0.7524E+01 -0.5483E+01 0.4965E+01 0.7809E+01
-0.1292E+01 -0.8309E+01 -0.2196E+01 0.8771E+01
0.1194E+02 0.1194E+02 0.8771E+01 -0.2196E+01
-0.8309E+01 -0.1292E+01 0.7809E+01 0.4965E+01
-0.5483E+01 -0.7524E+01 0.1971E+01 0.8444E+01
0.1971E+01 -0.7524E+01 -0.5483E+01 0.4965E+01
0.7809E+01 -0.1292E+01 -0.8309E+01 -0.2196E+01
0.8771E+01 0.1194E+02

Nodal rotation about transverse axis for the 11th mode of landing structure

-0.4630E-03 0.5676E+01 -0.5884E+01 -0.8123E+01
0.4267E+01 0.8715E+01 -0.2917E+01 -0.9177E+01
0.1476E+01 0.9408E+01 0.0000E+00 -0.9408E+01
-0.1476E+01 0.9177E+01 0.2917E+01 -0.8715E+01
-0.4267E+01 0.8123E+01 0.5884E+01 -0.5676E+01
0.4630E-03 -0.4630E-03 0.5676E+01 -0.5884E+01
-0.8123E+01 0.4267E+01 0.8715E+01 -0.2917E+01
-0.9177E+01 0.1476E+01 0.9408E+01 0.0000E+00
-0.9408E+01 -0.1476E+01 0.9177E+01 0.2917E+01
-0.8715E+01 -0.4267E+01 0.8123E+01 0.5884E+01
-0.5676E+01 0.4630E-03

Nodal rotation about transverse axis for the 12th mode of landing structure

0.1475E+02 0.8192E+01 -0.8166E+01 -0.5398E+01
0.9304E+01 0.3994E+01 -0.9920E+01 -0.2435E+01
0.1030E+02 0.8184E+00 -0.1043E+02 0.8184E+00
0.1030E+02 -0.2435E+01 -0.9920E+01 0.3994E+01
0.9304E+01 -0.5398E+01 -0.8166E+01 0.8192E+01
0.1475E+02 0.1475E+02 0.8192E+01 -0.8166E+01
-0.5398E+01 0.9304E+01 0.3994E+01 -0.9920E+01
-0.2435E+01 0.1030E+02 0.8184E+00 -0.1043E+02
0.8184E+00 0.1030E+02 -0.2435E+01 -0.9920E+01
0.3994E+01 0.9304E+01 -0.5398E+01 -0.8166E+01
0.8192E+01 0.1475E+02

Nodal rotation about transverse axis for the 13th mode of landing structure

-0.6736E-03 0.4643E+01 -0.1108E+02 -0.9325E+00
0.1128E+02 -0.4373E+01 -0.9243E+01 0.8687E+01
0.5187E+01 -0.1111E+02 0.0000E+00 0.1111E+02
-0.5187E+01 -0.8687E+01 0.9243E+01 0.4373E+01
-0.1128E+02 0.9325E+00 0.1108E+02 -0.4643E+01
0.6736E-03 -0.6736E-03 0.4643E+01 -0.1108E+02
-0.9325E+00 0.1128E+02 -0.4373E+01 -0.9243E+01
0.8687E+01 0.5187E+01 -0.1111E+02 0.0000E+00
0.1111E+02 -0.5187E+01 -0.8687E+01 0.9243E+01
0.4373E+01 -0.1128E+02 0.9325E+00 0.1108E+02
-0.4643E+01 0.6736E-03

Nodal rotation about transverse axis for the 14th mode of landing structure

0.1756E+02 0.5985E+01 -0.1224E+02 0.4776E+01
0.8784E+01 -0.1147E+02 -0.1620E-03 0.1147E+02
-0.8781E+01 -0.4752E+01 0.1242E+02 -0.4752E+01
-0.8781E+01 0.1147E+02 -0.1620E-03 -0.1147E+02
0.8784E+01 0.4776E+01 -0.1224E+02 0.5985E+01
0.1756E+02 0.1756E+02 0.5985E+01 -0.1224E+02
0.4776E+01 0.8784E+01 -0.1147E+02 -0.1620E-03
0.1147E+02 -0.8781E+01 -0.4752E+01 0.1242E+02
-0.4752E+01 -0.8781E+01 0.1147E+02 -0.1620E-03
-0.1147E+02 0.8784E+01 0.4776E+01 -0.1224E+02
0.5985E+01 0.1756E+02

Nodal rotation about transverse axis for the 15th mode of landing structure

-0.9235E-03 0.1994E+01 -0.1289E+02 0.1018E+02
0.2096E+01 -0.1239E+02 0.1085E+02 0.1052E+01
-0.1195E+02 0.1143E+02 0.0000E+00 -0.1143E+02
0.1195E+02 -0.1052E+01 -0.1085E+02 0.1239E+02
-0.2096E+01 -0.1018E+02 0.1289E+02 -0.1994E+01
0.9235E-03 -0.9235E-03 0.1994E+01 -0.1289E+02
0.1018E+02 0.2096E+01 -0.1239E+02 0.1085E+02
0.1052E+01 -0.1195E+02 0.1143E+02 0.0000E+00
-0.1143E+02 0.1195E+02 -0.1052E+01 -0.1085E+02
0.1239E+02 -0.2096E+01 -0.1018E+02 0.1289E+02
-0.1994E+01 0.9235E-03

Nodal rotation about transverse axis for the 16th mode of landing structure

0.2037E+02	0.2174E+01	-0.1155E+02	0.1402E+02
-0.6539E+01	-0.5512E+01	0.1370E+02	-0.1228E+02
0.2254E+01	0.9356E+01	-0.1441E+02	0.9356E+01
0.2254E+01	-0.1228E+02	0.1370E+02	-0.5512E+01
-0.6539E+01	0.1402E+02	-0.1155E+02	0.2174E+01
0.2037E+02	0.2037E+02	0.2174E+01	-0.1155E+02
0.1402E+02	-0.6539E+01	-0.5512E+01	0.1370E+02
-0.1228E+02	0.2254E+01	0.9356E+01	-0.1441E+02
0.9356E+01	0.2254E+01	-0.1228E+02	0.1370E+02
-0.5512E+01	-0.6539E+01	0.1402E+02	-0.1155E+02
0.2174E+01	0.2037E+02		

Longitudinal nodal coordinate of floating structure

-0.7500E+01	-0.7200E+01	-0.6900E+01	-0.6600E+01
-0.6300E+01	-0.6000E+01	-0.5700E+01	-0.5400E+01
-0.5100E+01	-0.4800E+01	-0.4500E+01	-0.4200E+01
-0.3900E+01	-0.3600E+01	-0.3300E+01	-0.3000E+01
-0.2700E+01	-0.2400E+01	-0.2100E+01	-0.1800E+01
-0.1500E+01	-0.1200E+01	-0.9000E+00	-0.6000E+00
-0.3000E+00	0.0000E+00	0.3000E+00	0.6000E+00
0.9000E+00	0.1200E+01	0.1500E+01	0.1800E+01
0.2100E+01	0.2400E+01	0.2700E+01	0.3000E+01
0.3300E+01	0.3600E+01	0.3900E+01	0.4200E+01
0.4500E+01	0.4800E+01	0.5100E+01	0.5400E+01
0.5700E+01	0.6000E+01	0.6300E+01	0.6600E+01
0.6900E+01	0.7200E+01	0.7500E+01	-0.7500E+01
-0.7200E+01	-0.6900E+01	-0.6600E+01	-0.6300E+01
-0.6000E+01	-0.5700E+01	-0.5400E+01	-0.5100E+01
-0.4800E+01	-0.4500E+01	-0.4200E+01	-0.3900E+01
-0.3600E+01	-0.3300E+01	-0.3000E+01	-0.2700E+01
-0.2400E+01	-0.2100E+01	-0.1800E+01	-0.1500E+01
-0.1200E+01	-0.9000E+00	-0.6000E+00	-0.3000E+00
0.0000E+00	0.3000E+00	0.6000E+00	0.9000E+00
0.1200E+01	0.1500E+01	0.1800E+01	0.2100E+01
0.2400E+01	0.2700E+01	0.3000E+01	0.3300E+01
0.3600E+01	0.3900E+01	0.4200E+01	0.4500E+01
0.4800E+01	0.5100E+01	0.5400E+01	0.5700E+01
0.6000E+01	0.6300E+01	0.6600E+01	0.6900E+01
0.7200E+01	0.7500E+01		

Transverse nodal coordinate of floating structure

-0.5000E+00	-0.5000E+00	-0.5000E+00	-0.5000E+00
-0.5000E+00	-0.5000E+00	-0.5000E+00	-0.5000E+00
-0.5000E+00	-0.5000E+00	-0.5000E+00	-0.5000E+00
-0.5000E+00	-0.5000E+00	-0.5000E+00	-0.5000E+00
-0.5000E+00	-0.5000E+00	-0.5000E+00	-0.5000E+00
-0.5000E+00	-0.5000E+00	-0.5000E+00	-0.5000E+00
-0.5000E+00	-0.5000E+00	-0.5000E+00	-0.5000E+00
-0.5000E+00	-0.5000E+00	-0.5000E+00	-0.5000E+00
-0.5000E+00	-0.5000E+00	-0.5000E+00	-0.5000E+00
-0.5000E+00	-0.5000E+00	-0.5000E+00	-0.5000E+00
-0.5000E+00	-0.5000E+00	-0.5000E+00	-0.5000E+00
-0.5000E+00	-0.5000E+00	-0.5000E+00	-0.5000E+00
-0.5000E+00	-0.5000E+00	-0.5000E+00	0.5000E+00
0.5000E+00	0.5000E+00	0.5000E+00	0.5000E+00
0.5000E+00	0.5000E+00	0.5000E+00	0.5000E+00
0.5000E+00	0.5000E+00	0.5000E+00	0.5000E+00
0.5000E+00	0.5000E+00	0.5000E+00	0.5000E+00
0.5000E+00	0.5000E+00	0.5000E+00	0.5000E+00
0.5000E+00	0.5000E+00	0.5000E+00	0.5000E+00
0.5000E+00	0.5000E+00	0.5000E+00	0.5000E+00
0.5000E+00	0.5000E+00	0.5000E+00	0.5000E+00
0.5000E+00	0.5000E+00	0.5000E+00	0.5000E+00
0.5000E+00	0.5000E+00	0.5000E+00	0.5000E+00
0.5000E+00	0.5000E+00	0.5000E+00	0.5000E+00
0.5000E+00	0.5000E+00	0.5000E+00	0.5000E+00
0.5000E+00	0.5000E+00		

Natural frequency of floating structure

0.0000E+00	0.0000E+00	0.1001E+00	0.2759E+00
0.5409E+00	0.8941E+00	0.1336E+01	0.1866E+01
0.2484E+01	0.3190E+01	0.3985E+01	0.4868E+01
0.5839E+01	0.6899E+01	0.8047E+01	0.9283E+01

Nodal vertical displacement for the 1st mode of floating structure

0.3651E-01	0.3651E-01	0.3651E-01	0.3651E-01
0.3651E-01	0.3651E-01	0.3651E-01	0.3651E-01
0.3651E-01	0.3651E-01	0.3651E-01	0.3651E-01
0.3651E-01	0.3651E-01	0.3651E-01	0.3651E-01
0.3651E-01	0.3651E-01	0.3651E-01	0.3651E-01
0.3651E-01	0.3651E-01	0.3651E-01	0.3651E-01
0.3651E-01	0.3651E-01	0.3651E-01	0.3651E-01
0.3651E-01	0.3651E-01	0.3651E-01	0.3651E-01
0.3651E-01	0.3651E-01	0.3651E-01	0.3651E-01
0.3651E-01	0.3651E-01	0.3651E-01	0.3651E-01
0.3651E-01	0.3651E-01	0.3651E-01	0.3651E-01
0.3651E-01	0.3651E-01	0.3651E-01	0.3651E-01

```
 0.3651E-01  0.3651E-01  0.3651E-01  0.3651E-01
 0.3651E-01  0.3651E-01  0.3651E-01  0.3651E-01
 0.3651E-01  0.3651E-01  0.3651E-01  0.3651E-01
 0.3651E-01  0.3651E-01  0.3651E-01  0.3651E-01
 0.3651E-01  0.3651E-01  0.3651E-01  0.3651E-01
 0.3651E-01  0.3651E-01  0.3651E-01  0.3651E-01
 0.3651E-01  0.3651E-01  0.3651E-01  0.3651E-01
 0.3651E-01  0.3651E-01  0.3651E-01  0.3651E-01
 0.3651E-01  0.3651E-01  0.3651E-01  0.3651E-01
 0.3651E-01  0.3651E-01  0.3651E-01  0.3651E-01
 0.3651E-01  0.3651E-01  0.3651E-01  0.3651E-01
 0.3651E-01  0.3651E-01  0.3651E-01  0.3651E-01
 0.3651E-01  0.3651E-01  0.3651E-01  0.3651E-01
 0.3651E-01  0.3651E-01
```

Nodal vertical displacement for the 2nd mode of floating structure

```
-0.6325E-01 -0.6072E-01 -0.5819E-01 -0.5566E-01
-0.5313E-01 -0.5060E-01 -0.4807E-01 -0.4554E-01
-0.4301E-01 -0.4048E-01 -0.3795E-01 -0.3542E-01
-0.3289E-01 -0.3036E-01 -0.2783E-01 -0.2530E-01
-0.2277E-01 -0.2024E-01 -0.1771E-01 -0.1518E-01
-0.1265E-01 -0.1012E-01 -0.7589E-02 -0.5060E-02
-0.2530E-02  0.0000E+00  0.2530E-02  0.5060E-02
 0.7589E-02  0.1012E-01  0.1265E-01  0.1518E-01
 0.1771E-01  0.2024E-01  0.2277E-01  0.2530E-01
 0.2783E-01  0.3036E-01  0.3289E-01  0.3542E-01
 0.3795E-01  0.4048E-01  0.4301E-01  0.4554E-01
 0.4807E-01  0.5060E-01  0.5313E-01  0.5566E-01
 0.5819E-01  0.6072E-01  0.6325E-01 -0.6325E-01
-0.6072E-01 -0.5819E-01 -0.5566E-01 -0.5313E-01
-0.5060E-01 -0.4807E-01 -0.4554E-01 -0.4301E-01
-0.4048E-01 -0.3795E-01 -0.3542E-01 -0.3289E-01
-0.3036E-01 -0.2783E-01 -0.2530E-01 -0.2277E-01
-0.2024E-01 -0.1771E-01 -0.1518E-01 -0.1265E-01
-0.1012E-01 -0.7589E-02 -0.5060E-02 -0.2530E-02
 0.0000E+00  0.2530E-02  0.5060E-02  0.7589E-02
 0.1012E-01  0.1265E-01  0.1518E-01  0.1771E-01
 0.2024E-01  0.2277E-01  0.2530E-01  0.2783E-01
 0.3036E-01  0.3289E-01  0.3542E-01  0.3795E-01
 0.4048E-01  0.4301E-01  0.4554E-01  0.4807E-01
 0.5060E-01  0.5313E-01  0.5566E-01  0.5819E-01
 0.6072E-01  0.6325E-01
```

Nodal vertical displacement for the 3rd mode of floating structure

```
 0.7303E-01  0.6624E-01  0.5946E-01  0.5268E-01
 0.4594E-01  0.3923E-01  0.3258E-01  0.2602E-01
 0.1958E-01  0.1327E-01  0.7136E-02  0.1204E-02
-0.4494E-02 -0.9926E-02 -0.1506E-01 -0.1987E-01
-0.2431E-01 -0.2837E-01 -0.3202E-01 -0.3524E-01
-0.3799E-01 -0.4028E-01 -0.4207E-01 -0.4335E-01
-0.4413E-01 -0.4439E-01 -0.4413E-01 -0.4335E-01
-0.4207E-01 -0.4028E-01 -0.3799E-01 -0.3524E-01
-0.3202E-01 -0.2837E-01 -0.2431E-01 -0.1987E-01
-0.1506E-01 -0.9926E-02 -0.4494E-02  0.1204E-02
 0.7136E-02  0.1327E-01  0.1958E-01  0.2602E-01
 0.3258E-01  0.3923E-01  0.4594E-01  0.5268E-01
 0.5946E-01  0.6624E-01  0.7303E-01  0.7303E-01
 0.6624E-01  0.5946E-01  0.5268E-01  0.4594E-01
 0.3923E-01  0.3258E-01  0.2602E-01  0.1958E-01
 0.1327E-01  0.7136E-02  0.1204E-02 -0.4494E-02
-0.9926E-02 -0.1506E-01 -0.1987E-01 -0.2431E-01
-0.2837E-01 -0.3202E-01 -0.3524E-01 -0.3799E-01
-0.4028E-01 -0.4207E-01 -0.4335E-01 -0.4413E-01
-0.4439E-01 -0.4413E-01 -0.4335E-01 -0.4207E-01
-0.4028E-01 -0.3799E-01 -0.3524E-01 -0.3202E-01
-0.2837E-01 -0.2431E-01 -0.1987E-01 -0.1506E-01
-0.9926E-02 -0.4494E-02  0.1204E-02  0.7136E-02
 0.1327E-01  0.1958E-01  0.2602E-01  0.3258E-01
 0.3923E-01  0.4594E-01  0.5268E-01  0.5946E-01
 0.6624E-01  0.7303E-01
```

Nodal vertical displacement for the 4th mode of floating structure

```
-0.7303E-01 -0.6155E-01 -0.5010E-01 -0.3873E-01
-0.2753E-01 -0.1661E-01 -0.6102E-02  0.3854E-02
 0.1312E-01  0.2155E-01  0.2901E-01  0.3539E-01
 0.4058E-01  0.4450E-01  0.4710E-01  0.4835E-01
 0.4824E-01  0.4681E-01  0.4410E-01  0.4022E-01
 0.3528E-01  0.2940E-01  0.2275E-01  0.1550E-01
 0.7853E-02  0.0000E+00 -0.7853E-02 -0.1550E-01
-0.2275E-01 -0.2940E-01 -0.3528E-01 -0.4022E-01
-0.4410E-01 -0.4681E-01 -0.4824E-01 -0.4835E-01
-0.4710E-01 -0.4450E-01 -0.4058E-01 -0.3539E-01
-0.2901E-01 -0.2155E-01 -0.1312E-01 -0.3854E-02
 0.6102E-02  0.1661E-01  0.2753E-01  0.3873E-01
 0.5010E-01  0.6155E-01  0.7303E-01 -0.7303E-01
```

-0.6155E-01 -0.5010E-01 -0.3873E-01 -0.2753E-01
-0.1661E-01 -0.6102E-02 0.3854E-02 0.1312E-01
0.2155E-01 0.2901E-01 0.3539E-01 0.4058E-01
0.4450E-01 0.4710E-01 0.4835E-01 0.4824E-01
0.4681E-01 0.4410E-01 0.4022E-01 0.3528E-01
0.2940E-01 0.2275E-01 0.1550E-01 0.7853E-02
0.0000E+00 -0.7853E-02 -0.1550E-01 -0.2275E-01
-0.2940E-01 -0.3528E-01 -0.4022E-01 -0.4410E-01
-0.4681E-01 -0.4824E-01 -0.4835E-01 -0.4710E-01
-0.4450E-01 -0.4058E-01 -0.3539E-01 -0.2901E-01
-0.2155E-01 -0.1312E-01 -0.3854E-02 0.6102E-02
0.1661E-01 0.2753E-01 0.3873E-01 0.5010E-01
0.6155E-01 0.7303E-01

Nodal vertical displacement for the 5th mode of floating structure

0.7303E-01 0.5698E-01 0.4101E-01 0.2535E-01
0.1029E-01 -0.3795E-02 -0.1652E-01 -0.2751E-01
-0.3642E-01 -0.4296E-01 -0.4695E-01 -0.4828E-01
-0.4697E-01 -0.4315E-01 -0.3704E-01 -0.2899E-01
-0.1941E-01 -0.8782E-02 0.2351E-02 0.1344E-01
0.2394E-01 0.3334E-01 0.4117E-01 0.4705E-01
0.5070E-01 0.5194E-01 0.5070E-01 0.4705E-01
0.4117E-01 0.3334E-01 0.2394E-01 0.1344E-01
0.2351E-02 -0.8782E-02 -0.1941E-01 -0.2899E-01
-0.3704E-01 -0.4315E-01 -0.4697E-01 -0.4828E-01
-0.4695E-01 -0.4296E-01 -0.3642E-01 -0.2751E-01
-0.1652E-01 -0.3795E-02 0.1029E-01 0.2535E-01
0.4101E-01 0.5698E-01 0.7303E-01 0.7303E-01
0.5698E-01 0.4101E-01 0.2535E-01 0.1029E-01
-0.3795E-02 -0.1652E-01 -0.2751E-01 -0.3642E-01
-0.4296E-01 -0.4695E-01 -0.4828E-01 -0.4697E-01
-0.4315E-01 -0.3704E-01 -0.2899E-01 -0.1941E-01
-0.8782E-02 0.2351E-02 0.1344E-01 0.2394E-01
0.3334E-01 0.4117E-01 0.4705E-01 0.5070E-01
0.5194E-01 0.5070E-01 0.4705E-01 0.4117E-01
0.3334E-01 0.2394E-01 0.1344E-01 0.2351E-02
-0.8782E-02 -0.1941E-01 -0.2899E-01 -0.3704E-01
-0.4315E-01 -0.4697E-01 -0.4828E-01 -0.4695E-01
-0.4296E-01 -0.3642E-01 -0.2751E-01 -0.1652E-01
-0.3795E-02 0.1029E-01 0.2535E-01 0.4101E-01
0.5698E-01 0.7303E-01

Nodal vertical displacement for the 6th mode of floating structure

-0.7303E-01 -0.5240E-01 -0.3201E-01 -0.1239E-01
0.5707E-02 0.2147E-01 0.3411E-01 0.4297E-01
0.4761E-01 0.4786E-01 0.4385E-01 0.3602E-01
0.2506E-01 0.1192E-01 -0.2317E-02 -0.1648E-01
-0.2942E-01 -0.4008E-01 -0.4761E-01 -0.5140E-01
-0.5112E-01 -0.4681E-01 -0.3879E-01 -0.2771E-01
-0.1442E-01 0.0000E+00 0.1442E-01 0.2771E-01
0.3879E-01 0.4681E-01 0.5112E-01 0.5140E-01
0.4761E-01 0.4008E-01 0.2942E-01 0.1648E-01
0.2317E-02 -0.1192E-01 -0.2506E-01 -0.3602E-01
-0.4385E-01 -0.4786E-01 -0.4761E-01 -0.4297E-01
-0.3411E-01 -0.2147E-01 -0.5707E-02 0.1239E-01
0.3201E-01 0.5240E-01 0.7303E-01 -0.7303E-01
-0.5240E-01 -0.3201E-01 -0.1239E-01 0.5707E-02
0.2147E-01 0.3411E-01 0.4297E-01 0.4761E-01
0.4786E-01 0.4385E-01 0.3602E-01 0.2506E-01
0.1192E-01 -0.2317E-02 -0.1648E-01 -0.2942E-01
-0.4008E-01 -0.4761E-01 -0.5140E-01 -0.5112E-01
-0.4681E-01 -0.3879E-01 -0.2771E-01 -0.1442E-01
0.0000E+00 0.1442E-01 0.2771E-01 0.3879E-01
0.4681E-01 0.5112E-01 0.5140E-01 0.4761E-01
0.4008E-01 0.2942E-01 0.1648E-01 0.2317E-02
-0.1192E-01 -0.2506E-01 -0.3602E-01 -0.4385E-01
-0.4786E-01 -0.4761E-01 -0.4297E-01 -0.3411E-01
-0.2147E-01 -0.5707E-02 0.1239E-01 0.3201E-01
0.5240E-01 0.7303E-01

Nodal vertical displacement for the 7th mode of floating structure

0.7303E-01 0.4783E-01 0.2315E-01 0.1075E-03
-0.1986E-01 -0.3529E-01 -0.4500E-01 -0.4829E-01
-0.4509E-01 -0.3602E-01 -0.2229E-01 -0.5657E-02
0.1184E-01 0.2808E-01 0.4109E-01 0.4932E-01
0.5176E-01 0.4812E-01 0.3881E-01 0.2493E-01
0.8116E-02 -0.9649E-02 -0.2627E-01 -0.3977E-01
-0.4857E-01 -0.5163E-01 -0.4857E-01 -0.3977E-01
-0.2627E-01 -0.9649E-02 0.8116E-02 0.2493E-01
0.3881E-01 0.4812E-01 0.5176E-01 0.4932E-01
0.4109E-01 0.2808E-01 0.1184E-01 -0.5657E-02
-0.2229E-01 -0.3602E-01 -0.4509E-01 -0.4829E-01
-0.4500E-01 -0.3529E-01 -0.1986E-01 0.1075E-03
0.2315E-01 0.4783E-01 0.7303E-01 0.7303E-01
0.4783E-01 0.2315E-01 0.1075E-03 -0.1986E-01

-0.3529E-01 -0.4500E-01 -0.4829E-01 -0.4509E-01
-0.3602E-01 -0.2229E-01 -0.5657E-02 0.1184E-01
0.2808E-01 0.4109E-01 0.4932E-01 0.5176E-01
0.4812E-01 0.3881E-01 0.2493E-01 0.8116E-02
-0.9649E-02 -0.2627E-01 -0.3977E-01 -0.4857E-01
-0.5163E-01 -0.4857E-01 -0.3977E-01 -0.2627E-01
-0.9649E-02 0.8116E-02 0.2493E-01 0.3881E-01
0.4812E-01 0.5176E-01 0.4932E-01 0.4109E-01
0.2808E-01 0.1184E-01 -0.5657E-02 -0.2229E-01
-0.3602E-01 -0.4509E-01 -0.4829E-01 -0.4500E-01
-0.3529E-01 -0.1986E-01 0.1075E-03 0.2315E-01
0.4783E-01 0.7303E-01

Nodal vertical displacement for the 8th mode of floating structure

-0.7303E-01 -0.4328E-01 -0.1451E-01 0.1126E-01
0.3161E-01 0.4437E-01 0.4826E-01 0.4316E-01
0.3026E-01 0.1192E-01 -0.8692E-02 -0.2808E-01
-0.4298E-01 -0.5090E-01 -0.5052E-01 -0.4186E-01
-0.2634E-01 -0.6508E-02 0.1438E-01 0.3290E-01
0.4600E-01 0.5153E-01 0.4858E-01 0.3764E-01
0.2051E-01 0.0000E+00 -0.2051E-01 -0.3764E-01
-0.4858E-01 -0.5153E-01 -0.4600E-01 -0.3290E-01
-0.1438E-01 0.6508E-02 0.2634E-01 0.4186E-01
0.5052E-01 0.5090E-01 0.4298E-01 0.2808E-01
0.8692E-02 -0.1192E-01 -0.3026E-01 -0.4316E-01
-0.4826E-01 -0.4437E-01 -0.3161E-01 -0.1126E-01
0.1451E-01 0.4328E-01 0.7303E-01 -0.7303E-01
-0.4328E-01 -0.1451E-01 0.1126E-01 0.3161E-01
0.4437E-01 0.4826E-01 0.4316E-01 0.3026E-01
0.1192E-01 -0.8692E-02 -0.2808E-01 -0.4298E-01
-0.5090E-01 -0.5052E-01 -0.4186E-01 -0.2634E-01
-0.6508E-02 0.1438E-01 0.3290E-01 0.4600E-01
0.5153E-01 0.4858E-01 0.3764E-01 0.2051E-01
0.0000E+00 -0.2051E-01 -0.3764E-01 -0.4858E-01
-0.5153E-01 -0.4600E-01 -0.3290E-01 -0.1438E-01
0.6508E-02 0.2634E-01 0.4186E-01 0.5052E-01
0.5090E-01 0.4298E-01 0.2808E-01 0.8692E-02
-0.1192E-01 -0.3026E-01 -0.4316E-01 -0.4826E-01
-0.4437E-01 -0.3161E-01 -0.1126E-01 0.1451E-01
0.4328E-01 0.7303E-01

Nodal vertical displacement for the 9th mode of floating structure

0.7303E-01 0.3875E-01 0.6152E-02 -0.2147E-01
-0.4047E-01 -0.4818E-01 -0.4385E-01 -0.2900E-01
-0.7237E-02 0.1648E-01 0.3684E-01 0.4932E-01
0.5113E-01 0.4186E-01 0.2349E-01 0.3166E-04
-0.2342E-01 -0.4176E-01 -0.5099E-01 -0.4911E-01
-0.3651E-01 -0.1596E-01 0.8079E-02 0.3035E-01
0.4601E-01 0.5164E-01 0.4601E-01 0.3035E-01
0.8079E-02 -0.1596E-01 -0.3651E-01 -0.4911E-01
-0.5099E-01 -0.4176E-01 -0.2342E-01 0.3166E-04
0.2349E-01 0.4186E-01 0.5113E-01 0.4932E-01
0.3684E-01 0.1648E-01 -0.7237E-02 -0.2900E-01
-0.4385E-01 -0.4818E-01 -0.4047E-01 -0.2147E-01
0.6152E-02 0.3875E-01 0.7303E-01 0.7303E-01
0.3875E-01 0.6152E-02 -0.2147E-01 -0.4047E-01
-0.4818E-01 -0.4385E-01 -0.2900E-01 -0.7237E-02
0.1648E-01 0.3684E-01 0.4932E-01 0.5113E-01
0.4186E-01 0.2349E-01 0.3166E-04 -0.2342E-01
-0.4176E-01 -0.5099E-01 -0.4911E-01 -0.3651E-01
-0.1596E-01 0.8079E-02 0.3035E-01 0.4601E-01
0.5164E-01 0.4601E-01 0.3035E-01 0.8079E-02
-0.1596E-01 -0.3651E-01 -0.4911E-01 -0.5099E-01
-0.4176E-01 -0.2342E-01 0.3166E-04 0.2349E-01
0.4186E-01 0.5113E-01 0.4932E-01 0.3684E-01
0.1648E-01 -0.7237E-02 -0.2900E-01 -0.4385E-01
-0.4818E-01 -0.4047E-01 -0.2147E-01 0.6152E-02
0.3875E-01 0.7303E-01

Nodal vertical displacement for the 10th mode of floating structure

-0.7303E-01 -0.3425E-01 0.1857E-02 0.3029E-01
0.4608E-01 0.4658E-01 0.3267E-01 0.8808E-02
-0.1800E-01 -0.4009E-01 -0.5118E-01 -0.4811E-01
-0.3171E-01 -0.6508E-02 0.2049E-01 0.4176E-01
0.5140E-01 0.4672E-01 0.2902E-01 0.3241E-02
-0.2344E-01 -0.4360E-01 -0.5161E-01 -0.4525E-01
-0.2629E-01 0.0000E+00 0.2629E-01 0.4525E-01
0.5161E-01 0.4360E-01 0.2344E-01 -0.3241E-02
-0.2902E-01 -0.4672E-01 -0.5140E-01 -0.4176E-01
-0.2049E-01 0.6508E-02 0.3171E-01 0.4811E-01
0.5118E-01 0.4009E-01 0.1800E-01 -0.8808E-02
-0.3267E-01 -0.4658E-01 -0.4608E-01 -0.3029E-01
-0.1857E-02 0.3425E-01 0.7303E-01 -0.7303E-01
-0.3425E-01 0.1857E-02 0.3029E-01 0.4608E-01
0.4658E-01 0.3267E-01 0.8808E-02 -0.1800E-01

-0.4009E-01 -0.5118E-01 -0.4811E-01 -0.3171E-01
-0.6508E-02 0.2049E-01 0.4176E-01 0.5140E-01
0.4672E-01 0.2902E-01 0.3241E-02 -0.2344E-01
-0.4360E-01 -0.5161E-01 -0.4525E-01 -0.2629E-01
0.0000E+00 0.2629E-01 0.4525E-01 0.5161E-01
0.4360E-01 0.2344E-01 -0.3241E-02 -0.2902E-01
-0.4672E-01 -0.5140E-01 -0.4176E-01 -0.2049E-01
0.6508E-02 0.3171E-01 0.4811E-01 0.5118E-01
0.4009E-01 0.1800E-01 -0.8808E-02 -0.3267E-01
-0.4658E-01 -0.4608E-01 -0.3029E-01 -0.1857E-02
0.3425E-01 0.7303E-01

Nodal vertical displacement for the 11th mode of floating structure

0.7303E-01 0.2978E-01 -0.9440E-02 -0.3751E-01
-0.4826E-01 -0.3993E-01 -0.1648E-01 0.1340E-01
0.3904E-01 0.5140E-01 0.4610E-01 0.2493E-01
-0.4830E-02 -0.3290E-01 -0.4958E-01 -0.4911E-01
-0.3165E-01 -0.3242E-02 0.2629E-01 0.4672E-01
0.5100E-01 0.3764E-01 0.1126E-01 -0.1901E-01
-0.4271E-01 -0.5164E-01 -0.4271E-01 -0.1901E-01
0.1126E-01 0.3764E-01 0.5100E-01 0.4672E-01
0.2629E-01 -0.3242E-02 -0.3165E-01 -0.4911E-01
-0.4958E-01 -0.3290E-01 -0.4830E-02 0.2493E-01
0.4610E-01 0.5140E-01 0.3904E-01 0.1340E-01
-0.1648E-01 -0.3993E-01 -0.4826E-01 -0.3751E-01
-0.9440E-02 0.2978E-01 0.7303E-01 0.7303E-01
0.2978E-01 -0.9440E-02 -0.3751E-01 -0.4826E-01
-0.3993E-01 -0.1648E-01 0.1340E-01 0.3904E-01
0.5140E-01 0.4610E-01 0.2493E-01 -0.4830E-02
-0.3290E-01 -0.4958E-01 -0.4911E-01 -0.3165E-01
-0.3242E-02 0.2629E-01 0.4672E-01 0.5100E-01
0.3764E-01 0.1126E-01 -0.1901E-01 -0.4271E-01
-0.5164E-01 -0.4271E-01 -0.1901E-01 0.1126E-01
0.3764E-01 0.5100E-01 0.4672E-01 0.2629E-01
-0.3242E-02 -0.3165E-01 -0.4911E-01 -0.4958E-01
-0.3290E-01 -0.4830E-02 0.2493E-01 0.4610E-01
0.5140E-01 0.3904E-01 0.1340E-01 -0.1648E-01
-0.3993E-01 -0.4826E-01 -0.3751E-01 -0.9440E-02
0.2978E-01 0.7303E-01

Nodal vertical displacement for the 12th mode of floating structure

-0.7303E-01 -0.2535E-01 0.1652E-01 0.4297E-01
0.4698E-01 0.2900E-01 -0.2318E-02 -0.3327E-01
-0.5058E-01 -0.4682E-01 -0.2349E-01 0.9649E-02
0.3872E-01 0.5153E-01 0.4271E-01 0.1596E-01
-0.1749E-01 -0.4360E-01 -0.5141E-01 -0.3764E-01
-0.8078E-02 0.2488E-01 0.4739E-01 0.5002E-01
0.3165E-01 0.0000E+00 -0.3165E-01 -0.5002E-01
-0.4739E-01 -0.2488E-01 0.8078E-02 0.3764E-01
0.5141E-01 0.4360E-01 0.1749E-01 -0.1596E-01
-0.4271E-01 -0.5153E-01 -0.3872E-01 -0.9649E-02
0.2349E-01 0.4682E-01 0.5058E-01 0.3327E-01
0.2318E-02 -0.2900E-01 -0.4698E-01 -0.4297E-01
-0.1652E-01 0.2535E-01 0.7303E-01 -0.7303E-01
-0.2535E-01 0.1652E-01 0.4297E-01 0.4698E-01
0.2900E-01 -0.2318E-02 -0.3327E-01 -0.5058E-01
-0.4682E-01 -0.2349E-01 0.9649E-02 0.3872E-01
0.5153E-01 0.4271E-01 0.1596E-01 -0.1749E-01
-0.4360E-01 -0.5141E-01 -0.3764E-01 -0.8078E-02
0.2488E-01 0.4739E-01 0.5002E-01 0.3165E-01
0.0000E+00 -0.3165E-01 -0.5002E-01 -0.4739E-01
-0.2488E-01 0.8078E-02 0.3764E-01 0.5141E-01
0.4360E-01 0.1749E-01 -0.1596E-01 -0.4271E-01
-0.5153E-01 -0.3872E-01 -0.9649E-02 0.2349E-01
0.4682E-01 0.5058E-01 0.3327E-01 0.2318E-02
-0.2900E-01 -0.4698E-01 -0.4297E-01 -0.1652E-01
0.2535E-01 0.7303E-01

Nodal vertical displacement for the 13th mode of floating structure

0.7303E-01 0.2097E-01 -0.2304E-01 -0.4654E-01
-0.4242E-01 -0.1497E-01 0.2098E-01 0.4695E-01
0.4970E-01 0.2772E-01 -0.8050E-02 -0.3977E-01
-0.5161E-01 -0.3764E-01 -0.4859E-02 0.3035E-01
0.5039E-01 0.4525E-01 0.1749E-01 -0.1901E-01
-0.4601E-01 -0.5002E-01 -0.2902E-01 0.6472E-02
0.3873E-01 0.5164E-01 0.3873E-01 0.6472E-02
-0.2902E-01 -0.5002E-01 -0.4601E-01 -0.1901E-01
0.1749E-01 0.4525E-01 0.5039E-01 0.3035E-01
-0.4859E-02 -0.3764E-01 -0.5161E-01 -0.3977E-01
-0.8050E-02 0.2772E-01 0.4970E-01 0.4695E-01
0.2098E-01 -0.1497E-01 -0.4242E-01 -0.4654E-01
-0.2304E-01 0.2097E-01 0.7303E-01 0.7303E-01
0.2097E-01 -0.2304E-01 -0.4654E-01 -0.4242E-01
-0.1497E-01 0.2098E-01 0.4695E-01 0.4970E-01
0.2772E-01 -0.8050E-02 -0.3977E-01 -0.5161E-01

-0.3764E-01 -0.4859E-02 0.3035E-01 0.5039E-01
0.4525E-01 0.1749E-01 -0.1901E-01 -0.4601E-01
-0.5002E-01 -0.2902E-01 0.6472E-02 0.3873E-01
0.5164E-01 0.3873E-01 0.6472E-02 -0.2902E-01
-0.5002E-01 -0.4601E-01 -0.1901E-01 0.1749E-01
0.4525E-01 0.5039E-01 0.3035E-01 -0.4859E-02
-0.3764E-01 -0.5161E-01 -0.3977E-01 -0.8050E-02
0.2772E-01 0.4970E-01 0.4695E-01 0.2098E-01
-0.1497E-01 -0.4242E-01 -0.4654E-01 -0.2304E-01
0.2097E-01 0.7303E-01

Nodal vertical displacement for the 14th mode of floating structure

-0.7303E-01 -0.1665E-01 0.2892E-01 0.4818E-01
0.3494E-01 -0.7175E-03 -0.3684E-01 -0.5179E-01
-0.3658E-01 -0.3261E-04 0.3650E-01 0.5163E-01
0.3651E-01 -0.1998E-06 -0.3651E-01 -0.5164E-01
-0.3651E-01 -0.8205E-06 0.3651E-01 0.5164E-01
0.3651E-01 0.3787E-06 -0.3651E-01 -0.5164E-01
-0.3651E-01 0.0000E+00 0.3651E-01 0.5164E-01
0.3651E-01 -0.3787E-06 -0.3651E-01 -0.5164E-01
-0.3651E-01 0.8205E-06 0.3651E-01 0.5164E-01
0.3651E-01 0.1998E-06 -0.3651E-01 -0.5163E-01
-0.3650E-01 0.3261E-04 0.3658E-01 0.5179E-01
0.3684E-01 0.7175E-03 -0.3494E-01 -0.4818E-01
-0.2892E-01 0.1665E-01 0.7303E-01 -0.7303E-01
-0.1665E-01 0.2892E-01 0.4818E-01 0.3494E-01
-0.7175E-03 -0.3684E-01 -0.5179E-01 -0.3658E-01
-0.3261E-04 0.3650E-01 0.5163E-01 0.3651E-01
-0.1998E-06 -0.3651E-01 -0.5164E-01 -0.3651E-01
-0.8205E-06 0.3651E-01 0.5164E-01 0.3651E-01
0.3787E-06 -0.3651E-01 -0.5164E-01 -0.3651E-01
0.0000E+00 0.3651E-01 0.5164E-01 0.3651E-01
-0.3787E-06 -0.3651E-01 -0.5164E-01 -0.3651E-01
0.8205E-06 0.3651E-01 0.5164E-01 0.3651E-01
0.1998E-06 -0.3651E-01 -0.5163E-01 -0.3650E-01
0.3261E-04 0.3658E-01 0.5179E-01 0.3684E-01
0.7175E-03 -0.3494E-01 -0.4818E-01 -0.2892E-01
0.1665E-01 0.7303E-01

Nodal vertical displacement for the 15th mode of floating structure

0.7303E-01 0.1239E-01 -0.3411E-01 -0.4786E-01
-0.2506E-01 0.1648E-01 0.4761E-01 0.4682E-01
0.1445E-01 -0.2765E-01 -0.5099E-01 -0.3978E-01
-0.1622E-02 0.3764E-01 0.5141E-01 0.3035E-01
-0.1126E-01 -0.4525E-01 -0.4858E-01 -0.1901E-01
0.2344E-01 0.5001E-01 0.4271E-01 0.6472E-02
-0.3415E-01 -0.5164E-01 -0.3415E-01 0.6472E-02
0.4271E-01 0.5001E-01 0.2344E-01 -0.1901E-01
-0.4858E-01 -0.4525E-01 -0.1126E-01 0.3035E-01
0.5141E-01 0.3764E-01 -0.1622E-02 -0.3978E-01
-0.5099E-01 -0.2765E-01 0.1445E-01 0.4682E-01
0.4761E-01 0.1648E-01 -0.2506E-01 -0.4786E-01
-0.3411E-01 0.1239E-01 0.7303E-01 0.7303E-01
0.1239E-01 -0.3411E-01 -0.4786E-01 -0.2506E-01
0.1648E-01 0.4761E-01 0.4682E-01 0.1445E-01
-0.2765E-01 -0.5099E-01 -0.3978E-01 -0.1622E-02
0.3764E-01 0.5141E-01 0.3035E-01 -0.1126E-01
-0.4525E-01 -0.4858E-01 -0.1901E-01 0.2344E-01
0.5001E-01 0.4271E-01 0.6472E-02 -0.3415E-01
-0.5164E-01 -0.3415E-01 0.6472E-02 0.4271E-01
0.5001E-01 0.2344E-01 -0.1901E-01 -0.4858E-01
-0.4525E-01 -0.1126E-01 0.3035E-01 0.5141E-01
0.3764E-01 -0.1622E-02 -0.3978E-01 -0.5099E-01
-0.2765E-01 0.1445E-01 0.4682E-01 0.4761E-01
0.1648E-01 -0.2506E-01 -0.4786E-01 -0.3411E-01
0.1239E-01 0.7303E-01

Nodal vertical displacement for the 16th mode of floating structure

-0.7303E-01 -0.8208E-02 0.3855E-01 0.4564E-01
0.1345E-01 -0.3074E-01 -0.5177E-01 -0.3298E-01
0.1124E-01 0.4672E-01 0.4601E-01 0.9674E-02
-0.3415E-01 -0.5154E-01 -0.2903E-01 0.1596E-01
0.4859E-01 0.4360E-01 0.4859E-02 -0.3765E-01
-0.5101E-01 -0.2488E-01 0.2051E-01 0.5002E-01
0.4081E-01 0.0000E+00 -0.4081E-01 -0.5002E-01
-0.2051E-01 0.2488E-01 0.5101E-01 0.3765E-01
-0.4859E-02 -0.4360E-01 -0.4859E-01 -0.1596E-01
0.2903E-01 0.5154E-01 0.3415E-01 -0.9674E-02
-0.4601E-01 -0.4672E-01 -0.1124E-01 0.3298E-01
0.5177E-01 0.3074E-01 -0.1345E-01 -0.4564E-01
-0.3855E-01 0.8208E-02 0.7303E-01 -0.7303E-01
-0.8208E-02 0.3855E-01 0.4564E-01 0.1345E-01
-0.3074E-01 -0.5177E-01 -0.3298E-01 0.1124E-01
0.4672E-01 0.4601E-01 0.9674E-02 -0.3415E-01
-0.5154E-01 -0.2903E-01 0.1596E-01 0.4859E-01

0.4360E-01 0.4859E-02 -0.3765E-01 -0.5101E-01
-0.2488E-01 0.2051E-01 0.5002E-01 0.4081E-01
0.0000E+00 -0.4081E-01 -0.5002E-01 -0.2051E-01
0.2488E-01 0.5101E-01 0.3765E-01 -0.4859E-02
-0.4360E-01 -0.4859E-01 -0.1596E-01 0.2903E-01
0.5154E-01 0.3415E-01 -0.9674E-02 -0.4601E-01
-0.4672E-01 -0.1124E-01 0.3298E-01 0.5177E-01
0.3074E-01 -0.1345E-01 -0.4564E-01 -0.3855E-01
0.8208E-02 0.7303E-01

Nodal rotation about longitudinal axis for the 1st mode of floating structure

0.0000E+00 0.0000E+00 0.0000E+00 0.0000E+00
0.0000E+00 0.0000E+00 0.0000E+00 0.0000E+00
0.0000E+00 0.0000E+00 0.0000E+00 0.0000E+00
0.0000E+00 0.0000E+00 0.0000E+00 0.0000E+00
0.0000E+00 0.0000E+00 0.0000E+00 0.0000E+00
0.0000E+00 0.0000E+00 0.0000E+00 0.0000E+00
0.0000E+00 0.0000E+00 0.0000E+00 0.0000E+00
0.0000E+00 0.0000E+00 0.0000E+00 0.0000E+00
0.0000E+00 0.0000E+00 0.0000E+00 0.0000E+00
0.0000E+00 0.0000E+00 0.0000E+00 0.0000E+00
0.0000E+00 0.0000E+00 0.0000E+00 0.0000E+00
0.0000E+00 0.0000E+00 0.0000E+00 0.0000E+00
0.0000E+00 0.0000E+00 0.0000E+00 0.0000E+00
0.0000E+00 0.0000E+00 0.0000E+00 0.0000E+00
0.0000E+00 0.0000E+00 0.0000E+00 0.0000E+00
0.0000E+00 0.0000E+00 0.0000E+00 0.0000E+00
0.0000E+00 0.0000E+00 0.0000E+00 0.0000E+00
0.0000E+00 0.0000E+00 0.0000E+00 0.0000E+00
0.0000E+00 0.0000E+00 0.0000E+00 0.0000E+00
0.0000E+00 0.0000E+00 0.0000E+00 0.0000E+00
0.0000E+00 0.0000E+00 0.0000E+00 0.0000E+00
0.0000E+00 0.0000E+00 0.0000E+00 0.0000E+00
0.0000E+00 0.0000E+00 0.0000E+00 0.0000E+00
0.0000E+00 0.0000E+00 0.0000E+00 0.0000E+00
0.0000E+00 0.0000E+00 0.0000E+00 0.0000E+00
0.0000E+00 0.0000E+00

Nodal rotation about longitudinal axis for the 2nd mode of floating structure

0.0000E+00 0.0000E+00 0.0000E+00 0.0000E+00
0.0000E+00 0.0000E+00 0.0000E+00 0.0000E+00
0.0000E+00 0.0000E+00 0.0000E+00 0.0000E+00
0.0000E+00 0.0000E+00 0.0000E+00 0.0000E+00
0.0000E+00 0.0000E+00 0.0000E+00 0.0000E+00
0.0000E+00 0.0000E+00 0.0000E+00 0.0000E+00
0.0000E+00 0.0000E+00 0.0000E+00 0.0000E+00
0.0000E+00 0.0000E+00 0.0000E+00 0.0000E+00
0.0000E+00 0.0000E+00 0.0000E+00 0.0000E+00
0.0000E+00 0.0000E+00 0.0000E+00 0.0000E+00
0.0000E+00 0.0000E+00 0.0000E+00 0.0000E+00
0.0000E+00 0.0000E+00 0.0000E+00 0.0000E+00
0.0000E+00 0.0000E+00 0.0000E+00 0.0000E+00
0.0000E+00 0.0000E+00 0.0000E+00 0.0000E+00
0.0000E+00 0.0000E+00 0.0000E+00 0.0000E+00
0.0000E+00 0.0000E+00 0.0000E+00 0.0000E+00
0.0000E+00 0.0000E+00 0.0000E+00 0.0000E+00
0.0000E+00 0.0000E+00 0.0000E+00 0.0000E+00
0.0000E+00 0.0000E+00 0.0000E+00 0.0000E+00
0.0000E+00 0.0000E+00 0.0000E+00 0.0000E+00
0.0000E+00 0.0000E+00 0.0000E+00 0.0000E+00
0.0000E+00 0.0000E+00 0.0000E+00 0.0000E+00
0.0000E+00 0.0000E+00 0.0000E+00 0.0000E+00
0.0000E+00 0.0000E+00 0.0000E+00 0.0000E+00
0.0000E+00 0.0000E+00 0.0000E+00 0.0000E+00
0.0000E+00 0.0000E+00

Nodal rotation about longitudinal axis for the 3rd mode of floating structure

0.0000E+00 0.0000E+00 0.0000E+00 0.0000E+00
0.0000E+00 0.0000E+00 0.0000E+00 0.0000E+00
0.0000E+00 0.0000E+00 0.0000E+00 0.0000E+00
0.0000E+00 0.0000E+00 0.0000E+00 0.0000E+00
0.0000E+00 0.0000E+00 0.0000E+00 0.0000E+00
0.0000E+00 0.0000E+00 0.0000E+00 0.0000E+00
0.0000E+00 0.0000E+00 0.0000E+00 0.0000E+00
0.0000E+00 0.0000E+00 0.0000E+00 0.0000E+00
0.0000E+00 0.0000E+00 0.0000E+00 0.0000E+00
0.0000E+00 0.0000E+00 0.0000E+00 0.0000E+00
0.0000E+00 0.0000E+00 0.0000E+00 0.0000E+00
0.0000E+00 0.0000E+00 0.0000E+00 0.0000E+00
0.0000E+00 0.0000E+00 0.0000E+00 0.0000E+00
0.0000E+00 0.0000E+00 0.0000E+00 0.0000E+00
0.0000E+00 0.0000E+00 0.0000E+00 0.0000E+00
0.0000E+00 0.0000E+00 0.0000E+00 0.0000E+00
0.0000E+00 0.0000E+00 0.0000E+00 0.0000E+00
0.0000E+00 0.0000E+00 0.0000E+00 0.0000E+00

0.0000E+00 0.0000E+00 0.0000E+00 0.0000E+00
0.0000E+00 0.0000E+00 0.0000E+00 0.0000E+00
0.0000E+00 0.0000E+00 0.0000E+00 0.0000E+00
0.0000E+00 0.0000E+00 0.0000E+00 0.0000E+00
0.0000E+00 0.0000E+00 0.0000E+00 0.0000E+00
0.0000E+00 0.0000E+00 0.0000E+00 0.0000E+00
0.0000E+00 0.0000E+00 0.0000E+00 0.0000E+00
0.0000E+00 0.0000E+00

Nodal rotation about longitudinal axis for the 4th mode of floating structure

0.0000E+00 0.0000E+00 0.0000E+00 0.0000E+00
0.0000E+00 0.0000E+00 0.0000E+00 0.0000E+00
0.0000E+00 0.0000E+00 0.0000E+00 0.0000E+00
0.0000E+00 0.0000E+00 0.0000E+00 0.0000E+00
0.0000E+00 0.0000E+00 0.0000E+00 0.0000E+00
0.0000E+00 0.0000E+00 0.0000E+00 0.0000E+00
0.0000E+00 0.0000E+00 0.0000E+00 0.0000E+00
0.0000E+00 0.0000E+00 0.0000E+00 0.0000E+00
0.0000E+00 0.0000E+00 0.0000E+00 0.0000E+00
0.0000E+00 0.0000E+00 0.0000E+00 0.0000E+00
0.0000E+00 0.0000E+00 0.0000E+00 0.0000E+00
0.0000E+00 0.0000E+00 0.0000E+00 0.0000E+00
0.0000E+00 0.0000E+00 0.0000E+00 0.0000E+00
0.0000E+00 0.0000E+00 0.0000E+00 0.0000E+00
0.0000E+00 0.0000E+00 0.0000E+00 0.0000E+00
0.0000E+00 0.0000E+00 0.0000E+00 0.0000E+00
0.0000E+00 0.0000E+00 0.0000E+00 0.0000E+00
0.0000E+00 0.0000E+00 0.0000E+00 0.0000E+00
0.0000E+00 0.0000E+00 0.0000E+00 0.0000E+00
0.0000E+00 0.0000E+00 0.0000E+00 0.0000E+00
0.0000E+00 0.0000E+00 0.0000E+00 0.0000E+00
0.0000E+00 0.0000E+00 0.0000E+00 0.0000E+00
0.0000E+00 0.0000E+00 0.0000E+00 0.0000E+00
0.0000E+00 0.0000E+00 0.0000E+00 0.0000E+00
0.0000E+00 0.0000E+00 0.0000E+00 0.0000E+00
0.0000E+00 0.0000E+00

Nodal rotation about longitudinal axis for the 5th mode of floating structure

0.0000E+00 0.0000E+00 0.0000E+00 0.0000E+00
0.0000E+00 0.0000E+00 0.0000E+00 0.0000E+00
0.0000E+00 0.0000E+00 0.0000E+00 0.0000E+00
0.0000E+00 0.0000E+00 0.0000E+00 0.0000E+00
0.0000E+00 0.0000E+00 0.0000E+00 0.0000E+00
0.0000E+00 0.0000E+00 0.0000E+00 0.0000E+00
0.0000E+00 0.0000E+00 0.0000E+00 0.0000E+00
0.0000E+00 0.0000E+00 0.0000E+00 0.0000E+00
0.0000E+00 0.0000E+00 0.0000E+00 0.0000E+00
0.0000E+00 0.0000E+00 0.0000E+00 0.0000E+00
0.0000E+00 0.0000E+00 0.0000E+00 0.0000E+00
0.0000E+00 0.0000E+00 0.0000E+00 0.0000E+00
0.0000E+00 0.0000E+00 0.0000E+00 0.0000E+00
0.0000E+00 0.0000E+00 0.0000E+00 0.0000E+00
0.0000E+00 0.0000E+00 0.0000E+00 0.0000E+00
0.0000E+00 0.0000E+00 0.0000E+00 0.0000E+00
0.0000E+00 0.0000E+00 0.0000E+00 0.0000E+00
0.0000E+00 0.0000E+00 0.0000E+00 0.0000E+00
0.0000E+00 0.0000E+00 0.0000E+00 0.0000E+00
0.0000E+00 0.0000E+00 0.0000E+00 0.0000E+00
0.0000E+00 0.0000E+00 0.0000E+00 0.0000E+00
0.0000E+00 0.0000E+00 0.0000E+00 0.0000E+00
0.0000E+00 0.0000E+00 0.0000E+00 0.0000E+00
0.0000E+00 0.0000E+00 0.0000E+00 0.0000E+00
0.0000E+00 0.0000E+00 0.0000E+00 0.0000E+00
0.0000E+00 0.0000E+00

Nodal rotation about longitudinal axis for the 6th mode of floating structure

0.0000E+00 0.0000E+00 0.0000E+00 0.0000E+00
0.0000E+00 0.0000E+00 0.0000E+00 0.0000E+00
0.0000E+00 0.0000E+00 0.0000E+00 0.0000E+00
0.0000E+00 0.0000E+00 0.0000E+00 0.0000E+00
0.0000E+00 0.0000E+00 0.0000E+00 0.0000E+00
0.0000E+00 0.0000E+00 0.0000E+00 0.0000E+00
0.0000E+00 0.0000E+00 0.0000E+00 0.0000E+00
0.0000E+00 0.0000E+00 0.0000E+00 0.0000E+00
0.0000E+00 0.0000E+00 0.0000E+00 0.0000E+00
0.0000E+00 0.0000E+00 0.0000E+00 0.0000E+00
0.0000E+00 0.0000E+00 0.0000E+00 0.0000E+00
0.0000E+00 0.0000E+00 0.0000E+00 0.0000E+00
0.0000E+00 0.0000E+00 0.0000E+00 0.0000E+00
0.0000E+00 0.0000E+00 0.0000E+00 0.0000E+00
0.0000E+00 0.0000E+00 0.0000E+00 0.0000E+00
0.0000E+00 0.0000E+00 0.0000E+00 0.0000E+00
0.0000E+00 0.0000E+00 0.0000E+00 0.0000E+00
0.0000E+00 0.0000E+00 0.0000E+00 0.0000E+00
0.0000E+00 0.0000E+00 0.0000E+00 0.0000E+00

0.0000E+00	0.0000E+00	0.0000E+00	0.0000E+00
0.0000E+00	0.0000E+00	0.0000E+00	0.0000E+00
0.0000E+00	0.0000E+00	0.0000E+00	0.0000E+00
0.0000E+00	0.0000E+00	0.0000E+00	0.0000E+00
0.0000E+00	0.0000E+00	0.0000E+00	0.0000E+00
0.0000E+00	0.0000E+00	0.0000E+00	0.0000E+00
0.0000E+00	0.0000E+00		

Nodal rotation about longitudinal axis for the 7th mode of floating structure

0.0000E+00	0.0000E+00	0.0000E+00	0.0000E+00
0.0000E+00	0.0000E+00	0.0000E+00	0.0000E+00
0.0000E+00	0.0000E+00	0.0000E+00	0.0000E+00
0.0000E+00	0.0000E+00	0.0000E+00	0.0000E+00
0.0000E+00	0.0000E+00	0.0000E+00	0.0000E+00
0.0000E+00	0.0000E+00	0.0000E+00	0.0000E+00
0.0000E+00	0.0000E+00	0.0000E+00	0.0000E+00
0.0000E+00	0.0000E+00	0.0000E+00	0.0000E+00
0.0000E+00	0.0000E+00	0.0000E+00	0.0000E+00
0.0000E+00	0.0000E+00	0.0000E+00	0.0000E+00
0.0000E+00	0.0000E+00	0.0000E+00	0.0000E+00
0.0000E+00	0.0000E+00	0.0000E+00	0.0000E+00
0.0000E+00	0.0000E+00	0.0000E+00	0.0000E+00
0.0000E+00	0.0000E+00	0.0000E+00	0.0000E+00
0.0000E+00	0.0000E+00	0.0000E+00	0.0000E+00
0.0000E+00	0.0000E+00	0.0000E+00	0.0000E+00
0.0000E+00	0.0000E+00	0.0000E+00	0.0000E+00
0.0000E+00	0.0000E+00	0.0000E+00	0.0000E+00
0.0000E+00	0.0000E+00	0.0000E+00	0.0000E+00
0.0000E+00	0.0000E+00	0.0000E+00	0.0000E+00
0.0000E+00	0.0000E+00	0.0000E+00	0.0000E+00
0.0000E+00	0.0000E+00	0.0000E+00	0.0000E+00
0.0000E+00	0.0000E+00	0.0000E+00	0.0000E+00
0.0000E+00	0.0000E+00	0.0000E+00	0.0000E+00
0.0000E+00	0.0000E+00	0.0000E+00	0.0000E+00
0.0000E+00	0.0000E+00		

Nodal rotation about longitudinal axis for the 8th mode of floating structure

0.0000E+00	0.0000E+00	0.0000E+00	0.0000E+00
0.0000E+00	0.0000E+00	0.0000E+00	0.0000E+00
0.0000E+00	0.0000E+00	0.0000E+00	0.0000E+00
0.0000E+00	0.0000E+00	0.0000E+00	0.0000E+00
0.0000E+00	0.0000E+00	0.0000E+00	0.0000E+00
0.0000E+00	0.0000E+00	0.0000E+00	0.0000E+00
0.0000E+00	0.0000E+00	0.0000E+00	0.0000E+00
0.0000E+00	0.0000E+00	0.0000E+00	0.0000E+00
0.0000E+00	0.0000E+00	0.0000E+00	0.0000E+00
0.0000E+00	0.0000E+00	0.0000E+00	0.0000E+00
0.0000E+00	0.0000E+00	0.0000E+00	0.0000E+00
0.0000E+00	0.0000E+00	0.0000E+00	0.0000E+00
0.0000E+00	0.0000E+00	0.0000E+00	0.0000E+00
0.0000E+00	0.0000E+00	0.0000E+00	0.0000E+00
0.0000E+00	0.0000E+00	0.0000E+00	0.0000E+00
0.0000E+00	0.0000E+00	0.0000E+00	0.0000E+00
0.0000E+00	0.0000E+00	0.0000E+00	0.0000E+00
0.0000E+00	0.0000E+00	0.0000E+00	0.0000E+00
0.0000E+00	0.0000E+00	0.0000E+00	0.0000E+00
0.0000E+00	0.0000E+00	0.0000E+00	0.0000E+00
0.0000E+00	0.0000E+00	0.0000E+00	0.0000E+00
0.0000E+00	0.0000E+00	0.0000E+00	0.0000E+00
0.0000E+00	0.0000E+00	0.0000E+00	0.0000E+00
0.0000E+00	0.0000E+00	0.0000E+00	0.0000E+00
0.0000E+00	0.0000E+00	0.0000E+00	0.0000E+00
0.0000E+00	0.0000E+00		

Nodal rotation about longitudinal axis for the 9th mode of floating structure

0.0000E+00	0.0000E+00	0.0000E+00	0.0000E+00
0.0000E+00	0.0000E+00	0.0000E+00	0.0000E+00
0.0000E+00	0.0000E+00	0.0000E+00	0.0000E+00
0.0000E+00	0.0000E+00	0.0000E+00	0.0000E+00
0.0000E+00	0.0000E+00	0.0000E+00	0.0000E+00
0.0000E+00	0.0000E+00	0.0000E+00	0.0000E+00
0.0000E+00	0.0000E+00	0.0000E+00	0.0000E+00
0.0000E+00	0.0000E+00	0.0000E+00	0.0000E+00
0.0000E+00	0.0000E+00	0.0000E+00	0.0000E+00
0.0000E+00	0.0000E+00	0.0000E+00	0.0000E+00
0.0000E+00	0.0000E+00	0.0000E+00	0.0000E+00
0.0000E+00	0.0000E+00	0.0000E+00	0.0000E+00
0.0000E+00	0.0000E+00	0.0000E+00	0.0000E+00
0.0000E+00	0.0000E+00	0.0000E+00	0.0000E+00
0.0000E+00	0.0000E+00	0.0000E+00	0.0000E+00
0.0000E+00	0.0000E+00	0.0000E+00	0.0000E+00
0.0000E+00	0.0000E+00	0.0000E+00	0.0000E+00
0.0000E+00	0.0000E+00	0.0000E+00	0.0000E+00
0.0000E+00	0.0000E+00	0.0000E+00	0.0000E+00
0.0000E+00	0.0000E+00	0.0000E+00	0.0000E+00

0.0000E+00 0.0000E+00 0.0000E+00 0.0000E+00
0.0000E+00 0.0000E+00 0.0000E+00 0.0000E+00
0.0000E+00 0.0000E+00 0.0000E+00 0.0000E+00
0.0000E+00 0.0000E+00 0.0000E+00 0.0000E+00
0.0000E+00 0.0000E+00 0.0000E+00 0.0000E+00
0.0000E+00 0.0000E+00

Nodal rotation about longitudinal axis for the 10th mode of floating structure

0.0000E+00 0.0000E+00 0.0000E+00 0.0000E+00
0.0000E+00 0.0000E+00 0.0000E+00 0.0000E+00
0.0000E+00 0.0000E+00 0.0000E+00 0.0000E+00
0.0000E+00 0.0000E+00 0.0000E+00 0.0000E+00
0.0000E+00 0.0000E+00 0.0000E+00 0.0000E+00
0.0000E+00 0.0000E+00 0.0000E+00 0.0000E+00
0.0000E+00 0.0000E+00 0.0000E+00 0.0000E+00
0.0000E+00 0.0000E+00 0.0000E+00 0.0000E+00
0.0000E+00 0.0000E+00 0.0000E+00 0.0000E+00
0.0000E+00 0.0000E+00 0.0000E+00 0.0000E+00
0.0000E+00 0.0000E+00 0.0000E+00 0.0000E+00
0.0000E+00 0.0000E+00 0.0000E+00 0.0000E+00
0.0000E+00 0.0000E+00 0.0000E+00 0.0000E+00
0.0000E+00 0.0000E+00 0.0000E+00 0.0000E+00
0.0000E+00 0.0000E+00 0.0000E+00 0.0000E+00
0.0000E+00 0.0000E+00 0.0000E+00 0.0000E+00
0.0000E+00 0.0000E+00 0.0000E+00 0.0000E+00
0.0000E+00 0.0000E+00 0.0000E+00 0.0000E+00
0.0000E+00 0.0000E+00 0.0000E+00 0.0000E+00
0.0000E+00 0.0000E+00 0.0000E+00 0.0000E+00
0.0000E+00 0.0000E+00 0.0000E+00 0.0000E+00
0.0000E+00 0.0000E+00 0.0000E+00 0.0000E+00
0.0000E+00 0.0000E+00 0.0000E+00 0.0000E+00
0.0000E+00 0.0000E+00 0.0000E+00 0.0000E+00
0.0000E+00 0.0000E+00 0.0000E+00 0.0000E+00
0.0000E+00 0.0000E+00

Nodal rotation about longitudinal axis for the 11th mode of floating structure

0.0000E+00 0.0000E+00 0.0000E+00 0.0000E+00
0.0000E+00 0.0000E+00 0.0000E+00 0.0000E+00
0.0000E+00 0.0000E+00 0.0000E+00 0.0000E+00
0.0000E+00 0.0000E+00 0.0000E+00 0.0000E+00
0.0000E+00 0.0000E+00 0.0000E+00 0.0000E+00
0.0000E+00 0.0000E+00 0.0000E+00 0.0000E+00
0.0000E+00 0.0000E+00 0.0000E+00 0.0000E+00
0.0000E+00 0.0000E+00 0.0000E+00 0.0000E+00
0.0000E+00 0.0000E+00 0.0000E+00 0.0000E+00
0.0000E+00 0.0000E+00 0.0000E+00 0.0000E+00
0.0000E+00 0.0000E+00 0.0000E+00 0.0000E+00
0.0000E+00 0.0000E+00 0.0000E+00 0.0000E+00
0.0000E+00 0.0000E+00 0.0000E+00 0.0000E+00
0.0000E+00 0.0000E+00 0.0000E+00 0.0000E+00
0.0000E+00 0.0000E+00 0.0000E+00 0.0000E+00
0.0000E+00 0.0000E+00 0.0000E+00 0.0000E+00
0.0000E+00 0.0000E+00 0.0000E+00 0.0000E+00
0.0000E+00 0.0000E+00 0.0000E+00 0.0000E+00
0.0000E+00 0.0000E+00 0.0000E+00 0.0000E+00
0.0000E+00 0.0000E+00 0.0000E+00 0.0000E+00
0.0000E+00 0.0000E+00 0.0000E+00 0.0000E+00
0.0000E+00 0.0000E+00 0.0000E+00 0.0000E+00
0.0000E+00 0.0000E+00 0.0000E+00 0.0000E+00
0.0000E+00 0.0000E+00 0.0000E+00 0.0000E+00
0.0000E+00 0.0000E+00 0.0000E+00 0.0000E+00
0.0000E+00 0.0000E+00

Nodal rotation about longitudinal axis for the 12th mode of floating structure

0.0000E+00 0.0000E+00 0.0000E+00 0.0000E+00
0.0000E+00 0.0000E+00 0.0000E+00 0.0000E+00
0.0000E+00 0.0000E+00 0.0000E+00 0.0000E+00
0.0000E+00 0.0000E+00 0.0000E+00 0.0000E+00
0.0000E+00 0.0000E+00 0.0000E+00 0.0000E+00
0.0000E+00 0.0000E+00 0.0000E+00 0.0000E+00
0.0000E+00 0.0000E+00 0.0000E+00 0.0000E+00
0.0000E+00 0.0000E+00 0.0000E+00 0.0000E+00
0.0000E+00 0.0000E+00 0.0000E+00 0.0000E+00
0.0000E+00 0.0000E+00 0.0000E+00 0.0000E+00
0.0000E+00 0.0000E+00 0.0000E+00 0.0000E+00
0.0000E+00 0.0000E+00 0.0000E+00 0.0000E+00
0.0000E+00 0.0000E+00 0.0000E+00 0.0000E+00
0.0000E+00 0.0000E+00 0.0000E+00 0.0000E+00
0.0000E+00 0.0000E+00 0.0000E+00 0.0000E+00
0.0000E+00 0.0000E+00 0.0000E+00 0.0000E+00
0.0000E+00 0.0000E+00 0.0000E+00 0.0000E+00
0.0000E+00 0.0000E+00 0.0000E+00 0.0000E+00
0.0000E+00 0.0000E+00 0.0000E+00 0.0000E+00
0.0000E+00 0.0000E+00 0.0000E+00 0.0000E+00
0.0000E+00 0.0000E+00 0.0000E+00 0.0000E+00

0.0000E+00 0.0000E+00 0.0000E+00 0.0000E+00
0.0000E+00 0.0000E+00 0.0000E+00 0.0000E+00
0.0000E+00 0.0000E+00 0.0000E+00 0.0000E+00
0.0000E+00 0.0000E+00 0.0000E+00 0.0000E+00
0.0000E+00 0.0000E+00

Nodal rotation about longitudinal axis for the 13th mode of floating structure

0.0000E+00 0.0000E+00 0.0000E+00 0.0000E+00
0.0000E+00 0.0000E+00 0.0000E+00 0.0000E+00
0.0000E+00 0.0000E+00 0.0000E+00 0.0000E+00
0.0000E+00 0.0000E+00 0.0000E+00 0.0000E+00
0.0000E+00 0.0000E+00 0.0000E+00 0.0000E+00
0.0000E+00 0.0000E+00 0.0000E+00 0.0000E+00
0.0000E+00 0.0000E+00 0.0000E+00 0.0000E+00
0.0000E+00 0.0000E+00 0.0000E+00 0.0000E+00
0.0000E+00 0.0000E+00 0.0000E+00 0.0000E+00
0.0000E+00 0.0000E+00 0.0000E+00 0.0000E+00
0.0000E+00 0.0000E+00 0.0000E+00 0.0000E+00
0.0000E+00 0.0000E+00 0.0000E+00 0.0000E+00
0.0000E+00 0.0000E+00 0.0000E+00 0.0000E+00
0.0000E+00 0.0000E+00 0.0000E+00 0.0000E+00
0.0000E+00 0.0000E+00 0.0000E+00 0.0000E+00
0.0000E+00 0.0000E+00 0.0000E+00 0.0000E+00
0.0000E+00 0.0000E+00 0.0000E+00 0.0000E+00
0.0000E+00 0.0000E+00 0.0000E+00 0.0000E+00
0.0000E+00 0.0000E+00 0.0000E+00 0.0000E+00
0.0000E+00 0.0000E+00 0.0000E+00 0.0000E+00
0.0000E+00 0.0000E+00 0.0000E+00 0.0000E+00
0.0000E+00 0.0000E+00 0.0000E+00 0.0000E+00
0.0000E+00 0.0000E+00 0.0000E+00 0.0000E+00
0.0000E+00 0.0000E+00 0.0000E+00 0.0000E+00
0.0000E+00 0.0000E+00 0.0000E+00 0.0000E+00
0.0000E+00 0.0000E+00

Nodal rotation about longitudinal axis for the 14th mode of floating structure

0.0000E+00 0.0000E+00 0.0000E+00 0.0000E+00
0.0000E+00 0.0000E+00 0.0000E+00 0.0000E+00
0.0000E+00 0.0000E+00 0.0000E+00 0.0000E+00
0.0000E+00 0.0000E+00 0.0000E+00 0.0000E+00
0.0000E+00 0.0000E+00 0.0000E+00 0.0000E+00
0.0000E+00 0.0000E+00 0.0000E+00 0.0000E+00
0.0000E+00 0.0000E+00 0.0000E+00 0.0000E+00
0.0000E+00 0.0000E+00 0.0000E+00 0.0000E+00
0.0000E+00 0.0000E+00 0.0000E+00 0.0000E+00
0.0000E+00 0.0000E+00 0.0000E+00 0.0000E+00
0.0000E+00 0.0000E+00 0.0000E+00 0.0000E+00
0.0000E+00 0.0000E+00 0.0000E+00 0.0000E+00
0.0000E+00 0.0000E+00 0.0000E+00 0.0000E+00
0.0000E+00 0.0000E+00 0.0000E+00 0.0000E+00
0.0000E+00 0.0000E+00 0.0000E+00 0.0000E+00
0.0000E+00 0.0000E+00 0.0000E+00 0.0000E+00
0.0000E+00 0.0000E+00 0.0000E+00 0.0000E+00
0.0000E+00 0.0000E+00 0.0000E+00 0.0000E+00
0.0000E+00 0.0000E+00 0.0000E+00 0.0000E+00
0.0000E+00 0.0000E+00 0.0000E+00 0.0000E+00
0.0000E+00 0.0000E+00 0.0000E+00 0.0000E+00
0.0000E+00 0.0000E+00 0.0000E+00 0.0000E+00
0.0000E+00 0.0000E+00 0.0000E+00 0.0000E+00
0.0000E+00 0.0000E+00 0.0000E+00 0.0000E+00
0.0000E+00 0.0000E+00 0.0000E+00 0.0000E+00
0.0000E+00 0.0000E+00

Nodal rotation about longitudinal axis for the 15th mode of floating structure

0.0000E+00 0.0000E+00 0.0000E+00 0.0000E+00
0.0000E+00 0.0000E+00 0.0000E+00 0.0000E+00
0.0000E+00 0.0000E+00 0.0000E+00 0.0000E+00
0.0000E+00 0.0000E+00 0.0000E+00 0.0000E+00
0.0000E+00 0.0000E+00 0.0000E+00 0.0000E+00
0.0000E+00 0.0000E+00 0.0000E+00 0.0000E+00
0.0000E+00 0.0000E+00 0.0000E+00 0.0000E+00
0.0000E+00 0.0000E+00 0.0000E+00 0.0000E+00
0.0000E+00 0.0000E+00 0.0000E+00 0.0000E+00
0.0000E+00 0.0000E+00 0.0000E+00 0.0000E+00
0.0000E+00 0.0000E+00 0.0000E+00 0.0000E+00
0.0000E+00 0.0000E+00 0.0000E+00 0.0000E+00
0.0000E+00 0.0000E+00 0.0000E+00 0.0000E+00
0.0000E+00 0.0000E+00 0.0000E+00 0.0000E+00
0.0000E+00 0.0000E+00 0.0000E+00 0.0000E+00
0.0000E+00 0.0000E+00 0.0000E+00 0.0000E+00
0.0000E+00 0.0000E+00 0.0000E+00 0.0000E+00
0.0000E+00 0.0000E+00 0.0000E+00 0.0000E+00
0.0000E+00 0.0000E+00 0.0000E+00 0.0000E+00
0.0000E+00 0.0000E+00 0.0000E+00 0.0000E+00
0.0000E+00 0.0000E+00 0.0000E+00 0.0000E+00
0.0000E+00 0.0000E+00 0.0000E+00 0.0000E+00

0.0000E+00	0.0000E+00	0.0000E+00	0.0000E+00
0.0000E+00	0.0000E+00	0.0000E+00	0.0000E+00
0.0000E+00	0.0000E+00	0.0000E+00	0.0000E+00
0.0000E+00	0.0000E+00		

Nodal rotation about longitudinal axis for the 16th mode of floating structure

0.0000E+00	0.0000E+00	0.0000E+00	0.0000E+00
0.0000E+00	0.0000E+00	0.0000E+00	0.0000E+00
0.0000E+00	0.0000E+00	0.0000E+00	0.0000E+00
0.0000E+00	0.0000E+00	0.0000E+00	0.0000E+00
0.0000E+00	0.0000E+00	0.0000E+00	0.0000E+00
0.0000E+00	0.0000E+00	0.0000E+00	0.0000E+00
0.0000E+00	0.0000E+00	0.0000E+00	0.0000E+00
0.0000E+00	0.0000E+00	0.0000E+00	0.0000E+00
0.0000E+00	0.0000E+00	0.0000E+00	0.0000E+00
0.0000E+00	0.0000E+00	0.0000E+00	0.0000E+00
0.0000E+00	0.0000E+00	0.0000E+00	0.0000E+00
0.0000E+00	0.0000E+00	0.0000E+00	0.0000E+00
0.0000E+00	0.0000E+00	0.0000E+00	0.0000E+00
0.0000E+00	0.0000E+00	0.0000E+00	0.0000E+00
0.0000E+00	0.0000E+00	0.0000E+00	0.0000E+00
0.0000E+00	0.0000E+00	0.0000E+00	0.0000E+00
0.0000E+00	0.0000E+00	0.0000E+00	0.0000E+00
0.0000E+00	0.0000E+00	0.0000E+00	0.0000E+00
0.0000E+00	0.0000E+00	0.0000E+00	0.0000E+00
0.0000E+00	0.0000E+00	0.0000E+00	0.0000E+00
0.0000E+00	0.0000E+00	0.0000E+00	0.0000E+00
0.0000E+00	0.0000E+00	0.0000E+00	0.0000E+00
0.0000E+00	0.0000E+00	0.0000E+00	0.0000E+00
0.0000E+00	0.0000E+00	0.0000E+00	0.0000E+00
0.0000E+00	0.0000E+00	0.0000E+00	0.0000E+00
0.0000E+00	0.0000E+00		

Nodal rotation about transverse axis for the 1st mode of floating structure

0.0000E+00	0.0000E+00	0.0000E+00	0.0000E+00
0.0000E+00	0.0000E+00	0.0000E+00	0.0000E+00
0.0000E+00	0.0000E+00	0.0000E+00	0.0000E+00
0.0000E+00	0.0000E+00	0.0000E+00	0.0000E+00
0.0000E+00	0.0000E+00	0.0000E+00	0.0000E+00
0.0000E+00	0.0000E+00	0.0000E+00	0.0000E+00
0.0000E+00	0.0000E+00	0.0000E+00	0.0000E+00
0.0000E+00	0.0000E+00	0.0000E+00	0.0000E+00
0.0000E+00	0.0000E+00	0.0000E+00	0.0000E+00
0.0000E+00	0.0000E+00	0.0000E+00	0.0000E+00
0.0000E+00	0.0000E+00	0.0000E+00	0.0000E+00
0.0000E+00	0.0000E+00	0.0000E+00	0.0000E+00
0.0000E+00	0.0000E+00	0.0000E+00	0.0000E+00
0.0000E+00	0.0000E+00	0.0000E+00	0.0000E+00
0.0000E+00	0.0000E+00	0.0000E+00	0.0000E+00
0.0000E+00	0.0000E+00	0.0000E+00	0.0000E+00
0.0000E+00	0.0000E+00	0.0000E+00	0.0000E+00
0.0000E+00	0.0000E+00	0.0000E+00	0.0000E+00
0.0000E+00	0.0000E+00	0.0000E+00	0.0000E+00
0.0000E+00	0.0000E+00	0.0000E+00	0.0000E+00
0.0000E+00	0.0000E+00	0.0000E+00	0.0000E+00
0.0000E+00	0.0000E+00	0.0000E+00	0.0000E+00
0.0000E+00	0.0000E+00	0.0000E+00	0.0000E+00
0.0000E+00	0.0000E+00	0.0000E+00	0.0000E+00
0.0000E+00	0.0000E+00	0.0000E+00	0.0000E+00
0.0000E+00	0.0000E+00		

Nodal rotation about transverse axis for the 2nd mode of floating structure

0.8433E-02	0.8433E-02	0.8433E-02	0.8433E-02
0.8433E-02	0.8433E-02	0.8433E-02	0.8433E-02
0.8433E-02	0.8433E-02	0.8433E-02	0.8433E-02
0.8433E-02	0.8433E-02	0.8433E-02	0.8433E-02
0.8433E-02	0.8433E-02	0.8433E-02	0.8433E-02
0.8433E-02	0.8433E-02	0.8433E-02	0.8433E-02
0.8433E-02	0.8433E-02	0.8433E-02	0.8433E-02
0.8433E-02	0.8433E-02	0.8433E-02	0.8433E-02
0.8433E-02	0.8433E-02	0.8433E-02	0.8433E-02
0.8433E-02	0.8433E-02	0.8433E-02	0.8433E-02
0.8433E-02	0.8433E-02	0.8433E-02	0.8433E-02
0.8433E-02	0.8433E-02	0.8433E-02	0.8433E-02
0.8433E-02	0.8433E-02	0.8433E-02	0.8433E-02
0.8433E-02	0.8433E-02	0.8433E-02	0.8433E-02
0.8433E-02	0.8433E-02	0.8433E-02	0.8433E-02
0.8433E-02	0.8433E-02	0.8433E-02	0.8433E-02
0.8433E-02	0.8433E-02	0.8433E-02	0.8433E-02
0.8433E-02	0.8433E-02	0.8433E-02	0.8433E-02
0.8433E-02	0.8433E-02	0.8433E-02	0.8433E-02
0.8433E-02	0.8433E-02	0.8433E-02	0.8433E-02
0.8433E-02	0.8433E-02	0.8433E-02	0.8433E-02
0.8433E-02	0.8433E-02	0.8433E-02	0.8433E-02
0.8433E-02	0.8433E-02	0.8433E-02	0.8433E-02

0.8433E-02 0.8433E-02 0.8433E-02 0.8433E-02
0.8433E-02 0.8433E-02 0.8433E-02 0.8433E-02
0.8433E-02 0.8433E-02

Nodal rotation about transverse axis for the 3rd mode of floating structure

0.4689E-06 0.2078E-02 0.3953E-02 0.5625E-02
0.7096E-02 0.8366E-02 0.9437E-02 0.1031E-01
0.1099E-01 0.1148E-01 0.1178E-01 0.1191E-01
0.1186E-01 0.1164E-01 0.1127E-01 0.1075E-01
0.1009E-01 0.9301E-02 0.8399E-02 0.7395E-02
0.6301E-02 0.5132E-02 0.3903E-02 0.2628E-02
0.1322E-02 0.0000E+00 -0.1322E-02 -0.2628E-02
-0.3903E-02 -0.5132E-02 -0.6301E-02 -0.7395E-02
-0.8399E-02 -0.9301E-02 -0.1009E-01 -0.1075E-01
-0.1127E-01 -0.1164E-01 -0.1186E-01 -0.1191E-01
-0.1178E-01 -0.1148E-01 -0.1099E-01 -0.1031E-01
-0.9437E-02 -0.8366E-02 -0.7096E-02 -0.5625E-02
-0.3953E-02 -0.2078E-02 -0.4689E-06 0.4689E-06
0.2078E-02 0.3953E-02 0.5625E-02 0.7096E-02
0.8366E-02 0.9437E-02 0.1031E-01 0.1099E-01
0.1148E-01 0.1178E-01 0.1191E-01 0.1186E-01
0.1164E-01 0.1127E-01 0.1075E-01 0.1009E-01
0.9301E-02 0.8399E-02 0.7395E-02 0.6301E-02
0.5132E-02 0.3903E-02 0.2628E-02 0.1322E-02
0.0000E+00 -0.1322E-02 -0.2628E-02 -0.3903E-02
-0.5132E-02 -0.6301E-02 -0.7395E-02 -0.8399E-02
-0.9301E-02 -0.1009E-01 -0.1075E-01 -0.1127E-01
-0.1164E-01 -0.1186E-01 -0.1191E-01 -0.1178E-01
-0.1148E-01 -0.1099E-01 -0.1031E-01 -0.9437E-02
-0.8366E-02 -0.7096E-02 -0.5625E-02 -0.3953E-02
-0.2078E-02 -0.4689E-06

Nodal rotation about transverse axis for the 4th mode of floating structure

0.3826E-01 0.3824E-01 0.3808E-01 0.3768E-01
0.3693E-01 0.3578E-01 0.3418E-01 0.3211E-01
0.2957E-01 0.2656E-01 0.2313E-01 0.1933E-01
0.1523E-01 0.1089E-01 0.6415E-02 0.1887E-02
-0.2594E-02 -0.6929E-02 -0.1102E-01 -0.1479E-01
-0.1813E-01 -0.2097E-01 -0.2326E-01 -0.2493E-01
-0.2595E-01 -0.2629E-01 -0.2595E-01 -0.2493E-01
-0.2326E-01 -0.2097E-01 -0.1813E-01 -0.1479E-01
-0.1102E-01 -0.6929E-02 -0.2594E-02 0.1887E-02
0.6415E-02 0.1089E-01 0.1523E-01 0.1933E-01
0.2313E-01 0.2656E-01 0.2957E-01 0.3211E-01
0.3418E-01 0.3578E-01 0.3693E-01 0.3768E-01
0.3808E-01 0.3824E-01 0.3826E-01 0.3826E-01
0.3824E-01 0.3808E-01 0.3768E-01 0.3693E-01
0.3578E-01 0.3418E-01 0.3211E-01 0.2957E-01
0.2656E-01 0.2313E-01 0.1933E-01 0.1523E-01
0.1089E-01 0.6415E-02 0.1887E-02 -0.2594E-02
-0.6929E-02 -0.1102E-01 -0.1479E-01 -0.1813E-01
-0.2097E-01 -0.2326E-01 -0.2493E-01 -0.2595E-01
-0.2629E-01 -0.2595E-01 -0.2493E-01 -0.2326E-01
-0.2097E-01 -0.1813E-01 -0.1479E-01 -0.1102E-01
-0.6929E-02 -0.2594E-02 0.1887E-02 0.6415E-02
0.1089E-01 0.1523E-01 0.1933E-01 0.2313E-01
0.2656E-01 0.2957E-01 0.3211E-01 0.3418E-01
0.3578E-01 0.3693E-01 0.3768E-01 0.3808E-01
0.3824E-01 0.3826E-01

Nodal rotation about transverse axis for the 5th mode of floating structure

0.2166E-06 0.1048E-01 0.1837E-01 0.2372E-01
0.2658E-01 0.2709E-01 0.2543E-01 0.2185E-01
0.1667E-01 0.1024E-01 0.2958E-02 -0.4754E-02
-0.1247E-01 -0.1976E-01 -0.2625E-01 -0.3160E-01
-0.3552E-01 -0.3780E-01 -0.3832E-01 -0.3705E-01
-0.3402E-01 -0.2939E-01 -0.2336E-01 -0.1622E-01
-0.8306E-02 0.0000E+00 0.8306E-02 0.1622E-01
0.2336E-01 0.2939E-01 0.3402E-01 0.3705E-01
0.3832E-01 0.3780E-01 0.3552E-01 0.3160E-01
0.2625E-01 0.1976E-01 0.1247E-01 0.4754E-02
-0.2958E-02 -0.1024E-01 -0.1667E-01 -0.2185E-01
-0.2543E-01 -0.2709E-01 -0.2658E-01 -0.2372E-01
-0.1837E-01 -0.1048E-01 -0.2166E-06 0.2166E-06
0.1048E-01 0.1837E-01 0.2372E-01 0.2658E-01
0.2709E-01 0.2543E-01 0.2185E-01 0.1667E-01
0.1024E-01 0.2958E-02 -0.4754E-02 -0.1247E-01
-0.1976E-01 -0.2625E-01 -0.3160E-01 -0.3552E-01
-0.3780E-01 -0.3832E-01 -0.3705E-01 -0.3402E-01
-0.2939E-01 -0.2336E-01 -0.1622E-01 -0.8306E-02
0.0000E+00 0.8306E-02 0.1622E-01 0.2336E-01
0.2939E-01 0.3402E-01 0.3705E-01 0.3832E-01
0.3780E-01 0.3552E-01 0.3160E-01 0.2625E-01
0.1976E-01 0.1247E-01 0.4754E-02 -0.2958E-02
-0.1024E-01 -0.1667E-01 -0.2185E-01 -0.2543E-01

-0.2709E-01 -0.2658E-01 -0.2372E-01 -0.1837E-01
-0.1048E-01 -0.2166E-06

Nodal rotation about transverse axis for the 6th mode of floating structure

0.6883E-01 0.6859E-01 0.6705E-01 0.6331E-01
0.5690E-01 0.4775E-01 0.3614E-01 0.2267E-01
0.8165E-02 -0.6417E-02 -0.2006E-01 -0.3178E-01
-0.4073E-01 -0.4627E-01 -0.4799E-01 -0.4579E-01
-0.3988E-01 -0.3074E-01 -0.1911E-01 -0.5935E-02
0.7741E-02 0.2082E-01 0.3227E-01 0.4116E-01
0.4680E-01 0.4873E-01 0.4680E-01 0.4116E-01
0.3227E-01 0.2082E-01 0.7741E-02 -0.5935E-02
-0.1911E-01 -0.3074E-01 -0.3988E-01 -0.4579E-01
-0.4799E-01 -0.4627E-01 -0.4073E-01 -0.3178E-01
-0.2006E-01 -0.6417E-02 0.8165E-02 0.2267E-01
0.3614E-01 0.4775E-01 0.5690E-01 0.6331E-01
0.6705E-01 0.6859E-01 0.6883E-01 0.6883E-01
0.6859E-01 0.6705E-01 0.6331E-01 0.5690E-01
0.4775E-01 0.3614E-01 0.2267E-01 0.8165E-02
-0.6417E-02 -0.2006E-01 -0.3178E-01 -0.4073E-01
-0.4627E-01 -0.4799E-01 -0.4579E-01 -0.3988E-01
-0.3074E-01 -0.1911E-01 -0.5935E-02 0.7741E-02
0.2082E-01 0.3227E-01 0.4116E-01 0.4680E-01
0.4873E-01 0.4680E-01 0.4116E-01 0.3227E-01
0.2082E-01 0.7741E-02 -0.5935E-02 -0.1911E-01
-0.3074E-01 -0.3988E-01 -0.4579E-01 -0.4799E-01
-0.4627E-01 -0.4073E-01 -0.3178E-01 -0.2006E-01
-0.6417E-02 0.8165E-02 0.2267E-01 0.3614E-01
0.4775E-01 0.5690E-01 0.6331E-01 0.6705E-01
0.6859E-01 0.6883E-01

Nodal rotation about transverse axis for the 7th mode of floating structure

-0.1657E-05 0.2405E-01 0.3815E-01 0.4270E-01
0.3864E-01 0.2749E-01 0.1131E-01 -0.7478E-02
-0.2627E-01 -0.4259E-01 -0.5433E-01 -0.5995E-01
-0.5872E-01 -0.5069E-01 -0.3679E-01 -0.1862E-01
0.1701E-02 0.2178E-01 0.3925E-01 0.5207E-01
0.5871E-01 0.5840E-01 0.5118E-01 0.3791E-01
0.2014E-01 0.0000E+00 -0.2014E-01 -0.3791E-01
-0.5118E-01 -0.5840E-01 -0.5871E-01 -0.5207E-01
-0.3925E-01 -0.2178E-01 -0.1701E-02 0.1862E-01
0.3679E-01 0.5069E-01 0.5872E-01 0.5995E-01
0.5433E-01 0.4259E-01 0.2627E-01 0.7478E-02
-0.1131E-01 -0.2749E-01 -0.3864E-01 -0.4270E-01
-0.3815E-01 -0.2405E-01 0.1657E-05 -0.1657E-05
0.2405E-01 0.3815E-01 0.4270E-01 0.3864E-01
0.2749E-01 0.1131E-01 -0.7478E-02 -0.2627E-01
-0.4259E-01 -0.5433E-01 -0.5995E-01 -0.5872E-01
-0.5069E-01 -0.3679E-01 -0.1862E-01 0.1701E-02
0.2178E-01 0.3925E-01 0.5207E-01 0.5871E-01
0.5840E-01 0.5118E-01 0.3791E-01 0.2014E-01
0.0000E+00 -0.2014E-01 -0.3791E-01 -0.5118E-01
-0.5840E-01 -0.5871E-01 -0.5207E-01 -0.3925E-01
-0.2178E-01 -0.1701E-02 0.1862E-01 0.3679E-01
0.5069E-01 0.5872E-01 0.5995E-01 0.5433E-01
0.4259E-01 0.2627E-01 0.7478E-02 -0.1131E-01
-0.2749E-01 -0.3864E-01 -0.4270E-01 -0.3815E-01
-0.2405E-01 0.1657E-05

Nodal rotation about transverse axis for the 8th mode of floating structure

0.9942E-01 0.9840E-01 0.9223E-01 0.7821E-01
0.5619E-01 0.2818E-01 -0.2327E-02 -0.3102E-01
-0.5365E-01 -0.6683E-01 -0.6860E-01 -0.5880E-01
-0.3914E-01 -0.1293E-01 0.1550E-01 0.4143E-01
0.6058E-01 0.6979E-01 0.6754E-01 0.5419E-01
0.3193E-01 0.4424E-02 -0.2381E-01 -0.4812E-01
-0.6451E-01 -0.7029E-01 -0.6451E-01 -0.4812E-01
-0.2381E-01 0.4424E-02 0.3193E-01 0.5419E-01
0.6754E-01 0.6979E-01 0.6058E-01 0.4143E-01
0.1550E-01 -0.1293E-01 -0.3914E-01 -0.5880E-01
-0.6860E-01 -0.6683E-01 -0.5365E-01 -0.3102E-01
-0.2327E-02 0.2818E-01 0.5619E-01 0.7821E-01
0.9223E-01 0.9840E-01 0.9942E-01 0.9942E-01
0.9840E-01 0.9223E-01 0.7821E-01 0.5619E-01
0.2818E-01 -0.2327E-02 -0.3102E-01 -0.5365E-01
-0.6683E-01 -0.6860E-01 -0.5880E-01 -0.3914E-01
-0.1293E-01 0.1550E-01 0.4143E-01 0.6058E-01
0.6979E-01 0.6754E-01 0.5419E-01 0.3193E-01
0.4424E-02 -0.2381E-01 -0.4812E-01 -0.6451E-01
-0.7029E-01 -0.6451E-01 -0.4812E-01 -0.2381E-01
0.4424E-02 0.3193E-01 0.5419E-01 0.6754E-01
0.6979E-01 0.6058E-01 0.4143E-01 0.1550E-01
-0.1293E-01 -0.3914E-01 -0.5880E-01 -0.6860E-01
-0.6683E-01 -0.5365E-01 -0.3102E-01 -0.2327E-02
0.2818E-01 0.5619E-01 0.7821E-01 0.9223E-01

0.9840E-01 0.9942E-01

Nodal rotation about transverse axis for the 9th mode of floating structure

-0.3176E-05 0.4134E-01 0.5777E-01 0.5167E-01
0.2812E-01 -0.5435E-02 -0.4022E-01 -0.6774E-01
-0.8144E-01 -0.7797E-01 -0.5787E-01 -0.2539E-01
0.1249E-01 0.4755E-01 0.7219E-01 0.8106E-01
0.7224E-01 0.4766E-01 0.1268E-01 -0.2507E-01
-0.5736E-01 -0.7715E-01 -0.8012E-01 -0.6562E-01
-0.3683E-01 0.0000E+00 0.3683E-01 0.6562E-01
0.8012E-01 0.7715E-01 0.5736E-01 0.2507E-01
-0.1268E-01 -0.4766E-01 -0.7224E-01 -0.8106E-01
-0.7219E-01 -0.4755E-01 -0.1249E-01 0.2539E-01
0.5787E-01 0.7797E-01 0.8144E-01 0.6774E-01
0.4022E-01 0.5435E-02 -0.2812E-01 -0.5167E-01
-0.5777E-01 -0.4134E-01 0.3176E-05 -0.3176E-05
0.4134E-01 0.5777E-01 0.5167E-01 0.2812E-01
-0.5435E-02 -0.4022E-01 -0.6774E-01 -0.8144E-01
-0.7797E-01 -0.5787E-01 -0.2539E-01 0.1249E-01
0.4755E-01 0.7219E-01 0.8106E-01 0.7224E-01
0.4766E-01 0.1268E-01 -0.2507E-01 -0.5736E-01
-0.7715E-01 -0.8012E-01 -0.6562E-01 -0.3683E-01
0.0000E+00 0.3683E-01 0.6562E-01 0.8012E-01
0.7715E-01 0.5736E-01 0.2507E-01 -0.1268E-01
-0.4766E-01 -0.7224E-01 -0.8106E-01 -0.7219E-01
-0.4755E-01 -0.1249E-01 0.2539E-01 0.5787E-01
0.7797E-01 0.8144E-01 0.6774E-01 0.4022E-01
0.5435E-02 -0.2812E-01 -0.5167E-01 -0.5777E-01
-0.4134E-01 0.3176E-05

Nodal rotation about transverse axis for the 10th mode of floating structure

0.1300E+00 0.1271E+00 0.1106E+00 0.7603E-01
0.2773E-01 -0.2391E-01 -0.6632E-01 -0.8875E-01
-0.8559E-01 -0.5807E-01 -0.1407E-01 0.3402E-01
0.7274E-01 0.9127E-01 0.8440E-01 0.5406E-01
0.8665E-02 -0.3913E-01 -0.7603E-01 -0.9174E-01
-0.8191E-01 -0.4926E-01 -0.2887E-02 0.4429E-01
0.7913E-01 0.9193E-01 0.7913E-01 0.4429E-01
-0.2887E-02 -0.4926E-01 -0.8191E-01 -0.9174E-01
-0.7603E-01 -0.3913E-01 0.8665E-02 0.5406E-01
0.8440E-01 0.9127E-01 0.7274E-01 0.3402E-01
-0.1407E-01 -0.5807E-01 -0.8559E-01 -0.8875E-01
-0.6632E-01 -0.2391E-01 0.2773E-01 0.7603E-01
0.1106E+00 0.1271E+00 0.1300E+00 0.1300E+00
0.1271E+00 0.1106E+00 0.7603E-01 0.2773E-01
-0.2391E-01 -0.6632E-01 -0.8875E-01 -0.8559E-01
-0.5807E-01 -0.1407E-01 0.3402E-01 0.7274E-01
0.9127E-01 0.8440E-01 0.5406E-01 0.8665E-02
-0.3913E-01 -0.7603E-01 -0.9174E-01 -0.8191E-01
-0.4926E-01 -0.2887E-02 0.4429E-01 0.7913E-01
0.9193E-01 0.7913E-01 0.4429E-01 -0.2887E-02
-0.4926E-01 -0.8191E-01 -0.9174E-01 -0.7603E-01
-0.3913E-01 0.8665E-02 0.5406E-01 0.8440E-01
0.9127E-01 0.7274E-01 0.3402E-01 -0.1407E-01
-0.5807E-01 -0.8559E-01 -0.8875E-01 -0.6632E-01
-0.2391E-01 0.2773E-01 0.7603E-01 0.1106E+00
0.1271E+00 0.1300E+00

Nodal rotation about transverse axis for the 11th mode of floating structure

-0.5040E-05 0.6093E-01 0.7228E-01 0.4293E-01
-0.9897E-02 -0.6406E-01 -0.9869E-01 -0.1006E+00
-0.6856E-01 -0.1322E-01 0.4646E-01 0.8993E-01
0.1022E+00 0.7913E-01 0.2865E-01 -0.3176E-01
-0.8119E-01 -0.1025E+00 -0.8844E-01 -0.4375E-01
0.1607E-01 0.7033E-01 0.1003E+00 0.9553E-01
0.5775E-01 0.0000E+00 -0.5775E-01 -0.9553E-01
-0.1003E+00 -0.7033E-01 -0.1607E-01 0.4375E-01
0.8844E-01 0.1025E+00 0.8119E-01 0.3176E-01
-0.2865E-01 -0.7913E-01 -0.1022E+00 -0.8993E-01
-0.4646E-01 0.1322E-01 0.6856E-01 0.1006E+00
0.9869E-01 0.6406E-01 0.9897E-02 -0.4293E-01
-0.7228E-01 -0.6093E-01 0.5040E-05 -0.5040E-05
0.6093E-01 0.7228E-01 0.4293E-01 -0.9897E-02
-0.6406E-01 -0.9869E-01 -0.1006E+00 -0.6856E-01
-0.1322E-01 0.4646E-01 0.8993E-01 0.1022E+00
0.7913E-01 0.2865E-01 -0.3176E-01 -0.8119E-01
-0.1025E+00 -0.8844E-01 -0.4375E-01 0.1607E-01
0.7033E-01 0.1003E+00 0.9553E-01 0.5775E-01
0.0000E+00 -0.5775E-01 -0.9553E-01 -0.1003E+00
-0.7033E-01 -0.1607E-01 0.4375E-01 0.8844E-01
0.1025E+00 0.8119E-01 0.3176E-01 -0.2865E-01
-0.7913E-01 -0.1022E+00 -0.8993E-01 -0.4646E-01
0.1322E-01 0.6856E-01 0.1006E+00 0.9869E-01
0.6406E-01 0.9897E-02 -0.4293E-01 -0.7228E-01
-0.6093E-01 0.5040E-05

Nodal rotation about transverse axis for the 12th mode of floating structure

0.1606E+00 0.1542E+00 0.1192E+00 0.5290E-01
-0.2594E-01 -0.8890E-01 -0.1120E+00 -0.8671E-01
-0.2436E-01 0.4856E-01 0.1013E+00 0.1116E+00
0.7513E-01 0.7148E-02 -0.6382E-01 -0.1080E+00
-0.1068E+00 -0.6085E-01 0.1069E-01 0.7774E-01
0.1122E+00 0.9951E-01 0.4510E-01 -0.2824E-01
-0.8973E-01 -0.1136E+00 -0.8973E-01 -0.2824E-01
0.4510E-01 0.9951E-01 0.1122E+00 0.7774E-01
0.1069E-01 -0.6085E-01 -0.1068E+00 -0.1080E+00
-0.6382E-01 0.7148E-02 0.7513E-01 0.1116E+00
0.1013E+00 0.4856E-01 -0.2436E-01 -0.8671E-01
-0.1120E+00 -0.8890E-01 -0.2594E-01 0.5290E-01
0.1192E+00 0.1542E+00 0.1606E+00 0.1606E+00
0.1542E+00 0.1192E+00 0.5290E-01 -0.2594E-01
-0.8890E-01 -0.1120E+00 -0.8671E-01 -0.2436E-01
0.4856E-01 0.1013E+00 0.1116E+00 0.7513E-01
0.7148E-02 -0.6382E-01 -0.1080E+00 -0.1068E+00
-0.6085E-01 0.1069E-01 0.7774E-01 0.1122E+00
0.9951E-01 0.4510E-01 -0.2824E-01 -0.8973E-01
-0.1136E+00 -0.8973E-01 -0.2824E-01 0.4510E-01
0.9951E-01 0.1122E+00 0.7774E-01 0.1069E-01
-0.6085E-01 -0.1068E+00 -0.1080E+00 -0.6382E-01
0.7148E-02 0.7513E-01 0.1116E+00 0.1013E+00
0.4856E-01 -0.2436E-01 -0.8671E-01 -0.1120E+00
-0.8890E-01 -0.2594E-01 0.5290E-01 0.1192E+00
0.1542E+00 0.1606E+00

Nodal rotation about transverse axis for the 13th mode of floating structure

-0.7333E-05 0.8143E-01 0.7755E-01 0.1324E-01
-0.6819E-01 -0.1207E+00 -0.1153E+00 -0.5352E-01
0.3442E-01 0.1049E+00 0.1228E+00 0.7925E-01
-0.3919E-02 -0.8514E-01 -0.1238E+00 -0.1006E+00
-0.2713E-01 0.5991E-01 0.1170E+00 0.1156E+00
0.5646E-01 -0.3093E-01 -0.1029E+00 -0.1234E+00
-0.8225E-01 0.0000E+00 0.8225E-01 0.1234E+00
0.1029E+00 0.3093E-01 -0.5646E-01 -0.1156E+00
-0.1170E+00 -0.5991E-01 0.2713E-01 0.1006E+00
0.1238E+00 0.8514E-01 0.3919E-02 -0.7925E-01
-0.1228E+00 -0.1049E+00 -0.3442E-01 0.5352E-01
0.1153E+00 0.1207E+00 0.6819E-01 -0.1324E-01
-0.7755E-01 -0.8143E-01 0.7333E-05 -0.7333E-05
0.8143E-01 0.7755E-01 0.1324E-01 -0.6819E-01
-0.1207E+00 -0.1153E+00 -0.5352E-01 0.3442E-01
0.1049E+00 0.1228E+00 0.7925E-01 -0.3919E-02
-0.8514E-01 -0.1238E+00 -0.1006E+00 -0.2713E-01
0.5991E-01 0.1170E+00 0.1156E+00 0.5646E-01
-0.3093E-01 -0.1029E+00 -0.1234E+00 -0.8225E-01
0.0000E+00 0.8225E-01 0.1234E+00 0.1029E+00
0.3093E-01 -0.5646E-01 -0.1156E+00 -0.1170E+00
-0.5991E-01 0.2713E-01 0.1006E+00 0.1238E+00
0.8514E-01 0.3919E-02 -0.7925E-01 -0.1228E+00
-0.1049E+00 -0.3442E-01 0.5352E-01 0.1153E+00
0.1207E+00 0.6819E-01 -0.1324E-01 -0.7755E-01
-0.8143E-01 0.7333E-05

Nodal rotation about transverse axis for the 14th mode of floating structure

0.1912E+00 0.1788E+00 0.1155E+00 0.9066E-02
-0.9146E-01 -0.1333E+00 -0.9474E-01 0.3870E-03
0.9577E-01 0.1353E+00 0.9563E-01 0.2041E-04
-0.9558E-01 -0.1352E+00 -0.9559E-01 -0.1764E-05
0.9559E-01 0.1352E+00 0.9559E-01 0.1529E-05
-0.9559E-01 -0.1352E+00 -0.9559E-01 -0.4976E-06
0.9559E-01 0.1352E+00 0.9559E-01 -0.4976E-06
-0.9559E-01 -0.1352E+00 -0.9559E-01 0.1529E-05
0.9559E-01 0.1352E+00 0.9559E-01 -0.1764E-05
-0.9559E-01 -0.1352E+00 -0.9558E-01 0.2041E-04
0.9563E-01 0.1353E+00 0.9577E-01 0.3870E-03
-0.9474E-01 -0.1333E+00 -0.9146E-01 0.9066E-02
0.1155E+00 0.1788E+00 0.1912E+00 0.1912E+00
0.1788E+00 0.1155E+00 0.9066E-02 -0.9146E-01
-0.1333E+00 -0.9474E-01 0.3870E-03 0.9577E-01
0.1353E+00 0.9563E-01 0.2041E-04 -0.9558E-01
-0.1352E+00 -0.9559E-01 -0.1764E-05 0.9559E-01
0.1352E+00 0.9559E-01 0.1529E-05 -0.9559E-01
-0.1352E+00 -0.9559E-01 -0.4976E-06 0.9559E-01
0.1352E+00 0.9559E-01 -0.4976E-06 -0.9559E-01
-0.1352E+00 -0.9559E-01 0.1529E-05 0.9559E-01
0.1352E+00 0.9559E-01 -0.1764E-05 -0.9559E-01
-0.1352E+00 -0.9558E-01 0.2041E-04 0.9563E-01
0.1353E+00 0.9577E-01 0.3870E-03 -0.9474E-01
-0.1333E+00 -0.9146E-01 0.9066E-02 0.1155E+00
0.1788E+00 0.1912E+00

Nodal rotation about transverse axis for the 15th mode of floating structure

-0.1005E-04 0.1015E+00 0.7056E-01 -0.3546E-01
-0.1291E+00 -0.1403E+00 -0.5863E-01 0.6189E-01
0.1401E+00 0.1232E+00 0.2282E-01 -0.9307E-01
-0.1459E+00 -0.9995E-01 0.1374E-01 0.1181E+00
0.1425E+00 0.7034E-01 -0.4945E-01 -0.1357E+00
-0.1301E+00 -0.3631E-01 0.8206E-01 0.1448E+00
0.1095E+00 0.0000E+00 -0.1095E+00 -0.1448E+00
-0.8206E-01 0.3631E-01 0.1301E+00 0.1357E+00
0.4945E-01 -0.7034E-01 -0.1425E+00 -0.1181E+00
-0.1374E-01 0.9995E-01 0.1459E+00 0.9307E-01
-0.2282E-01 -0.1232E+00 -0.1401E+00 -0.6189E-01
0.5863E-01 0.1403E+00 0.1291E+00 0.3546E-01
-0.7056E-01 -0.1015E+00 0.1005E-04 -0.1005E-04
0.1015E+00 0.7056E-01 -0.3546E-01 -0.1291E+00
-0.1403E+00 -0.5863E-01 0.6189E-01 0.1401E+00
0.1232E+00 0.2282E-01 -0.9307E-01 -0.1459E+00
-0.9995E-01 0.1374E-01 0.1181E+00 0.1425E+00
0.7034E-01 -0.4945E-01 -0.1357E+00 -0.1301E+00
-0.3631E-01 0.8206E-01 0.1448E+00 0.1095E+00
0.0000E+00 -0.1095E+00 -0.1448E+00 -0.8206E-01
0.3631E-01 0.1301E+00 0.1357E+00 0.4945E-01
-0.7034E-01 -0.1425E+00 -0.1181E+00 -0.1374E-01
0.9995E-01 0.1459E+00 0.9307E-01 -0.2282E-01
-0.1232E+00 -0.1401E+00 -0.6189E-01 0.5863E-01
0.1403E+00 0.1291E+00 0.3546E-01 -0.7056E-01
-0.1015E+00 0.1005E-04

Nodal rotation about transverse axis for the 16th mode of floating structure

0.2218E+00 0.2002E+00 0.9776E-01 -0.5053E-01
-0.1477E+00 -0.1257E+00 -0.4452E-02 0.1210E+00
0.1531E+00 0.6680E-01 -0.7119E-01 -0.1540E+00
-0.1176E+00 0.9852E-02 0.1297E+00 0.1492E+00
0.5312E-01 -0.8404E-01 -0.1561E+00 -0.1074E+00
0.2454E-01 0.1374E+00 0.1439E+00 0.3900E-01
-0.9612E-01 -0.1568E+00 -0.9612E-01 0.3900E-01
0.1439E+00 0.1374E+00 0.2454E-01 -0.1074E+00
-0.1561E+00 -0.8404E-01 0.5312E-01 0.1492E+00
0.1297E+00 0.9852E-02 -0.1176E+00 -0.1540E+00
-0.7119E-01 0.6680E-01 0.1531E+00 0.1210E+00
-0.4452E-02 -0.1257E+00 -0.1477E+00 -0.5053E-01
0.9776E-01 0.2002E+00 0.2218E+00 0.2218E+00
0.2002E+00 0.9776E-01 -0.5053E-01 -0.1477E+00
-0.1257E+00 -0.4452E-02 0.1210E+00 0.1531E+00
0.6680E-01 -0.7119E-01 -0.1540E+00 -0.1176E+00
0.9852E-02 0.1297E+00 0.1492E+00 0.5312E-01
-0.8404E-01 -0.1561E+00 -0.1074E+00 0.2454E-01
0.1374E+00 0.1439E+00 0.3900E-01 -0.9612E-01
-0.1568E+00 -0.9612E-01 0.3900E-01 0.1439E+00
0.1374E+00 0.2454E-01 -0.1074E+00 -0.1561E+00
-0.8404E-01 0.5312E-01 0.1492E+00 0.1297E+00
0.9852E-02 -0.1176E+00 -0.1540E+00 -0.7119E-01
0.6680E-01 0.1531E+00 0.1210E+00 -0.4452E-02
-0.1257E+00 -0.1477E+00 -0.5053E-01 0.9776E-01
0.2002E+00 0.2218E+00

Appendix E: Output file for landing beam-floating beam-water interaction system in 2D fluid domain

****
Output file for Program MMFBEP
Unit system: m for displacement and coordinate,
m/s for velocity, m/s**2 for acceleration,
s for time, N for force and N/m**2 for pressure.
****

Time step 200, Time= 1.00s
Displacement distribution of landing structure:

X	Y	WZ2
-0.5000	-0.0500	-0.0320
-0.4500	-0.0500	-0.0310
-0.4000	-0.0500	-0.0301
-0.3500	-0.0500	-0.0292
-0.3000	-0.0500	-0.0283
-0.2500	-0.0500	-0.0275
-0.2000	-0.0500	-0.0267
-0.1500	-0.0500	-0.0261
-0.1000	-0.0500	-0.0255
-0.0500	-0.0500	-0.0252
0.0000	-0.0500	-0.0251
0.0500	-0.0500	-0.0252
0.1000	-0.0500	-0.0255
0.1500	-0.0500	-0.0261
0.2000	-0.0500	-0.0267
0.2500	-0.0500	-0.0275
0.3000	-0.0500	-0.0283
0.3500	-0.0500	-0.0292
0.4000	-0.0500	-0.0301
0.4500	-0.0500	-0.0310
0.5000	-0.0500	-0.0320
-0.5000	0.0500	-0.0320
-0.4500	0.0500	-0.0310
-0.4000	0.0500	-0.0301
-0.3500	0.0500	-0.0292
-0.3000	0.0500	-0.0283
-0.2500	0.0500	-0.0275
-0.2000	0.0500	-0.0267
-0.1500	0.0500	-0.0261
-0.1000	0.0500	-0.0255
-0.0500	0.0500	-0.0252
0.0000	0.0500	-0.0251
0.0500	0.0500	-0.0252
0.1000	0.0500	-0.0255
0.1500	0.0500	-0.0261
0.2000	0.0500	-0.0267
0.2500	0.0500	-0.0275
0.3000	0.0500	-0.0283
0.3500	0.0500	-0.0292
0.4000	0.0500	-0.0301
0.4500	0.0500	-0.0310
0.5000	0.0500	-0.0320

Displacement distribution of floating structure:

X	Y	W1
-7.5000	-0.5000	0.0024
-7.2000	-0.5000	0.0022
-6.9000	-0.5000	0.0021
-6.6000	-0.5000	0.0020
-6.3000	-0.5000	0.0020
-6.0000	-0.5000	0.0021
-5.7000	-0.5000	0.0023
-5.4000	-0.5000	0.0025
-5.1000	-0.5000	0.0026
-4.8000	-0.5000	0.0024
-4.5000	-0.5000	0.0017
-4.2000	-0.5000	0.0008
-3.9000	-0.5000	-0.0004
-3.6000	-0.5000	-0.0013
-3.3000	-0.5000	-0.0021
-3.0000	-0.5000	-0.0027
-2.7000	-0.5000	-0.0034
-2.4000	-0.5000	-0.0046
-2.1000	-0.5000	-0.0064
-1.8000	-0.5000	-0.0089
-1.5000	-0.5000	-0.0114
-1.2000	-0.5000	-0.0133

-0.9000	-0.5000	-0.0138
-0.6000	-0.5000	-0.0127
-0.3000	-0.5000	-0.0099
0.0000	-0.5000	-0.0060
0.3000	-0.5000	-0.0018
0.6000	-0.5000	0.0022
0.9000	-0.5000	0.0052
1.2000	-0.5000	0.0072
1.5000	-0.5000	0.0080
1.8000	-0.5000	0.0077
2.1000	-0.5000	0.0066
2.4000	-0.5000	0.0049
2.7000	-0.5000	0.0028
3.0000	-0.5000	0.0009
3.3000	-0.5000	-0.0006
3.6000	-0.5000	-0.0014
3.9000	-0.5000	-0.0015
4.2000	-0.5000	-0.0011
4.5000	-0.5000	-0.0003
4.8000	-0.5000	0.0004
5.1000	-0.5000	0.0011
5.4000	-0.5000	0.0015
5.7000	-0.5000	0.0017
6.0000	-0.5000	0.0017
6.3000	-0.5000	0.0014
6.6000	-0.5000	0.0008
6.9000	-0.5000	0.0000
7.2000	-0.5000	-0.0011
7.5000	-0.5000	-0.0022
-7.5000	0.5000	0.0024
-7.2000	0.5000	0.0022
-6.9000	0.5000	0.0021
-6.6000	0.5000	0.0020
-6.3000	0.5000	0.0020
-6.0000	0.5000	0.0021
-5.7000	0.5000	0.0023
-5.4000	0.5000	0.0025
-5.1000	0.5000	0.0026
-4.8000	0.5000	0.0024
-4.5000	0.5000	0.0017
-4.2000	0.5000	0.0008
-3.9000	0.5000	-0.0004
-3.6000	0.5000	-0.0013
-3.3000	0.5000	-0.0021
-3.0000	0.5000	-0.0027
-2.7000	0.5000	-0.0034
-2.4000	0.5000	-0.0046
-2.1000	0.5000	-0.0064
-1.8000	0.5000	-0.0089
-1.5000	0.5000	-0.0114
-1.2000	0.5000	-0.0133
-0.9000	0.5000	-0.0138
-0.6000	0.5000	-0.0127
-0.3000	0.5000	-0.0099
0.0000	0.5000	-0.0060
0.3000	0.5000	-0.0018
0.6000	0.5000	0.0022
0.9000	0.5000	0.0052
1.2000	0.5000	0.0072
1.5000	0.5000	0.0080
1.8000	0.5000	0.0077
2.1000	0.5000	0.0066
2.4000	0.5000	0.0049
2.7000	0.5000	0.0028
3.0000	0.5000	0.0009
3.3000	0.5000	-0.0006
3.6000	0.5000	-0.0014
3.9000	0.5000	-0.0015
4.2000	0.5000	-0.0011
4.5000	0.5000	-0.0003
4.8000	0.5000	0.0004
5.1000	0.5000	0.0011
5.4000	0.5000	0.0015
5.7000	0.5000	0.0017
6.0000	0.5000	0.0017
6.3000	0.5000	0.0014
6.6000	0.5000	0.0008
6.9000	0.5000	0.0000
7.2000	0.5000	-0.0011
7.5000	0.5000	-0.0022

Water pressure distribution along floating structure:

X	Y	PD
-7.3500	0.0000	-2.4237
-7.0500	0.0000	8.5607
-6.7500	0.0000	4.2947
-6.4500	0.0000	-9.2520
-6.1500	0.0000	-22.7722
-5.8500	0.0000	-24.9780

-5.5500	0.0000	-10.6159
-5.2500	0.0000	14.7009
-4.9500	0.0000	35.7017
-4.6500	0.0000	37.7293
-4.3500	0.0000	16.2461
-4.0500	0.0000	-18.1613
-3.7500	0.0000	-45.4382
-3.4500	0.0000	-48.3286
-3.1500	0.0000	-23.2726
-2.8500	0.0000	17.3703
-2.5500	0.0000	53.0071
-2.2500	0.0000	67.6320
-1.9500	0.0000	59.0971
-1.6500	0.0000	40.1072
-1.3500	0.0000	26.8184
-1.0500	0.0000	30.3775
-0.7500	0.0000	48.0355
-0.4500	0.0000	66.8528
-0.1500	0.0000	73.9326
0.1500	0.0000	64.6798
0.4500	0.0000	45.4453
0.7500	0.0000	28.6650
1.0500	0.0000	22.9711
1.3500	0.0000	27.9907
1.6500	0.0000	34.4103
1.9500	0.0000	31.6156
2.2500	0.0000	14.7821
2.5500	0.0000	-11.1017
2.8500	0.0000	-34.5555
3.1500	0.0000	-44.8178
3.4500	0.0000	-38.4095
3.7500	0.0000	-20.4216
4.0500	0.0000	-1.0538
4.3500	0.0000	11.0388
4.6500	0.0000	13.0575
4.9500	0.0000	8.5985
5.2500	0.0000	4.0992
5.5500	0.0000	3.9493
5.8500	0.0000	7.9387
6.1500	0.0000	11.6574
6.4500	0.0000	9.9485
6.7500	0.0000	1.1354
7.0500	0.0000	-10.1906
7.3500	0.0000	-8.4586

Time step 400, Time= 2.00s

Displacement distribution of landing structure:

X	Y	WZ2
-0.5000	-0.0500	-0.0352
-0.4500	-0.0500	-0.0340
-0.4000	-0.0500	-0.0328
-0.3500	-0.0500	-0.0317
-0.3000	-0.0500	-0.0306
-0.2500	-0.0500	-0.0295
-0.2000	-0.0500	-0.0285
-0.1500	-0.0500	-0.0277
-0.1000	-0.0500	-0.0271
-0.0500	-0.0500	-0.0266
0.0000	-0.0500	-0.0265
0.0500	-0.0500	-0.0266
0.1000	-0.0500	-0.0271
0.1500	-0.0500	-0.0277
0.2000	-0.0500	-0.0285
0.2500	-0.0500	-0.0295
0.3000	-0.0500	-0.0306
0.3500	-0.0500	-0.0317
0.4000	-0.0500	-0.0328
0.4500	-0.0500	-0.0340
0.5000	-0.0500	-0.0352
-0.5000	0.0500	-0.0352
-0.4500	0.0500	-0.0340
-0.4000	0.0500	-0.0328
-0.3500	0.0500	-0.0317
-0.3000	0.0500	-0.0306
-0.2500	0.0500	-0.0295
-0.2000	0.0500	-0.0285
-0.1500	0.0500	-0.0277
-0.1000	0.0500	-0.0271
-0.0500	0.0500	-0.0266
0.0000	0.0500	-0.0265
0.0500	0.0500	-0.0266
0.1000	0.0500	-0.0271
0.1500	0.0500	-0.0277
0.2000	0.0500	-0.0285
0.2500	0.0500	-0.0295
0.3000	0.0500	-0.0306
0.3500	0.0500	-0.0317
0.4000	0.0500	-0.0328
0.4500	0.0500	-0.0340

0.5000	0.0500	−0.0352

Displacement distribution of floating structure:

X	Y	W1
−7.5000	−0.5000	−0.0016
−7.2000	−0.5000	−0.0015
−6.9000	−0.5000	−0.0015
−6.6000	−0.5000	−0.0015
−6.3000	−0.5000	−0.0017
−6.0000	−0.5000	−0.0018
−5.7000	−0.5000	−0.0019
−5.4000	−0.5000	−0.0017
−5.1000	−0.5000	−0.0014
−4.8000	−0.5000	−0.0010
−4.5000	−0.5000	−0.0007
−4.2000	−0.5000	−0.0004
−3.9000	−0.5000	−0.0001
−3.6000	−0.5000	0.0001
−3.3000	−0.5000	0.0002
−3.0000	−0.5000	0.0004
−2.7000	−0.5000	0.0005
−2.4000	−0.5000	0.0007
−2.1000	−0.5000	0.0008
−1.8000	−0.5000	0.0010
−1.5000	−0.5000	0.0009
−1.2000	−0.5000	0.0003
−0.9000	−0.5000	−0.0012
−0.6000	−0.5000	−0.0036
−0.3000	−0.5000	−0.0070
0.0000	−0.5000	−0.0108
0.3000	−0.5000	−0.0141
0.6000	−0.5000	−0.0163
0.9000	−0.5000	−0.0168
1.2000	−0.5000	−0.0156
1.5000	−0.5000	−0.0132
1.8000	−0.5000	−0.0101
2.1000	−0.5000	−0.0070
2.4000	−0.5000	−0.0043
2.7000	−0.5000	−0.0021
3.0000	−0.5000	−0.0003
3.3000	−0.5000	0.0012
3.6000	−0.5000	0.0025
3.9000	−0.5000	0.0036
4.2000	−0.5000	0.0045
4.5000	−0.5000	0.0052
4.8000	−0.5000	0.0056
5.1000	−0.5000	0.0057
5.4000	−0.5000	0.0056
5.7000	−0.5000	0.0052
6.0000	−0.5000	0.0042
6.3000	−0.5000	0.0027
6.6000	−0.5000	0.0004
6.9000	−0.5000	−0.0023
7.2000	−0.5000	−0.0055
7.5000	−0.5000	−0.0087
−7.5000	0.5000	−0.0016
−7.2000	0.5000	−0.0015
−6.9000	0.5000	−0.0015
−6.6000	0.5000	−0.0015
−6.3000	0.5000	−0.0017
−6.0000	0.5000	−0.0018
−5.7000	0.5000	−0.0019
−5.4000	0.5000	−0.0017
−5.1000	0.5000	−0.0014
−4.8000	0.5000	−0.0010
−4.5000	0.5000	−0.0007
−4.2000	0.5000	−0.0004
−3.9000	0.5000	−0.0001
−3.6000	0.5000	0.0001
−3.3000	0.5000	0.0002
−3.0000	0.5000	0.0004
−2.7000	0.5000	0.0005
−2.4000	0.5000	0.0007
−2.1000	0.5000	0.0008
−1.8000	0.5000	0.0010
−1.5000	0.5000	0.0009
−1.2000	0.5000	0.0003
−0.9000	0.5000	−0.0012
−0.6000	0.5000	−0.0036
−0.3000	0.5000	−0.0070
0.0000	0.5000	−0.0108
0.3000	0.5000	−0.0141
0.6000	0.5000	−0.0163
0.9000	0.5000	−0.0168
1.2000	0.5000	−0.0156
1.5000	0.5000	−0.0132
1.8000	0.5000	−0.0101
2.1000	0.5000	−0.0070
2.4000	0.5000	−0.0043

2.7000	0.5000	-0.0021
3.0000	0.5000	-0.0003
3.3000	0.5000	0.0012
3.6000	0.5000	0.0025
3.9000	0.5000	0.0036
4.2000	0.5000	0.0045
4.5000	0.5000	0.0052
4.8000	0.5000	0.0056
5.1000	0.5000	0.0057
5.4000	0.5000	0.0056
5.7000	0.5000	0.0052
6.0000	0.5000	0.0042
6.3000	0.5000	0.0027
6.6000	0.5000	0.0004
6.9000	0.5000	-0.0023
7.2000	0.5000	-0.0055
7.5000	0.5000	-0.0087

Water pressure distribution along floating structure:

X	Y	PD
-7.3500	0.0000	2.8397
-7.0500	0.0000	-0.6604
-6.7500	0.0000	1.8334
-6.4500	0.0000	5.3955
-6.1500	0.0000	5.8057
-5.8500	0.0000	1.6646
-5.5500	0.0000	-5.6159
-5.2500	0.0000	-11.9057
-4.9500	0.0000	-12.5446
-4.6500	0.0000	-5.7906
-4.3500	0.0000	5.8036
-4.0500	0.0000	15.4963
-3.7500	0.0000	17.5203
-3.4500	0.0000	9.1459
-3.1500	0.0000	-6.0319
-2.8500	0.0000	-20.7385
-2.5500	0.0000	-27.8658
-2.2500	0.0000	-24.2675
-1.9500	0.0000	-12.2284
-1.6500	0.0000	4.5249
-1.3500	0.0000	20.8280
-1.0500	0.0000	36.3089
-0.7500	0.0000	51.4036
-0.4500	0.0000	65.5919
-0.1500	0.0000	77.2009
0.1500	0.0000	83.2829
0.4500	0.0000	81.3987
0.7500	0.0000	73.3725
1.0500	0.0000	62.9643
1.3500	0.0000	54.7260
1.6500	0.0000	50.1961
1.9500	0.0000	46.2277
2.2500	0.0000	37.7771
2.5500	0.0000	23.1919
2.8500	0.0000	5.5786
3.1500	0.0000	-8.6757
3.4500	0.0000	-13.2901
3.7500	0.0000	-8.5521
4.0500	0.0000	-0.6243
4.3500	0.0000	2.0854
4.6500	0.0000	-3.9104
4.9500	0.0000	-14.4052
5.2500	0.0000	-19.0194
5.5500	0.0000	-10.0026
5.8500	0.0000	11.2542
6.1500	0.0000	32.0133
6.4500	0.0000	35.0597
6.7500	0.0000	13.4175
7.0500	0.0000	-20.9791
7.3500	0.0000	-19.2223

Time step 600, Time= 3.00s

Displacement distribution of landing structure:

X	Y	WZ2
-0.5000	-0.0500	-0.0256
-0.4500	-0.0500	-0.0244
-0.4000	-0.0500	-0.0233
-0.3500	-0.0500	-0.0222
-0.3000	-0.0500	-0.0212
-0.2500	-0.0500	-0.0202
-0.2000	-0.0500	-0.0192
-0.1500	-0.0500	-0.0184
-0.1000	-0.0500	-0.0178
-0.0500	-0.0500	-0.0174
0.0000	-0.0500	-0.0172
0.0500	-0.0500	-0.0174
0.1000	-0.0500	-0.0178
0.1500	-0.0500	-0.0184
0.2000	-0.0500	-0.0192

0.2500	−0.0500	−0.0202
0.3000	−0.0500	−0.0212
0.3500	−0.0500	−0.0222
0.4000	−0.0500	−0.0233
0.4500	−0.0500	−0.0244
0.5000	−0.0500	−0.0256
−0.5000	0.0500	−0.0256
−0.4500	0.0500	−0.0244
−0.4000	0.0500	−0.0233
−0.3500	0.0500	−0.0222
−0.3000	0.0500	−0.0212
−0.2500	0.0500	−0.0202
−0.2000	0.0500	−0.0192
−0.1500	0.0500	−0.0184
−0.1000	0.0500	−0.0178
−0.0500	0.0500	−0.0174
0.0000	0.0500	−0.0172
0.0500	0.0500	−0.0174
0.1000	0.0500	−0.0178
0.1500	0.0500	−0.0184
0.2000	0.0500	−0.0192
0.2500	0.0500	−0.0202
0.3000	0.0500	−0.0212
0.3500	0.0500	−0.0222
0.4000	0.0500	−0.0233
0.4500	0.0500	−0.0244
0.5000	0.0500	−0.0256

Displacement distribution of floating structure:

X	Y	W1
−7.5000	−0.5000	0.0000
−7.2000	−0.5000	0.0000
−6.9000	−0.5000	0.0002
−6.6000	−0.5000	0.0005
−6.3000	−0.5000	0.0009
−6.0000	−0.5000	0.0012
−5.7000	−0.5000	0.0013
−5.4000	−0.5000	0.0010
−5.1000	−0.5000	0.0005
−4.8000	−0.5000	0.0002
−4.5000	−0.5000	0.0002
−4.2000	−0.5000	0.0004
−3.9000	−0.5000	0.0006
−3.6000	−0.5000	0.0005
−3.3000	−0.5000	0.0003
−3.0000	−0.5000	−0.0001
−2.7000	−0.5000	−0.0003
−2.4000	−0.5000	0.0001
−2.1000	−0.5000	0.0008
−1.8000	−0.5000	0.0017
−1.5000	−0.5000	0.0024
−1.2000	−0.5000	0.0025
−0.9000	−0.5000	0.0020
−0.6000	−0.5000	0.0012
−0.3000	−0.5000	0.0001
0.0000	−0.5000	−0.0011
0.3000	−0.5000	−0.0025
0.6000	−0.5000	−0.0041
0.9000	−0.5000	−0.0058
1.2000	−0.5000	−0.0072
1.5000	−0.5000	−0.0082
1.8000	−0.5000	−0.0083
2.1000	−0.5000	−0.0078
2.4000	−0.5000	−0.0068
2.7000	−0.5000	−0.0058
3.0000	−0.5000	−0.0050
3.3000	−0.5000	−0.0046
3.6000	−0.5000	−0.0045
3.9000	−0.5000	−0.0047
4.2000	−0.5000	−0.0051
4.5000	−0.5000	−0.0058
4.8000	−0.5000	−0.0066
5.1000	−0.5000	−0.0071
5.4000	−0.5000	−0.0072
5.7000	−0.5000	−0.0063
6.0000	−0.5000	−0.0047
6.3000	−0.5000	−0.0025
6.6000	−0.5000	−0.0001
6.9000	−0.5000	0.0021
7.2000	−0.5000	0.0041
7.5000	−0.5000	0.0060
−7.5000	0.5000	0.0000
−7.2000	0.5000	0.0000
−6.9000	0.5000	0.0002
−6.6000	0.5000	0.0005
−6.3000	0.5000	0.0009
−6.0000	0.5000	0.0012
−5.7000	0.5000	0.0013
−5.4000	0.5000	0.0010

-5.1000	0.5000	0.0005
-4.8000	0.5000	0.0002
-4.5000	0.5000	0.0002
-4.2000	0.5000	0.0004
-3.9000	0.5000	0.0006
-3.6000	0.5000	0.0005
-3.3000	0.5000	0.0003
-3.0000	0.5000	-0.0001
-2.7000	0.5000	-0.0003
-2.4000	0.5000	0.0001
-2.1000	0.5000	0.0008
-1.8000	0.5000	0.0017
-1.5000	0.5000	0.0024
-1.2000	0.5000	0.0025
-0.9000	0.5000	0.0020
-0.6000	0.5000	0.0012
-0.3000	0.5000	0.0001
0.0000	0.5000	-0.0011
0.3000	0.5000	-0.0025
0.6000	0.5000	-0.0041
0.9000	0.5000	-0.0058
1.2000	0.5000	-0.0072
1.5000	0.5000	-0.0082
1.8000	0.5000	-0.0083
2.1000	0.5000	-0.0078
2.4000	0.5000	-0.0068
2.7000	0.5000	-0.0058
3.0000	0.5000	-0.0050
3.3000	0.5000	-0.0046
3.6000	0.5000	-0.0045
3.9000	0.5000	-0.0047
4.2000	0.5000	-0.0051
4.5000	0.5000	-0.0058
4.8000	0.5000	-0.0066
5.1000	0.5000	-0.0071
5.4000	0.5000	-0.0072
5.7000	0.5000	-0.0063
6.0000	0.5000	-0.0047
6.3000	0.5000	-0.0025
6.6000	0.5000	-0.0001
6.9000	0.5000	0.0021
7.2000	0.5000	0.0041
7.5000	0.5000	0.0060

Water pressure distribution along floating structure:

X	Y	PD
-7.3500	0.0000	22.0273
-7.0500	0.0000	-12.9620
-6.7500	0.0000	-32.9776
-6.4500	0.0000	-19.7380
-6.1500	0.0000	14.7840
-5.8500	0.0000	42.1712
-5.5500	0.0000	39.0798
-5.2500	0.0000	5.4588
-4.9500	0.0000	-34.3938
-4.6500	0.0000	-50.2308
-4.3500	0.0000	-28.3233
-4.0500	0.0000	16.3478
-3.7500	0.0000	51.8142
-3.4500	0.0000	50.7805
-3.1500	0.0000	11.5274
-2.8500	0.0000	-40.2656
-2.5500	0.0000	-69.7906
-2.2500	0.0000	-57.1782
-1.9500	0.0000	-11.2758
-1.6500	0.0000	39.0646
-1.3500	0.0000	62.0588
-1.0500	0.0000	48.0701
-0.7500	0.0000	10.8423
-0.4500	0.0000	-23.4813
-0.1500	0.0000	-33.5089
0.1500	0.0000	-16.6004
0.4500	0.0000	15.9560
0.7500	0.0000	49.0705
1.0500	0.0000	74.9549
1.3500	0.0000	95.4461
1.6500	0.0000	112.8290
1.9500	0.0000	122.6541
2.2500	0.0000	113.8572
2.5500	0.0000	81.3280
2.8500	0.0000	32.3221
3.1500	0.0000	-11.9347
3.4500	0.0000	-27.9486
3.7500	0.0000	-8.7785
4.0500	0.0000	28.8922
4.3500	0.0000	54.1497
4.6500	0.0000	42.8528
4.9500	0.0000	-2.9248
5.2500	0.0000	-55.0935

5.5500	0.0000	-78.1239
5.8500	0.0000	-53.3323
6.1500	0.0000	4.2773
6.4500	0.0000	54.7422
6.7500	0.0000	61.8439
7.0500	0.0000	16.9444
7.3500	0.0000	-39.2756

Time step 800, Time= 4.00s

Displacement distribution of landing structure:

X	Y	WZ2
-0.5000	-0.0500	-0.0279
-0.4500	-0.0500	-0.0267
-0.4000	-0.0500	-0.0256
-0.3500	-0.0500	-0.0245
-0.3000	-0.0500	-0.0235
-0.2500	-0.0500	-0.0225
-0.2000	-0.0500	-0.0215
-0.1500	-0.0500	-0.0208
-0.1000	-0.0500	-0.0201
-0.0500	-0.0500	-0.0197
0.0000	-0.0500	-0.0196
0.0500	-0.0500	-0.0197
0.1000	-0.0500	-0.0201
0.1500	-0.0500	-0.0208
0.2000	-0.0500	-0.0215
0.2500	-0.0500	-0.0225
0.3000	-0.0500	-0.0235
0.3500	-0.0500	-0.0245
0.4000	-0.0500	-0.0256
0.4500	-0.0500	-0.0267
0.5000	-0.0500	-0.0279
-0.5000	0.0500	-0.0279
-0.4500	0.0500	-0.0267
-0.4000	0.0500	-0.0256
-0.3500	0.0500	-0.0245
-0.3000	0.0500	-0.0235
-0.2500	0.0500	-0.0225
-0.2000	0.0500	-0.0215
-0.1500	0.0500	-0.0208
-0.1000	0.0500	-0.0201
-0.0500	0.0500	-0.0197
0.0000	0.0500	-0.0196
0.0500	0.0500	-0.0197
0.1000	0.0500	-0.0201
0.1500	0.0500	-0.0208
0.2000	0.0500	-0.0215
0.2500	0.0500	-0.0225
0.3000	0.0500	-0.0235
0.3500	0.0500	-0.0245
0.4000	0.0500	-0.0256
0.4500	0.0500	-0.0267
0.5000	0.0500	-0.0279

Displacement distribution of floating structure:

X	Y	W1
-7.5000	-0.5000	-0.0031
-7.2000	-0.5000	-0.0015
-6.9000	-0.5000	0.0000
-6.6000	-0.5000	0.0014
-6.3000	-0.5000	0.0024
-6.0000	-0.5000	0.0027
-5.7000	-0.5000	0.0025
-5.4000	-0.5000	0.0018
-5.1000	-0.5000	0.0008
-4.8000	-0.5000	0.0001
-4.5000	-0.5000	-0.0002
-4.2000	-0.5000	0.0000
-3.9000	-0.5000	0.0005
-3.6000	-0.5000	0.0010
-3.3000	-0.5000	0.0011
-3.0000	-0.5000	0.0009
-2.7000	-0.5000	0.0005
-2.4000	-0.5000	0.0002
-2.1000	-0.5000	0.0002
-1.8000	-0.5000	0.0006
-1.5000	-0.5000	0.0012
-1.2000	-0.5000	0.0018
-0.9000	-0.5000	0.0020
-0.6000	-0.5000	0.0019
-0.3000	-0.5000	0.0016
0.0000	-0.5000	0.0010
0.3000	-0.5000	0.0002
0.6000	-0.5000	-0.0009
0.9000	-0.5000	-0.0024
1.2000	-0.5000	-0.0044
1.5000	-0.5000	-0.0066
1.8000	-0.5000	-0.0085
2.1000	-0.5000	-0.0097

2.4000	−0.5000	−0.0097
2.7000	−0.5000	−0.0083
3.0000	−0.5000	−0.0060
3.3000	−0.5000	−0.0031
3.6000	−0.5000	−0.0003
3.9000	−0.5000	0.0019
4.2000	−0.5000	0.0034
4.5000	−0.5000	0.0041
4.8000	−0.5000	0.0042
5.1000	−0.5000	0.0038
5.4000	−0.5000	0.0031
5.7000	−0.5000	0.0021
6.0000	−0.5000	0.0009
6.3000	−0.5000	−0.0004
6.6000	−0.5000	−0.0017
6.9000	−0.5000	−0.0029
7.2000	−0.5000	−0.0041
7.5000	−0.5000	−0.0053
−7.5000	0.5000	−0.0031
−7.2000	0.5000	−0.0015
−6.9000	0.5000	0.0000
−6.6000	0.5000	0.0014
−6.3000	0.5000	0.0024
−6.0000	0.5000	0.0027
−5.7000	0.5000	0.0025
−5.4000	0.5000	0.0018
−5.1000	0.5000	0.0008
−4.8000	0.5000	0.0001
−4.5000	0.5000	−0.0002
−4.2000	0.5000	0.0000
−3.9000	0.5000	0.0005
−3.6000	0.5000	0.0010
−3.3000	0.5000	0.0011
−3.0000	0.5000	0.0009
−2.7000	0.5000	0.0005
−2.4000	0.5000	0.0002
−2.1000	0.5000	0.0002
−1.8000	0.5000	0.0006
−1.5000	0.5000	0.0012
−1.2000	0.5000	0.0018
−0.9000	0.5000	0.0020
−0.6000	0.5000	0.0019
−0.3000	0.5000	0.0016
0.0000	0.5000	0.0010
0.3000	0.5000	0.0002
0.6000	0.5000	−0.0009
0.9000	0.5000	−0.0024
1.2000	0.5000	−0.0044
1.5000	0.5000	−0.0066
1.8000	0.5000	−0.0085
2.1000	0.5000	−0.0097
2.4000	0.5000	−0.0097
2.7000	0.5000	−0.0083
3.0000	0.5000	−0.0060
3.3000	0.5000	−0.0031
3.6000	0.5000	−0.0003
3.9000	0.5000	0.0019
4.2000	0.5000	0.0034
4.5000	0.5000	0.0041
4.8000	0.5000	0.0042
5.1000	0.5000	0.0038
5.4000	0.5000	0.0031
5.7000	0.5000	0.0021
6.0000	0.5000	0.0009
6.3000	0.5000	−0.0004
6.6000	0.5000	−0.0017
6.9000	0.5000	−0.0029
7.2000	0.5000	−0.0041
7.5000	0.5000	−0.0053

Water pressure distribution along floating structure:

X	Y	PD
−7.3500	0.0000	−6.1802
−7.0500	0.0000	−25.7944
−6.7500	0.0000	−12.8040
−6.4500	0.0000	16.6712
−6.1500	0.0000	44.6611
−5.8500	0.0000	52.8145
−5.5500	0.0000	32.0132
−5.2500	0.0000	−9.4234
−4.9500	0.0000	−49.1233
−4.6500	0.0000	−63.6386
−4.3500	0.0000	−43.6604
−4.0500	0.0000	−1.1233
−3.7500	0.0000	38.9930
−3.4500	0.0000	53.2325
−3.1500	0.0000	34.6281
−2.8500	0.0000	−2.7572
−2.5500	0.0000	−35.0227

-2.2500	0.0000	-43.6785
-1.9500	0.0000	-27.0159
-1.6500	0.0000	2.1602
-1.3500	0.0000	23.6318
-1.0500	0.0000	26.5704
-0.7500	0.0000	13.5590
-0.4500	0.0000	-4.2565
-0.1500	0.0000	-13.5717
0.1500	0.0000	-10.0059
0.4500	0.0000	3.7082
0.7500	0.0000	20.8163
1.0500	0.0000	36.4602
1.3500	0.0000	51.7935
1.6500	0.0000	69.3636
1.9500	0.0000	87.2512
2.2500	0.0000	98.4960
2.5500	0.0000	96.7273
2.8500	0.0000	79.5533
3.1500	0.0000	52.5459
3.4500	0.0000	28.3386
3.7500	0.0000	15.6613
4.0500	0.0000	16.5749
4.3500	0.0000	22.2378
4.6500	0.0000	22.1750
4.9500	0.0000	11.8670
5.2500	0.0000	-5.5621
5.5500	0.0000	-19.8959
5.8500	0.0000	-22.2147
6.1500	0.0000	-12.2530
6.4500	0.0000	1.4176
6.7500	0.0000	9.8331
7.0500	0.0000	5.4240
7.3500	0.0000	-8.7133

Time step 1000, Time= 5.00s

Displacement distribution of landing structure:

X	Y	WZ2
-0.5000	-0.0500	-0.0280
-0.4500	-0.0500	-0.0269
-0.4000	-0.0500	-0.0257
-0.3500	-0.0500	-0.0246
-0.3000	-0.0500	-0.0235
-0.2500	-0.0500	-0.0225
-0.2000	-0.0500	-0.0216
-0.1500	-0.0500	-0.0208
-0.1000	-0.0500	-0.0202
-0.0500	-0.0500	-0.0197
0.0000	-0.0500	-0.0196
0.0500	-0.0500	-0.0197
0.1000	-0.0500	-0.0202
0.1500	-0.0500	-0.0208
0.2000	-0.0500	-0.0216
0.2500	-0.0500	-0.0225
0.3000	-0.0500	-0.0235
0.3500	-0.0500	-0.0246
0.4000	-0.0500	-0.0257
0.4500	-0.0500	-0.0269
0.5000	-0.0500	-0.0280
-0.5000	0.0500	-0.0280
-0.4500	0.0500	-0.0269
-0.4000	0.0500	-0.0257
-0.3500	0.0500	-0.0246
-0.3000	0.0500	-0.0235
-0.2500	0.0500	-0.0225
-0.2000	0.0500	-0.0216
-0.1500	0.0500	-0.0208
-0.1000	0.0500	-0.0202
-0.0500	0.0500	-0.0197
0.0000	0.0500	-0.0196
0.0500	0.0500	-0.0197
0.1000	0.0500	-0.0202
0.1500	0.0500	-0.0208
0.2000	0.0500	-0.0216
0.2500	0.0500	-0.0225
0.3000	0.0500	-0.0235
0.3500	0.0500	-0.0246
0.4000	0.0500	-0.0257
0.4500	0.0500	-0.0269
0.5000	0.0500	-0.0280

Displacement distribution of floating structure:

X	Y	W1
-7.5000	-0.5000	-0.0006
-7.2000	-0.5000	-0.0003
-6.9000	-0.5000	0.0000
-6.6000	-0.5000	0.0001
-6.3000	-0.5000	0.0000
-6.0000	-0.5000	0.0000
-5.7000	-0.5000	0.0001

−5.4000	−0.5000	0.0003	−7.5000	0.5000	−0.0006
−5.1000	−0.5000	0.0007	−7.2000	0.5000	−0.0003
−4.8000	−0.5000	0.0011	−6.9000	0.5000	0.0000
−4.5000	−0.5000	0.0013	−6.6000	0.5000	0.0001
−4.2000	−0.5000	0.0013	−6.3000	0.5000	0.0000
−3.9000	−0.5000	0.0011	−6.0000	0.5000	0.0000
−3.6000	−0.5000	0.0009	−5.7000	0.5000	0.0001
−3.3000	−0.5000	0.0008	−5.4000	0.5000	0.0003
−3.0000	−0.5000	0.0006	−5.1000	0.5000	0.0007
−2.7000	−0.5000	0.0005	−4.8000	0.5000	0.0011
−2.4000	−0.5000	0.0004	−4.5000	0.5000	0.0013
−2.1000	−0.5000	0.0004	−4.2000	0.5000	0.0013
−1.8000	−0.5000	0.0007	−3.9000	0.5000	0.0011
−1.5000	−0.5000	0.0012	−3.6000	0.5000	0.0009
−1.2000	−0.5000	0.0016	−3.3000	0.5000	0.0008
−0.9000	−0.5000	0.0019	−3.0000	0.5000	0.0006
−0.6000	−0.5000	0.0019	−2.7000	0.5000	0.0005
−0.3000	−0.5000	0.0016	−2.4000	0.5000	0.0004
0.0000	−0.5000	0.0012	−2.1000	0.5000	0.0004
0.3000	−0.5000	0.0007	−1.8000	0.5000	0.0007
0.6000	−0.5000	0.0001	−1.5000	0.5000	0.0012
0.9000	−0.5000	−0.0007	−1.2000	0.5000	0.0016
1.2000	−0.5000	−0.0020	−0.9000	0.5000	0.0019
1.5000	−0.5000	−0.0039	−0.6000	0.5000	0.0019
1.8000	−0.5000	−0.0062	−0.3000	0.5000	0.0016
2.1000	−0.5000	−0.0084	0.0000	0.5000	0.0012
2.4000	−0.5000	−0.0097	0.3000	0.5000	0.0007
2.7000	−0.5000	−0.0099	0.6000	0.5000	0.0001
3.0000	−0.5000	−0.0089	0.9000	0.5000	−0.0007
3.3000	−0.5000	−0.0071	1.2000	0.5000	−0.0020
3.6000	−0.5000	−0.0051	1.5000	0.5000	−0.0039
3.9000	−0.5000	−0.0033	1.8000	0.5000	−0.0062
4.2000	−0.5000	−0.0018	2.1000	0.5000	−0.0084
4.5000	−0.5000	−0.0006	2.4000	0.5000	−0.0097
4.8000	−0.5000	0.0005	2.7000	0.5000	−0.0099
5.1000	−0.5000	0.0012	3.0000	0.5000	−0.0089
5.4000	−0.5000	0.0016	3.3000	0.5000	−0.0071
5.7000	−0.5000	0.0015	3.6000	0.5000	−0.0051
6.0000	−0.5000	0.0013	3.9000	0.5000	−0.0033
6.3000	−0.5000	0.0012	4.2000	0.5000	−0.0018
6.6000	−0.5000	0.0018	4.5000	0.5000	−0.0006
6.9000	−0.5000	0.0032	4.8000	0.5000	0.0005
7.2000	−0.5000	0.0053	5.1000	0.5000	0.0012
7.5000	−0.5000	0.0076	5.4000	0.5000	0.0016

5.7000	0.5000	0.0015
6.0000	0.5000	0.0013
6.3000	0.5000	0.0012
6.6000	0.5000	0.0018
6.9000	0.5000	0.0032
7.2000	0.5000	0.0053
7.5000	0.5000	0.0076

Water pressure distribution along floating structure:

X	Y	PD
-7.3500	0.0000	-16.4630
-7.0500	0.0000	4.8514
-6.7500	0.0000	23.3471
-6.4500	0.0000	19.8293
-6.1500	0.0000	-1.5349
-5.8500	0.0000	-23.1048
-5.5500	0.0000	-27.9903
-5.2500	0.0000	-13.1518
-4.9500	0.0000	9.4660
-4.6500	0.0000	23.3906
-4.3500	0.0000	19.9230
-4.0500	0.0000	4.1310
-3.7500	0.0000	-9.1009
-3.4500	0.0000	-9.3624
-3.1500	0.0000	1.5941
-2.8500	0.0000	12.1373
-2.5500	0.0000	10.2035
-2.2500	0.0000	-5.3774
-1.9500	0.0000	-23.5808
-1.6500	0.0000	-27.7373
-1.3500	0.0000	-12.8390
-1.0500	0.0000	12.4419
-0.7500	0.0000	29.6749
-0.4500	0.0000	24.0760
-0.1500	0.0000	-1.4846
0.1500	0.0000	-29.2310
0.4500	0.0000	-36.4958
0.7500	0.0000	-13.4434
1.0500	0.0000	29.9383
1.3500	0.0000	72.7868
1.6500	0.0000	97.0758
1.9500	0.0000	98.7766
2.2500	0.0000	88.4170
2.5500	0.0000	81.4921
2.8500	0.0000	82.2874
3.1500	0.0000	81.3896
3.4500	0.0000	66.4690
3.7500	0.0000	32.6930
4.0500	0.0000	-5.5827
4.3500	0.0000	-26.6005
4.6500	0.0000	-15.6403
4.9500	0.0000	20.8481
5.2500	0.0000	54.5931
5.5500	0.0000	55.7983
5.8500	0.0000	15.8374
6.1500	0.0000	-43.3294
6.4500	0.0000	-81.0878
6.7500	0.0000	-63.2410
7.0500	0.0000	5.1864
7.3500	0.0000	68.1717

Time history of displacement at node NL1:

-0.5962E-03	-0.1542E-02	-0.3101E-02	-0.5128E-02
-0.7074E-02	-0.8852E-02	-0.1072E-01	-0.1265E-01
-0.1456E-01	-0.1612E-01	-0.1708E-01	-0.1773E-01
-0.1816E-01	-0.1829E-01	-0.1800E-01	-0.1719E-01
-0.1603E-01	-0.1479E-01	-0.1351E-01	-0.1207E-01
-0.1057E-01	-0.9081E-02	-0.7838E-02	-0.6973E-02
-0.6336E-02	-0.5949E-02	-0.5875E-02	-0.6195E-02
-0.6954E-02	-0.8042E-02	-0.9300E-02	-0.1073E-01
-0.1236E-01	-0.1410E-01	-0.1586E-01	-0.1749E-01
-0.1890E-01	-0.2014E-01	-0.2115E-01	-0.2188E-01
-0.2226E-01	-0.2225E-01	-0.2194E-01	-0.2139E-01
-0.2059E-01	-0.1957E-01	-0.1838E-01	-0.1711E-01
-0.1588E-01	-0.1475E-01	-0.1371E-01	-0.1285E-01
-0.1223E-01	-0.1190E-01	-0.1189E-01	-0.1216E-01
-0.1271E-01	-0.1352E-01	-0.1458E-01	-0.1584E-01
-0.1722E-01	-0.1865E-01	-0.2006E-01	-0.2143E-01
-0.2268E-01	-0.2375E-01	-0.2459E-01	-0.2516E-01
-0.2547E-01	-0.2551E-01	-0.2527E-01	-0.2479E-01
-0.2408E-01	-0.2322E-01	-0.2224E-01	-0.2122E-01
-0.2019E-01	-0.1922E-01	-0.1837E-01	-0.1769E-01
-0.1723E-01	-0.1699E-01	-0.1700E-01	-0.1727E-01
-0.1779E-01	-0.1854E-01	-0.1948E-01	-0.2058E-01
-0.2178E-01	-0.2303E-01	-0.2429E-01	-0.2548E-01
-0.2657E-01	-0.2749E-01	-0.2823E-01	-0.2875E-01
-0.2903E-01	-0.2907E-01	-0.2887E-01	-0.2845E-01
-0.2785E-01	-0.2711E-01	-0.2625E-01	-0.2534E-01
-0.2442E-01	-0.2355E-01	-0.2278E-01	-0.2214E-01

-0.2167E-01 -0.2140E-01 -0.2134E-01 -0.2150E-01 -0.3484E-01 -0.3523E-01 -0.3563E-01 -0.3602E-01
-0.2188E-01 -0.2245E-01 -0.2320E-01 -0.2408E-01 -0.3639E-01 -0.3672E-01 -0.3700E-01 -0.3721E-01
-0.2507E-01 -0.2611E-01 -0.2716E-01 -0.2817E-01 -0.3736E-01 -0.3742E-01 -0.3742E-01 -0.3733E-01
-0.2910E-01 -0.2991E-01 -0.3057E-01 -0.3105E-01 -0.3718E-01 -0.3698E-01 -0.3673E-01 -0.3644E-01
-0.3134E-01 -0.3143E-01 -0.3133E-01 -0.3104E-01 -0.3615E-01 -0.3585E-01 -0.3557E-01 -0.3531E-01
-0.3059E-01 -0.3001E-01 -0.2934E-01 -0.2861E-01 -0.3510E-01 -0.3495E-01 -0.3485E-01 -0.3482E-01
-0.2787E-01 -0.2716E-01 -0.2651E-01 -0.2597E-01 -0.3485E-01 -0.3495E-01 -0.3510E-01 -0.3530E-01
-0.2557E-01 -0.2532E-01 -0.2525E-01 -0.2535E-01 -0.3553E-01 -0.3579E-01 -0.3606E-01 -0.3632E-01
-0.2564E-01 -0.2608E-01 -0.2668E-01 -0.2739E-01 -0.3657E-01 -0.3679E-01 -0.3697E-01 -0.3710E-01
-0.2818E-01 -0.2903E-01 -0.2988E-01 -0.3071E-01 -0.3718E-01 -0.3720E-01 -0.3716E-01 -0.3707E-01
-0.3147E-01 -0.3213E-01 -0.3266E-01 -0.3305E-01 -0.3693E-01 -0.3676E-01 -0.3656E-01 -0.3634E-01
-0.3327E-01 -0.3333E-01 -0.3322E-01 -0.3295E-01 -0.3612E-01 -0.3592E-01 -0.3573E-01 -0.3558E-01
-0.3256E-01 -0.3205E-01 -0.3146E-01 -0.3083E-01 -0.3547E-01 -0.3541E-01 -0.3541E-01 -0.3546E-01
-0.3019E-01 -0.2958E-01 -0.2903E-01 -0.2857E-01 -0.3556E-01 -0.3571E-01 -0.3590E-01 -0.3611E-01
-0.2823E-01 -0.2803E-01 -0.2799E-01 -0.2809E-01 -0.3635E-01 -0.3658E-01 -0.3681E-01 -0.3702E-01
-0.2835E-01 -0.2876E-01 -0.2929E-01 -0.2992E-01 -0.3719E-01 -0.3731E-01 -0.3739E-01 -0.3740E-01
-0.3063E-01 -0.3138E-01 -0.3214E-01 -0.3287E-01 -0.3735E-01 -0.3725E-01 -0.3708E-01 -0.3686E-01
-0.3354E-01 -0.3414E-01 -0.3462E-01 -0.3497E-01 -0.3660E-01 -0.3630E-01 -0.3598E-01 -0.3565E-01
-0.3519E-01 -0.3526E-01 -0.3518E-01 -0.3498E-01 -0.3533E-01 -0.3503E-01 -0.3476E-01 -0.3453E-01
-0.3465E-01 -0.3423E-01 -0.3374E-01 -0.3320E-01 -0.3436E-01 -0.3423E-01 -0.3418E-01 -0.3418E-01
-0.3265E-01 -0.3211E-01 -0.3162E-01 -0.3121E-01 -0.3424E-01 -0.3436E-01 -0.3453E-01 -0.3474E-01
-0.3088E-01 -0.3067E-01 -0.3058E-01 -0.3062E-01 -0.3498E-01 -0.3524E-01 -0.3550E-01 -0.3576E-01
-0.3079E-01 -0.3108E-01 -0.3148E-01 -0.3197E-01 -0.3600E-01 -0.3621E-01 -0.3638E-01 -0.3651E-01
-0.3252E-01 -0.3311E-01 -0.3372E-01 -0.3431E-01 -0.3660E-01 -0.3663E-01 -0.3661E-01 -0.3655E-01
-0.3487E-01 -0.3535E-01 -0.3576E-01 -0.3606E-01 -0.3645E-01 -0.3631E-01 -0.3614E-01 -0.3596E-01
-0.3625E-01 -0.3633E-01 -0.3628E-01 -0.3613E-01 -0.3577E-01 -0.3557E-01 -0.3539E-01 -0.3523E-01
-0.3588E-01 -0.3554E-01 -0.3515E-01 -0.3472E-01 -0.3509E-01 -0.3498E-01 -0.3490E-01 -0.3485E-01
-0.3427E-01 -0.3383E-01 -0.3343E-01 -0.3308E-01 -0.3484E-01 -0.3485E-01 -0.3489E-01 -0.3494E-01
-0.3281E-01 -0.3263E-01 -0.3255E-01 -0.3257E-01 -0.3500E-01 -0.3507E-01 -0.3513E-01 -0.3518E-01
-0.3269E-01 -0.3291E-01 -0.3321E-01 -0.3358E-01 -0.3520E-01 -0.3521E-01 -0.3518E-01 -0.3511E-01
-0.3401E-01 -0.3446E-01 -0.3492E-01 -0.3537E-01 -0.3501E-01 -0.3488E-01 -0.3471E-01 -0.3452E-01
-0.3578E-01 -0.3613E-01 -0.3641E-01 -0.3661E-01 -0.3430E-01 -0.3406E-01 -0.3382E-01 -0.3357E-01
-0.3671E-01 -0.3671E-01 -0.3661E-01 -0.3643E-01 -0.3333E-01 -0.3310E-01 -0.3290E-01 -0.3272E-01
-0.3616E-01 -0.3583E-01 -0.3544E-01 -0.3503E-01 -0.3257E-01 -0.3246E-01 -0.3238E-01 -0.3234E-01
-0.3460E-01 -0.3419E-01 -0.3381E-01 -0.3348E-01 -0.3233E-01 -0.3235E-01 -0.3240E-01 -0.3247E-01
-0.3322E-01 -0.3304E-01 -0.3294E-01 -0.3293E-01 -0.3254E-01 -0.3262E-01 -0.3270E-01 -0.3277E-01
-0.3302E-01 -0.3318E-01 -0.3343E-01 -0.3374E-01 -0.3282E-01 -0.3285E-01 -0.3285E-01 -0.3282E-01
-0.3409E-01 -0.3447E-01 -0.3486E-01 -0.3524E-01 -0.3276E-01 -0.3267E-01 -0.3255E-01 -0.3241E-01
-0.3559E-01 -0.3590E-01 -0.3614E-01 -0.3632E-01 -0.3224E-01 -0.3206E-01 -0.3187E-01 -0.3168E-01
-0.3641E-01 -0.3643E-01 -0.3636E-01 -0.3622E-01 -0.3149E-01 -0.3131E-01 -0.3114E-01 -0.3100E-01
-0.3601E-01 -0.3574E-01 -0.3543E-01 -0.3510E-01 -0.3088E-01 -0.3080E-01 -0.3074E-01 -0.3071E-01
-0.3477E-01 -0.3444E-01 -0.3415E-01 -0.3390E-01 -0.3071E-01 -0.3074E-01 -0.3079E-01 -0.3086E-01
-0.3371E-01 -0.3359E-01 -0.3355E-01 -0.3358E-01 -0.3094E-01 -0.3102E-01 -0.3111E-01 -0.3119E-01
-0.3370E-01 -0.3390E-01 -0.3416E-01 -0.3448E-01 -0.3127E-01 -0.3132E-01 -0.3135E-01 -0.3136E-01

-0.3135E-01 -0.3131E-01 -0.3124E-01 -0.3114E-01 -0.2603E-01 -0.2605E-01 -0.2608E-01 -0.2609E-01
-0.3103E-01 -0.3089E-01 -0.3074E-01 -0.3058E-01 -0.2611E-01 -0.2613E-01 -0.2614E-01 -0.2615E-01
-0.3041E-01 -0.3024E-01 -0.3008E-01 -0.2992E-01 -0.2615E-01 -0.2615E-01 -0.2615E-01 -0.2615E-01
-0.2978E-01 -0.2965E-01 -0.2955E-01 -0.2946E-01 -0.2614E-01 -0.2612E-01 -0.2610E-01 -0.2607E-01
-0.2939E-01 -0.2934E-01 -0.2931E-01 -0.2930E-01 -0.2604E-01 -0.2600E-01 -0.2595E-01 -0.2590E-01
-0.2929E-01 -0.2930E-01 -0.2932E-01 -0.2934E-01 -0.2584E-01 -0.2577E-01 -0.2570E-01 -0.2563E-01
-0.2936E-01 -0.2938E-01 -0.2939E-01 -0.2939E-01 -0.2556E-01 -0.2549E-01 -0.2541E-01 -0.2535E-01
-0.2938E-01 -0.2937E-01 -0.2934E-01 -0.2930E-01 -0.2529E-01 -0.2523E-01 -0.2518E-01 -0.2514E-01
-0.2926E-01 -0.2921E-01 -0.2915E-01 -0.2909E-01 -0.2511E-01 -0.2509E-01 -0.2508E-01 -0.2508E-01
-0.2903E-01 -0.2897E-01 -0.2892E-01 -0.2887E-01 -0.2508E-01 -0.2510E-01 -0.2512E-01 -0.2515E-01
-0.2883E-01 -0.2881E-01 -0.2879E-01 -0.2879E-01 -0.2518E-01 -0.2521E-01 -0.2525E-01 -0.2528E-01
-0.2881E-01 -0.2883E-01 -0.2887E-01 -0.2891E-01 -0.2531E-01 -0.2534E-01 -0.2536E-01 -0.2538E-01
-0.2896E-01 -0.2902E-01 -0.2908E-01 -0.2914E-01 -0.2539E-01 -0.2540E-01 -0.2540E-01 -0.2540E-01
-0.2919E-01 -0.2924E-01 -0.2928E-01 -0.2931E-01 -0.2539E-01 -0.2538E-01 -0.2536E-01 -0.2535E-01
-0.2932E-01 -0.2933E-01 -0.2932E-01 -0.2929E-01 -0.2534E-01 -0.2533E-01 -0.2532E-01 -0.2532E-01
-0.2925E-01 -0.2920E-01 -0.2914E-01 -0.2907E-01 -0.2532E-01 -0.2533E-01 -0.2535E-01 -0.2538E-01
-0.2900E-01 -0.2893E-01 -0.2886E-01 -0.2879E-01 -0.2542E-01 -0.2546E-01 -0.2551E-01 -0.2557E-01
-0.2873E-01 -0.2868E-01 -0.2864E-01 -0.2862E-01 -0.2563E-01 -0.2570E-01 -0.2577E-01 -0.2584E-01
-0.2861E-01 -0.2861E-01 -0.2863E-01 -0.2866E-01 -0.2592E-01 -0.2599E-01 -0.2606E-01 -0.2612E-01
-0.2870E-01 -0.2875E-01 -0.2882E-01 -0.2888E-01 -0.2619E-01 -0.2624E-01 -0.2630E-01 -0.2634E-01
-0.2895E-01 -0.2902E-01 -0.2909E-01 -0.2915E-01 -0.2639E-01 -0.2642E-01 -0.2646E-01 -0.2649E-01
-0.2920E-01 -0.2924E-01 -0.2927E-01 -0.2928E-01 -0.2651E-01 -0.2654E-01 -0.2656E-01 -0.2659E-01
-0.2928E-01 -0.2927E-01 -0.2924E-01 -0.2920E-01 -0.2662E-01 -0.2665E-01 -0.2668E-01 -0.2672E-01
-0.2915E-01 -0.2908E-01 -0.2901E-01 -0.2892E-01 -0.2676E-01 -0.2681E-01 -0.2686E-01 -0.2691E-01
-0.2884E-01 -0.2874E-01 -0.2865E-01 -0.2855E-01 -0.2697E-01 -0.2703E-01 -0.2710E-01 -0.2716E-01
-0.2845E-01 -0.2835E-01 -0.2825E-01 -0.2816E-01 -0.2722E-01 -0.2729E-01 -0.2735E-01 -0.2740E-01
-0.2807E-01 -0.2797E-01 -0.2788E-01 -0.2780E-01 -0.2745E-01 -0.2750E-01 -0.2755E-01 -0.2758E-01
-0.2771E-01 -0.2762E-01 -0.2753E-01 -0.2744E-01 -0.2762E-01 -0.2764E-01 -0.2767E-01 -0.2769E-01
-0.2734E-01 -0.2725E-01 -0.2715E-01 -0.2705E-01 -0.2771E-01 -0.2772E-01 -0.2774E-01 -0.2775E-01
-0.2695E-01 -0.2684E-01 -0.2674E-01 -0.2664E-01 -0.2777E-01 -0.2778E-01 -0.2781E-01 -0.2783E-01
-0.2654E-01 -0.2644E-01 -0.2634E-01 -0.2625E-01 -0.2786E-01 -0.2789E-01 -0.2792E-01 -0.2796E-01
-0.2616E-01 -0.2609E-01 -0.2601E-01 -0.2595E-01 -0.2800E-01 -0.2804E-01 -0.2809E-01 -0.2813E-01
-0.2589E-01 -0.2584E-01 -0.2580E-01 -0.2577E-01 -0.2817E-01 -0.2821E-01 -0.2824E-01 -0.2827E-01
-0.2573E-01 -0.2571E-01 -0.2569E-01 -0.2566E-01 -0.2829E-01 -0.2831E-01 -0.2832E-01 -0.2832E-01
-0.2564E-01 -0.2562E-01 -0.2560E-01 -0.2558E-01 -0.2831E-01 -0.2829E-01 -0.2827E-01 -0.2824E-01
-0.2555E-01 -0.2552E-01 -0.2549E-01 -0.2545E-01 -0.2820E-01 -0.2816E-01 -0.2812E-01 -0.2807E-01
-0.2541E-01 -0.2537E-01 -0.2532E-01 -0.2528E-01 -0.2802E-01 -0.2798E-01 -0.2793E-01 -0.2789E-01
-0.2523E-01 -0.2519E-01 -0.2515E-01 -0.2512E-01 -0.2785E-01 -0.2781E-01 -0.2778E-01 -0.2776E-01
-0.2509E-01 -0.2507E-01 -0.2506E-01 -0.2506E-01 -0.2774E-01 -0.2773E-01 -0.2772E-01 -0.2773E-01
-0.2507E-01 -0.2508E-01 -0.2511E-01 -0.2514E-01 -0.2773E-01 -0.2774E-01 -0.2776E-01 -0.2778E-01
-0.2518E-01 -0.2523E-01 -0.2529E-01 -0.2535E-01 -0.2780E-01 -0.2782E-01 -0.2784E-01 -0.2786E-01
-0.2541E-01 -0.2547E-01 -0.2554E-01 -0.2560E-01 -0.2789E-01 -0.2791E-01 -0.2793E-01 -0.2795E-01
-0.2567E-01 -0.2573E-01 -0.2578E-01 -0.2583E-01 -0.2797E-01 -0.2798E-01 -0.2799E-01 -0.2800E-01
-0.2588E-01 -0.2593E-01 -0.2596E-01 -0.2600E-01 -0.2800E-01 -0.2800E-01 -0.2800E-01 -0.2800E-01

-0.2799E-01 -0.2798E-01 -0.2796E-01 -0.2794E-01
-0.2791E-01 -0.2788E-01 -0.2785E-01 -0.2781E-01
-0.2776E-01 -0.2771E-01 -0.2766E-01 -0.2760E-01
-0.2753E-01 -0.2746E-01 -0.2739E-01 -0.2732E-01
-0.2724E-01 -0.2717E-01 -0.2709E-01 -0.2702E-01
-0.2695E-01 -0.2689E-01 -0.2683E-01 -0.2679E-01
-0.2675E-01 -0.2672E-01 -0.2670E-01 -0.2669E-01
-0.2670E-01 -0.2671E-01 -0.2674E-01 -0.2678E-01
-0.2683E-01 -0.2689E-01 -0.2696E-01 -0.2703E-01
-0.2711E-01 -0.2720E-01 -0.2728E-01 -0.2737E-01
-0.2745E-01 -0.2753E-01 -0.2761E-01 -0.2768E-01
-0.2775E-01 -0.2780E-01 -0.2785E-01 -0.2789E-01
-0.2792E-01 -0.2794E-01 -0.2795E-01 -0.2796E-01
-0.2795E-01 -0.2794E-01 -0.2791E-01 -0.2789E-01
-0.2785E-01 -0.2781E-01 -0.2777E-01 -0.2772E-01
-0.2766E-01 -0.2761E-01 -0.2755E-01 -0.2749E-01
-0.2743E-01 -0.2737E-01 -0.2731E-01 -0.2725E-01
-0.2719E-01 -0.2714E-01 -0.2708E-01 -0.2703E-01
-0.2698E-01 -0.2693E-01 -0.2688E-01 -0.2684E-01
-0.2680E-01 -0.2677E-01 -0.2674E-01 -0.2672E-01
-0.2670E-01 -0.2669E-01 -0.2668E-01 -0.2668E-01
-0.2669E-01 -0.2669E-01 -0.2671E-01 -0.2672E-01
-0.2674E-01 -0.2677E-01 -0.2679E-01 -0.2681E-01
-0.2684E-01 -0.2686E-01 -0.2688E-01 -0.2690E-01
-0.2692E-01 -0.2693E-01 -0.2694E-01 -0.2695E-01
-0.2695E-01 -0.2695E-01 -0.2695E-01 -0.2694E-01
-0.2693E-01 -0.2691E-01 -0.2690E-01 -0.2689E-01
-0.2688E-01 -0.2686E-01 -0.2686E-01 -0.2685E-01
-0.2685E-01 -0.2686E-01 -0.2687E-01 -0.2689E-01
-0.2692E-01 -0.2695E-01 -0.2700E-01 -0.2704E-01
-0.2710E-01 -0.2716E-01 -0.2723E-01 -0.2731E-01
-0.2739E-01 -0.2748E-01 -0.2757E-01 -0.2766E-01
-0.2776E-01 -0.2785E-01 -0.2795E-01 -0.2805E-01
-0.2815E-01 -0.2824E-01 -0.2833E-01 -0.2842E-01
-0.2851E-01 -0.2859E-01 -0.2867E-01 -0.2874E-01
-0.2881E-01 -0.2887E-01 -0.2893E-01 -0.2897E-01
-0.2901E-01 -0.2904E-01 -0.2907E-01 -0.2908E-01
-0.2909E-01 -0.2908E-01 -0.2907E-01 -0.2906E-01
-0.2903E-01 -0.2899E-01 -0.2895E-01 -0.2891E-01
-0.2885E-01 -0.2879E-01 -0.2873E-01 -0.2867E-01
-0.2860E-01 -0.2853E-01 -0.2846E-01 -0.2839E-01
-0.2833E-01 -0.2827E-01 -0.2821E-01 -0.2816E-01
-0.2811E-01 -0.2807E-01 -0.2803E-01 -0.2800E-01
-0.2798E-01 -0.2796E-01 -0.2795E-01 -0.2794E-01
-0.2794E-01 -0.2794E-01 -0.2795E-01 -0.2796E-01
-0.2797E-01 -0.2798E-01 -0.2798E-01 -0.2799E-01
-0.2800E-01 -0.2800E-01 -0.2800E-01 -0.2800E-01

Time history of displacement at node NL2:

-0.3021E-03 -0.3833E-03 -0.4574E-03 -0.5316E-03
-0.5974E-03 -0.6830E-03 -0.8246E-03 -0.1006E-02
-0.1176E-02 -0.1349E-02 -0.1547E-02 -0.1773E-02
-0.2035E-02 -0.2291E-02 -0.2522E-02 -0.2767E-02
-0.3019E-02 -0.3273E-02 -0.3519E-02 -0.3728E-02
-0.3921E-02 -0.4117E-02 -0.4304E-02 -0.4473E-02
-0.4619E-02 -0.4746E-02 -0.4875E-02 -0.5014E-02
-0.5140E-02 -0.5263E-02 -0.5385E-02 -0.5514E-02
-0.5668E-02 -0.5828E-02 -0.5991E-02 -0.6164E-02
-0.6352E-02 -0.6556E-02 -0.6772E-02 -0.6990E-02
-0.7205E-02 -0.7430E-02 -0.7655E-02 -0.7882E-02
-0.8101E-02 -0.8305E-02 -0.8504E-02 -0.8696E-02
-0.8876E-02 -0.9042E-02 -0.9192E-02 -0.9329E-02
-0.9459E-02 -0.9581E-02 -0.9691E-02 -0.9794E-02
-0.9894E-02 -0.9992E-02 -0.1010E-01 -0.1020E-01
-0.1031E-01 -0.1043E-01 -0.1055E-01 -0.1070E-01
-0.1085E-01 -0.1101E-01 -0.1117E-01 -0.1136E-01
-0.1154E-01 -0.1174E-01 -0.1194E-01 -0.1214E-01
-0.1234E-01 -0.1253E-01 -0.1272E-01 -0.1290E-01
-0.1308E-01 -0.1324E-01 -0.1339E-01 -0.1353E-01
-0.1367E-01 -0.1380E-01 -0.1392E-01 -0.1403E-01
-0.1415E-01 -0.1426E-01 -0.1438E-01 -0.1449E-01
-0.1461E-01 -0.1474E-01 -0.1488E-01 -0.1502E-01
-0.1516E-01 -0.1531E-01 -0.1547E-01 -0.1563E-01
-0.1579E-01 -0.1595E-01 -0.1611E-01 -0.1627E-01
-0.1643E-01 -0.1657E-01 -0.1671E-01 -0.1684E-01
-0.1696E-01 -0.1707E-01 -0.1718E-01 -0.1727E-01
-0.1735E-01 -0.1743E-01 -0.1751E-01 -0.1758E-01
-0.1766E-01 -0.1773E-01 -0.1781E-01 -0.1790E-01
-0.1799E-01 -0.1809E-01 -0.1820E-01 -0.1831E-01
-0.1844E-01 -0.1857E-01 -0.1870E-01 -0.1885E-01
-0.1899E-01 -0.1914E-01 -0.1928E-01 -0.1943E-01
-0.1957E-01 -0.1970E-01 -0.1983E-01 -0.1995E-01
-0.2007E-01 -0.2017E-01 -0.2027E-01 -0.2036E-01
-0.2044E-01 -0.2051E-01 -0.2058E-01 -0.2064E-01
-0.2070E-01 -0.2076E-01 -0.2081E-01 -0.2087E-01
-0.2093E-01 -0.2099E-01 -0.2106E-01 -0.2113E-01
-0.2121E-01 -0.2130E-01 -0.2139E-01 -0.2148E-01
-0.2158E-01 -0.2169E-01 -0.2179E-01 -0.2190E-01

-0.2201E-01 -0.2211E-01 -0.2221E-01 -0.2231E-01 -0.2813E-01 -0.2815E-01 -0.2816E-01 -0.2816E-01
-0.2240E-01 -0.2249E-01 -0.2258E-01 -0.2266E-01 -0.2816E-01 -0.2815E-01 -0.2814E-01 -0.2811E-01
-0.2273E-01 -0.2280E-01 -0.2286E-01 -0.2293E-01 -0.2809E-01 -0.2806E-01 -0.2803E-01 -0.2799E-01
-0.2299E-01 -0.2305E-01 -0.2311E-01 -0.2318E-01 -0.2796E-01 -0.2792E-01 -0.2788E-01 -0.2784E-01
-0.2324E-01 -0.2332E-01 -0.2339E-01 -0.2347E-01 -0.2779E-01 -0.2775E-01 -0.2771E-01 -0.2766E-01
-0.2356E-01 -0.2365E-01 -0.2374E-01 -0.2384E-01 -0.2762E-01 -0.2757E-01 -0.2752E-01 -0.2748E-01
-0.2393E-01 -0.2403E-01 -0.2413E-01 -0.2422E-01 -0.2743E-01 -0.2739E-01 -0.2735E-01 -0.2731E-01
-0.2431E-01 -0.2440E-01 -0.2448E-01 -0.2455E-01 -0.2727E-01 -0.2723E-01 -0.2720E-01 -0.2718E-01
-0.2462E-01 -0.2468E-01 -0.2474E-01 -0.2479E-01 -0.2715E-01 -0.2714E-01 -0.2713E-01 -0.2712E-01
-0.2483E-01 -0.2487E-01 -0.2490E-01 -0.2494E-01 -0.2712E-01 -0.2712E-01 -0.2713E-01 -0.2715E-01
-0.2497E-01 -0.2500E-01 -0.2503E-01 -0.2507E-01 -0.2717E-01 -0.2719E-01 -0.2722E-01 -0.2725E-01
-0.2511E-01 -0.2515E-01 -0.2520E-01 -0.2525E-01 -0.2728E-01 -0.2731E-01 -0.2734E-01 -0.2736E-01
-0.2531E-01 -0.2537E-01 -0.2544E-01 -0.2551E-01 -0.2738E-01 -0.2740E-01 -0.2741E-01 -0.2741E-01
-0.2558E-01 -0.2565E-01 -0.2573E-01 -0.2580E-01 -0.2740E-01 -0.2739E-01 -0.2737E-01 -0.2733E-01
-0.2587E-01 -0.2594E-01 -0.2601E-01 -0.2607E-01 -0.2730E-01 -0.2725E-01 -0.2719E-01 -0.2713E-01
-0.2612E-01 -0.2617E-01 -0.2621E-01 -0.2625E-01 -0.2706E-01 -0.2699E-01 -0.2691E-01 -0.2682E-01
-0.2627E-01 -0.2630E-01 -0.2631E-01 -0.2632E-01 -0.2674E-01 -0.2665E-01 -0.2656E-01 -0.2647E-01
-0.2633E-01 -0.2633E-01 -0.2633E-01 -0.2634E-01 -0.2638E-01 -0.2628E-01 -0.2619E-01 -0.2610E-01
-0.2634E-01 -0.2634E-01 -0.2634E-01 -0.2635E-01 -0.2601E-01 -0.2593E-01 -0.2584E-01 -0.2575E-01
-0.2636E-01 -0.2637E-01 -0.2638E-01 -0.2640E-01 -0.2566E-01 -0.2558E-01 -0.2549E-01 -0.2541E-01
-0.2641E-01 -0.2643E-01 -0.2645E-01 -0.2646E-01 -0.2532E-01 -0.2524E-01 -0.2516E-01 -0.2507E-01
-0.2648E-01 -0.2649E-01 -0.2650E-01 -0.2651E-01 -0.2499E-01 -0.2491E-01 -0.2482E-01 -0.2474E-01
-0.2652E-01 -0.2652E-01 -0.2652E-01 -0.2651E-01 -0.2466E-01 -0.2458E-01 -0.2451E-01 -0.2443E-01
-0.2651E-01 -0.2650E-01 -0.2649E-01 -0.2647E-01 -0.2436E-01 -0.2429E-01 -0.2422E-01 -0.2415E-01
-0.2646E-01 -0.2644E-01 -0.2643E-01 -0.2642E-01 -0.2409E-01 -0.2403E-01 -0.2397E-01 -0.2391E-01
-0.2641E-01 -0.2640E-01 -0.2640E-01 -0.2640E-01 -0.2385E-01 -0.2379E-01 -0.2374E-01 -0.2368E-01
-0.2641E-01 -0.2642E-01 -0.2644E-01 -0.2645E-01 -0.2363E-01 -0.2357E-01 -0.2351E-01 -0.2346E-01
-0.2648E-01 -0.2650E-01 -0.2653E-01 -0.2656E-01 -0.2340E-01 -0.2335E-01 -0.2329E-01 -0.2324E-01
-0.2659E-01 -0.2662E-01 -0.2665E-01 -0.2669E-01 -0.2318E-01 -0.2313E-01 -0.2308E-01 -0.2303E-01
-0.2672E-01 -0.2675E-01 -0.2678E-01 -0.2682E-01 -0.2298E-01 -0.2293E-01 -0.2288E-01 -0.2284E-01
-0.2685E-01 -0.2688E-01 -0.2691E-01 -0.2694E-01 -0.2280E-01 -0.2276E-01 -0.2272E-01 -0.2268E-01
-0.2698E-01 -0.2701E-01 -0.2705E-01 -0.2709E-01 -0.2264E-01 -0.2260E-01 -0.2256E-01 -0.2253E-01
-0.2713E-01 -0.2717E-01 -0.2722E-01 -0.2726E-01 -0.2249E-01 -0.2244E-01 -0.2240E-01 -0.2235E-01
-0.2731E-01 -0.2736E-01 -0.2741E-01 -0.2745E-01 -0.2230E-01 -0.2225E-01 -0.2219E-01 -0.2214E-01
-0.2750E-01 -0.2755E-01 -0.2760E-01 -0.2764E-01 -0.2207E-01 -0.2201E-01 -0.2194E-01 -0.2187E-01
-0.2768E-01 -0.2772E-01 -0.2775E-01 -0.2778E-01 -0.2180E-01 -0.2173E-01 -0.2166E-01 -0.2158E-01
-0.2780E-01 -0.2782E-01 -0.2783E-01 -0.2784E-01 -0.2151E-01 -0.2144E-01 -0.2138E-01 -0.2131E-01
-0.2784E-01 -0.2784E-01 -0.2783E-01 -0.2782E-01 -0.2125E-01 -0.2120E-01 -0.2114E-01 -0.2110E-01
-0.2781E-01 -0.2780E-01 -0.2778E-01 -0.2777E-01 -0.2105E-01 -0.2101E-01 -0.2098E-01 -0.2095E-01
-0.2775E-01 -0.2774E-01 -0.2773E-01 -0.2773E-01 -0.2092E-01 -0.2090E-01 -0.2088E-01 -0.2086E-01
-0.2773E-01 -0.2773E-01 -0.2774E-01 -0.2775E-01 -0.2084E-01 -0.2083E-01 -0.2082E-01 -0.2081E-01
-0.2777E-01 -0.2779E-01 -0.2782E-01 -0.2785E-01 -0.2080E-01 -0.2079E-01 -0.2078E-01 -0.2078E-01
-0.2789E-01 -0.2792E-01 -0.2796E-01 -0.2799E-01 -0.2078E-01 -0.2077E-01 -0.2077E-01 -0.2077E-01
-0.2803E-01 -0.2806E-01 -0.2809E-01 -0.2811E-01 -0.2077E-01 -0.2077E-01 -0.2077E-01 -0.2077E-01

-0.2077E-01 -0.2076E-01 -0.2076E-01 -0.2076E-01 -0.1699E-01 -0.1700E-01 -0.1701E-01 -0.1703E-01
-0.2076E-01 -0.2076E-01 -0.2075E-01 -0.2075E-01 -0.1704E-01 -0.1705E-01 -0.1707E-01 -0.1709E-01
-0.2074E-01 -0.2074E-01 -0.2073E-01 -0.2072E-01 -0.1711E-01 -0.1712E-01 -0.1715E-01 -0.1717E-01
-0.2071E-01 -0.2071E-01 -0.2070E-01 -0.2069E-01 -0.1719E-01 -0.1722E-01 -0.1725E-01 -0.1727E-01
-0.2068E-01 -0.2067E-01 -0.2066E-01 -0.2065E-01 -0.1731E-01 -0.1734E-01 -0.1737E-01 -0.1741E-01
-0.2064E-01 -0.2064E-01 -0.2063E-01 -0.2063E-01 -0.1745E-01 -0.1749E-01 -0.1753E-01 -0.1757E-01
-0.2063E-01 -0.2062E-01 -0.2062E-01 -0.2063E-01 -0.1761E-01 -0.1766E-01 -0.1771E-01 -0.1775E-01
-0.2063E-01 -0.2063E-01 -0.2064E-01 -0.2064E-01 -0.1780E-01 -0.1785E-01 -0.1790E-01 -0.1794E-01
-0.2065E-01 -0.2065E-01 -0.2066E-01 -0.2066E-01 -0.1799E-01 -0.1804E-01 -0.1809E-01 -0.1814E-01
-0.2067E-01 -0.2067E-01 -0.2066E-01 -0.2066E-01 -0.1818E-01 -0.1823E-01 -0.1828E-01 -0.1833E-01
-0.2065E-01 -0.2063E-01 -0.2061E-01 -0.2059E-01 -0.1837E-01 -0.1842E-01 -0.1846E-01 -0.1851E-01
-0.2056E-01 -0.2053E-01 -0.2048E-01 -0.2044E-01 -0.1855E-01 -0.1860E-01 -0.1864E-01 -0.1869E-01
-0.2038E-01 -0.2033E-01 -0.2026E-01 -0.2019E-01 -0.1873E-01 -0.1877E-01 -0.1881E-01 -0.1886E-01
-0.2012E-01 -0.2004E-01 -0.1996E-01 -0.1987E-01 -0.1890E-01 -0.1894E-01 -0.1898E-01 -0.1902E-01
-0.1978E-01 -0.1969E-01 -0.1959E-01 -0.1950E-01 -0.1906E-01 -0.1910E-01 -0.1914E-01 -0.1918E-01
-0.1940E-01 -0.1931E-01 -0.1921E-01 -0.1911E-01 -0.1922E-01 -0.1926E-01 -0.1929E-01 -0.1933E-01
-0.1902E-01 -0.1892E-01 -0.1883E-01 -0.1874E-01 -0.1937E-01 -0.1940E-01 -0.1944E-01 -0.1947E-01
-0.1865E-01 -0.1857E-01 -0.1848E-01 -0.1840E-01 -0.1950E-01 -0.1953E-01 -0.1957E-01 -0.1959E-01
-0.1832E-01 -0.1824E-01 -0.1817E-01 -0.1810E-01 -0.1962E-01 -0.1965E-01 -0.1968E-01 -0.1970E-01
-0.1803E-01 -0.1796E-01 -0.1790E-01 -0.1783E-01 -0.1972E-01 -0.1974E-01 -0.1976E-01 -0.1978E-01
-0.1777E-01 -0.1772E-01 -0.1766E-01 -0.1760E-01 -0.1979E-01 -0.1981E-01 -0.1982E-01 -0.1982E-01
-0.1755E-01 -0.1750E-01 -0.1746E-01 -0.1741E-01 -0.1983E-01 -0.1983E-01 -0.1983E-01 -0.1983E-01
-0.1737E-01 -0.1732E-01 -0.1728E-01 -0.1725E-01 -0.1983E-01 -0.1982E-01 -0.1981E-01 -0.1980E-01
-0.1721E-01 -0.1718E-01 -0.1715E-01 -0.1712E-01 -0.1979E-01 -0.1978E-01 -0.1976E-01 -0.1975E-01
-0.1709E-01 -0.1707E-01 -0.1705E-01 -0.1703E-01 -0.1973E-01 -0.1971E-01 -0.1969E-01 -0.1967E-01
-0.1701E-01 -0.1700E-01 -0.1699E-01 -0.1699E-01 -0.1966E-01 -0.1964E-01 -0.1962E-01 -0.1961E-01
-0.1698E-01 -0.1698E-01 -0.1698E-01 -0.1699E-01 -0.1959E-01 -0.1958E-01 -0.1957E-01 -0.1956E-01
-0.1700E-01 -0.1701E-01 -0.1703E-01 -0.1704E-01 -0.1956E-01 -0.1955E-01 -0.1955E-01 -0.1955E-01
-0.1707E-01 -0.1709E-01 -0.1712E-01 -0.1715E-01 -0.1955E-01 -0.1956E-01 -0.1956E-01 -0.1957E-01
-0.1718E-01 -0.1721E-01 -0.1725E-01 -0.1728E-01 -0.1958E-01 -0.1958E-01 -0.1959E-01 -0.1960E-01
-0.1732E-01 -0.1736E-01 -0.1740E-01 -0.1744E-01 -0.1960E-01 -0.1961E-01 -0.1961E-01 -0.1961E-01
-0.1748E-01 -0.1752E-01 -0.1756E-01 -0.1759E-01 -0.1961E-01 -0.1961E-01 -0.1960E-01 -0.1959E-01
-0.1762E-01 -0.1765E-01 -0.1768E-01 -0.1770E-01 -0.1958E-01 -0.1956E-01 -0.1954E-01 -0.1951E-01
-0.1772E-01 -0.1773E-01 -0.1774E-01 -0.1774E-01 -0.1948E-01 -0.1945E-01 -0.1942E-01 -0.1938E-01
-0.1774E-01 -0.1773E-01 -0.1772E-01 -0.1771E-01 -0.1934E-01 -0.1929E-01 -0.1925E-01 -0.1920E-01
-0.1769E-01 -0.1767E-01 -0.1764E-01 -0.1761E-01 -0.1915E-01 -0.1910E-01 -0.1906E-01 -0.1901E-01
-0.1758E-01 -0.1755E-01 -0.1751E-01 -0.1747E-01 -0.1896E-01 -0.1892E-01 -0.1888E-01 -0.1884E-01
-0.1744E-01 -0.1740E-01 -0.1736E-01 -0.1732E-01 -0.1881E-01 -0.1878E-01 -0.1875E-01 -0.1873E-01
-0.1728E-01 -0.1724E-01 -0.1721E-01 -0.1718E-01 -0.1871E-01 -0.1870E-01 -0.1870E-01 -0.1870E-01
-0.1714E-01 -0.1711E-01 -0.1709E-01 -0.1706E-01 -0.1870E-01 -0.1871E-01 -0.1873E-01 -0.1875E-01
-0.1704E-01 -0.1702E-01 -0.1700E-01 -0.1699E-01 -0.1878E-01 -0.1881E-01 -0.1884E-01 -0.1888E-01
-0.1698E-01 -0.1697E-01 -0.1696E-01 -0.1696E-01 -0.1892E-01 -0.1896E-01 -0.1900E-01 -0.1905E-01
-0.1695E-01 -0.1695E-01 -0.1695E-01 -0.1696E-01 -0.1909E-01 -0.1914E-01 -0.1918E-01 -0.1922E-01
-0.1696E-01 -0.1697E-01 -0.1697E-01 -0.1698E-01 -0.1926E-01 -0.1930E-01 -0.1933E-01 -0.1936E-01

-0.1938E-01 -0.1940E-01 -0.1942E-01 -0.1943E-01
-0.1943E-01 -0.1943E-01 -0.1942E-01 -0.1941E-01
-0.1939E-01 -0.1937E-01 -0.1934E-01 -0.1931E-01
-0.1928E-01 -0.1924E-01 -0.1920E-01 -0.1916E-01
-0.1912E-01 -0.1907E-01 -0.1903E-01 -0.1898E-01
-0.1893E-01 -0.1889E-01 -0.1885E-01 -0.1881E-01
-0.1877E-01 -0.1873E-01 -0.1869E-01 -0.1866E-01
-0.1863E-01 -0.1861E-01 -0.1859E-01 -0.1857E-01
-0.1855E-01 -0.1854E-01 -0.1853E-01 -0.1852E-01
-0.1851E-01 -0.1851E-01 -0.1851E-01 -0.1851E-01
-0.1851E-01 -0.1851E-01 -0.1852E-01 -0.1852E-01
-0.1853E-01 -0.1854E-01 -0.1854E-01 -0.1855E-01
-0.1856E-01 -0.1856E-01 -0.1857E-01 -0.1857E-01
-0.1858E-01 -0.1858E-01 -0.1859E-01 -0.1860E-01
-0.1860E-01 -0.1861E-01 -0.1862E-01 -0.1863E-01
-0.1864E-01 -0.1865E-01 -0.1867E-01 -0.1868E-01
-0.1870E-01 -0.1873E-01 -0.1875E-01 -0.1878E-01
-0.1882E-01 -0.1886E-01 -0.1890E-01 -0.1894E-01
-0.1899E-01 -0.1904E-01 -0.1910E-01 -0.1916E-01
-0.1923E-01 -0.1929E-01 -0.1936E-01 -0.1943E-01
-0.1951E-01 -0.1958E-01 -0.1966E-01 -0.1973E-01
-0.1981E-01 -0.1988E-01 -0.1996E-01 -0.2003E-01
-0.2010E-01 -0.2016E-01 -0.2022E-01 -0.2028E-01
-0.2033E-01 -0.2038E-01 -0.2042E-01 -0.2046E-01
-0.2049E-01 -0.2052E-01 -0.2053E-01 -0.2055E-01
-0.2055E-01 -0.2056E-01 -0.2055E-01 -0.2054E-01
-0.2053E-01 -0.2051E-01 -0.2048E-01 -0.2046E-01
-0.2042E-01 -0.2039E-01 -0.2035E-01 -0.2031E-01
-0.2027E-01 -0.2023E-01 -0.2019E-01 -0.2015E-01
-0.2011E-01 -0.2007E-01 -0.2003E-01 -0.1999E-01
-0.1995E-01 -0.1992E-01 -0.1989E-01 -0.1986E-01
-0.1983E-01 -0.1981E-01 -0.1978E-01 -0.1976E-01
-0.1975E-01 -0.1973E-01 -0.1971E-01 -0.1970E-01
-0.1969E-01 -0.1967E-01 -0.1966E-01 -0.1965E-01
-0.1964E-01 -0.1962E-01 -0.1961E-01 -0.1959E-01

Time history of vertical velocity at node NL1:

-0.1385E+00 -0.2400E+00 -0.3836E+00 -0.4270E+00
-0.3515E+00 -0.3594E+00 -0.3879E+00 -0.3826E+00
-0.3811E+00 -0.2440E+00 -0.1415E+00 -0.1170E+00
-0.5531E-01 0.4237E-02 0.1112E+00 0.2110E+00
0.2554E+00 0.2391E+00 0.2728E+00 0.3018E+00
0.2984E+00 0.2988E+00 0.1985E+00 0.1475E+00
0.1073E+00 0.4745E-01 -0.1799E-01 -0.1098E+00

-0.1940E+00 -0.2413E+00 -0.2616E+00 -0.3125E+00
-0.3372E+00 -0.3578E+00 -0.3483E+00 -0.3022E+00
-0.2608E+00 -0.2360E+00 -0.1704E+00 -0.1188E+00
-0.3473E-01 0.3855E-01 0.8494E-01 0.1375E+00
0.1807E+00 0.2293E+00 0.2450E+00 0.2622E+00
0.2315E+00 0.2214E+00 0.1938E+00 0.1482E+00
0.1015E+00 0.3181E-01 -0.2897E-01 -0.8160E-01
-0.1364E+00 -0.1888E+00 -0.2348E+00 -0.2672E+00
-0.2863E+00 -0.2840E+00 -0.2815E+00 -0.2669E+00
-0.2324E+00 -0.1964E+00 -0.1393E+00 -0.8789E-01
-0.3570E-01 0.1942E-01 0.7370E-01 0.1200E+00
0.1624E+00 0.1851E+00 0.2033E+00 0.2063E+00
0.2061E+00 0.1822E+00 0.1578E+00 0.1147E+00
0.6985E-01 0.2666E-01 -0.3151E-01 -0.7596E-01
-0.1323E+00 -0.1691E+00 -0.2085E+00 -0.2293E+00
-0.2497E+00 -0.2537E+00 -0.2472E+00 -0.2315E+00
-0.2013E+00 -0.1685E+00 -0.1268E+00 -0.8078E-01
-0.3132E-01 0.1616E-01 0.6394E-01 0.1014E+00
0.1376E+00 0.1622E+00 0.1800E+00 0.1855E+00
0.1809E+00 0.1670E+00 0.1421E+00 0.1144E+00
0.7330E-01 0.3482E-01 -0.1147E-01 -0.5455E-01
-0.9496E-01 -0.1343E+00 -0.1637E+00 -0.1907E+00
-0.2035E+00 -0.2125E+00 -0.2071E+00 -0.1971E+00
-0.1762E+00 -0.1484E+00 -0.1155E+00 -0.7741E-01
-0.3795E-01 0.1540E-02 0.4024E-01 0.7469E-01
0.1043E+00 0.1272E+00 0.1420E+00 0.1493E+00
0.1474E+00 0.1383E+00 0.1198E+00 0.9626E-01
0.6594E-01 0.3264E-01 -0.3068E-02 -0.3909E-01
-0.7437E-01 -0.1046E+00 -0.1332E+00 -0.1512E+00
-0.1675E+00 -0.1705E+00 -0.1715E+00 -0.1592E+00
-0.1444E+00 -0.1203E+00 -0.9240E-01 -0.6201E-01
-0.2660E-01 0.4424E-02 0.3968E-01 0.6559E-01
0.9353E-01 0.1093E+00 0.1250E+00 0.1274E+00
0.1282E+00 0.1168E+00 0.1030E+00 0.8019E-01
0.5509E-01 0.2533E-01 -0.6113E-02 -0.3656E-01
-0.6822E-01 -0.9337E-01 -0.1189E+00 -0.1343E+00
-0.1484E+00 -0.1514E+00 -0.1516E+00 -0.1418E+00
-0.1286E+00 -0.1080E+00 -0.8467E-01 -0.5708E-01
-0.2893E-01 0.9214E-03 0.2808E-01 0.5442E-01
0.7548E-01 0.9321E-01 0.1046E+00 0.1105E+00
0.1104E+00 0.1036E+00 0.9241E-01 0.7449E-01
0.5485E-01 0.2965E-01 0.5426E-02 -0.2200E-01
-0.4574E-01 -0.7018E-01 -0.8865E-01 -0.1057E+00
-0.1154E+00 -0.1218E+00 -0.1212E+00 -0.1160E+00

-0.1055E+00 -0.8994E-01 -0.7179E-01 -0.4921E-01 0.2482E-01 0.3099E-01 0.3546E-01 0.3823E-01
-0.2708E-01 -0.2310E-02 0.1961E-01 0.4153E-01 0.3861E-01 0.3784E-01 0.3455E-01 0.3093E-01
0.5926E-01 0.7405E-01 0.8415E-01 0.8924E-01 0.2493E-01 0.1948E-01 0.1223E-01 0.6528E-02
0.8985E-01 0.8486E-01 0.7603E-01 0.6240E-01 -0.2191E-03 -0.4752E-02 -0.9576E-02 -0.1184E-01
0.4597E-01 0.2688E-01 0.6345E-02 -0.1415E-01 -0.1361E-01 -0.1294E-01 -0.1131E-01 -0.7809E-02
-0.3464E-01 -0.5241E-01 -0.6878E-01 -0.8018E-01 -0.3143E-02 0.2585E-02 0.9362E-02 0.1614E-01
-0.8933E-01 -0.9215E-01 -0.9246E-01 -0.8626E-01 0.2360E-01 0.3007E-01 0.3673E-01 0.4160E-01
-0.7772E-01 -0.6391E-01 -0.4832E-01 -0.2983E-01 0.4612E-01 0.4833E-01 0.4986E-01 0.4895E-01
-0.1025E-01 0.9226E-02 0.2895E-01 0.4558E-01 0.4727E-01 0.4337E-01 0.3882E-01 0.3264E-01
0.6155E-01 0.7227E-01 0.8146E-01 0.8433E-01 0.2619E-01 0.1885E-01 0.1181E-01 0.4692E-02
0.8513E-01 0.7963E-01 0.7218E-01 0.5947E-01 -0.1586E-02 -0.7167E-02 -0.1150E-01 -0.1457E-01
0.4560E-01 0.2809E-01 0.1077E-01 -0.8196E-02 -0.1617E-01 -0.1623E-01 -0.1491E-01 -0.1202E-01
-0.2538E-01 -0.4207E-01 -0.5569E-01 -0.6683E-01 -0.8182E-02 -0.3015E-02 0.2489E-02 0.8860E-02
-0.7439E-01 -0.7803E-01 -0.7827E-01 -0.7378E-01 0.1486E-01 0.2116E-01 0.2637E-01 0.3139E-01
-0.6690E-01 -0.5532E-01 -0.4305E-01 -0.2672E-01 0.3480E-01 0.3767E-01 0.3867E-01 0.3886E-01
-0.1171E-01 0.6182E-02 0.2070E-01 0.3668E-01 0.3717E-01 0.3472E-01 0.3069E-01 0.2614E-01
0.4769E-01 0.5873E-01 0.6408E-01 0.6803E-01 0.2052E-01 0.1474E-01 0.8546E-02 0.2628E-02
0.6669E-01 0.6283E-01 0.5514E-01 0.4430E-01 -0.2992E-02 -0.7978E-02 -0.1203E-01 -0.1524E-01
0.3178E-01 0.1605E-01 0.1138E-02 -0.1637E-01 -0.1702E-01 -0.1794E-01 -0.1718E-01 -0.1578E-01
-0.3081E-01 -0.4678E-01 -0.5805E-01 -0.6951E-01 -0.1265E-01 -0.9290E-02 -0.4382E-02 0.2440E-03
-0.7538E-01 -0.8033E-01 -0.7971E-01 -0.7745E-01 0.6012E-02 0.1100E-01 0.1666E-01 0.2112E-01
-0.7049E-01 -0.6162E-01 -0.4959E-01 -0.3601E-01 0.2572E-01 0.2889E-01 0.3170E-01 0.3314E-01
-0.2121E-01 -0.5664E-02 0.9138E-02 0.2377E-01 0.3383E-01 0.3341E-01 0.3198E-01 0.2992E-01
0.3588E-01 0.4678E-01 0.5391E-01 0.5910E-01 0.2679E-01 0.2364E-01 0.1945E-01 0.1586E-01
0.6008E-01 0.5902E-01 0.5382E-01 0.4694E-01 0.1141E-01 0.8086E-02 0.4146E-02 0.1679E-02
0.3665E-01 0.2575E-01 0.1266E-01 0.1649E-03 -0.1180E-02 -0.2454E-02 -0.3893E-02 -0.3864E-02
-0.1317E-01 -0.2471E-01 -0.3561E-01 -0.4378E-01 -0.3855E-02 -0.2729E-02 -0.1547E-02 0.2890E-03
-0.5010E-01 -0.5344E-01 -0.5415E-01 -0.5208E-01 0.2216E-02 0.4225E-02 0.6320E-02 0.7971E-02
-0.4721E-01 -0.4031E-01 -0.3108E-01 -0.2099E-01 0.9804E-02 0.1084E-01 0.1204E-01 0.1202E-01
-0.9436E-02 0.1675E-02 0.1310E-01 0.2285E-01 0.1222E-01 0.1110E-01 0.1033E-01 0.8286E-02
0.3170E-01 0.3795E-01 0.4251E-01 0.4399E-01 0.6621E-02 0.3862E-02 0.1649E-02 -0.1272E-02
0.4337E-01 0.3972E-01 0.3415E-01 0.2618E-01 -0.3549E-02 -0.6135E-02 -0.8105E-02 -0.9928E-02
0.1704E-01 0.6342E-02 -0.4326E-02 -0.1546E-01 -0.1112E-01 -0.1179E-01 -0.1197E-01 -0.1138E-01
-0.2524E-01 -0.3437E-01 -0.4097E-01 -0.4592E-01 -0.1054E-01 -0.8774E-02 -0.6994E-02 -0.4319E-02
-0.4761E-01 -0.4726E-01 -0.4387E-01 -0.3821E-01 -0.1949E-02 0.1129E-02 0.3631E-02 0.6643E-02
-0.3023E-01 -0.2010E-01 -0.9002E-02 0.3521E-02 0.8856E-02 0.1126E-01 0.1270E-01 0.1407E-01
0.1541E-01 0.2811E-01 0.3864E-01 0.4918E-01 0.1449E-01 0.1467E-01 0.1395E-01 0.1287E-01
0.5622E-01 0.6247E-01 0.6465E-01 0.6565E-01 0.1110E-01 0.8984E-02 0.6466E-02 0.3694E-02
0.6255E-01 0.5813E-01 0.5024E-01 0.4118E-01 0.8210E-03 -0.2164E-02 -0.4891E-02 -0.7577E-02
0.3004E-01 0.1813E-01 0.5704E-02 -0.6911E-02 -0.9708E-02 -0.1168E-01 -0.1288E-01 -0.1383E-01
-0.1845E-01 -0.2953E-01 -0.3806E-01 -0.4573E-01 -0.1386E-01 -0.1369E-01 -0.1256E-01 -0.1134E-01
-0.4992E-01 -0.5304E-01 -0.5229E-01 -0.5057E-01 -0.9223E-02 -0.7146E-02 -0.4356E-02 -0.1769E-02
-0.4519E-01 -0.3935E-01 -0.3054E-01 -0.2195E-01 0.1307E-02 0.4033E-02 0.6984E-02 0.9502E-02
-0.1146E-01 -0.1895E-02 0.8247E-02 0.1687E-01 0.1200E-01 0.1404E-01 0.1586E-01 0.1730E-01

0.1835E-01	0.1917E-01	0.1950E-01	0.1982E-01	-0.1207E-01	-0.1240E-01	-0.1280E-01	-0.1274E-01
0.1960E-01	0.1959E-01	0.1904E-01	0.1890E-01	-0.1270E-01	-0.1220E-01	-0.1175E-01	-0.1092E-01
0.1827E-01	0.1823E-01	0.1773E-01	0.1786E-01	-0.1013E-01	-0.9083E-02	-0.8102E-02	-0.7021E-02
0.1760E-01	0.1797E-01	0.1801E-01	0.1857E-01	-0.6072E-02	-0.5140E-02	-0.4335E-02	-0.3699E-02
0.1883E-01	0.1943E-01	0.1980E-01	0.2026E-01	-0.3195E-02	-0.2997E-02	-0.2887E-02	-0.3084E-02
0.2057E-01	0.2071E-01	0.2080E-01	0.2048E-01	-0.3319E-02	-0.3892E-02	-0.4407E-02	-0.5214E-02
0.2025E-01	0.1941E-01	0.1881E-01	0.1750E-01	-0.5839E-02	-0.6666E-02	-0.7237E-02	-0.7922E-02
0.1656E-01	0.1490E-01	0.1374E-01	0.1195E-01	-0.8259E-02	-0.8600E-02	-0.8530E-02	-0.8396E-02
0.1075E-01	0.9038E-02	0.7925E-02	0.6526E-02	-0.7885E-02	-0.7245E-02	-0.6284E-02	-0.5169E-02
0.5709E-02	0.4818E-02	0.4380E-02	0.4039E-02	-0.3838E-02	-0.2378E-02	-0.8590E-03	0.7709E-03
0.3979E-02	0.4216E-02	0.4507E-02	0.5182E-02	0.2318E-02	0.3925E-02	0.5281E-02	0.6654E-02
0.5660E-02	0.6552E-02	0.7033E-02	0.7948E-02	0.7642E-02	0.8616E-02	0.9129E-02	0.9593E-02
0.8249E-02	0.8901E-02	0.8823E-02	0.9025E-02	0.9550E-02	0.9485E-02	0.8952E-02	0.8415E-02
0.8489E-02	0.8135E-02	0.7070E-02	0.6117E-02	0.7473E-02	0.6529E-02	0.5334E-02	0.4169E-02
0.4615E-02	0.3166E-02	0.1384E-02	-0.3861E-03	0.2882E-02	0.1655E-02	0.4591E-03	-0.6903E-03
-0.2269E-02	-0.4154E-02	-0.5900E-02	-0.7661E-02	-0.1673E-02	-0.2617E-02	-0.3288E-02	-0.3946E-02
-0.9055E-02	-0.1049E-01	-0.1141E-01	-0.1238E-01	-0.4280E-02	-0.4655E-02	-0.4659E-02	-0.4754E-02
-0.1272E-01	-0.1315E-01	-0.1295E-01	-0.1288E-01	-0.4478E-02	-0.4327E-02	-0.3868E-02	-0.3543E-02
-0.1221E-01	-0.1172E-01	-0.1076E-01	-0.1003E-01	-0.2951E-02	-0.2501E-02	-0.1847E-02	-0.1306E-02
-0.8971E-02	-0.8155E-02	-0.7139E-02	-0.6352E-02	-0.6373E-03	0.3210E-05	0.6900E-03	0.1408E-02
-0.5507E-02	-0.4831E-02	-0.4190E-02	-0.3586E-02	0.2130E-02	0.2943E-02	0.3725E-02	0.4673E-02
-0.3090E-02	-0.2521E-02	-0.2080E-02	-0.1445E-02	0.5505E-02	0.6564E-02	0.7473E-02	0.8602E-02
-0.9405E-03	-0.1284E-03	0.5267E-03	0.1560E-02	0.9537E-02	0.1067E-01	0.1156E-01	0.1259E-01
0.2447E-02	0.3736E-02	0.4823E-02	0.6289E-02	0.1334E-01	0.1412E-01	0.1459E-01	0.1501E-01
0.7488E-02	0.8983E-02	0.1017E-01	0.1151E-01	0.1510E-01	0.1503E-01	0.1465E-01	0.1401E-01
0.1249E-01	0.1347E-01	0.1405E-01	0.1452E-01	0.1311E-01	0.1190E-01	0.1047E-01	0.8723E-02
0.1459E-01	0.1440E-01	0.1387E-01	0.1300E-01	0.6857E-02	0.4687E-02	0.2536E-02	0.1283E-03
0.1192E-01	0.1046E-01	0.8940E-02	0.7024E-02	-0.2164E-02	-0.4598E-02	-0.6800E-02	-0.9040E-02
0.5265E-02	0.3173E-02	0.1412E-02	-0.6034E-03	-0.1093E-01	-0.1278E-01	-0.1422E-01	-0.1549E-01
-0.2138E-02	-0.3813E-02	-0.4875E-02	-0.5988E-02	-0.1634E-01	-0.1695E-01	-0.1715E-01	-0.1708E-01
-0.6472E-02	-0.6938E-02	-0.6831E-02	-0.6634E-02	-0.1664E-01	-0.1590E-01	-0.1491E-01	-0.1364E-01
-0.5975E-02	-0.5215E-02	-0.4209E-02	-0.3105E-02	-0.1222E-01	-0.1057E-01	-0.8856E-02	-0.6970E-02
-0.1979E-02	-0.7623E-03	0.2458E-03	0.1308E-02	-0.5169E-02	-0.3226E-02	-0.1459E-02	0.3957E-03
0.1934E-02	0.2609E-02	0.2711E-02	0.2862E-02	0.2027E-02	0.3678E-02	0.5052E-02	0.6432E-02
0.2363E-02	0.1930E-02	0.8417E-03	-0.1337E-03	0.7529E-02	0.8619E-02	0.9447E-02	0.1022E-01
-0.1653E-02	-0.3002E-02	-0.4733E-02	-0.6275E-02	0.1077E-01	0.1126E-01	0.1160E-01	0.1185E-01
-0.8002E-02	-0.9489E-02	-0.1094E-01	-0.1216E-01	0.1199E-01	0.1202E-01	0.1201E-01	0.1186E-01
-0.1316E-01	-0.1398E-01	-0.1439E-01	-0.1468E-01	0.1169E-01	0.1134E-01	0.1103E-01	0.1050E-01
-0.1448E-01	-0.1429E-01	-0.1359E-01	-0.1300E-01	0.1004E-01	0.9354E-02	0.8712E-02	0.7840E-02
-0.1192E-01	-0.1107E-01	-0.9842E-02	-0.8948E-02	0.7047E-02	0.6039E-02	0.5113E-02	0.4015E-02
-0.7806E-02	-0.7030E-02	-0.6139E-02	-0.5645E-02	0.2991E-02	0.1864E-02	0.8216E-03	-0.2422E-03
-0.5167E-02	-0.5048E-02	-0.5035E-02	-0.5303E-02	-0.1213E-02	-0.2137E-02	-0.2977E-02	-0.3642E-02
-0.5765E-02	-0.6364E-02	-0.7157E-02	-0.7935E-02	-0.4229E-02	-0.4595E-02	-0.4892E-02	-0.4922E-02
-0.8913E-02	-0.9730E-02	-0.1070E-01	-0.1133E-01	-0.4897E-02	-0.4579E-02	-0.4257E-02	-0.3649E-02

-0.3096E-02 -0.2315E-02 -0.1622E-02 -0.7701E-03
-0.5413E-04 0.7319E-03 0.1349E-02 0.1934E-02
0.2345E-02 0.2614E-02 0.2708E-02 0.2599E-02
0.2331E-02 0.1821E-02 0.1177E-02 0.2595E-03
-0.7101E-03 -0.1934E-02 -0.3160E-02 -0.4627E-02
-0.6022E-02 -0.7591E-02 -0.9025E-02 -0.1056E-01
-0.1194E-01 -0.1336E-01 -0.1458E-01 -0.1575E-01
-0.1674E-01 -0.1763E-01 -0.1835E-01 -0.1891E-01
-0.1929E-01 -0.1950E-01 -0.1960E-01 -0.1949E-01
-0.1932E-01 -0.1889E-01 -0.1841E-01 -0.1770E-01
-0.1700E-01 -0.1605E-01 -0.1511E-01 -0.1393E-01
-0.1276E-01 -0.1143E-01 -0.1008E-01 -0.8574E-02
-0.7064E-02 -0.5434E-02 -0.3817E-02 -0.2121E-02
-0.4316E-03 0.1257E-02 0.2929E-02 0.4537E-02
0.6118E-02 0.7566E-02 0.8973E-02 0.1014E-01
0.1125E-01 0.1209E-01 0.1284E-01 0.1331E-01
0.1366E-01 0.1368E-01 0.1359E-01 0.1321E-01
0.1273E-01 0.1198E-01 0.1113E-01 0.1007E-01
0.8981E-02 0.7783E-02 0.6557E-02 0.5290E-02
0.4033E-02 0.2886E-02 0.1772E-02 0.8246E-03
-0.8119E-04 -0.7638E-03 -0.1343E-02 -0.1657E-02
-0.1895E-02 -0.1856E-02 -0.1742E-02 -0.1366E-02
-0.9241E-03 -0.2652E-03 0.4349E-03 0.1315E-02

Time history of vertical velocity at node NL2:

-0.2085E-01 -0.1161E-01 -0.1803E-01 -0.1164E-01
-0.1470E-01 -0.1951E-01 -0.3714E-01 -0.3527E-01
-0.3275E-01 -0.3639E-01 -0.4301E-01 -0.4732E-01
-0.5733E-01 -0.4519E-01 -0.4721E-01 -0.5071E-01
-0.5005E-01 -0.5181E-01 -0.4660E-01 -0.3675E-01
-0.4074E-01 -0.3764E-01 -0.3694E-01 -0.3060E-01
-0.2805E-01 -0.2279E-01 -0.2866E-01 -0.2694E-01
-0.2328E-01 -0.2605E-01 -0.2290E-01 -0.2874E-01
-0.3292E-01 -0.3072E-01 -0.3472E-01 -0.3458E-01
-0.4030E-01 -0.4133E-01 -0.4523E-01 -0.4179E-01
-0.4421E-01 -0.4604E-01 -0.4397E-01 -0.4659E-01
-0.4105E-01 -0.4049E-01 -0.3922E-01 -0.3754E-01
-0.3448E-01 -0.3213E-01 -0.2787E-01 -0.2678E-01
-0.2534E-01 -0.2323E-01 -0.2097E-01 -0.2029E-01
-0.1941E-01 -0.1996E-01 -0.2204E-01 -0.1976E-01
-0.2389E-01 -0.2330E-01 -0.2713E-01 -0.2924E-01
-0.3055E-01 -0.3341E-01 -0.3414E-01 -0.3837E-01
-0.3735E-01 -0.4107E-01 -0.3879E-01 -0.4035E-01
-0.3976E-01 -0.3834E-01 -0.3765E-01 -0.3490E-01
-0.3355E-01 -0.3122E-01 -0.3021E-01 -0.2718E-01
-0.2653E-01 -0.2398E-01 -0.2411E-01 -0.2257E-01
-0.2346E-01 -0.2191E-01 -0.2380E-01 -0.2346E-01
-0.2510E-01 -0.2643E-01 -0.2682E-01 -0.2897E-01
-0.2931E-01 -0.3124E-01 -0.3144E-01 -0.3244E-01
-0.3227E-01 -0.3236E-01 -0.3215E-01 -0.3111E-01
-0.3007E-01 -0.2885E-01 -0.2646E-01 -0.2590E-01
-0.2249E-01 -0.2197E-01 -0.1864E-01 -0.1830E-01
-0.1597E-01 -0.1587E-01 -0.1473E-01 -0.1467E-01
-0.1510E-01 -0.1521E-01 -0.1684E-01 -0.1727E-01
-0.1953E-01 -0.2009E-01 -0.2302E-01 -0.2315E-01
-0.2635E-01 -0.2595E-01 -0.2867E-01 -0.2808E-01
-0.2971E-01 -0.2906E-01 -0.2919E-01 -0.2870E-01
-0.2728E-01 -0.2707E-01 -0.2449E-01 -0.2417E-01
-0.2130E-01 -0.2060E-01 -0.1808E-01 -0.1710E-01
-0.1510E-01 -0.1414E-01 -0.1280E-01 -0.1211E-01
-0.1142E-01 -0.1124E-01 -0.1115E-01 -0.1161E-01
-0.1217E-01 -0.1303E-01 -0.1414E-01 -0.1517E-01
-0.1648E-01 -0.1762E-01 -0.1872E-01 -0.1975E-01
-0.2042E-01 -0.2107E-01 -0.2129E-01 -0.2136E-01
-0.2120E-01 -0.2058E-01 -0.2023E-01 -0.1898E-01
-0.1854E-01 -0.1701E-01 -0.1641E-01 -0.1506E-01
-0.1435E-01 -0.1348E-01 -0.1282E-01 -0.1254E-01
-0.1214E-01 -0.1241E-01 -0.1249E-01 -0.1313E-01
-0.1379E-01 -0.1458E-01 -0.1570E-01 -0.1651E-01
-0.1770E-01 -0.1823E-01 -0.1915E-01 -0.1925E-01
-0.1970E-01 -0.1933E-01 -0.1920E-01 -0.1845E-01
-0.1768E-01 -0.1671E-01 -0.1535E-01 -0.1443E-01
-0.1260E-01 -0.1195E-01 -0.9911E-02 -0.9624E-02
-0.7754E-02 -0.7786E-02 -0.6465E-02 -0.6712E-02
-0.6168E-02 -0.6552E-02 -0.6854E-02 -0.7303E-02
-0.8308E-02 -0.8772E-02 -0.1022E-01 -0.1065E-01
-0.1224E-01 -0.1251E-01 -0.1397E-01 -0.1396E-01
-0.1507E-01 -0.1470E-01 -0.1526E-01 -0.1452E-01
-0.1444E-01 -0.1339E-01 -0.1269E-01 -0.1142E-01
-0.1023E-01 -0.8889E-02 -0.7439E-02 -0.6202E-02
-0.4734E-02 -0.3762E-02 -0.2448E-02 -0.1917E-02
-0.8514E-03 -0.8504E-03 -0.6302E-04 -0.5674E-03
-0.5546E-04 -0.9290E-03 -0.6668E-03 -0.1659E-02
-0.1618E-02 -0.2467E-02 -0.2595E-02 -0.3086E-02
-0.3286E-02 -0.3311E-02 -0.3501E-02 -0.3050E-02
-0.3160E-02 -0.2309E-02 -0.2303E-02 -0.1209E-02
-0.1097E-02 0.6409E-04 0.2541E-03 0.1290E-02
0.1511E-02 0.2252E-02 0.2457E-02 0.2809E-02

0.2895E-02	0.2755E-02	0.2592E-02	0.2029E-02	0.1258E-01	0.1230E-01	0.1188E-01	0.1163E-01
0.1599E-02	0.7606E-03	0.1075E-03	-0.8262E-03	0.1140E-01	0.1121E-01	0.1120E-01	0.1105E-01
-0.1617E-02	-0.2518E-02	-0.3304E-02	-0.4074E-02	0.1119E-01	0.1104E-01	0.1124E-01	0.1105E-01
-0.4721E-02	-0.5307E-02	-0.5731E-02	-0.6124E-02	0.1126E-01	0.1102E-01	0.1116E-01	0.1085E-01
-0.6291E-02	-0.6523E-02	-0.6474E-02	-0.6601E-02	0.1087E-01	0.1050E-01	0.1039E-01	0.9974E-02
-0.6416E-02	-0.6509E-02	-0.6283E-02	-0.6415E-02	0.9733E-02	0.9321E-02	0.8993E-02	0.8638E-02
-0.6242E-02	-0.6461E-02	-0.6412E-02	-0.6723E-02	0.8289E-02	0.8045E-02	0.7747E-02	0.7668E-02
-0.6841E-02	-0.7228E-02	-0.7501E-02	-0.7912E-02	0.7488E-02	0.7613E-02	0.7596E-02	0.7935E-02
-0.8281E-02	-0.8660E-02	-0.9048E-02	-0.9317E-02	0.8104E-02	0.8638E-02	0.8984E-02	0.9661E-02
-0.9627E-02	-0.9711E-02	-0.9860E-02	-0.9699E-02	0.1014E-01	0.1088E-01	0.1142E-01	0.1214E-01
-0.9655E-02	-0.9209E-02	-0.9003E-02	-0.8270E-02	0.1267E-01	0.1327E-01	0.1369E-01	0.1409E-01
-0.7881E-02	-0.6857E-02	-0.6285E-02	-0.5018E-02	0.1433E-01	0.1446E-01	0.1448E-01	0.1431E-01
-0.4292E-02	-0.2924E-02	-0.2125E-02	-0.8456E-03	0.1408E-01	0.1362E-01	0.1315E-01	0.1244E-01
-0.4560E-04	0.9780E-03	0.1679E-02	0.2281E-02	0.1178E-01	0.1089E-01	0.1010E-01	0.9133E-02
0.2790E-02	0.2880E-02	0.3158E-02	0.2719E-02	0.8312E-02	0.7353E-02	0.6590E-02	0.5736E-02
0.2733E-02	0.1821E-02	0.1582E-02	0.3461E-03	0.5106E-02	0.4423E-02	0.3957E-02	0.3406E-02
-0.1052E-03	-0.1488E-02	-0.2083E-02	-0.3409E-02	0.3019E-02	0.2554E-02	0.2226E-02	0.1835E-02
-0.4057E-02	-0.5132E-02	-0.5731E-02	-0.6414E-02	0.1559E-02	0.1260E-02	0.1031E-02	0.8150E-03
-0.6859E-02	-0.7064E-02	-0.7261E-02	-0.6960E-02	0.6146E-03	0.4831E-03	0.3158E-03	0.2783E-03
-0.6866E-02	-0.6095E-02	-0.5688E-02	-0.4526E-02	0.1339E-03	0.1732E-03	0.5764E-04	0.1736E-03
-0.3842E-02	-0.2404E-02	-0.1505E-02	0.9640E-04	0.9641E-04	0.2754E-03	0.2339E-03	0.4563E-03
0.1138E-02	0.2654E-02	0.3527E-02	0.4700E-02	0.4614E-03	0.7085E-03	0.7632E-03	0.1004E-02
0.5354E-02	0.6178E-02	0.6649E-02	0.7182E-02	0.1095E-02	0.1303E-02	0.1424E-02	0.1575E-02
0.7580E-02	0.7874E-02	0.8222E-02	0.8338E-02	0.1706E-02	0.1763E-02	0.1877E-02	0.1837E-02
0.8684E-02	0.8683E-02	0.9045E-02	0.8926E-02	0.1916E-02	0.1765E-02	0.1787E-02	0.1528E-02
0.9252E-02	0.9037E-02	0.9276E-02	0.8963E-02	0.1485E-02	0.1142E-02	0.1033E-02	0.6343E-03
0.9027E-02	0.8580E-02	0.8405E-02	0.7813E-02	0.4721E-03	0.6377E-04	-0.1220E-03	-0.4832E-03
0.7351E-02	0.6607E-02	0.5843E-02	0.4945E-02	-0.6614E-03	-0.9180E-03	-0.1041E-02	-0.1139E-02
0.3936E-02	0.2924E-02	0.1751E-02	0.6846E-03	-0.1162E-02	-0.1054E-02	-0.9360E-03	-0.5889E-03
-0.5429E-03	-0.1562E-02	-0.2693E-02	-0.3558E-02	-0.2939E-03	0.2990E-03	0.7888E-03	0.1618E-02
-0.4464E-02	-0.5056E-02	-0.5612E-02	-0.5818E-02	0.2306E-02	0.3339E-02	0.4203E-02	0.5384E-02
-0.5936E-02	-0.5686E-02	-0.5325E-02	-0.4580E-02	0.6390E-02	0.7649E-02	0.8742E-02	0.9999E-02
-0.3746E-02	-0.2517E-02	-0.1267E-02	0.3610E-03	0.1112E-01	0.1229E-01	0.1336E-01	0.1439E-01
0.1891E-02	0.3704E-02	0.5328E-02	0.7147E-02	0.1536E-01	0.1619E-01	0.1700E-01	0.1761E-01
0.8724E-02	0.1039E-01	0.1182E-01	0.1321E-01	0.1823E-01	0.1860E-01	0.1902E-01	0.1917E-01
0.1440E-01	0.1542E-01	0.1632E-01	0.1696E-01	0.1938E-01	0.1932E-01	0.1934E-01	0.1911E-01
0.1758E-01	0.1785E-01	0.1823E-01	0.1820E-01	0.1897E-01	0.1861E-01	0.1834E-01	0.1789E-01
0.1838E-01	0.1815E-01	0.1821E-01	0.1787E-01	0.1752E-01	0.1703E-01	0.1659E-01	0.1609E-01
0.1788E-01	0.1753E-01	0.1753E-01	0.1723E-01	0.1561E-01	0.1511E-01	0.1461E-01	0.1415E-01
0.1723E-01	0.1702E-01	0.1703E-01	0.1691E-01	0.1365E-01	0.1321E-01	0.1272E-01	0.1232E-01
0.1690E-01	0.1686E-01	0.1678E-01	0.1677E-01	0.1183E-01	0.1146E-01	0.1098E-01	0.1063E-01
0.1659E-01	0.1658E-01	0.1627E-01	0.1623E-01	0.1016E-01	0.9817E-02	0.9345E-02	0.8997E-02
0.1577E-01	0.1568E-01	0.1510E-01	0.1494E-01	0.8527E-02	0.8166E-02	0.7693E-02	0.7306E-02
0.1429E-01	0.1407E-01	0.1342E-01	0.1316E-01	0.6823E-02	0.6403E-02	0.5913E-02	0.5453E-02

0.4950E-02	0.4441E-02	0.3926E-02	0.3368E-02	0.3575E-02	0.3630E-02	0.3691E-02	0.3613E-02
0.2839E-02	0.2231E-02	0.1685E-02	0.1031E-02	0.3548E-02	0.3346E-02	0.3162E-02	0.2852E-02
0.4763E-03	-0.2140E-03	-0.7798E-03	-0.1491E-02	0.2566E-02	0.2175E-02	0.1816E-02	0.1380E-02
-0.2057E-02	-0.2769E-02	-0.3322E-02	-0.4005E-02	0.9792E-03	0.5465E-03	0.1503E-03	-0.2388E-03
-0.4533E-02	-0.5159E-02	-0.5640E-02	-0.6173E-02	-0.5873E-03	-0.8873E-03	-0.1147E-02	-0.1320E-02
-0.6584E-02	-0.6993E-02	-0.7321E-02	-0.7593E-02	-0.1453E-02	-0.1472E-02	-0.1454E-02	-0.1302E-02
-0.7818E-02	-0.7913E-02	-0.7996E-02	-0.7885E-02	-0.1120E-02	-0.7958E-03	-0.4520E-03	0.3302E-04
-0.7790E-02	-0.7454E-02	-0.7167E-02	-0.6618E-02	0.5241E-03	0.1143E-02	0.1753E-02	0.2463E-02
-0.6141E-02	-0.5405E-02	-0.4757E-02	-0.3877E-02	0.3154E-02	0.3913E-02	0.4633E-02	0.5384E-02
-0.3094E-02	-0.2130E-02	-0.1257E-02	-0.2687E-03	0.6085E-02	0.6771E-02	0.7401E-02	0.7973E-02
0.6396E-03	0.1587E-02	0.2478E-02	0.3328E-02	0.8477E-02	0.8888E-02	0.9227E-02	0.9437E-02
0.4151E-02	0.4861E-02	0.5570E-02	0.6108E-02	0.9582E-02	0.9565E-02	0.9488E-02	0.9239E-02
0.6672E-02	0.7020E-02	0.7415E-02	0.7572E-02	0.8936E-02	0.8454E-02	0.7932E-02	0.7241E-02
0.7788E-02	0.7764E-02	0.7805E-02	0.7622E-02	0.6515E-02	0.5644E-02	0.4754E-02	0.3748E-02
0.7500E-02	0.7185E-02	0.6919E-02	0.6509E-02	0.2737E-02	0.1651E-02	0.5700E-03	-0.5363E-03
0.6127E-02	0.5654E-02	0.5184E-02	0.4685E-02	-0.1626E-02	-0.2689E-02	-0.3721E-02	-0.4680E-02
0.4162E-02	0.3665E-02	0.3116E-02	0.2643E-02	-0.5600E-02	-0.6395E-02	-0.7144E-02	-0.7730E-02
0.2102E-02	0.1673E-02	0.1161E-02	0.7850E-03	-0.8262E-02	-0.8607E-02	-0.8886E-02	-0.8965E-02
0.3168E-03	-0.4445E-05	-0.4144E-03	-0.6829E-03	-0.8977E-02	-0.8785E-02	-0.8526E-02	-0.8082E-02
-0.1034E-02	-0.1261E-02	-0.1559E-02	-0.1760E-02	-0.7563E-02	-0.6890E-02	-0.6149E-02	-0.5293E-02
-0.2013E-02	-0.2201E-02	-0.2426E-02	-0.2621E-02	-0.4381E-02	-0.3398E-02	-0.2365E-02	-0.1315E-02
-0.2834E-02	-0.3053E-02	-0.3268E-02	-0.3520E-02	-0.2295E-03	0.8271E-03	0.1905E-02	0.2908E-02
-0.3754E-02	-0.4051E-02	-0.4309E-02	-0.4650E-02	0.3920E-02	0.4815E-02	0.5704E-02	0.6449E-02
-0.4931E-02	-0.5310E-02	-0.5617E-02	-0.6020E-02	0.7167E-02	0.7732E-02	0.8255E-02	0.8616E-02
-0.6339E-02	-0.6748E-02	-0.7063E-02	-0.7459E-02	0.8921E-02	0.9076E-02	0.9164E-02	0.9122E-02
-0.7758E-02	-0.8115E-02	-0.8380E-02	-0.8678E-02	0.9002E-02	0.8778E-02	0.8477E-02	0.8105E-02
-0.8898E-02	-0.9127E-02	-0.9292E-02	-0.9439E-02	0.7655E-02	0.7168E-02	0.6609E-02	0.6048E-02
-0.9548E-02	-0.9617E-02	-0.9678E-02	-0.9675E-02	0.5424E-02	0.4829E-02	0.4181E-02	0.3589E-02
-0.9695E-02	-0.9637E-02	-0.9636E-02	-0.9549E-02	0.2960E-02	0.2404E-02	0.1831E-02	0.1339E-02
-0.9538E-02	-0.9427E-02	-0.9407E-02	-0.9285E-02	0.8427E-03	0.4343E-03	0.3709E-04	-0.2757E-03
-0.9258E-02	-0.9132E-02	-0.9094E-02	-0.8973E-02	-0.5656E-03	-0.7859E-03	-0.9724E-03	-0.1104E-02
-0.8930E-02	-0.8819E-02	-0.8764E-02	-0.8667E-02	-0.1195E-02	-0.1253E-02	-0.1268E-02	-0.1279E-02
-0.8603E-02	-0.8527E-02	-0.8451E-02	-0.8390E-02	-0.1245E-02	-0.1231E-02	-0.1181E-02	-0.1170E-02
-0.8298E-02	-0.8252E-02	-0.8146E-02	-0.8111E-02	-0.1136E-02	-0.1165E-02	-0.1180E-02	-0.1274E-02
-0.7985E-02	-0.7950E-02	-0.7810E-02	-0.7769E-02	-0.1368E-02	-0.1552E-02	-0.1750E-02	-0.2043E-02
-0.7615E-02	-0.7556E-02	-0.7386E-02	-0.7306E-02	-0.2360E-02	-0.2770E-02	-0.3217E-02	-0.3743E-02
-0.7128E-02	-0.7014E-02	-0.6822E-02	-0.6667E-02	-0.4313E-02	-0.4943E-02	-0.5622E-02	-0.6337E-02
-0.6461E-02	-0.6265E-02	-0.6045E-02	-0.5796E-02	-0.7095E-02	-0.7861E-02	-0.8663E-02	-0.9444E-02
-0.5555E-02	-0.5254E-02	-0.4987E-02	-0.4634E-02	-0.1025E-01	-0.1100E-01	-0.1175E-01	-0.1242E-01
-0.4334E-02	-0.3927E-02	-0.3591E-02	-0.3139E-02	-0.1309E-01	-0.1364E-01	-0.1415E-01	-0.1454E-01
-0.2765E-02	-0.2276E-02	-0.1864E-02	-0.1351E-02	-0.1487E-01	-0.1507E-01	-0.1519E-01	-0.1517E-01
-0.9111E-03	-0.3947E-03	0.5908E-04	0.5611E-03	-0.1505E-01	-0.1480E-01	-0.1444E-01	-0.1397E-01
0.1010E-02	0.1467E-02	0.1887E-02	0.2273E-02	-0.1338E-01	-0.1269E-01	-0.1189E-01	-0.1102E-01
0.2638E-02	0.2934E-02	0.3216E-02	0.3396E-02	-0.1004E-01	-0.9027E-02	-0.7915E-02	-0.6791E-02

-0.5593E-02 -0.4419E-02 -0.3190E-02 -0.2014E-02
-0.8124E-03 0.3180E-03 0.1439E-02 0.2477E-02
0.3475E-02 0.4376E-02 0.5212E-02 0.5945E-02
0.6591E-02 0.7139E-02 0.7581E-02 0.7930E-02
0.8162E-02 0.8316E-02 0.8348E-02 0.8325E-02
0.8177E-02 0.7993E-02 0.7699E-02 0.7387E-02
0.6989E-02 0.6589E-02 0.6123E-02 0.5677E-02
0.5198E-02 0.4754E-02 0.4303E-02 0.3895E-02
0.3515E-02 0.3186E-02 0.2912E-02 0.2692E-02
0.2545E-02 0.2449E-02 0.2446E-02 0.2486E-02
0.2623E-02 0.2795E-02 0.3059E-02 0.3346E-02

Time history of vertical acceleration at node NL1:

-0.1539E+02 -0.2524E+02 -0.3216E+02 0.1477E+02
0.1543E+02 -0.1858E+02 0.7175E+01 -0.5063E+01
0.5680E+01 0.4915E+02 -0.8121E+01 0.1790E+02
0.6788E+01 0.1703E+02 0.2577E+02 0.1411E+02
0.3655E+01 -0.1017E+02 0.2365E+02 -0.1205E+02
0.1070E+02 -0.1054E+02 -0.2961E+02 0.9242E+01
-0.2535E+02 0.1423E+01 -0.2760E+02 -0.9130E+01
-0.2453E+02 0.5593E+01 -0.1371E+02 -0.6656E+01
-0.3219E+01 -0.5016E+01 0.8801E+01 0.9659E+01
0.6917E+01 0.2987E+01 0.2325E+02 -0.2586E+01
0.3620E+02 -0.6887E+01 0.2544E+02 -0.4429E+01
0.2171E+02 -0.2279E+01 0.8569E+01 -0.1700E+01
-0.1057E+02 0.6548E+01 -0.1760E+02 -0.6392E+00
-0.1803E+02 -0.9858E+01 -0.1445E+02 -0.6599E+01
-0.1534E+02 -0.5605E+01 -0.1278E+02 -0.1929E+00
-0.7434E+01 0.8319E+01 -0.7286E+01 0.1310E+02
0.7178E+00 0.1365E+02 0.9186E+01 0.1140E+02
0.9479E+01 0.1257E+02 0.9143E+01 0.9378E+01
0.7587E+01 0.1472E+01 0.5842E+01 -0.4657E+01
0.4580E+01 -0.1415E+02 0.4377E+01 -0.2159E+02
0.3642E+01 -0.2092E+02 -0.2346E+01 -0.1543E+02
-0.7122E+01 -0.7594E+01 -0.8147E+01 -0.1643E+00
-0.8017E+01 0.6414E+01 -0.3821E+01 0.1013E+02
0.1928E+01 0.1119E+02 0.5488E+01 0.1293E+02
0.6857E+01 0.1213E+02 0.6982E+01 0.7993E+01
0.6489E+01 0.3370E+01 0.3754E+01 -0.1587E+01
-0.2334E+00 -0.5334E+01 -0.4622E+01 -0.6454E+01
-0.9988E+01 -0.5403E+01 -0.1311E+02 -0.4122E+01
-0.1204E+02 -0.3702E+01 -0.8041E+01 -0.2768E+01
-0.2333E+01 -0.1290E+01 0.3449E+01 0.5706E+00
0.7756E+01 0.3363E+01 0.9798E+01 0.5454E+01
0.1033E+02 0.5465E+01 0.1001E+02 0.3767E+01
0.8072E+01 0.1095E+01 0.4839E+01 -0.1939E+01
0.1179E+01 -0.4829E+01 -0.2538E+01 -0.6895E+01
-0.5232E+01 -0.8088E+01 -0.6195E+01 -0.8212E+01
-0.5902E+01 -0.6192E+01 -0.5226E+01 -0.1984E+01
-0.4555E+01 0.3361E+01 -0.3751E+01 0.8661E+01
-0.2738E+01 0.1239E+02 -0.1249E+01 0.1341E+02
0.7575E+00 0.1165E+02 0.2450E+01 0.7914E+01
0.3261E+01 0.3044E+01 0.3236E+01 -0.2266E+01
0.2563E+01 -0.7098E+01 0.1577E+01 -0.1071E+02
0.6664E+00 -0.1257E+02 -0.7707E-02 -0.1217E+02
-0.4985E+00 -0.9559E+01 -0.6345E+00 -0.5533E+01
-0.1048E+00 -0.1122E+01 0.1064E+01 0.2831E+01
0.2483E+01 0.5743E+01 0.3585E+01 0.7451E+01
0.3811E+01 0.8128E+01 0.2734E+01 0.7804E+01
0.6182E+00 0.6475E+01 -0.1905E+01 0.4258E+01
-0.4295E+01 0.1544E+01 -0.6001E+01 -0.1164E+01
-0.6696E+01 -0.3384E+01 -0.6303E+01 -0.4668E+01
-0.4826E+01 -0.4950E+01 -0.2440E+01 -0.4384E+01
0.4927E+00 -0.3057E+01 0.3321E+01 -0.1235E+01
0.5438E+01 0.7728E+00 0.6485E+01 0.2549E+01
0.6303E+01 0.3604E+01 0.5164E+01 0.3603E+01
0.3488E+01 0.2430E+01 0.1608E+01 0.4294E+00
-0.1865E+00 -0.1810E+01 -0.1721E+01 -0.3732E+01
-0.2838E+01 -0.4800E+01 -0.3413E+01 -0.4784E+01
-0.3410E+01 -0.3702E+01 -0.2844E+01 -0.1717E+01
-0.1940E+01 0.8112E+00 -0.9336E+00 0.3410E+01
0.7180E-02 0.5515E+01 0.7221E+00 0.6676E+01
0.1153E+01 0.6638E+01 0.1251E+01 0.5404E+01
0.9828E+00 0.3303E+01 0.3727E+00 0.7750E+00
-0.4547E+00 -0.1743E+01 -0.1236E+01 -0.3849E+01
-0.1700E+01 -0.5305E+01 -0.1624E+01 -0.5961E+01
-0.9119E+00 -0.5765E+01 0.3185E+00 -0.4775E+01
0.1751E+01 -0.3210E+01 0.3114E+01 -0.1317E+01
0.4069E+01 0.5650E+00 0.4340E+01 0.2195E+01
0.3807E+01 0.3351E+01 0.2456E+01 0.3935E+01
0.4704E+00 0.3947E+01 -0.1807E+01 0.3386E+01
-0.3920E+01 0.2376E+01 -0.5451E+01 0.1114E+01
-0.6124E+01 -0.1660E+00 -0.5800E+01 -0.1203E+01
-0.4574E+01 -0.1814E+01 -0.2694E+01 -0.1890E+01
-0.4609E+00 -0.1517E+01 0.1762E+01 -0.8555E+00
0.3638E+01 -0.8829E-01 0.4898E+01 0.5354E+00
0.5384E+01 0.8359E+00 0.5085E+01 0.7661E+00
0.4080E+01 0.2818E+00 0.2567E+01 -0.4910E+00

0.8844E+00	-0.1310E+01	-0.7691E+00	-0.1981E+01	-0.3456E+00	-0.9848E+00	-0.5913E+00	-0.3955E+00
-0.2137E+01	-0.2224E+01	-0.3010E+01	-0.1990E+01	-0.7479E+00	0.2380E+00	-0.8133E+00	0.8247E+00
-0.3345E+01	-0.1270E+01	-0.3090E+01	-0.1765E+00	-0.8210E+00	0.1271E+01	-0.7983E+00	0.1533E+01
-0.2355E+01	0.1022E+01	-0.1309E+01	0.2136E+01	-0.7616E+00	0.1565E+01	-0.7272E+00	0.1388E+01
-0.1852E+00	0.2945E+01	0.7479E+00	0.3288E+01	-0.6547E+00	0.1067E+01	-0.5840E+00	0.5757E+00
0.1333E+01	0.3111E+01	0.1457E+01	0.2447E+01	-0.4971E+00	0.4951E-01	-0.3589E+00	-0.4570E+00
0.1091E+01	0.1410E+01	0.4117E+00	0.1808E+00	-0.2092E+00	-0.8942E+00	0.8740E-02	-0.1177E+01
-0.4268E+00	-0.1033E+01	-0.1197E+01	-0.1993E+01	0.2662E+00	-0.1301E+01	0.5123E+00	-0.1242E+01
-0.1659E+01	-0.2622E+01	-0.1645E+01	-0.2808E+01	0.7635E+00	-0.1031E+01	0.9579E+00	-0.7207E+00
-0.1103E+01	-0.2549E+01	-0.9138E-01	-0.1887E+01	0.1055E+01	-0.3471E+00	0.1059E+01	0.1117E-01
0.1211E+01	-0.1071E+01	0.2426E+01	-0.1606E+00	0.9368E+00	0.2942E+00	0.7067E+00	0.4982E+00
0.3350E+01	0.7029E+00	0.3737E+01	0.1272E+01	0.3869E+00	0.5752E+00	-0.7243E-03	0.5511E+00
0.3485E+01	0.1595E+01	0.2616E+01	0.1600E+01	-0.3860E+00	0.4578E+00	-0.7457E+00	0.3149E+00
0.1215E+01	0.1286E+01	-0.4153E+00	0.8173E+00	-0.1024E+01	0.1786E+00	-0.1186E+01	0.7712E-01
-0.2057E+01	0.2865E+00	-0.3442E+01	-0.1799E+00	-0.1226E+01	0.3223E-01	-0.1123E+01	0.4853E-01
-0.4277E+01	-0.4858E+00	-0.4486E+01	-0.5602E+00	-0.9011E+00	0.1116E+00	-0.5893E+00	0.2068E+00
-0.4055E+01	-0.3776E+00	-0.3037E+01	-0.2831E-01	-0.2176E+00	0.2834E+00	0.1688E+00	0.3209E+00
-0.1650E+01	0.4004E+00	-0.9670E-01	0.7818E+00	0.5259E+00	0.3047E+00	0.8115E+00	0.2232E+00
0.1372E+01	0.9627E+00	0.2563E+01	0.8741E+00	0.1007E+01	0.8351E-01	0.1097E+01	-0.9004E-01
0.3322E+01	0.5026E+00	0.3554E+01	-0.1071E+00	0.1088E+01	-0.2698E+00	0.9979E+00	-0.4230E+00
0.3288E+01	-0.8210E+00	0.2612E+01	-0.1506E+01	0.8433E+00	-0.5141E+00	0.6472E+00	-0.5221E+00
0.1660E+01	-0.1968E+01	0.6526E+00	-0.2100E+01	0.4341E+00	-0.4389E+00	0.2189E+00	-0.2740E+00
-0.3024E+00	-0.1877E+01	-0.1021E+01	-0.1261E+01	0.2408E-01	-0.4324E-01	-0.1564E+00	0.2091E+00
-0.1438E+01	-0.3752E+00	-0.1554E+01	0.6472E+00	-0.3106E+00	0.4586E+00	-0.4426E+00	0.6641E+00
-0.1352E+01	0.1618E+01	-0.9643E+00	0.2363E+01	-0.5578E+00	0.7955E+00	-0.6461E+00	0.8287E+00
-0.4966E+00	0.2788E+01	-0.7669E-01	0.2789E+01	-0.7038E+00	0.7605E+00	-0.7238E+00	0.5957E+00
0.1944E+00	0.2391E+01	0.2737E+00	0.1677E+01	-0.6891E+00	0.3535E+00	-0.5930E+00	0.6874E-01
0.1302E+00	0.7530E+00	-0.1402E+00	-0.2242E+00	-0.4456E+00	-0.2179E+00	-0.2445E+00	-0.4726E+00
-0.4467E+00	-0.1116E+01	-0.7012E+00	-0.1774E+01	-0.9593E-02	-0.6740E+00	0.2288E+00	-0.7888E+00
-0.8034E+00	-0.2134E+01	-0.6842E+00	-0.2162E+01	0.4623E+00	-0.8187E+00	0.6435E+00	-0.7800E+00
-0.3496E+00	-0.1883E+01	0.1499E+00	-0.1377E+01	0.7559E+00	-0.6608E+00	0.7770E+00	-0.5069E+00
0.7342E+00	-0.7567E+00	0.1284E+01	-0.1285E+00	0.6979E+00	-0.3411E+00	0.5338E+00	-0.1681E+00
0.1665E+01	0.4023E+00	0.1799E+01	0.7493E+00	0.2886E+00	-0.2777E-01	-0.3335E-02	0.8415E-01
0.1649E+01	0.8715E+00	0.1216E+01	0.7892E+00	-0.2986E+00	0.1568E+00	-0.5824E+00	0.2009E+00
0.5777E+00	0.5671E+00	-0.1651E+00	0.2410E+00	-0.8013E+00	0.2216E+00	-0.9343E+00	0.2261E+00
-0.9193E+00	-0.5997E-01	-0.1552E+01	-0.2672E+00	-0.9794E+00	0.2257E+00	-0.9241E+00	0.2197E+00
-0.1979E+01	-0.3346E+00	-0.2143E+01	-0.2243E+00	-0.7773E+00	0.2015E+00	-0.5665E+00	0.1780E+00
-0.2024E+01	0.2929E-01	-0.1649E+01	0.3652E+00	-0.3137E+00	0.1398E+00	-0.5799E-01	0.8346E-01
-0.1077E+01	0.7089E+00	-0.4049E+00	0.9645E+00	0.1849E+00	0.1230E-01	0.3727E+00	-0.8171E-01
0.2863E+00	0.1059E+01	0.9039E+00	0.9465E+00	0.5053E+00	-0.1789E+00	0.5853E+00	-0.2702E+00
0.1361E+01	0.6343E+00	0.1632E+01	0.1515E+00	0.6080E+00	-0.3375E+00	0.5939E+00	-0.3523E+00
0.1689E+01	-0.4239E+00	0.1549E+01	-0.9726E+00	0.5505E+00	-0.3226E+00	0.4987E+00	-0.2445E+00
0.1248E+01	-0.1417E+01	0.8469E+00	-0.1670E+01	0.4463E+00	-0.1214E+00	0.3835E+00	0.2975E-01
0.4140E+00	-0.1674E+01	-0.4510E-03	-0.1435E+01	0.3252E+00	0.1903E+00	0.2445E+00	0.3418E+00

0.1381E+00	0.4596E+00	0.1369E-01	0.5251E+00	-0.2302E+00	0.2029E+00	-0.3569E+00	0.1029E+00
-0.1362E+00	0.5311E+00	-0.3002E+00	0.4886E+00	-0.4641E+00	-0.1986E-01	-0.5514E+00	-0.1471E+00
-0.4596E+00	0.3814E+00	-0.5929E+00	0.2444E+00	-0.5992E+00	-0.2688E+00	-0.5916E+00	-0.3716E+00
-0.6739E+00	0.8982E-01	-0.6996E+00	-0.6673E-01	-0.5452E+00	-0.4288E+00	-0.4517E+00	-0.4444E+00
-0.6367E+00	-0.2003E+00	-0.5040E+00	-0.3021E+00	-0.3134E+00	-0.4263E+00	-0.1490E+00	-0.3602E+00
-0.3118E+00	-0.3580E+00	-0.6699E-01	-0.3779E+00	0.2048E-01	-0.2646E+00	0.1860E+00	-0.1588E+00
0.1842E+00	-0.3708E+00	0.4138E+00	-0.3351E+00	0.3374E+00	-0.4302E-01	0.4410E+00	0.6483E-01
0.5988E+00	-0.2947E+00	0.6973E+00	-0.2559E+00	0.5046E+00	0.1560E+00	0.5280E+00	0.2262E+00
0.7064E+00	-0.2197E+00	0.6230E+00	-0.1981E+00	0.4944E+00	0.2829E+00	0.4237E+00	0.3182E+00
0.4485E+00	-0.1786E+00	0.2197E+00	-0.1593E+00	0.3342E+00	0.3263E+00	0.2231E+00	0.3289E+00
-0.4023E-01	-0.1331E+00	-0.3022E+00	-0.8799E-01	0.1101E+00	0.3256E+00	0.5818E-02	0.3016E+00
-0.5197E+00	-0.1979E-01	-0.6729E+00	0.5612E-01	-0.8145E-01	0.2790E+00	-0.1440E+00	0.2439E+00
-0.7467E+00	0.1519E+00	-0.7342E+00	0.2466E+00	-0.1866E+00	0.1980E+00	-0.2027E+00	0.1414E+00
-0.6455E+00	0.3184E+00	-0.4826E+00	0.3660E+00	-0.2069E+00	0.6768E-01	-0.1942E+00	-0.1520E-01
-0.2864E+00	0.3627E+00	-0.8354E-01	0.3207E+00	-0.1696E+00	-0.1055E+00	-0.1515E+00	-0.1971E+00
0.1121E+00	0.2270E+00	0.2641E+00	0.9349E-01	-0.1201E+00	-0.2832E+00	-0.8716E-01	-0.3521E+00
0.3632E+00	-0.5263E-01	0.4088E+00	-0.2110E+00	-0.5762E-01	-0.3931E+00	-0.2377E-01	-0.4018E+00
0.4020E+00	-0.3542E+00	0.3593E+00	-0.4664E+00	0.1365E-01	-0.3833E+00	0.4724E-01	-0.3132E+00
0.2814E+00	-0.5211E+00	0.2039E+00	-0.5151E+00	0.7819E-01	-0.2245E+00	0.1057E+00	-0.1178E+00
0.1240E+00	-0.4507E+00	0.6425E-01	-0.3188E+00	0.1279E+00	-0.5927E-03	0.1293E+00	0.1140E+00
0.2530E-01	-0.1574E+00	-0.4452E-02	0.2821E-01	0.1071E+00	0.2055E+00	0.7176E-01	0.2688E+00
-0.1068E-01	0.2088E+00	-0.2708E-01	0.3594E+00	0.1762E-01	0.2968E+00	-0.4991E-01	0.2837E+00
-0.4551E-01	0.4656E+00	-0.7350E-01	0.5060E+00	-0.1193E+00	0.2269E+00	-0.1893E+00	0.1457E+00
-0.1262E+00	0.4987E+00	-0.1768E+00	0.4313E+00	-0.2531E+00	0.4934E-01	-0.3070E+00	-0.5995E-01
-0.2296E+00	0.3088E+00	-0.2650E+00	0.1862E+00	-0.3279E+00	-0.1617E+00	-0.3287E+00	-0.2583E+00
-0.2803E+00	0.5122E-01	-0.2572E+00	-0.6564E-01	-0.2997E+00	-0.3277E+00	-0.2458E+00	-0.3684E+00
-0.1844E+00	-0.1461E+00	-0.8251E-01	-0.1916E+00	-0.1843E+00	-0.3836E+00	-0.1028E+00	-0.3658E+00
0.5691E-01	-0.1933E+00	0.2213E+00	-0.1676E+00	-0.2997E-01	-0.3246E+00	0.3535E-01	-0.2595E+00
0.3721E+00	-0.1163E+00	0.5008E+00	-0.5467E-01	0.1070E+00	-0.1905E+00	0.1509E+00	-0.1095E+00
0.5869E+00	-0.2907E-02	0.6106E+00	0.4135E-01	0.1791E+00	-0.6466E-02	0.1985E+00	0.8273E-01
0.5776E+00	0.6521E-01	0.4771E+00	0.7221E-01	0.1998E+00	0.1804E+00	0.1933E+00	0.2784E+00
0.3230E+00	0.6650E-01	0.1388E+00	0.4645E-01	0.1896E+00	0.3452E+00	0.1957E+00	0.4050E+00
-0.6365E-01	0.3794E-01	-0.2514E+00	0.3664E-01	0.1991E+00	0.4529E+00	0.1939E+00	0.4842E+00
-0.4132E+00	0.3549E-01	-0.5136E+00	0.4747E-01	0.1918E+00	0.4836E+00	0.1853E+00	0.4578E+00
-0.5620E+00	0.7111E-01	-0.5494E+00	0.8963E-01	0.1746E+00	0.4047E+00	0.1579E+00	0.3093E+00
-0.4827E+00	0.1050E+00	-0.3733E+00	0.1104E+00	0.1344E+00	0.2026E+00	0.9701E-01	0.9075E-01
-0.2440E+00	0.9394E-01	-0.9552E-01	0.5748E-01	0.4795E-01	-0.3770E-01	0.9475E-03	-0.1532E+00
0.5291E-01	0.7460E-02	0.1763E+00	-0.4636E-01	-0.3948E-01	-0.2608E+00	-0.8020E-01	-0.3406E+00
0.2830E+00	-0.1029E+00	0.3645E+00	-0.1484E+00	-0.9656E-01	-0.3827E+00	-0.1076E+00	-0.3992E+00
0.4159E+00	-0.1597E+00	0.4344E+00	-0.1473E+00	-0.1035E+00	-0.3556E+00	-0.8980E-01	-0.2893E+00
0.4362E+00	-0.1113E+00	0.4242E+00	-0.4485E-01	-0.7304E-01	-0.2000E+00	-0.3179E-01	-0.9365E-01
0.3777E+00	0.4605E-01	0.3174E+00	0.1341E+00	-0.1466E-02	0.1709E-01	0.2840E-01	0.1220E+00
0.2400E+00	0.2145E+00	0.1385E+00	0.2736E+00	0.5470E-01	0.2089E+00	0.7120E-01	0.2807E+00
0.2723E-01	0.2869E+00	-0.9824E-01	0.2650E+00				

Time history of vertical acceleration at node NL2:

0.3166E+02	-0.2796E+02	0.2540E+02	-0.2284E+02	-0.2256E+00	-0.9218E-01	-0.3559E+00	0.3408E-01
0.2162E+02	-0.2354E+02	0.1649E+02	-0.1574E+02	-0.5134E+00	0.3019E+00	-0.6691E+00	0.6286E+00
0.1675E+02	-0.1821E+02	0.1556E+02	-0.1728E+02	-0.8080E+00	0.9569E+00	-0.9047E+00	0.1204E+01
0.1328E+02	-0.8429E+01	0.7619E+01	-0.9019E+01	-0.8955E+00	0.1281E+01	-0.7364E+00	0.1105E+01
0.9286E+01	-0.9992E+01	0.1208E+02	-0.8138E+01	-0.3751E+00	0.6347E+00	0.1828E+00	-0.6794E-01
0.6545E+01	-0.5308E+01	0.5588E+01	-0.3050E+01	0.8160E+00	-0.8290E+00	0.1358E+01	-0.1456E+01
0.4069E+01	-0.1963E+01	-0.3877E+00	0.1078E+01	0.1673E+01	-0.1827E+01	0.1706E+01	-0.1885E+01
0.3869E+00	-0.1494E+01	0.2755E+01	-0.5093E+01	0.1483E+01	-0.1668E+01	0.1090E+01	-0.1263E+01
0.3420E+01	-0.2539E+01	0.9404E+00	-0.8849E+00	0.6283E+00	-0.7363E+00	0.1514E+00	-0.1466E+00
-0.1404E+01	0.9921E+00	-0.2549E+01	0.3924E+01	-0.2963E+00	0.4436E+00	-0.6678E+00	0.9640E+00
-0.4890E+01	0.4155E+01	-0.3325E+01	0.2277E+01	-0.9349E+00	0.1357E+01	-0.1079E+01	0.1589E+01
-0.6046E-01	0.2849E+00	0.2209E+00	0.4516E+00	-0.1112E+01	0.1648E+01	-0.1068E+01	0.1562E+01
0.7717E+00	0.1692E+00	0.1535E+01	-0.1097E+01	-0.9749E+00	0.1364E+01	-0.8381E+00	0.1050E+01
0.1670E+01	-0.8258E+00	0.1732E+01	-0.1458E+01	-0.6244E+00	0.6248E+00	-0.3098E+00	0.1081E+00
0.1810E+01	-0.2031E+01	0.1198E+01	-0.2847E+00	0.9670E-01	-0.4461E+00	0.5510E+00	-0.9479E+00
-0.1367E+01	0.1602E+01	-0.3134E+01	0.2288E+01	0.9643E+00	-0.1304E+01	0.1252E+01	-0.1449E+01
-0.2810E+01	0.1667E+01	-0.1961E+01	0.2686E+00	0.1369E+01	-0.1379E+01	0.1303E+01	-0.1123E+01
0.1414E+00	-0.1630E+01	0.2543E+01	-0.3170E+01	0.1079E+01	-0.7392E+00	0.7418E+00	-0.3042E+00
0.3406E+01	-0.2837E+01	0.3113E+01	-0.2013E+01	0.3488E+00	0.1158E+00	-0.3983E-01	0.4540E+00
0.2552E+01	-0.1618E+01	0.2023E+01	-0.8116E+00	-0.3653E+00	0.6617E+00	-0.5799E+00	0.7208E+00
0.1071E+01	-0.5020E-01	-0.2051E-02	0.6180E+00	-0.6866E+00	0.6306E+00	-0.6957E+00	0.4703E+00
-0.9727E+00	0.1593E+01	-0.2349E+01	0.2484E+01	-0.6423E+00	0.3071E+00	-0.5683E+00	0.1949E+00
-0.3142E+01	0.2613E+01	-0.2769E+01	0.1909E+01	-0.5110E+00	0.1505E+00	-0.4650E+00	0.1571E+00
-0.2047E+01	0.1273E+01	-0.1349E+01	0.9462E+00	-0.4159E+00	0.1815E+00	-0.3509E+00	0.1936E+00
-0.8770E+00	0.8426E+00	-0.7599E+00	0.1176E+01	-0.2603E+00	0.1674E+00	-0.1474E+00	0.9647E-01
-0.7608E+00	0.1251E+01	-0.2943E+00	0.5163E+00	-0.2261E-01	-0.1429E-01	0.1045E+00	-0.1572E+00
0.8507E+00	-0.6426E+00	0.1971E+01	-0.1832E+01	0.2266E+00	-0.3143E+00	0.3339E+00	-0.4585E+00
0.2765E+01	-0.2728E+01	0.3185E+01	-0.3161E+01	0.4115E+00	-0.5663E+00	0.4570E+00	-0.6211E+00
0.2990E+01	-0.3033E+01	0.2379E+01	-0.2549E+01	0.4733E+00	-0.6248E+00	0.4697E+00	-0.5774E+00
0.1642E+01	-0.1866E+01	0.6960E+00	-0.7508E+00	0.4535E+00	-0.4873E+00	0.4280E+00	-0.3636E+00
-0.5276E+00	0.6893E+00	-0.1778E+01	0.2012E+01	0.3811E+00	-0.2028E+00	0.2851E+00	0.8235E-02
-0.2662E+01	0.2924E+01	-0.2976E+01	0.3171E+01	0.1473E+00	0.2621E+00	-0.3341E-01	0.5403E+00
-0.2601E+01	0.2683E+01	-0.1650E+01	0.1779E+01	-0.2499E+00	0.7973E+00	-0.4777E+00	0.9896E+00
-0.6331E+00	0.9143E+00	0.9372E-01	0.2965E+00	-0.6696E+00	0.1079E+01	-0.7985E+00	0.1039E+01
0.5046E+00	-0.1209E+00	0.6567E+00	-0.3804E+00	-0.8354E+00	0.8715E+00	-0.7601E+00	0.5846E+00
0.6580E+00	-0.5888E+00	0.6257E+00	-0.8094E+00	-0.5791E+00	0.2144E+00	-0.3099E+00	-0.1846E+00
0.5852E+00	-0.9281E+00	0.4833E+00	-0.8959E+00	0.4070E-02	-0.5573E+00	0.3194E+00	-0.8499E+00
0.3711E+00	-0.8257E+00	0.3838E+00	-0.7926E+00	0.5908E+00	-0.1021E+01	0.7815E+00	-0.1055E+01
0.5225E+00	-0.7803E+00	0.6923E+00	-0.7234E+00	0.8771E+00	-0.9592E+00	0.8805E+00	-0.7601E+00
0.7893E+00	-0.5429E+00	0.6862E+00	-0.1887E+00	0.7979E+00	-0.4897E+00	0.6525E+00	-0.1879E+00
0.3671E+00	0.2445E+00	-0.6989E-02	0.5466E+00	0.4618E+00	0.1132E+00	0.2466E+00	0.3940E+00
-0.2609E+00	0.6069E+00	-0.3398E+00	0.4499E+00	0.2259E-01	0.5841E+00	-0.2350E+00	0.7042E+00
-0.2900E+00	0.1823E+00	-0.2146E+00	-0.3883E-01	-0.4429E+00	0.7725E+00	-0.5839E+00	0.7969E+00
				-0.6376E+00	0.7554E+00	-0.6161E+00	0.6623E+00

-0.5239E+00 0.5237E+00 -0.3792E+00 0.3320E+00 -0.2461E+00 0.1860E+00 -0.1775E+00 0.7405E-01
-0.2017E+00 0.1155E+00 -0.1980E-01 -0.1052E+00 -0.9105E-01 -0.4648E-01 0.3143E-02 -0.1627E+00
0.1308E+00 -0.3095E+00 0.2392E+00 -0.4759E+00 0.9782E-01 -0.2611E+00 0.1868E+00 -0.3313E+00
0.2909E+00 -0.5885E+00 0.2830E+00 -0.6422E+00 0.2600E+00 -0.3627E+00 0.3134E+00 -0.3523E+00
0.2385E+00 -0.6432E+00 0.1737E+00 -0.6001E+00 0.3430E+00 -0.3000E+00 0.3473E+00 -0.2085E+00
0.1091E+00 -0.5166E+00 0.6410E-01 -0.4100E+00 0.3265E+00 -0.8929E-01 0.2852E+00 0.4665E-01
0.4738E-01 -0.2840E+00 0.6150E-01 -0.1438E+00 0.2282E+00 0.1852E+00 0.1603E+00 0.3121E+00
0.9655E-01 0.3289E-02 0.1411E+00 0.1571E+00 0.9043E-01 0.4129E+00 0.2440E-01 0.4785E+00
0.1763E+00 0.3151E+00 0.1852E+00 0.4660E+00 -0.3213E-01 0.5022E+00 -0.7333E-01 0.4843E+00
0.1461E+00 0.5790E+00 0.7061E-01 0.6569E+00 -0.9753E-01 0.4303E+00 -0.1054E+00 0.3481E+00
-0.2577E-01 0.6914E+00 -0.1204E+00 0.6776E+00 -0.9748E-01 0.2457E+00 -0.7813E-01 0.1349E+00
-0.2026E+00 0.6113E+00 -0.2496E+00 0.5039E+00 -0.4936E-01 0.2492E-01 -0.1544E-01 -0.7667E-01
-0.2540E+00 0.3628E+00 -0.2146E+00 0.2026E+00 0.1965E-01 -0.1627E+00 0.5242E-01 -0.2292E+00
-0.1284E+00 0.3512E-01 -0.8154E-02 -0.1284E+00 0.7917E-01 -0.2742E+00 0.9652E-01 -0.2973E+00
0.1317E+00 -0.2712E+00 0.2692E+00 -0.3880E+00 0.1053E+00 -0.3023E+00 0.1029E+00 -0.2892E+00
0.3893E+00 -0.4746E+00 0.4782E+00 -0.5240E+00 0.8874E-01 -0.2618E+00 0.6441E-01 -0.2238E+00
0.5179E+00 -0.5350E+00 0.5031E+00 -0.5050E+00 0.2832E-01 -0.1774E+00 -0.1447E-01 -0.1260E+00
0.4311E+00 -0.4325E+00 0.3052E+00 -0.3184E+00 -0.6205E-01 -0.7536E-01 -0.1133E+00 -0.2586E-01
0.1343E+00 -0.1712E+00 -0.6009E-01 -0.4616E-02 -0.1623E+00 0.1816E-01 -0.2073E+00 0.5220E-01
-0.2546E+00 0.1660E+00 -0.4274E+00 0.3235E+00 -0.2453E+00 0.7720E-01 -0.2732E+00 0.8931E-01
-0.5557E+00 0.4465E+00 -0.6178E+00 0.5205E+00 -0.2905E+00 0.8674E-01 -0.2926E+00 0.6946E-01
-0.6135E+00 0.5387E+00 -0.5431E+00 0.4840E+00 -0.2809E+00 0.3744E-01 -0.2556E+00 -0.6057E-02
-0.4296E+00 0.3676E+00 -0.2843E+00 0.2075E+00 -0.2158E+00 -0.6028E-01 -0.1660E+00 -0.1183E+00
-0.1242E+00 0.2674E-01 0.3123E-01 -0.1564E+00 -0.1084E+00 -0.1764E+00 -0.4467E-01 -0.2286E+00
0.1661E+00 -0.3151E+00 0.2691E+00 -0.4335E+00 0.1744E-01 -0.2676E+00 0.7498E-01 -0.2879E+00
0.3371E+00 -0.5018E+00 0.3706E+00 -0.5127E+00 0.1232E+00 -0.2866E+00 0.1552E+00 -0.2637E+00
0.3731E+00 -0.4706E+00 0.3514E+00 -0.3831E+00 0.1737E+00 -0.2118E+00 0.1785E+00 -0.1341E+00
0.3114E+00 -0.2615E+00 0.2549E+00 -0.1196E+00 0.1722E+00 -0.3777E-01 0.1524E+00 0.6711E-01
0.1873E+00 0.2609E-01 0.1127E+00 0.1579E+00 0.1238E+00 0.1707E+00 0.8853E-01 0.2633E+00
0.3232E-01 0.2655E+00 -0.4942E-01 0.3382E+00 0.5019E-01 0.3351E+00 0.1439E-01 0.3808E+00
-0.1292E+00 0.3692E+00 -0.2009E+00 0.3603E+00 -0.1745E-01 0.3962E+00 -0.3979E-01 0.3800E+00
-0.2630E+00 0.3156E+00 -0.3089E+00 0.2416E+00 -0.5072E-01 0.3347E+00 -0.5109E-01 0.2660E+00
-0.3341E+00 0.1512E+00 -0.3395E+00 0.5600E-01 -0.4001E-01 0.1791E+00 -0.2112E-01 0.8400E-01
-0.3216E+00 -0.3358E-01 -0.2798E+00 -0.1087E+00 0.2257E-02 -0.1195E-01 0.2867E-01 -0.1020E+00
-0.2199E+00 -0.1633E+00 -0.1421E+00 -0.1997E+00 0.5322E-01 -0.1790E+00 0.7232E-01 -0.2361E+00
-0.5200E-01 -0.2213E+00 0.3485E-01 -0.2552E+00 0.8318E-01 -0.2722E+00 0.8419E-01 -0.2838E+00
0.1007E+00 -0.2869E+00 0.1557E+00 -0.3123E+00 0.7454E-01 -0.2733E+00 0.5384E-01 -0.2431E+00
0.2020E+00 -0.3213E+00 0.2294E+00 -0.3157E+00 0.2637E-01 -0.1979E+00 -0.6841E-02 -0.1434E+00
0.2355E+00 -0.2881E+00 0.2212E+00 -0.2362E+00 -0.4389E-01 -0.8461E-01 -0.7936E-01 -0.2807E-01
0.1784E+00 -0.1627E+00 0.1164E+00 -0.7004E-01 -0.1123E+00 0.2131E-01 -0.1404E+00 0.6015E-01
0.3915E-01 0.3245E-01 -0.4907E-01 0.1381E+00 -0.1613E+00 0.8598E-01 -0.1759E+00 0.9782E-01
-0.1360E+00 0.2349E+00 -0.2130E+00 0.3093E+00 -0.1833E+00 0.9601E-01 -0.1820E+00 0.8084E-01
-0.2729E+00 0.3563E+00 -0.3080E+00 0.3683E+00 -0.1745E+00 0.5579E-01 -0.1589E+00 0.2261E-01
-0.3161E+00 0.3392E+00 -0.2937E+00 0.2775E+00 -0.1353E+00 -0.1614E-01 -0.1066E+00 -0.5496E-01

-0.7249E-01 -0.9093E-01 -0.3534E-01 -0.1231E+00
0.3773E-02 -0.1466E+00 0.4074E-01 -0.1600E+00
0.7205E-01 -0.1637E+00 0.9775E-01 -0.1566E+00
0.1132E+00 -0.1408E+00 0.1164E+00 -0.1153E+00
0.1073E+00 -0.8422E-01 0.8459E-01 -0.4957E-01
0.5395E-01 -0.9701E-02 0.1772E-01 0.3121E-01
-0.2036E-01 0.7074E-01 -0.5561E-01 0.1041E+00
-0.8714E-01 0.1319E+00 -0.1100E+00 0.1489E+00
-0.1234E+00 0.1537E+00 -0.1231E+00 0.1471E+00
-0.1101E+00 0.1284E+00 -0.8610E-01 0.1003E+00
-0.4968E-01 0.6365E-01 -0.7646E-02 0.2392E-01
0.3778E-01 -0.1441E-01 0.8248E-01 -0.5041E-01
0.1216E+00 -0.7602E-01 0.1527E+00 -0.9036E-01
0.1726E+00 -0.9414E-01 0.1821E+00 -0.8247E-01
0.1788E+00 -0.5819E-01 0.1648E+00 -0.2368E-01
0.1436E+00 0.1918E-01 0.1154E+00 0.6545E-01
0.8425E-01 0.1111E+00 0.5405E-01 0.1510E+00
0.2496E-01 0.1816E+00 -0.1333E-03 0.2009E+00
-0.2128E-01 0.2041E+00 -0.3648E-01 0.1911E+00
-0.4518E-01 0.1635E+00 -0.5058E-01 0.1228E+00
-0.5118E-01 0.7313E-01 -0.4866E-01 0.1740E-01
-0.4358E-01 -0.3729E-01 -0.3612E-01 -0.8778E-01
-0.2675E-01 -0.1296E+00 -0.1423E-01 -0.1600E+00
-0.3384E-03 -0.1728E+00 0.1431E-01 -0.1699E+00
0.3054E-01 -0.1505E+00 0.4681E-01 -0.1162E+00
0.6310E-01 -0.7101E-01 0.7833E-01 -0.1768E-01
0.9078E-01 0.3876E-01 0.9875E-01 0.9526E-01
0.1012E+00 0.1465E+00 0.9738E-01 0.1868E+00
0.8958E-01 0.2138E+00 0.7439E-01 0.2261E+00
0.5436E-01 0.2200E+00 0.3194E-01 0.1967E+00
0.5064E-02 0.1592E+00 -0.2337E-01 0.1073E+00
-0.4946E-01 0.4283E-01 -0.7351E-01 -0.2636E-01
-0.9460E-01 -0.9830E-01 -0.1106E+00 -0.1659E+00
-0.1242E+00 -0.2242E+00 -0.1319E+00 -0.2707E+00
-0.1336E+00 -0.3007E+00 -0.1317E+00 -0.3108E+00
-0.1251E+00 -0.3001E+00 -0.1130E+00 -0.2705E+00
-0.9747E-01 -0.2206E+00 -0.7905E-01 -0.1554E+00
-0.5718E-01 -0.8102E-01 -0.3036E-01 -0.1289E-02
-0.3392E-02 0.7985E-01 0.2389E-01 0.1537E+00
0.5393E-01 0.2155E+00 0.8070E-01 0.2617E+00
0.1034E+00 0.2896E+00 0.1238E+00 0.2959E+00
0.1384E+00 0.2842E+00 0.1469E+00 0.2543E+00
0.1507E+00 0.2072E+00 0.1483E+00 0.1499E+00
0.1372E+00 0.8888E-01 0.1201E+00 0.2424E-01
0.9786E-01 -0.3577E-01 0.7083E-01 -0.8748E-01
0.3942E-01 -0.1290E+00 0.8349E-02 -0.1569E+00
-0.2327E-01 -0.1713E+00 -0.5228E-01 -0.1722E+00
-0.7746E-01 -0.1605E+00 -0.9871E-01 -0.1380E+00
-0.1139E+00 -0.1083E+00 -0.1212E+00 -0.7560E-01
-0.1228E+00 -0.4057E-01 -0.1183E+00 -0.6824E-02
-0.1091E+00 0.2103E-01 -0.9562E-01 0.4309E-01
-0.7940E-01 0.5594E-01 -0.6190E-01 0.5771E-01
-0.4446E-01 0.5038E-01 -0.3031E-01 0.3432E-01
-0.2048E-01 0.8675E-02 -0.1451E-01 -0.2298E-01
-0.1467E-01 -0.5911E-01 -0.1981E-01 -0.9761E-01
-0.2919E-01 -0.1349E+00 -0.4372E-01 -0.1669E+00
-0.6111E-01 -0.1908E+00 -0.8068E-01 -0.2055E+00
-0.9748E-01 -0.2092E+00 -0.1115E+00 -0.2008E+00
-0.1208E+00 -0.1795E+00 -0.1223E+00 -0.1462E+00
-0.1185E+00 -0.1016E+00 -0.1053E+00 -0.4951E-01
-0.8408E-01 0.6555E-02 -0.5510E-01 0.6390E-01
-0.1689E-01 0.1164E+00 0.2624E-01 0.1642E+00
0.7009E-01 0.2060E+00 0.1135E+00 0.2347E+00
0.1567E+00 0.2501E+00 0.1949E+00 0.2547E+00
0.2245E+00 0.2451E+00 0.2464E+00 0.2241E+00
0.2565E+00 0.1957E+00 0.2527E+00 0.1625E+00
0.2366E+00 0.1238E+00 0.2105E+00 0.8280E-01
0.1757E+00 0.4341E-01 0.1332E+00 0.6517E-02
0.8617E-01 -0.2449E-01 0.3717E-01 -0.4623E-01
-0.1283E-01 -0.6097E-01 -0.5665E-01 -0.6821E-01
-0.9099E-01 -0.6905E-01 -0.1171E+00 -0.6156E-01
-0.1299E+00 -0.4790E-01 -0.1323E+00 -0.3117E-01
-0.1208E+00 -0.1053E-01 -0.9929E-01 0.1149E-01
-0.7044E-01 0.3193E-01 -0.3284E-01 0.4873E-01
0.6194E-02 0.6246E-01 0.4324E-01 0.7128E-01

Time history of displacement at node NF1:

0.7573E-06 0.3407E-05 0.8155E-05 0.1473E-04
0.2277E-04 0.3226E-04 0.4418E-04 0.5977E-04
0.7898E-04 0.1010E-03 0.1258E-03 0.1534E-03
0.1842E-03 0.2178E-03 0.2526E-03 0.2873E-03
0.3214E-03 0.3541E-03 0.3844E-03 0.4107E-03
0.4312E-03 0.4454E-03 0.4526E-03 0.4523E-03
0.4438E-03 0.4264E-03 0.4001E-03 0.3657E-03
0.3238E-03 0.2748E-03 0.2196E-03 0.1593E-03
0.9538E-04 0.2951E-04 -0.3702E-04 -0.1028E-03
-0.1662E-03 -0.2256E-03 -0.2794E-03 -0.3262E-03
-0.3651E-03 -0.3948E-03 -0.4143E-03 -0.4231E-03

-0.4206E-03	-0.4070E-03	-0.3824E-03	-0.3470E-03	0.3840E-02	0.3820E-02	0.3792E-02	0.3757E-02
-0.3012E-03	-0.2457E-03	-0.1814E-03	-0.1091E-03	0.3715E-02	0.3668E-02	0.3616E-02	0.3560E-02
-0.2981E-04	0.5568E-04	0.1463E-03	0.2410E-03	0.3502E-02	0.3442E-02	0.3382E-02	0.3323E-02
0.3387E-03	0.4384E-03	0.5390E-03	0.6396E-03	0.3266E-02	0.3211E-02	0.3161E-02	0.3115E-02
0.7389E-03	0.8361E-03	0.9300E-03	0.1020E-02	0.3075E-02	0.3041E-02	0.3014E-02	0.2994E-02
0.1104E-02	0.1183E-02	0.1255E-02	0.1320E-02	0.2982E-02	0.2978E-02	0.2982E-02	0.2993E-02
0.1377E-02	0.1426E-02	0.1466E-02	0.1498E-02	0.3013E-02	0.3039E-02	0.3073E-02	0.3112E-02
0.1522E-02	0.1538E-02	0.1546E-02	0.1547E-02	0.3158E-02	0.3209E-02	0.3265E-02	0.3324E-02
0.1541E-02	0.1529E-02	0.1512E-02	0.1490E-02	0.3387E-02	0.3452E-02	0.3518E-02	0.3585E-02
0.1464E-02	0.1435E-02	0.1402E-02	0.1368E-02	0.3652E-02	0.3719E-02	0.3784E-02	0.3847E-02
0.1332E-02	0.1295E-02	0.1257E-02	0.1218E-02	0.3907E-02	0.3963E-02	0.4016E-02	0.4065E-02
0.1180E-02	0.1141E-02	0.1102E-02	0.1063E-02	0.4108E-02	0.4146E-02	0.4179E-02	0.4205E-02
0.1023E-02	0.9827E-03	0.9408E-03	0.8972E-03	0.4226E-02	0.4240E-02	0.4248E-02	0.4249E-02
0.8514E-03	0.8031E-03	0.7516E-03	0.6966E-03	0.4245E-02	0.4235E-02	0.4220E-02	0.4199E-02
0.6378E-03	0.5748E-03	0.5073E-03	0.4352E-03	0.4174E-02	0.4144E-02	0.4111E-02	0.4075E-02
0.3582E-03	0.2763E-03	0.1893E-03	0.9737E-04	0.4037E-02	0.3997E-02	0.3956E-02	0.3915E-02
0.3394E-06	-0.1017E-03	-0.2088E-03	-0.3210E-03	0.3875E-02	0.3835E-02	0.3797E-02	0.3761E-02
-0.4380E-03	-0.5600E-03	-0.6867E-03	-0.8181E-03	0.3727E-02	0.3696E-02	0.3668E-02	0.3643E-02
-0.9539E-03	-0.1094E-02	-0.1238E-02	-0.1385E-02	0.3622E-02	0.3604E-02	0.3589E-02	0.3577E-02
-0.1535E-02	-0.1688E-02	-0.1842E-02	-0.1998E-02	0.3567E-02	0.3560E-02	0.3554E-02	0.3550E-02
-0.2153E-02	-0.2307E-02	-0.2458E-02	-0.2607E-02	0.3546E-02	0.3541E-02	0.3536E-02	0.3528E-02
-0.2751E-02	-0.2889E-02	-0.3021E-02	-0.3145E-02	0.3519E-02	0.3506E-02	0.3490E-02	0.3469E-02
-0.3259E-02	-0.3363E-02	-0.3456E-02	-0.3537E-02	0.3444E-02	0.3413E-02	0.3377E-02	0.3336E-02
-0.3606E-02	-0.3661E-02	-0.3703E-02	-0.3731E-02	0.3288E-02	0.3235E-02	0.3177E-02	0.3113E-02
-0.3745E-02	-0.3746E-02	-0.3733E-02	-0.3708E-02	0.3044E-02	0.2971E-02	0.2894E-02	0.2814E-02
-0.3670E-02	-0.3621E-02	-0.3562E-02	-0.3492E-02	0.2731E-02	0.2646E-02	0.2561E-02	0.2476E-02
-0.3414E-02	-0.3327E-02	-0.3234E-02	-0.3134E-02	0.2392E-02	0.2309E-02	0.2230E-02	0.2155E-02
-0.3030E-02	-0.2920E-02	-0.2807E-02	-0.2691E-02	0.2085E-02	0.2020E-02	0.1962E-02	0.1912E-02
-0.2573E-02	-0.2453E-02	-0.2332E-02	-0.2210E-02	0.1869E-02	0.1834E-02	0.1808E-02	0.1790E-02
-0.2087E-02	-0.1965E-02	-0.1843E-02	-0.1722E-02	0.1782E-02	0.1782E-02	0.1790E-02	0.1806E-02
-0.1602E-02	-0.1483E-02	-0.1365E-02	-0.1249E-02	0.1830E-02	0.1860E-02	0.1895E-02	0.1935E-02
-0.1135E-02	-0.1022E-02	-0.9102E-03	-0.8002E-03	0.1979E-02	0.2024E-02	0.2070E-02	0.2116E-02
-0.6917E-03	-0.5844E-03	-0.4784E-03	-0.3733E-03	0.2159E-02	0.2198E-02	0.2233E-02	0.2261E-02
-0.2690E-03	-0.1654E-03	-0.6224E-04	0.4085E-04	0.2282E-02	0.2293E-02	0.2295E-02	0.2285E-02
0.1441E-03	0.2478E-03	0.3523E-03	0.4579E-03	0.2263E-02	0.2229E-02	0.2181E-02	0.2120E-02
0.5649E-03	0.6735E-03	0.7841E-03	0.8967E-03	0.2044E-02	0.1955E-02	0.1852E-02	0.1736E-02
0.1012E-02	0.1129E-02	0.1248E-02	0.1370E-02	0.1608E-02	0.1467E-02	0.1315E-02	0.1153E-02
0.1493E-02	0.1618E-02	0.1745E-02	0.1873E-02	0.9824E-03	0.8043E-03	0.6202E-03	0.4316E-03
0.2001E-02	0.2130E-02	0.2258E-02	0.2385E-02	0.2401E-03	0.4750E-04	-0.1446E-03	-0.3344E-03
0.2510E-02	0.2634E-02	0.2755E-02	0.2872E-02	-0.5203E-03	-0.7007E-03	-0.8738E-03	-0.1038E-02
0.2985E-02	0.3094E-02	0.3198E-02	0.3295E-02	-0.1193E-02	-0.1336E-02	-0.1466E-02	-0.1583E-02
0.3387E-02	0.3472E-02	0.3549E-02	0.3618E-02	-0.1686E-02	-0.1774E-02	-0.1847E-02	-0.1905E-02
0.3679E-02	0.3732E-02	0.3775E-02	0.3809E-02	-0.1948E-02	-0.1975E-02	-0.1988E-02	-0.1988E-02
0.3834E-02	0.3849E-02	0.3855E-02	0.3852E-02	-0.1974E-02	-0.1948E-02	-0.1912E-02	-0.1867E-02

-0.1814E-02	-0.1754E-02	-0.1690E-02	-0.1623E-02	0.3592E-03	0.2283E-03	0.1071E-03	-0.3464E-05
-0.1555E-02	-0.1487E-02	-0.1422E-02	-0.1360E-02	-0.1028E-03	-0.1905E-03	-0.2661E-03	-0.3296E-03
-0.1303E-02	-0.1253E-02	-0.1210E-02	-0.1176E-02	-0.3810E-03	-0.4204E-03	-0.4483E-03	-0.4651E-03
-0.1152E-02	-0.1138E-02	-0.1135E-02	-0.1143E-02	-0.4716E-03	-0.4685E-03	-0.4567E-03	-0.4372E-03
-0.1163E-02	-0.1195E-02	-0.1237E-02	-0.1291E-02	-0.4111E-03	-0.3795E-03	-0.3436E-03	-0.3045E-03
-0.1355E-02	-0.1429E-02	-0.1511E-02	-0.1602E-02	-0.2634E-03	-0.2216E-03	-0.1800E-03	-0.1398E-03
-0.1699E-02	-0.1801E-02	-0.1908E-02	-0.2019E-02	-0.1019E-03	-0.6724E-04	-0.3666E-04	-0.1082E-04
-0.2131E-02	-0.2243E-02	-0.2355E-02	-0.2464E-02	0.9715E-05	0.2452E-04	0.3327E-04	0.3578E-04
-0.2571E-02	-0.2672E-02	-0.2769E-02	-0.2859E-02	0.3200E-04	0.2205E-04	0.6158E-05	-0.1536E-04
-0.2942E-02	-0.3016E-02	-0.3083E-02	-0.3140E-02	-0.4208E-04	-0.7345E-04	-0.1088E-03	-0.1474E-03
-0.3189E-02	-0.3228E-02	-0.3258E-02	-0.3279E-02	-0.1886E-03	-0.2314E-03	-0.2751E-03	-0.3186E-03
-0.3292E-02	-0.3296E-02	-0.3292E-02	-0.3281E-02	-0.3612E-03	-0.4019E-03	-0.4400E-03	-0.4747E-03
-0.3264E-02	-0.3242E-02	-0.3215E-02	-0.3184E-02	-0.5053E-03	-0.5310E-03	-0.5515E-03	-0.5661E-03
-0.3151E-02	-0.3116E-02	-0.3081E-02	-0.3047E-02	-0.5744E-03	-0.5764E-03	-0.5716E-03	-0.5602E-03
-0.3014E-02	-0.2984E-02	-0.2957E-02	-0.2934E-02	-0.5421E-03	-0.5177E-03	-0.4870E-03	-0.4506E-03
-0.2916E-02	-0.2904E-02	-0.2897E-02	-0.2897E-02	-0.4089E-03	-0.3625E-03	-0.3120E-03	-0.2580E-03
-0.2903E-02	-0.2916E-02	-0.2936E-02	-0.2962E-02	-0.2014E-03	-0.1428E-03	-0.8300E-04	-0.2281E-04
-0.2994E-02	-0.3032E-02	-0.3075E-02	-0.3122E-02	0.3700E-04	0.9573E-04	0.1527E-03	0.2073E-03
-0.3174E-02	-0.3229E-02	-0.3286E-02	-0.3346E-02	0.2590E-03	0.3073E-03	0.3519E-03	0.3924E-03
-0.3406E-02	-0.3466E-02	-0.3525E-02	-0.3583E-02	0.4287E-03	0.4607E-03	0.4884E-03	0.5121E-03
-0.3639E-02	-0.3691E-02	-0.3740E-02	-0.3784E-02	0.5318E-03	0.5480E-03	0.5610E-03	0.5712E-03
-0.3823E-02	-0.3857E-02	-0.3886E-02	-0.3908E-02	0.5794E-03	0.5859E-03	0.5916E-03	0.5972E-03
-0.3925E-02	-0.3935E-02	-0.3939E-02	-0.3937E-02	0.6032E-03	0.6104E-03	0.6194E-03	0.6310E-03
-0.3929E-02	-0.3916E-02	-0.3897E-02	-0.3873E-02	0.6458E-03	0.6643E-03	0.6871E-03	0.7146E-03
-0.3845E-02	-0.3813E-02	-0.3777E-02	-0.3738E-02	0.7472E-03	0.7851E-03	0.8285E-03	0.8775E-03
-0.3695E-02	-0.3651E-02	-0.3604E-02	-0.3555E-02	0.9320E-03	0.9921E-03	0.1057E-02	0.1127E-02
-0.3504E-02	-0.3452E-02	-0.3399E-02	-0.3344E-02	0.1202E-02	0.1281E-02	0.1363E-02	0.1448E-02
-0.3288E-02	-0.3230E-02	-0.3171E-02	-0.3109E-02	0.1535E-02	0.1623E-02	0.1713E-02	0.1802E-02
-0.3045E-02	-0.2978E-02	-0.2908E-02	-0.2834E-02	0.1891E-02	0.1978E-02	0.2063E-02	0.2146E-02
-0.2756E-02	-0.2672E-02	-0.2584E-02	-0.2490E-02	0.2225E-02	0.2301E-02	0.2373E-02	0.2441E-02
-0.2389E-02	-0.2281E-02	-0.2166E-02	-0.2043E-02	0.2504E-02	0.2563E-02	0.2618E-02	0.2669E-02
-0.1912E-02	-0.1772E-02	-0.1625E-02	-0.1469E-02	0.2716E-02	0.2759E-02	0.2800E-02	0.2838E-02
-0.1305E-02	-0.1133E-02	-0.9535E-03	-0.7671E-03	0.2876E-02	0.2912E-02	0.2949E-02	0.2987E-02
-0.5745E-03	-0.3765E-03	-0.1738E-03	0.3229E-04	0.3027E-02	0.3071E-02	0.3118E-02	0.3170E-02
0.2408E-03	0.4504E-03	0.6598E-03	0.8676E-03	0.3228E-02	0.3293E-02	0.3365E-02	0.3445E-02
0.1072E-02	0.1273E-02	0.1467E-02	0.1654E-02	0.3533E-02	0.3630E-02	0.3737E-02	0.3852E-02
0.1833E-02	0.2000E-02	0.2157E-02	0.2300E-02	0.3977E-02	0.4111E-02	0.4253E-02	0.4402E-02
0.2429E-02	0.2544E-02	0.2642E-02	0.2723E-02	0.4559E-02	0.4722E-02	0.4889E-02	0.5060E-02
0.2787E-02	0.2833E-02	0.2861E-02	0.2871E-02	0.5234E-02	0.5408E-02	0.5581E-02	0.5751E-02
0.2862E-02	0.2836E-02	0.2792E-02	0.2731E-02	0.5916E-02	0.6075E-02	0.6225E-02	0.6365E-02
0.2655E-02	0.2563E-02	0.2457E-02	0.2339E-02	0.6493E-02	0.6606E-02	0.6704E-02	0.6785E-02
0.2210E-02	0.2070E-02	0.1923E-02	0.1768E-02	0.6847E-02	0.6889E-02	0.6909E-02	0.6906E-02
0.1609E-02	0.1447E-02	0.1283E-02	0.1120E-02	0.6881E-02	0.6831E-02	0.6758E-02	0.6660E-02
0.9578E-03	0.7994E-03	0.6459E-03	0.4987E-03	0.6537E-02	0.6391E-02	0.6221E-02	0.6028E-02

0.5813E-02 0.5578E-02 0.5324E-02 0.5051E-02
0.4763E-02 0.4461E-02 0.4146E-02 0.3820E-02
0.3486E-02 0.3146E-02 0.2802E-02 0.2456E-02
0.2110E-02 0.1766E-02 0.1426E-02 0.1092E-02
0.7650E-03 0.4472E-03 0.1399E-03 -0.1556E-03
-0.4384E-03 -0.7074E-03 -0.9621E-03 -0.1202E-02
-0.1426E-02 -0.1635E-02 -0.1828E-02 -0.2005E-02
-0.2168E-02 -0.2315E-02 -0.2448E-02 -0.2568E-02
-0.2674E-02 -0.2768E-02 -0.2850E-02 -0.2921E-02
-0.2983E-02 -0.3035E-02 -0.3079E-02 -0.3115E-02
-0.3144E-02 -0.3167E-02 -0.3184E-02 -0.3196E-02
-0.3203E-02 -0.3205E-02 -0.3203E-02 -0.3197E-02
-0.3186E-02 -0.3171E-02 -0.3152E-02 -0.3128E-02
-0.3099E-02 -0.3065E-02 -0.3026E-02 -0.2981E-02
-0.2930E-02 -0.2873E-02 -0.2808E-02 -0.2737E-02
-0.2659E-02 -0.2573E-02 -0.2480E-02 -0.2379E-02
-0.2271E-02 -0.2156E-02 -0.2034E-02 -0.1905E-02
-0.1770E-02 -0.1630E-02 -0.1484E-02 -0.1335E-02
-0.1182E-02 -0.1027E-02 -0.8696E-03 -0.7121E-03
-0.5551E-03 -0.3996E-03 -0.2465E-03 -0.9699E-04
0.4808E-04 0.1877E-03 0.3211E-03 0.4475E-03
0.5661E-03 0.6765E-03 0.7780E-03 0.8704E-03
0.9534E-03 0.1027E-02 0.1091E-02 0.1146E-02
0.1192E-02 0.1229E-02 0.1259E-02 0.1280E-02
0.1296E-02 0.1305E-02 0.1310E-02 0.1311E-02
0.1309E-02 0.1305E-02 0.1300E-02 0.1296E-02
0.1293E-02 0.1291E-02 0.1293E-02 0.1299E-02
0.1309E-02 0.1324E-02 0.1345E-02 0.1371E-02
0.1404E-02 0.1443E-02 0.1488E-02 0.1539E-02
0.1596E-02 0.1657E-02 0.1723E-02 0.1793E-02
0.1865E-02 0.1940E-02 0.2015E-02 0.2090E-02
0.2164E-02 0.2236E-02 0.2304E-02 0.2367E-02
0.2425E-02 0.2476E-02 0.2519E-02 0.2554E-02
0.2579E-02 0.2595E-02 0.2600E-02 0.2595E-02
0.2579E-02 0.2553E-02 0.2515E-02 0.2468E-02
0.2411E-02 0.2344E-02 0.2270E-02 0.2188E-02
0.2100E-02 0.2006E-02 0.1910E-02 0.1810E-02
0.1710E-02 0.1610E-02 0.1512E-02 0.1418E-02
0.1328E-02 0.1244E-02 0.1168E-02 0.1101E-02
0.1043E-02 0.9966E-03 0.9613E-03 0.9382E-03
0.9277E-03 0.9303E-03 0.9459E-03 0.9745E-03
0.1016E-02 0.1070E-02 0.1135E-02 0.1211E-02
0.1298E-02 0.1393E-02 0.1495E-02 0.1604E-02
0.1718E-02 0.1836E-02 0.1955E-02 0.2074E-02
0.2193E-02 0.2308E-02 0.2419E-02 0.2524E-02
0.2622E-02 0.2711E-02 0.2791E-02 0.2860E-02
0.2917E-02 0.2962E-02 0.2995E-02 0.3014E-02
0.3019E-02 0.3011E-02 0.2990E-02 0.2956E-02
0.2909E-02 0.2850E-02 0.2780E-02 0.2700E-02
0.2610E-02 0.2511E-02 0.2406E-02 0.2295E-02
0.2178E-02 0.2058E-02 0.1936E-02 0.1813E-02
0.1690E-02 0.1568E-02 0.1448E-02 0.1332E-02
0.1219E-02 0.1112E-02 0.1009E-02 0.9129E-03
0.8227E-03 0.7390E-03 0.6618E-03 0.5913E-03
0.5272E-03 0.4693E-03 0.4172E-03 0.3707E-03
0.3290E-03 0.2918E-03 0.2584E-03 0.2281E-03
0.2004E-03 0.1744E-03 0.1497E-03 0.1255E-03
0.1014E-03 0.7674E-04 0.5115E-04 0.2424E-04
-0.4290E-05 -0.3464E-04 -0.6691E-04 -0.1011E-03
-0.1371E-03 -0.1748E-03 -0.2139E-03 -0.2541E-03
-0.2948E-03 -0.3357E-03 -0.3762E-03 -0.4156E-03
-0.4535E-03 -0.4892E-03 -0.5221E-03 -0.5515E-03
-0.5769E-03 -0.5978E-03 -0.6137E-03 -0.6242E-03

Time history of displacement at node NF2:

-0.4102E-06 -0.1841E-05 -0.4385E-05 -0.7880E-05
-0.1215E-04 -0.1718E-04 -0.2340E-04 -0.3135E-04
-0.4099E-04 -0.5200E-04 -0.6429E-04 -0.7796E-04
-0.9311E-04 -0.1096E-03 -0.1268E-03 -0.1442E-03
-0.1617E-03 -0.1790E-03 -0.1956E-03 -0.2109E-03
-0.2244E-03 -0.2355E-03 -0.2441E-03 -0.2497E-03
-0.2519E-03 -0.2503E-03 -0.2446E-03 -0.2349E-03
-0.2208E-03 -0.2024E-03 -0.1794E-03 -0.1519E-03
-0.1200E-03 -0.8362E-04 -0.4290E-04 0.2168E-05
0.5151E-04 0.1050E-03 0.1627E-03 0.2244E-03
0.2901E-03 0.3598E-03 0.4334E-03 0.5107E-03
0.5918E-03 0.6765E-03 0.7646E-03 0.8560E-03
0.9506E-03 0.1048E-02 0.1148E-02 0.1251E-02
0.1355E-02 0.1462E-02 0.1570E-02 0.1680E-02
0.1790E-02 0.1901E-02 0.2013E-02 0.2125E-02
0.2237E-02 0.2349E-02 0.2461E-02 0.2573E-02
0.2684E-02 0.2794E-02 0.2904E-02 0.3013E-02
0.3121E-02 0.3228E-02 0.3334E-02 0.3439E-02
0.3542E-02 0.3643E-02 0.3742E-02 0.3838E-02
0.3932E-02 0.4023E-02 0.4110E-02 0.4194E-02
0.4274E-02 0.4350E-02 0.4422E-02 0.4490E-02
0.4553E-02 0.4613E-02 0.4668E-02 0.4719E-02
0.4767E-02 0.4811E-02 0.4852E-02 0.4890E-02

0.4926E-02	0.4959E-02	0.4990E-02	0.5019E-02	-0.1422E-01	-0.1429E-01	-0.1437E-01	-0.1444E-01
0.5046E-02	0.5072E-02	0.5095E-02	0.5117E-02	-0.1452E-01	-0.1460E-01	-0.1468E-01	-0.1475E-01
0.5137E-02	0.5154E-02	0.5169E-02	0.5181E-02	-0.1483E-01	-0.1490E-01	-0.1498E-01	-0.1505E-01
0.5189E-02	0.5194E-02	0.5196E-02	0.5192E-02	-0.1513E-01	-0.1520E-01	-0.1527E-01	-0.1533E-01
0.5185E-02	0.5173E-02	0.5155E-02	0.5133E-02	-0.1540E-01	-0.1547E-01	-0.1553E-01	-0.1559E-01
0.5106E-02	0.5074E-02	0.5037E-02	0.4995E-02	-0.1565E-01	-0.1571E-01	-0.1577E-01	-0.1582E-01
0.4949E-02	0.4898E-02	0.4844E-02	0.4787E-02	-0.1588E-01	-0.1593E-01	-0.1598E-01	-0.1603E-01
0.4726E-02	0.4662E-02	0.4595E-02	0.4526E-02	-0.1608E-01	-0.1613E-01	-0.1617E-01	-0.1621E-01
0.4455E-02	0.4381E-02	0.4305E-02	0.4227E-02	-0.1625E-01	-0.1628E-01	-0.1632E-01	-0.1634E-01
0.4147E-02	0.4064E-02	0.3978E-02	0.3890E-02	-0.1637E-01	-0.1639E-01	-0.1641E-01	-0.1642E-01
0.3799E-02	0.3704E-02	0.3606E-02	0.3505E-02	-0.1643E-01	-0.1644E-01	-0.1644E-01	-0.1644E-01
0.3400E-02	0.3292E-02	0.3179E-02	0.3064E-02	-0.1643E-01	-0.1642E-01	-0.1641E-01	-0.1640E-01
0.2945E-02	0.2822E-02	0.2697E-02	0.2569E-02	-0.1638E-01	-0.1636E-01	-0.1634E-01	-0.1632E-01
0.2439E-02	0.2307E-02	0.2173E-02	0.2039E-02	-0.1629E-01	-0.1626E-01	-0.1623E-01	-0.1620E-01
0.1903E-02	0.1767E-02	0.1630E-02	0.1493E-02	-0.1616E-01	-0.1613E-01	-0.1609E-01	-0.1605E-01
0.1357E-02	0.1221E-02	0.1085E-02	0.9492E-03	-0.1601E-01	-0.1596E-01	-0.1591E-01	-0.1586E-01
0.8138E-03	0.6786E-03	0.5434E-03	0.4081E-03	-0.1581E-01	-0.1575E-01	-0.1570E-01	-0.1564E-01
0.2725E-03	0.1365E-03	-0.1638E-06	-0.1376E-03	-0.1557E-01	-0.1551E-01	-0.1544E-01	-0.1537E-01
-0.2760E-03	-0.4154E-03	-0.5560E-03	-0.6979E-03	-0.1530E-01	-0.1523E-01	-0.1515E-01	-0.1508E-01
-0.8410E-03	-0.9855E-03	-0.1131E-02	-0.1278E-02	-0.1500E-01	-0.1492E-01	-0.1484E-01	-0.1476E-01
-0.1427E-02	-0.1577E-02	-0.1728E-02	-0.1880E-02	-0.1468E-01	-0.1459E-01	-0.1451E-01	-0.1442E-01
-0.2034E-02	-0.2189E-02	-0.2345E-02	-0.2503E-02	-0.1433E-01	-0.1425E-01	-0.1416E-01	-0.1407E-01
-0.2662E-02	-0.2823E-02	-0.2986E-02	-0.3150E-02	-0.1398E-01	-0.1389E-01	-0.1379E-01	-0.1370E-01
-0.3317E-02	-0.3485E-02	-0.3655E-02	-0.3828E-02	-0.1361E-01	-0.1351E-01	-0.1342E-01	-0.1332E-01
-0.4002E-02	-0.4179E-02	-0.4357E-02	-0.4538E-02	-0.1322E-01	-0.1313E-01	-0.1303E-01	-0.1294E-01
-0.4721E-02	-0.4905E-02	-0.5092E-02	-0.5280E-02	-0.1284E-01	-0.1275E-01	-0.1266E-01	-0.1256E-01
-0.5470E-02	-0.5661E-02	-0.5853E-02	-0.6046E-02	-0.1247E-01	-0.1238E-01	-0.1230E-01	-0.1221E-01
-0.6240E-02	-0.6435E-02	-0.6631E-02	-0.6826E-02	-0.1213E-01	-0.1205E-01	-0.1197E-01	-0.1189E-01
-0.7022E-02	-0.7218E-02	-0.7414E-02	-0.7609E-02	-0.1182E-01	-0.1175E-01	-0.1168E-01	-0.1161E-01
-0.7804E-02	-0.7998E-02	-0.8190E-02	-0.8382E-02	-0.1154E-01	-0.1148E-01	-0.1142E-01	-0.1136E-01
-0.8571E-02	-0.8759E-02	-0.8945E-02	-0.9128E-02	-0.1131E-01	-0.1125E-01	-0.1120E-01	-0.1115E-01
-0.9308E-02	-0.9485E-02	-0.9659E-02	-0.9829E-02	-0.1110E-01	-0.1105E-01	-0.1100E-01	-0.1095E-01
-0.9994E-02	-0.1016E-01	-0.1031E-01	-0.1047E-01	-0.1091E-01	-0.1086E-01	-0.1082E-01	-0.1077E-01
-0.1061E-01	-0.1076E-01	-0.1089E-01	-0.1103E-01	-0.1073E-01	-0.1069E-01	-0.1064E-01	-0.1060E-01
-0.1116E-01	-0.1128E-01	-0.1140E-01	-0.1151E-01	-0.1055E-01	-0.1050E-01	-0.1046E-01	-0.1041E-01
-0.1162E-01	-0.1173E-01	-0.1184E-01	-0.1193E-01	-0.1035E-01	-0.1030E-01	-0.1025E-01	-0.1019E-01
-0.1203E-01	-0.1212E-01	-0.1222E-01	-0.1230E-01	-0.1013E-01	-0.1006E-01	-0.1000E-01	-0.9931E-02
-0.1239E-01	-0.1247E-01	-0.1255E-01	-0.1263E-01	-0.9860E-02	-0.9786E-02	-0.9709E-02	-0.9629E-02
-0.1270E-01	-0.1278E-01	-0.1285E-01	-0.1292E-01	-0.9546E-02	-0.9460E-02	-0.9370E-02	-0.9278E-02
-0.1298E-01	-0.1305E-01	-0.1311E-01	-0.1317E-01	-0.9182E-02	-0.9084E-02	-0.8982E-02	-0.8878E-02
-0.1323E-01	-0.1329E-01	-0.1335E-01	-0.1341E-01	-0.8771E-02	-0.8662E-02	-0.8550E-02	-0.8436E-02
-0.1347E-01	-0.1352E-01	-0.1358E-01	-0.1364E-01	-0.8320E-02	-0.8202E-02	-0.8082E-02	-0.7961E-02
-0.1370E-01	-0.1376E-01	-0.1382E-01	-0.1388E-01	-0.7838E-02	-0.7715E-02	-0.7591E-02	-0.7467E-02
-0.1394E-01	-0.1401E-01	-0.1408E-01	-0.1415E-01	-0.7342E-02	-0.7217E-02	-0.7093E-02	-0.6970E-02

-0.6847E-02 -0.6725E-02 -0.6604E-02 -0.6485E-02 -0.8635E-03 -0.8186E-03 -0.7717E-03 -0.7228E-03
-0.6368E-02 -0.6252E-02 -0.6139E-02 -0.6027E-02 -0.6723E-03 -0.6204E-03 -0.5673E-03 -0.5133E-03
-0.5918E-02 -0.5811E-02 -0.5706E-02 -0.5604E-02 -0.4585E-03 -0.4033E-03 -0.3480E-03 -0.2927E-03
-0.5504E-02 -0.5406E-02 -0.5311E-02 -0.5218E-02 -0.2377E-03 -0.1833E-03 -0.1297E-03 -0.7723E-04
-0.5127E-02 -0.5039E-02 -0.4953E-02 -0.4869E-02 -0.2605E-04 0.2359E-04 0.7148E-04 0.1174E-03
-0.4787E-02 -0.4708E-02 -0.4630E-02 -0.4554E-02 0.1612E-03 0.2027E-03 0.2417E-03 0.2781E-03
-0.4480E-02 -0.4407E-02 -0.4336E-02 -0.4267E-02 0.3118E-03 0.3426E-03 0.3705E-03 0.3955E-03
-0.4199E-02 -0.4131E-02 -0.4065E-02 -0.4000E-02 0.4174E-03 0.4363E-03 0.4522E-03 0.4651E-03
-0.3935E-02 -0.3871E-02 -0.3807E-02 -0.3743E-02 0.4750E-03 0.4821E-03 0.4863E-03 0.4879E-03
-0.3679E-02 -0.3616E-02 -0.3552E-02 -0.3487E-02 0.4868E-03 0.4833E-03 0.4775E-03 0.4695E-03
-0.3422E-02 -0.3356E-02 -0.3290E-02 -0.3222E-02 0.4596E-03 0.4479E-03 0.4347E-03 0.4201E-03
-0.3154E-02 -0.3085E-02 -0.3014E-02 -0.2942E-02 0.4044E-03 0.3878E-03 0.3705E-03 0.3527E-03
-0.2870E-02 -0.2796E-02 -0.2721E-02 -0.2645E-02 0.3347E-03 0.3167E-03 0.2990E-03 0.2817E-03
-0.2568E-02 -0.2490E-02 -0.2412E-02 -0.2332E-02 0.2651E-03 0.2493E-03 0.2347E-03 0.2213E-03
-0.2252E-02 -0.2172E-02 -0.2091E-02 -0.2010E-02 0.2094E-03 0.1991E-03 0.1906E-03 0.1839E-03
-0.1929E-02 -0.1848E-02 -0.1767E-02 -0.1686E-02 0.1793E-03 0.1769E-03 0.1766E-03 0.1786E-03
-0.1606E-02 -0.1526E-02 -0.1447E-02 -0.1369E-02 0.1830E-03 0.1898E-03 0.1989E-03 0.2105E-03
-0.1292E-02 -0.1215E-02 -0.1140E-02 -0.1066E-02 0.2244E-03 0.2406E-03 0.2592E-03 0.2800E-03
-0.9938E-03 -0.9228E-03 -0.8535E-03 -0.7859E-03 0.3029E-03 0.3279E-03 0.3549E-03 0.3837E-03
-0.7201E-03 -0.6563E-03 -0.5946E-03 -0.5350E-03 0.4142E-03 0.4464E-03 0.4799E-03 0.5148E-03
-0.4776E-03 -0.4225E-03 -0.3698E-03 -0.3196E-03 0.5508E-03 0.5877E-03 0.6255E-03 0.6640E-03
-0.2718E-03 -0.2265E-03 -0.1837E-03 -0.1435E-03 0.7029E-03 0.7422E-03 0.7816E-03 0.8210E-03
-0.1059E-03 -0.7081E-04 -0.3822E-04 -0.8122E-05 0.8603E-03 0.8994E-03 0.9379E-03 0.9760E-03
0.1954E-04 0.4481E-04 0.6775E-04 0.8843E-04 0.1013E-02 0.1050E-02 0.1085E-02 0.1120E-02
0.1069E-03 0.1233E-03 0.1376E-03 0.1500E-03 0.1154E-02 0.1186E-02 0.1217E-02 0.1247E-02
0.1605E-03 0.1691E-03 0.1760E-03 0.1812E-03 0.1275E-02 0.1302E-02 0.1328E-02 0.1353E-02
0.1847E-03 0.1866E-03 0.1869E-03 0.1858E-03 0.1375E-02 0.1397E-02 0.1417E-02 0.1436E-02
0.1831E-03 0.1790E-03 0.1734E-03 0.1663E-03 0.1454E-02 0.1470E-02 0.1485E-02 0.1499E-02
0.1578E-03 0.1479E-03 0.1365E-03 0.1237E-03 0.1511E-02 0.1523E-02 0.1533E-02 0.1543E-02
0.1094E-03 0.9372E-04 0.7658E-04 0.5799E-04 0.1551E-02 0.1559E-02 0.1566E-02 0.1572E-02
0.3797E-04 0.1653E-04 -0.6340E-05 -0.3061E-04 0.1577E-02 0.1582E-02 0.1586E-02 0.1589E-02
-0.5627E-04 -0.8328E-04 -0.1116E-03 -0.1413E-03 0.1592E-02 0.1595E-02 0.1596E-02 0.1598E-02
-0.1722E-03 -0.2043E-03 -0.2375E-03 -0.2719E-03 0.1599E-02 0.1599E-02 0.1599E-02 0.1598E-02
-0.3072E-03 -0.3435E-03 -0.3807E-03 -0.4186E-03 0.1597E-02 0.1596E-02 0.1594E-02 0.1592E-02
-0.4571E-03 -0.4963E-03 -0.5358E-03 -0.5756E-03 0.1589E-02 0.1585E-02 0.1581E-02 0.1577E-02
-0.6156E-03 -0.6556E-03 -0.6954E-03 -0.7350E-03 0.1571E-02 0.1565E-02 0.1559E-02 0.1552E-02
-0.7740E-03 -0.8124E-03 -0.8500E-03 -0.8865E-03 0.1544E-02 0.1535E-02 0.1525E-02 0.1515E-02
-0.9219E-03 -0.9558E-03 -0.9882E-03 -0.1019E-02 0.1503E-02 0.1491E-02 0.1479E-02 0.1465E-02
-0.1047E-02 -0.1074E-02 -0.1098E-02 -0.1120E-02 0.1450E-02 0.1435E-02 0.1419E-02 0.1402E-02
-0.1139E-02 -0.1156E-02 -0.1169E-02 -0.1180E-02 0.1385E-02 0.1367E-02 0.1348E-02 0.1329E-02
-0.1187E-02 -0.1191E-02 -0.1192E-02 -0.1190E-02 0.1309E-02 0.1289E-02 0.1269E-02 0.1249E-02
-0.1184E-02 -0.1175E-02 -0.1163E-02 -0.1147E-02 0.1228E-02 0.1207E-02 0.1187E-02 0.1166E-02
-0.1127E-02 -0.1105E-02 -0.1079E-02 -0.1050E-02 0.1146E-02 0.1126E-02 0.1107E-02 0.1088E-02
-0.1019E-02 -0.9838E-03 -0.9463E-03 -0.9061E-03 0.1070E-02 0.1052E-02 0.1035E-02 0.1019E-02

0.1003E-02 0.9889E-03 0.9755E-03 0.9630E-03 0.9837E-03 0.9788E-03 0.9744E-03 0.9706E-03
0.9515E-03 0.9411E-03 0.9317E-03 0.9233E-03 0.9674E-03 0.9649E-03 0.9632E-03 0.9622E-03
0.9158E-03 0.9094E-03 0.9039E-03 0.8992E-03 0.9621E-03 0.9628E-03 0.9645E-03 0.9671E-03
0.8954E-03 0.8923E-03 0.8898E-03 0.8879E-03 0.9708E-03 0.9755E-03 0.9813E-03 0.9883E-03
0.8864E-03 0.8853E-03 0.8844E-03 0.8836E-03 0.9964E-03 0.1006E-02 0.1016E-02 0.1028E-02
0.8828E-03 0.8818E-03 0.8804E-03 0.8786E-03 0.1041E-02 0.1055E-02 0.1071E-02 0.1087E-02
0.8762E-03 0.8730E-03 0.8689E-03 0.8638E-03 0.1105E-02 0.1124E-02 0.1144E-02 0.1165E-02
0.8574E-03 0.8498E-03 0.8407E-03 0.8300E-03
0.8177E-03 0.8036E-03 0.7876E-03 0.7697E-03 Time history of displacement at node NF3:
0.7498E-03 0.7278E-03 0.7037E-03 0.6775E-03 -0.4198E-06 -0.1879E-05 -0.4455E-05 -0.7949E-05
0.6491E-03 0.6186E-03 0.5861E-03 0.5514E-03 -0.1214E-04 -0.1694E-04 -0.2276E-04 -0.3006E-04
0.5148E-03 0.4762E-03 0.4358E-03 0.3937E-03 -0.3871E-04 -0.4824E-04 -0.5845E-04 -0.6925E-04
0.3499E-03 0.3047E-03 0.2581E-03 0.2104E-03 -0.8056E-04 -0.9200E-04 -0.1028E-03 -0.1123E-03
0.1616E-03 0.1121E-03 0.6193E-04 0.1138E-04 -0.1201E-03 -0.1256E-03 -0.1285E-03 -0.1282E-03
-0.3934E-04 -0.9000E-04 -0.1404E-03 -0.1902E-03 -0.1241E-03 -0.1160E-03 -0.1038E-03 -0.8741E-04
-0.2393E-03 -0.2873E-03 -0.3341E-03 -0.3793E-03 -0.6696E-04 -0.4261E-04 -0.1466E-04 0.1650E-04
-0.4228E-03 -0.4643E-03 -0.5035E-03 -0.5403E-03 0.5035E-04 0.8630E-04 0.1237E-03 0.1619E-03
-0.5744E-03 -0.6055E-03 -0.6336E-03 -0.6584E-03 0.2003E-03 0.2380E-03 0.2745E-03 0.3088E-03
-0.6798E-03 -0.6976E-03 -0.7116E-03 -0.7218E-03 0.3404E-03 0.3683E-03 0.3921E-03 0.4109E-03
-0.7280E-03 -0.7303E-03 -0.7284E-03 -0.7225E-03 0.4240E-03 0.4309E-03 0.4309E-03 0.4238E-03
-0.7125E-03 -0.6983E-03 -0.6801E-03 -0.6579E-03 0.4092E-03 0.3872E-03 0.3577E-03 0.3209E-03
-0.6317E-03 -0.6017E-03 -0.5680E-03 -0.5307E-03 0.2773E-03 0.2274E-03 0.1717E-03 0.1109E-03
-0.4900E-03 -0.4460E-03 -0.3989E-03 -0.3490E-03 0.4592E-04 -0.2221E-04 -0.9248E-04 -0.1638E-03
-0.2964E-03 -0.2414E-03 -0.1843E-03 -0.1252E-03 -0.2348E-03 -0.3044E-03 -0.3710E-03 -0.4334E-03
-0.6448E-04 -0.2354E-05 0.6089E-04 0.1250E-03 -0.4902E-03 -0.5400E-03 -0.5815E-03 -0.6137E-03
0.1897E-03 0.2546E-03 0.3197E-03 0.3845E-03 -0.6353E-03 -0.6456E-03 -0.6441E-03 -0.6302E-03
0.4488E-03 0.5123E-03 0.5749E-03 0.6363E-03 -0.6038E-03 -0.5650E-03 -0.5144E-03 -0.4526E-03
0.6962E-03 0.7545E-03 0.8109E-03 0.8654E-03 -0.3806E-03 -0.2995E-03 -0.2107E-03 -0.1157E-03
0.9176E-03 0.9676E-03 0.1015E-02 0.1060E-02 -0.1592E-04 0.8692E-04 0.1912E-03 0.2954E-03
0.1102E-02 0.1142E-02 0.1179E-02 0.1213E-02 0.3979E-03 0.4971E-03 0.5915E-03 0.6798E-03
0.1244E-02 0.1272E-02 0.1298E-02 0.1320E-02 0.7609E-03 0.8337E-03 0.8972E-03 0.9508E-03
0.1340E-02 0.1358E-02 0.1373E-02 0.1385E-02 0.9939E-03 0.1026E-02 0.1047E-02 0.1057E-02
0.1395E-02 0.1402E-02 0.1407E-02 0.1411E-02 0.1056E-02 0.1044E-02 0.1021E-02 0.9883E-03
0.1412E-02 0.1411E-02 0.1409E-02 0.1405E-02 0.9462E-03 0.8952E-03 0.8360E-03 0.7694E-03
0.1400E-02 0.1393E-02 0.1385E-02 0.1376E-02 0.6961E-03 0.6170E-03 0.5328E-03 0.4445E-03
0.1366E-02 0.1356E-02 0.1344E-02 0.1333E-02 0.3530E-03 0.2593E-03 0.1642E-03 0.6881E-04
0.1320E-02 0.1307E-02 0.1294E-02 0.1281E-02 -0.2584E-04 -0.1187E-03 -0.2088E-03 -0.2950E-03
0.1268E-02 0.1255E-02 0.1241E-02 0.1228E-02 -0.3763E-03 -0.4517E-03 -0.5204E-03 -0.5814E-03
0.1215E-02 0.1202E-02 0.1189E-02 0.1176E-02 -0.6340E-03 -0.6775E-03 -0.7113E-03 -0.7352E-03
0.1164E-02 0.1152E-02 0.1140E-02 0.1129E-02 -0.7487E-03 -0.7517E-03 -0.7443E-03 -0.7265E-03
0.1118E-02 0.1107E-02 0.1096E-02 0.1086E-02 -0.6986E-03 -0.6610E-03 -0.6142E-03 -0.5587E-03
0.1076E-02 0.1066E-02 0.1057E-02 0.1048E-02 -0.4951E-03 -0.4241E-03 -0.3466E-03 -0.2631E-03
0.1040E-02 0.1031E-02 0.1023E-02 0.1016E-02 -0.1746E-03 -0.8175E-04 0.1464E-04 0.1138E-03
0.1008E-02 0.1002E-02 0.9952E-03 0.9892E-03 0.2151E-03 0.3177E-03 0.4211E-03 0.5245E-03

0.6276E-03	0.7297E-03	0.8305E-03	0.9294E-03	0.5991E-02	0.5904E-02	0.5823E-02	0.5748E-02
0.1026E-02	0.1120E-02	0.1211E-02	0.1299E-02	0.5679E-02	0.5616E-02	0.5557E-02	0.5502E-02
0.1384E-02	0.1464E-02	0.1541E-02	0.1613E-02	0.5450E-02	0.5401E-02	0.5353E-02	0.5306E-02
0.1681E-02	0.1744E-02	0.1801E-02	0.1854E-02	0.5257E-02	0.5206E-02	0.5152E-02	0.5094E-02
0.1901E-02	0.1943E-02	0.1980E-02	0.2010E-02	0.5031E-02	0.4961E-02	0.4884E-02	0.4799E-02
0.2035E-02	0.2055E-02	0.2068E-02	0.2075E-02	0.4706E-02	0.4603E-02	0.4491E-02	0.4370E-02
0.2077E-02	0.2072E-02	0.2061E-02	0.2044E-02	0.4238E-02	0.4097E-02	0.3947E-02	0.3788E-02
0.2020E-02	0.1989E-02	0.1951E-02	0.1905E-02	0.3620E-02	0.3444E-02	0.3260E-02	0.3070E-02
0.1852E-02	0.1792E-02	0.1723E-02	0.1645E-02	0.2874E-02	0.2672E-02	0.2467E-02	0.2258E-02
0.1560E-02	0.1465E-02	0.1362E-02	0.1251E-02	0.2047E-02	0.1834E-02	0.1620E-02	0.1405E-02
0.1131E-02	0.1002E-02	0.8654E-03	0.7206E-03	0.1191E-02	0.9785E-03	0.7671E-03	0.5576E-03
0.5679E-03	0.4080E-03	0.2412E-03	0.6806E-04	0.3504E-03	0.1456E-03	-0.5674E-04	-0.2565E-03
-0.1108E-03	-0.2946E-03	-0.4827E-03	-0.6743E-03	-0.4540E-03	-0.6492E-03	-0.8426E-03	-0.1034E-02
-0.8686E-03	-0.1065E-02	-0.1262E-02	-0.1459E-02	-0.1225E-02	-0.1416E-02	-0.1607E-02	-0.1798E-02
-0.1655E-02	-0.1850E-02	-0.2042E-02	-0.2231E-02	-0.1992E-02	-0.2187E-02	-0.2386E-02	-0.2588E-02
-0.2415E-02	-0.2594E-02	-0.2768E-02	-0.2934E-02	-0.2795E-02	-0.3007E-02	-0.3225E-02	-0.3449E-02
-0.3094E-02	-0.3245E-02	-0.3388E-02	-0.3521E-02	-0.3679E-02	-0.3916E-02	-0.4160E-02	-0.4411E-02
-0.3644E-02	-0.3756E-02	-0.3857E-02	-0.3946E-02	-0.4668E-02	-0.4932E-02	-0.5201E-02	-0.5476E-02
-0.4023E-02	-0.4087E-02	-0.4138E-02	-0.4175E-02	-0.5754E-02	-0.6037E-02	-0.6321E-02	-0.6606E-02
-0.4199E-02	-0.4209E-02	-0.4206E-02	-0.4189E-02	-0.6891E-02	-0.7174E-02	-0.7453E-02	-0.7726E-02
-0.4159E-02	-0.4117E-02	-0.4062E-02	-0.3996E-02	-0.7993E-02	-0.8251E-02	-0.8498E-02	-0.8733E-02
-0.3919E-02	-0.3832E-02	-0.3735E-02	-0.3630E-02	-0.8954E-02	-0.9159E-02	-0.9347E-02	-0.9517E-02
-0.3518E-02	-0.3400E-02	-0.3275E-02	-0.3146E-02	-0.9666E-02	-0.9795E-02	-0.9902E-02	-0.9986E-02
-0.3014E-02	-0.2878E-02	-0.2740E-02	-0.2601E-02	-0.1005E-01	-0.1008E-01	-0.1010E-01	-0.1009E-01
-0.2461E-02	-0.2320E-02	-0.2179E-02	-0.2038E-02	-0.1006E-01	-0.9999E-02	-0.9920E-02	-0.9819E-02
-0.1897E-02	-0.1756E-02	-0.1616E-02	-0.1476E-02	-0.9697E-02	-0.9557E-02	-0.9398E-02	-0.9222E-02
-0.1335E-02	-0.1195E-02	-0.1053E-02	-0.9099E-03	-0.9031E-02	-0.8826E-02	-0.8609E-02	-0.8382E-02
-0.7650E-03	-0.6177E-03	-0.4674E-03	-0.3135E-03	-0.8146E-02	-0.7903E-02	-0.7656E-02	-0.7404E-02
-0.1555E-03	0.7174E-05	0.1750E-03	0.3486E-03	-0.7150E-02	-0.6896E-02	-0.6643E-02	-0.6391E-02
0.5283E-03	0.7146E-03	0.9078E-03	0.1108E-02	-0.6142E-02	-0.5897E-02	-0.5656E-02	-0.5420E-02
0.1316E-02	0.1531E-02	0.1753E-02	0.1983E-02	-0.5190E-02	-0.4964E-02	-0.4745E-02	-0.4531E-02
0.2220E-02	0.2463E-02	0.2712E-02	0.2968E-02	-0.4322E-02	-0.4117E-02	-0.3917E-02	-0.3721E-02
0.3228E-02	0.3492E-02	0.3759E-02	0.4029E-02	-0.3528E-02	-0.3337E-02	-0.3148E-02	-0.2960E-02
0.4299E-02	0.4570E-02	0.4838E-02	0.5104E-02	-0.2772E-02	-0.2583E-02	-0.2392E-02	-0.2199E-02
0.5366E-02	0.5622E-02	0.5870E-02	0.6111E-02	-0.2003E-02	-0.1803E-02	-0.1600E-02	-0.1392E-02
0.6341E-02	0.6560E-02	0.6767E-02	0.6961E-02	-0.1179E-02	-0.9612E-03	-0.7387E-03	-0.5113E-03
0.7140E-02	0.7304E-02	0.7452E-02	0.7583E-02	-0.2794E-03	-0.4328E-04	0.1965E-03	0.4395E-03
0.7697E-02	0.7794E-02	0.7873E-02	0.7934E-02	0.6848E-03	0.9317E-03	0.1179E-02	0.1427E-02
0.7977E-02	0.8003E-02	0.8012E-02	0.8005E-02	0.1673E-02	0.1917E-02	0.2157E-02	0.2393E-02
0.7982E-02	0.7943E-02	0.7891E-02	0.7826E-02	0.2623E-02	0.2846E-02	0.3061E-02	0.3268E-02
0.7749E-02	0.7662E-02	0.7566E-02	0.7462E-02	0.3465E-02	0.3652E-02	0.3827E-02	0.3991E-02
0.7351E-02	0.7235E-02	0.7116E-02	0.6995E-02	0.4143E-02	0.4281E-02	0.4408E-02	0.4521E-02
0.6873E-02	0.6751E-02	0.6631E-02	0.6513E-02	0.4621E-02	0.4709E-02	0.4785E-02	0.4849E-02
0.6398E-02	0.6289E-02	0.6184E-02	0.6084E-02	0.4903E-02	0.4946E-02	0.4980E-02	0.5006E-02

0.5024E-02	0.5037E-02	0.5045E-02	0.5049E-02	-0.6090E-02	-0.6258E-02	-0.6431E-02	-0.6607E-02
0.5050E-02	0.5050E-02	0.5051E-02	0.5052E-02	-0.6786E-02	-0.6970E-02	-0.7156E-02	-0.7346E-02
0.5055E-02	0.5061E-02	0.5071E-02	0.5085E-02	-0.7538E-02	-0.7731E-02	-0.7926E-02	-0.8121E-02
0.5105E-02	0.5131E-02	0.5162E-02	0.5201E-02	-0.8315E-02	-0.8508E-02	-0.8699E-02	-0.8886E-02
0.5246E-02	0.5297E-02	0.5355E-02	0.5420E-02	-0.9068E-02	-0.9245E-02	-0.9415E-02	-0.9577E-02
0.5491E-02	0.5568E-02	0.5650E-02	0.5737E-02	-0.9732E-02	-0.9877E-02	-0.1001E-01	-0.1014E-01
0.5828E-02	0.5923E-02	0.6021E-02	0.6121E-02	-0.1025E-01	-0.1035E-01	-0.1044E-01	-0.1052E-01
0.6223E-02	0.6326E-02	0.6430E-02	0.6534E-02	-0.1059E-01	-0.1065E-01	-0.1069E-01	-0.1072E-01
0.6637E-02	0.6739E-02	0.6839E-02	0.6938E-02	-0.1075E-01	-0.1076E-01	-0.1077E-01	-0.1077E-01
0.7035E-02	0.7130E-02	0.7222E-02	0.7312E-02	-0.1076E-01	-0.1074E-01	-0.1072E-01	-0.1070E-01
0.7400E-02	0.7486E-02	0.7570E-02	0.7652E-02	-0.1067E-01	-0.1065E-01	-0.1062E-01	-0.1059E-01
0.7733E-02	0.7813E-02	0.7893E-02	0.7972E-02	-0.1057E-01	-0.1054E-01	-0.1053E-01	-0.1051E-01
0.8051E-02	0.8131E-02	0.8212E-02	0.8294E-02	-0.1050E-01	-0.1050E-01	-0.1050E-01	-0.1051E-01
0.8377E-02	0.8463E-02	0.8550E-02	0.8639E-02	-0.1052E-01	-0.1054E-01	-0.1057E-01	-0.1060E-01
0.8731E-02	0.8825E-02	0.8920E-02	0.9018E-02	-0.1064E-01	-0.1068E-01	-0.1073E-01	-0.1078E-01
0.9116E-02	0.9216E-02	0.9316E-02	0.9416E-02	-0.1083E-01	-0.1088E-01	-0.1093E-01	-0.1098E-01
0.9516E-02	0.9613E-02	0.9708E-02	0.9800E-02	-0.1103E-01	-0.1108E-01	-0.1112E-01	-0.1116E-01
0.9888E-02	0.9970E-02	0.1005E-01	0.1011E-01	-0.1119E-01	-0.1121E-01	-0.1123E-01	-0.1124E-01
0.1017E-01	0.1023E-01	0.1027E-01	0.1030E-01	-0.1124E-01	-0.1123E-01	-0.1121E-01	-0.1118E-01
0.1031E-01	0.1032E-01	0.1031E-01	0.1029E-01	-0.1113E-01	-0.1108E-01	-0.1102E-01	-0.1095E-01
0.1025E-01	0.1020E-01	0.1014E-01	0.1006E-01	-0.1087E-01	-0.1079E-01	-0.1069E-01	-0.1059E-01
0.9966E-02	0.9860E-02	0.9740E-02	0.9608E-02	-0.1048E-01	-0.1037E-01	-0.1025E-01	-0.1013E-01
0.9464E-02	0.9308E-02	0.9143E-02	0.8970E-02	-0.1001E-01	-0.9890E-02	-0.9767E-02	-0.9645E-02
0.8788E-02	0.8600E-02	0.8407E-02	0.8210E-02	-0.9525E-02	-0.9407E-02	-0.9292E-02	-0.9182E-02
0.8010E-02	0.7809E-02	0.7609E-02	0.7410E-02	-0.9075E-02	-0.8973E-02	-0.8876E-02	-0.8784E-02
0.7213E-02	0.7020E-02	0.6832E-02	0.6649E-02	-0.8697E-02	-0.8615E-02	-0.8537E-02	-0.8463E-02
0.6473E-02	0.6303E-02	0.6142E-02	0.5988E-02	-0.8393E-02	-0.8326E-02	-0.8261E-02	-0.8197E-02
0.5842E-02	0.5704E-02	0.5574E-02	0.5452E-02	-0.8134E-02	-0.8071E-02	-0.8006E-02	-0.7940E-02
0.5337E-02	0.5229E-02	0.5128E-02	0.5031E-02	-0.7870E-02	-0.7797E-02	-0.7719E-02	-0.7635E-02
0.4939E-02	0.4850E-02	0.4763E-02	0.4677E-02	-0.7545E-02	-0.7448E-02	-0.7344E-02	-0.7231E-02
0.4592E-02	0.4505E-02	0.4416E-02	0.4323E-02	-0.7111E-02	-0.6983E-02	-0.6846E-02	-0.6701E-02
0.4225E-02	0.4122E-02	0.4012E-02	0.3894E-02	-0.6548E-02	-0.6388E-02	-0.6220E-02	-0.6047E-02
0.3768E-02	0.3632E-02	0.3487E-02	0.3331E-02	-0.5867E-02	-0.5683E-02	-0.5496E-02	-0.5305E-02
0.3165E-02	0.2989E-02	0.2802E-02	0.2604E-02	-0.5113E-02	-0.4920E-02	-0.4728E-02	-0.4538E-02
0.2396E-02	0.2179E-02	0.1952E-02	0.1717E-02	-0.4350E-02	-0.4167E-02	-0.3989E-02	-0.3816E-02
0.1474E-02	0.1225E-02	0.9693E-03	0.7094E-03	-0.3651E-02	-0.3494E-02	-0.3345E-02	-0.3205E-02
0.4459E-03	0.1799E-03	-0.8729E-04	-0.3547E-03	-0.3075E-02	-0.2955E-02	-0.2844E-02	-0.2744E-02
-0.6211E-03	-0.8855E-03	-0.1147E-02	-0.1404E-02	-0.2653E-02	-0.2572E-02	-0.2500E-02	-0.2436E-02
-0.1657E-02	-0.1904E-02	-0.2145E-02	-0.2379E-02	-0.2380E-02	-0.2331E-02	-0.2288E-02	-0.2249E-02
-0.2606E-02	-0.2826E-02	-0.3039E-02	-0.3244E-02	-0.2215E-02	-0.2184E-02	-0.2154E-02	-0.2124E-02
-0.3442E-02	-0.3633E-02	-0.3818E-02	-0.3996E-02	-0.2094E-02	-0.2062E-02	-0.2027E-02	-0.1989E-02
-0.4169E-02	-0.4337E-02	-0.4501E-02	-0.4662E-02	-0.1945E-02	-0.1895E-02	-0.1840E-02	-0.1777E-02
-0.4821E-02	-0.4977E-02	-0.5133E-02	-0.5288E-02	-0.1706E-02	-0.1628E-02	-0.1541E-02	-0.1447E-02
-0.5445E-02	-0.5603E-02	-0.5762E-02	-0.5925E-02	-0.1344E-02	-0.1234E-02	-0.1116E-02	-0.9909E-03

-0.8597E-03 -0.7228E-03 -0.5811E-03 -0.4356E-03 0.6508E-02 0.6939E-02 0.6971E-02 0.6916E-02
-0.2872E-03 -0.1368E-03 0.1429E-04 0.1652E-03 0.6721E-02 0.6360E-02 0.5760E-02 0.4733E-02
0.3148E-03 0.4622E-03 0.6062E-03 0.7460E-03 0.3485E-02 0.2174E-02 0.7363E-03 -0.8499E-03
0.8808E-03 0.1010E-02 0.1132E-02 0.1248E-02 -0.2579E-02 -0.4390E-02 -0.6106E-02 -0.7642E-02
0.1356E-02 0.1457E-02 0.1550E-02 0.1636E-02 -0.9129E-02 -0.1047E-01 -0.1162E-01 -0.1252E-01
0.1714E-02 0.1785E-02 0.1849E-02 0.1908E-02 -0.1304E-01 -0.1331E-01 -0.1331E-01 -0.1300E-01
0.1961E-02 0.2010E-02 0.2055E-02 0.2098E-02 -0.1237E-01 -0.1140E-01 -0.1012E-01 -0.8613E-02
0.2140E-02 0.2182E-02 0.2225E-02 0.2270E-02 -0.6916E-02 -0.4964E-02 -0.2862E-02 -0.6366E-03
0.2318E-02 0.2371E-02 0.2429E-02 0.2495E-02 0.1621E-02 0.3826E-02 0.6019E-02 0.8149E-02
0.2567E-02 0.2649E-02 0.2739E-02 0.2839E-02 0.1016E-01 0.1203E-01 0.1371E-01 0.1520E-01
0.2950E-02 0.3070E-02 0.3201E-02 0.3343E-02 0.1653E-01 0.1767E-01 0.1859E-01 0.1929E-01
0.3495E-02 0.3657E-02 0.3828E-02 0.4008E-02 0.1979E-01 0.2008E-01 0.2017E-01 0.2004E-01
0.4196E-02 0.4391E-02 0.4591E-02 0.4796E-02 0.1970E-01 0.1916E-01 0.1841E-01 0.1749E-01
0.5005E-02 0.5216E-02 0.5427E-02 0.5637E-02 0.1638E-01 0.1511E-01 0.1370E-01 0.1219E-01
0.5846E-02 0.6051E-02 0.6251E-02 0.6445E-02 0.1058E-01 0.8927E-02 0.7247E-02 0.5575E-02
0.6631E-02 0.6809E-02 0.6977E-02 0.7134E-02 0.3944E-02 0.2378E-02 0.8948E-03 -0.4910E-03
0.7279E-02 0.7413E-02 0.7533E-02 0.7641E-02 -0.1767E-02 -0.2922E-02 -0.3948E-02 -0.4840E-02
0.7735E-02 0.7815E-02 0.7882E-02 0.7935E-02 -0.5597E-02 -0.6219E-02 -0.6712E-02 -0.7085E-02
0.7976E-02 0.8004E-02 0.8020E-02 0.8024E-02 -0.7353E-02 -0.7530E-02 -0.7636E-02 -0.7692E-02
0.8019E-02 0.8003E-02 0.7979E-02 0.7947E-02 -0.7722E-02 -0.7752E-02 -0.7796E-02 -0.7878E-02
0.7909E-02 0.7864E-02 0.7815E-02 0.7762E-02 -0.8017E-02 -0.8230E-02 -0.8528E-02 -0.8915E-02
0.7707E-02 0.7649E-02 0.7591E-02 0.7532E-02 -0.9394E-02 -0.9962E-02 -0.1062E-01 -0.1136E-01
0.7474E-02 0.7417E-02 0.7361E-02 0.7307E-02 -0.1217E-01 -0.1304E-01 -0.1395E-01 -0.1490E-01
0.7256E-02 0.7207E-02 0.7160E-02 0.7116E-02 -0.1588E-01 -0.1688E-01 -0.1789E-01 -0.1890E-01
0.7074E-02 0.7034E-02 0.6997E-02 0.6961E-02 -0.1991E-01 -0.2092E-01 -0.2193E-01 -0.2292E-01
0.6926E-02 0.6892E-02 0.6859E-02 0.6825E-02 -0.2391E-01 -0.2487E-01 -0.2582E-01 -0.2673E-01
0.6792E-02 0.6757E-02 0.6722E-02 0.6685E-02 -0.2760E-01 -0.2841E-01 -0.2915E-01 -0.2979E-01
0.6646E-02 0.6606E-02 0.6563E-02 0.6519E-02 -0.3033E-01 -0.3073E-01 -0.3099E-01 -0.3107E-01
0.6472E-02 0.6424E-02 0.6374E-02 0.6324E-02 -0.3096E-01 -0.3064E-01 -0.3009E-01 -0.2932E-01
0.6272E-02 0.6220E-02 0.6169E-02 0.6118E-02 -0.2831E-01 -0.2706E-01 -0.2557E-01 -0.2385E-01
0.6069E-02 0.6023E-02 0.5980E-02 0.5941E-02 -0.2191E-01 -0.1977E-01 -0.1746E-01 -0.1499E-01
0.5907E-02 0.5879E-02 0.5857E-02 0.5842E-02 -0.1240E-01 -0.9720E-02 -0.6987E-02 -0.4232E-02
0.5834E-02 0.5835E-02 0.5845E-02 0.5863E-02 -0.1490E-02 0.1206E-02 0.3823E-02 0.6330E-02
0.5891E-02 0.5928E-02 0.5975E-02 0.6030E-02 0.8701E-02 0.1092E-01 0.1297E-01 0.1484E-01
0.6094E-02 0.6166E-02 0.6245E-02 0.6331E-02 0.1652E-01 0.1802E-01 0.1934E-01 0.2048E-01
0.6423E-02 0.6519E-02 0.6619E-02 0.6721E-02 0.2145E-01 0.2226E-01 0.2293E-01 0.2346E-01
0.6823E-02 0.6925E-02 0.7024E-02 0.7120E-02 0.2387E-01 0.2416E-01 0.2436E-01 0.2446E-01
0.7210E-02 0.7293E-02 0.7367E-02 0.7432E-02 0.2448E-01 0.2443E-01 0.2431E-01 0.2413E-01
0.7484E-02 0.7524E-02 0.7550E-02 0.7560E-02 0.2391E-01 0.2366E-01 0.2338E-01 0.2307E-01
0.2276E-01 0.2245E-01 0.2214E-01 0.2185E-01

Time history of vertical velocity at node NF1:

0.2157E-01 0.2133E-01 0.2111E-01 0.2092E-01
0.3029E-03 0.7570E-03 0.1142E-02 0.1486E-02 0.2077E-01 0.2067E-01 0.2062E-01 0.2062E-01
0.1733E-02 0.2060E-02 0.2708E-02 0.3531E-02 0.2068E-01 0.2081E-01 0.2099E-01 0.2124E-01
0.4153E-02 0.4666E-02 0.5226E-02 0.5826E-02 0.2155E-01 0.2191E-01 0.2231E-01 0.2274E-01

0.2319E-01	0.2365E-01	0.2410E-01	0.2452E-01	-0.2700E-01	-0.2931E-01	-0.3143E-01	-0.3332E-01
0.2490E-01	0.2522E-01	0.2547E-01	0.2563E-01	-0.3495E-01	-0.3630E-01	-0.3735E-01	-0.3809E-01
0.2571E-01	0.2568E-01	0.2555E-01	0.2530E-01	-0.3849E-01	-0.3856E-01	-0.3828E-01	-0.3766E-01
0.2493E-01	0.2444E-01	0.2383E-01	0.2310E-01	-0.3671E-01	-0.3543E-01	-0.3383E-01	-0.3195E-01
0.2224E-01	0.2127E-01	0.2017E-01	0.1896E-01	-0.2979E-01	-0.2740E-01	-0.2480E-01	-0.2203E-01
0.1764E-01	0.1621E-01	0.1468E-01	0.1306E-01	-0.1913E-01	-0.1613E-01	-0.1308E-01	-0.1002E-01
0.1136E-01	0.9586E-02	0.7758E-02	0.5896E-02	-0.6991E-02	-0.4042E-02	-0.1206E-02	0.1479E-02
0.4015E-02	0.2136E-02	0.2852E-03	-0.1512E-02	0.3967E-02	0.6226E-02	0.8225E-02	0.9937E-02
-0.3238E-02	-0.4868E-02	-0.6376E-02	-0.7743E-02	0.1134E-01	0.1242E-01	0.1318E-01	0.1360E-01
-0.8948E-02	-0.9977E-02	-0.1081E-01	-0.1143E-01	0.1368E-01	0.1342E-01	0.1284E-01	0.1196E-01
-0.1183E-01	-0.1201E-01	-0.1197E-01	-0.1171E-01	0.1079E-01	0.9365E-02	0.7720E-02	0.5872E-02
-0.1123E-01	-0.1055E-01	-0.9680E-02	-0.8637E-02	0.3850E-02	0.1700E-02	-0.5418E-03	-0.2837E-02
-0.7440E-02	-0.6115E-02	-0.4691E-02	-0.3189E-02	-0.5146E-02	-0.7433E-02	-0.9661E-02	-0.1179E-01
-0.1630E-02	-0.4539E-04	0.1538E-02	0.3095E-02	-0.1381E-01	-0.1567E-01	-0.1734E-01	-0.1880E-01
0.4598E-02	0.6027E-02	0.7367E-02	0.8601E-02	-0.2004E-01	-0.2105E-01	-0.2180E-01	-0.2228E-01
0.9712E-02	0.1069E-01	0.1153E-01	0.1223E-01	-0.2251E-01	-0.2247E-01	-0.2218E-01	-0.2164E-01
0.1278E-01	0.1316E-01	0.1339E-01	0.1347E-01	-0.2086E-01	-0.1987E-01	-0.1868E-01	-0.1732E-01
0.1339E-01	0.1318E-01	0.1282E-01	0.1233E-01	-0.1579E-01	-0.1415E-01	-0.1241E-01	-0.1061E-01
0.1171E-01	0.1099E-01	0.1014E-01	0.9199E-02	-0.8776E-02	-0.6935E-02	-0.5112E-02	-0.3332E-02
0.8175E-02	0.7074E-02	0.5909E-02	0.4702E-02	-0.1626E-02	-0.1855E-04	0.1469E-02	0.2813E-02
0.3467E-02	0.2215E-02	0.9688E-03	-0.2540E-03	0.4000E-02	0.5006E-02	0.5816E-02	0.6428E-02
-0.1445E-02	-0.2579E-02	-0.3642E-02	-0.4619E-02	0.6832E-02	0.7022E-02	0.7004E-02	0.6782E-02
-0.5494E-02	-0.6266E-02	-0.6921E-02	-0.7446E-02	0.6365E-02	0.5767E-02	0.5005E-02	0.4095E-02
-0.7843E-02	-0.8106E-02	-0.8225E-02	-0.8206E-02	0.3051E-02	0.1908E-02	0.6838E-03	-0.6047E-03
-0.8063E-02	-0.7809E-02	-0.7454E-02	-0.7006E-02	-0.1926E-02	-0.3250E-02	-0.4554E-02	-0.5813E-02
-0.6482E-02	-0.5897E-02	-0.5269E-02	-0.4619E-02	-0.7004E-02	-0.8105E-02	-0.9099E-02	-0.9971E-02
-0.3958E-02	-0.3307E-02	-0.2691E-02	-0.2131E-02	-0.1070E-01	-0.1129E-01	-0.1172E-01	-0.1198E-01
-0.1648E-02	-0.1260E-02	-0.9920E-03	-0.8483E-03	-0.1207E-01	-0.1199E-01	-0.1175E-01	-0.1136E-01
-0.8347E-03	-0.9633E-03	-0.1233E-02	-0.1648E-02	-0.1082E-01	-0.1013E-01	-0.9319E-02	-0.8387E-02
-0.2202E-02	-0.2884E-02	-0.3683E-02	-0.4581E-02	-0.7361E-02	-0.6261E-02	-0.5101E-02	-0.3898E-02
-0.5573E-02	-0.6637E-02	-0.7745E-02	-0.8882E-02	-0.2672E-02	-0.1435E-02	-0.2084E-03	0.9860E-03
-0.1003E-01	-0.1116E-01	-0.1225E-01	-0.1327E-01	0.2137E-02	0.3233E-02	0.4259E-02	0.5206E-02
-0.1421E-01	-0.1505E-01	-0.1577E-01	-0.1636E-01	0.6075E-02	0.6858E-02	0.7554E-02	0.8168E-02
-0.1678E-01	-0.1704E-01	-0.1711E-01	-0.1700E-01	0.8708E-02	0.9174E-02	0.9581E-02	0.9940E-02
-0.1668E-01	-0.1617E-01	-0.1547E-01	-0.1458E-01	0.1026E-01	0.1055E-01	0.1082E-01	0.1110E-01
-0.1351E-01	-0.1228E-01	-0.1091E-01	-0.9404E-02	0.1140E-01	0.1173E-01	0.1211E-01	0.1256E-01
-0.7798E-02	-0.6108E-02	-0.4365E-02	-0.2603E-02	0.1307E-01	0.1368E-01	0.1439E-01	0.1519E-01
-0.8512E-03	0.8581E-03	0.2494E-02	0.4017E-02	0.1611E-01	0.1713E-01	0.1826E-01	0.1950E-01
0.5397E-02	0.6604E-02	0.7609E-02	0.8391E-02	0.2085E-01	0.2229E-01	0.2381E-01	0.2539E-01
0.8933E-02	0.9213E-02	0.9214E-02	0.8933E-02	0.2702E-01	0.2869E-01	0.3035E-01	0.3200E-01
0.8363E-02	0.7503E-02	0.6359E-02	0.4938E-02	0.3361E-01	0.3516E-01	0.3661E-01	0.3793E-01
0.3261E-02	0.1346E-02	-0.7872E-03	-0.3107E-02	0.3911E-01	0.4012E-01	0.4093E-01	0.4152E-01
-0.5587E-02	-0.8200E-02	-0.1091E-01	-0.1366E-01	0.4187E-01	0.4197E-01	0.4179E-01	0.4134E-01
-0.1644E-01	-0.1920E-01	-0.2191E-01	-0.2452E-01	0.4060E-01	0.3956E-01	0.3823E-01	0.3660E-01

0.3468E-01	0.3248E-01	0.3002E-01	0.2732E-01	0.2584E-01	0.2757E-01	0.2920E-01	0.3068E-01
0.2440E-01	0.2128E-01	0.1800E-01	0.1457E-01	0.3199E-01	0.3309E-01	0.3394E-01	0.3452E-01
0.1103E-01	0.7413E-02	0.3762E-02	0.1059E-03	0.3481E-01	0.3476E-01	0.3437E-01	0.3362E-01
-0.3512E-02	-0.7055E-02	-0.1049E-01	-0.1378E-01	0.3250E-01	0.3100E-01	0.2912E-01	0.2687E-01
-0.1689E-01	-0.1979E-01	-0.2246E-01	-0.2486E-01	0.2425E-01	0.2127E-01	0.1795E-01	0.1432E-01
-0.2697E-01	-0.2878E-01	-0.3026E-01	-0.3141E-01	0.1040E-01	0.6226E-02	0.1826E-02	-0.2753E-02
-0.3223E-01	-0.3270E-01	-0.3282E-01	-0.3261E-01	-0.7476E-02	-0.1230E-01	-0.1718E-01	-0.2206E-01
-0.3209E-01	-0.3126E-01	-0.3014E-01	-0.2874E-01	-0.2691E-01	-0.3168E-01	-0.3631E-01	-0.4078E-01
-0.2710E-01	-0.2525E-01	-0.2321E-01	-0.2103E-01	-0.4504E-01	-0.4904E-01	-0.5275E-01	-0.5614E-01
-0.1872E-01	-0.1634E-01	-0.1391E-01	-0.1148E-01	-0.5919E-01	-0.6186E-01	-0.6414E-01	-0.6601E-01
-0.9067E-02	-0.6712E-02	-0.4444E-02	-0.2293E-02	-0.6747E-01	-0.6851E-01	-0.6912E-01	-0.6932E-01
-0.2910E-03	0.1538E-02	0.3179E-02	0.4614E-02	-0.6911E-01	-0.6850E-01	-0.6753E-01	-0.6619E-01
0.5826E-02	0.6809E-02	0.7560E-02	0.8074E-02	-0.6453E-01	-0.6257E-01	-0.6034E-01	-0.5788E-01
0.8351E-02	0.8401E-02	0.8234E-02	0.7858E-02	-0.5522E-01	-0.5240E-01	-0.4945E-01	-0.4640E-01
0.7293E-02	0.6560E-02	0.5674E-02	0.4661E-02	-0.4330E-01	-0.4018E-01	-0.3706E-01	-0.3398E-01
0.3553E-02	0.2369E-02	0.1132E-02	-0.1293E-03	-0.3096E-01	-0.2803E-01	-0.2521E-01	-0.2251E-01
-0.1382E-02	-0.2598E-02	-0.3760E-02	-0.4848E-02	-0.1996E-01	-0.1756E-01	-0.1532E-01	-0.1324E-01
-0.5840E-02	-0.6708E-02	-0.7435E-02	-0.8016E-02	-0.1133E-01	-0.9573E-02	-0.7969E-02	-0.6508E-02
-0.8442E-02	-0.8693E-02	-0.8766E-02	-0.8658E-02	-0.5182E-02	-0.3973E-02	-0.2869E-02	-0.1856E-02
-0.8374E-02	-0.7922E-02	-0.7314E-02	-0.6557E-02	-0.9093E-03	-0.1261E-04	0.8504E-03	0.1698E-02
-0.5664E-02	-0.4648E-02	-0.3522E-02	-0.2312E-02	0.2548E-02	0.3414E-02	0.4310E-02	0.5249E-02
-0.1041E-02	0.2745E-03	0.1616E-02	0.2955E-02	0.6240E-02	0.7291E-02	0.8406E-02	0.9588E-02
0.4267E-02	0.5530E-02	0.6726E-02	0.7834E-02	0.1084E-01	0.1215E-01	0.1353E-01	0.1495E-01
0.8842E-02	0.9730E-02	0.1048E-01	0.1110E-01	0.1641E-01	0.1789E-01	0.1938E-01	0.2087E-01
0.1156E-01	0.1188E-01	0.1204E-01	0.1204E-01	0.2233E-01	0.2376E-01	0.2512E-01	0.2640E-01
0.1189E-01	0.1160E-01	0.1119E-01	0.1065E-01	0.2757E-01	0.2862E-01	0.2953E-01	0.3029E-01
0.1002E-01	0.9303E-02	0.8519E-02	0.7687E-02	0.3087E-01	0.3128E-01	0.3149E-01	0.3150E-01
0.6832E-02	0.5973E-02	0.5130E-02	0.4324E-02	0.3131E-01	0.3091E-01	0.3031E-01	0.2951E-01
0.3573E-02	0.2892E-02	0.2299E-02	0.1810E-02	0.2852E-01	0.2735E-01	0.2601E-01	0.2453E-01
0.1437E-02	0.1195E-02	0.1088E-02	0.1117E-02	0.2292E-01	0.2121E-01	0.1941E-01	0.1755E-01
0.1288E-02	0.1593E-02	0.2034E-02	0.2609E-02	0.1566E-01	0.1376E-01	0.1189E-01	0.1006E-01
0.3303E-02	0.4106E-02	0.5009E-02	0.5991E-02	0.8297E-02	0.6636E-02	0.5094E-02	0.3694E-02
0.7034E-02	0.8123E-02	0.9237E-02	0.1036E-01	0.2453E-02	0.1388E-02	0.5113E-03	-0.1670E-03
0.1147E-01	0.1254E-01	0.1356E-01	0.1450E-01	-0.6406E-03	-0.9089E-03	-0.9711E-03	-0.8308E-03
0.1536E-01	0.1610E-01	0.1673E-01	0.1724E-01	-0.4978E-03	0.1668E-04	0.6998E-03	0.1533E-02
0.1760E-01	0.1783E-01	0.1790E-01	0.1783E-01	0.2497E-02	0.3569E-02	0.4721E-02	0.5932E-02
0.1762E-01	0.1728E-01	0.1681E-01	0.1623E-01	0.7171E-02	0.8411E-02	0.9619E-02	0.1077E-01
0.1555E-01	0.1480E-01	0.1398E-01	0.1312E-01	0.1183E-01	0.1278E-01	0.1360E-01	0.1426E-01
0.1224E-01	0.1137E-01	0.1053E-01	0.9732E-02	0.1474E-01	0.1503E-01	0.1511E-01	0.1497E-01
0.9017E-02	0.8400E-02	0.7901E-02	0.7542E-02	0.1460E-01	0.1400E-01	0.1319E-01	0.1215E-01
0.7340E-02	0.7308E-02	0.7451E-02	0.7775E-02	0.1091E-01	0.9467E-02	0.7848E-02	0.6070E-02
0.8293E-02	0.9000E-02	0.9896E-02	0.1097E-01	0.4161E-02	0.2142E-02	0.4231E-04	-0.2103E-02
0.1223E-01	0.1363E-01	0.1517E-01	0.1682E-01	-0.4261E-02	-0.6403E-02	-0.8496E-02	-0.1051E-01
0.1857E-01	0.2037E-01	0.2220E-01	0.2404E-01	-0.1240E-01	-0.1414E-01	-0.1571E-01	-0.1706E-01

-0.1820E-01 -0.1908E-01 -0.1970E-01 -0.2004E-01
-0.2009E-01 -0.1985E-01 -0.1932E-01 -0.1849E-01
-0.1739E-01 -0.1602E-01 -0.1439E-01 -0.1254E-01
-0.1049E-01 -0.8250E-02 -0.5871E-02 -0.3376E-02
-0.8002E-03 0.1817E-02 0.4436E-02 0.7022E-02
0.9538E-02 0.1194E-01 0.1421E-01 0.1630E-01
0.1819E-01 0.1985E-01 0.2125E-01 0.2237E-01
0.2320E-01 0.2373E-01 0.2394E-01 0.2384E-01
0.2342E-01 0.2269E-01 0.2166E-01 0.2035E-01
0.1878E-01 0.1696E-01 0.1492E-01 0.1269E-01
0.1030E-01 0.7775E-02 0.5160E-02 0.2484E-02
-0.2177E-03 -0.2910E-02 -0.5561E-02 -0.8138E-02
-0.1061E-01 -0.1294E-01 -0.1511E-01 -0.1710E-01
-0.1888E-01 -0.2044E-01 -0.2176E-01 -0.2284E-01
-0.2367E-01 -0.2425E-01 -0.2459E-01 -0.2469E-01
-0.2456E-01 -0.2421E-01 -0.2367E-01 -0.2294E-01
-0.2205E-01 -0.2103E-01 -0.1990E-01 -0.1868E-01
-0.1741E-01 -0.1609E-01 -0.1477E-01 -0.1346E-01
-0.1219E-01 -0.1097E-01 -0.9837E-02 -0.8792E-02
-0.7853E-02 -0.7033E-02 -0.6337E-02 -0.5770E-02
-0.5337E-02 -0.5034E-02 -0.4859E-02 -0.4805E-02
-0.4857E-02 -0.5004E-02 -0.5233E-02 -0.5532E-02
-0.5881E-02 -0.6259E-02 -0.6647E-02 -0.7028E-02
-0.7386E-02 -0.7697E-02 -0.7942E-02 -0.8110E-02
-0.8188E-02 -0.8164E-02 -0.8026E-02 -0.7768E-02
-0.7388E-02 -0.6882E-02 -0.6254E-02 -0.5510E-02
-0.4658E-02 -0.3700E-02 -0.2658E-02 -0.1548E-02

Time history of vertical velocity at node NF2:

-0.1641E-03 -0.4084E-03 -0.6091E-03 -0.7889E-03
-0.9206E-03 -0.1090E-02 -0.1398E-02 -0.1781E-02
-0.2076E-02 -0.2326E-02 -0.2593E-02 -0.2875E-02
-0.3185E-02 -0.3402E-02 -0.3474E-02 -0.3511E-02
-0.3494E-02 -0.3411E-02 -0.3234E-02 -0.2898E-02
-0.2468E-02 -0.1990E-02 -0.1439E-02 -0.8021E-03
-0.7785E-04 0.7186E-03 0.1541E-02 0.2370E-02
0.3243E-02 0.4138E-02 0.5045E-02 0.5952E-02
0.6830E-02 0.7707E-02 0.8582E-02 0.9445E-02
0.1029E-01 0.1112E-01 0.1194E-01 0.1275E-01
0.1354E-01 0.1433E-01 0.1510E-01 0.1585E-01
0.1658E-01 0.1729E-01 0.1796E-01 0.1861E-01
0.1922E-01 0.1978E-01 0.2028E-01 0.2074E-01
0.2114E-01 0.2149E-01 0.2178E-01 0.2200E-01
0.2218E-01 0.2230E-01 0.2239E-01 0.2242E-01
0.2242E-01 0.2239E-01 0.2233E-01 0.2226E-01
0.2216E-01 0.2204E-01 0.2189E-01 0.2173E-01
0.2154E-01 0.2132E-01 0.2106E-01 0.2075E-01
0.2041E-01 0.2001E-01 0.1956E-01 0.1905E-01
0.1847E-01 0.1783E-01 0.1715E-01 0.1641E-01
0.1563E-01 0.1481E-01 0.1397E-01 0.1312E-01
0.1229E-01 0.1146E-01 0.1065E-01 0.9891E-02
0.9170E-02 0.8515E-02 0.7905E-02 0.7353E-02
0.6856E-02 0.6408E-02 0.6004E-02 0.5626E-02
0.5265E-02 0.4902E-02 0.4535E-02 0.4141E-02
0.3706E-02 0.3225E-02 0.2675E-02 0.2069E-02
0.1390E-02 0.6418E-03 -0.1730E-03 -0.1052E-02
-0.1978E-02 -0.2947E-02 -0.3937E-02 -0.4948E-02
-0.5948E-02 -0.6937E-02 -0.7889E-02 -0.8801E-02
-0.9660E-02 -0.1046E-01 -0.1120E-01 -0.1188E-01
-0.1250E-01 -0.1306E-01 -0.1358E-01 -0.1405E-01
-0.1451E-01 -0.1495E-01 -0.1540E-01 -0.1585E-01
-0.1633E-01 -0.1683E-01 -0.1737E-01 -0.1795E-01
-0.1856E-01 -0.1922E-01 -0.1991E-01 -0.2062E-01
-0.2135E-01 -0.2208E-01 -0.2279E-01 -0.2349E-01
-0.2415E-01 -0.2476E-01 -0.2532E-01 -0.2582E-01
-0.2624E-01 -0.2659E-01 -0.2687E-01 -0.2707E-01
-0.2721E-01 -0.2729E-01 -0.2732E-01 -0.2731E-01
-0.2727E-01 -0.2722E-01 -0.2715E-01 -0.2710E-01
-0.2705E-01 -0.2703E-01 -0.2704E-01 -0.2708E-01
-0.2715E-01 -0.2726E-01 -0.2740E-01 -0.2758E-01
-0.2778E-01 -0.2800E-01 -0.2824E-01 -0.2849E-01
-0.2876E-01 -0.2902E-01 -0.2929E-01 -0.2956E-01
-0.2982E-01 -0.3008E-01 -0.3034E-01 -0.3061E-01
-0.3087E-01 -0.3114E-01 -0.3143E-01 -0.3172E-01
-0.3203E-01 -0.3236E-01 -0.3271E-01 -0.3307E-01
-0.3345E-01 -0.3385E-01 -0.3426E-01 -0.3468E-01
-0.3510E-01 -0.3552E-01 -0.3594E-01 -0.3635E-01
-0.3674E-01 -0.3712E-01 -0.3746E-01 -0.3779E-01
-0.3808E-01 -0.3834E-01 -0.3856E-01 -0.3876E-01
-0.3891E-01 -0.3904E-01 -0.3912E-01 -0.3917E-01
-0.3919E-01 -0.3917E-01 -0.3910E-01 -0.3900E-01
-0.3885E-01 -0.3866E-01 -0.3842E-01 -0.3812E-01
-0.3777E-01 -0.3735E-01 -0.3688E-01 -0.3634E-01
-0.3574E-01 -0.3508E-01 -0.3436E-01 -0.3358E-01
-0.3275E-01 -0.3188E-01 -0.3097E-01 -0.3003E-01
-0.2906E-01 -0.2809E-01 -0.2712E-01 -0.2616E-01
-0.2522E-01 -0.2430E-01 -0.2342E-01 -0.2258E-01
-0.2177E-01 -0.2101E-01 -0.2030E-01 -0.1962E-01

-0.1899E-01	-0.1839E-01	-0.1783E-01	-0.1729E-01	0.1227E-01	0.1280E-01	0.1335E-01	0.1392E-01
-0.1678E-01	-0.1629E-01	-0.1581E-01	-0.1534E-01	0.1450E-01	0.1510E-01	0.1572E-01	0.1633E-01
-0.1488E-01	-0.1443E-01	-0.1400E-01	-0.1358E-01	0.1695E-01	0.1758E-01	0.1819E-01	0.1880E-01
-0.1317E-01	-0.1280E-01	-0.1245E-01	-0.1214E-01	0.1940E-01	0.1999E-01	0.2056E-01	0.2111E-01
-0.1187E-01	-0.1166E-01	-0.1150E-01	-0.1140E-01	0.2164E-01	0.2213E-01	0.2260E-01	0.2304E-01
-0.1136E-01	-0.1139E-01	-0.1148E-01	-0.1163E-01	0.2343E-01	0.2378E-01	0.2410E-01	0.2436E-01
-0.1185E-01	-0.1211E-01	-0.1241E-01	-0.1275E-01	0.2458E-01	0.2474E-01	0.2486E-01	0.2492E-01
-0.1311E-01	-0.1348E-01	-0.1384E-01	-0.1419E-01	0.2494E-01	0.2490E-01	0.2480E-01	0.2466E-01
-0.1451E-01	-0.1480E-01	-0.1503E-01	-0.1522E-01	0.2447E-01	0.2424E-01	0.2397E-01	0.2365E-01
-0.1535E-01	-0.1541E-01	-0.1542E-01	-0.1536E-01	0.2331E-01	0.2293E-01	0.2252E-01	0.2210E-01
-0.1525E-01	-0.1508E-01	-0.1488E-01	-0.1463E-01	0.2165E-01	0.2119E-01	0.2072E-01	0.2024E-01
-0.1435E-01	-0.1406E-01	-0.1375E-01	-0.1343E-01	0.1977E-01	0.1929E-01	0.1881E-01	0.1834E-01
-0.1311E-01	-0.1280E-01	-0.1250E-01	-0.1220E-01	0.1787E-01	0.1742E-01	0.1698E-01	0.1655E-01
-0.1191E-01	-0.1163E-01	-0.1135E-01	-0.1107E-01	0.1614E-01	0.1574E-01	0.1536E-01	0.1500E-01
-0.1077E-01	-0.1046E-01	-0.1013E-01	-0.9770E-02	0.1466E-01	0.1435E-01	0.1406E-01	0.1379E-01
-0.9373E-02	-0.8934E-02	-0.8451E-02	-0.7922E-02	0.1355E-01	0.1334E-01	0.1316E-01	0.1301E-01
-0.7347E-02	-0.6728E-02	-0.6066E-02	-0.5369E-02	0.1289E-01	0.1280E-01	0.1275E-01	0.1272E-01
-0.4639E-02	-0.3888E-02	-0.3119E-02	-0.2347E-02	0.1273E-01	0.1278E-01	0.1285E-01	0.1295E-01
-0.1576E-02	-0.8189E-03	-0.7907E-04	0.6328E-03	0.1307E-01	0.1322E-01	0.1339E-01	0.1358E-01
0.1315E-02	0.1960E-02	0.2568E-02	0.3137E-02	0.1378E-01	0.1400E-01	0.1422E-01	0.1444E-01
0.3669E-02	0.4167E-02	0.4633E-02	0.5075E-02	0.1466E-01	0.1488E-01	0.1509E-01	0.1529E-01
0.5494E-02	0.5902E-02	0.6301E-02	0.6701E-02	0.1548E-01	0.1565E-01	0.1580E-01	0.1593E-01
0.7102E-02	0.7512E-02	0.7932E-02	0.8368E-02	0.1604E-01	0.1612E-01	0.1618E-01	0.1622E-01
0.8819E-02	0.9286E-02	0.9765E-02	0.1026E-01	0.1623E-01	0.1621E-01	0.1617E-01	0.1610E-01
0.1075E-01	0.1125E-01	0.1175E-01	0.1224E-01	0.1601E-01	0.1588E-01	0.1574E-01	0.1557E-01
0.1272E-01	0.1318E-01	0.1362E-01	0.1404E-01	0.1537E-01	0.1515E-01	0.1491E-01	0.1464E-01
0.1443E-01	0.1480E-01	0.1513E-01	0.1544E-01	0.1435E-01	0.1403E-01	0.1370E-01	0.1334E-01
0.1573E-01	0.1599E-01	0.1623E-01	0.1646E-01	0.1296E-01	0.1256E-01	0.1214E-01	0.1170E-01
0.1667E-01	0.1687E-01	0.1707E-01	0.1727E-01	0.1125E-01	0.1078E-01	0.1030E-01	0.9810E-02
0.1746E-01	0.1765E-01	0.1784E-01	0.1804E-01	0.9310E-02	0.8804E-02	0.8294E-02	0.7783E-02
0.1822E-01	0.1841E-01	0.1858E-01	0.1874E-01	0.7273E-02	0.6767E-02	0.6267E-02	0.5774E-02
0.1888E-01	0.1901E-01	0.1910E-01	0.1916E-01	0.5290E-02	0.4818E-02	0.4359E-02	0.3914E-02
0.1919E-01	0.1919E-01	0.1914E-01	0.1904E-01	0.3483E-02	0.3067E-02	0.2667E-02	0.2280E-02
0.1891E-01	0.1873E-01	0.1851E-01	0.1824E-01	0.1908E-02	0.1548E-02	0.1201E-02	0.8663E-03
0.1794E-01	0.1760E-01	0.1724E-01	0.1684E-01	0.5417E-03	0.2256E-03	-0.8308E-04	-0.3851E-03
0.1642E-01	0.1599E-01	0.1553E-01	0.1507E-01	-0.6820E-03	-0.9754E-03	-0.1267E-02	-0.1556E-02
0.1461E-01	0.1414E-01	0.1368E-01	0.1323E-01	-0.1844E-02	-0.2131E-02	-0.2419E-02	-0.2707E-02
0.1278E-01	0.1235E-01	0.1193E-01	0.1153E-01	-0.2996E-02	-0.3284E-02	-0.3573E-02	-0.3861E-02
0.1114E-01	0.1078E-01	0.1045E-01	0.1014E-01	-0.4147E-02	-0.4432E-02	-0.4714E-02	-0.4994E-02
0.9853E-02	0.9599E-02	0.9377E-02	0.9188E-02	-0.5268E-02	-0.5538E-02	-0.5801E-02	-0.6056E-02
0.9036E-02	0.8920E-02	0.8844E-02	0.8810E-02	-0.6302E-02	-0.6538E-02	-0.6763E-02	-0.6974E-02
0.8817E-02	0.8869E-02	0.8965E-02	0.9106E-02	-0.7170E-02	-0.7349E-02	-0.7511E-02	-0.7653E-02
0.9293E-02	0.9524E-02	0.9799E-02	0.1012E-01	-0.7774E-02	-0.7871E-02	-0.7943E-02	-0.7988E-02
0.1047E-01	0.1087E-01	0.1131E-01	0.1177E-01	-0.8005E-02	-0.7991E-02	-0.7946E-02	-0.7868E-02

-0.7755E-02 -0.7606E-02 -0.7421E-02 -0.7199E-02 -0.1685E-02 -0.1841E-02 -0.2000E-02 -0.2162E-02
-0.6939E-02 -0.6642E-02 -0.6307E-02 -0.5935E-02 -0.2326E-02 -0.2491E-02 -0.2655E-02 -0.2817E-02
-0.5527E-02 -0.5085E-02 -0.4609E-02 -0.4101E-02 -0.2977E-02 -0.3131E-02 -0.3280E-02 -0.3421E-02
-0.3564E-02 -0.2999E-02 -0.2409E-02 -0.1798E-02 -0.3553E-02 -0.3674E-02 -0.3784E-02 -0.3881E-02
-0.1167E-02 -0.5205E-03 0.1389E-03 0.8079E-03 -0.3963E-02 -0.4030E-02 -0.4081E-02 -0.4114E-02
0.1483E-02 0.2160E-02 0.2836E-02 0.3508E-02 -0.4130E-02 -0.4129E-02 -0.4109E-02 -0.4070E-02
0.4171E-02 0.4823E-02 0.5458E-02 0.6075E-02 -0.4013E-02 -0.3939E-02 -0.3847E-02 -0.3737E-02
0.6669E-02 0.7238E-02 0.7778E-02 0.8286E-02 -0.3612E-02 -0.3472E-02 -0.3318E-02 -0.3152E-02
0.8759E-02 0.9195E-02 0.9590E-02 0.9943E-02 -0.2975E-02 -0.2789E-02 -0.2595E-02 -0.2395E-02
0.1025E-01 0.1051E-01 0.1073E-01 0.1089E-01 -0.2192E-02 -0.1987E-02 -0.1783E-02 -0.1581E-02
0.1101E-01 0.1107E-01 0.1108E-01 0.1104E-01 -0.1384E-02 -0.1195E-02 -0.1015E-02 -0.8461E-03
0.1095E-01 0.1081E-01 0.1062E-01 0.1038E-01 -0.6914E-03 -0.5523E-03 -0.4311E-03 -0.3300E-03
0.1009E-01 0.9764E-02 0.9392E-02 0.8982E-02 -0.2505E-03 -0.1943E-03 -0.1626E-03 -0.1576E-03
0.8535E-02 0.8056E-02 0.7547E-02 0.7012E-02 -0.1799E-03 -0.2300E-03 -0.3089E-03 -0.4172E-03
0.6455E-02 0.5879E-02 0.5290E-02 0.4691E-02 -0.5545E-03 -0.7208E-03 -0.9161E-03 -0.1140E-02
0.4086E-02 0.3480E-02 0.2877E-02 0.2280E-02 -0.1390E-02 -0.1667E-02 -0.1969E-02 -0.2294E-02
0.1694E-02 0.1123E-02 0.5706E-03 0.4023E-04 -0.2640E-02 -0.3005E-02 -0.3386E-02 -0.3783E-02
-0.4647E-03 -0.9408E-03 -0.1385E-02 -0.1795E-02 -0.4190E-02 -0.4608E-02 -0.5031E-02 -0.5457E-02
-0.2167E-02 -0.2500E-02 -0.2792E-02 -0.3041E-02 -0.5883E-02 -0.6306E-02 -0.6723E-02 -0.7130E-02
-0.3246E-02 -0.3406E-02 -0.3520E-02 -0.3587E-02 -0.7524E-02 -0.7902E-02 -0.8260E-02 -0.8596E-02
-0.3609E-02 -0.3585E-02 -0.3515E-02 -0.3401E-02 -0.8907E-02 -0.9190E-02 -0.9441E-02 -0.9658E-02
-0.3245E-02 -0.3048E-02 -0.2811E-02 -0.2538E-02 -0.9838E-02 -0.9980E-02 -0.1008E-01 -0.1014E-01
-0.2230E-02 -0.1891E-02 -0.1522E-02 -0.1128E-02 -0.1015E-01 -0.1012E-01 -0.1003E-01 -0.9903E-02
-0.7119E-03 -0.2763E-03 0.1752E-03 0.6390E-03 -0.9723E-02 -0.9493E-02 -0.9214E-02 -0.8886E-02
0.1112E-02 0.1589E-02 0.2069E-02 0.2547E-02 -0.8508E-02 -0.8083E-02 -0.7611E-02 -0.7095E-02
0.3020E-02 0.3484E-02 0.3938E-02 0.4378E-02 -0.6535E-02 -0.5935E-02 -0.5297E-02 -0.4624E-02
0.4801E-02 0.5203E-02 0.5584E-02 0.5941E-02 -0.3920E-02 -0.3187E-02 -0.2428E-02 -0.1649E-02
0.6272E-02 0.6575E-02 0.6849E-02 0.7092E-02 -0.8523E-03 -0.4260E-04 0.7756E-03 0.1598E-02
0.7304E-02 0.7484E-02 0.7631E-02 0.7746E-02 0.2420E-02 0.3238E-02 0.4047E-02 0.4843E-02
0.7828E-02 0.7878E-02 0.7895E-02 0.7882E-02 0.5622E-02 0.6379E-02 0.7110E-02 0.7813E-02
0.7838E-02 0.7766E-02 0.7666E-02 0.7541E-02 0.8482E-02 0.9115E-02 0.9709E-02 0.1026E-01
0.7391E-02 0.7219E-02 0.7027E-02 0.6816E-02 0.1077E-01 0.1123E-01 0.1163E-01 0.1199E-01
0.6589E-02 0.6348E-02 0.6095E-02 0.5833E-02 0.1230E-01 0.1255E-01 0.1275E-01 0.1289E-01
0.5564E-02 0.5289E-02 0.5010E-02 0.4730E-02 0.1298E-01 0.1301E-01 0.1299E-01 0.1292E-01
0.4451E-02 0.4174E-02 0.3901E-02 0.3633E-02 0.1280E-01 0.1263E-01 0.1241E-01 0.1214E-01
0.3373E-02 0.3119E-02 0.2874E-02 0.2639E-02 0.1183E-01 0.1148E-01 0.1110E-01 0.1068E-01
0.2414E-02 0.2200E-02 0.1996E-02 0.1803E-02 0.1023E-01 0.9749E-02 0.9248E-02 0.8727E-02
0.1622E-02 0.1450E-02 0.1290E-02 0.1140E-02 0.8190E-02 0.7641E-02 0.7082E-02 0.6517E-02
0.9986E-03 0.8667E-03 0.7431E-03 0.6269E-03 0.5951E-02 0.5387E-02 0.4827E-02 0.4274E-02
0.5173E-03 0.4133E-03 0.3139E-03 0.2186E-03 0.3733E-02 0.3204E-02 0.2692E-02 0.2197E-02
0.1260E-03 0.3507E-04 -0.5532E-04 -0.1462E-03 0.1722E-02 0.1269E-02 0.8394E-03 0.4335E-03
-0.2389E-03 -0.3336E-03 -0.4308E-03 -0.5316E-03 0.5261E-04 -0.3023E-03 -0.6308E-03 -0.9328E-03
-0.6373E-03 -0.7482E-03 -0.8646E-03 -0.9868E-03 -0.1208E-02 -0.1457E-02 -0.1680E-02 -0.1877E-02
-0.1115E-02 -0.1249E-02 -0.1389E-02 -0.1534E-02 -0.2049E-02 -0.2198E-02 -0.2323E-02 -0.2427E-02

-0.2510E-02 -0.2575E-02 -0.2622E-02 -0.2653E-02
-0.2669E-02 -0.2672E-02 -0.2663E-02 -0.2644E-02
-0.2616E-02 -0.2581E-02 -0.2539E-02 -0.2491E-02
-0.2439E-02 -0.2383E-02 -0.2326E-02 -0.2266E-02
-0.2205E-02 -0.2143E-02 -0.2081E-02 -0.2019E-02
-0.1956E-02 -0.1892E-02 -0.1828E-02 -0.1763E-02
-0.1697E-02 -0.1629E-02 -0.1558E-02 -0.1484E-02
-0.1407E-02 -0.1325E-02 -0.1238E-02 -0.1144E-02
-0.1045E-02 -0.9379E-03 -0.8227E-03 -0.6989E-03
-0.5664E-03 -0.4247E-03 -0.2736E-03 -0.1126E-03
0.5840E-04 0.2390E-03 0.4290E-03 0.6281E-03
0.8361E-03 0.1052E-02 0.1276E-02 0.1506E-02
0.1742E-02 0.1982E-02 0.2226E-02 0.2471E-02
0.2717E-02 0.2962E-02 0.3205E-02 0.3444E-02
0.3678E-02 0.3904E-02 0.4120E-02 0.4326E-02

Time history of vertical velocity at node NF3:

-0.1679E-03 -0.4159E-03 -0.6144E-03 -0.7833E-03
-0.8926E-03 -0.1029E-02 -0.1297E-02 -0.1623E-02
-0.1837E-02 -0.1977E-02 -0.2106E-02 -0.2215E-02
-0.2309E-02 -0.2270E-02 -0.2048E-02 -0.1748E-02
-0.1359E-02 -0.8735E-03 -0.2853E-03 0.4292E-03
0.1214E-02 0.2024E-02 0.2855E-02 0.3686E-02
0.4494E-02 0.5248E-02 0.5932E-02 0.6529E-02
0.7011E-02 0.7372E-02 0.7596E-02 0.7684E-02
0.7650E-02 0.7463E-02 0.7119E-02 0.6623E-02
0.5983E-02 0.5208E-02 0.4292E-02 0.3228E-02
0.2022E-02 0.7113E-03 -0.6928E-03 -0.2156E-02
-0.3655E-02 -0.5165E-02 -0.6641E-02 -0.8055E-02
-0.9383E-02 -0.1060E-01 -0.1169E-01 -0.1262E-01
-0.1336E-01 -0.1389E-01 -0.1421E-01 -0.1430E-01
-0.1413E-01 -0.1370E-01 -0.1297E-01 -0.1198E-01
-0.1072E-01 -0.9198E-02 -0.7431E-02 -0.5421E-02
-0.3233E-02 -0.8991E-03 0.1531E-02 0.4029E-02
0.6525E-02 0.8965E-02 0.1129E-01 0.1343E-01
0.1537E-01 0.1706E-01 0.1846E-01 0.1956E-01
0.2034E-01 0.2080E-01 0.2093E-01 0.2074E-01
0.2024E-01 0.1943E-01 0.1834E-01 0.1700E-01
0.1544E-01 0.1367E-01 0.1174E-01 0.9685E-02
0.7531E-02 0.5325E-02 0.3086E-02 0.8510E-03
-0.1349E-02 -0.3488E-02 -0.5544E-02 -0.7503E-02
-0.9342E-02 -0.1105E-01 -0.1262E-01 -0.1403E-01
-0.1529E-01 -0.1637E-01 -0.1729E-01 -0.1803E-01
-0.1858E-01 -0.1893E-01 -0.1909E-01 -0.1905E-01
-0.1881E-01 -0.1835E-01 -0.1768E-01 -0.1680E-01
-0.1572E-01 -0.1445E-01 -0.1300E-01 -0.1139E-01
-0.9639E-02 -0.7763E-02 -0.5788E-02 -0.3744E-02
-0.1657E-02 0.4443E-03 0.2532E-02 0.4582E-02
0.6567E-02 0.8469E-02 0.1027E-01 0.1194E-01
0.1349E-01 0.1489E-01 0.1614E-01 0.1724E-01
0.1818E-01 0.1896E-01 0.1959E-01 0.2008E-01
0.2042E-01 0.2063E-01 0.2071E-01 0.2068E-01
0.2054E-01 0.2031E-01 0.1998E-01 0.1958E-01
0.1910E-01 0.1855E-01 0.1793E-01 0.1726E-01
0.1652E-01 0.1573E-01 0.1489E-01 0.1399E-01
0.1305E-01 0.1208E-01 0.1106E-01 0.1001E-01
0.8935E-02 0.7835E-02 0.6711E-02 0.5572E-02
0.4421E-02 0.3256E-02 0.2077E-02 0.8850E-03
-0.3260E-03 -0.1564E-02 -0.2828E-02 -0.4129E-02
-0.5476E-02 -0.6872E-02 -0.8319E-02 -0.9817E-02
-0.1137E-01 -0.1297E-01 -0.1462E-01 -0.1629E-01
-0.1799E-01 -0.1971E-01 -0.2144E-01 -0.2317E-01
-0.2488E-01 -0.2655E-01 -0.2819E-01 -0.2977E-01
-0.3128E-01 -0.3270E-01 -0.3402E-01 -0.3523E-01
-0.3630E-01 -0.3723E-01 -0.3801E-01 -0.3864E-01
-0.3909E-01 -0.3937E-01 -0.3947E-01 -0.3940E-01
-0.3914E-01 -0.3871E-01 -0.3811E-01 -0.3733E-01
-0.3640E-01 -0.3530E-01 -0.3405E-01 -0.3265E-01
-0.3110E-01 -0.2941E-01 -0.2759E-01 -0.2563E-01
-0.2355E-01 -0.2135E-01 -0.1903E-01 -0.1661E-01
-0.1410E-01 -0.1150E-01 -0.8840E-02 -0.6139E-02
-0.3414E-02 -0.6896E-03 0.2012E-02 0.4669E-02
0.7254E-02 0.9745E-02 0.1212E-01 0.1437E-01
0.1647E-01 0.1841E-01 0.2017E-01 0.2174E-01
0.2313E-01 0.2433E-01 0.2535E-01 0.2619E-01
0.2686E-01 0.2737E-01 0.2775E-01 0.2801E-01
0.2816E-01 0.2822E-01 0.2822E-01 0.2818E-01
0.2813E-01 0.2807E-01 0.2803E-01 0.2804E-01
0.2810E-01 0.2823E-01 0.2845E-01 0.2877E-01
0.2919E-01 0.2973E-01 0.3039E-01 0.3116E-01
0.3204E-01 0.3303E-01 0.3412E-01 0.3531E-01
0.3659E-01 0.3793E-01 0.3934E-01 0.4079E-01
0.4227E-01 0.4375E-01 0.4522E-01 0.4664E-01
0.4802E-01 0.4931E-01 0.5050E-01 0.5156E-01
0.5248E-01 0.5321E-01 0.5375E-01 0.5406E-01
0.5414E-01 0.5397E-01 0.5353E-01 0.5281E-01
0.5181E-01 0.5053E-01 0.4897E-01 0.4713E-01
0.4503E-01 0.4268E-01 0.4011E-01 0.3733E-01

0.3435E-01	0.3121E-01	0.2793E-01	0.2454E-01	0.4682E-01	0.4762E-01	0.4831E-01	0.4886E-01
0.2108E-01	0.1755E-01	0.1400E-01	0.1045E-01	0.4927E-01	0.4950E-01	0.4955E-01	0.4940E-01
0.6939E-02	0.3487E-02	0.1295E-03	-0.3103E-02	0.4904E-01	0.4846E-01	0.4765E-01	0.4662E-01
-0.6182E-02	-0.9080E-02	-0.1178E-01	-0.1425E-01	0.4538E-01	0.4393E-01	0.4227E-01	0.4043E-01
-0.1647E-01	-0.1844E-01	-0.2013E-01	-0.2154E-01	0.3841E-01	0.3624E-01	0.3395E-01	0.3154E-01
-0.2268E-01	-0.2354E-01	-0.2411E-01	-0.2442E-01	0.2905E-01	0.2651E-01	0.2394E-01	0.2137E-01
-0.2447E-01	-0.2428E-01	-0.2387E-01	-0.2325E-01	0.1883E-01	0.1636E-01	0.1398E-01	0.1172E-01
-0.2245E-01	-0.2151E-01	-0.2044E-01	-0.1927E-01	0.9611E-02	0.7675E-02	0.5927E-02	0.4383E-02
-0.1805E-01	-0.1680E-01	-0.1556E-01	-0.1437E-01	0.3064E-02	0.1971E-02	0.1110E-02	0.4923E-03
-0.1324E-01	-0.1222E-01	-0.1132E-01	-0.1058E-01	0.1179E-03	-0.2092E-04	0.6797E-04	0.3734E-03
-0.1002E-01	-0.9658E-02	-0.9505E-02	-0.9575E-02	0.8767E-03	0.1562E-02	0.2410E-02	0.3398E-02
-0.9871E-02	-0.1040E-01	-0.1115E-01	-0.1212E-01	0.4506E-02	0.5714E-02	0.6990E-02	0.8313E-02
-0.1329E-01	-0.1464E-01	-0.1615E-01	-0.1781E-01	0.9654E-02	0.1099E-01	0.1230E-01	0.1357E-01
-0.1958E-01	-0.2143E-01	-0.2334E-01	-0.2528E-01	0.1478E-01	0.1590E-01	0.1692E-01	0.1784E-01
-0.2722E-01	-0.2913E-01	-0.3100E-01	-0.3278E-01	0.1864E-01	0.1931E-01	0.1986E-01	0.2027E-01
-0.3445E-01	-0.3600E-01	-0.3741E-01	-0.3867E-01	0.2056E-01	0.2072E-01	0.2076E-01	0.2070E-01
-0.3977E-01	-0.4071E-01	-0.4147E-01	-0.4206E-01	0.2054E-01	0.2029E-01	0.1997E-01	0.1958E-01
-0.4249E-01	-0.4276E-01	-0.4288E-01	-0.4285E-01	0.1916E-01	0.1872E-01	0.1825E-01	0.1780E-01
-0.4270E-01	-0.4245E-01	-0.4211E-01	-0.4168E-01	0.1737E-01	0.1697E-01	0.1661E-01	0.1631E-01
-0.4122E-01	-0.4071E-01	-0.4021E-01	-0.3971E-01	0.1608E-01	0.1592E-01	0.1583E-01	0.1583E-01
-0.3925E-01	-0.3884E-01	-0.3851E-01	-0.3826E-01	0.1590E-01	0.1604E-01	0.1625E-01	0.1653E-01
-0.3811E-01	-0.3810E-01	-0.3821E-01	-0.3846E-01	0.1687E-01	0.1725E-01	0.1767E-01	0.1810E-01
-0.3886E-01	-0.3940E-01	-0.4008E-01	-0.4091E-01	0.1853E-01	0.1895E-01	0.1933E-01	0.1964E-01
-0.4187E-01	-0.4295E-01	-0.4414E-01	-0.4540E-01	0.1988E-01	0.2002E-01	0.2006E-01	0.1997E-01
-0.4672E-01	-0.4808E-01	-0.4945E-01	-0.5081E-01	0.1973E-01	0.1932E-01	0.1874E-01	0.1798E-01
-0.5211E-01	-0.5333E-01	-0.5443E-01	-0.5538E-01	0.1701E-01	0.1585E-01	0.1449E-01	0.1292E-01
-0.5615E-01	-0.5671E-01	-0.5703E-01	-0.5707E-01	0.1115E-01	0.9190E-02	0.7055E-02	0.4750E-02
-0.5682E-01	-0.5626E-01	-0.5536E-01	-0.5412E-01	0.2294E-02	-0.2887E-03	-0.2980E-02	-0.5756E-02
-0.5253E-01	-0.5059E-01	-0.4829E-01	-0.4565E-01	-0.8588E-02	-0.1145E-01	-0.1432E-01	-0.1716E-01
-0.4268E-01	-0.3940E-01	-0.3583E-01	-0.3199E-01	-0.1994E-01	-0.2264E-01	-0.2523E-01	-0.2768E-01
-0.2791E-01	-0.2362E-01	-0.1916E-01	-0.1456E-01	-0.2997E-01	-0.3207E-01	-0.3395E-01	-0.3561E-01
-0.9870E-02	-0.5123E-02	-0.3668E-03	0.4365E-02	-0.3702E-01	-0.3819E-01	-0.3909E-01	-0.3972E-01
0.9037E-02	0.1360E-01	0.1802E-01	0.2226E-01	-0.4009E-01	-0.4019E-01	-0.4003E-01	-0.3964E-01
0.2628E-01	0.3005E-01	0.3356E-01	0.3677E-01	-0.3901E-01	-0.3817E-01	-0.3714E-01	-0.3594E-01
0.3968E-01	0.4225E-01	0.4449E-01	0.4638E-01	-0.3459E-01	-0.3314E-01	-0.3159E-01	-0.2999E-01
0.4793E-01	0.4914E-01	0.5002E-01	0.5058E-01	-0.2836E-01	-0.2675E-01	-0.2517E-01	-0.2365E-01
0.5084E-01	0.5083E-01	0.5058E-01	0.5010E-01	-0.2224E-01	-0.2095E-01	-0.1981E-01	-0.1884E-01
0.4944E-01	0.4863E-01	0.4769E-01	0.4667E-01	-0.1807E-01	-0.1751E-01	-0.1717E-01	-0.1706E-01
0.4559E-01	0.4448E-01	0.4338E-01	0.4231E-01	-0.1718E-01	-0.1755E-01	-0.1815E-01	-0.1898E-01
0.4131E-01	0.4039E-01	0.3958E-01	0.3889E-01	-0.2003E-01	-0.2130E-01	-0.2275E-01	-0.2438E-01
0.3834E-01	0.3794E-01	0.3770E-01	0.3762E-01	-0.2616E-01	-0.2806E-01	-0.3006E-01	-0.3214E-01
0.3770E-01	0.3794E-01	0.3834E-01	0.3888E-01	-0.3425E-01	-0.3638E-01	-0.3850E-01	-0.4056E-01
0.3954E-01	0.4030E-01	0.4116E-01	0.4207E-01	-0.4256E-01	-0.4446E-01	-0.4622E-01	-0.4783E-01
0.4304E-01	0.4402E-01	0.4500E-01	0.4594E-01	-0.4927E-01	-0.5053E-01	-0.5158E-01	-0.5240E-01

-0.5300E-01	-0.5337E-01	-0.5352E-01	-0.5344E-01	0.2507E-01	0.2309E-01	0.2109E-01	0.1911E-01
-0.5313E-01	-0.5262E-01	-0.5192E-01	-0.5104E-01	0.1717E-01	0.1532E-01	0.1356E-01	0.1194E-01
-0.5000E-01	-0.4883E-01	-0.4754E-01	-0.4616E-01	0.1047E-01	0.9177E-02	0.8080E-02	0.7192E-02
-0.4473E-01	-0.4326E-01	-0.4178E-01	-0.4032E-01	0.6522E-02	0.6082E-02	0.5875E-02	0.5900E-02
-0.3890E-01	-0.3755E-01	-0.3628E-01	-0.3511E-01	0.6155E-02	0.6633E-02	0.7322E-02	0.8208E-02
-0.3408E-01	-0.3319E-01	-0.3245E-01	-0.3186E-01	0.9272E-02	0.1049E-01	0.1185E-01	0.1332E-01
-0.3145E-01	-0.3119E-01	-0.3110E-01	-0.3116E-01	0.1487E-01	0.1647E-01	0.1810E-01	0.1973E-01
-0.3137E-01	-0.3171E-01	-0.3218E-01	-0.3274E-01	0.2132E-01	0.2286E-01	0.2431E-01	0.2565E-01
-0.3338E-01	-0.3408E-01	-0.3482E-01	-0.3557E-01	0.2685E-01	0.2790E-01	0.2877E-01	0.2945E-01
-0.3630E-01	-0.3699E-01	-0.3762E-01	-0.3816E-01	0.2993E-01	0.3020E-01	0.3026E-01	0.3011E-01
-0.3859E-01	-0.3888E-01	-0.3902E-01	-0.3899E-01	0.2975E-01	0.2918E-01	0.2843E-01	0.2750E-01
-0.3878E-01	-0.3838E-01	-0.3777E-01	-0.3696E-01	0.2641E-01	0.2519E-01	0.2385E-01	0.2242E-01
-0.3595E-01	-0.3474E-01	-0.3333E-01	-0.3174E-01	0.2092E-01	0.1939E-01	0.1785E-01	0.1634E-01
-0.2998E-01	-0.2807E-01	-0.2603E-01	-0.2387E-01	0.1489E-01	0.1352E-01	0.1225E-01	0.1113E-01
-0.2163E-01	-0.1932E-01	-0.1699E-01	-0.1464E-01	0.1017E-01	0.9384E-02	0.8800E-02	0.8430E-02
-0.1231E-01	-0.1003E-01	-0.7827E-02	-0.5725E-02	0.8288E-02	0.8378E-02	0.8705E-02	0.9271E-02
-0.3750E-02	-0.1925E-02	-0.2681E-03	0.1206E-02	0.1007E-01	0.1110E-01	0.1233E-01	0.1376E-01
0.2479E-02	0.3538E-02	0.4374E-02	0.4985E-02	0.1537E-01	0.1713E-01	0.1903E-01	0.2103E-01
0.5371E-02	0.5531E-02	0.5474E-02	0.5208E-02	0.2309E-01	0.2519E-01	0.2730E-01	0.2938E-01
0.4747E-02	0.4108E-02	0.3310E-02	0.2372E-02	0.3140E-01	0.3334E-01	0.3515E-01	0.3682E-01
0.1320E-02	0.1748E-03	-0.1033E-02	-0.2273E-02	0.3830E-01	0.3958E-01	0.4063E-01	0.4144E-01
-0.3518E-02	-0.4739E-02	-0.5905E-02	-0.6992E-02	0.4199E-01	0.4227E-01	0.4226E-01	0.4198E-01
-0.7973E-02	-0.8821E-02	-0.9518E-02	-0.1004E-01	0.4141E-01	0.4056E-01	0.3945E-01	0.3807E-01
-0.1038E-01	-0.1052E-01	-0.1044E-01	-0.1015E-01	0.3645E-01	0.3460E-01	0.3255E-01	0.3032E-01
-0.9649E-02	-0.8931E-02	-0.8003E-02	-0.6875E-02	0.2793E-01	0.2542E-01	0.2281E-01	0.2014E-01
-0.5564E-02	-0.4084E-02	-0.2455E-02	-0.6953E-03	0.1743E-01	0.1471E-01	0.1202E-01	0.9382E-02
0.1169E-02	0.3112E-02	0.5109E-02	0.7131E-02	0.6820E-02	0.4362E-02	0.2034E-02	-0.1485E-03
0.9149E-02	0.1114E-01	0.1306E-01	0.1491E-01	-0.2168E-02	-0.4006E-02	-0.5653E-02	-0.7102E-02
0.1664E-01	0.1824E-01	0.1969E-01	0.2097E-01	-0.8350E-02	-0.9395E-02	-0.1024E-01	-0.1088E-01
0.2207E-01	0.2298E-01	0.2369E-01	0.2420E-01	-0.1135E-01	-0.1163E-01	-0.1175E-01	-0.1172E-01
0.2451E-01	0.2462E-01	0.2454E-01	0.2428E-01	-0.1157E-01	-0.1131E-01	-0.1096E-01	-0.1054E-01
0.2385E-01	0.2327E-01	0.2257E-01	0.2176E-01	-0.1008E-01	-0.9584E-02	-0.9085E-02	-0.8596E-02
0.2086E-01	0.1990E-01	0.1891E-01	0.1792E-01	-0.8132E-02	-0.7713E-02	-0.7349E-02	-0.7054E-02
0.1694E-01	0.1600E-01	0.1514E-01	0.1437E-01	-0.6837E-02	-0.6700E-02	-0.6646E-02	-0.6678E-02
0.1371E-01	0.1319E-01	0.1282E-01	0.1261E-01	-0.6792E-02	-0.6979E-02	-0.7234E-02	-0.7547E-02
0.1257E-01	0.1272E-01	0.1305E-01	0.1356E-01	-0.7905E-02	-0.8293E-02	-0.8693E-02	-0.9089E-02
0.1426E-01	0.1513E-01	0.1616E-01	0.1735E-01	-0.9465E-02	-0.9800E-02	-0.1007E-01	-0.1027E-01
0.1867E-01	0.2010E-01	0.2163E-01	0.2323E-01	-0.1037E-01	-0.1036E-01	-0.1023E-01	-0.9961E-02
0.2487E-01	0.2653E-01	0.2818E-01	0.2979E-01	-0.9543E-02	-0.8970E-02	-0.8237E-02	-0.7342E-02
0.3134E-01	0.3280E-01	0.3414E-01	0.3534E-01	-0.6291E-02	-0.5087E-02	-0.3738E-02	-0.2259E-02
0.3637E-01	0.3723E-01	0.3789E-01	0.3833E-01	-0.6621E-03	0.1034E-02	0.2805E-02	0.4628E-02
0.3855E-01	0.3855E-01	0.3831E-01	0.3784E-01	0.6482E-02	0.8337E-02	0.1016E-01	0.1193E-01
0.3714E-01	0.3622E-01	0.3509E-01	0.3378E-01	0.1361E-01	0.1517E-01	0.1659E-01	0.1783E-01
0.3229E-01	0.3065E-01	0.2888E-01	0.2701E-01	0.1887E-01	0.1968E-01	0.2023E-01	0.2051E-01

0.2050E-01 0.2019E-01 0.1957E-01 0.1864E-01
0.1738E-01 0.1581E-01 0.1393E-01 0.1176E-01
0.9302E-02 0.6589E-02 0.3640E-02 0.4851E-03

Time history of vertical acceleration at node NF1:

0.1212E+00 0.6047E-01 0.9363E-01 0.4385E-01
0.5486E-01 0.7613E-01 0.1829E+00 0.1463E+00
0.1026E+00 0.1025E+00 0.1214E+00 0.1185E+00
0.1545E+00 0.1791E-01 -0.5108E-02 -0.1711E-01
-0.6068E-01 -0.8369E-01 -0.1562E+00 -0.2550E+00
-0.2439E+00 -0.2808E+00 -0.2941E+00 -0.3404E+00
-0.3513E+00 -0.3730E+00 -0.3135E+00 -0.3008E+00
-0.2940E+00 -0.2405E+00 -0.2202E+00 -0.1400E+00
-0.6952E-01 -0.3623E-01 0.3656E-01 0.8484E-01
0.1680E+00 0.2213E+00 0.2903E+00 0.3116E+00
0.3673E+00 0.4136E+00 0.4269E+00 0.4635E+00
0.4396E+00 0.4426E+00 0.4343E+00 0.4177E+00
0.3877E+00 0.3577E+00 0.3139E+00 0.2837E+00
0.2484E+00 0.2063E+00 0.1616E+00 0.1210E+00
0.7796E-01 0.3752E-01 -0.1783E-03 -0.5120E-01
-0.8590E-01 -0.1314E+00 -0.1668E+00 -0.2039E+00
-0.2390E+00 -0.2680E+00 -0.2945E+00 -0.3127E+00
-0.3283E+00 -0.3345E+00 -0.3372E+00 -0.3317E+00
-0.3206E+00 -0.3059E+00 -0.2872E+00 -0.2671E+00
-0.2434E+00 -0.2186E+00 -0.1916E+00 -0.1652E+00
-0.1378E+00 -0.1109E+00 -0.8638E-01 -0.6282E-01
-0.4429E-01 -0.2641E-01 -0.1594E-01 -0.6704E-02
-0.5365E-02 -0.6684E-02 -0.1059E-01 -0.2247E-01
-0.3317E-01 -0.5192E-01 -0.6727E-01 -0.8740E-01
-0.1041E+00 -0.1232E+00 -0.1409E+00 -0.1551E+00
-0.1679E+00 -0.1801E+00 -0.1841E+00 -0.1976E+00
-0.1944E+00 -0.2049E+00 -0.1982E+00 -0.2054E+00
-0.1993E+00 -0.2034E+00 -0.1994E+00 -0.1979E+00
-0.1967E+00 -0.1900E+00 -0.1885E+00 -0.1765E+00
-0.1715E+00 -0.1525E+00 -0.1425E+00 -0.1146E+00
-0.9999E-01 -0.6258E-01 -0.3837E-01 0.5553E-02
0.3946E-01 0.8780E-01 0.1309E+00 0.1774E+00
0.2282E+00 0.2710E+00 0.3248E+00 0.3627E+00
0.4118E+00 0.4438E+00 0.4822E+00 0.5054E+00
0.5303E+00 0.5421E+00 0.5513E+00 0.5507E+00
0.5460E+00 0.5326E+00 0.5141E+00 0.4888E+00
0.4595E+00 0.4274E+00 0.3925E+00 0.3558E+00
0.3183E+00 0.2810E+00 0.2460E+00 0.2104E+00
0.1782E+00 0.1467E+00 0.1187E+00 0.9339E-01
0.6942E-01 0.4899E-01 0.2914E-01 0.1271E-01
-0.4393E-02 -0.1763E-01 -0.3084E-01 -0.3924E-01
-0.4821E-01 -0.5366E-01 -0.5837E-01 -0.6296E-01
-0.6172E-01 -0.6247E-01 -0.6051E-01 -0.5728E-01
-0.5327E-01 -0.4583E-01 -0.4128E-01 -0.3369E-01
-0.2557E-01 -0.1595E-01 -0.5433E-02 0.6778E-02
0.1806E-01 0.3265E-01 0.4233E-01 0.5620E-01
0.6604E-01 0.7807E-01 0.8366E-01 0.8827E-01
0.9223E-01 0.9161E-01 0.8857E-01 0.7954E-01
0.7007E-01 0.5780E-01 0.4205E-01 0.2508E-01
0.5134E-02 -0.1605E-01 -0.3852E-01 -0.6133E-01
-0.8549E-01 -0.1106E+00 -0.1333E+00 -0.1595E+00
-0.1829E+00 -0.2075E+00 -0.2292E+00 -0.2546E+00
-0.2734E+00 -0.2984E+00 -0.3138E+00 -0.3339E+00
-0.3479E+00 -0.3618E+00 -0.3697E+00 -0.3750E+00
-0.3773E+00 -0.3740E+00 -0.3665E+00 -0.3525E+00
-0.3378E+00 -0.3139E+00 -0.2895E+00 -0.2572E+00
-0.2249E+00 -0.1866E+00 -0.1458E+00 -0.1019E+00
-0.5982E-01 -0.1284E-01 0.2904E-01 0.7672E-01
0.1155E+00 0.1560E+00 0.1920E+00 0.2250E+00
0.2540E+00 0.2760E+00 0.2937E+00 0.3069E+00
0.3166E+00 0.3173E+00 0.3162E+00 0.3063E+00
0.2952E+00 0.2763E+00 0.2596E+00 0.2340E+00
0.2101E+00 0.1821E+00 0.1548E+00 0.1248E+00
0.9202E-01 0.6121E-01 0.2973E-01 0.2089E-02
-0.3021E-01 -0.5741E-01 -0.8461E-01 -0.1116E+00
-0.1347E+00 -0.1571E+00 -0.1800E+00 -0.1973E+00
-0.2122E+00 -0.2282E+00 -0.2382E+00 -0.2446E+00
-0.2495E+00 -0.2512E+00 -0.2472E+00 -0.2419E+00
-0.2343E+00 -0.2194E+00 -0.2059E+00 -0.1850E+00
-0.1649E+00 -0.1439E+00 -0.1180E+00 -0.9221E-01
-0.6664E-01 -0.3830E-01 -0.9519E-02 0.1711E-01
0.4019E-01 0.6159E-01 0.8021E-01 0.9892E-01
0.1110E+00 0.1229E+00 0.1283E+00 0.1315E+00
0.1331E+00 0.1272E+00 0.1193E+00 0.1046E+00
0.8882E-01 0.6627E-01 0.4100E-01 0.1649E-01
-0.1104E-01 -0.4041E-01 -0.6759E-01 -0.9807E-01
-0.1237E+00 -0.1493E+00 -0.1703E+00 -0.1886E+00
-0.2082E+00 -0.2176E+00 -0.2258E+00 -0.2290E+00
-0.2294E+00 -0.2222E+00 -0.2132E+00 -0.1965E+00
-0.1797E+00 -0.1570E+00 -0.1311E+00 -0.1021E+00
-0.6823E-01 -0.3430E-01 0.4151E-02 0.4291E-01
0.8208E-01 0.1217E+00 0.1592E+00 0.1966E+00
0.2307E+00 0.2610E+00 0.2893E+00 0.3123E+00

0.3304E+00	0.3456E+00	0.3516E+00	0.3531E+00	0.1121E+00	0.1317E+00	0.1494E+00	0.1722E+00
0.3475E+00	0.3362E+00	0.3180E+00	0.2915E+00	0.1939E+00	0.2146E+00	0.2374E+00	0.2598E+00
0.2603E+00	0.2224E+00	0.1797E+00	0.1330E+00	0.2797E+00	0.2963E+00	0.3109E+00	0.3229E+00
0.8406E-01	0.2804E-01	-0.2780E-01	-0.8477E-01	0.3293E+00	0.3361E+00	0.3310E+00	0.3280E+00
-0.1430E+00	-0.2010E+00	-0.2568E+00	-0.3114E+00	0.3170E+00	0.3010E+00	0.2780E+00	0.2516E+00
-0.3595E+00	-0.4066E+00	-0.4466E+00	-0.4814E+00	0.2197E+00	0.1844E+00	0.1406E+00	0.9621E-01
-0.5103E+00	-0.5352E+00	-0.5473E+00	-0.5546E+00	0.4410E-01	-0.7139E-02	-0.6281E-01	-0.1186E+00
-0.5572E+00	-0.5482E+00	-0.5338E+00	-0.5111E+00	-0.1770E+00	-0.2381E+00	-0.2961E+00	-0.3550E+00
-0.4808E+00	-0.4440E+00	-0.4020E+00	-0.3523E+00	-0.4134E+00	-0.4660E+00	-0.5163E+00	-0.5630E+00
-0.3004E+00	-0.2408E+00	-0.1797E+00	-0.1153E+00	-0.6050E+00	-0.6431E+00	-0.6721E+00	-0.6992E+00
-0.4716E-01	0.2190E-01	0.8983E-01	0.1577E+00	-0.7175E+00	-0.7276E+00	-0.7328E+00	-0.7297E+00
0.2241E+00	0.2871E+00	0.3499E+00	0.4053E+00	-0.7173E+00	-0.6999E+00	-0.6734E+00	-0.6420E+00
0.4567E+00	0.5016E+00	0.5373E+00	0.5696E+00	-0.6027E+00	-0.5583E+00	-0.5085E+00	-0.4528E+00
0.5903E+00	0.6101E+00	0.6116E+00	0.6111E+00	-0.3922E+00	-0.3297E+00	-0.2646E+00	-0.1961E+00
0.6002E+00	0.5796E+00	0.5547E+00	0.5193E+00	-0.1289E+00	-0.5901E-01	0.9576E-02	0.7299E-01
0.4758E+00	0.4280E+00	0.3716E+00	0.3131E+00	0.1352E+00	0.1975E+00	0.2529E+00	0.3061E+00
0.2487E+00	0.1844E+00	0.1178E+00	0.4885E-01	0.3498E+00	0.3907E+00	0.4233E+00	0.4515E+00
-0.1664E-01	-0.8485E-01	-0.1475E+00	-0.2073E+00	0.4702E+00	0.4829E+00	0.4878E+00	0.4859E+00
-0.2601E+00	-0.3084E+00	-0.3500E+00	-0.3891E+00	0.4786E+00	0.4636E+00	0.4433E+00	0.4171E+00
-0.4194E+00	-0.4409E+00	-0.4557E+00	-0.4622E+00	0.3838E+00	0.3479E+00	0.3085E+00	0.2652E+00
-0.4616E+00	-0.4531E+00	-0.4379E+00	-0.4151E+00	0.2197E+00	0.1733E+00	0.1273E+00	0.7836E-01
-0.3906E+00	-0.3538E+00	-0.3145E+00	-0.2705E+00	0.3214E-01	-0.1210E-01	-0.5472E-01	-0.9543E-01
-0.2252E+00	-0.1765E+00	-0.1239E+00	-0.7146E-01	-0.1308E+00	-0.1624E+00	-0.1917E+00	-0.2136E+00
-0.1911E-01	0.3431E-01	0.8326E-01	0.1327E+00	-0.2296E+00	-0.2439E+00	-0.2510E+00	-0.2535E+00
0.1769E+00	0.2200E+00	0.2556E+00	0.2917E+00	-0.2475E+00	-0.2389E+00	-0.2258E+00	-0.2096E+00
0.3177E+00	0.3409E+00	0.3541E+00	0.3646E+00	-0.1869E+00	-0.1603E+00	-0.1306E+00	-0.1020E+00
0.3694E+00	0.3672E+00	0.3617E+00	0.3506E+00	-0.6838E-01	-0.3178E-01	0.2606E-02	0.4028E-01
0.3318E+00	0.3110E+00	0.2841E+00	0.2537E+00	0.7367E-01	0.1069E+00	0.1365E+00	0.1660E+00
0.2210E+00	0.1814E+00	0.1427E+00	0.1020E+00	0.1912E+00	0.2156E+00	0.2348E+00	0.2491E+00
0.5937E-01	0.1674E-01	-0.2406E-01	-0.6440E-01	0.2593E+00	0.2670E+00	0.2696E+00	0.2662E+00
-0.1025E+00	-0.1369E+00	-0.1679E+00	-0.1962E+00	0.2585E+00	0.2470E+00	0.2312E+00	0.2122E+00
-0.2210E+00	-0.2365E+00	-0.2531E+00	-0.2623E+00	0.1909E+00	0.1642E+00	0.1370E+00	0.1085E+00
-0.2662E+00	-0.2634E+00	-0.2581E+00	-0.2456E+00	0.7779E-01	0.4753E-01	0.1664E-01	-0.1587E-01
-0.2306E+00	-0.2101E+00	-0.1872E+00	-0.1615E+00	-0.4383E-01	-0.7041E-01	-0.9534E-01	-0.1184E+00
-0.1319E+00	-0.1020E+00	-0.6874E-01	-0.3536E-01	-0.1353E+00	-0.1513E+00	-0.1626E+00	-0.1699E+00
-0.8994E-03	0.3224E-01	0.6253E-01	0.9302E-01	-0.1722E+00	-0.1712E+00	-0.1663E+00	-0.1560E+00
0.1232E+00	0.1515E+00	0.1750E+00	0.1976E+00	-0.1446E+00	-0.1277E+00	-0.1092E+00	-0.8636E-01
0.2130E+00	0.2272E+00	0.2367E+00	0.2443E+00	-0.6289E-01	-0.3421E-01	-0.8345E-02	0.1999E-01
0.2461E+00	0.2485E+00	0.2423E+00	0.2355E+00	0.4813E-01	0.7406E-01	0.1024E+00	0.1276E+00
0.2250E+00	0.2135E+00	0.1967E+00	0.1822E+00	0.1501E+00	0.1711E+00	0.1897E+00	0.2033E+00
0.1653E+00	0.1479E+00	0.1305E+00	0.1151E+00	0.2138E+00	0.2218E+00	0.2242E+00	0.2242E+00
0.1008E+00	0.8570E-01	0.7691E-01	0.6703E-01	0.2190E+00	0.2102E+00	0.1970E+00	0.1814E+00
0.5999E-01	0.5514E-01	0.5448E-01	0.5747E-01	0.1593E+00	0.1383E+00	0.1141E+00	0.8834E-01
0.6267E-01	0.6997E-01	0.8214E-01	0.9539E-01	0.5882E-01	0.3019E-01	0.6031E-03	-0.2816E-01

-0.5586E-01 -0.8154E-01 -0.1055E+00 -0.1263E+00
-0.1456E+00 -0.1580E+00 -0.1697E+00 -0.1738E+00
-0.1761E+00 -0.1728E+00 -0.1655E+00 -0.1516E+00
-0.1346E+00 -0.1123E+00 -0.8722E-01 -0.5624E-01
-0.2461E-01 0.1158E-01 0.4562E-01 0.8428E-01
0.1225E+00 0.1606E+00 0.1976E+00 0.2340E+00
0.2662E+00 0.2950E+00 0.3206E+00 0.3415E+00
0.3555E+00 0.3648E+00 0.3693E+00 0.3661E+00
0.3545E+00 0.3373E+00 0.3130E+00 0.2810E+00
0.2421E+00 0.1964E+00 0.1454E+00 0.8765E-01
0.2533E-01 -0.4346E-01 -0.1130E+00 -0.1870E+00
-0.2619E+00 -0.3372E+00 -0.4138E+00 -0.4875E+00
-0.5606E+00 -0.6304E+00 -0.6963E+00 -0.7563E+00
-0.8115E+00 -0.8595E+00 -0.9003E+00 -0.9315E+00
-0.9576E+00 -0.9722E+00 -0.9790E+00 -0.9750E+00
-0.9639E+00 -0.9425E+00 -0.9125E+00 -0.8744E+00
-0.8281E+00 -0.7728E+00 -0.7120E+00 -0.6443E+00
-0.5734E+00 -0.4961E+00 -0.4158E+00 -0.3337E+00
-0.2500E+00 -0.1648E+00 -0.8063E-01 0.2779E-02
0.8178E-01 0.1592E+00 0.2322E+00 0.3012E+00
0.3631E+00 0.4206E+00 0.4707E+00 0.5141E+00
0.5501E+00 0.5794E+00 0.6010E+00 0.6167E+00
0.6236E+00 0.6256E+00 0.6220E+00 0.6109E+00
0.5958E+00 0.5768E+00 0.5526E+00 0.5249E+00
0.4958E+00 0.4647E+00 0.4318E+00 0.3989E+00
0.3664E+00 0.3360E+00 0.3055E+00 0.2786E+00
0.2521E+00 0.2314E+00 0.2099E+00 0.1954E+00
0.1833E+00 0.1754E+00 0.1698E+00 0.1693E+00
0.1705E+00 0.1759E+00 0.1825E+00 0.1931E+00
0.2035E+00 0.2168E+00 0.2291E+00 0.2436E+00
0.2562E+00 0.2700E+00 0.2789E+00 0.2891E+00
0.2951E+00 0.2987E+00 0.2984E+00 0.2965E+00
0.2894E+00 0.2798E+00 0.2645E+00 0.2467E+00
0.2229E+00 0.1973E+00 0.1672E+00 0.1349E+00
0.9882E-01 0.6239E-01 0.2265E-01 -0.1756E-01
-0.5951E-01 -0.1002E+00 -0.1405E+00 -0.1792E+00
-0.2172E+00 -0.2511E+00 -0.2821E+00 -0.3098E+00
-0.3342E+00 -0.3517E+00 -0.3680E+00 -0.3758E+00
-0.3806E+00 -0.3784E+00 -0.3719E+00 -0.3603E+00
-0.3432E+00 -0.3213E+00 -0.2954E+00 -0.2647E+00
-0.2316E+00 -0.1944E+00 -0.1563E+00 -0.1150E+00
-0.7440E-01 -0.3290E-01 0.7994E-02 0.4812E-01
0.8511E-01 0.1207E+00 0.1526E+00 0.1808E+00
0.2048E+00 0.2238E+00 0.2373E+00 0.2470E+00
0.2488E+00 0.2471E+00 0.2365E+00 0.2225E+00
0.2025E+00 0.1785E+00 0.1483E+00 0.1151E+00
0.7800E-01 0.3741E-01 -0.5882E-02 -0.5071E-01
-0.9660E-01 -0.1411E+00 -0.1857E+00 -0.2278E+00
-0.2700E+00 -0.3064E+00 -0.3414E+00 -0.3696E+00
-0.3943E+00 -0.4132E+00 -0.4266E+00 -0.4315E+00
-0.4319E+00 -0.4250E+00 -0.4122E+00 -0.3913E+00
-0.3653E+00 -0.3322E+00 -0.2942E+00 -0.2493E+00
-0.2031E+00 -0.1513E+00 -0.9610E-01 -0.3901E-01
0.1882E-01 0.7717E-01 0.1355E+00 0.1939E+00
0.2485E+00 0.3006E+00 0.3478E+00 0.3925E+00
0.4307E+00 0.4633E+00 0.4885E+00 0.5093E+00
0.5211E+00 0.5258E+00 0.5219E+00 0.5125E+00
0.4938E+00 0.4686E+00 0.4376E+00 0.3998E+00
0.3556E+00 0.3070E+00 0.2533E+00 0.1962E+00
0.1362E+00 0.7429E-01 0.1068E-01 -0.5188E-01
-0.1162E+00 -0.1759E+00 -0.2349E+00 -0.2890E+00
-0.3408E+00 -0.3872E+00 -0.4293E+00 -0.4624E+00
-0.4937E+00 -0.5150E+00 -0.5311E+00 -0.5393E+00
-0.5414E+00 -0.5354E+00 -0.5253E+00 -0.5055E+00
-0.4818E+00 -0.4507E+00 -0.4179E+00 -0.3774E+00
-0.3346E+00 -0.2888E+00 -0.2411E+00 -0.1904E+00
-0.1416E+00 -0.9189E-01 -0.4275E-01 0.3653E-02
0.4812E-01 0.9018E-01 0.1281E+00 0.1630E+00
0.1917E+00 0.2170E+00 0.2357E+00 0.2504E+00
0.2604E+00 0.2655E+00 0.2648E+00 0.2589E+00
0.2495E+00 0.2358E+00 0.2183E+00 0.1997E+00
0.1759E+00 0.1524E+00 0.1261E+00 0.1005E+00
0.7283E-01 0.4817E-01 0.2183E-01 0.9196E-04
-0.2096E-01 -0.3793E-01 -0.5357E-01 -0.6597E-01
-0.7397E-01 -0.7715E-01 -0.7792E-01 -0.7473E-01
-0.6826E-01 -0.5606E-01 -0.4212E-01 -0.2502E-01
-0.6157E-02 0.1585E-01 0.3938E-01 0.6354E-01
0.8877E-01 0.1133E+00 0.1381E+00 0.1591E+00
0.1821E+00 0.2009E+00 0.2160E+00 0.2280E+00

Time history of vertical acceleration at node NF2:

-0.6563E-01 -0.3207E-01 -0.4824E-01 -0.2365E-01
-0.2904E-01 -0.3868E-01 -0.8474E-01 -0.6820E-01
-0.4996E-01 -0.4990E-01 -0.5702E-01 -0.5562E-01
-0.6839E-01 -0.1857E-01 -0.1005E-01 -0.4910E-02
0.1164E-01 0.2179E-01 0.4901E-01 0.8520E-01
0.8668E-01 0.1046E+00 0.1161E+00 0.1386E+00
0.1511E+00 0.1675E+00 0.1616E+00 0.1697E+00

0.1797E+00	0.1781E+00	0.1848E+00	0.1778E+00	-0.1070E-03	0.9451E-02	0.1539E-01	0.2593E-01
0.1737E+00	0.1771E+00	0.1728E+00	0.1724E+00	0.3279E-01	0.4475E-01	0.5266E-01	0.6585E-01
0.1667E+00	0.1651E+00	0.1614E+00	0.1615E+00	0.7564E-01	0.8918E-01	0.1005E+00	0.1138E+00
0.1581E+00	0.1550E+00	0.1523E+00	0.1487E+00	0.1261E+00	0.1383E+00	0.1507E+00	0.1607E+00
0.1439E+00	0.1387E+00	0.1326E+00	0.1255E+00	0.1715E+00	0.1781E+00	0.1867E+00	0.1894E+00
0.1168E+00	0.1075E+00	0.9565E-01	0.8605E-01	0.1952E+00	0.1928E+00	0.1957E+00	0.1884E+00
0.7551E-01	0.6360E-01	0.5087E-01	0.4019E-01	0.1886E+00	0.1778E+00	0.1754E+00	0.1626E+00
0.2903E-01	0.2031E-01	0.1477E-01	-0.3893E-04	0.1583E+00	0.1460E+00	0.1399E+00	0.1299E+00
-0.4246E-03	-0.1188E-01	-0.1211E-01	-0.1667E-01	0.1228E+00	0.1164E+00	0.1088E+00	0.1063E+00
-0.2352E-01	-0.2554E-01	-0.3409E-01	-0.3087E-01	0.9866E-01	0.9949E-01	0.9221E-01	0.9518E-01
-0.4523E-01	-0.4231E-01	-0.6051E-01	-0.6327E-01	0.8808E-01	0.9091E-01	0.8361E-01	0.8464E-01
-0.7344E-01	-0.8594E-01	-0.9449E-01	-0.1110E+00	0.7678E-01	0.7382E-01	0.6516E-01	0.5833E-01
-0.1206E+00	-0.1337E+00	-0.1399E+00	-0.1551E+00	0.4856E-01	0.3739E-01	0.2721E-01	0.1292E-01
-0.1577E+00	-0.1694E+00	-0.1664E+00	-0.1718E+00	0.1724E-02	-0.1309E-01	-0.2420E-01	-0.3756E-01
-0.1635E+00	-0.1685E+00	-0.1533E+00	-0.1511E+00	-0.4720E-01	-0.5772E-01	-0.6469E-01	-0.7040E-01
-0.1371E+00	-0.1250E+00	-0.1189E+00	-0.1019E+00	-0.7309E-01	-0.7390E-01	-0.7139E-01	-0.6797E-01
-0.9699E-01	-0.8216E-01	-0.7940E-01	-0.7176E-01	-0.6053E-01	-0.5337E-01	-0.4180E-01	-0.3221E-01
-0.7276E-01	-0.7242E-01	-0.7448E-01	-0.8294E-01	-0.1855E-01	-0.8156E-02	0.6655E-02	0.1586E-01
-0.9123E-01	-0.1011E+00	-0.1191E+00	-0.1233E+00	0.2911E-01	0.3652E-01	0.4705E-01	0.5166E-01
-0.1482E+00	-0.1510E+00	-0.1749E+00	-0.1767E+00	0.5842E-01	0.6045E-01	0.6341E-01	0.6307E-01
-0.1939E+00	-0.1938E+00	-0.2021E+00	-0.2021E+00	0.6309E-01	0.6184E-01	0.6001E-01	0.5830E-01
-0.1982E+00	-0.1970E+00	-0.1840E+00	-0.1807E+00	0.5655E-01	0.5666E-01	0.5576E-01	0.5831E-01
-0.1629E+00	-0.1587E+00	-0.1362E+00	-0.1355E+00	0.5894E-01	0.6483E-01	0.6765E-01	0.7703E-01
-0.1105E+00	-0.1143E+00	-0.9308E-01	-0.9811E-01	0.8170E-01	0.9391E-01	0.9922E-01	0.1125E+00
-0.8516E-01	-0.9013E-01	-0.8838E-01	-0.9120E-01	0.1177E+00	0.1301E+00	0.1345E+00	0.1444E+00
-0.1006E+00	-0.9976E-01	-0.1168E+00	-0.1150E+00	0.1474E+00	0.1530E+00	0.1545E+00	0.1544E+00
-0.1321E+00	-0.1312E+00	-0.1432E+00	-0.1420E+00	0.1540E+00	0.1487E+00	0.1472E+00	0.1375E+00
-0.1477E+00	-0.1442E+00	-0.1429E+00	-0.1356E+00	0.1355E+00	0.1226E+00	0.1206E+00	0.1071E+00
-0.1284E+00	-0.1173E+00	-0.1060E+00	-0.9160E-01	0.1055E+00	0.9368E-01	0.9301E-01	0.8375E-01
-0.7758E-01	-0.6277E-01	-0.4771E-01	-0.3456E-01	0.8383E-01	0.7929E-01	0.8039E-01	0.7954E-01
-0.2133E-01	-0.1050E-01	-0.1576E-02	0.5683E-02	0.8076E-01	0.8317E-01	0.8480E-01	0.8970E-01
0.9687E-02	0.1263E-01	0.1219E-01	0.1048E-01	0.9062E-01	0.9616E-01	0.9558E-01	0.1007E+00
0.6967E-02	0.1071E-02	-0.3481E-02	-0.1248E-01	0.9832E-01	0.1020E+00	0.9750E-01	0.9871E-01
-0.1693E-01	-0.2620E-01	-0.3078E-01	-0.3819E-01	0.9252E-01	0.9159E-01	0.8488E-01	0.8200E-01
-0.4229E-01	-0.4667E-01	-0.4995E-01	-0.5124E-01	0.7506E-01	0.7042E-01	0.6452E-01	0.5941E-01
-0.5349E-01	-0.5292E-01	-0.5375E-01	-0.5273E-01	0.5449E-01	0.4991E-01	0.4712E-01	0.4296E-01
-0.5257E-01	-0.5246E-01	-0.5208E-01	-0.5308E-01	0.4222E-01	0.3909E-01	0.4026E-01	0.3772E-01
-0.5349E-01	-0.5565E-01	-0.5730E-01	-0.6071E-01	0.3967E-01	0.3735E-01	0.3952E-01	0.3684E-01
-0.6344E-01	-0.6753E-01	-0.7084E-01	-0.7468E-01	0.3822E-01	0.3512E-01	0.3429E-01	0.2996E-01
-0.7798E-01	-0.8078E-01	-0.8311E-01	-0.8435E-01	0.2733E-01	0.2150E-01	0.1616E-01	0.9438E-02
-0.8496E-01	-0.8437E-01	-0.8291E-01	-0.8038E-01	0.2257E-02	-0.5510E-02	-0.1437E-01	-0.2260E-01
-0.7663E-01	-0.7266E-01	-0.6694E-01	-0.6181E-01	-0.3185E-01	-0.3982E-01	-0.4861E-01	-0.5658E-01
-0.5506E-01	-0.4876E-01	-0.4211E-01	-0.3475E-01	-0.6416E-01	-0.7074E-01	-0.7648E-01	-0.8158E-01
-0.2829E-01	-0.2037E-01	-0.1454E-01	-0.5797E-02	-0.8587E-01	-0.8913E-01	-0.9139E-01	-0.9262E-01

-0.9327E-01	-0.9279E-01	-0.9221E-01	-0.9030E-01	-0.5734E-01	-0.5768E-01	-0.5750E-01	-0.5776E-01
-0.8816E-01	-0.8538E-01	-0.8213E-01	-0.7826E-01	-0.5760E-01	-0.5777E-01	-0.5770E-01	-0.5732E-01
-0.7419E-01	-0.6990E-01	-0.6488E-01	-0.5961E-01	-0.5730E-01	-0.5660E-01	-0.5642E-01	-0.5526E-01
-0.5373E-01	-0.4782E-01	-0.4107E-01	-0.3441E-01	-0.5464E-01	-0.5310E-01	-0.5208E-01	-0.5006E-01
-0.2654E-01	-0.1960E-01	-0.1078E-01	-0.3021E-02	-0.4847E-01	-0.4600E-01	-0.4368E-01	-0.4077E-01
0.6041E-02	0.1440E-01	0.2409E-01	0.3253E-01	-0.3764E-01	-0.3421E-01	-0.3043E-01	-0.2641E-01
0.4201E-01	0.5042E-01	0.5956E-01	0.6743E-01	-0.2181E-01	-0.1713E-01	-0.1168E-01	-0.6390E-02
0.7571E-01	0.8317E-01	0.9036E-01	0.9673E-01	-0.2070E-03	0.5603E-02	0.1249E-01	0.1883E-01
0.1028E+00	0.1075E+00	0.1123E+00	0.1158E+00	0.2646E-01	0.3301E-01	0.4092E-01	0.4792E-01
0.1189E+00	0.1212E+00	0.1233E+00	0.1238E+00	0.5593E-01	0.6302E-01	0.7102E-01	0.7780E-01
0.1247E+00	0.1239E+00	0.1233E+00	0.1210E+00	0.8525E-01	0.9171E-01	0.9869E-01	0.1044E+00
0.1191E+00	0.1154E+00	0.1125E+00	0.1073E+00	0.1105E+00	0.1155E+00	0.1203E+00	0.1243E+00
0.1030E+00	0.9639E-01	0.9067E-01	0.8282E-01	0.1280E+00	0.1307E+00	0.1331E+00	0.1345E+00
0.7512E-01	0.6654E-01	0.5778E-01	0.4831E-01	0.1354E+00	0.1356E+00	0.1349E+00	0.1338E+00
0.3833E-01	0.2851E-01	0.1758E-01	0.8000E-02	0.1315E+00	0.1290E+00	0.1253E+00	0.1214E+00
-0.3146E-02	-0.1309E-01	-0.2366E-01	-0.3265E-01	0.1164E+00	0.1111E+00	0.1048E+00	0.9838E-01
-0.4265E-01	-0.5059E-01	-0.5918E-01	-0.6623E-01	0.9092E-01	0.8332E-01	0.7495E-01	0.6621E-01
-0.7286E-01	-0.7841E-01	-0.8340E-01	-0.8753E-01	0.5712E-01	0.4771E-01	0.3793E-01	0.2785E-01
-0.9057E-01	-0.9319E-01	-0.9455E-01	-0.9605E-01	0.1785E-01	0.7290E-02	-0.2629E-02	-0.1329E-01
-0.9566E-01	-0.9625E-01	-0.9450E-01	-0.9397E-01	-0.2306E-01	-0.3360E-01	-0.4293E-01	-0.5261E-01
-0.9133E-01	-0.9009E-01	-0.8677E-01	-0.8483E-01	-0.6143E-01	-0.7043E-01	-0.7812E-01	-0.8604E-01
-0.8059E-01	-0.7824E-01	-0.7349E-01	-0.7019E-01	-0.9258E-01	-0.9925E-01	-0.1044E+00	-0.1095E+00
-0.6527E-01	-0.6084E-01	-0.5574E-01	-0.5090E-01	-0.1134E+00	-0.1167E+00	-0.1190E+00	-0.1206E+00
-0.4513E-01	-0.3919E-01	-0.3319E-01	-0.2672E-01	-0.1212E+00	-0.1212E+00	-0.1202E+00	-0.1185E+00
-0.2078E-01	-0.1398E-01	-0.7851E-02	-0.1068E-02	-0.1159E+00	-0.1126E+00	-0.1085E+00	-0.1037E+00
0.5022E-02	0.1149E-01	0.1699E-01	0.2288E-01	-0.9827E-01	-0.9218E-01	-0.8557E-01	-0.7832E-01
0.2767E-01	0.3231E-01	0.3576E-01	0.3945E-01	-0.7067E-01	-0.6255E-01	-0.5418E-01	-0.4547E-01
0.4153E-01	0.4365E-01	0.4438E-01	0.4490E-01	-0.3652E-01	-0.2740E-01	-0.1810E-01	-0.8921E-02
0.4398E-01	0.4336E-01	0.4114E-01	0.3897E-01	0.3557E-03	0.9356E-02	0.1843E-01	0.2703E-01
0.3554E-01	0.3237E-01	0.2819E-01	0.2400E-01	0.3554E-01	0.4340E-01	0.5117E-01	0.5820E-01
0.1957E-01	0.1439E-01	0.9883E-02	0.4162E-02	0.6491E-01	0.7083E-01	0.7647E-01	0.8116E-01
-0.4765E-03	-0.6422E-02	-0.1073E-01	-0.1676E-01	0.8541E-01	0.8883E-01	0.9175E-01	0.9380E-01
-0.2102E-01	-0.2725E-01	-0.3112E-01	-0.3718E-01	0.9525E-01	0.9586E-01	0.9594E-01	0.9517E-01
-0.4109E-01	-0.4689E-01	-0.5080E-01	-0.5642E-01	0.9399E-01	0.9194E-01	0.8960E-01	0.8634E-01
-0.6031E-01	-0.6532E-01	-0.6944E-01	-0.7395E-01	0.8261E-01	0.7844E-01	0.7396E-01	0.6886E-01
-0.7812E-01	-0.8188E-01	-0.8578E-01	-0.8892E-01	0.6342E-01	0.5774E-01	0.5182E-01	0.4556E-01
-0.9263E-01	-0.9452E-01	-0.9770E-01	-0.9870E-01	0.3924E-01	0.3269E-01	0.2624E-01	0.1964E-01
-0.1012E+00	-0.1013E+00	-0.1027E+00	-0.1017E+00	0.1317E-01	0.6681E-02	0.4312E-03	-0.5814E-02
-0.1021E+00	-0.1003E+00	-0.9974E-01	-0.9749E-01	-0.1165E-01	-0.1731E-01	-0.2255E-01	-0.2762E-01
-0.9582E-01	-0.9301E-01	-0.9055E-01	-0.8776E-01	-0.3226E-01	-0.3652E-01	-0.4035E-01	-0.4399E-01
-0.8448E-01	-0.8183E-01	-0.7834E-01	-0.7625E-01	-0.4688E-01	-0.4952E-01	-0.5148E-01	-0.5335E-01
-0.7279E-01	-0.7103E-01	-0.6764E-01	-0.6641E-01	-0.5452E-01	-0.5548E-01	-0.5593E-01	-0.5606E-01
-0.6343E-01	-0.6300E-01	-0.6047E-01	-0.6033E-01	-0.5564E-01	-0.5515E-01	-0.5414E-01	-0.5285E-01
-0.5846E-01	-0.5890E-01	-0.5759E-01	-0.5796E-01	-0.5138E-01	-0.4995E-01	-0.4802E-01	-0.4605E-01

-0.4393E-01 -0.4189E-01 -0.3963E-01 -0.3744E-01
-0.3526E-01 -0.3323E-01 -0.3092E-01 -0.2923E-01
-0.2713E-01 -0.2563E-01 -0.2383E-01 -0.2264E-01
-0.2121E-01 -0.2041E-01 -0.1934E-01 -0.1879E-01
-0.1825E-01 -0.1813E-01 -0.1802E-01 -0.1834E-01
-0.1871E-01 -0.1920E-01 -0.1967E-01 -0.2065E-01
-0.2163E-01 -0.2272E-01 -0.2385E-01 -0.2501E-01
-0.2623E-01 -0.2733E-01 -0.2862E-01 -0.2972E-01
-0.3063E-01 -0.3157E-01 -0.3213E-01 -0.3262E-01
-0.3292E-01 -0.3302E-01 -0.3264E-01 -0.3232E-01
-0.3148E-01 -0.3044E-01 -0.2894E-01 -0.2741E-01
-0.2540E-01 -0.2324E-01 -0.2060E-01 -0.1807E-01
-0.1481E-01 -0.1193E-01 -0.8453E-02 -0.5035E-02
-0.1327E-02 0.2045E-02 0.5917E-02 0.9423E-02
0.1331E-01 0.1650E-01 0.2034E-01 0.2343E-01
0.2664E-01 0.2938E-01 0.3219E-01 0.3435E-01
0.3636E-01 0.3810E-01 0.3957E-01 0.4035E-01
0.4081E-01 0.4105E-01 0.4075E-01 0.3992E-01
0.3880E-01 0.3700E-01 0.3508E-01 0.3237E-01
0.2952E-01 0.2613E-01 0.2235E-01 0.1809E-01
0.1369E-01 0.8818E-02 0.3828E-02 -0.1814E-02
-0.7109E-02 -0.1291E-01 -0.1867E-01 -0.2465E-01
-0.3028E-01 -0.3623E-01 -0.4187E-01 -0.4758E-01
-0.5273E-01 -0.5802E-01 -0.6264E-01 -0.6728E-01
-0.7107E-01 -0.7487E-01 -0.7790E-01 -0.8061E-01
-0.8249E-01 -0.8438E-01 -0.8500E-01 -0.8548E-01
-0.8497E-01 -0.8411E-01 -0.8247E-01 -0.8034E-01
-0.7732E-01 -0.7382E-01 -0.6962E-01 -0.6489E-01
-0.5946E-01 -0.5348E-01 -0.4690E-01 -0.3990E-01
-0.3234E-01 -0.2424E-01 -0.1590E-01 -0.7003E-02
0.2174E-02 0.1159E-01 0.2110E-01 0.3107E-01
0.4095E-01 0.5082E-01 0.6086E-01 0.7058E-01
0.8040E-01 0.8966E-01 0.9898E-01 0.1077E+00
0.1161E+00 0.1239E+00 0.1313E+00 0.1378E+00
0.1440E+00 0.1492E+00 0.1541E+00 0.1577E+00
0.1610E+00 0.1629E+00 0.1644E+00 0.1645E+00
0.1643E+00 0.1627E+00 0.1609E+00 0.1576E+00
0.1539E+00 0.1490E+00 0.1436E+00 0.1373E+00
0.1305E+00 0.1228E+00 0.1147E+00 0.1059E+00
0.9654E-01 0.8688E-01 0.7683E-01 0.6637E-01
0.5578E-01 0.4504E-01 0.3405E-01 0.2316E-01
0.1223E-01 0.1431E-02 -0.9107E-02 -0.1965E-01
-0.2974E-01 -0.3955E-01 -0.4871E-01 -0.5761E-01
-0.6584E-01 -0.7366E-01 -0.8064E-01 -0.8718E-01
-0.9297E-01 -0.9810E-01 -0.1023E+00 -0.1060E+00
-0.1088E+00 -0.1111E+00 -0.1124E+00 -0.1133E+00
-0.1132E+00 -0.1127E+00 -0.1113E+00 -0.1096E+00
-0.1071E+00 -0.1043E+00 -0.1008E+00 -0.9712E-01
-0.9277E-01 -0.8840E-01 -0.8358E-01 -0.7880E-01
-0.7354E-01 -0.6843E-01 -0.6298E-01 -0.5784E-01
-0.5232E-01 -0.4720E-01 -0.4189E-01 -0.3688E-01
-0.3204E-01 -0.2738E-01 -0.2277E-01 -0.1877E-01
-0.1471E-01 -0.1111E-01 -0.7636E-02 -0.4649E-02
-0.1863E-02 0.6271E-03 0.2903E-02 0.4735E-02
0.6448E-02 0.7767E-02 0.9003E-02 0.9975E-02
0.1093E-01 0.1125E-01 0.1185E-01 0.1188E-01
0.1249E-01 0.1232E-01 0.1252E-01 0.1247E-01
0.1273E-01 0.1270E-01 0.1290E-01 0.1313E-01
0.1348E-01 0.1375E-01 0.1449E-01 0.1497E-01
0.1599E-01 0.1685E-01 0.1807E-01 0.1918E-01
0.2068E-01 0.2209E-01 0.2399E-01 0.2555E-01
0.2741E-01 0.2927E-01 0.3118E-01 0.3322E-01
0.3517E-01 0.3708E-01 0.3892E-01 0.4072E-01
0.4248E-01 0.4394E-01 0.4555E-01 0.4654E-01
0.4773E-01 0.4838E-01 0.4901E-01 0.4918E-01
0.4921E-01 0.4882E-01 0.4840E-01 0.4727E-01
0.4609E-01 0.4424E-01 0.4241E-01 0.4000E-01

Time history of vertical acceleration at node NF3:

-0.6717E-01 -0.3200E-01 -0.4740E-01 -0.2016E-01
-0.2358E-01 -0.3109E-01 -0.7584E-01 -0.5465E-01
-0.3091E-01 -0.2535E-01 -0.2618E-01 -0.1717E-01
-0.2043E-01 0.3594E-01 0.5294E-01 0.6676E-01
0.8905E-01 0.1051E+00 0.1302E+00 0.1556E+00
0.1584E+00 0.1657E+00 0.1668E+00 0.1656E+00
0.1575E+00 0.1442E+00 0.1294E+00 0.1092E+00
0.8380E-01 0.6058E-01 0.2901E-01 0.6199E-02
-0.1960E-01 -0.5528E-01 -0.8250E-01 -0.1160E+00
-0.1397E+00 -0.1706E+00 -0.1957E+00 -0.2299E+00
-0.2525E+00 -0.2718E+00 -0.2898E+00 -0.2955E+00
-0.3041E+00 -0.3000E+00 -0.2904E+00 -0.2751E+00
-0.2562E+00 -0.2310E+00 -0.2048E+00 -0.1677E+00
-0.1275E+00 -0.8584E-01 -0.4210E-01 0.8205E-02
0.5889E-01 0.1153E+00 0.1763E+00 0.2185E+00
0.2843E+00 0.3253E+00 0.3813E+00 0.4228E+00
0.4523E+00 0.4813E+00 0.4907E+00 0.5085E+00
0.4900E+00 0.4862E+00 0.4431E+00 0.4128E+00
0.3648E+00 0.3091E+00 0.2535E+00 0.1862E+00

0.1249E+00	0.5811E-01	-0.3739E-02	-0.7246E-01	0.1878E+00	0.2072E+00	0.2280E+00	0.2488E+00
-0.1299E+00	-0.1930E+00	-0.2422E+00	-0.2939E+00	0.2621E+00	0.2768E+00	0.2869E+00	0.2925E+00
-0.3320E+00	-0.3741E+00	-0.3980E+00	-0.4244E+00	0.2977E+00	0.2968E+00	0.2897E+00	0.2802E+00
-0.4373E+00	-0.4448E+00	-0.4509E+00	-0.4432E+00	0.2695E+00	0.2484E+00	0.2256E+00	0.2007E+00
-0.4369E+00	-0.4186E+00	-0.4040E+00	-0.3794E+00	0.1651E+00	0.1278E+00	0.8694E-01	0.3914E-01
-0.3564E+00	-0.3282E+00	-0.2976E+00	-0.2671E+00	-0.8276E-02	-0.6050E-01	-0.1160E+00	-0.1713E+00
-0.2352E+00	-0.1997E+00	-0.1679E+00	-0.1257E+00	-0.2268E+00	-0.2859E+00	-0.3401E+00	-0.3934E+00
-0.9428E-01	-0.4859E-01	-0.1537E-01	0.3075E-01	-0.4464E+00	-0.4938E+00	-0.5368E+00	-0.5757E+00
0.6890E-01	0.1142E+00	0.1541E+00	0.1953E+00	-0.6127E+00	-0.6433E+00	-0.6691E+00	-0.6864E+00
0.2367E+00	0.2720E+00	0.3074E+00	0.3365E+00	-0.7007E+00	-0.7091E+00	-0.7111E+00	-0.7083E+00
0.3654E+00	0.3850E+00	0.4050E+00	0.4128E+00	-0.6977E+00	-0.6830E+00	-0.6600E+00	-0.6332E+00
0.4217E+00	0.4190E+00	0.4160E+00	0.4039E+00	-0.5981E+00	-0.5613E+00	-0.5183E+00	-0.4702E+00
0.3903E+00	0.3704E+00	0.3483E+00	0.3231E+00	-0.4190E+00	-0.3671E+00	-0.3097E+00	-0.2558E+00
0.2946E+00	0.2656E+00	0.2346E+00	0.2037E+00	-0.1994E+00	-0.1429E+00	-0.8714E-01	-0.3429E-01
0.1727E+00	0.1414E+00	0.1111E+00	0.8269E-01	0.1361E-01	0.6149E-01	0.1049E+00	0.1431E+00
0.5482E-01	0.2888E-01	0.4333E-02	-0.1757E-01	0.1733E+00	0.2036E+00	0.2242E+00	0.2430E+00
-0.3769E-01	-0.5618E-01	-0.7318E-01	-0.8934E-01	0.2477E+00	0.2508E+00	0.2441E+00	0.2340E+00
-0.1033E+00	-0.1162E+00	-0.1302E+00	-0.1402E+00	0.2169E+00	0.1929E+00	0.1646E+00	0.1311E+00
-0.1536E+00	-0.1630E+00	-0.1742E+00	-0.1833E+00	0.9320E-01	0.5273E-01	0.8731E-02	-0.3704E-01
-0.1921E+00	-0.1993E+00	-0.2073E+00	-0.2124E+00	-0.8110E-01	-0.1303E+00	-0.1705E+00	-0.2162E+00
-0.2178E+00	-0.2221E+00	-0.2273E+00	-0.2285E+00	-0.2522E+00	-0.2878E+00	-0.3177E+00	-0.3447E+00
-0.2319E+00	-0.2341E+00	-0.2375E+00	-0.2394E+00	-0.3630E+00	-0.3776E+00	-0.3852E+00	-0.3904E+00
-0.2450E+00	-0.2504E+00	-0.2550E+00	-0.2656E+00	-0.3868E+00	-0.3797E+00	-0.3648E+00	-0.3475E+00
-0.2732E+00	-0.2852E+00	-0.2934E+00	-0.3059E+00	-0.3219E+00	-0.2972E+00	-0.2681E+00	-0.2363E+00
-0.3152E+00	-0.3259E+00	-0.3330E+00	-0.3369E+00	-0.2043E+00	-0.1694E+00	-0.1353E+00	-0.1027E+00
-0.3426E+00	-0.3448E+00	-0.3464E+00	-0.3443E+00	-0.6861E-01	-0.3781E-01	-0.8747E-02	0.1873E-01
-0.3397E+00	-0.3311E+00	-0.3220E+00	-0.3104E+00	0.4028E-01	0.5991E-01	0.7833E-01	0.9055E-01
-0.2932E+00	-0.2761E+00	-0.2533E+00	-0.2283E+00	0.9727E-01	0.1028E+00	0.1011E+00	0.9542E-01
-0.2003E+00	-0.1725E+00	-0.1405E+00	-0.1088E+00	0.8906E-01	0.7513E-01	0.5957E-01	0.4025E-01
-0.7152E-01	-0.4069E-01	-0.1706E-02	0.3244E-01	0.1649E-01	-0.8818E-02	-0.3566E-01	-0.6557E-01
0.6892E-01	0.1029E+00	0.1379E+00	0.1730E+00	-0.9273E-01	-0.1233E+00	-0.1517E+00	-0.1797E+00
0.2021E+00	0.2357E+00	0.2647E+00	0.2970E+00	-0.2041E+00	-0.2287E+00	-0.2443E+00	-0.2603E+00
0.3229E+00	0.3521E+00	0.3757E+00	0.4065E+00	-0.2693E+00	-0.2746E+00	-0.2740E+00	-0.2673E+00
0.4267E+00	0.4540E+00	0.4728E+00	0.4950E+00	-0.2550E+00	-0.2320E+00	-0.2075E+00	-0.1750E+00
0.5119E+00	0.5266E+00	0.5371E+00	0.5434E+00	-0.1334E+00	-0.9033E-01	-0.3617E-01	0.1906E-01
0.5465E+00	0.5434E+00	0.5372E+00	0.5256E+00	0.8043E-01	0.1462E+00	0.2128E+00	0.2835E+00
0.5085E+00	0.4877E+00	0.4641E+00	0.4352E+00	0.3513E+00	0.4247E+00	0.4942E+00	0.5623E+00
0.4045E+00	0.3701E+00	0.3336E+00	0.2964E+00	0.6270E+00	0.6849E+00	0.7427E+00	0.7933E+00
0.2600E+00	0.2209E+00	0.1860E+00	0.1493E+00	0.8387E+00	0.8781E+00	0.9074E+00	0.9308E+00
0.1186E+00	0.8734E-01	0.6249E-01	0.4004E-01	0.9453E+00	0.9533E+00	0.9492E+00	0.9433E+00
0.2022E-01	0.6751E-02	-0.6680E-02	-0.9334E-02	0.9258E+00	0.9005E+00	0.8665E+00	0.8284E+00
-0.1298E-01	-0.1024E-01	-0.4478E-02	0.7114E-02	0.7791E+00	0.7296E+00	0.6739E+00	0.6133E+00
0.1770E-01	0.3429E-01	0.5351E-01	0.7360E-01	0.5481E+00	0.4819E+00	0.4136E+00	0.3424E+00
0.9586E-01	0.1193E+00	0.1430E+00	0.1655E+00	0.2754E+00	0.2086E+00	0.1440E+00	0.8050E-01

0.2299E-01	-0.2595E-01	-0.7457E-01	-0.1153E+00
-0.1496E+00	-0.1763E+00	-0.1973E+00	-0.2113E+00
-0.2206E+00	-0.2229E+00	-0.2198E+00	-0.2077E+00
-0.1930E+00	-0.1736E+00	-0.1500E+00	-0.1255E+00
-0.9582E-01	-0.6452E-01	-0.3228E-01	-0.1867E-03
0.3295E-01	0.6486E-01	0.9414E-01	0.1204E+00
0.1440E+00	0.1627E+00	0.1780E+00	0.1894E+00
0.1954E+00	0.1987E+00	0.1932E+00	0.1834E+00
0.1687E+00	0.1502E+00	0.1248E+00	0.9743E-01
0.6495E-01	0.2920E-01	-0.1074E-01	-0.5004E-01
-0.9429E-01	-0.1382E+00	-0.1838E+00	-0.2275E+00
-0.2688E+00	-0.3121E+00	-0.3511E+00	-0.3873E+00
-0.4188E+00	-0.4480E+00	-0.4704E+00	-0.4915E+00
-0.5044E+00	-0.5142E+00	-0.5149E+00	-0.5121E+00
-0.5019E+00	-0.4874E+00	-0.4642E+00	-0.4390E+00
-0.4053E+00	-0.3692E+00	-0.3299E+00	-0.2878E+00
-0.2401E+00	-0.1969E+00	-0.1476E+00	-0.9928E-01
-0.5046E-01	-0.5089E-02	0.4064E-01	0.8152E-01
0.1198E+00	0.1542E+00	0.1849E+00	0.2102E+00
0.2333E+00	0.2498E+00	0.2606E+00	0.2685E+00
0.2681E+00	0.2665E+00	0.2575E+00	0.2497E+00
0.2336E+00	0.2150E+00	0.1942E+00	0.1729E+00
0.1482E+00	0.1209E+00	0.9641E-01	0.6961E-01
0.4394E-01	0.2099E-01	-0.3985E-02	-0.2163E-01
-0.4109E-01	-0.5831E-01	-0.7116E-01	-0.8253E-01
-0.8673E-01	-0.9186E-01	-0.9252E-01	-0.8891E-01
-0.8308E-01	-0.7729E-01	-0.6648E-01	-0.5260E-01
-0.3944E-01	-0.2679E-01	-0.7847E-02	0.6643E-02
0.2119E-01	0.3588E-01	0.4905E-01	0.6244E-01
0.7258E-01	0.8065E-01	0.8664E-01	0.8651E-01
0.8484E-01	0.8156E-01	0.7014E-01	0.5442E-01
0.4068E-01	0.1887E-01	-0.3574E-02	-0.3324E-01
-0.6380E-01	-0.9826E-01	-0.1337E+00	-0.1731E+00
-0.2123E+00	-0.2525E+00	-0.2930E+00	-0.3345E+00
-0.3732E+00	-0.4101E+00	-0.4440E+00	-0.4779E+00
-0.5048E+00	-0.5281E+00	-0.5486E+00	-0.5618E+00
-0.5710E+00	-0.5754E+00	-0.5723E+00	-0.5630E+00
-0.5499E+00	-0.5303E+00	-0.5049E+00	-0.4757E+00
-0.4390E+00	-0.3992E+00	-0.3555E+00	-0.3067E+00
-0.2597E+00	-0.2070E+00	-0.1525E+00	-0.1001E+00
-0.4578E-01	0.5647E-02	0.5527E-01	0.1031E+00
0.1472E+00	0.1884E+00	0.2253E+00	0.2551E+00
0.2822E+00	0.3010E+00	0.3164E+00	0.3240E+00
0.3271E+00	0.3204E+00	0.3112E+00	0.2942E+00
0.2703E+00	0.2445E+00	0.2125E+00	0.1744E+00
0.1349E+00	0.8973E-01	0.4585E-01	-0.1737E-02
-0.4755E-01	-0.9714E-01	-0.1438E+00	-0.1892E+00
-0.2322E+00	-0.2730E+00	-0.3093E+00	-0.3420E+00
-0.3683E+00	-0.3924E+00	-0.4097E+00	-0.4209E+00
-0.4243E+00	-0.4273E+00	-0.4190E+00	-0.4076E+00
-0.3909E+00	-0.3669E+00	-0.3388E+00	-0.3067E+00
-0.2691E+00	-0.2320E+00	-0.1879E+00	-0.1422E+00
-0.9723E-01	-0.5216E-01	-0.6510E-02	0.3923E-01
0.8242E-01	0.1219E+00	0.1593E+00	0.1939E+00
0.2212E+00	0.2480E+00	0.2675E+00	0.2827E+00
0.2915E+00	0.2963E+00	0.2955E+00	0.2886E+00
0.2777E+00	0.2643E+00	0.2441E+00	0.2209E+00
0.1938E+00	0.1627E+00	0.1327E+00	0.1004E+00
0.6719E-01	0.3517E-01	0.1927E-02	-0.2799E-01
-0.5589E-01	-0.8135E-01	-0.1030E+00	-0.1217E+00
-0.1346E+00	-0.1460E+00	-0.1497E+00	-0.1504E+00
-0.1430E+00	-0.1339E+00	-0.1183E+00	-0.9764E-01
-0.7160E-01	-0.4422E-01	-0.1224E-01	0.2291E-01
0.6093E-01	0.1002E+00	0.1420E+00	0.1819E+00
0.2226E+00	0.2622E+00	0.3006E+00	0.3357E+00
0.3681E+00	0.3963E+00	0.4218E+00	0.4409E+00
0.4563E+00	0.4652E+00	0.4700E+00	0.4693E+00
0.4614E+00	0.4501E+00	0.4320E+00	0.4089E+00
0.3810E+00	0.3489E+00	0.3140E+00	0.2755E+00
0.2338E+00	0.1897E+00	0.1449E+00	0.9972E-01
0.5444E-01	0.9764E-02	-0.3279E-01	-0.7369E-01
-0.1105E+00	-0.1450E+00	-0.1743E+00	-0.2006E+00
-0.2205E+00	-0.2375E+00	-0.2456E+00	-0.2505E+00
-0.2475E+00	-0.2406E+00	-0.2258E+00	-0.2092E+00
-0.1829E+00	-0.1562E+00	-0.1228E+00	-0.8715E-01
-0.4738E-01	-0.6901E-02	0.3618E-01	0.7904E-01
0.1228E+00	0.1645E+00	0.2066E+00	0.2445E+00
0.2802E+00	0.3115E+00	0.3404E+00	0.3633E+00
0.3824E+00	0.3949E+00	0.4038E+00	0.4050E+00
0.4022E+00	0.3925E+00	0.3791E+00	0.3583E+00
0.3339E+00	0.3056E+00	0.2740E+00	0.2390E+00
0.2018E+00	0.1617E+00	0.1221E+00	0.8148E-01
0.4164E-01	0.2134E-02	-0.3414E-01	-0.6985E-01
-0.1006E+00	-0.1304E+00	-0.1516E+00	-0.1729E+00
-0.1860E+00	-0.1967E+00	-0.1994E+00	-0.1992E+00
-0.1917E+00	-0.1820E+00	-0.1640E+00	-0.1440E+00
-0.1183E+00	-0.9131E-01	-0.5771E-01	-0.2516E-01
0.1100E-01	0.4714E-01	0.8426E-01	0.1212E+00

0.1571E+00 0.1905E+00 0.2234E+00 0.2510E+00
0.2767E+00 0.2965E+00 0.3151E+00 0.3251E+00
0.3320E+00 0.3328E+00 0.3271E+00 0.3167E+00
0.3022E+00 0.2802E+00 0.2554E+00 0.2246E+00
0.1908E+00 0.1517E+00 0.1110E+00 0.6668E-01
0.2250E-01 -0.2522E-01 -0.7119E-01 -0.1176E+00
-0.1621E+00 -0.2053E+00 -0.2446E+00 -0.2817E+00
-0.3145E+00 -0.3421E+00 -0.3642E+00 -0.3829E+00
-0.3933E+00 -0.4002E+00 -0.3998E+00 -0.3930E+00
-0.3803E+00 -0.3628E+00 -0.3387E+00 -0.3101E+00
-0.2772E+00 -0.2403E+00 -0.1987E+00 -0.1567E+00
-0.1111E+00 -0.6472E-01 -0.1823E-01 0.2805E-01
0.7398E-01 0.1173E+00 0.1582E+00 0.1961E+00
0.2297E+00 0.2592E+00 0.2838E+00 0.3023E+00
0.3171E+00 0.3244E+00 0.3272E+00 0.3240E+00
0.3151E+00 0.3002E+00 0.2799E+00 0.2554E+00
0.2261E+00 0.1922E+00 0.1555E+00 0.1160E+00
0.7555E-01 0.3259E-01 -0.8127E-02 -0.5185E-01
-0.9298E-01 -0.1327E+00 -0.1679E+00 -0.2030E+00
-0.2322E+00 -0.2579E+00 -0.2787E+00 -0.2941E+00
-0.3042E+00 -0.3084E+00 -0.3055E+00 -0.2982E+00
-0.2838E+00 -0.2655E+00 -0.2398E+00 -0.2101E+00
-0.1751E+00 -0.1372E+00 -0.9642E-01 -0.5148E-01
-0.5308E-02 0.4106E-01 0.8997E-01 0.1363E+00
0.1837E+00 0.2265E+00 0.2681E+00 0.3042E+00
0.3389E+00 0.3666E+00 0.3912E+00 0.4073E+00
0.4182E+00 0.4226E+00 0.4204E+00 0.4117E+00
0.3985E+00 0.3763E+00 0.3491E+00 0.3151E+00
0.2784E+00 0.2336E+00 0.1875E+00 0.1353E+00
0.8419E-01 0.2717E-01 -0.2832E-01 -0.8587E-01
-0.1411E+00 -0.1968E+00 -0.2492E+00 -0.3011E+00
-0.3479E+00 -0.3919E+00 -0.4291E+00 -0.4636E+00
-0.4902E+00 -0.5148E+00 -0.5288E+00 -0.5410E+00
-0.5437E+00 -0.5423E+00 -0.5339E+00 -0.5215E+00
-0.5031E+00 -0.4801E+00 -0.4515E+00 -0.4213E+00
-0.3863E+00 -0.3493E+00 -0.3095E+00 -0.2699E+00
-0.2293E+00 -0.1887E+00 -0.1484E+00 -0.1103E+00
-0.7401E-01 -0.3946E-01 -0.8631E-02 0.1893E-01
0.4248E-01 0.6169E-01 0.7802E-01 0.8916E-01
0.9699E-01 0.1000E+00 0.9952E-01 0.9620E-01
0.8923E-01 0.7839E-01 0.6721E-01 0.5087E-01
0.3585E-01 0.1896E-01 0.2746E-02 -0.1555E-01
-0.3000E-01 -0.4501E-01 -0.5699E-01 -0.6801E-01
-0.7533E-01 -0.7978E-01 -0.8027E-01 -0.7801E-01
-0.7234E-01 -0.6169E-01 -0.4740E-01 -0.3090E-01
-0.9592E-02 0.1271E-01 0.3992E-01 0.6793E-01
0.9916E-01 0.1300E+00 0.1632E+00 0.1946E+00
0.2260E+00 0.2556E+00 0.2839E+00 0.3079E+00
0.3308E+00 0.3476E+00 0.3610E+00 0.3682E+00
0.3732E+00 0.3689E+00 0.3615E+00 0.3461E+00
0.3259E+00 0.2991E+00 0.2676E+00 0.2290E+00
0.1860E+00 0.1363E+00 0.8488E-01 0.2722E-01
-0.3066E-01 -0.9227E-01 -0.1556E+00 -0.2194E+00
-0.2820E+00 -0.3457E+00 -0.4063E+00 -0.4642E+00
-0.5175E+00 -0.5680E+00 -0.6114E+00 -0.6505E+00

Time history of water pressure at element NEF1:

-0.1078E+02 -0.5418E+01 -0.8449E+01 -0.3967E+01
-0.4992E+01 -0.6965E+01 -0.1683E+02 -0.1349E+02
-0.9470E+01 -0.9469E+01 -0.1122E+02 -0.1097E+02
-0.1436E+02 -0.1703E+01 0.3806E+00 0.1418E+01
0.5397E+01 0.7437E+01 0.1416E+02 0.2340E+02
0.2221E+02 0.2560E+02 0.2672E+02 0.3108E+02
0.3203E+02 0.3409E+02 0.2815E+02 0.2687E+02
0.2621E+02 0.2091E+02 0.1897E+02 0.1098E+02
0.3977E+01 0.8235E+00 -0.6376E+01 -0.1105E+02
-0.1927E+02 -0.2443E+02 -0.3116E+02 -0.3298E+02
-0.3833E+02 -0.4277E+02 -0.4386E+02 -0.4737E+02
-0.4478E+02 -0.4502E+02 -0.4407E+02 -0.4236E+02
-0.3932E+02 -0.3631E+02 -0.3192E+02 -0.2895E+02
-0.2556E+02 -0.2139E+02 -0.1704E+02 -0.1309E+02
-0.8987E+01 -0.5147E+01 -0.1651E+01 0.3350E+01
0.6486E+01 0.1091E+02 0.1416E+02 0.1769E+02
0.2115E+02 0.2395E+02 0.2675E+02 0.2854E+02
0.3047E+02 0.3119E+02 0.3207E+02 0.3196E+02
0.3133E+02 0.3053E+02 0.2913E+02 0.2792E+02
0.2609E+02 0.2433E+02 0.2219E+02 0.2038E+02
0.1817E+02 0.1608E+02 0.1412E+02 0.1229E+02
0.1088E+02 0.9605E+01 0.8789E+01 0.8245E+01
0.8429E+01 0.8660E+01 0.9296E+01 0.1059E+02
0.1183E+02 0.1389E+02 0.1553E+02 0.1762E+02
0.1931E+02 0.2142E+02 0.2316E+02 0.2480E+02
0.2600E+02 0.2745E+02 0.2782E+02 0.2928E+02
0.2914E+02 0.3022E+02 0.2962E+02 0.3023E+02
0.2967E+02 0.3005E+02 0.2976E+02 0.2958E+02
0.2951E+02 0.2881E+02 0.2869E+02 0.2748E+02
0.2701E+02 0.2516E+02 0.2398E+02 0.2148E+02
0.2017E+02 0.1664E+02 0.1422E+02 0.9985E+01

0.6711E+01	0.1830E+01	-0.2182E+01	-0.6634E+01	-0.6162E+00	0.2053E+01	0.4190E+01	0.7482E+01
-0.1146E+02	-0.1565E+02	-0.2091E+02	-0.2455E+02	0.9541E+01	0.1192E+02	0.1339E+02	0.1467E+02
-0.2956E+02	-0.3259E+02	-0.3655E+02	-0.3869E+02	0.1747E+02	0.1758E+02	0.1817E+02	0.1849E+02
-0.4131E+02	-0.4235E+02	-0.4345E+02	-0.4357E+02	0.1858E+02	0.1769E+02	0.1683E+02	0.1456E+02
-0.4351E+02	-0.4244E+02	-0.4072E+02	-0.3829E+02	0.1344E+02	0.1127E+02	0.8751E+01	0.6676E+01
-0.3537E+02	-0.3251E+02	-0.2938E+02	-0.2577E+02	0.3001E+01	0.1274E+00	-0.3874E+01	-0.7432E+01
-0.2241E+02	-0.1896E+02	-0.1596E+02	-0.1262E+02	-0.1096E+02	-0.1462E+02	-0.1784E+02	-0.2109E+02
-0.9726E+01	-0.6853E+01	-0.4398E+01	-0.2437E+01	-0.2427E+02	-0.2623E+02	-0.2910E+02	-0.3069E+02
-0.3314E+00	0.1211E+01	0.2830E+01	0.4124E+01	-0.3209E+02	-0.3354E+02	-0.3364E+02	-0.3333E+02
0.5432E+01	0.6740E+01	0.7644E+01	0.7903E+01	-0.3264E+02	-0.3138E+02	-0.2966E+02	-0.2644E+02
0.8362E+01	0.8391E+01	0.8466E+01	0.8968E+01	-0.2320E+02	-0.1904E+02	-0.1492E+02	-0.1024E+02
0.8053E+01	0.8118E+01	0.7769E+01	0.7185E+01	-0.5923E+01	0.1608E+00	0.5642E+01	0.1095E+02
0.6710E+01	0.5268E+01	0.4922E+01	0.3733E+01	0.1667E+02	0.2265E+02	0.2811E+02	0.3376E+02
0.2557E+01	0.1572E+01	0.1438E+00	-0.1246E+01	0.3810E+02	0.4290E+02	0.4670E+02	0.4997E+02
-0.2580E+01	-0.4664E+01	-0.5473E+01	-0.7430E+01	0.5276E+02	0.5602E+02	0.5615E+02	0.5692E+02
-0.8541E+01	-0.1081E+02	-0.1130E+02	-0.1233E+02	0.5782E+02	0.5666E+02	0.5540E+02	0.5324E+02
-0.1328E+02	-0.1387E+02	-0.1390E+02	-0.1311E+02	0.4996E+02	0.4669E+02	0.4265E+02	0.3782E+02
-0.1258E+02	-0.1181E+02	-0.1064E+02	-0.9427E+01	0.3302E+02	0.2735E+02	0.2165E+02	0.1591E+02
-0.7762E+01	-0.5995E+01	-0.4175E+01	-0.2424E+01	0.8782E+01	0.2444E+01	-0.3939E+01	-0.1023E+02
-0.7115E-01	0.1916E+01	0.3875E+01	0.6143E+01	-0.1665E+02	-0.2212E+02	-0.2903E+02	-0.3372E+02
0.8298E+01	0.1018E+02	0.1231E+02	0.1450E+02	-0.3894E+02	-0.4292E+02	-0.4596E+02	-0.4898E+02
0.1587E+02	0.1832E+02	0.1923E+02	0.2111E+02	-0.5045E+02	-0.5352E+02	-0.5225E+02	-0.5224E+02
0.2217E+02	0.2318E+02	0.2368E+02	0.2375E+02	-0.5140E+02	-0.4853E+02	-0.4717E+02	-0.4329E+02
0.2390E+02	0.2347E+02	0.2250E+02	0.2074E+02	-0.3886E+02	-0.3433E+02	-0.2851E+02	-0.2303E+02
0.1967E+02	0.1697E+02	0.1471E+02	0.1139E+02	-0.1632E+02	-0.1036E+02	-0.4164E+01	0.2840E+01
0.8342E+01	0.4950E+01	0.5624E+00	-0.3481E+01	0.8999E+01	0.1659E+02	0.2258E+02	0.2865E+02
-0.7491E+01	-0.1189E+02	-0.1597E+02	-0.2088E+02	0.3352E+02	0.3782E+02	0.4191E+02	0.4644E+02
-0.2429E+02	-0.2798E+02	-0.3173E+02	-0.3487E+02	0.4976E+02	0.5163E+02	0.5349E+02	0.5406E+02
-0.3779E+02	-0.3952E+02	-0.4091E+02	-0.4245E+02	0.5410E+02	0.5342E+02	0.5210E+02	0.5007E+02
-0.4332E+02	-0.4341E+02	-0.4310E+02	-0.4224E+02	0.4859E+02	0.4468E+02	0.4057E+02	0.3669E+02
-0.4066E+02	-0.3874E+02	-0.3734E+02	-0.3450E+02	0.3247E+02	0.2861E+02	0.2307E+02	0.1854E+02
-0.3217E+02	-0.2944E+02	-0.2693E+02	-0.2393E+02	0.1343E+02	0.8404E+01	0.3880E+01	-0.6043E+00
-0.2010E+02	-0.1668E+02	-0.1347E+02	-0.1106E+02	-0.4748E+01	-0.9232E+01	-0.1228E+02	-0.1657E+02
-0.7324E+01	-0.4522E+01	-0.1879E+01	0.1391E+01	-0.1888E+02	-0.2147E+02	-0.2237E+02	-0.2352E+02
0.3585E+01	0.6040E+01	0.9055E+01	0.1080E+02	-0.2404E+02	-0.2370E+02	-0.2365E+02	-0.2314E+02
0.1212E+02	0.1485E+02	0.1585E+02	0.1642E+02	-0.2103E+02	-0.1982E+02	-0.1721E+02	-0.1464E+02
0.1737E+02	0.1806E+02	0.1748E+02	0.1756E+02	-0.1191E+02	-0.8032E+01	-0.4508E+01	-0.9112E+00
0.1741E+02	0.1585E+02	0.1537E+02	0.1319E+02	0.3190E+01	0.7273E+01	0.1091E+02	0.1495E+02
0.1172E+02	0.1090E+02	0.8179E+01	0.6258E+01	0.1838E+02	0.2177E+02	0.2427E+02	0.2737E+02
0.4322E+01	0.1526E+01	-0.1652E+01	-0.4258E+01	0.2989E+02	0.3041E+02	0.3250E+02	0.3371E+02
-0.6104E+01	-0.7889E+01	-0.9163E+01	-0.1143E+02	0.3394E+02	0.3336E+02	0.3316E+02	0.3166E+02
-0.1195E+02	-0.1333E+02	-0.1344E+02	-0.1378E+02	0.3025E+02	0.2819E+02	0.2589E+02	0.2354E+02
-0.1414E+02	-0.1341E+02	-0.1268E+02	-0.1122E+02	0.2040E+02	0.1787E+02	0.1431E+02	0.1117E+02
-0.1014E+02	-0.7923E+01	-0.4874E+01	-0.3372E+01	0.7302E+01	0.4138E+01	0.1581E+01	-0.1394E+01

-0.4929E+01	-0.8056E+01	-0.1051E+02	-0.1322E+02	0.1224E+02	0.1043E+02	0.8581E+01	0.6186E+01
-0.1465E+02	-0.1619E+02	-0.1742E+02	-0.1862E+02	0.3813E+01	0.3955E+00	-0.1953E+01	-0.4794E+01
-0.1920E+02	-0.2038E+02	-0.1998E+02	-0.1979E+02	-0.7780E+01	-0.9633E+01	-0.1315E+02	-0.1566E+02
-0.1940E+02	-0.1905E+02	-0.1750E+02	-0.1696E+02	-0.1783E+02	-0.2015E+02	-0.2245E+02	-0.2374E+02
-0.1604E+02	-0.1466E+02	-0.1357E+02	-0.1280E+02	-0.2481E+02	-0.2619E+02	-0.2648E+02	-0.2712E+02
-0.1224E+02	-0.1093E+02	-0.1146E+02	-0.1084E+02	-0.2687E+02	-0.2641E+02	-0.2541E+02	-0.2461E+02
-0.1058E+02	-0.1023E+02	-0.1071E+02	-0.1151E+02	-0.2194E+02	-0.2086E+02	-0.1919E+02	-0.1744E+02
-0.1245E+02	-0.1311E+02	-0.1489E+02	-0.1628E+02	-0.1463E+02	-0.1248E+02	-0.9978E+01	-0.7698E+01
-0.1804E+02	-0.2045E+02	-0.2160E+02	-0.2446E+02	-0.5468E+01	-0.3608E+01	-0.1889E+01	-0.4078E+00
-0.2645E+02	-0.2798E+02	-0.3047E+02	-0.3297E+02	0.1361E+01	0.1566E+01	0.2762E+01	0.2276E+01
-0.3511E+02	-0.3621E+02	-0.3762E+02	-0.3886E+02	0.2409E+01	0.1829E+01	0.1043E+01	-0.8613E+00
-0.3895E+02	-0.4036E+02	-0.3862E+02	-0.3896E+02	-0.2593E+01	-0.5154E+01	-0.7561E+01	-0.1111E+02
-0.3767E+02	-0.3597E+02	-0.3315E+02	-0.3041E+02	-0.1404E+02	-0.1791E+02	-0.2041E+02	-0.2432E+02
-0.2735E+02	-0.2399E+02	-0.1905E+02	-0.1490E+02	-0.2790E+02	-0.3134E+02	-0.3480E+02	-0.3834E+02
-0.9075E+01	-0.4274E+01	0.1214E+01	0.6309E+01	-0.4104E+02	-0.4338E+02	-0.4554E+02	-0.4717E+02
0.1182E+02	0.1848E+02	0.2369E+02	0.2969E+02	-0.4788E+02	-0.4825E+02	-0.4869E+02	-0.4791E+02
0.3597E+02	0.4055E+02	0.4549E+02	0.4985E+02	-0.4592E+02	-0.4379E+02	-0.4105E+02	-0.3728E+02
0.5407E+02	0.5777E+02	0.6012E+02	0.6325E+02	-0.3295E+02	-0.2789E+02	-0.2257E+02	-0.1631E+02
0.6516E+02	0.6566E+02	0.6659E+02	0.6637E+02	-0.9753E+01	-0.2124E+01	0.5033E+01	0.1292E+02
0.6467E+02	0.6312E+02	0.6022E+02	0.5732E+02	0.2067E+02	0.2842E+02	0.3656E+02	0.4410E+02
0.5354E+02	0.4934E+02	0.4476E+02	0.3921E+02	0.5175E+02	0.5926E+02	0.6633E+02	0.7270E+02
0.3308E+02	0.2730E+02	0.2111E+02	0.1437E+02	0.7873E+02	0.8406E+02	0.8860E+02	0.9179E+02
0.8257E+01	0.1246E+01	-0.5733E+01	-0.1087E+02	0.9529E+02	0.9710E+02	0.9828E+02	0.9821E+02
-0.1655E+02	-0.2314E+02	-0.2826E+02	-0.3383E+02	0.9776E+02	0.9627E+02	0.9381E+02	0.9089E+02
-0.3747E+02	-0.4158E+02	-0.4445E+02	-0.4763E+02	0.8672E+02	0.8168E+02	0.7609E+02	0.6995E+02
-0.4912E+02	-0.5021E+02	-0.5026E+02	-0.4989E+02	0.6377E+02	0.5665E+02	0.4918E+02	0.4174E+02
-0.4933E+02	-0.4773E+02	-0.4572E+02	-0.4336E+02	0.3393E+02	0.2596E+02	0.1799E+02	0.1007E+02
-0.3930E+02	-0.3573E+02	-0.3193E+02	-0.2741E+02	0.2831E+01	-0.4458E+01	-0.1161E+02	-0.1822E+02
-0.2272E+02	-0.1816E+02	-0.1377E+02	-0.8433E+01	-0.2400E+02	-0.2961E+02	-0.3456E+02	-0.3851E+02
-0.3574E+01	0.5894E+00	0.5046E+01	0.9571E+01	-0.4206E+02	-0.4480E+02	-0.4687E+02	-0.4851E+02
0.1315E+02	0.1626E+02	0.2000E+02	0.2203E+02	-0.4906E+02	-0.4912E+02	-0.4936E+02	-0.4798E+02
0.2352E+02	0.2572E+02	0.2677E+02	0.2762E+02	-0.4676E+02	-0.4501E+02	-0.4276E+02	-0.3983E+02
0.2668E+02	0.2616E+02	0.2530E+02	0.2471E+02	-0.3725E+02	-0.3424E+02	-0.3109E+02	-0.2776E+02
0.2264E+02	0.2025E+02	0.1715E+02	0.1560E+02	-0.2470E+02	-0.2180E+02	-0.1875E+02	-0.1615E+02
0.1237E+02	0.8462E+01	0.5673E+01	0.1415E+01	-0.1338E+02	-0.1148E+02	-0.9023E+01	-0.7519E+01
-0.1423E+01	-0.4420E+01	-0.6760E+01	-0.9550E+01	-0.6347E+01	-0.5362E+01	-0.4744E+01	-0.4549E+01
-0.1180E+02	-0.1460E+02	-0.1654E+02	-0.1771E+02	-0.4478E+01	-0.4845E+01	-0.5308E+01	-0.6180E+01
-0.1877E+02	-0.1987E+02	-0.2058E+02	-0.2024E+02	-0.6913E+01	-0.8124E+01	-0.9074E+01	-0.1041E+02
-0.1950E+02	-0.1875E+02	-0.1738E+02	-0.1599E+02	-0.1164E+02	-0.1306E+02	-0.1361E+02	-0.1472E+02
-0.1463E+02	-0.1200E+02	-0.9766E+01	-0.7911E+01	-0.1539E+02	-0.1571E+02	-0.1582E+02	-0.1590E+02
-0.5047E+01	-0.2720E+01	-0.3500E-01	0.3355E+01	-0.1559E+02	-0.1504E+02	-0.1387E+02	-0.1250E+02
0.5557E+01	0.7648E+01	0.9858E+01	0.1205E+02	-0.1040E+02	-0.8360E+01	-0.5991E+01	-0.3297E+01
0.1291E+02	0.1441E+02	0.1529E+02	0.1575E+02	-0.4080E+00	0.2414E+01	0.5613E+01	0.8938E+01
0.1554E+02	0.1538E+02	0.1477E+02	0.1326E+02	0.1236E+02	0.1567E+02	0.1876E+02	0.2191E+02

0.2488E+02 0.2739E+02 0.2962E+02 0.3159E+02
0.3330E+02 0.3406E+02 0.3525E+02 0.3513E+02
0.3497E+02 0.3402E+02 0.3282E+02 0.3124E+02
0.2884E+02 0.2626E+02 0.2326E+02 0.1975E+02
0.1610E+02 0.1205E+02 0.8036E+01 0.3637E+01
-0.6154E+00 -0.4788E+01 -0.9198E+01 -0.1324E+02
-0.1698E+02 -0.2062E+02 -0.2405E+02 -0.2680E+02
-0.2953E+02 -0.3137E+02 -0.3282E+02 -0.3409E+02
-0.3428E+02 -0.3439E+02 -0.3320E+02 -0.3193E+02
-0.3017E+02 -0.2804E+02 -0.2523E+02 -0.2217E+02
-0.1894E+02 -0.1495E+02 -0.1095E+02 -0.6426E+01
-0.2181E+01 0.2020E+01 0.5991E+01 0.9960E+01
0.1408E+02 0.1746E+02 0.2088E+02 0.2348E+02
0.2573E+02 0.2783E+02 0.2910E+02 0.2947E+02
0.2953E+02 0.2906E+02 0.2801E+02 0.2608E+02
0.2360E+02 0.2064E+02 0.1690E+02 0.1260E+02
0.8451E+01 0.3886E+01 -0.1610E+01 -0.6665E+01
-0.1208E+02 -0.1715E+02 -0.2266E+02 -0.2815E+02
-0.3316E+02 -0.3776E+02 -0.4195E+02 -0.4605E+02
-0.4953E+02 -0.5223E+02 -0.5432E+02 -0.5622E+02
-0.5713E+02 -0.5705E+02 -0.5632E+02 -0.5514E+02
-0.5289E+02 -0.4994E+02 -0.4690E+02 -0.4282E+02
-0.3823E+02 -0.3316E+02 -0.2775E+02 -0.2170E+02
-0.1574E+02 -0.9279E+01 -0.2851E+01 0.3489E+01
0.1034E+02 0.1623E+02 0.2221E+02 0.2764E+02
0.3298E+02 0.3793E+02 0.4231E+02 0.4545E+02
0.4921E+02 0.5151E+02 0.5332E+02 0.5452E+02
0.5492E+02 0.5471E+02 0.5431E+02 0.5255E+02
0.5045E+02 0.4761E+02 0.4506E+02 0.4133E+02
0.3714E+02 0.3307E+02 0.2849E+02 0.2357E+02
0.1903E+02 0.1444E+02 0.9528E+01 0.5351E+01
0.9493E+00 -0.3161E+01 -0.6976E+01 -0.1047E+02
-0.1327E+02 -0.1589E+02 -0.1770E+02 -0.1912E+02
-0.2058E+02 -0.2128E+02 -0.2148E+02 -0.2093E+02
-0.2037E+02 -0.1922E+02 -0.1780E+02 -0.1655E+02
-0.1429E+02 -0.1240E+02 -0.1014E+02 -0.7879E+01
-0.5289E+01 -0.3274E+01 -0.5869E+00 0.1320E+01
0.3122E+01 0.4523E+01 0.5984E+01 0.7579E+01
0.8075E+01 0.8344E+01 0.8491E+01 0.8471E+01
0.8084E+01 0.6820E+01 0.5551E+01 0.4236E+01
0.2660E+01 0.8037E+00 -0.1268E+01 -0.3159E+01
-0.5412E+01 -0.7346E+01 -0.9637E+01 -0.1078E+02
-0.1327E+02 -0.1474E+02 -0.1581E+02 -0.1646E+02

Time history of water pressure at element NEF2:

0.2028E+02 0.1020E+02 0.1567E+02 0.8237E+01
0.1037E+02 0.1390E+02 0.2911E+02 0.2423E+02
0.1888E+02 0.1922E+02 0.2172E+02 0.2185E+02
0.2641E+02 0.1294E+02 0.1175E+02 0.1171E+02
0.8356E+01 0.7008E+01 0.1895E+00 -0.1004E+02
-0.9000E+01 -0.1385E+02 -0.1679E+02 -0.2447E+02
-0.2890E+02 -0.3565E+02 -0.3279E+02 -0.3681E+02
-0.4252E+02 -0.4247E+02 -0.4781E+02 -0.4505E+02
-0.4416E+02 -0.4904E+02 -0.4848E+02 -0.5160E+02
-0.4996E+02 -0.5246E+02 -0.5288E+02 -0.5874E+02
-0.6019E+02 -0.6199E+02 -0.6570E+02 -0.6628E+02
-0.7036E+02 -0.7111E+02 -0.7155E+02 -0.7136E+02
-0.7093E+02 -0.6945E+02 -0.6773E+02 -0.6449E+02
-0.6073E+02 -0.5647E+02 -0.5184E+02 -0.4640E+02
-0.4085E+02 -0.3477E+02 -0.2856E+02 -0.2250E+02
-0.1622E+02 -0.1026E+02 -0.4477E+01 0.1020E+01
0.6137E+01 0.1074E+02 0.1505E+02 0.1837E+02
0.2193E+02 0.2424E+02 0.2685E+02 0.2838E+02
0.2984E+02 0.3100E+02 0.3147E+02 0.3235E+02
0.3250E+02 0.3284E+02 0.3254E+02 0.3316E+02
0.3243E+02 0.3299E+02 0.3180E+02 0.3179E+02
0.3011E+02 0.3063E+02 0.2817E+02 0.2797E+02
0.2604E+02 0.2466E+02 0.2443E+02 0.2251E+02
0.2289E+02 0.2176E+02 0.2290E+02 0.2349E+02
0.2585E+02 0.2826E+02 0.3098E+02 0.3541E+02
0.3965E+02 0.4447E+02 0.5063E+02 0.5451E+02
0.6190E+02 0.6551E+02 0.7216E+02 0.7497E+02
0.7994E+02 0.8175E+02 0.8477E+02 0.8622E+02
0.8656E+02 0.8698E+02 0.8511E+02 0.8446E+02
0.8100E+02 0.7947E+02 0.7447E+02 0.7278E+02
0.6627E+02 0.6495E+02 0.5858E+02 0.5732E+02
0.5214E+02 0.5074E+02 0.4795E+02 0.4618E+02
0.4597E+02 0.4366E+02 0.4577E+02 0.4386E+02
0.4645E+02 0.4520E+02 0.4733E+02 0.4649E+02
0.4773E+02 0.4720E+02 0.4763E+02 0.4676E+02
0.4652E+02 0.4549E+02 0.4442E+02 0.4335E+02
0.4223E+02 0.4107E+02 0.3974E+02 0.3882E+02
0.3842E+02 0.3770E+02 0.3768E+02 0.3800E+02
0.3842E+02 0.3947E+02 0.4055E+02 0.4248E+02
0.4417E+02 0.4644E+02 0.4839E+02 0.5109E+02
0.5282E+02 0.5530E+02 0.5728E+02 0.5925E+02
0.6051E+02 0.6232E+02 0.6311E+02 0.6377E+02
0.6446E+02 0.6475E+02 0.6513E+02 0.6513E+02

0.6537E+02	0.6612E+02	0.6685E+02	0.6792E+02	0.9062E+02	0.9463E+02	0.9457E+02	0.9788E+02
0.6904E+02	0.7019E+02	0.7137E+02	0.7251E+02	0.9688E+02	0.9894E+02	0.9717E+02	0.9970E+02
0.7370E+02	0.7447E+02	0.7526E+02	0.7588E+02	0.9656E+02	0.9860E+02	0.9700E+02	0.9900E+02
0.7620E+02	0.7605E+02	0.7569E+02	0.7546E+02	0.9853E+02	0.1011E+03	0.1021E+03	0.1040E+03
0.7386E+02	0.7381E+02	0.7187E+02	0.7138E+02	0.1058E+03	0.1090E+03	0.1122E+03	0.1143E+03
0.6903E+02	0.6910E+02	0.6670E+02	0.6712E+02	0.1181E+03	0.1200E+03	0.1229E+03	0.1250E+03
0.6549E+02	0.6524E+02	0.6530E+02	0.6468E+02	0.1264E+03	0.1271E+03	0.1271E+03	0.1264E+03
0.6536E+02	0.6484E+02	0.6670E+02	0.6563E+02	0.1256E+03	0.1240E+03	0.1206E+03	0.1176E+03
0.6728E+02	0.6615E+02	0.6770E+02	0.6612E+02	0.1143E+03	0.1094E+03	0.1064E+03	0.1015E+03
0.6653E+02	0.6363E+02	0.6375E+02	0.6014E+02	0.9809E+02	0.9284E+02	0.9096E+02	0.8666E+02
0.5882E+02	0.5482E+02	0.5230E+02	0.4816E+02	0.8436E+02	0.8299E+02	0.8072E+02	0.8024E+02
0.4490E+02	0.4113E+02	0.3667E+02	0.3373E+02	0.7991E+02	0.7949E+02	0.7985E+02	0.8017E+02
0.3007E+02	0.2835E+02	0.2508E+02	0.2413E+02	0.8046E+02	0.8242E+02	0.8153E+02	0.8328E+02
0.2148E+02	0.2337E+02	0.2193E+02	0.2589E+02	0.8318E+02	0.8482E+02	0.8225E+02	0.8308E+02
0.2549E+02	0.3043E+02	0.3075E+02	0.3669E+02	0.8067E+02	0.7931E+02	0.7667E+02	0.7549E+02
0.3784E+02	0.4343E+02	0.4442E+02	0.4835E+02	0.7218E+02	0.6837E+02	0.6532E+02	0.6141E+02
0.5044E+02	0.5218E+02	0.5414E+02	0.5349E+02	0.5760E+02	0.5456E+02	0.5122E+02	0.4807E+02
0.5638E+02	0.5361E+02	0.5570E+02	0.5169E+02	0.4611E+02	0.4191E+02	0.3967E+02	0.3741E+02
0.5400E+02	0.5017E+02	0.5282E+02	0.5048E+02	0.3557E+02	0.3357E+02	0.3366E+02	0.3182E+02
0.5312E+02	0.5349E+02	0.5674E+02	0.5869E+02	0.3271E+02	0.3181E+02	0.3245E+02	0.3278E+02
0.6319E+02	0.6824E+02	0.7289E+02	0.7997E+02	0.3388E+02	0.3449E+02	0.3572E+02	0.3788E+02
0.8560E+02	0.9353E+02	0.9939E+02	0.1071E+03	0.4063E+02	0.4341E+02	0.4522E+02	0.4887E+02
0.1123E+03	0.1194E+03	0.1235E+03	0.1274E+03	0.5124E+02	0.5530E+02	0.5803E+02	0.6119E+02
0.1294E+03	0.1311E+03	0.1305E+03	0.1294E+03	0.6468E+02	0.6912E+02	0.7256E+02	0.7659E+02
0.1266E+03	0.1238E+03	0.1182E+03	0.1135E+03	0.8115E+02	0.8407E+02	0.8862E+02	0.9261E+02
0.1071E+03	0.1019E+03	0.9408E+02	0.8990E+02	0.9592E+02	0.9874E+02	0.1023E+03	0.1049E+03
0.8295E+02	0.8012E+02	0.7467E+02	0.7313E+02	0.1070E+03	0.1084E+03	0.1097E+03	0.1105E+03
0.7018E+02	0.6979E+02	0.6961E+02	0.7105E+02	0.1104E+03	0.1088E+03	0.1078E+03	0.1056E+03
0.7267E+02	0.7494E+02	0.7754E+02	0.8102E+02	0.1035E+03	0.9979E+02	0.9743E+02	0.9322E+02
0.8304E+02	0.8480E+02	0.8722E+02	0.8724E+02	0.8855E+02	0.8487E+02	0.7931E+02	0.7408E+02
0.8853E+02	0.8672E+02	0.8722E+02	0.8395E+02	0.6908E+02	0.6336E+02	0.5867E+02	0.5404E+02
0.8338E+02	0.7834E+02	0.7842E+02	0.7359E+02	0.4862E+02	0.4317E+02	0.3926E+02	0.3447E+02
0.7351E+02	0.6904E+02	0.6933E+02	0.6626E+02	0.3111E+02	0.2761E+02	0.2483E+02	0.2231E+02
0.6755E+02	0.6624E+02	0.6798E+02	0.7030E+02	0.1942E+02	0.1839E+02	0.1691E+02	0.1641E+02
0.7281E+02	0.7739E+02	0.7993E+02	0.8748E+02	0.1527E+02	0.1646E+02	0.1722E+02	0.1864E+02
0.8959E+02	0.9800E+02	0.9957E+02	0.1079E+03	0.2042E+02	0.2379E+02	0.2621E+02	0.2938E+02
0.1080E+03	0.1145E+03	0.1129E+03	0.1178E+03	0.3255E+02	0.3531E+02	0.3892E+02	0.4218E+02
0.1153E+03	0.1152E+03	0.1111E+03	0.1086E+03	0.4642E+02	0.4867E+02	0.5244E+02	0.5481E+02
0.1043E+03	0.9882E+02	0.9426E+02	0.8604E+02	0.5846E+02	0.6093E+02	0.6338E+02	0.6530E+02
0.8106E+02	0.7320E+02	0.6949E+02	0.6146E+02	0.6781E+02	0.6894E+02	0.6986E+02	0.6975E+02
0.6051E+02	0.5338E+02	0.5405E+02	0.5017E+02	0.7123E+02	0.7069E+02	0.7118E+02	0.6939E+02
0.5282E+02	0.5066E+02	0.5379E+02	0.5477E+02	0.6894E+02	0.6791E+02	0.6645E+02	0.6473E+02
0.5969E+02	0.6347E+02	0.6730E+02	0.7149E+02	0.6223E+02	0.6080E+02	0.5877E+02	0.5656E+02
0.7691E+02	0.8087E+02	0.8473E+02	0.8880E+02	0.5530E+02	0.5258E+02	0.5105E+02	0.4924E+02

0.4841E+02	0.4583E+02	0.4558E+02	0.4378E+02	0.2212E+01	0.2974E+01	0.4306E+01	0.4382E+01
0.4367E+02	0.4255E+02	0.4267E+02	0.4198E+02	0.5123E+01	0.5281E+01	0.5660E+01	0.5439E+01
0.4255E+02	0.4181E+02	0.4298E+02	0.4333E+02	0.5644E+01	0.5109E+01	0.5274E+01	0.4957E+01
0.4377E+02	0.4431E+02	0.4531E+02	0.4629E+02	0.5039E+01	0.4432E+01	0.4319E+01	0.4333E+01
0.4719E+02	0.4768E+02	0.4931E+02	0.5057E+02	0.4917E+01	0.4741E+01	0.5046E+01	0.5613E+01
0.5250E+02	0.5308E+02	0.5429E+02	0.5484E+02	0.6334E+01	0.7349E+01	0.8616E+01	0.9601E+01
0.5616E+02	0.5693E+02	0.5772E+02	0.5814E+02	0.1100E+02	0.1214E+02	0.1423E+02	0.1518E+02
0.5772E+02	0.5855E+02	0.5805E+02	0.5746E+02	0.1700E+02	0.1872E+02	0.2070E+02	0.2194E+02
0.5744E+02	0.5607E+02	0.5555E+02	0.5370E+02	0.2392E+02	0.2501E+02	0.2694E+02	0.2779E+02
0.5180E+02	0.5014E+02	0.4791E+02	0.4533E+02	0.2929E+02	0.3007E+02	0.3098E+02	0.3091E+02
0.4311E+02	0.4028E+02	0.3806E+02	0.3552E+02	0.3135E+02	0.3114E+02	0.3080E+02	0.3028E+02
0.3316E+02	0.2976E+02	0.2775E+02	0.2449E+02	0.2952E+02	0.2846E+02	0.2722E+02	0.2566E+02
0.2257E+02	0.1984E+02	0.1783E+02	0.1508E+02	0.2409E+02	0.2188E+02	0.2015E+02	0.1794E+02
0.1322E+02	0.1140E+02	0.1036E+02	0.8637E+01	0.1628E+02	0.1379E+02	0.1176E+02	0.9322E+01
0.7346E+01	0.5957E+01	0.4696E+01	0.3035E+01	0.7710E+01	0.5610E+01	0.4113E+01	0.2272E+01
0.2898E+01	0.1981E+01	0.6998E+00	0.1767E+00	0.1234E+01	-0.2802E+00	-0.8941E+00	-0.1710E+01
-0.1437E+01	-0.1784E+01	-0.3147E+01	-0.4232E+01	-0.1870E+01	-0.2214E+01	-0.1788E+01	-0.1734E+01
-0.5048E+01	-0.7059E+01	-0.8618E+01	-0.9466E+01	-0.5995E+00	-0.3157E-01	0.1137E+01	0.2148E+01
-0.1111E+02	-0.1301E+02	-0.1446E+02	-0.1660E+02	0.4053E+01	0.5362E+01	0.6920E+01	0.8535E+01
-0.1885E+02	-0.2030E+02	-0.2218E+02	-0.2445E+02	0.1062E+02	0.1177E+02	0.1368E+02	0.1480E+02
-0.2594E+02	-0.2820E+02	-0.3026E+02	-0.3141E+02	0.1635E+02	0.1714E+02	0.1858E+02	0.1843E+02
-0.3311E+02	-0.3443E+02	-0.3602E+02	-0.3695E+02	0.1922E+02	0.1901E+02	0.1897E+02	0.1821E+02
-0.3768E+02	-0.3806E+02	-0.3746E+02	-0.3817E+02	0.1741E+02	0.1607E+02	0.1474E+02	0.1266E+02
-0.3695E+02	-0.3603E+02	-0.3396E+02	-0.3252E+02	0.1063E+02	0.8041E+01	0.5512E+01	0.2416E+01
-0.2981E+02	-0.2710E+02	-0.2351E+02	-0.1977E+02	-0.1632E+00	-0.3737E+01	-0.6609E+01	-0.1001E+02
-0.1597E+02	-0.1155E+02	-0.6491E+01	-0.1676E+01	-0.1263E+02	-0.1641E+02	-0.1902E+02	-0.2201E+02
0.4498E+01	0.9685E+01	0.1588E+02	0.2165E+02	-0.2440E+02	-0.2687E+02	-0.2855E+02	-0.3038E+02
0.2746E+02	0.3453E+02	0.4044E+02	0.4491E+02	-0.3117E+02	-0.3233E+02	-0.3248E+02	-0.3252E+02
0.5160E+02	0.5674E+02	0.6230E+02	0.6667E+02	-0.3157E+02	-0.3092E+02	-0.2896E+02	-0.2696E+02
0.7092E+02	0.7489E+02	0.7819E+02	0.8080E+02	-0.2409E+02	-0.2154E+02	-0.1770E+02	-0.1431E+02
0.8333E+02	0.8433E+02	0.8547E+02	0.8518E+02	-0.1014E+02	-0.5991E+01	-0.1028E+01	0.3386E+01
0.8479E+02	0.8333E+02	0.8174E+02	0.7888E+02	0.8622E+01	0.1315E+02	0.1840E+02	0.2283E+02
0.7585E+02	0.7178E+02	0.6781E+02	0.6292E+02	0.2762E+02	0.3168E+02	0.3623E+02	0.3969E+02
0.5824E+02	0.5236E+02	0.4677E+02	0.4051E+02	0.4335E+02	0.4620E+02	0.4880E+02	0.5052E+02
0.3441E+02	0.2804E+02	0.2224E+02	0.1552E+02	0.5237E+02	0.5282E+02	0.5367E+02	0.5307E+02
0.9675E+01	0.3265E+01	-0.2710E+01	-0.8521E+01	0.5265E+02	0.5097E+02	0.4924E+02	0.4658E+02
-0.1322E+02	-0.1840E+02	-0.2278E+02	-0.2708E+02	0.4385E+02	0.4000E+02	0.3637E+02	0.3185E+02
-0.3067E+02	-0.3368E+02	-0.3608E+02	-0.3861E+02	0.2753E+02	0.2195E+02	0.1743E+02	0.1157E+02
-0.3935E+02	-0.4060E+02	-0.4101E+02	-0.4131E+02	0.6300E+01	0.3375E+00	-0.4673E+01	-0.1089E+02
-0.4028E+02	-0.3999E+02	-0.3840E+02	-0.3700E+02	-0.1581E+02	-0.2136E+02	-0.2627E+02	-0.3137E+02
-0.3464E+02	-0.3274E+02	-0.3012E+02	-0.2784E+02	-0.3572E+02	-0.4004E+02	-0.4360E+02	-0.4742E+02
-0.2487E+02	-0.2244E+02	-0.1950E+02	-0.1713E+02	-0.4988E+02	-0.5301E+02	-0.5460E+02	-0.5647E+02
-0.1355E+02	-0.1116E+02	-0.8680E+01	-0.6841E+01	-0.5723E+02	-0.5837E+02	-0.5858E+02	-0.5866E+02
-0.3869E+01	-0.2477E+01	-0.5547E+00	0.7167E+00	-0.5807E+02	-0.5741E+02	-0.5597E+02	-0.5465E+02

-0.5279E+02 -0.5102E+02 -0.4885E+02 -0.4690E+02
-0.4404E+02 -0.4214E+02 -0.3921E+02 -0.3720E+02
-0.3442E+02 -0.3247E+02 -0.2987E+02 -0.2790E+02
-0.2518E+02 -0.2359E+02 -0.2139E+02 -0.1963E+02
-0.1762E+02 -0.1655E+02 -0.1440E+02 -0.1336E+02
-0.1138E+02 -0.1040E+02 -0.8687E+01 -0.7369E+01
-0.5451E+01 -0.4338E+01 -0.2469E+01 -0.1274E+01
0.8180E+00 0.2328E+01 0.4553E+01 0.6206E+01
0.8775E+01 0.1061E+02 0.1321E+02 0.1516E+02
0.1807E+02 0.2019E+02 0.2328E+02 0.2554E+02
0.2832E+02 0.3056E+02 0.3347E+02 0.3546E+02
0.3805E+02 0.3979E+02 0.4207E+02 0.4328E+02
0.4513E+02 0.4586E+02 0.4705E+02 0.4757E+02
0.4799E+02 0.4774E+02 0.4731E+02 0.4643E+02
0.4528E+02 0.4361E+02 0.4171E+02 0.3910E+02
0.3683E+02 0.3367E+02 0.3073E+02 0.2736E+02
0.2399E+02 0.2012E+02 0.1655E+02 0.1260E+02
0.9215E+01 0.5071E+01 0.1691E+01 -0.2177E+01
-0.5138E+01 -0.8689E+01 -0.1102E+02 -0.1417E+02
-0.1626E+02 -0.1835E+02 -0.1967E+02 -0.2086E+02
-0.2189E+02 -0.2224E+02 -0.2181E+02 -0.2186E+02
-0.2083E+02 -0.2012E+02 -0.1817E+02 -0.1733E+02
-0.1490E+02 -0.1307E+02 -0.1064E+02 -0.8467E+01
-0.5860E+01 -0.3767E+01 -0.1060E+01 0.1203E+01
0.3695E+01 0.5294E+01 0.7104E+01 0.8584E+01
0.1021E+02 0.1074E+02 0.1200E+02 0.1185E+02
0.1221E+02 0.1132E+02 0.1119E+02 0.9541E+01
0.8603E+01 0.6633E+01 0.4652E+01 0.2335E+01
0.3389E-01 -0.3019E+01 -0.5383E+01 -0.8666E+01
-0.1113E+02 -0.1444E+02 -0.1714E+02 -0.2029E+02
-0.2245E+02 -0.2511E+02 -0.2674E+02 -0.2923E+02

Time history of water pressure at element NEF3:

0.6113E+01 0.2900E+01 0.4273E+01 0.1810E+01
0.2099E+01 0.2743E+01 0.6642E+01 0.4720E+01
0.2590E+01 0.2034E+01 0.2005E+01 0.1121E+01
0.1237E+01 -0.3565E+01 -0.5107E+01 -0.6391E+01
-0.8321E+01 -0.9748E+01 -0.1179E+02 -0.1368E+02
-0.1399E+02 -0.1447E+02 -0.1446E+02 -0.1403E+02
-0.1311E+02 -0.1163E+02 -0.1047E+02 -0.8503E+01
-0.5998E+01 -0.3983E+01 -0.9194E+00 0.8735E+00
0.3069E+01 0.6403E+01 0.8708E+01 0.1172E+02
0.1358E+02 0.1632E+02 0.1838E+02 0.2156E+02
0.2341E+02 0.2498E+02 0.2660E+02 0.2686E+02
0.2774E+02 0.2723E+02 0.2621E+02 0.2465E+02
0.2285E+02 0.2040E+02 0.1798E+02 0.1435E+02
0.1048E+02 0.6488E+01 0.2334E+01 -0.2516E+01
-0.7349E+01 -0.1280E+02 -0.1868E+02 -0.2265E+02
-0.2899E+02 -0.3282E+02 -0.3821E+02 -0.4217E+02
-0.4487E+02 -0.4754E+02 -0.4840E+02 -0.4997E+02
-0.4811E+02 -0.4758E+02 -0.4323E+02 -0.4027E+02
-0.3553E+02 -0.3008E+02 -0.2463E+02 -0.1795E+02
-0.1214E+02 -0.5634E+01 0.4139E+00 0.7124E+01
0.1267E+02 0.1881E+02 0.2364E+02 0.2862E+02
0.3236E+02 0.3636E+02 0.3881E+02 0.4133E+02
0.4266E+02 0.4337E+02 0.4409E+02 0.4341E+02
0.4274E+02 0.4097E+02 0.3979E+02 0.3729E+02
0.3512E+02 0.3240E+02 0.2940E+02 0.2630E+02
0.2334E+02 0.1968E+02 0.1652E+02 0.1229E+02
0.9029E+01 0.4359E+01 0.1007E+01 -0.3683E+01
-0.7678E+01 -0.1223E+02 -0.1633E+02 -0.2045E+02
-0.2491E+02 -0.2840E+02 -0.3182E+02 -0.3490E+02
-0.3794E+02 -0.4000E+02 -0.4221E+02 -0.4311E+02
-0.4412E+02 -0.4411E+02 -0.4391E+02 -0.4301E+02
-0.4180E+02 -0.4014E+02 -0.3816E+02 -0.3591E+02
-0.3315E+02 -0.3053E+02 -0.2769E+02 -0.2474E+02
-0.2194E+02 -0.1873E+02 -0.1582E+02 -0.1306E+02
-0.1021E+02 -0.7468E+01 -0.4767E+01 -0.2270E+01
-0.8392E-01 0.2057E+01 0.4089E+01 0.6305E+01
0.8032E+01 0.9758E+01 0.1190E+02 0.1304E+02
0.1547E+02 0.1665E+02 0.1857E+02 0.1986E+02
0.2127E+02 0.2223E+02 0.2365E+02 0.2431E+02
0.2528E+02 0.2620E+02 0.2722E+02 0.2764E+02
0.2806E+02 0.2899E+02 0.2945E+02 0.2981E+02
0.3081E+02 0.3173E+02 0.3190E+02 0.3378E+02
0.3466E+02 0.3624E+02 0.3689E+02 0.3859E+02
0.3952E+02 0.4105E+02 0.4169E+02 0.4202E+02
0.4287E+02 0.4333E+02 0.4356E+02 0.4359E+02
0.4290E+02 0.4181E+02 0.4105E+02 0.4018E+02
0.3813E+02 0.3665E+02 0.3442E+02 0.3148E+02
0.2882E+02 0.2583E+02 0.2321E+02 0.1951E+02
0.1607E+02 0.1302E+02 0.9296E+01 0.5608E+01
0.2255E+01 -0.1250E+01 -0.4750E+01 -0.8459E+01
-0.1083E+02 -0.1422E+02 -0.1737E+02 -0.2058E+02
-0.2326E+02 -0.2567E+02 -0.2822E+02 -0.3155E+02
-0.3346E+02 -0.3623E+02 -0.3838E+02 -0.4057E+02
-0.4265E+02 -0.4391E+02 -0.4540E+02 -0.4593E+02
-0.4669E+02 -0.4628E+02 -0.4615E+02 -0.4530E+02

−0.4355E+02 −0.4206E+02 −0.4002E+02 −0.3785E+02 0.3074E+01 −0.4843E+01 −0.1233E+02 −0.1922E+02
−0.3510E+02 −0.3235E+02 −0.2878E+02 −0.2607E+02 −0.2605E+02 −0.3099E+02 −0.3777E+02 −0.4272E+02
−0.2296E+02 −0.1975E+02 −0.1694E+02 −0.1389E+02 −0.4815E+02 −0.5283E+02 −0.5610E+02 −0.5866E+02
−0.1157E+02 −0.8954E+01 −0.7549E+01 −0.6058E+01 −0.6075E+02 −0.6238E+02 −0.6222E+02 −0.6298E+02
−0.4677E+01 −0.3959E+01 −0.2773E+01 −0.3663E+01 −0.6230E+02 −0.6046E+02 −0.5798E+02 −0.5519E+02
−0.3777E+01 −0.4264E+01 −0.5669E+01 −0.7548E+01 −0.5071E+02 −0.4721E+02 −0.4340E+02 −0.3816E+02
−0.8723E+01 −0.1074E+02 −0.1365E+02 −0.1577E+02 −0.3300E+02 −0.2717E+02 −0.2186E+02 −0.1517E+02
−0.1893E+02 −0.2174E+02 −0.2490E+02 −0.2764E+02 −0.1006E+02 −0.4384E+01 0.8239E+00 0.6768E+01
−0.3041E+02 −0.3221E+02 −0.3506E+02 −0.3817E+02 0.1132E+02 0.1443E+02 0.1851E+02 0.2151E+02
−0.3941E+02 −0.4157E+02 −0.4307E+02 −0.4372E+02 0.2376E+02 0.2538E+02 0.2647E+02 0.2698E+02
−0.4509E+02 −0.4525E+02 −0.4463E+02 −0.4390E+02 0.2717E+02 0.2677E+02 0.2550E+02 0.2287E+02
−0.4422E+02 −0.4181E+02 −0.4018E+02 −0.3905E+02 0.2061E+02 0.1766E+02 0.1455E+02 0.1176E+02
−0.3525E+02 −0.3213E+02 −0.2880E+02 −0.2400E+02 0.8000E+01 0.4112E+01 0.2422E+00 −0.3476E+01
−0.2025E+02 −0.1535E+02 −0.1011E+02 −0.5090E+01 −0.7722E+01 −0.1168E+02 −0.1537E+02 −0.1830E+02
−0.2958E+00 0.6218E+01 0.1058E+02 0.1550E+02 −0.2169E+02 −0.2364E+02 −0.2613E+02 −0.2761E+02
0.2079E+02 0.2488E+02 0.2841E+02 0.3196E+02 −0.2921E+02 −0.3094E+02 −0.3101E+02 −0.3031E+02
0.3551E+02 0.3852E+02 0.4115E+02 0.4219E+02 −0.2990E+02 −0.2896E+02 −0.2705E+02 −0.2520E+02
0.4374E+02 0.4479E+02 0.4502E+02 0.4489E+02 −0.2310E+02 −0.2011E+02 −0.1707E+02 −0.1407E+02
0.4378E+02 0.4249E+02 0.4033E+02 0.3803E+02 −0.1042E+02 −0.6600E+01 −0.2835E+01 0.9146E+00
0.3437E+02 0.3135E+02 0.2784E+02 0.2301E+02 0.3743E+01 0.7736E+01 0.1109E+02 0.1401E+02
0.1851E+02 0.1389E+02 0.8075E+01 0.3926E+01 0.1639E+02 0.1879E+02 0.2023E+02 0.2218E+02
−0.1052E+01 −0.6353E+01 −0.1165E+02 −0.1631E+02 0.2306E+02 0.2411E+02 0.2362E+02 0.2323E+02
−0.1996E+02 −0.2405E+02 −0.2834E+02 −0.3100E+02 0.2199E+02 0.2051E+02 0.1781E+02 0.1547E+02
−0.3328E+02 −0.3571E+02 −0.3744E+02 −0.3903E+02 0.1177E+02 0.7996E+01 0.4544E+01 0.4517E+00
−0.3837E+02 −0.3785E+02 −0.3668E+02 −0.3447E+02 −0.4724E+01 −0.8073E+01 −0.1312E+02 −0.1817E+02
−0.3276E+02 −0.2923E+02 −0.2622E+02 −0.2214E+02 −0.2316E+02 −0.2753E+02 −0.3247E+02 −0.3641E+02
−0.1768E+02 −0.1316E+02 −0.7815E+01 −0.2512E+01 −0.3999E+02 −0.4327E+02 −0.4637E+02 −0.4864E+02
0.2406E+01 0.8936E+01 0.1305E+02 0.1902E+02 −0.5130E+02 −0.5280E+02 −0.5388E+02 −0.5497E+02
0.2344E+02 0.2768E+02 0.3191E+02 0.3576E+02 −0.5440E+02 −0.5458E+02 −0.5320E+02 −0.5349E+02
0.3852E+02 0.4062E+02 0.4250E+02 0.4466E+02 −0.5171E+02 −0.4964E+02 −0.4782E+02 −0.4624E+02
0.4582E+02 0.4676E+02 0.4629E+02 0.4608E+02 −0.4400E+02 −0.4081E+02 −0.3896E+02 −0.3617E+02
0.4436E+02 0.4370E+02 0.4233E+02 0.4053E+02 −0.3348E+02 −0.3201E+02 −0.2855E+02 −0.2787E+02
0.3884E+02 0.3696E+02 0.3485E+02 0.3365E+02 −0.2538E+02 −0.2349E+02 −0.2179E+02 −0.2044E+02
0.3101E+02 0.2969E+02 0.2780E+02 0.2647E+02 −0.2022E+02 −0.1935E+02 −0.1861E+02 −0.1928E+02
0.2554E+02 0.2539E+02 0.2357E+02 0.2376E+02 −0.1928E+02 −0.1927E+02 −0.1976E+02 −0.2142E+02
0.2425E+02 0.2444E+02 0.2565E+02 0.2714E+02 −0.2200E+02 −0.2230E+02 −0.2456E+02 −0.2522E+02
0.2780E+02 0.3040E+02 0.3224E+02 0.3458E+02 −0.2583E+02 −0.2681E+02 −0.2737E+02 −0.2857E+02
0.3760E+02 0.4055E+02 0.4351E+02 0.4706E+02 −0.2912E+02 −0.2950E+02 −0.3018E+02 −0.2912E+02
0.4934E+02 0.5291E+02 0.5573E+02 0.5879E+02 −0.2869E+02 −0.2854E+02 −0.2651E+02 −0.2399E+02
0.6087E+02 0.6394E+02 0.6433E+02 0.6638E+02 −0.2348E+02 −0.2064E+02 −0.1888E+02 −0.1528E+02
0.6680E+02 0.6734E+02 0.6729E+02 0.6662E+02 −0.1224E+02 −0.8615E+01 −0.5159E+01 −0.9701E+00
0.6564E+02 0.6207E+02 0.6039E+02 0.5696E+02 0.2889E+01 0.6872E+01 0.1093E+02 0.1535E+02
0.5218E+02 0.4858E+02 0.4191E+02 0.3692E+02 0.1919E+02 0.2259E+02 0.2589E+02 0.2968E+02
0.3039E+02 0.2362E+02 0.1684E+02 0.9526E+01 0.3220E+02 0.3411E+02 0.3652E+02 0.3734E+02

0.3851E+02	0.3913E+02	0.3885E+02	0.3761E+02	-0.2093E+02	-0.1885E+02	-0.1625E+02	-0.1362E+02
0.3679E+02	0.3505E+02	0.3283E+02	0.3050E+02	-0.1047E+02	-0.7059E+01	-0.3699E+01	-0.6210E+00
0.2684E+02	0.2323E+02	0.1924E+02	0.1425E+02	0.2875E+01	0.6139E+01	0.9242E+01	0.1217E+02
0.1093E+02	0.5841E+01	0.3885E+00	-0.3911E+01	0.1478E+02	0.1740E+02	0.1860E+02	0.2061E+02
-0.9252E+01	-0.1353E+02	-0.1783E+02	-0.2195E+02	0.2138E+02	0.2215E+02	0.2211E+02	0.2169E+02
-0.2559E+02	-0.2934E+02	-0.3265E+02	-0.3443E+02	0.2085E+02	0.1972E+02	0.1760E+02	0.1534E+02
-0.3696E+02	-0.3787E+02	-0.3913E+02	-0.3928E+02	0.1277E+02	0.1007E+02	0.6369E+01	0.3148E+01
-0.3953E+02	-0.3756E+02	-0.3656E+02	-0.3433E+02	-0.3161E+00	-0.4024E+01	-0.7415E+01	-0.1140E+02
-0.3081E+02	-0.2840E+02	-0.2481E+02	-0.2003E+02	-0.1473E+02	-0.1814E+02	-0.2142E+02	-0.2418E+02
-0.1585E+02	-0.1030E+02	-0.5927E+01	-0.5147E+00	-0.2662E+02	-0.2860E+02	-0.3074E+02	-0.3160E+02
0.3826E+01	0.9980E+01	0.1503E+02	0.1997E+02	-0.3242E+02	-0.3274E+02	-0.3199E+02	-0.3119E+02
0.2482E+02	0.2961E+02	0.3381E+02	0.3770E+02	-0.3011E+02	-0.2801E+02	-0.2587E+02	-0.2315E+02
0.4048E+02	0.4414E+02	0.4647E+02	0.4826E+02	-0.2004E+02	-0.1649E+02	-0.1282E+02	-0.8713E+01
0.4853E+02	0.5057E+02	0.4989E+02	0.4972E+02	-0.4778E+01	-0.2523E+00	0.3962E+01	0.8039E+01
0.4933E+02	0.4744E+02	0.4566E+02	0.4342E+02	0.1227E+02	0.1613E+02	0.1967E+02	0.2301E+02
0.4023E+02	0.3844E+02	0.3443E+02	0.3029E+02	0.2625E+02	0.2845E+02	0.3027E+02	0.3212E+02
0.2695E+02	0.2352E+02	0.1993E+02	0.1579E+02	0.3275E+02	0.3342E+02	0.3330E+02	0.3236E+02
0.1213E+02	0.9237E+01	0.6137E+01	0.3204E+01	0.3100E+02	0.2917E+02	0.2668E+02	0.2376E+02
0.1842E+01	-0.8758E+00	-0.2078E+01	-0.3128E+01	0.2053E+02	0.1691E+02	0.1258E+02	0.8667E+01
-0.3362E+01	-0.3538E+01	-0.3234E+01	-0.1857E+01	0.4106E+01	-0.4823E+00	-0.4947E+01	-0.9494E+01
-0.5992E+00	0.4070E+00	0.2766E+01	0.5235E+01	-0.1408E+02	-0.1840E+02	-0.2231E+02	-0.2628E+02
0.8304E+01	0.1198E+02	0.1463E+02	0.1799E+02	-0.2940E+02	-0.3241E+02	-0.3479E+02	-0.3667E+02
0.2132E+02	0.2439E+02	0.2813E+02	0.3101E+02	-0.3834E+02	-0.3918E+02	-0.3957E+02	-0.3969E+02
0.3362E+02	0.3626E+02	0.3813E+02	0.4025E+02	-0.3896E+02	-0.3791E+02	-0.3590E+02	-0.3411E+02
0.4124E+02	0.4306E+02	0.4316E+02	0.4370E+02	-0.3133E+02	-0.2843E+02	-0.2482E+02	-0.2152E+02
0.4247E+02	0.4213E+02	0.4071E+02	0.3871E+02	-0.1775E+02	-0.1399E+02	-0.1052E+02	-0.6593E+01
0.3598E+02	0.3379E+02	0.3099E+02	0.2761E+02	-0.2625E+01	0.6617E+00	0.3647E+01	0.6790E+01
0.2407E+02	0.2026E+02	0.1609E+02	0.1251E+02	0.9449E+01	0.1145E+02	0.1350E+02	0.1444E+02
0.8701E+01	0.4909E+01	0.1065E+01	-0.2238E+01	0.1560E+02	0.1546E+02	0.1510E+02	0.1403E+02
-0.5386E+01	-0.7991E+01	-0.1080E+02	-0.1249E+02	0.1262E+02	0.1066E+02	0.8119E+01	0.4807E+01
-0.1412E+02	-0.1481E+02	-0.1559E+02	-0.1587E+02	0.1414E+01	-0.2523E+01	-0.6124E+01	-0.1096E+02
-0.1499E+02	-0.1435E+02	-0.1285E+02	-0.1068E+02	-0.1529E+02	-0.1986E+02	-0.2468E+02	-0.2929E+02
-0.8268E+01	-0.5298E+01	-0.2412E+01	0.7909E+00	-0.3399E+02	-0.3819E+02	-0.4211E+02	-0.4564E+02
0.4559E+01	0.8724E+01	0.1264E+02	0.1658E+02	-0.4912E+02	-0.5197E+02	-0.5441E+02	-0.5612E+02
0.2050E+02	0.2459E+02	0.2822E+02	0.3194E+02	-0.5682E+02	-0.5753E+02	-0.5693E+02	-0.5645E+02
0.3493E+02	0.3785E+02	0.4004E+02	0.4234E+02	-0.5524E+02	-0.5332E+02	-0.5044E+02	-0.4736E+02
0.4383E+02	0.4542E+02	0.4550E+02	0.4584E+02	-0.4388E+02	-0.3950E+02	-0.3502E+02	-0.2993E+02
0.4491E+02	0.4421E+02	0.4212E+02	0.4068E+02	-0.2529E+02	-0.1958E+02	-0.1418E+02	-0.8737E+01
0.3730E+02	0.3472E+02	0.3115E+02	0.2741E+02	-0.3320E+01	0.1946E+01	0.7161E+01	0.1237E+02
0.2309E+02	0.1896E+02	0.1449E+02	0.1011E+02	0.1718E+02	0.2155E+02	0.2528E+02	0.2873E+02
0.5554E+01	0.1232E+01	-0.3252E+01	-0.7125E+01	0.3140E+02	0.3431E+02	0.3560E+02	0.3720E+02
-0.1092E+02	-0.1406E+02	-0.1738E+02	-0.1994E+02	0.3762E+02	0.3765E+02	0.3721E+02	0.3622E+02
-0.2229E+02	-0.2368E+02	-0.2531E+02	-0.2561E+02	0.3497E+02	0.3282E+02	0.3040E+02	0.2780E+02
-0.2600E+02	-0.2534E+02	-0.2471E+02	-0.2291E+02	0.2493E+02	0.2129E+02	0.1778E+02	0.1404E+02

0.1078E+02 0.6696E+01 0.3173E+01 -0.5704E+00
-0.3553E+01 -0.7260E+01 -0.9807E+01 -0.1275E+02
-0.1452E+02 -0.1658E+02 -0.1790E+02 -0.1923E+02
-0.1980E+02 -0.2049E+02 -0.2005E+02 -0.2033E+02
-0.1954E+02 -0.1878E+02 -0.1790E+02 -0.1632E+02
-0.1493E+02 -0.1374E+02 -0.1226E+02 -0.1054E+02
-0.9357E+01 -0.8207E+01 -0.7014E+01 -0.6105E+01
-0.5308E+01 -0.5147E+01 -0.4984E+01 -0.5359E+01
-0.5444E+01 -0.6798E+01 -0.7904E+01 -0.9383E+01
-0.1122E+02 -0.1307E+02 -0.1529E+02 -0.1791E+02
-0.2049E+02 -0.2324E+02 -0.2602E+02 -0.2880E+02
-0.3112E+02 -0.3380E+02 -0.3583E+02 -0.3767E+02
-0.3933E+02 -0.4052E+02 -0.4100E+02 -0.4111E+02
-0.4125E+02 -0.4015E+02 -0.3883E+02 -0.3683E+02
-0.3414E+02 -0.3129E+02 -0.2761E+02 -0.2352E+02
-0.1862E+02 -0.1327E+02 -0.7858E+01 -0.1721E+01
0.4277E+01 0.1042E+02 0.1741E+02 0.2369E+02
0.3018E+02 0.3678E+02 0.4328E+02 0.4909E+02
0.5454E+02 0.5975E+02 0.6429E+02 0.6817E+02

Time history of relative displacement at landing gear 1

-0.3001E-03 -0.3742E-03 -0.4356E-03 -0.4920E-03
-0.5356E-03 -0.5944E-03 -0.7022E-03 -0.8389E-03
-0.9540E-03 -0.1063E-02 -0.1188E-02 -0.1330E-02
-0.1498E-02 -0.1650E-02 -0.1770E-02 -0.1899E-02
-0.2031E-02 -0.2163E-02 -0.2285E-02 -0.2370E-02
-0.2444E-02 -0.2524E-02 -0.2599E-02 -0.2661E-02
-0.2705E-02 -0.2736E-02 -0.2774E-02 -0.2826E-02
-0.2868E-02 -0.2910E-02 -0.2953E-02 -0.3003E-02
-0.3078E-02 -0.3157E-02 -0.3237E-02 -0.3324E-02
-0.3423E-02 -0.3534E-02 -0.3654E-02 -0.3772E-02
-0.3885E-02 -0.4010E-02 -0.4136E-02 -0.4264E-02
-0.4384E-02 -0.4491E-02 -0.4595E-02 -0.4692E-02
-0.4781E-02 -0.4858E-02 -0.4924E-02 -0.4981E-02
-0.5038E-02 -0.5092E-02 -0.5141E-02 -0.5188E-02
-0.5238E-02 -0.5292E-02 -0.5356E-02 -0.5423E-02
-0.5495E-02 -0.5575E-02 -0.5660E-02 -0.5755E-02
-0.5851E-02 -0.5948E-02 -0.6043E-02 -0.6137E-02
-0.6226E-02 -0.6308E-02 -0.6379E-02 -0.6435E-02
-0.6483E-02 -0.6532E-02 -0.6584E-02 -0.6637E-02
-0.6688E-02 -0.6738E-02 -0.6787E-02 -0.6835E-02
-0.6880E-02 -0.6923E-02 -0.6966E-02 -0.7012E-02
-0.7059E-02 -0.7109E-02 -0.7163E-02 -0.7222E-02
-0.7286E-02 -0.7358E-02 -0.7434E-02 -0.7515E-02
-0.7600E-02 -0.7690E-02 -0.7782E-02 -0.7874E-02
-0.7965E-02 -0.8054E-02 -0.8140E-02 -0.8221E-02
-0.8295E-02 -0.8363E-02 -0.8423E-02 -0.8477E-02
-0.8525E-02 -0.8567E-02 -0.8606E-02 -0.8640E-02
-0.8671E-02 -0.8700E-02 -0.8727E-02 -0.8753E-02
-0.8781E-02 -0.8810E-02 -0.8843E-02 -0.8880E-02
-0.8922E-02 -0.8969E-02 -0.9023E-02 -0.9081E-02
-0.9146E-02 -0.9214E-02 -0.9286E-02 -0.9360E-02
-0.9434E-02 -0.9509E-02 -0.9580E-02 -0.9649E-02
-0.9712E-02 -0.9770E-02 -0.9821E-02 -0.9865E-02
-0.9901E-02 -0.9930E-02 -0.9953E-02 -0.9970E-02
-0.9982E-02 -0.9991E-02 -0.9999E-02 -0.1001E-01
-0.1002E-01 -0.1004E-01 -0.1008E-01 -0.1012E-01
-0.1017E-01 -0.1023E-01 -0.1029E-01 -0.1037E-01
-0.1045E-01 -0.1053E-01 -0.1062E-01 -0.1071E-01
-0.1080E-01 -0.1089E-01 -0.1097E-01 -0.1105E-01
-0.1112E-01 -0.1119E-01 -0.1124E-01 -0.1129E-01
-0.1132E-01 -0.1135E-01 -0.1136E-01 -0.1137E-01
-0.1137E-01 -0.1136E-01 -0.1135E-01 -0.1133E-01
-0.1131E-01 -0.1128E-01 -0.1125E-01 -0.1122E-01
-0.1119E-01 -0.1116E-01 -0.1113E-01 -0.1109E-01
-0.1108E-01 -0.1108E-01 -0.1111E-01 -0.1115E-01
-0.1120E-01 -0.1126E-01 -0.1133E-01 -0.1141E-01
-0.1149E-01 -0.1157E-01 -0.1166E-01 -0.1174E-01
-0.1182E-01 -0.1190E-01 -0.1198E-01 -0.1205E-01
-0.1212E-01 -0.1218E-01 -0.1223E-01 -0.1228E-01
-0.1233E-01 -0.1237E-01 -0.1240E-01 -0.1243E-01
-0.1245E-01 -0.1247E-01 -0.1248E-01 -0.1248E-01
-0.1247E-01 -0.1246E-01 -0.1243E-01 -0.1239E-01
-0.1234E-01 -0.1227E-01 -0.1219E-01 -0.1209E-01
-0.1198E-01 -0.1189E-01 -0.1181E-01 -0.1175E-01
-0.1170E-01 -0.1167E-01 -0.1166E-01 -0.1165E-01
-0.1165E-01 -0.1166E-01 -0.1168E-01 -0.1171E-01
-0.1174E-01 -0.1178E-01 -0.1183E-01 -0.1188E-01
-0.1193E-01 -0.1199E-01 -0.1205E-01 -0.1211E-01
-0.1218E-01 -0.1224E-01 -0.1230E-01 -0.1235E-01
-0.1240E-01 -0.1244E-01 -0.1248E-01 -0.1251E-01
-0.1252E-01 -0.1253E-01 -0.1252E-01 -0.1250E-01
-0.1247E-01 -0.1243E-01 -0.1237E-01 -0.1230E-01
-0.1222E-01 -0.1212E-01 -0.1202E-01 -0.1190E-01
-0.1180E-01 -0.1171E-01 -0.1164E-01 -0.1159E-01
-0.1155E-01 -0.1153E-01 -0.1151E-01 -0.1151E-01
-0.1152E-01 -0.1153E-01 -0.1156E-01 -0.1158E-01
-0.1162E-01 -0.1165E-01 -0.1169E-01 -0.1172E-01

-0.1175E-01 -0.1179E-01 -0.1181E-01 -0.1184E-01 -0.9678E-02 -0.9666E-02 -0.9650E-02 -0.9631E-02
-0.1185E-01 -0.1187E-01 -0.1188E-01 -0.1188E-01 -0.9609E-02 -0.9585E-02 -0.9559E-02 -0.9531E-02
-0.1188E-01 -0.1187E-01 -0.1186E-01 -0.1185E-01 -0.9502E-02 -0.9472E-02 -0.9442E-02 -0.9411E-02
-0.1183E-01 -0.1181E-01 -0.1179E-01 -0.1177E-01 -0.9380E-02 -0.9350E-02 -0.9319E-02 -0.9289E-02
-0.1176E-01 -0.1174E-01 -0.1172E-01 -0.1170E-01 -0.9260E-02 -0.9231E-02 -0.9203E-02 -0.9176E-02
-0.1168E-01 -0.1167E-01 -0.1165E-01 -0.1164E-01 -0.9150E-02 -0.9124E-02 -0.9099E-02 -0.9075E-02
-0.1162E-01 -0.1161E-01 -0.1161E-01 -0.1160E-01 -0.9051E-02 -0.9029E-02 -0.9007E-02 -0.8986E-02
-0.1160E-01 -0.1159E-01 -0.1159E-01 -0.1159E-01 -0.8965E-02 -0.8946E-02 -0.8927E-02 -0.8910E-02
-0.1158E-01 -0.1158E-01 -0.1158E-01 -0.1157E-01 -0.8893E-02 -0.8878E-02 -0.8863E-02 -0.8851E-02
-0.1157E-01 -0.1157E-01 -0.1156E-01 -0.1156E-01 -0.8839E-02 -0.8829E-02 -0.8820E-02 -0.8814E-02
-0.1156E-01 -0.1155E-01 -0.1155E-01 -0.1155E-01 -0.8809E-02 -0.8806E-02 -0.8805E-02 -0.8807E-02
-0.1156E-01 -0.1156E-01 -0.1156E-01 -0.1157E-01 -0.8812E-02 -0.8819E-02 -0.8828E-02 -0.8836E-02
-0.1157E-01 -0.1158E-01 -0.1158E-01 -0.1159E-01 -0.8843E-02 -0.8848E-02 -0.8852E-02 -0.8853E-02
-0.1159E-01 -0.1159E-01 -0.1159E-01 -0.1159E-01 -0.8853E-02 -0.8850E-02 -0.8845E-02 -0.8838E-02
-0.1159E-01 -0.1158E-01 -0.1157E-01 -0.1157E-01 -0.8829E-02 -0.8818E-02 -0.8805E-02 -0.8790E-02
-0.1156E-01 -0.1155E-01 -0.1155E-01 -0.1155E-01 -0.8773E-02 -0.8755E-02 -0.8736E-02 -0.8716E-02
-0.1155E-01 -0.1156E-01 -0.1158E-01 -0.1160E-01 -0.8696E-02 -0.8675E-02 -0.8655E-02 -0.8634E-02
-0.1164E-01 -0.1167E-01 -0.1170E-01 -0.1173E-01 -0.8613E-02 -0.8593E-02 -0.8574E-02 -0.8555E-02
-0.1175E-01 -0.1177E-01 -0.1178E-01 -0.1178E-01 -0.8537E-02 -0.8520E-02 -0.8503E-02 -0.8488E-02
-0.1179E-01 -0.1178E-01 -0.1177E-01 -0.1176E-01 -0.8473E-02 -0.8459E-02 -0.8445E-02 -0.8432E-02
-0.1174E-01 -0.1171E-01 -0.1168E-01 -0.1164E-01 -0.8420E-02 -0.8408E-02 -0.8397E-02 -0.8387E-02
-0.1160E-01 -0.1155E-01 -0.1149E-01 -0.1143E-01 -0.8376E-02 -0.8367E-02 -0.8358E-02 -0.8349E-02
-0.1136E-01 -0.1129E-01 -0.1121E-01 -0.1113E-01 -0.8341E-02 -0.8333E-02 -0.8326E-02 -0.8320E-02
-0.1105E-01 -0.1097E-01 -0.1088E-01 -0.1080E-01 -0.8315E-02 -0.8310E-02 -0.8307E-02 -0.8304E-02
-0.1072E-01 -0.1064E-01 -0.1056E-01 -0.1049E-01 -0.8302E-02 -0.8301E-02 -0.8301E-02 -0.8302E-02
-0.1042E-01 -0.1036E-01 -0.1030E-01 -0.1025E-01 -0.8304E-02 -0.8307E-02 -0.8311E-02 -0.8315E-02
-0.1021E-01 -0.1017E-01 -0.1014E-01 -0.1012E-01 -0.8321E-02 -0.8328E-02 -0.8335E-02 -0.8343E-02
-0.1011E-01 -0.1011E-01 -0.1012E-01 -0.1013E-01 -0.8352E-02 -0.8362E-02 -0.8373E-02 -0.8386E-02
-0.1016E-01 -0.1019E-01 -0.1024E-01 -0.1029E-01 -0.8399E-02 -0.8412E-02 -0.8427E-02 -0.8442E-02
-0.1034E-01 -0.1038E-01 -0.1041E-01 -0.1044E-01 -0.8458E-02 -0.8474E-02 -0.8491E-02 -0.8508E-02
-0.1046E-01 -0.1047E-01 -0.1048E-01 -0.1048E-01 -0.8526E-02 -0.8543E-02 -0.8562E-02 -0.8580E-02
-0.1047E-01 -0.1046E-01 -0.1045E-01 -0.1044E-01 -0.8599E-02 -0.8618E-02 -0.8637E-02 -0.8656E-02
-0.1042E-01 -0.1039E-01 -0.1037E-01 -0.1034E-01 -0.8675E-02 -0.8694E-02 -0.8713E-02 -0.8732E-02
-0.1031E-01 -0.1028E-01 -0.1025E-01 -0.1021E-01 -0.8751E-02 -0.8769E-02 -0.8788E-02 -0.8805E-02
-0.1017E-01 -0.1013E-01 -0.1009E-01 -0.1004E-01 -0.8823E-02 -0.8840E-02 -0.8857E-02 -0.8873E-02
-0.9999E-02 -0.9953E-02 -0.9906E-02 -0.9859E-02 -0.8889E-02 -0.8904E-02 -0.8919E-02 -0.8933E-02
-0.9811E-02 -0.9764E-02 -0.9718E-02 -0.9673E-02 -0.8947E-02 -0.8960E-02 -0.8973E-02 -0.8986E-02
-0.9630E-02 -0.9589E-02 -0.9551E-02 -0.9516E-02 -0.8998E-02 -0.9009E-02 -0.9019E-02 -0.9029E-02
-0.9486E-02 -0.9459E-02 -0.9437E-02 -0.9420E-02 -0.9038E-02 -0.9047E-02 -0.9054E-02 -0.9061E-02
-0.9407E-02 -0.9400E-02 -0.9398E-02 -0.9401E-02 -0.9067E-02 -0.9072E-02 -0.9076E-02 -0.9079E-02
-0.9409E-02 -0.9423E-02 -0.9442E-02 -0.9465E-02 -0.9081E-02 -0.9082E-02 -0.9082E-02 -0.9082E-02
-0.9494E-02 -0.9527E-02 -0.9563E-02 -0.9595E-02 -0.9080E-02 -0.9078E-02 -0.9076E-02 -0.9073E-02
-0.9623E-02 -0.9646E-02 -0.9664E-02 -0.9678E-02 -0.9070E-02 -0.9067E-02 -0.9064E-02 -0.9061E-02
-0.9687E-02 -0.9691E-02 -0.9691E-02 -0.9687E-02 -0.9059E-02 -0.9058E-02 -0.9058E-02 -0.9059E-02

-0.9061E-02 -0.9064E-02 -0.9070E-02 -0.9077E-02 -0.9848E-02 -0.9848E-02 -0.9849E-02 -0.9849E-02
-0.9086E-02 -0.9097E-02 -0.9109E-02 -0.9122E-02 -0.9849E-02 -0.9849E-02 -0.9849E-02 -0.9848E-02
-0.9135E-02 -0.9148E-02 -0.9161E-02 -0.9174E-02 -0.9848E-02 -0.9847E-02 -0.9846E-02 -0.9844E-02
-0.9188E-02 -0.9202E-02 -0.9216E-02 -0.9230E-02 -0.9843E-02 -0.9842E-02 -0.9840E-02 -0.9839E-02
-0.9244E-02 -0.9259E-02 -0.9273E-02 -0.9288E-02 -0.9838E-02 -0.9837E-02 -0.9836E-02 -0.9835E-02
-0.9303E-02 -0.9318E-02 -0.9333E-02 -0.9348E-02 -0.9834E-02 -0.9833E-02 -0.9832E-02 -0.9832E-02
-0.9363E-02 -0.9377E-02 -0.9392E-02 -0.9406E-02 -0.9831E-02 -0.9831E-02 -0.9830E-02 -0.9830E-02
-0.9420E-02 -0.9434E-02 -0.9447E-02 -0.9459E-02 -0.9829E-02 -0.9829E-02 -0.9828E-02 -0.9827E-02
-0.9470E-02 -0.9480E-02 -0.9489E-02 -0.9497E-02 -0.9826E-02 -0.9824E-02 -0.9822E-02 -0.9820E-02
-0.9504E-02 -0.9509E-02 -0.9513E-02 -0.9516E-02 -0.9818E-02 -0.9815E-02 -0.9811E-02 -0.9808E-02
-0.9517E-02 -0.9517E-02 -0.9515E-02 -0.9512E-02 -0.9804E-02 -0.9799E-02 -0.9795E-02 -0.9790E-02
-0.9508E-02 -0.9502E-02 -0.9496E-02 -0.9489E-02 -0.9785E-02 -0.9779E-02 -0.9774E-02 -0.9769E-02
-0.9481E-02 -0.9473E-02 -0.9464E-02 -0.9456E-02 -0.9764E-02 -0.9759E-02 -0.9754E-02 -0.9749E-02
-0.9447E-02 -0.9439E-02 -0.9431E-02 -0.9424E-02 -0.9745E-02 -0.9741E-02 -0.9737E-02 -0.9734E-02
-0.9417E-02 -0.9411E-02 -0.9406E-02 -0.9401E-02 -0.9731E-02 -0.9729E-02 -0.9727E-02 -0.9725E-02
-0.9398E-02 -0.9395E-02 -0.9393E-02 -0.9391E-02 -0.9724E-02 -0.9724E-02 -0.9723E-02 -0.9723E-02
-0.9391E-02 -0.9391E-02 -0.9391E-02 -0.9392E-02 -0.9724E-02 -0.9725E-02 -0.9726E-02 -0.9728E-02
-0.9393E-02 -0.9394E-02 -0.9396E-02 -0.9397E-02 -0.9729E-02 -0.9731E-02 -0.9733E-02 -0.9735E-02
-0.9398E-02 -0.9399E-02 -0.9400E-02 -0.9401E-02 -0.9737E-02 -0.9738E-02 -0.9740E-02 -0.9742E-02
-0.9401E-02 -0.9401E-02 -0.9401E-02 -0.9401E-02 -0.9743E-02 -0.9744E-02 -0.9746E-02 -0.9746E-02
-0.9400E-02 -0.9399E-02 -0.9399E-02 -0.9398E-02 -0.9747E-02 -0.9748E-02 -0.9748E-02 -0.9748E-02
-0.9397E-02 -0.9397E-02 -0.9396E-02 -0.9396E-02 -0.9748E-02 -0.9748E-02 -0.9748E-02 -0.9748E-02
-0.9396E-02 -0.9396E-02 -0.9397E-02 -0.9398E-02 -0.9747E-02 -0.9746E-02 -0.9745E-02 -0.9745E-02
-0.9399E-02 -0.9401E-02 -0.9403E-02 -0.9406E-02 -0.9744E-02 -0.9743E-02 -0.9742E-02 -0.9740E-02
-0.9409E-02 -0.9412E-02 -0.9416E-02 -0.9420E-02 -0.9739E-02 -0.9738E-02 -0.9738E-02 -0.9737E-02
-0.9424E-02 -0.9429E-02 -0.9433E-02 -0.9438E-02 -0.9736E-02 -0.9736E-02 -0.9735E-02 -0.9735E-02
-0.9443E-02 -0.9448E-02 -0.9454E-02 -0.9459E-02 -0.9735E-02 -0.9736E-02 -0.9736E-02 -0.9737E-02
-0.9465E-02 -0.9471E-02 -0.9477E-02 -0.9484E-02 -0.9738E-02 -0.9739E-02 -0.9741E-02 -0.9743E-02
-0.9491E-02 -0.9498E-02 -0.9506E-02 -0.9514E-02 -0.9744E-02 -0.9746E-02 -0.9748E-02 -0.9750E-02
-0.9522E-02 -0.9531E-02 -0.9540E-02 -0.9550E-02 -0.9752E-02 -0.9754E-02 -0.9756E-02 -0.9758E-02
-0.9560E-02 -0.9570E-02 -0.9580E-02 -0.9590E-02 -0.9760E-02 -0.9762E-02 -0.9763E-02 -0.9764E-02
-0.9600E-02 -0.9610E-02 -0.9619E-02 -0.9629E-02 -0.9765E-02 -0.9766E-02 -0.9767E-02 -0.9767E-02
-0.9638E-02 -0.9646E-02 -0.9655E-02 -0.9662E-02 -0.9768E-02 -0.9768E-02 -0.9768E-02 -0.9767E-02
-0.9670E-02 -0.9677E-02 -0.9683E-02 -0.9689E-02 -0.9767E-02 -0.9767E-02 -0.9767E-02 -0.9766E-02
-0.9695E-02 -0.9700E-02 -0.9705E-02 -0.9709E-02 -0.9766E-02 -0.9766E-02 -0.9766E-02 -0.9766E-02
-0.9714E-02 -0.9718E-02 -0.9722E-02 -0.9726E-02 -0.9766E-02 -0.9766E-02 -0.9767E-02 -0.9768E-02
-0.9730E-02 -0.9735E-02 -0.9739E-02 -0.9743E-02 -0.9769E-02 -0.9770E-02 -0.9771E-02 -0.9773E-02
-0.9748E-02 -0.9752E-02 -0.9757E-02 -0.9761E-02 -0.9774E-02 -0.9776E-02 -0.9778E-02 -0.9781E-02
-0.9766E-02 -0.9771E-02 -0.9776E-02 -0.9781E-02 -0.9783E-02 -0.9786E-02 -0.9788E-02 -0.9791E-02
-0.9785E-02 -0.9790E-02 -0.9795E-02 -0.9799E-02 -0.9794E-02 -0.9797E-02 -0.9800E-02 -0.9804E-02
-0.9804E-02 -0.9808E-02 -0.9812E-02 -0.9816E-02 -0.9807E-02 -0.9810E-02 -0.9813E-02 -0.9816E-02
-0.9820E-02 -0.9824E-02 -0.9827E-02 -0.9830E-02 -0.9819E-02 -0.9822E-02 -0.9825E-02 -0.9828E-02
-0.9833E-02 -0.9835E-02 -0.9838E-02 -0.9840E-02 -0.9830E-02 -0.9832E-02 -0.9834E-02 -0.9836E-02
-0.9842E-02 -0.9844E-02 -0.9845E-02 -0.9847E-02 -0.9837E-02 -0.9839E-02 -0.9839E-02 -0.9840E-02

-0.9840E-02 -0.9840E-02 -0.9840E-02 -0.9839E-02
-0.9838E-02 -0.9837E-02 -0.9836E-02 -0.9835E-02
-0.9833E-02 -0.9831E-02 -0.9829E-02 -0.9828E-02
-0.9826E-02 -0.9824E-02 -0.9823E-02 -0.9821E-02
-0.9820E-02 -0.9819E-02 -0.9818E-02 -0.9817E-02
-0.9817E-02 -0.9816E-02 -0.9816E-02 -0.9817E-02
-0.9817E-02 -0.9818E-02 -0.9818E-02 -0.9819E-02

Time history of force provided by landing gear system

-0.2065E+03 -0.1035E+03 -0.1585E+03 -0.8612E+02
-0.1100E+03 -0.1493E+03 -0.3095E+03 -0.2706E+03
-0.2285E+03 -0.2492E+03 -0.2980E+03 -0.3219E+03
-0.4003E+03 -0.2612E+03 -0.2705E+03 -0.2951E+03
-0.2796E+03 -0.2903E+03 -0.2345E+03 -0.1388E+03
-0.1841E+03 -0.1587E+03 -0.1584E+03 -0.1036E+03
-0.8873E+02 -0.4807E+02 -0.1175E+03 -0.1085E+03
-0.8064E+02 -0.1163E+03 -0.9194E+02 -0.1559E+03
-0.1995E+03 -0.1783E+03 -0.2184E+03 -0.2160E+03
-0.2708E+03 -0.2770E+03 -0.3109E+03 -0.2723E+03
-0.2934E+03 -0.3074E+03 -0.2823E+03 -0.3040E+03
-0.2452E+03 -0.2384E+03 -0.2255E+03 -0.2097E+03
-0.1821E+03 -0.1635E+03 -0.1281E+03 -0.1260E+03
-0.1213E+03 -0.1106E+03 -0.9934E+02 -0.1041E+03
-0.1066E+03 -0.1226E+03 -0.1519E+03 -0.1363E+03
-0.1828E+03 -0.1795E+03 -0.2178E+03 -0.2358E+03
-0.2432E+03 -0.2639E+03 -0.2616E+03 -0.2924E+03
-0.2698E+03 -0.2947E+03 -0.2603E+03 -0.2666E+03
-0.2530E+03 -0.2334E+03 -0.2231E+03 -0.1943E+03
-0.1816E+03 -0.1608E+03 -0.1546E+03 -0.1298E+03
-0.1300E+03 -0.1121E+03 -0.1216E+03 -0.1147E+03
-0.1320E+03 -0.1248E+03 -0.1518E+03 -0.1557E+03
-0.1788E+03 -0.1976E+03 -0.2063E+03 -0.2316E+03
-0.2379E+03 -0.2591E+03 -0.2619E+03 -0.2723E+03
-0.2703E+03 -0.2707E+03 -0.2680E+03 -0.2571E+03
-0.2467E+03 -0.2351E+03 -0.2128E+03 -0.2097E+03
-0.1792E+03 -0.1787E+03 -0.1501E+03 -0.1510E+03
-0.1316E+03 -0.1343E+03 -0.1259E+03 -0.1279E+03
-0.1341E+03 -0.1365E+03 -0.1533E+03 -0.1574E+03
-0.1792E+03 -0.1834E+03 -0.2107E+03 -0.2099E+03
-0.2393E+03 -0.2327E+03 -0.2575E+03 -0.2493E+03
-0.2635E+03 -0.2553E+03 -0.2556E+03 -0.2502E+03
-0.2362E+03 -0.2351E+03 -0.2111E+03 -0.2106E+03
-0.1856E+03 -0.1832E+03 -0.1635E+03 -0.1601E+03
-0.1472E+03 -0.1455E+03 -0.1405E+03 -0.1425E+03
-0.1444E+03 -0.1510E+03 -0.1575E+03 -0.1683E+03
-0.1787E+03 -0.1905E+03 -0.2032E+03 -0.2134E+03
-0.2250E+03 -0.2335E+03 -0.2405E+03 -0.2459E+03
-0.2471E+03 -0.2477E+03 -0.2440E+03 -0.2391E+03
-0.2321E+03 -0.2213E+03 -0.2140E+03 -0.1987E+03
-0.1925E+03 -0.1767E+03 -0.1713E+03 -0.1595E+03
-0.1550E+03 -0.1499E+03 -0.1473E+03 -0.1491E+03
-0.1497E+03 -0.1569E+03 -0.1618E+03 -0.1716E+03
-0.1808E+03 -0.1905E+03 -0.2024E+03 -0.2104E+03
-0.2222E+03 -0.2275E+03 -0.2368E+03 -0.2382E+03
-0.2433E+03 -0.2406E+03 -0.2407E+03 -0.2349E+03
-0.2294E+03 -0.2223E+03 -0.2117E+03 -0.2058E+03
-0.1912E+03 -0.1885E+03 -0.1721E+03 -0.1732E+03
-0.1585E+03 -0.1627E+03 -0.1530E+03 -0.1588E+03
-0.1561E+03 -0.1623E+03 -0.1669E+03 -0.1725E+03
-0.1829E+03 -0.1872E+03 -0.2007E+03 -0.2035E+03
-0.2174E+03 -0.2177E+03 -0.2297E+03 -0.2270E+03
-0.2356E+03 -0.2299E+03 -0.2340E+03 -0.2259E+03
-0.2254E+03 -0.2163E+03 -0.2119E+03 -0.2030E+03
-0.1961E+03 -0.1887E+03 -0.1812E+03 -0.1765E+03
-0.1700E+03 -0.1688E+03 -0.1643E+03 -0.1674E+03
-0.1649E+03 -0.1725E+03 -0.1716E+03 -0.1828E+03
-0.1830E+03 -0.1961E+03 -0.1969E+03 -0.2093E+03
-0.2105E+03 -0.2199E+03 -0.2213E+03 -0.2259E+03
-0.2270E+03 -0.2261E+03 -0.2266E+03 -0.2207E+03
-0.2203E+03 -0.2106E+03 -0.2095E+03 -0.1979E+03
-0.1966E+03 -0.1851E+03 -0.1839E+03 -0.1746E+03
-0.1740E+03 -0.1685E+03 -0.1688E+03 -0.1678E+03
-0.1692E+03 -0.1722E+03 -0.1749E+03 -0.1809E+03
-0.1848E+03 -0.1921E+03 -0.1968E+03 -0.2036E+03
-0.2082E+03 -0.2133E+03 -0.2167E+03 -0.2194E+03
-0.2205E+03 -0.2207E+03 -0.2191E+03 -0.2171E+03
-0.2128E+03 -0.2093E+03 -0.2030E+03 -0.1988E+03
-0.1917E+03 -0.1877E+03 -0.1810E+03 -0.1783E+03
-0.1731E+03 -0.1723E+03 -0.1695E+03 -0.1708E+03
-0.1709E+03 -0.1742E+03 -0.1770E+03 -0.1817E+03
-0.1864E+03 -0.1918E+03 -0.1976E+03 -0.2026E+03
-0.2084E+03 -0.2121E+03 -0.2167E+03 -0.2184E+03
-0.2214E+03 -0.2203E+03 -0.2215E+03 -0.2175E+03
-0.2173E+03 -0.2110E+03 -0.2097E+03 -0.2020E+03
-0.2001E+03 -0.1923E+03 -0.1905E+03 -0.1841E+03
-0.1825E+03 -0.1786E+03 -0.1776E+03 -0.1771E+03
-0.1768E+03 -0.1797E+03 -0.1796E+03 -0.1855E+03
-0.1856E+03 -0.1935E+03 -0.1933E+03 -0.2017E+03

-0.2010E+03 -0.2085E+03 -0.2072E+03 -0.2125E+03 -0.1971E+03 -0.1971E+03 -0.1960E+03 -0.1957E+03
-0.2106E+03 -0.2129E+03 -0.2106E+03 -0.2098E+03 -0.1946E+03 -0.1941E+03 -0.1932E+03 -0.1927E+03
-0.2074E+03 -0.2038E+03 -0.2017E+03 -0.1963E+03 -0.1923E+03 -0.1918E+03 -0.1920E+03 -0.1915E+03
-0.1950E+03 -0.1890E+03 -0.1888E+03 -0.1832E+03 -0.1924E+03 -0.1920E+03 -0.1936E+03 -0.1933E+03
-0.1846E+03 -0.1804E+03 -0.1835E+03 -0.1812E+03 -0.1953E+03 -0.1950E+03 -0.1972E+03 -0.1970E+03
-0.1858E+03 -0.1854E+03 -0.1907E+03 -0.1920E+03 -0.1991E+03 -0.1988E+03 -0.2004E+03 -0.2001E+03
-0.1975E+03 -0.2001E+03 -0.2050E+03 -0.2080E+03 -0.2012E+03 -0.2008E+03 -0.2010E+03 -0.2005E+03
-0.2111E+03 -0.2139E+03 -0.2149E+03 -0.2168E+03 -0.1999E+03 -0.1996E+03 -0.1982E+03 -0.1980E+03
-0.2153E+03 -0.2159E+03 -0.2119E+03 -0.2115E+03 -0.1961E+03 -0.1960E+03 -0.1939E+03 -0.1941E+03
-0.2056E+03 -0.2042E+03 -0.1974E+03 -0.1953E+03 -0.1919E+03 -0.1925E+03 -0.1906E+03 -0.1916E+03
-0.1886E+03 -0.1865E+03 -0.1811E+03 -0.1794E+03 -0.1902E+03 -0.1914E+03 -0.1907E+03 -0.1920E+03
-0.1760E+03 -0.1752E+03 -0.1743E+03 -0.1746E+03 -0.1920E+03 -0.1934E+03 -0.1940E+03 -0.1952E+03
-0.1760E+03 -0.1776E+03 -0.1809E+03 -0.1835E+03 -0.1964E+03 -0.1972E+03 -0.1989E+03 -0.1992E+03
-0.1881E+03 -0.1912E+03 -0.1961E+03 -0.1991E+03 -0.2010E+03 -0.2008E+03 -0.2026E+03 -0.2019E+03
-0.2036E+03 -0.2060E+03 -0.2093E+03 -0.2105E+03 -0.2034E+03 -0.2023E+03 -0.2036E+03 -0.2022E+03
-0.2124E+03 -0.2122E+03 -0.2126E+03 -0.2109E+03 -0.2030E+03 -0.2016E+03 -0.2020E+03 -0.2007E+03
-0.2102E+03 -0.2072E+03 -0.2058E+03 -0.2021E+03 -0.2006E+03 -0.1997E+03 -0.1992E+03 -0.1987E+03
-0.2005E+03 -0.1967E+03 -0.1953E+03 -0.1922E+03 -0.1980E+03 -0.1979E+03 -0.1971E+03 -0.1973E+03
-0.1914E+03 -0.1896E+03 -0.1896E+03 -0.1892E+03 -0.1964E+03 -0.1970E+03 -0.1961E+03 -0.1969E+03
-0.1899E+03 -0.1911E+03 -0.1923E+03 -0.1947E+03 -0.1960E+03 -0.1968E+03 -0.1959E+03 -0.1967E+03
-0.1959E+03 -0.1992E+03 -0.2000E+03 -0.2035E+03 -0.1958E+03 -0.1964E+03 -0.1956E+03 -0.1960E+03
-0.2035E+03 -0.2066E+03 -0.2056E+03 -0.2079E+03 -0.1952E+03 -0.1953E+03 -0.1947E+03 -0.1946E+03
-0.2059E+03 -0.2069E+03 -0.2041E+03 -0.2039E+03 -0.1941E+03 -0.1938E+03 -0.1935E+03 -0.1931E+03
-0.2006E+03 -0.1994E+03 -0.1961E+03 -0.1942E+03 -0.1931E+03 -0.1926E+03 -0.1929E+03 -0.1924E+03
-0.1915E+03 -0.1893E+03 -0.1877E+03 -0.1856E+03 -0.1930E+03 -0.1926E+03 -0.1935E+03 -0.1931E+03
-0.1855E+03 -0.1837E+03 -0.1853E+03 -0.1840E+03 -0.1941E+03 -0.1938E+03 -0.1948E+03 -0.1946E+03
-0.1870E+03 -0.1864E+03 -0.1905E+03 -0.1903E+03 -0.1955E+03 -0.1953E+03 -0.1961E+03 -0.1958E+03
-0.1949E+03 -0.1950E+03 -0.1993E+03 -0.1996E+03 -0.1963E+03 -0.1960E+03 -0.1962E+03 -0.1958E+03
-0.2029E+03 -0.2032E+03 -0.2051E+03 -0.2052E+03 -0.1957E+03 -0.1954E+03 -0.1949E+03 -0.1946E+03
-0.2053E+03 -0.2053E+03 -0.2037E+03 -0.2035E+03 -0.1939E+03 -0.1938E+03 -0.1929E+03 -0.1930E+03
-0.2004E+03 -0.2001E+03 -0.1961E+03 -0.1960E+03 -0.1920E+03 -0.1923E+03 -0.1914E+03 -0.1920E+03
-0.1918E+03 -0.1920E+03 -0.1881E+03 -0.1887E+03 -0.1913E+03 -0.1921E+03 -0.1915E+03 -0.1925E+03
-0.1858E+03 -0.1868E+03 -0.1853E+03 -0.1867E+03 -0.1922E+03 -0.1932E+03 -0.1932E+03 -0.1941E+03
-0.1865E+03 -0.1883E+03 -0.1895E+03 -0.1913E+03 -0.1944E+03 -0.1951E+03 -0.1956E+03 -0.1961E+03
-0.1934E+03 -0.1950E+03 -0.1978E+03 -0.1989E+03 -0.1967E+03 -0.1969E+03 -0.1977E+03 -0.1975E+03
-0.2017E+03 -0.2022E+03 -0.2047E+03 -0.2043E+03 -0.1985E+03 -0.1980E+03 -0.1989E+03 -0.1983E+03
-0.2062E+03 -0.2050E+03 -0.2060E+03 -0.2041E+03 -0.1992E+03 -0.1985E+03 -0.1994E+03 -0.1986E+03
-0.2044E+03 -0.2020E+03 -0.2015E+03 -0.1990E+03 -0.1994E+03 -0.1989E+03 -0.1995E+03 -0.1991E+03
-0.1980E+03 -0.1957E+03 -0.1945E+03 -0.1928E+03 -0.1996E+03 -0.1995E+03 -0.1996E+03 -0.1998E+03
-0.1916E+03 -0.1906E+03 -0.1896E+03 -0.1895E+03 -0.1996E+03 -0.1999E+03 -0.1994E+03 -0.1999E+03
-0.1889E+03 -0.1895E+03 -0.1893E+03 -0.1906E+03 -0.1991E+03 -0.1995E+03 -0.1984E+03 -0.1988E+03
-0.1906E+03 -0.1923E+03 -0.1925E+03 -0.1943E+03 -0.1975E+03 -0.1978E+03 -0.1964E+03 -0.1965E+03
-0.1945E+03 -0.1962E+03 -0.1962E+03 -0.1976E+03 -0.1952E+03 -0.1951E+03 -0.1940E+03 -0.1938E+03
-0.1973E+03 -0.1983E+03 -0.1977E+03 -0.1981E+03 -0.1929E+03 -0.1927E+03 -0.1922E+03 -0.1920E+03

-0.1919E+03 -0.1917E+03 -0.1921E+03 -0.1919E+03 -0.1912E+03 -0.1915E+03 -0.1925E+03 -0.1929E+03
-0.1927E+03 -0.1926E+03 -0.1936E+03 -0.1935E+03 -0.1940E+03 -0.1946E+03 -0.1958E+03 -0.1963E+03
-0.1947E+03 -0.1947E+03 -0.1958E+03 -0.1958E+03 -0.1974E+03 -0.1979E+03 -0.1989E+03 -0.1993E+03
-0.1968E+03 -0.1967E+03 -0.1974E+03 -0.1972E+03 -0.2001E+03 -0.2004E+03 -0.2010E+03 -0.2012E+03
-0.1976E+03 -0.1973E+03 -0.1973E+03 -0.1970E+03 -0.2014E+03 -0.2016E+03 -0.2015E+03 -0.2015E+03
-0.1967E+03 -0.1963E+03 -0.1957E+03 -0.1953E+03 -0.2013E+03 -0.2012E+03 -0.2008E+03 -0.2007E+03
-0.1946E+03 -0.1944E+03 -0.1936E+03 -0.1936E+03 -0.2000E+03 -0.2000E+03 -0.1992E+03 -0.1991E+03
-0.1929E+03 -0.1930E+03 -0.1925E+03 -0.1929E+03 -0.1984E+03 -0.1982E+03 -0.1975E+03 -0.1974E+03
-0.1925E+03 -0.1931E+03 -0.1929E+03 -0.1937E+03 -0.1967E+03 -0.1965E+03 -0.1960E+03 -0.1957E+03
-0.1937E+03 -0.1946E+03 -0.1947E+03 -0.1955E+03 -0.1953E+03 -0.1950E+03 -0.1947E+03 -0.1943E+03
-0.1958E+03 -0.1965E+03 -0.1968E+03 -0.1972E+03 -0.1941E+03 -0.1937E+03 -0.1937E+03 -0.1933E+03
-0.1974E+03 -0.1976E+03 -0.1978E+03 -0.1976E+03 -0.1933E+03 -0.1930E+03 -0.1931E+03 -0.1928E+03
-0.1978E+03 -0.1974E+03 -0.1975E+03 -0.1968E+03 -0.1931E+03 -0.1929E+03 -0.1933E+03 -0.1932E+03
-0.1970E+03 -0.1962E+03 -0.1963E+03 -0.1955E+03 -0.1936E+03 -0.1937E+03 -0.1942E+03 -0.1943E+03
-0.1957E+03 -0.1950E+03 -0.1953E+03 -0.1947E+03 -0.1948E+03 -0.1951E+03 -0.1955E+03 -0.1959E+03
-0.1951E+03 -0.1948E+03 -0.1951E+03 -0.1951E+03 -0.1962E+03 -0.1966E+03 -0.1968E+03 -0.1971E+03
-0.1955E+03 -0.1957E+03 -0.1960E+03 -0.1965E+03 -0.1972E+03 -0.1975E+03 -0.1974E+03 -0.1975E+03
-0.1966E+03 -0.1972E+03 -0.1972E+03 -0.1978E+03 -0.1972E+03 -0.1973E+03 -0.1969E+03 -0.1968E+03
-0.1976E+03 -0.1982E+03 -0.1977E+03 -0.1983E+03 -0.1962E+03 -0.1961E+03 -0.1954E+03 -0.1952E+03
-0.1977E+03 -0.1980E+03 -0.1973E+03 -0.1975E+03 -0.1946E+03 -0.1942E+03 -0.1937E+03 -0.1933E+03
-0.1969E+03 -0.1969E+03 -0.1964E+03 -0.1963E+03 -0.1929E+03 -0.1926E+03 -0.1923E+03 -0.1921E+03
-0.1959E+03 -0.1958E+03 -0.1957E+03 -0.1955E+03 -0.1920E+03 -0.1918E+03 -0.1919E+03 -0.1918E+03
-0.1957E+03 -0.1956E+03 -0.1961E+03 -0.1960E+03 -0.1921E+03 -0.1921E+03 -0.1926E+03 -0.1927E+03
-0.1967E+03 -0.1966E+03 -0.1974E+03 -0.1974E+03 -0.1933E+03 -0.1935E+03 -0.1941E+03 -0.1944E+03
-0.1983E+03 -0.1983E+03 -0.1991E+03 -0.1990E+03 -0.1951E+03 -0.1954E+03 -0.1961E+03 -0.1965E+03
-0.1997E+03 -0.1995E+03 -0.1999E+03 -0.1997E+03 -0.1971E+03 -0.1975E+03 -0.1981E+03 -0.1985E+03
-0.1998E+03 -0.1995E+03 -0.1993E+03 -0.1990E+03 -0.1990E+03 -0.1995E+03 -0.1998E+03 -0.2003E+03
-0.1984E+03 -0.1981E+03 -0.1974E+03 -0.1971E+03 -0.2005E+03 -0.2010E+03 -0.2010E+03 -0.2014E+03
-0.1962E+03 -0.1960E+03 -0.1951E+03 -0.1950E+03 -0.2014E+03 -0.2017E+03 -0.2016E+03 -0.2018E+03
-0.1941E+03 -0.1942E+03 -0.1935E+03 -0.1936E+03 -0.2015E+03 -0.2016E+03 -0.2013E+03 -0.2012E+03
-0.1932E+03 -0.1934E+03 -0.1932E+03 -0.1935E+03 -0.2008E+03 -0.2005E+03 -0.2000E+03 -0.1997E+03
-0.1935E+03 -0.1939E+03 -0.1941E+03 -0.1944E+03 -0.1991E+03 -0.1986E+03 -0.1981E+03 -0.1974E+03
-0.1948E+03 -0.1951E+03 -0.1956E+03 -0.1958E+03 -0.1969E+03 -0.1962E+03 -0.1958E+03 -0.1951E+03
-0.1964E+03 -0.1965E+03 -0.1971E+03 -0.1971E+03 -0.1948E+03 -0.1942E+03 -0.1940E+03 -0.1935E+03
-0.1977E+03 -0.1977E+03 -0.1982E+03 -0.1981E+03 -0.1934E+03 -0.1930E+03 -0.1931E+03 -0.1930E+03
-0.1987E+03 -0.1985E+03 -0.1990E+03 -0.1989E+03 -0.1932E+03 -0.1932E+03 -0.1935E+03 -0.1937E+03
-0.1992E+03 -0.1991E+03 -0.1994E+03 -0.1992E+03 -0.1941E+03 -0.1944E+03 -0.1948E+03 -0.1953E+03
-0.1994E+03 -0.1993E+03 -0.1992E+03 -0.1991E+03 -0.1956E+03 -0.1962E+03 -0.1965E+03 -0.1971E+03
-0.1989E+03 -0.1987E+03 -0.1983E+03 -0.1981E+03 -0.1973E+03 -0.1978E+03 -0.1980E+03 -0.1984E+03
-0.1974E+03 -0.1972E+03 -0.1963E+03 -0.1960E+03
-0.1950E+03 -0.1947E+03 -0.1937E+03 -0.1933E+03 Time history of total force from water pressure
-0.1924E+03 -0.1920E+03 -0.1912E+03 -0.1909E+03 0.2056E+03 0.1030E+03 0.1578E+03 0.8574E+02
-0.1903E+03 -0.1901E+03 -0.1898E+03 -0.1898E+03 0.1095E+03 0.1486E+03 0.3082E+03 0.2695E+03
-0.1898E+03 -0.1899E+03 -0.1902E+03 -0.1905E+03 0.2275E+03 0.2482E+03 0.2967E+03 0.3205E+03

0.3986E+03	0.2601E+03	0.2693E+03	0.2938E+03	0.1877E+03	0.1854E+03	0.1723E+03	0.1687E+03
0.2783E+03	0.2890E+03	0.2333E+03	0.1380E+03	0.1574E+03	0.1605E+03	0.1532E+03	0.1587E+03
0.1831E+03	0.1577E+03	0.1574E+03	0.1028E+03	0.1570E+03	0.1607E+03	0.1679E+03	0.1705E+03
0.8795E+02	0.4743E+02	0.1166E+03	0.1076E+03	0.1846E+03	0.1854E+03	0.2026E+03	0.2023E+03
0.7989E+02	0.1155E+03	0.9129E+02	0.1550E+03	0.2158E+03	0.2182E+03	0.2317E+03	0.2305E+03
0.1985E+03	0.1774E+03	0.2173E+03	0.2151E+03	0.2358E+03	0.2288E+03	0.2328E+03	0.2250E+03
0.2697E+03	0.2760E+03	0.3099E+03	0.2714E+03	0.2254E+03	0.2156E+03	0.2102E+03	0.2001E+03
0.2925E+03	0.3064E+03	0.2816E+03	0.3031E+03	0.1935E+03	0.1895E+03	0.1778E+03	0.1751E+03
0.2445E+03	0.2377E+03	0.2250E+03	0.2092E+03	0.1713E+03	0.1712E+03	0.1677E+03	0.1659E+03
0.1818E+03	0.1628E+03	0.1280E+03	0.1255E+03	0.1626E+03	0.1734E+03	0.1739E+03	0.1842E+03
0.1208E+03	0.1107E+03	0.9920E+02	0.1044E+03	0.1887E+03	0.1988E+03	0.1982E+03	0.2091E+03
0.1065E+03	0.1224E+03	0.1516E+03	0.1360E+03	0.2139E+03	0.2261E+03	0.2184E+03	0.2246E+03
0.1827E+03	0.1789E+03	0.2172E+03	0.2350E+03	0.2239E+03	0.2279E+03	0.2254E+03	0.2185E+03
0.2424E+03	0.2630E+03	0.2605E+03	0.2911E+03	0.2233E+03	0.2142E+03	0.2100E+03	0.1951E+03
0.2686E+03	0.2938E+03	0.2590E+03	0.2656E+03	0.1972E+03	0.1848E+03	0.1819E+03	0.1776E+03
0.2520E+03	0.2324E+03	0.2214E+03	0.1934E+03	0.1713E+03	0.1697E+03	0.1682E+03	0.1651E+03
0.1794E+03	0.1589E+03	0.1528E+03	0.1286E+03	0.1684E+03	0.1742E+03	0.1762E+03	0.1783E+03
0.1286E+03	0.1105E+03	0.1203E+03	0.1130E+03	0.1827E+03	0.1912E+03	0.1944E+03	0.2030E+03
0.1301E+03	0.1232E+03	0.1498E+03	0.1537E+03	0.2061E+03	0.2182E+03	0.2175E+03	0.2208E+03
0.1767E+03	0.1953E+03	0.2045E+03	0.2296E+03	0.2150E+03	0.2233E+03	0.2196E+03	0.2101E+03
0.2352E+03	0.2568E+03	0.2596E+03	0.2696E+03	0.2127E+03	0.2083E+03	0.2028E+03	0.1948E+03
0.2676E+03	0.2691E+03	0.2649E+03	0.2548E+03	0.1900E+03	0.1828E+03	0.1795E+03	0.1737E+03
0.2444E+03	0.2333E+03	0.2104E+03	0.2081E+03	0.1687E+03	0.1778E+03	0.1698E+03	0.1708E+03
0.1775E+03	0.1780E+03	0.1495E+03	0.1498E+03	0.1729E+03	0.1691E+03	0.1734E+03	0.1737E+03
0.1309E+03	0.1327E+03	0.1255E+03	0.1286E+03	0.1809E+03	0.1864E+03	0.1937E+03	0.2001E+03
0.1345E+03	0.1363E+03	0.1543E+03	0.1574E+03	0.2020E+03	0.2087E+03	0.2154E+03	0.2170E+03
0.1790E+03	0.1838E+03	0.2105E+03	0.2102E+03	0.2197E+03	0.2184E+03	0.2233E+03	0.2209E+03
0.2403E+03	0.2330E+03	0.2584E+03	0.2503E+03	0.2135E+03	0.2066E+03	0.2122E+03	0.2039E+03
0.2646E+03	0.2557E+03	0.2574E+03	0.2516E+03	0.2010E+03	0.1938E+03	0.1845E+03	0.1853E+03
0.2385E+03	0.2365E+03	0.2125E+03	0.2139E+03	0.1833E+03	0.1750E+03	0.1731E+03	0.1696E+03
0.1868E+03	0.1857E+03	0.1653E+03	0.1619E+03	0.1753E+03	0.1751E+03	0.1725E+03	0.1850E+03
0.1493E+03	0.1482E+03	0.1440E+03	0.1442E+03	0.1856E+03	0.1916E+03	0.1949E+03	0.1967E+03
0.1458E+03	0.1514E+03	0.1567E+03	0.1706E+03	0.2022E+03	0.2071E+03	0.2006E+03	0.2197E+03
0.1819E+03	0.1925E+03	0.2042E+03	0.2126E+03	0.2116E+03	0.2128E+03	0.2048E+03	0.2078E+03
0.2290E+03	0.2335E+03	0.2411E+03	0.2465E+03	0.2056E+03	0.2028E+03	0.2061E+03	0.1991E+03
0.2467E+03	0.2483E+03	0.2423E+03	0.2385E+03	0.1898E+03	0.1950E+03	0.1848E+03	0.1807E+03
0.2309E+03	0.2203E+03	0.2142E+03	0.1987E+03	0.1897E+03	0.1800E+03	0.1855E+03	0.1878E+03
0.1904E+03	0.1775E+03	0.1730E+03	0.1580E+03	0.1934E+03	0.1855E+03	0.1847E+03	0.1897E+03
0.1526E+03	0.1505E+03	0.1436E+03	0.1484E+03	0.1995E+03	0.2095E+03	0.2032E+03	0.2038E+03
0.1483E+03	0.1566E+03	0.1614E+03	0.1706E+03	0.2122E+03	0.2112E+03	0.2192E+03	0.2122E+03
0.1788E+03	0.1877E+03	0.2009E+03	0.2071E+03	0.2098E+03	0.2158E+03	0.2107E+03	0.2154E+03
0.2199E+03	0.2269E+03	0.2350E+03	0.2374E+03	0.2083E+03	0.2042E+03	0.1986E+03	0.2019E+03
0.2423E+03	0.2373E+03	0.2380E+03	0.2343E+03	0.1849E+03	0.1950E+03	0.1754E+03	0.1808E+03
0.2293E+03	0.2193E+03	0.2118E+03	0.2034E+03	0.1795E+03	0.1825E+03	0.1798E+03	0.1770E+03

0.1718E+03	0.1861E+03	0.1839E+03	0.1860E+03	0.1969E+03	0.1896E+03	0.1987E+03	0.1964E+03
0.1905E+03	0.1971E+03	0.2022E+03	0.2090E+03	0.2060E+03	0.1993E+03	0.2001E+03	0.1991E+03
0.2037E+03	0.2111E+03	0.2137E+03	0.2153E+03	0.2061E+03	0.1986E+03	0.2062E+03	0.2060E+03
0.2158E+03	0.2248E+03	0.2084E+03	0.2186E+03	0.1932E+03	0.1994E+03	0.1925E+03	0.1926E+03
0.2149E+03	0.2106E+03	0.2119E+03	0.2111E+03	0.1973E+03	0.1948E+03	0.1988E+03	0.1960E+03
0.2136E+03	0.1926E+03	0.2127E+03	0.2020E+03	0.1914E+03	0.1961E+03	0.1924E+03	0.1944E+03
0.1984E+03	0.2094E+03	0.1915E+03	0.2029E+03	0.1942E+03	0.1927E+03	0.1912E+03	0.2023E+03
0.2049E+03	0.2012E+03	0.2038E+03	0.1998E+03	0.2018E+03	0.1950E+03	0.1997E+03	0.1936E+03
0.2057E+03	0.2090E+03	0.2011E+03	0.2063E+03	0.1975E+03	0.1976E+03	0.1977E+03	0.1905E+03
0.2118E+03	0.2267E+03	0.2134E+03	0.2215E+03	0.1910E+03	0.1932E+03	0.1987E+03	0.2002E+03
0.2169E+03	0.2061E+03	0.2101E+03	0.2155E+03	0.1966E+03	0.1975E+03	0.1949E+03	0.1869E+03
0.2155E+03	0.1998E+03	0.2062E+03	0.1967E+03	0.1998E+03	0.2007E+03	0.1933E+03	0.2004E+03
0.1935E+03	0.1913E+03	0.1917E+03	0.1923E+03	0.1926E+03	0.1990E+03	0.1955E+03	0.1981E+03
0.1998E+03	0.1883E+03	0.1839E+03	0.1891E+03	0.2040E+03	0.1956E+03	0.1938E+03	0.2047E+03
0.1842E+03	0.1918E+03	0.1966E+03	0.1935E+03	0.2009E+03	0.2008E+03	0.2050E+03	0.2004E+03
0.2029E+03	0.2017E+03	0.2057E+03	0.2096E+03	0.1945E+03	0.2054E+03	0.2019E+03	0.2026E+03
0.2136E+03	0.2042E+03	0.2086E+03	0.2051E+03	0.2054E+03	0.1998E+03	0.1954E+03	0.2070E+03
0.2108E+03	0.2120E+03	0.2074E+03	0.2104E+03	0.2018E+03	0.2069E+03	0.1949E+03	0.2027E+03
0.2085E+03	0.2134E+03	0.2044E+03	0.1975E+03	0.1936E+03	0.1973E+03	0.2007E+03	0.1908E+03
0.1978E+03	0.1912E+03	0.1924E+03	0.1881E+03	0.1922E+03	0.1948E+03	0.1982E+03	0.1982E+03
0.1944E+03	0.1811E+03	0.1896E+03	0.1879E+03	0.1952E+03	0.2000E+03	0.1990E+03	0.2034E+03
0.1889E+03	0.1837E+03	0.1904E+03	0.1950E+03	0.1944E+03	0.2011E+03	0.1961E+03	0.1965E+03
0.1933E+03	0.1986E+03	0.1978E+03	0.2088E+03	0.2045E+03	0.1982E+03	0.2031E+03	0.2005E+03
0.2098E+03	0.1931E+03	0.2014E+03	0.2034E+03	0.1953E+03	0.2093E+03	0.2060E+03	0.1899E+03
0.2064E+03	0.1963E+03	0.2102E+03	0.2040E+03	0.2002E+03	0.1981E+03	0.2033E+03	0.2004E+03
0.2024E+03	0.2064E+03	0.2009E+03	0.1953E+03	0.1994E+03	0.2018E+03	0.2024E+03	0.2034E+03
0.1964E+03	0.1934E+03	0.1937E+03	0.1971E+03	0.2069E+03	0.2039E+03	0.2067E+03	0.2060E+03
0.1896E+03	0.1853E+03	0.1934E+03	0.1886E+03	0.2051E+03	0.2076E+03	0.2066E+03	0.2074E+03
0.1898E+03	0.1906E+03	0.1932E+03	0.1945E+03	0.2050E+03	0.2034E+03	0.2021E+03	0.2038E+03
0.1897E+03	0.1985E+03	0.1962E+03	0.1990E+03	0.2040E+03	0.2036E+03	0.1998E+03	0.2016E+03
0.1910E+03	0.1965E+03	0.1951E+03	0.1968E+03	0.1974E+03	0.2031E+03	0.2025E+03	0.2009E+03
0.1949E+03	0.2022E+03	0.2030E+03	0.2031E+03	0.2004E+03	0.2002E+03	0.1929E+03	0.1949E+03
0.2001E+03	0.2004E+03	0.2001E+03	0.1959E+03	0.1970E+03	0.1975E+03	0.1962E+03	0.1964E+03
0.2000E+03	0.1919E+03	0.1898E+03	0.1842E+03	0.1922E+03	0.1964E+03	0.1968E+03	0.1928E+03
0.1917E+03	0.1910E+03	0.1913E+03	0.1898E+03	0.2021E+03	0.2006E+03	0.2007E+03	0.1982E+03
0.1957E+03	0.1953E+03	0.1939E+03	0.1868E+03	0.2046E+03	0.1998E+03	0.2016E+03	0.2023E+03
0.2014E+03	0.1943E+03	0.2100E+03	0.1933E+03	0.2048E+03	0.2033E+03	0.2016E+03	0.2001E+03
0.2019E+03	0.2076E+03	0.2069E+03	0.2029E+03	0.2020E+03	0.1986E+03	0.1988E+03	0.1951E+03
0.1950E+03	0.2052E+03	0.2005E+03	0.1989E+03	0.2006E+03	0.2018E+03	0.1992E+03	0.1944E+03
0.2058E+03	0.1924E+03	0.2005E+03	0.1928E+03	0.2005E+03	0.1960E+03	0.1957E+03	0.1948E+03
0.1977E+03	0.1899E+03	0.1968E+03	0.1925E+03	0.1952E+03	0.1939E+03	0.1992E+03	0.1949E+03
0.1909E+03	0.1896E+03	0.1936E+03	0.1896E+03	0.1958E+03	0.1995E+03	0.1986E+03	0.1985E+03
0.1940E+03	0.1895E+03	0.1950E+03	0.1925E+03	0.1991E+03	0.2001E+03	0.2014E+03	0.2044E+03
0.1882E+03	0.1944E+03	0.1894E+03	0.1934E+03	0.2044E+03	0.2034E+03	0.1975E+03	0.1996E+03

0.2034E+03	0.2020E+03	0.1975E+03	0.2000E+03	0.1889E+03	0.1887E+03	0.1888E+03	0.1895E+03
0.1961E+03	0.2006E+03	0.1974E+03	0.1992E+03	0.1889E+03	0.1905E+03	0.1899E+03	0.1911E+03
0.1952E+03	0.1960E+03	0.1981E+03	0.1952E+03	0.1919E+03	0.1918E+03	0.1921E+03	0.1921E+03
0.1919E+03	0.1935E+03	0.1941E+03	0.1929E+03	0.1926E+03	0.1936E+03	0.1941E+03	0.1936E+03
0.1931E+03	0.1917E+03	0.1951E+03	0.1950E+03	0.1927E+03	0.1950E+03	0.1935E+03	0.1929E+03
0.1960E+03	0.1996E+03	0.1995E+03	0.1955E+03	0.1934E+03	0.1929E+03	0.1936E+03	0.1929E+03
0.1961E+03	0.1982E+03	0.1935E+03	0.1975E+03	0.1924E+03	0.1922E+03	0.1917E+03	0.1915E+03
0.1943E+03	0.1981E+03	0.1946E+03	0.1999E+03	0.1917E+03	0.1903E+03	0.1899E+03	0.1870E+03
0.1961E+03	0.1947E+03	0.1930E+03	0.1935E+03	0.1907E+03	0.1875E+03	0.1871E+03	0.1881E+03
0.1950E+03	0.1958E+03	0.1950E+03	0.1933E+03	0.1885E+03	0.1893E+03	0.1876E+03	0.1874E+03
0.1943E+03	0.1952E+03	0.1957E+03	0.1959E+03	0.1891E+03	0.1900E+03	0.1889E+03	0.1892E+03
0.1972E+03	0.1983E+03	0.1959E+03	0.1985E+03	0.1889E+03	0.1888E+03	0.1917E+03	0.1923E+03
0.1991E+03	0.1988E+03	0.1999E+03	0.2002E+03	0.1915E+03	0.1925E+03	0.1928E+03	0.1956E+03
0.2030E+03	0.2027E+03	0.2016E+03	0.2004E+03	0.1959E+03	0.1962E+03	0.1957E+03	0.1965E+03
0.2028E+03	0.2049E+03	0.1983E+03	0.2020E+03	0.1977E+03	0.1967E+03	0.1989E+03	0.1993E+03
0.2020E+03	0.2003E+03	0.2002E+03	0.1997E+03	0.1989E+03	0.1989E+03	0.1988E+03	0.2007E+03
0.1999E+03	0.1981E+03	0.1994E+03	0.1956E+03	0.1995E+03	0.2006E+03	0.2026E+03	0.2023E+03
0.1966E+03	0.1958E+03	0.1942E+03	0.1957E+03	0.2018E+03	0.2022E+03	0.2048E+03	0.2006E+03
0.1944E+03	0.1942E+03	0.1957E+03	0.1960E+03	0.2022E+03	0.2020E+03	0.2008E+03	0.2001E+03
0.1934E+03	0.1953E+03	0.1931E+03	0.1935E+03	0.2005E+03	0.1984E+03	0.1986E+03	0.2004E+03
0.1944E+03	0.1942E+03	0.1942E+03	0.1957E+03	0.1999E+03	0.1973E+03	0.1966E+03	0.1977E+03
0.1971E+03	0.1954E+03	0.1965E+03	0.1965E+03	0.1957E+03	0.1945E+03	0.1954E+03	0.1963E+03
0.1958E+03	0.1959E+03	0.1980E+03	0.1970E+03	0.1944E+03	0.1925E+03	0.1939E+03	0.1926E+03
0.1995E+03	0.1987E+03	0.1966E+03	0.1975E+03	0.1948E+03	0.1950E+03	0.1924E+03	0.1947E+03
0.1974E+03	0.1953E+03	0.1964E+03	0.1963E+03	0.1943E+03	0.1925E+03	0.1953E+03	0.1943E+03
0.1978E+03	0.1964E+03	0.1962E+03	0.1961E+03	0.1952E+03	0.1965E+03	0.1961E+03	0.1970E+03
0.1938E+03	0.1949E+03	0.1933E+03	0.1943E+03	0.1960E+03	0.1969E+03	0.2000E+03	0.1981E+03
0.1936E+03	0.1934E+03	0.1932E+03	0.1933E+03				
0.1909E+03	0.1901E+03	0.1903E+03	0.1895E+03				
0.1889E+03	0.1886E+03	0.1873E+03	0.1870E+03				
0.1864E+03	0.1853E+03	0.1861E+03	0.1855E+03				
0.1855E+03	0.1863E+03	0.1862E+03	0.1864E+03				
0.1866E+03	0.1866E+03	0.1882E+03	0.1890E+03				
0.1896E+03	0.1891E+03	0.1914E+03	0.1918E+03				
0.1932E+03	0.1925E+03	0.1941E+03	0.1936E+03				
0.1951E+03	0.1962E+03	0.1965E+03	0.1955E+03				
0.1966E+03	0.1965E+03	0.1970E+03	0.1963E+03				
0.1974E+03	0.1960E+03	0.1964E+03	0.1961E+03				
0.1953E+03	0.1951E+03	0.1942E+03	0.1948E+03				
0.1925E+03	0.1943E+03	0.1917E+03	0.1935E+03				
0.1909E+03	0.1925E+03	0.1908E+03	0.1912E+03				
0.1911E+03	0.1905E+03	0.1901E+03	0.1889E+03				
0.1899E+03	0.1893E+03	0.1902E+03	0.1898E+03				
0.1905E+03	0.1895E+03	0.1886E+03	0.1898E+03				